The Role of the Cell Cycle in Human Embryonic Stem Cell Self-Renewal and Pluripotency

(La función del ciclo celular en la auto-renovación y la pluripotencia de las células madre embrionarias humanas)

Cristina Menchón Najas

ADVERTIMENT. La consulta d'aquesta tesi queda condicionada a l'acceptació de les següents condicions d'ús: La difusió d'aquesta tesi per mitjà del servei TDX (**www.tdx.cat**) ha estat autoritzada pels titulars dels drets de propietat intel·lectual únicament per a usos privats emmarcats en activitats d'investigació i docència. No s'autoritza la seva reproducció amb finalitats de lucre ni la seva difusió i posada a disposició des d'un lloc aliè al servei TDX. No s'autoritza la presentació del seu contingut en una finestra o marc aliè a TDX (framing). Aquesta reserva de drets afecta tant al resum de presentació de la tesi com als seus continguts. En la utilització o cita de parts de la tesi és obligat indicar el nom de la persona autora.

ADVERTENCIA. La consulta de esta tesis queda condicionada a la aceptación de las siguientes condiciones de uso: La difusión de esta tesis por medio del servicio TDR (**www.tdx.cat**) ha sido autorizada por los titulares de los derechos de propiedad intelectual únicamente para usos privados enmarcados en actividades de investigación y docencia. No se autoriza su reproducción con finalidades de lucro ni su difusión y puesta a disposición desde un sitio ajeno al servicio TDR. No se autoriza la presentación de su contenido en una ventana o marco ajeno a TDR (framing). Esta reserva de derechos afecta tanto al resumen de presentación de la tesis como a sus contenidos. En la utilización o cita de partes de la tesis es obligado indicar el nombre de la persona autora.

WARNING. On having consulted this thesis you're accepting the following use conditions: Spreading this thesis by the TDX (**www.tdx.cat**) service has been authorized by the titular of the intellectual property rights only for private uses placed in investigation and teaching activities. Reproduction with lucrative aims is not authorized neither its spreading and availability from a site foreign to the TDX service. Introducing its content in a window or frame foreign to the TDX service is not authorized (framing). This rights affect to the presentation summary of the thesis as well as to its contents. In the using or citation of parts of the thesis it's obliged to indicate the name of the author.

THE ROLE OF THE CELL CYCLE IN HUMAN EMBRYONIC STEM CELL SELF-RENEWAL AND PLURIPOTENCY

LA FUNCIÓN DEL CICLO CELULAR EN LA AUTO-RENOVACIÓN Y LA PLURIPOTENCIA DE LAS CÉLULAS MADRE EMBRIONARIAS HUMANAS

CRISTINA MENCHÓN NAJAS

Barcelona, 2011

DEPARTAMENTO DE BIOQUÍMICA Y BIOLOGÍA MOLECULAR
FACULTAD DE BIOLOGÍA
UNIVERSIDAD DE BARCELONA
CENTRO DE MEDICINA REGENERATIVA DE BARCELONA

THE ROLE OF THE CELL CYCLE IN HUMAN EMBRYONIC STEM CELL SELF-RENEWAL AND PLURIPOTENCY

LA FUNCIÓN DEL CICLO CELULAR EN LA AUTO-RENOVACIÓN Y LA PLURIPOTENCIA DE LAS CÉLULAS MADRE EMBRIONARIAS HUMANAS

CRISTINA MENCHÓN NAJAS

Barcelona, 2011

THE ROLE OF THE CELL CYCLE IN HUMAN EMBRYONIC STEM CELL SELF-RENEWAL AND PLURIPOTENCY

LA FUNCIÓN DEL CICLO CELULAR EN LA AUTO-RENOVACIÓN Y LA PLURIPOTENCIA DE LAS CÉLULAS MADRE EMBRIONARIAS HUMANAS

Memoria presentada por **Cristina Menchón Najas**, Licenciada en Biología, para optar al Título de Doctora por la Universidad de Barcelona. Programa de Doctorado en Biomedicina (Bienio 2004-2006).

Tesis Doctoral realizada en el Centro de Medicina Regenerativa de Barcelona bajo la dirección del Dr. Juan Carlos Izpisúa Belmonte y Dr. Michael John Edel y bajo la tutoría de la Dra. Julia Peinado Onsurbe

La interesada

Cristina Menchón Najas

Directores de la Tesis Doctoral:

Dr. Juan Carlos Izpisúa Belmonte **Dr. Michael John Edel**

Tutora de la Tesis Doctoral:

Dra. Julia Peinado Onsurbe

AGRADECIMIENTOS

Y ya he llegado a mis últimas palabras y al fin de la tesis ¡por fin! Pensaba que no se acabaría nunca pero aquí está. Claro que esto no hubiera sido posible sin la ayuda de muchas personas que directamente o indirectamente han hecho que esto haya sido posible:

En primer lugar me gustaría agradecer al Ministerio de Educación y Ciencia la concesión de una beca FPU y al Centro de Medicina Regenerativa de Barcelona por financiarme durante el último año de tesis.

Me gustaría agradecer a Juan Carlos Izpisúa Belmonte la confianza depositada en mí y la oportunidad de poder realizar mi tesis en su laboratorio. Hace algunos años, estando en C.O.U. oí hablar del laboratorio de Juan Carlos y su trabajo con células madre, entonces pensé que algún día me gustaría trabajar con las células madre en su laboratorio, gracias por hacer mi sueño realidad.

This thesis would not have been possible without Michael Edel. Mike thanks for everything, for your support, for your infinite patience, for all your advices (Cris, focus…). I have learnt a lot from you. Thanks for all.

Me gustaría agradecer también a Julia Peinado su apoyo incondicional. Julia no habría podido llegar hasta aquí sin tu ayuda. Muchas gracias por estar siempre ahí para cualquier cosa que he necesitado y por todos tus consejos. Te estoy infinitamente agradecida.

También quisiera agradecer a todo el personal del Departamento de Biología Celular que tan bien me acogió cuando decidí venirme de Alicante y por todo lo que aprendí. Lo pasé muy bien durante esos años.

Esta tesis no hubiera sido posible sin las excelentes plataformas técnicas del Centro de Medicina Regenerativa de Barcelona, en especial a Facs Cytometry, Bioimaging y Cell Culture. Esta tesis no se hubiera hecho realidad sin vuestra ayuda. Gracias por todo lo que me habéis enseñado, por estar siempre dispuestos a poner a punto algún experimento, por los favores en el último momento (a veces del día). Gracias a todos por todo lo que me habéis enseñado y por los buenos momentos vividos.

Me gustaría hacer extensivo estos agradecimientos a todo el personal del Centro de Medicina Regenerativa de Barcelona, incluidos los que ya no están, porque todos y cada uno de vosotros me habéis aportado algo y siempre habéis estado ahí para

cualquier cosa que he necesitado. No puedo nombraros a todos porque no acabaría nunca y seguro que se me olvidaría alguno. También al personal de Administración por vuestra ayuda.

Me gustaría agradecer también al personal del Banco de líneas celulares su apoyo incondicional, su amabilidad y el haberme introducido en el complejo mundo de las células madres embrionarias, y enseñarme cómo cultivarlas entre otras muchas cosas ¡Gracias Yoli e Ignasi! ¡Muchas gracias a todos!

A los compañeros de fatigas, los becarios, algunos ya Doctores o en proceso (Adriana, Alex, Borja, Edu, Erika, Ignasi, Lorena, Raquel) por compartir frustaciones y *sopars becaris*. ¡Gracias a todos! Os echaré de menos.

Me gustaría agradecer también al personal del Instituto de Alta Tecnología de Barcelona por su apoyo para cualquier cosa que he necesitado, por la ayuda estadística y los programas informáticos. ¡Muchas gracias!

Me gustaría agradecer a Neil Forrest las correcciones del inglés gratuitas ¡en pro de la Ciencia! Thank you very much Neil.

También me gustaría agradecer a todas las personas que he conocido en Barcelona (y alrededores) durante estos años, tampoco puedo nombraros a todos porque no acabaría nunca: a todos los amigos (que son muchos), amigas de la resi, a mis compañeros de piso en especial a Montse por ser un apoyo incondicional para todo y a Sergi que me ha ayudado en el diseño de la portada. También a mi prima "Titi" que me cuidó durante San Juan. Muchas gracias a todos por hacerme sentir como en casa y por los buenos momentos compartidos. A Silvia y Sagrario por los tuppers de comida que me han salvado más de una vez. También a mis amigos de Alicante por estar siempre ahí aunque no vaya a menudo.

A toda mi familia en general, tíos, primos, cuñados… por confiar en mí y quererme.

A mi sobrino José Ángel por su ayuda informática. A mis sobrinas Natalia y Estefanía por su apoyo moral cuando no me salían los experimentos. A mis sobrinos más pequeños (Benito, Estrella, José Antonio y Loli) por la divulgación científica en el colegio de lo que hago en el laboratorio.

A Raúl (cari) por tu apoyo incondicional. Gracias por estar siempre ahí, por todos tus consejos, por los fines de semana y algún que otro verano sacrificado, por salir tan tarde del laboratorio... por lo feliz que me haces.

A mis hermanas, ¡tengo tanto que agradeceros! gracias por todo, por confiar en mí, por animarme siempre, por vuestros consejos, por quererme, por estar ahí cuando más lo he necesitado, por el vacío que nos ha quedado… espero que tengamos fuerzas para seguir el largo camino que nos queda.

Pero si a alguien tengo que agradecer el poder haber llegado hasta aquí es a mis padres. No tengo palabras para definir lo afortunada que soy por los padres que tengo. Gracias por vuestro infinito amor. Por vuestros consejos, por haberme apoyado en todas las decisiones de mi vida y darme la libertad de elegir. Por lo feliz que he sido con vosotros y porque me habéis enseñado que ante todo en la vida hay que ser una buena persona. A mi madre por su valentía, su bondad y su sabiduría.

A mi padre, muchas gracias por todo lo que nos has enseñado, qué buen ejemplo nos has dado, por ser tan bueno, por tus sabios consejos, tu serenidad y por cuidarnos. Hemos sido muy felices contigo. Espero que nos des fuerzas para seguir… Esta tesis va dedicada especialmente para ti.

Vivir en los corazones que dejamos
tras nosotros, eso no es morir
Thomas Campbell

A mi padre José Menchón Castellanos

ABSTRACT

Embryonic stem cells (ESC) are derived from the inner cell mass (ICM) of the blastocyst and have the capacity for unlimited proliferation while retaining their potential to differentiate into a wide variety of cell types when cultured *in vitro.* These properties have made of human embryonic stem cells (hESC) an excelent model on which to study the conditions required for differentiation into specific cell lineages, and consequently the possibility of transplanting specific cell types into damaged tissues.

The continued turn over of ESC while maintaining an undifferentiated state is dependent on unusual cell cycle properties. These unusual proliferative properties are responsible for the generation of tumours when these cells are injected into adult animals. Thus, the study of the unusual proliferative properties of hESC needs to be addressed if their potential is to be realized. To date, most studies of the cell cycle in hESC have been descriptive, lacking functional studies that reveal the mechanisms of how the cell cycle maintains pluripotency and self- renewal of hESC.

In this thesis we sought to understand the mechanisms of cell cycle control of hESC. We asked the question if a single cell cycle gene could regulate the self-renewal or pluripotency properties of hESC using a gain and loss of gene function strategy. We have identified that the protein expression of the $p27^{Kip1}$ cell cycle inhibitor was low in human pluripotent cells, but its expression increased during differentiation together with changes in the cell cycle structure of pluripotent cells. By adopting a gain and loss of function strategy we increased or reduced its expression in undifferentiating conditions to define its functional role in self-renewal and pluripotency of hESC. Using undifferentiation conditions, overexpression of $p27^{Kip1}$ in hESC lead to a G_1 phase arrest with an enlarged and flattened hESC morphology and consequently loss of self-renewal ability. Loss of $p27^{Kip1}$ caused an increase of self-renewal while maintaining an undifferentiated phenotype. Moreover, we have shown that a change in the balance of $p27^{Kip1}$ levels in undifferentiated hESC affects expression of the mesoderm markers: *BRACHYURY* and *TWIST*. We have found that expression changes of *TWIST1* are associated with the presence of $p27^{Kip1}$ protein in the *TWIST1* gene promoter.

The results presented in this thesis have interesting implications in stem cell biology. Firstly, these results define that the maintenance of $p27^{Kip1}$ protein levels at a certain level is essential for self-renewal and pluripotency of hESC. Secondly, $p27^{Kip1}$ is involved in the regulation of *TWIST* which is upregulated in several types of tumours and induces an epithelial-mesenchymal transition to facilitate tumor metastasis.

RESUMEN

Las células madre embrionarias son derivadas de la masa celular interna de los blastocistos y poseen la capacidad para dividirse ilimitadamente, reteniendo su potencial para diferenciarse hace una amplia variedad de tipos celulares, cuando son cultivadas *in vitro*. Estas propiedades hacen de las células madre embrionarias humanas un modelo excelente en el cual estudiar las condiciones requeridas para diferenciarse hacia linajes celulares específicos y, por lo tanto, la posibilidad de poder trasplantar tipos celulares específicos en tejidos dañados.

El continuo recambio de las células madre embrionarias al mismo tiempo que mantienen un estado de indiferenciación es dependiente de sus inusuales propiedades del ciclo celular. Estas inusuales propiedades proliferativas son responsables de la formación de tumores cuando estas células son inyectadas en modelos animales adultos. Así pues, el estudio de las propiedades proliferativas es necesario con el fin de poder aplicar las células madre embrionarias humanas en terapia celular. Actualmente, la mayoría de los estudios del ciclo celular de las células madre embrionarias han sido descriptivos, faltando estudios funcionales que revelen los mecanismos por los cuales el ciclo celular mantiene las propiedades de pluripotencia y auto-renovación de las células madre embrionarias humanas.

El objetivo de esta tesis doctoral fue el estudio de los mecanismos de control del ciclo celular de las células madre embrionarias humanas. Nos preguntamos si una única proteína del ciclo celular podría regular las propiedades auto-renovación o pluripotencia de las células madre embrionarias humanas mediante una estrategia de ganancia o perdida de función. Durante el desarrollo de esta tesis, hemos identificado que la expresión del inhibidor del ciclo celular $p27^{Kip1}$ era baja en células humanas pluripotentes pero sus niveles de expresión aumentaron dramáticamente durante la diferenciación, al mismo tiempo que la estructura del ciclo celular de las células pluripotentes cambió. Por medio de una estrategia de ganancia y pérdida de función, aumentamos o reducimos la expresión de $p27^{Kip1}$ con el fin de definir su función en la auto-renovación o pluripotancia de las células madre embrionarias humanas. En condiciones de indiferenciación, la sobreexpresión de $p27^{Kip1}$ en las células madre embrionarias humanas resultó en un arresto del ciclo celular en fase G_1 y un cambio hacia una morfología más grande y aplanada, y, por lo tanto, pérdida de la capacidad de auto-renovación. La pérdida de $p27^{Kip1}$ causó un aumento de la auto-renovación manteniendo un fenotipo indiferenciado.

También, hemos demostrado que un cambio en el balance de la expresión de $p27^{Kip1}$ en células madre embrionarias humanas indiferenciadas afecta la expresión de los reguladores de mesodermo: *BRACHYURY* y *TWIST*. Además, hemos descubierto que los cambios en la expresión de *TWIST1* están asociados con la presencia de la proteína $p27^{Kip1}$ en el promotor de *TWIST1*.

En su conjunto, los resultados presentados en esta tesis poseen implicaciones interesantes para la Biología de las células madre por varias razones. En primer lugar, estos resultados han revelado que los niveles de $p27^{Kip1}$ han de ser mantenidos a ciertos niveles para mantener las propiedades de auto-renovación y pluripotencia de las células madre embrionarias humanas. En segundo lugar, $p27^{Kip1}$ está implicada en la regulación de *TWIST*, cuya expresión está aumentada en múltiples tipos de tumores y, además, está implicado en el proceso de transición de epitelio a mesénquima para facilitar la formación de metástasis tumorales.

CONTENTS

ABBREVIATIONS

AP-1: activator protein 1
bFGF: basic fibroblast growth factor
bHLH: basic helix-loop-helix
BMP: bone morphogenetic protein
BSA: bovine serum albumin
CBP: Creb-binding protein
CDK: cyclin dependent kinase
cDNA: complementary DNA
CHX: cycloheximide
CKI: cyclin dependent kinase inhibitor
CM: conditioned medium
DAPI: 4', 6-dimidino-2-phenylindole
DGCR8: DiGeorge syndrome critical region gene 8
$DilC_1(5)$: 1,1′,3,3,3′,3′-hexamethylindodicarbo-cyanine iodide
DNMT3B: DNA (cytosine-5-) methyltransferase 3 beta
DOX: doxycycline
EB: embryoid bodies
EdU: 5-ethynyl-2'-deoxyuridine
EMT: epithelial to mesenchymal transition
EpiSC: epiblast stem cells
ERK: extracellular signal regulated kinase
ESC: embryonic stem cells
FACS: fluorescence activated cell sorting
FBS: fetal bovine serum
FiPSC: fibroblasts induced pluripotent stem cells
FOXO: Forkhead box group O
G_1 phase: Gap 1 phase
G_2 phase: Gap 2 phase
GATA 6: GATA binding protein 6
GBX2: gastrulation brain homeobox 2
GEF: guanine-nucleotide exchange factor
GFP: green fluorescent protein
GSK3-β: glycogen synthase kinase 3β
hESC: human embryonic stem cells
hFiPS: human fibroblast induced pluripotent stem cells
hiPSC: human induced pluripotent stem cells
hKiPS: human keratinocytes induced pluripotent stem cells
hKIS: human kinase interacting stathmin
ICM: inner cell mass
IGF: insulin-like growth factors
iPSC: induced pluripotent stem cells
JAB1: Jun activating binding protein 1
JAK: Janus-associated tyrosine kinase
KiPSC: keratinocytes induced pluripotent stem cells
KODMEM: Knockout Dulbecco´s Modified Eagle´s Medium
KPC: Kip1 ubiquitination promoting complex
KSR: knockout serum replacement
LB: Luria Bertani
LIF: leukaemia inhibitory factor

LIMK: LIM domain kinase
M phase: Mitosis phase
MAPK: mitogen activated protein kinase
MCM: mini chromosome maintenance protein
MEF: mouse embryonic fibroblast
mESC: mouse embryonic stem cells
MET: mesenchymal to epithelial transitions
MG-132: carbobenzoxy-L-leucyl-L-leucinal
miPSC: mouse induced pluripotent stem cells
miRNA: microRNAs
NF-κβ: nuclear factor kappa-light-chain-enhancer of activated B cells
NLS: nuclear localization signal
NT: non target
Oct3/4: octamer-binding transcription factor 3/4
PAK: p21-activated kinase
PBS: phosphate-buffered saline
PBST: PBS containing 0.1% Tween-20
PCNA: proliferating cell nuclear antigen
PI: propidium iodide
PI3K: phosphatidylinositol-3-OH-kinase
PKB: protein kinase B
PLZF: promyelocytic leukaemia zinc finger
qRT-PCR: quantitative reverse transcription polymerase chain reaction
R: Restriction point control
RA: Retinoic Acid
Rb: retinoblastoma
Rho: Ras homolog gene family
RhoA: Ras homolog gene family member A
RISC: RNA-induced silencing complex
ROCK: Rho-associated protein kinase
RTK: receptor tyrosine kinase
S phase: Synthesis phase
SAC: spindle assembly checkpoint
Ser: serine
shRNAs: short hairpin RNAs
Skp2: S-phase kinase associated protein 2
snRNA: small nuclear RNA
Sox2: Sex-determining region Y (SRY)-related HMG-box 2
STAT3: signal transducer and activator of transcription 3
T: Brachyury
TBS: Tris-buffered saline
TGFβ: transforming growth factor β
Thr: threonine
TKO: triple knockout
tTA: tetracycline transactivator
Tuj1: β-Tubulin III
Tyr: tyrosine
UTR: 3’ untranslated region
X-gal: 5-bromo-4-chloro-3-indolyl-βD-galactopyranoside

LIST OF FIGURES

LIST OF TABLES

INTRODUCTION

1. STEM CELLS

Stem cells are a type of cells that have the ability to renew themselves as well as the ability to differentiate into various cell types. According to their capacity to differentiate into other cell types they are classified as:

(1) **Totipotent**: these type of cells have a self-organizing ability to generate a whole organism and can differentiate into any cell type (Niwa 2007). In mammals only the zygote and early blastomeres are totipotent.

(2) **Pluripotent**: these cells can give rise to cell types of all three germ layers of the foetus: ectoderm, mesoderm, and endoderm. An example are the cells of the epiblast that are specific to the early embryo (Pera and Tam 2010).

(3) **Multipotent**: these are cells that can give rise to all cell types within one particular lineage. An example are hematopoietic stem cells.

(4) **Unipotent:** these type of cells can only generate one type of cells, an example are spermatogonial stem cells as they can only form sperm (Jaenisch and Young 2008).

According to their origin, stem cells can be classified into:

1. Embryonic: Pluripotent cells are present only transiently in embryos *in vivo* as they quickly differentiate into various somatic cells through development. However, the cells derived from the epiblast of blastocysts, namely embryonic stem cells, can be propagated indefinitely as a stable self-renewing population under appropriate conditions *in vitro* (Evans and Kaufman 1981; Thomson et al 1998).

Embryonic stem cells (ESC) are pluripotent which means that an individual cell can give rise to all cell types of the foetus even after prolonged culture. This has been shown conclusively in mouse embryonic stem cells (mESC) by their complete integration into a developing embryo after being reintroduced into the blastocyst (Beddington and Robertson 1989). These cells can efficiently colonize the germ line, resulting in chimaeric animals. In contrast to their behaviour when introduced into the early embryo, they produce teratomas, that is, mixed cell tumours comprising the three germ layers: ectoderm, mesoderm, and endoderm when they are injected into adult mice.

For human embryonic stem cells (hESC), where embryo transfer is not practical, the common test to assay pluripotency is their ability to form teratomas when injected into immunocompromised mice (Yu and Thomson 2008; Ohtsuka and Dalton 2008).

Both mESC and hESC can also undergo multilineage differentiation *in vitro* and produce a range of well differentiated progeny.

More recently, pluripotent epiblast stem cells (EpiSC) have been established from epiblast of mouse embryos at the post-implantation pre-gastrulation stage, but their properties differ markedly from those of mESC. Unlike mESC they cannot contibute to the germ line after introduction into host blastocysts but they can form teratomas (Yu and Thomson 2008). A similar developmental potential of mEpiSC and hESC to that of the epiblast of mouse embryos has been suggested given that they share key features with hESC, such as, the independence of leukaemia inhibitory factor (LIF) to maintain their state. However, there are crucial differences between the cell surface marker and gene expression of the two cell types (Pera and Tam 2010). Given the lack of data on gene expression during crucial phases of immediate post-implantation development in humans, it remains unclear precisely which embryonic cells are the counterpart of hESC (Pera and Tam 2010).

2. Germinal: embryonic germ cells (EGC) are pluripotent stem cells derived from primordial germ cells *in vitro*. In culture, mouse EGC are morphologically indistinguishable from mESC and express typical mESC markers. Upon blastocyst injection they can contribute extensively to chimaeric mice including germ cells (Yu and Thomson 2008).

Another type of pluripotent stem cells: multipotent germline stem cells (mGSC) more recently have been derived from both neonatal and adult mouse testis. These cells share a similar morphology with mESC, express typical mESC specific markers, differentiate into multiple lineages *in vitro*, form teratomas, and contribute extensively to chimaeras including germline cells upon injection into blastocysts. However, mGSC have an epigenetic status distinct from both mESC and mouse EGC (Yu and Thomson 2008).

3. Somatic: they are a type of undifferentiated cells found in adult or fetal somatic differentiated tissues that have limited self-renewal capacity and usually only can differentiate into cell types associated with the organ system in which they reside. Currently, it is known that niches of stem cells exist in many tissues, such as bone marrow, brain, liver, skin, skeletal muscle, the gastrointestinal tract, the pancreas, the

eye, blood, and dental pulp. A notable exception to the tissue specificity of adult stem cells is the mesenchymal stem cell or what is more recently called the multipotent adult progenitor cell (MAPC). This cell type is derived from bone marrow stroma and has been shown to differentiate *in vitro* into numerous tissue types including neuronal, adipose, muscle, liver, lungs, spleen, and gut but, notably, not bone marrow or gonads, though the generation of a single high-contribution postnatal chimaera from MAPC was reported, this result has not been independently confirmed to date, and the demonstration of functional integration of donor cells into, non only, midgestation embryos but viable late-stage embryos or postnatal chimaeras is needed to make this conclusion (Jaenisch and Young 2008).

This thesis will be focused in embryonic stem cells.

2. EMBRYONIC STEM CELLS

The first mESC lines were derived from the inner cell mass (ICM) of mouse blastocysts in 1981 (Evans and Kaufman 1981; Martin 1981). These cells have also been derived from cleavage stage embryos and even from individual blastomeres of two- to eight-cell stage embryos. Initially, mESC were cultured onto mitotically inactivated mouse embryonic fibroblast feeder cells (MEF) and serum. Posterior experiments demonstrated that they could be cultured in the absence of feeder cells with conditioned filtered medium obtained from these cells. Analysis of conditioned medium led to the identification of leukaemia inhibitory factor (LIF), a member of IL-6 family of cytokines, as a factor that sustained mESC. In serum-free medium, LIF alone was insufficient to prevent mESC differentiation, however in combination with bone morphogenetic protein (BMP), mESC state was sustained (Yu and Thomson 2008).

There was a considerable delay between the derivation of mESC in 1981 and the derivation of hESC in 1998 (Thomson et al 1998). This was due to species differences between both types of cells and suboptimal human embryo culture media. Initially hESC were derived using mitotically inactivated feeder layers and serum-containing medium. However, LIF and its related cytokines failed to support human and non human primate ESC. In contrast to mESC, basic fibroblast growth factor (bFGF) and transforming growth factor β (TGFβ)/Activin/Nodal signalling are of central importance for the culture of undifferentiated hESC (Yu and Thomson 2008). Because of the

dependence of hESC on bFGF, they are thought to be derived from a later stage of ICM development than mESC.

Because their fundamental properties: the ability to self-renew indefinitely and the developmental potential to differentiate to derivatives from the three germ layers, hESC are ideal candidates for their use in Regenerative Medicine and tissue engineering including gene therapy, cell replacement therapies and drug discovery.

2.1. THERAPEUTIC POTENTIAL OF HUMAN EMBRYONIC STEM CELLS

Human embryonic stem cells (hESC) are the *in vitro* counterparts of the early human embryo. This enables the study of the molecular events of human embryogenesis, until now very scarce due to ethical issues. Moreover, they can provide a platform where to isolate ESC from human embryos with genetic diseases and study the molecular mechanisms of these diseases and the way to treat them. This is particularly important for those diseases for which there are not animals models that reproduce the human disease. Besides this, hESC can be differentiated into various types of cells, and thus be used in functional assays and for evaluation of potential toxicity. Finally, hESC are ideal candidates for their use as cell replacement therapies or tissue engineering in several diseases because of their unlimited capacity to self-renew and capability to differentiate into any cell type of an embryo or adult. They could be used as a therapeutic delivery of factors that are not express in specific genetic diseases (Figure 1).

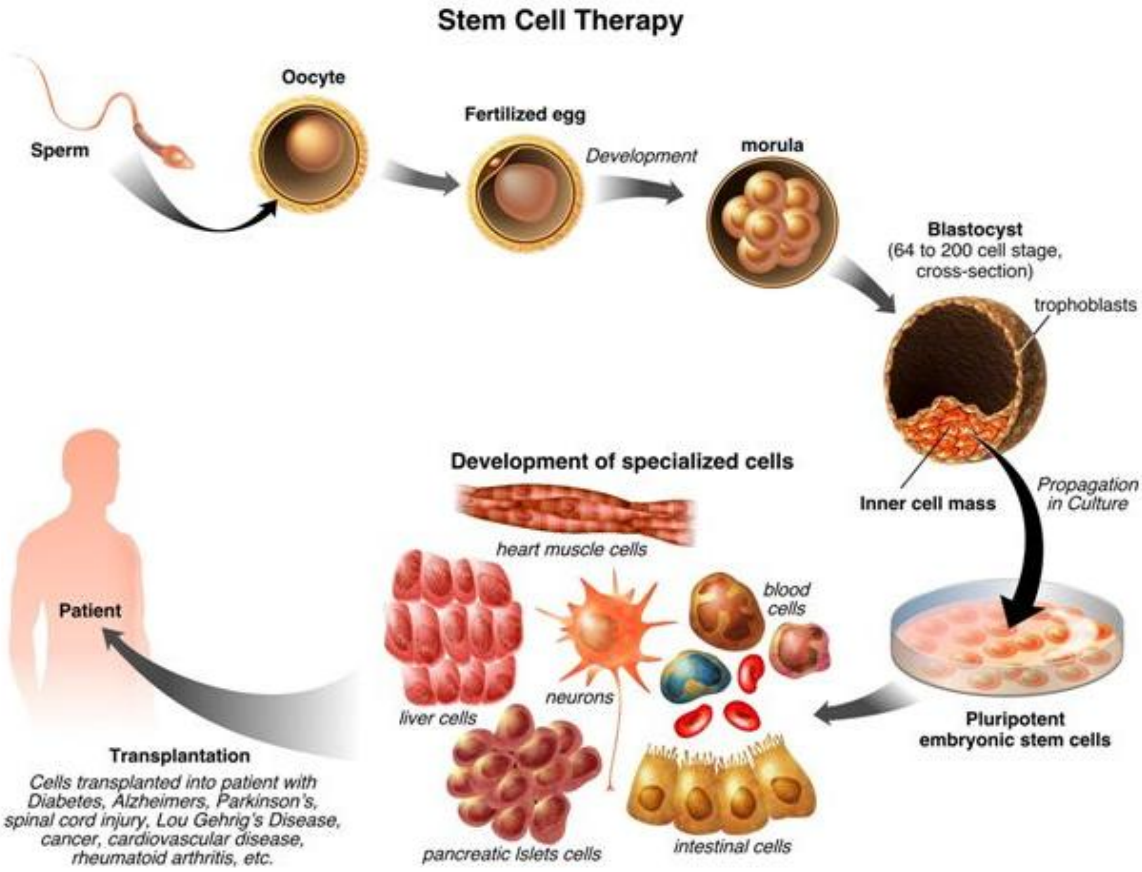

Figure 1. Cell replacement therapy. Human embryonic stem cells (hESC) are derived from the inner cell mass of human blastocysts. Like the inner cell mass cells, hESC are pluripotent and have the potential to give rise to all cell types of the foetus. Moreover, they can be propagated indefinitely *in vitro.* These properties make that hESC can be expanded in high numbers *in vitro*, differentiated into specific cell lineages, and transplanted into patients with specific damaged tissues. If they are manipulated to express a specific molecule, they could be used for therapeutic delivery of factors that are not expressed in specific genetic diseases.

Despite the advantages of therapeutic potential of hESC, they present some disadvantages, such as, allogenic hESC transplantation may result in graft rejection. Also, and importantly, if they are not properly differentiated, hESC can give rise to tumours comprising the three embryonic germ layers when grafted into an adult host.

Thus, many basic questions about the biology of these cells, and especially the study of the unusual proliferative properties need to be addressed if their potential is to be realized. On the other hand, they will shed light in the mechanisms underlying proliferation and acquisition of malignant properties, such as, undifferentiation of tumour cells.

2.2. PLURIPOTENCY AND SELF-RENEWAL

Embryonic stem cells can be expanded in large numbers *in vitro* owing to a process of symmetrical self-renewal, while maintaining their ability to generate all cell types of a foetus, that is, pluripotency. Thus, the self-renewal and pluripotency properties of ESC entail continuous proliferation in absence of differentiation. These properties are related to unsual cell cycle properties of ESC together with signalling networks, transcription factors, epigenetic regulators, and microRNAs.

The next sections will be dedicated to the mechanisms involved in the fundamental properties of hESC focusing in the unusual mechanisms of cell cycle control compared to somatic cells.

2.2.1. Signalling pathways

The key signalling pathways that maintain hESC in their pluripotent state are those mediated by activin A, basic fibroblast growth factor (bFGF, also known as FGF2), and insulin/insulin-like growth factors (IGF). These signalling pathways differ from those critical for maintaining mESC pluripotent state which depend on LIF. Besides LIF, phosphatidylinositol-3-OH-kinase (PI3K)/protein kinase B (PKB; Akt) pathway appears to be most critical, and may be activated as part of the LIF signalling pathway or from other factors in media (for example IGF) (Ohtsuka and Dalton 2008). The differences between hESC and mESC have been suggested to be a consequence of species-specific differences in development, or it is possible that hESC and mESC represent different stages of development (Pera and Tam 2010).

A summary table of the different signalling pathways involved in the maintenance of mESC and hESC is presented below (Table 1).

Origin ESC	Signalling pathway	Activators	Effectors	Effect	Reference
Human	TGF-β	TGFβ/Activin/Nodal	Smad-2/-3	Undifferentiation	(Wang, Zhang et al. 2005) (Vallier, Alexander et al. 2005) (James, Levine et al. 2005)
Mouse	TGF-β	TGFβ/Activin/Nodal	Smad-2/-3	Undifferentiation	(Shen 2007)
Human	TGF-β	BMP	Smad-1/-5/-8	Differentiation	(Xu, Chen et al. 2002)
Mouse	TGF-β	BMP	Smad-1/-5/-8	Suppression differentiation	(Ying, Nichols et al. 2003) (Qi, Li et al. 2004)
Human	Ras-Raf-ERK	bFGF	ERK	Undifferentiation	(Li, Wang et al. 2007) (Feng 2007) (Kang, Kim et al. 2005)
Mouse	Ras-Raf-ERK	Growth factors that bind RTK	ERK	Differentiation	(Kunath, Saba-El-Leil et al. 2007) (Burdon, Stracey et al. 1999)
Human	PI3K	IGF/insulin	Akt1	Suppression differentiation Survival	(McLean, D'Amour et al. 2007)
Mouse	PI3K	LIF/IGF	Akt1	Undifferentiation	(Storm, Bone et al. 2007) (Paling, Wheadon et al. 2004) (Amit, Carpenter et al. 2000)
Mouse	LIF-STAT3	LIF	JAK-STAT	Undifferentiation	(Matsuda, Nakamura et al. 1999) (Niwa, Burdon et al. 1998) (Raz, Lee et al. 1999)
Human	Wnt	Wnt	GSK3-β	proliferation	(Dravid, Ye et al. 2005)
Mouse	Wnt	Wnt	β-catenin/p300	Suppression differentiation	(Miyabayashi, Teo et al. 2007)

Table 1. Summary of signalling networks that regulate the maintenance of the properties of human and mouse embryonic stem cells. Signalling mediated by members of TGF-β family such as TGF-β, activin and nodal, and growth factors such as, IGF and bFGF, maintain hESC state. Signalling mediated by LIF, BMP, and IGF maintain mESC state. TGF-β, transforming growth factor-β; BMP, bone morphogenetic proteins; ERK, extracellular signal regulated kinase; bFGF, basic fibroblast growth factor; RTK, receptor tyrosine kinase; PI3K, phosphatidylinositol-3-OH kinase; IGF, insulin-like growth factors; LIF, leukaemia inhibitory factor; STAT3, signal transducer and activator of transcription 3; JAK, Janus-associated tyrosine kinase; GSK3-β, glycogen synthase kinase 3β.

2.2.2. Transcription factors

The genetic basis of pluripotency have been elaborated in ESC, in which a transcriptional network driven by the core transcription factors: octamer-binding transcription factor 3/4 (Oct3/4), Nanog, and Sex-determining region Y (SRY)-related HMG-box 2 (Sox2) are essential to maintain the undifferentiated state of both mESC and hESC. The transcription factors Oct3/4, Nanog, and Sox2 regulate their own expression and control a set of targets through mutual heterodimerization and/or shared promoter occupancy, thus forming a self-reinforcing circuit of pluripotency (Hemberger, Dean et al. 2009).

There are many transcription factors involved in maintaining pluripotency, however, this thesis will be focused on the main ones.

Oct3/4

Octamer-binding transcription factor 3/4 (Oct3/4), also known as Oct3, Oct4, or Pou5f1 is a POU-domain transcription factor. It is specifically expressed in ESC, early embryos, and germ cells. The transcription factor Oct3/4 is highly expressed in hESC and mESC and its expression diminishes when these cells differentiate and lose pluripotency. Its expression is essential for the development of the ICM *in vivo*, the derivation of ESC, and the maintenance of a pluripotent state. However, twofold overexpression of Oct3/4 in ESC causes differentiation into primitive endoderm and mesoderm. Thus a critical amount of Oct-3/4 is required to sustain ESC properties, and up- or downregulation induce divergent developmental programmes (Yamanaka 2008; Niwa, Miyazaki et al. 2000).

Sox2

Sex-determining region Y (SRY)-related HMG-box 2 (Sox2) family of transcription factors are part of a large family of 20 proteins that share a similar HMG box DNA-binding motif. The transcription factor Sox2 is expressed in ESC, in the extra-embryonic ectoderm, trophoblast stem cells, and neural stem cells. In these cell lineages, Sox2 expression is restricted to cells with stem cell characteristics and is no longer expressed in cells with a more restricted developmental potential (Avilion, Nicolis et al. 2003). Homozygous mutant blastocysts differentiate into trophoectoderm and primitive endoderm-like cells when cultured *in vitro*. In the same way, disruption of

Sox2 in mESC and hESC results in rapid differentiation (Fong, Hohenstein et al. 2008; Yamanaka 2008). The transcription factor Sox2 is involved in the self-renewal of ESC and has an important role in maintaining ESC pluripotency. Indeed it heterodimerizes in a complex with Oct3/4 (Yuan, Corbi et al. 1995).

A recent study in hESC showed the high frequency of co-occupancy within the same gene region by key pluripotency factors. Thus, among OCT3/4 bound genes, half of them are also bound by SOX2, and 87% of these sites also overlap with NANOG targets (Boyer, Lee et al. 2005).

Nanog

Nanog is an homeobox protein specifically expressed in pluripotent cells and is absent from differentiated cells. It is found in the interior cells of the compacted morula and the ICM of the blastocyst. On implantation, Nanog expression is detected only in the epiblast and is eventually restricted to primordial germ cells (Chambers, Colby et al. 2003). *Nanog*-null embryos show disoganization of extraembryonic tissues at E5.5, with no discernible epiblast. *Nanog*-deficient blastocysts appear to be morphologically normal, but the inner cell mass produces only parietal endoderm-like cells and not epiblast when cultured *in vitro*. Knockdown of Nanog leads to differentiation in both mESC and hESC. Importantly, overexpression of Nanog in mESC permits cells to self-renew in the absence of LIF, although the cells self-renewal capability is reduced. Likewise, overexpression of NANOG in hESC enabled growth without feeder cells (Yamanaka 2008).

More recently, a slightly more refined role of Nanog has been proposed. According to new data, loss of Nanog predisposes ESC to differentiation but does not mark commitment and is reversible (Chambers, Silva et al. 2007). Nanog expression is upregulated by Oct3/4 and Sox2. Also, FoxD3, a forkhead family transcription factor highly expressed in mESC and pluripotent cells of the early embryo, can activate *Nanog* promoter (Pan, Li et al. 2006). In this study it was shown that Oct3/4 maintains Nanog expression by directly binding to the *Nanog* promoter when present at a sub-steady level, but represses it when Oct3/4 is above the normal level. On the other hand, FoxD3 positively regulates Nanog to counter the repression effect of excess of Oct3/4. Conversely, Nanog and FoxD3 function as activators of Oct3/4 expression. When the expression level of Oct3/4 rises above a steady level, it represses its own promoter as

well as *Nanog*, thus exerting a negative feedback regulation loop to limit its own expression (Pan, Li et al. 2006). This negative feedback regulation loop keeps the expression of Oct3/4 at a steady level, thus maintaining ESC properties.

Overall, these data suggest that the key pluripotency factors work together rather than individually, to control a whole set of target genes, as well as each other, to maintain the pluripotency of ESC (Pan and Thomson 2007).

2.2.3. MicroRNAs regulation

MicroRNAs (miRNAs) are small (19–25 nucleotides) endogenous non-coding RNAs that bind to the 3′ untranslated region (UTR) of target messenger RNA (mRNA) to repress gene expression by inhibition of mRNA translation or direct cleavage of targeted mRNA (Bibikova, Laurent et al. 2008). Occasionally, miRNAs have also been observed to activate target mRNA translation and to regulate their stability.

MicroRNAs are produced via a multi-step process (Figure 2) which commences with the production of a long primary transcript (pri-miRNA) by RNA polymerase II or III (Borchert, Lanier et al. 2006; Lee, Kim et al. 2004).

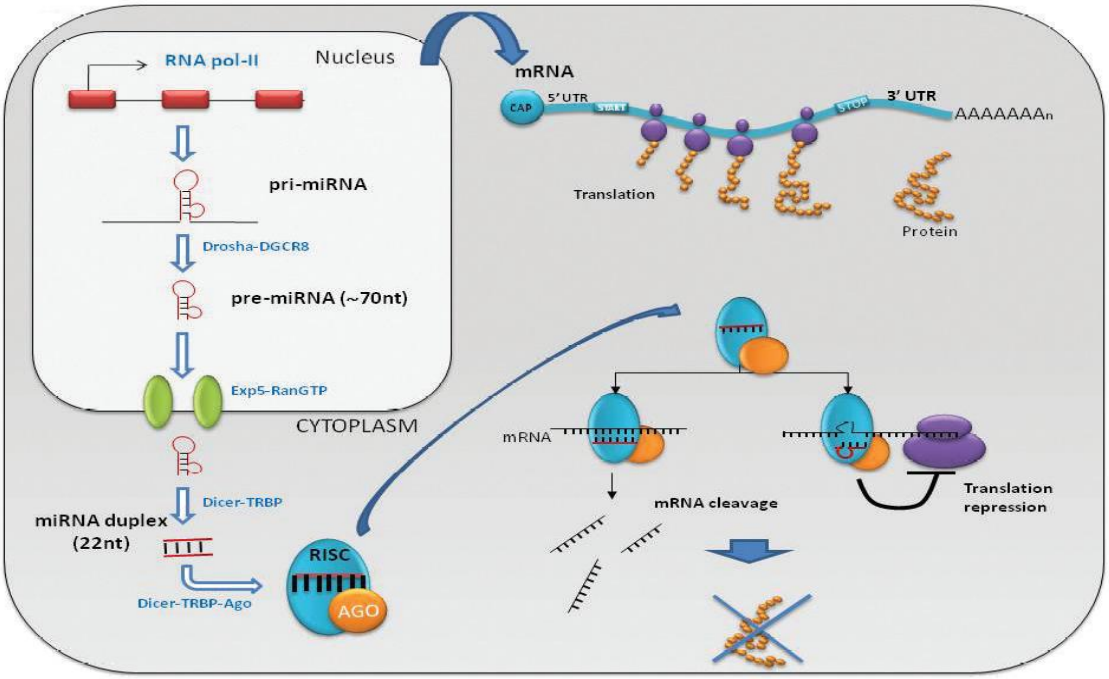

Figure 2. MicroRNAs biogenesis pathway. MicroRNAs (miRNAs) are produced via a multi-step process which commences with the production of a long primary transcript (pri-miRNA) by RNA polymerase II or III. The pri-miRNA folds into a stemloop structure and is subsequently processed by the Microprocessor protein complex containing Drosha, a nuclear RNase-III-like enzyme, and DiGeorge syndrome critical region gene 8 (DGCR8; also known as Pasha) proteins. The microprocessor protein complex-mediated cleavage yields a hairpin structure, ranging in size from 70-100 nucleotides, called precursor miRNA (pre-miRNA) that is translocated by the exportin 5–RanGTP shuttle system into the cytoplasm, in which another cleavage is performed by a second RNase-III-like enzyme called Dicer. This cleavage results in the formation of a small double stranded RNA duplex, containing both the mature miRNA and its complementary sequence, that is processed by RISC which produces and directs the mature miRNA to its targets which results either in repression of gene expression by inhibition of mRNA translation or direct cleavage of targeted mRNA. RISC, RNA-induced silencing complex. Adapted from (Navarro and Monzo 2010).

MicroRNAs have been shown to be powerful key regulator elements, since a particular miRNA sequence is thought to guide the regulation of several hundred different mRNAs. Additionally, an individual mRNA may be simultaneously targeted by multiple different miRNAs. Thus, miRNA-mediated gene regulation represents an extensive mechanism for modulating gene expression.

Since their discovery, research has been aimed at identifying the functions and target genes of miRNAs discovering important roles for miRNAs in ESC properties.

MicroRNAs functions in embryonic stem cells

These small, non-coding RNAs are believed to regulate more than a third of all protein coding genes, and they have been implicated in the control of virtually all biological processes, including the biology of ESC.

Small RNA profiling in different mammalian tissues and cell types has revealed a plethora of miRNAs, with more than 500 identified so far, some of which are cell type specific and others of which display a more widespread expression profile. Both mESC and hESC express only a very limited repertoire of miRNAs whose levels decrease as stem cells differentiate (Gangaraju and Lin 2009). Indeed, the ESC-specific miR-290 family (which includes miR-290, miR-291a, miR-291b, miR-292, miR-293, miR-294, miR-295) and miR-302 cluster (miR-302a, miR-302b, miR-302c, miR-302d, miR-367) in mice, and miR-371 family (miR-371, miR-372, miR-373) that is homologous to the mouse miR-290 family, and miR-302 family in humans, represent the majority of the total miRNA molecules expressed in undifferentiated ESC (Marson, Levine et al. 2008). Significantly, members of this set of ESC miRNAs possess the same or similar seed motif, suggesting common sets of target mRNAs (Gangaraju and Lin 2009).

The essential roles of miRNAs in the control of pluripotent ESC were clearly established by the finding that hESC lacking proteins required for miRNA biogenesis such as DICER and DROSHA were unable to downregulate stem cell specific markers and displayed defects in self-renewal by proliferation defects (Qi, Yu et al. 2009). The proliferation defect of DICER and DROSHA mutant ESC suggests that miRNAs are regulating cell cycle proteins. Indeed, a recent work demonstrated that two miRNAs, miR-195 and miR-372, could partially reverse the cell cycle delay in DICER knockdown hESC. Whereas miR-372 was shown to regulate the cyclin dependent kinase inhibitor $p21^{Cip1}$, miR-195 was shown to regulate the inhibitory kinase WEE1, one of the three kinases that negatively regulate the G_2 cyclin B-cyclin dependent kinase (CDK) complexes in mammalian cells (Qi, Yu et al. 2009).

In the same way, the reintroduction of the highly expressed miR-290 and miR-302 clusters into *Dgcr8*-deficient mESC partially rescued the proliferation and cell cycle defects of *Dgcr8*-deficient mESCs. These miRNA directly repressed several cell cycle proteins (Wang, Baskerville et al. 2008).

Numerous miRNAs have been shown to control the fate of ESC and to directly influence critical gene regulatory networks controlled by pluripotency factors. Thus, the

let-7 family of miRNAs is broadly expressed across differentiated tissues and is tightly regulated during ESC differentiation (Viswanathan, Daley et al. 2008). It was found that let-7 induces the differentiation of mESC by directly targeting the expression of several stemness factors, including c-Myc, Sal-like 4 *Drosophila* (Sall4), and Lin28, all of which have let-7 binding sites in their 3'UTR (Melton, Judson et al.).

Other miRNAs besides let-7 contribute to the restricted expression of pluripotency factors during ESC differentiation. A study in mESC uncovered evidence for the miR-134-, miR-296-, and miR-470 mediated regulation of the pluripotency factors Nanog, Oct4, and Sox2 (Tay, Zhang et al. 2008). Another work showed that miR-200c, miR-203, and miR-183 cooperate to repress the pluripotency factors Sox2 and Klf4 in mESC (Wellner, Schubert et al. 2009). Likewise, in hESC miR-145 represses OCT3/4, SOX2, and KLF4. Moreover, OCT3/4 transcriptionally repressed miR-145 expression (Xu, Papagiannakopoulos et al. 2009).

A growing list of tissue-specific miRNAs, which are silenced or not processed fully in ESC, has been found to promote differentiation upon their expression and proper processing. In this way, it has been demonstrated that the expression of either miR-1 or miR-133 in ESC results in enhanced mesoderm gene expression in differentiating embryoid bodies, and supression of differentiation into the ectodermal or endodermal cell lineages (Ivey, Muth et al. 2008). Additional evidence supporting the role for miRNAs in cell lineage determination, comes from a recent report where the elevation of miR-134 levels alone in mESC enhances differentiation toward ectodermal lineages, whereas inhibition of miR-134 blocks differentiation (Tay, Tam et al. 2008).

2.3. INDUCED PLURIPOTENT STEM CELLS

An important discovery that lead to a revolution in stem cells field came in 2006, when the reversion of differentiated somatic cells back to a pluripotent ESC like state was reported. The authors of this work selected twenty-four factors specifically expressed in mESC. Then, they introduced combinations of the genes into MEFs using a retroviral vector. Amazingly, they found that a combination of only four factors: Oct3/4, Sox2, Klf4, and c-myc, was sufficient to generate ESC like colonies. This process was called reprogramming, and the reprogrammed cells induced pluripotent stem cells (iPSC) (Takahashi and Yamanaka 2006). Following on this work, at the end of 2007, three groups demonstrated the isolation of iPSC from human embryonic neonatal and adult fibroblasts. Two groups used the same four factors that reprogram MEFs (Park, Zhao et al. 2008; Takahashi, Tanabe et al. 2007), whereas other group identified a different combination of four factors: Oct3/4, Sox2, Nanog, and a RNA binding protein Lin28 (Yu, Vodyanik et al. 2007). In addition to fibroblasts, mouse induced pluripotent stem cells (miPSC) have been generated from hepatocytes and gastric epithelial cells (Aoi, Yae et al. 2008), pancreatic cells (Stadtfeld, Brennand et al. 2008), neural stem cells (Kim, Zaehres et al. 2008; Silva, Barrandon et al. 2008), and B lymphocytes (Hanna, Markoulaki et al. 2008). In addition to fibroblasts, human induced pluripotent stem cells (hiPSC) have been generated from keratinocytes (KiPSC) (Aasen, Raya et al. 2008), and blood progenitor cells (Loh, Agarwal et al. 2009).

The potential to turn somatic cells into iPSC with comparable characteristics and developmental potential than ESC, has opened a new area in Regenerative Medicine. The iPSC technology offers the possibility to derive patient-specific iPSC that could be differentiate in the cell type damaged and transplanted into the host avoiding two important obstacles associated with hESC: immune rejection, and ethical concerns regarding the use of human embryos. However, the mechanism of reprogramming is a complex process that remains largely elusive and it will be necessary more research in this field before iPSC can be used in clinical applications. Also, the reprogramming vectors used in this process can cause insertional mutagenesis due to the integration of the provirus into critical areas of the host genome and lead to malignant transformation. Another concern is the long time required for the reprograming process which may induce chromosomal and genetic abnormalities, and also epigenetic instability that can induce the formation of tumours (Zhao and Daley 2008).

3. CELL CYCLE CONTROL OF SOMATIC CELLS

The genetic programmes controlling the properties of self-renewal and pluripotency are strictly linked to regulation of cell cycle. In fact, to hold self-renewal an ESC has to decide going into cell cycle, and bypass cell cycle exit, avoiding decisions such as differentiation, apoptosis, or senescence.

Embryonic stem cells have unusual proliferative properties that have been related to a unique cell cycle structure and mechanisms of cell cycle regulation that differ markedly from those observed in somatic cells.

In the next sections the current knowledge of cell cycle control mechanisms in differentiated mammalian cells and ESC will be summarized.

3.1. PHASES OF THE CELL CYCLE

The cell division cycle of eukaryotic cells is divided into four main phases, namely Gap 1 phase (G_1) where the cells grow and prepare for the Synthesis phase (S) where the chromosomes duplicate. After this process, the cells enter the Gap 2 phase (G_2) in which the cell continues to grow and prepares for Mitosis phase (M) during which the cell will actually divide (Figure 3). However most cells are not constantly proliferating and remain in a reversible resting state, often referred to, as quiescence or G_0. These cells can be stimulated to reenter the cycle and proliferate (Blomen and Boonstra 2007).

Collectively, G_1, S, and G_2 are called interphase, the cell cycle period distinct from division of the nucleus (mitosis) and cytoplasm (cytokinesis).

3.2. RESTRICTION POINT AND CHECKPOINTS

In culture, cells undergo a period of mitogen dependence in G_1 phase before they enter the cycle. In this period, they sense the amount of available nutrients or the intensity of the mitogenic information. If they receive positive stimuli they proceed to progress into cell cycle. This point is called the Restriction point (R) and represents a “point of no return” that commits cells to a new round of cell division. After a cell passes through this R point is no longer under the influence of growth factors and will enter the S phase even if deprived of mitogens. On the contrary, if they receive negative stimulus, such as, no availability of nutrients or differentiation stimuli, they exit the cell

cycle before the R point to undergo another cell fates, such as, differentiation, senescence, or apoptosis (Blomen and Boonstra 2007).

Proper progression through the cell cycle is monitored by checkpoints that check possible defects during cell cycle progression, such as DNA damage, and induce cell cycle arrest or apoptosis through modulation of cell cycle regulators (Figure 3). Also, these checkpoints prevent cells from entering into a new phase until they have succesfully completed the previous one. This pathway is essential for the maintenance of genome stability and prevention of tumour development. This manner, in the presence of DNA damage, the G_1/S checkpoint prevents replication of damaged DNA. During the S phase, intra S checkpoint inhibits replicative DNA synthesis of damaged DNA. Finally, the G_2/M checkpoint prevents damaged cells from entry into mitosis (Shimada and Nakanishi 2006). Cell cycle arrest allows cells to properly repair these defects, thus preventing their transmission to the resulting daughter cells. If repair is unsuccesful, cells may enter senescence or undergo apoptosis (Malumbres and Barbacid 2009).

One of the key players in these pathways is the transcription factor p53. p53 protein becomes stabilized and active upon DNA damage, and in turn regulates transcription of a large number of genes, among them the $p21^{Cip1/Waf1/WSdi1}$ cyclin dependent kinase inhibitor capable of silencing the cyclin dependent kinases which are essential for S phase entry (Sherr and Roberts 1999).

Finally, another checkpoint that is found in the cell cycle is the spindle assembly checkpoint (SAC) that controls proper chromosome segregation. Defects in the SAC can lead to premature separation of sister chromatids and could facilitate chromosomal instability (Malumbres and Barbacid 2009).

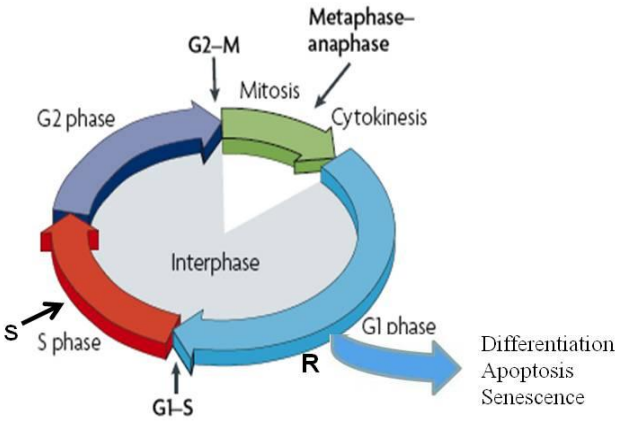

Figure 3. Restriction point and checkpoints during mammalian cell cycle. The cell division cycle is divided into four main phases: G_1, S, G_2, and M. During G_1 phase cells undergo a period of mitogen dependence during which they can decide if continue into cell cycle or exit to follow another cell fate. Beyond the restriction point (R) cells are irreversibly committed to S phase transition. DNA checkpoints at G_1 to S phase, intra S phase, G_2 to M phase, and spindle assembly checkpoint (SAC) sense possible defects during DNA synthesis and chromosome segregation.

3.3. CYCLINS AND CYCLIN DEPENDENT KINASES

In eukaryotic cells, the transition between cell cycle phases is governed by cyclin-dependent kinases (CDK) which belong to the class of protein serine-threonine kinases. The activity of CDK requires the binding of regulatory subunits known as cyclins. Cyclins are synthesized and destroyed at specific times during the cell cycle, thus regulating kinase activity in a timely manner (Figure 4A). The kinase is completely inactive without its cyclin partner, but in addition to the binding of cyclin, activation of the holoenzyme requires the activating phosphorylation of a key residue in the activation loop of the kinase subunit (Hochegger, Takeda et al. 2008). The active enzymes can be turned off in various ways, for example, the cyclin subunits can be degraded by highly specific ubiquitin-mediated proteolysis, the cyclin-CDK complexes can be subject to inhibitory phosphorylations, and finally, these complexes might associate with tight binding inhibitor proteins namely cyclin dependent kinase inhibitors (CKI).

Human cells contain multiple loci encoding CDK and cyclins. However, only a certain subset of CDK-cyclin complexes is directly involved in driving the cell cycle. They include three interphase CDK (CDK2, CDK4, and CDK6) a mitotic CDK (CDK1, also known as cell division control protein 2 (CDC2) and ten cyclins that belong to four different classes (the A-, B-, D- and E- type cyclins) (Malumbres and Barbacid 2009).

3.4. RETINOBLASTOMA-E2F PATHWAY

According to the "classical" model for the mammalian somatic cell cycle, specific cyclin-CDK complexes are responsible for driving the various events known to take place during cell cycle in a sequential and orderly fashion (Figure 4B). This manner, in early G_1 phase, mitogenic signals are first sensed by expression of D-type cyclins (D_1, D_2, and D_3) that preferentially bind and activate CDK4 and CDK6 and displace them from the CKI members of the INK4 family. When expressed at low levels, CKI members of the Cip/Kip family enhance the binding of Cyclin D_1 to the CDK4/6, acting as a bridge (Cheng, Olivier et al. 1999). In this way, cyclin D-CDK4/6 complexes sequester Cip/Kip proteins away from CDK2.

Activation of cyclin D-CDK4 and cyclin D-CDK6 complexes initiates phosphorylation of the retinoblastoma protein (Rb) Rb1 (also known as p105-Rb), and possibly other members of the family, comprising retinoblastoma-like protein 1 (Rbl1; also known as p107) and retinoblastoma-like protein 2 (Rbl2; also known as p130). Retinoblastoma protein family members or "pocket proteins" share sequence homology in a bipartite domain known as the pocket domain, which folds into a globular pocket-like structure owing to the presence of a flexible "spacer" region (Lapenna and Giordano 2009). The pocket domain mediates interactions with members of the E2F family of transcription factors and with proteins containing an LXCXE motif, such as, D-type cyclins, histone deacetylases, and viral oncoproteins (Lapenna and Giordano 2009). The activity of Rb family members is regulated by phosphorylation. Active hypophosphorylated Rb members inhibit the expression of genes that are required for entry into S phase by sequestering the E2F family of transcription factors (Lapenna and Giordano 2009).

Inactivation of the pocket proteins by cyclin D-CDK4 or cyclin D-CDK6 induces a partial release of E2F transcription factors which results in the activation and transcription of genes required for cell cycle progression, such as *E-type cyclins* and *cdc25A* genes. The cdc25A phosphatase removes inhibitory phosphates from CDK2, and the resulting cyclin E-CDK2 complexes then complete Rb proteins phosphorylation, leading to full release of E2F, activation of target genes, and entry into S phase (Harbour and Dean 2000). Cyclin E-CDK2 complexes also phosphorylate $p27^{Kip1}$, a CKI member of the Cip/Kip family, to target it for proteolysis, then reinforcing Rb proteins inactivation (Sheaff, Groudine et al. 1997).

A second pathway involves the *c-myc* protooncogene which directly stimulates transcription of the genes that encode cyclin E and cdc25A proteins to activate cyclin E-CDK2 complexes (Bartek and Lukas 2001).

Once S phase entry, CDK2 is subsequently activated by A-type cyclins. A-type cyclins are synthesized at the onset of the S phase and, together with CDK2, phosphorylate proteins involved in DNA replication and drive the transition from S phase to G_2 phase. Finally, CDK1 is thought to be activated by A-type cyclins to facilitate the onset of mitosis. Following nuclear envelope breakdown, A-type cyclins are degraded, facilitating the formation of the cyclin B-CDK1 complexes responsible for driving cells through mitosis (Satyanarayana and Kaldis 2009; Malumbres and Barbacid 2009).

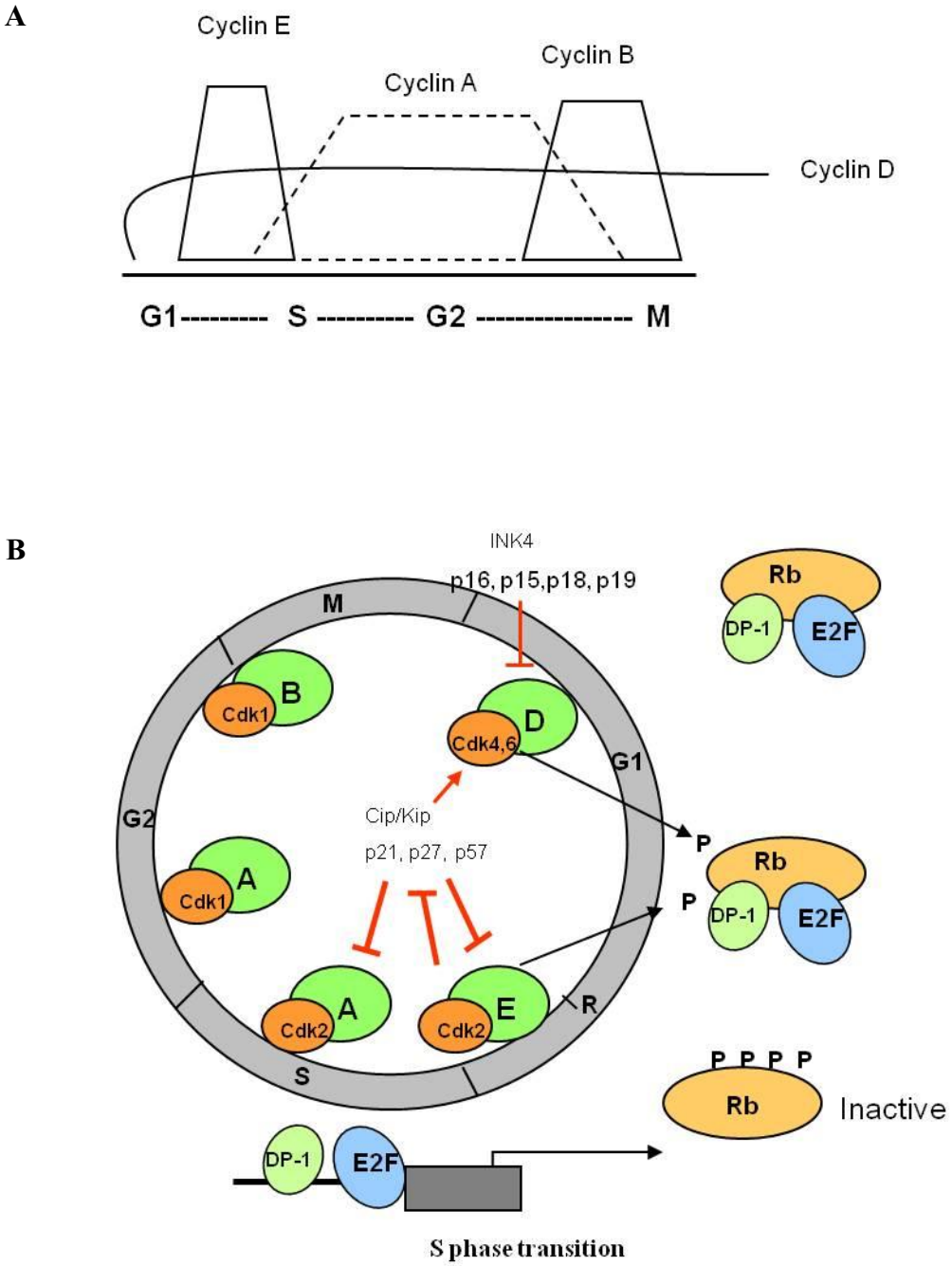

Figure 4. Model of mammalian somatic cell cycle control. (**A**) Cyclins E, A, and B are synthesized and destroyed at specific times during the cell cycle, thus regulating kinase activity in a timely and periodic manner. Cyclin D expression is regulated by extracellular signals. (**B**) During somatic cell cycle, each of the main events that take place during cell cycle is driven by unique cyclin dependent kinases (CDK) bound to specific cyclins. Proliferation of somatic cells is controlled primarily by regulating the progression through G_1 phase and entry into S phase. Inactivation of retinoblatoma protein (Rb) family by the sequential phosphorylation mediated by cyclin-CDK complexes leads to full release of E2F transcription factors and activation of target genes required for entry into S phase. The cyclin dependent kinase inhibitors (CKI) members of the INK4 and Cip/Kip family negatively regulate cyclin D-CDK4/6 and cyclin E/A-CDK2 kinases, respectively.

3.5. CYCLIN DEPENDENT KINASE INHIBITORS

Cell division relies on the coordinated activation of cyclins which bind to CDKs to induce cell cycle progression towards S phase, and later to initiate mitosis. One level of regulation of these cyclin-CDK complexes is provided by their binding to cyclin dependent kinase inhibitors (CKI). In metazoans, two CKI gene families have been defined based on their evolutionary origins, structure, and CDK specificities: INK4 and Cip/Kip gene families. The INK4 gene family encodes $p16^{INK4a}$, $p15^{INK4b}$, $p18^{INK4c}$, and $p19^{INK4d}$, all of which bind to CDK4 and CDK6 and inhibit their kinase activities by interfering with their association with D-type cyclins (Sherr and Roberts 1999). In contrast, CKIs of the Cip/Kip family bind to both cyclin and CDK subunits and can modulate the activities of cyclin D-, E-, A-, and B-CDK complexes (Sherr and Roberts 1999).

3.6. CIP/KIP PROTEINS

The Cip/Kip family members $p21^{Cip1/Waf1/WSdi1}$ (encoded by *Cdkn1a*) (el-Deiry, Tokino et al. 1993; Gu, Turck et al. 1993; Xiong, Hannon et al. 1993), $p27^{Kip1}$ (encoded by *Cdkn1b*) (Polyak, Lee et al. 1994; Polyak, Kato et al. 1994; Toyoshima and Hunter 1994), and $p57^{Kip2}$ (encoded by *Cdkn1c*) (Lee, Reynisdottir et al. 1995; Matsuoka, Edwards et al. 1995) share a conserved N-terminal domain that mediates binding to cyclins and CDKs, but diverge in the remainder of their sequence, suggesting that each of these proteins could have distinct functions and regulation.

A vast body of Literature has described the importance of $p21^{Cip1}$, $p27^{Kip1}$, and $p57^{Kip2}$ in restraining proliferation during development, differentiation, and response to cellular stresses (Sherr and Roberts 1999), although each has specific biological functions that distinguish it from the other family members. Thus, different anti-proliferative signals tend to cause elevated expression of only a subset of the Cip/Kip proteins. For example, $p21^{Cip1}$ is an important transcriptional target of p53 and mediates DNA-damage-induced cell cycle arrest. In contrast to $p21^{Cip1}$, $p27^{Kip1}$ expression is usually elevated in mitogen-starved cells and other quiescent states, and the protein is rapidly downregulated as cells enter the cell cycle (Besson, Dowdy et al. 2008).

The importance of the Cip/Kip proteins in cell cycle regulation is underscored by the phenotypes of the knockout mice for each of these proteins. $p27^{Kip1}$ null mice display an overall increased body size and multiple organ hyperplasia, revealing the

importance of $p27^{Kip1}$ in limiting growth (Fero, Rivkin et al. 1996; Nakayama, Ishida et al 1996). Although mice lacking $p21^{Cip1}$ do not display an overt hyperproliferative disorder, $p21^{Cip1}$ null cells fail to undergo DNA-damage-induced cell cycle arrest and can reach higher saturation density (Deng, Zhang et al. 1995).

Recently, it has been discovered that Cip/Kip proteins are also involved in the regulation of cellular processes beyond cell cycle regulation, including cell fate determination, transcriptional regulation, apoptosis, cell migration, and cytoskeletal dynamics (Besson, Dowdy et al. 2008). These functions rely on different subcellular localizations, stability, and different targets present either in the cytoplasm, in the nucleus, and probably also on DNA (Coqueret 2003).

This thesis will be focused on the regulation and diverse functions of $p27^{Kip1}$.

3.7. STRUCTURE AND REGULATION OF $p27^{Kip1}$

$p27^{Kip1}$ belongs to the growing family of "natively unfolded", "intrinsically disordered" or "intrinsically unstructured" proteins (Figure 5). Interestingly, many proteins involved in pivotal cellular processes exhibit characteristics of unfolded, rather that folded, proteins. A number of them undergoes folding transition from disorder to order upon binding target proteins or nucleic acids, and exhibit an extraordinary affinity for the target (Borriello, Cucciolla et al. 2007; Wright and Dyson 1999). This conformational flexibility suggests that phosphorylation events and protein-protein interactions may modify its binding specificity and their potency to inhibit its targets. Likewise, it may explain why $p27^{Kip1}$ is capable of interacting with a wide diversity of proteins to regulate various cellular functions (Borriello, Cucciolla et al. 2007).

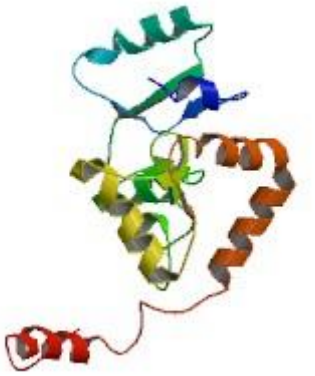

Figure 5. Three-dimensional structure model of $p27^{Kip1}$. Model provided by ModBase (Pieper, Eswar et al. 2009).

3.7.1. $p27^{Kip1}$ protein domains

The human gene (formally *CDKN1B*) encoding $p27^{Kip1}$ protein is located on chromosome 12p13 at the junction of 12p 12-12p 13.1. (Ponce-Castaneda, Lee et al. 1995). A detailed examination of the protein identified two major regions: the N-terminal which on the basis of homology with $p21^{Cip1}$ and $p57^{Kip2}$ showed the capability of inhibiting the kinase activity of cyclin-CDK complexes, and a C-terminal region with initially unknown functions. The C-terminal domain of $p27^{Kip1}$ has been reported to interact with several proteins involved in processes apparently not correlated to the cell cycle control. In particular, when localized at cytosolic cellular compartment, $p27^{Kip1}$ interacts, probably by means of the C-terminal domain, with various proteins including RhoA, Rac, Stathmin, Grb2, and 14-3-3 (Baldassarre, Belletti et al. 2005; Besson, Gurian-West et al. 2004; McAllister, Becker-Hapak et al. 2003; Fujita, Sato et al. 2002; Sugiyama, Tomoda et al. 2001).

Also, two additional regions have been identified in the $p27^{Kip1}$ sequence. The first region is a bipartite nuclear localization signal (NLS, 152/153-166/168) which is recognized by the alpha/beta importins, allowing $p27^{Kip1}$ transport into the nucleus (Zeng, Hirano et al. 2000). The second region is a putative nuclear export signal (NES) identified between aminoacids 32 and 45. However, other residues of the protein could be involved in the export process including serine 10 and arginine 90 (Connor, Kotchetkov et al. 2003).

3.7.2. $p27^{Kip1}$ regulation

The activity of $p27^{Kip1}$ is controlled by two different mechanisms. First, $p27^{Kip1}$ concentration is regulated at the level of transcription, translation, and protein stability. Second, $p27^{Kip1}$ function is modulated by its subcellular localization (Figure 6). These mechanisms are underlied by phosphorylation events and interactions with other cellular complexes and assemblies, thus, depending on the phosphorylated residue, $p27^{Kip1}$ is degraded in the nucleus, exported to the cytoplasm and degraded, or excluded from the nucleus and retained in the cytoplasm (le Sage, Nagel et al. 2007).

Although these $p27^{Kip1}$ inhibitory mechanisms are induced by different effectors, their common goal is to activate CDK1 and CDK2 complexes which are required for cell cycle transition. An accumulating amount of data on $p27^{Kip1}$ regulation suggests the convergence of mitogen-stimulated pathways to inhibit the function of $p27^{Kip1}$.

Mitogenic stimuli, like growth factors, cytokines, and hormones bind to cellular transmembrane receptors and activate the Ras and/or PI3K pathways, both important for cellular proliferation and self-renewal. Whereas Ras activity induces c-Myc, PI3K stimulation triggers Akt to become active. Both c-Myc and Akt negatively influence $p27^{Kip1}$ in multiple direct and indirect ways (le Sage, Nagel et al. 2007).

3.7.3. Transcriptional regulation of $p27^{Kip1}$

Although it is well established that the control of $p27^{Kip1}$ level is mostly due to the extent of degradation rate, several reports describe the ocurrence of a transcriptional modulation of the *CDKN1B* gene. In this manner, members of the Forkhead box group O (FOXO) transcription factor family (Stahl, Dijkers et al. 2002; Medema, Kops et al. 2000; Dijkers, Medema et al. 2000), E2F1 (Wang, Hou et al. 2005), c-myc (or c-Myc/Max complex) (Chandramohan, Jeay et al. 2004; Yang, Shen et al. 2001), Sp1 (Andres, Urena et al. 2001), and menin (Karnik, Hughes et al. 2005) have been described involved in *CDKN1B* transcriptional control.

Ras and PI3K pathways, both important for cellular proliferation and self-renewal, negatively influence $p27^{Kip1}$ in multiple direct and indirect ways (le Sage, Nagel et al. 2007). Ras activity induces c-myc, meanwhile that PI3K stimulation triggers Akt to become active. Thus, c-myc, besides being capable of directly repress $p27^{Kip1}$ transcription (Yang, Shen et al. 2001), it also induces transcription of cyclin D_1, cyclin D_2, and CDK4 which, when assembled into cyclin-CDK complexes, sequester $p27^{Kip1}$ from CDK2 (Perez-Roger, Kim et al. 1999; Bouchard, Thieke et al. 1999; Cheng, Olivier et al. 1999). On the other hand, $p27^{Kip1}$ transcription is affected by Akt through the inhibition of FOXO transcription factors that directly regulate $p27^{Kip1}$ transcription. FOXOs are phosphorylated by Akt, and exported to the cytoplasm, which eliminates $p27^{Kip1}$ transcription (Brownawell, Kops et al. 2001; Brunet, Bonni et al. 1999).

3.7.4. Regulation of $p27^{Kip1}$ degradation and localization

The phosphorylation of $p27^{Kip1}$ on Threonine 187 (Thr187) is catalyzed by cyclin E/A-CDK2 and by cyclin B-CDK1 complexes (Sheaff, Groudine et al. 1997). The Thr187 phosphorylation is required for the binding of $p27^{Kip1}$ to S-phase kinase associated protein 2 (Skp2), an F-box component of a Skp/Cullin/F-box (SCF^{Skp2}) ubiquitin ligase complex, which acts in the $p27^{Kip1}$ ubiquitinylation and its subsequent

degradation by the ubiquitin-proteasome system (Carrano, Eytan et al. 1999; Tsvetkov, Yeh et al. 1999; Shirane, Harumiya et al. 1999; Pagano, Tam et al. 1995). Additionally, c-Myc induces Cullin and (cdc kinase subunit 1) Cks1 which are, respectively, part of and cofactor for the SCF^{Skp2} complex, to enhance $p27^{Kip1}$ ubiquitination and degradation (le Sage, Nagel et al. 2007).

A number of reports have demonstrated that Akt phosphorylates human $p27^{Kip1}$ on threonine 157 (Shin, Yakes et al. 2002; Viglietto, Motti et al. 2002) and/or 198 (Fujita, Sato et al. 2002). Thr157 and Thr198 phosphorylations have been shown to induce the recruitment of the 14-3-3 protein to $p27^{Kip1}$ which, by masking the NLS of $p27^{Kip1}$, competes with importin alpha. The net effect is redistribution of $p27^{Kip1}$ to the cytoplasm where it is retained (Sekimoto, Fukumoto et al. 2004). Also, Akt regulates $p27^{Kip1}$ function by negative regulation of glycogen synthase kinase 3 β (GSK3β). GSK3β destabilizes cyclin D_1 through phosphorylation, and subsequent chromosome region maintenance 1 (CRM1)-dependent nuclear export (Diehl, Cheng et al. 1998), prior to ubiquitination by Kip1 ubiquitination promoting complex (KPC) and cytoplasmic proteasomal degradation. Since Akt inhibits GSK3β (Cross, Alessi et al. 1995), cyclin D-dependent CDK4/6 complexes remain functional for sequestering $p27^{Kip1}$ from CDK2 complexes (Sherr and Roberts 1999).

The phosphorylation of $p27^{Kip1}$ on Serine 10 (Ser10) represents the most abundant post-translational $p27^{Kip1}$ modification (Ishida, Kitagawa et al. 2000). Two enzymes have been supposed to catalyze the reaction in mitogen stimulated cells. These include human kinase interacting stathmin (hKIS) (Boehm, Yoshimoto et al. 2002), and mitogen activated protein kinase (MAPK) (Alessandrini, Chiaur et al. 1997). In proliferating cells, Ser10 phosphorylation induces $p27^{Kip1}$ nuclear export via CRM1, cytoplasmic ubiquitination by KPC, and proteasomal degradation (Kamura, Hara et al. 2004; Ishida, Hara et al. 2002).

Recently, two studies have shown that $p27^{Kip1}$ can also be phosphorylated on three different tyrosine residues (Tyr74, Tyr88, and Tyr89). Growth factor stimulation of receptor protein tyrosine kinases induces downstream protein tyrosine kinases such as sarcoma (Src), Lyn, and V-abl Abelson murine leukaemia viral oncogene homolog 1 (Abl). It has been reported that mitogen-activated Src phosphorylates $p27^{Kip1}$ at Tyr74, and, to a lesser extent, Tyr88 (Chu, Sun et al. 2007). On the other hand, it has also been demonstrated the potential of both, Lyn and Abl, to phosphorylate Tyr88 and Tyr89

residues of $p27^{Kip1}$ (Grimmler, Wang et al. 2007). In both cases, tyrosine phosphorylation inactivates $p27^{Kip1}$ inhibitory function towards CDK2, thereby making $p27^{Kip1}$ more susceptible to CDK2-mediated Thr187 phosphorylation and subsequent ubiquitination by SCF^{Skp2}.

3.7.5. Regulation of $p27^{Kip1}$ by microRNA

Recently, several reports have shown the involvement of miRNAs in the regulation of $p27^{Kip1}$. The pioneering work by Hatfield *et al*., already hinted the involvement of miRNAs in the regulation of the *Drosophila* $p27^{Kip1}$ orthologue Dacapo (Hatfield, Shcherbata et al. 2005). This work described the mutation of Dicer-1, an important gene for the biogenesis of miRNAs, in germline cyst production. Without miRNAs to aid in the process of germline cell proliferation, Dicer-1 mutant cells were delayed in their progression through G_1. This G_1 delay was found to depend on Dacapo, as knockdown of Dacapo restored germ cell growth (Hatfield, Shcherbata et al. 2005).

Recently, several groups have identified miR‑221 and miR-222 as regulators of $p27^{Kip1}$. In one study, it was reported a marked decrease in cellular proliferation by suppressing the endogenous expression of either miR‑221 or miR-222 in human glioblastoma cell lines (Gillies and Lorimer 2007). Furthermore, suppression of either miR‑221 or miR-222 led to the upregulation of $p27^{Kip1}$ which was suggested to cause the arrest (Gillies and Lorimer 2007). In a different study, three human prostate carcinoma cell lines were investigated for the expression of miR‑221 and miR-222. In all cell lines tested, an inverse relationship between the expression of miR-221 and miR-222 and $p27^{Kip1}$ was observed. Furthermore, miR-221 and miR-222 ectopic overexpression directly resulted in $p27^{Kip1}$ downregulation and an increase in the growth potential by inducing a G_1 to S shift in the cell cycle. Consistently, miR-221 and miR-222 knock-down increased $p27^{Kip1}$ and reduced the clonogenicity of prostate carcinoma cell lines *in vitro* (Galardi, Mercatelli et al. 2007).

In an unbiased approach to screen for miRNAs that regulate $p27^{Kip1}$, miRNA‑221 and miR‑222 were identified as potent regulators of $p27^{Kip1}$. In several human glioblastoma cell lines, among them U87, and in the human breast tumour cell line MDA‑MB‑231, miR‑221 and miR-222 were endogenously expressed. The suppression of miR‑221 and miR-222 expression in glioblastoma and breast tumour cell lines

resulted in a $p27^{Kip1}$ dependent G_1 growth arrest, as knocking down $p27^{Kip1}$ almost completely rescued this arrest (le Sage, Nagel et al. 2007).

Subsequently, an increasing number of reports have shown an inverse correlation between miR-221 and miR-222 up-regulation and down-regulation of the $p27^{Kip1}$ protein levels in human thyroid papillary carcinomas (Visone, Russo et al. 2007) and human hepatocellular carcinoma (Fornari, Gramantieri et al. 2008). In the last study, it was also shown that $p57^{Kip2}$ is also a target of miR-221, and a significant inverse correlation between miR-221, and both $p27^{Kip1}$ and $p57^{Kip2}$ was found in human hepatocellular carcinoma cells (Fornari, Gramantieri et al. 2008). Finally, another report identified the promyelocytic leukaemia zinc finger (PLZF) transcription factor as a repressor of miR-221 and miR-222 by direct binding to their putative regulatory region. Specifically, PLZF silencing in human melanomas unblocked miR-221 and miR-222 which, in turn, regulated the progression of the neoplasia through down-modulation of $p27^{Kip1}$ and c-KIT receptor, leading to enhanced proliferation and differentiation blockade of the melanoma cells, respectively (Felicetti, Errico et al. 2008).

Recently, miR-181a has been identified as a novel regulator of $p27^{Kip1}$ mRNA translation in human promyelocytic leukaemia (HL60) cells. MicroRNA-181a is highly expressed in undifferentiated HL60 cells and acts as a repressor of $p27^{Kip1}$ mRNA translation in undifferentiated HL60 cells. Phorbol-12- myristate-13-acetate (TPA) induced differentiation of these cells into monocytes/macrophages results in the relief of miR-181a mediated repression, allowing the accumulation of sufficient $p27^{Kip1}$ to ensure proper differentiation (Cuesta, Martinez-Sanchez et al. 2009).

The cell cycle inhibitor $p21^{Cip1}$ is also regulated by miRNA. In mESC it has been shown that miR-291a-3p, miR-294, and miR-295 downregulated $p21^{Cip1}$, and partially rescued the G_1 accumulation phenotype of *Dgcr8* knockout, thus regulating the G_1 to S transition in mESC (Wang, Baskerville et al. 2008). Likewise, a similar mechanism is observed in hESC where miR-372, a member of the miR-371 family that is homologous to the mouse miR-290 family, has been shown to downregulate $p21^{Cip1}$ (Qi, Yu et al. 2009).

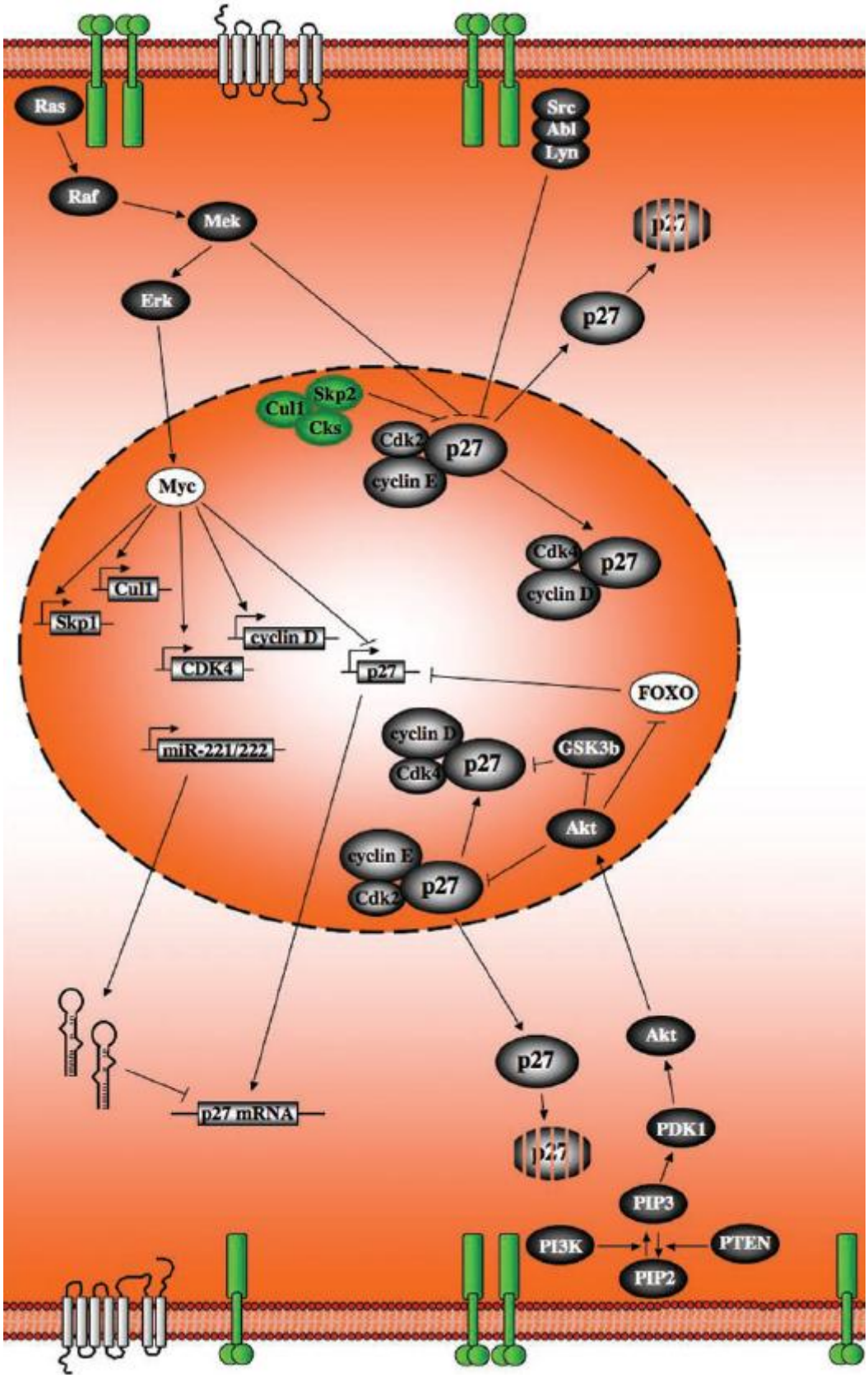

Figure 6. Schematic representation summarizing the pathways regulating $p27^{Kip1}$. The activity of $p27^{Kip1}$ is controlled by regulation of its concentration at the level of transcription, translation, and proteolysis, and by its subcellular localization. Mitogen-stimulated pathways important for embryonic stem cells maintenance converge to inhibit $p27^{Kip1}$. Adapted from (le Sage, Nagel et al. 2007).

3.8. FUNCTIONS OF $p27^{Kip1}$

$p27^{Kip1}$ was first identified as a cell cycle inhibitor mediating the growth inhibitory cues of upstream signalling pathways. Recently, it has been shown that $p27^{Kip1}$ has alternative functions beyond cell cycle regulation involved in differentiation, apoptosis, transcriptional regulation, cell migration, and cytoskeletal dynamics (Figure 7). These functions are essential for the maintenance of normal cell and tissue homeostasis, in processes ranging from embryonic development to tumour suppression.

3.8.1. $p27^{Kip1}$ protein as cell cycle inhibitor

The cell cycle inhibition was the first identified function of $p27^{Kip1}$ and the reason for what it is considered a tumour suppressor. Moreover, it was initially characterized as a strict inhibitor of all cyclin-CDK complexes, albeit displaying lower affinity towards cyclin B-CDK1 (Sherr and Roberts 1999). The crystal structure of the N-terminal cyclin and CDK-binding domains of $p27^{Kip1}$ (aa 22-106) bound to cyclin A-CDK2 revealed that the CKI occludes a substrate interaction domain on the cyclin subunit and inserts itself deep inside the catalytic cleft of the CDK subunit, thereby blocking ATP loading and catalytic activity. Important CDK2 conformational changes further lock the catalytic cleft in an inactive form (Russo, Jeffrey et al. 1996). Since the activated form of CDK2 is located in the nucleus, only nuclear forms of $p27^{Kip1}$ proteins should probably be considered as catalytic inhibitors of CDKs (Coqueret 2003).

$p27^{Kip1}$ protein is intrinsically unstructured, adopting specific tertiary conformations only after binding to other proteins (Lacy, Filippov et al. 2004). This conformational flexibility suggests that phosphorylation events and protein-protein interactions may modify its binding specificity and their potency to inhibit cyclin-CDK complexes. Indeed, the phosphorylation of $p27^{Kip1}$ on Tyr-74, -88 and/or -89 by Src, Lyn, or Abl greatly decreased the ability of $p27^{Kip1}$ to inhibit CDK2 containing complexes, as Tyr-88 is part of the 3_{10}-helix that normally inserts into the ATP-binding site of the CDK (Chu, Sun et al. 2007; Grimmler, Wang et al. 2007). As mentioned above, also a number of proteins can either enhance or diminish the inhibitory effect of $p27^{Kip1}$ on cyclin-CDK complexes by forming quaternary complexes and potentially altering the conformation of the $p27^{Kip1}$ bound to these complexes. In this manner, human papillomavirus-16 E7 protein can bind to $p21^{Cip1}$ and $p27^{Kip1}$ and abrogate their inhibitory activity towards CDK2-containing complexes (Funk and Galloway 1998).

The general conclusion is that $p27^{Kip1}$ is a potent inhibitor of cyclin-CDK complexes, although most of the findings in recent years have shown that its inhibitory potential is dependent on cellular context and regulated via phosphorylations and protein-protein interactions.

Cip/Kip proteins also modulate cell cycle progression, independently of cyclins and CDKs, via the inhibition of components of the replication machinery. Thus, $p21^{Cip1}$ has been reported to bind to proliferating cell nuclear antigen (PCNA), via its C terminus (aa 143-160), thereby blocking processive DNA synthesis (Luo, Hurwitz et al. 1995). Although no interaction between $p27^{Kip1}$ and PCNA has been reported, $p27^{Kip1}$ may also inhibit DNA synthesis via the interaction and inhibition of minichromosome maintenance-7 (MCM7), a subunit of the MCM2-7 replication fork helicase, through its C-terminal part (aa 144-198) (Nallamshetty, Crook et al. 2005).

A vast body of Literature has described the role of $p27^{Kip1}$ during differentiation in several cell types. In all cases differentiation was associated with cell cycle exit and a reduction in the overall amount of CDK activity in G_1. In this way, induction of $p27^{Kip1}$ resulted in the expression of erythroid differentiation markers in mouse erythroid progenitors (Li, Jia et al. 2006), and human myeloid leukaemia cells (Munoz-Alonso, Acosta et al. 2005). Despite these findings, the vast majority or reports demonstrate a key role for $p27^{Kip1}$ during neuronal differentiation (Galderisi, Jori et al. 2003). Thus, in rat embryonic forebrains, high expression of $p27^{Kip1}$ was detected in the cortical plate and preplate, basal telencephalon, and diencephalon (Lee, Nikolic et al. 1996). Moreover, $p27^{Kip1}$ expression correlated with the differentiation grade of neuronal cells in a multipotent embryonal carcinoma cell line induced to differentiate towards a neuronal phenotype by retinoic acid treatment (Baldassarre, Boccia et al. 2000). Another study reported a role for $p27^{Kip1}$ during differentiation of cerebellar granule cell precursors (GCP) (Miyazawa, Himi et al. 2000). This study suggested that $p27^{Kip1}$ gradually accumulates in GCP as they proliferate and not after cell cycle exit (Miyazawa, Himi et al. 2000). $p27^{Kip1}$ has also been shown to regulate neuronal differentiation associated with cell cycle arrest in oligodendrocytes (Durand, Gao et al. 1997), a neuroblastoma cell line (Perez-Juste and Aranda 1999), and mouse neural progenitor cells (Misumi, Kim et al. 2008).

3.8.2. $p27^{Kip1}$ protein and apoptosis

Cip/Kip proteins can modulate apoptosis in various ways. Although it has been well documented an apoptosis resistant phenotype when $p21^{Cip1}$ is present in the cytoplasm (Coqueret 2003; Asada, Yamada et al. 1999), the functions of $p27^{Kip1}$ in the apoptotic process remain unclear.

Numerous reports have suggested proapoptotic roles for $p27^{Kip1}$ by overexpression in cancer cell lines (Wang, Gorospe et al. 1997). However, in these studies $p27^{Kip1}$ was overexpressed using adenoviral vectors and their relevance to physiological conditions is uncertain. On the contrary, other studies have reported a function for $p27^{Kip1}$ in protection from apoptosis. Thus, $p27^{Kip1}$ has been reported to play a protective role in safeguarding normal tissues from excessive apoptosis during inflamatory injury (Ophascharoensuk, Fero et al. 1998). One way by which Cip/Kip proteins protect against apoptosis is via their CDK inhibitory activity. This was first shown in endothelial cells where caspase-mediated cleavage of $p21^{Cip1}$ and $p27^{Kip1}$ upregulated CDK2 activity, thereby enhancing the apoptotic program (Levkau, Koyama et al. 1998). However, in a study with mESC in which it was shown increased apoptosis in differentiating $p27^{Kip1}$ deficient mESC, neither CDK2 nor CDK4 associated kinase activities were altered in the absence of $p27^{Kip1}$. Although this study inferred that caspase independent apoptotic pathways were responsible for the massive cell death of differentiating $p27^{Kip1}$ deficient mESC, they did not provide a specific molecular mechanism or pathway by which $p27^{Kip1}$ protected mESC from differentiation associated apoptosis (Bryja, Pachernik et al. 2004).

Contrary to $p21^{Cip1}$ which directly interferes with apoptotic pathways (Shim, Lee et al. 1996; Suzuki, Tsutomi et al. 1998), there have not been any reports to suggest that $p27^{Kip1}$ can directly interfere with pro- or antiapoptotic pathways so far.

3.8.3. $p27^{Kip1}$ protein in the regulation of cytoskeletal dynamics and migration

In mammals, Ras homolog gene family (Rho) of GTPases, composed of at least 20 members, regulates multiple signalling pathways with pleiotropic cellular responses. Rho and its effector Rho-associated protein kinase (ROCK) are best known for their role in the regulation of actin-stress-fiber formation, focal-adhesion assembly, as well as actin-myosin contractility. Stress-fiber assembly is mediated by the activation of LIM

domain kinase (LIMK), by ROCK, which in turn phosphorylates and inactivates the actin-depolymerization factor cofilin to promote stress-fiber formation. On the other hand, Rac and its effector p21-activated kinase (PAK) induce actin rearrangements that control the formation of lamellipodia and new focal contacts at the cell edges (Ridley, Schwartz et al. 2003). Cell migration requieres a tight balance of Rho and Rac activities, and the dynamic activation and inhibiton of both GTPases are spatially and temporally coordinated.

The involvement of $p27^{Kip1}$ in the regulation of migration was first reported in hepatocellular carcinoma cells, in which transduction of a TAT-$p27^{Kip1}$ protein induced migration (Nagahara, Vocero-Akbani et al. 1998). Moreover, N-terminal phosphorylation of $p27^{Kip1}$ and cytoplasmic translocation have been reported to induce cell motility (Reed 2002). In support of this, a recent report showed that expression of even subphysiological levels of cytoplasmic $p27^{Kip1}$ in melanoma cells resulted in a profound increase of metastatic potential *in vivo* (Denicourt, Saenz et al. 2007).

Recent analysis have shown that the motility of $p27^{Kip1}$ null mouse fibroblasts was impaired due to an increase in Ras homolog gene family member A (RhoA) activity. Overexpression of $p27^{Kip1}$ experiments revealed that $p27^{Kip1}$ interacted with RhoA, thereby preventing RhoA activation by interfering with RhoA binding to its guanine-nucleotide exchange factor (GEF) (Besson, Gurian-West et al. 2004). Importantly, this function was independent of its role in cell cycle regulation. The regulation of RhoA by $p27^{Kip1}$ has been shown to be critical for proper migration of neuronal progenitor cells in the subventricular cortex of developing mice (Itoh, Masuyama et al. 2007; Nguyen, Besson et al. 2006; Nguyen, Besson et al. 2006).

3.8.4. $p27^{Kip1}$ protein and cell transformation

The firm evidence of a tumour suppressor role for $p27^{Kip1}$ was reported in $p27^{Kip-/-}$ mice which spontaneously developed adenomas of the intermediate lobe of the pituitary gland and were more susceptible to tumorigenesis induced by chemical carcinogens or irradiation (Nakayama, Ishida et al. 1996).

Later on, it has been shown that $p27^{Kip1}$ expression is a prognostic marker for clinical outcome in human cancers (Chu, Hengst et al. 2008). Low amounts of nuclear $p27^{Kip1}$ protein are frequently observed in a broad array of human malignancies, including carcinomas of the breast, colon, prostate, ovary, lung, brain, stomach, and

others, and they are associated with increased tumour aggressiveness (Besson, Assoian et al. 2004). Surprisingly, $p27^{Kip1}$ proteins do not fit Knudson's "two-mutation" criterion of tumour suppressor genes. Whereas loss of a single allele of $p27^{Kip1}$ has been reported, inactivating mutations of both copies of the $p27^{Kip1}$ gene are infrequent events. Notably, heterozygous $p27^{Kip1+/-}$ mice get tumours even with only one mutant allele (Coqueret 2003; Fero, Randel et al. 1998). Instead, $p27^{Kip1}$ is downregulated by other mechanisms, including aberrant proteolytic degradation, decreased transcription, and cytoplasmic mislocalization. In addition, the related miR-221 and miR-222 have been shown to repress $p27^{Kip1}$ mRNA expression in human cell lines derived from melanoma (Felicetti, Errico et al. 2008), hepatocellular carcinoma (Fornari, Gramantieri et al. 2008), prostate carcinoma (Galardi, Mercatelli et al. 2007), gliobastoma (Gillies and Lorimer 2007), breast tumours (le Sage, Nagel et al. 2007), and thyroid papillary carcinomas (Visone, Russo et al. 2007).

Not only the cytoplasmic mislocalization is a mechanism to downregulate nuclear $p27^{Kip1}$ expression levels, but increasing evidence points to the importance of cytoplasmic subcellular localization in the active contribution to tumorigenesis (Besson, Hwang et al. 2007; Besson, Assoian et al. 2004). In support of this, elevated cytoplasmic localization of $p27^{Kip1}$ is a negative prognostic factor in subsets of certain human tumour types, including carcinomas of the breast, cervix, esophagus, ovary, uterus, some leukemias and lymphomas, and in melanomas (Denicourt, Saenz et al. 2007; Besson, Assoian et al. 2004).

An active role for $p27^{Kip1}$ in promoting tumour formation has also been supported by several studies in mice. A knockin mouse model in which point mutations in $p27^{Kip1}$ prevented its interaction with cyclins and CDKs ($p27^{Kip1CK-}$) revealed that, in contrast to $p27^{Kip-/-}$ mice which spontaneously developed only pituitary tumours, $p27^{Kip1CK-}$ mice developed hyperplastic lesions and tumours in multiple organs, including the lung, retina, pituitary, ovary, adrenals, spleen, and lymphomas (Besson, Hwang et al. 2007). In the lung and retina of $p27^{Kip1CK-}$ mice, the development of tumours was associated with the expansion of stem/progenitor cell populations (Besson, Hwang et al. 2007) suggesting that, independently of its role as a CDK inhibitor, $p27^{Kip1}$ could function as an oncogene *in vivo*, possibly by deregulating the proliferation and/or differentiation of stem/progenitor cells. However, this study did not address whether that effect was

exerted in the nucleus or cytoplasm, and the mechanism by which it promotes tumorigenesis and stem cell amplification remains to be evaluated.

3.8.5. $p27^{Kip1}$ protein as transcriptional regulator

Cip/Kip proteins can repress transcription indirectly, by inhibiting cyclin-CDK complexes, in turn preventing the phosphorylation of Rb-family proteins (Rb1, p107, and p130). In their hypophosphorylated state, Rb related proteins sequester E2F family members, thereby repressing their transcriptional targets (Sherr and Roberts 1999). In addition, Cip/Kip proteins can also modulate the activity of transcription factors through direct binding to transcription factors.

$p21^{Cip1}$ is a potent regulator of several transcription factors. $p21^{Cip1}$ regulates NF-κβ indirectly through the inhibition of its CDK2 associated activity (Coqueret 2003). However, through direct binding, $p21^{Cip1}$ inhibits the activities of E2F1, c-Myc, and STAT3, independently of the CDK function (Vigneron, Cherier et al. 2006). On the other hand, $p21^{Cip1}$ can stimulate p300/Creb-binding protein (CBP) histone acetyl transferase complex-mediated transcriptional activation. Through direct binding to p300, $p21^{Cip1}$ can disrupt the activity of the cell cycle regulatory domain 1 (CRD1)-trancriptional-repression domain of p300 and derepress transcription of target genes, independently of the CDK function (Gregory, Garcia-Wilson et al. 2002; Snowden, Anderson et al. 2000).

$p57^{Kip2}$ can also modulate the activity of transcription factors through direct binding. The N-terminal cyclin-CDK binding region of $p57^{Kip2}$ can interact with MyoD, protecting MyoD from degradation, and thus promoting transactivation of muscle-specific genes (Reynaud, Leibovitch et al. 2000).

Interestingly, a similar mechanism is observed between $p27^{Kip1}$ and Neurogenin-2, and $p27^{Kip1}$-mediated stabilization of Neurogenin-2 promotes the differentiation of mouse neuronal progenitors in the cortex (Nguyen, Besson et al. 2006). This activity was independent of its role in cell cycle regulation and was carried out by the N-terminal half of $p27^{Kip1}$ (Nguyen, Besson et al. 2006). This interaction is evolutionary conserved, since in *Xenopus*, primary neurogenesis also relies on the stabilization of *Xenopus* Neurogenin related (X-NGNR1) transcription factor, a Neurogenin-2 homolog, by $p27^{Xic1}$. The ability of $p27^{Xic1}$ to stabilize X-NGNR1 and enhance neurogenesis localized to the N-terminal domain of the molecule and was separable from its ability to

inhibit the cell cycle (Vernon, Devine et al. 2003). *Xenopus* has only one described CKI, $p27^{Xic1}$, which shows structural and functional characteristics of $p21^{Cip1}$, $p27^{Kip1}$, and $p57^{Kip2}$ (Vernon, Devine et al. 2003). $p27^{Xic1}$ also regulates muscle differentiation, independently of the cell cycle regulation, in *Xenopus* (Vernon and Philpott 2003) in a similar way than $p57^{Kip2}$ in mammals (Reynaud, Leibovitch et al. 2000).

Moreover, in early G_1 phase, $p27^{Kip1}$ inhibits the activity of activator protein 1 (AP-1) through downregulation of its Jun activating binding protein (JAB1) cofactor. Although JAB1 translocates to the cytoplasm to increase the degradation of $p27^{Kip1}$, it functions also as a transcriptional cofactor for AP-1. Therefore, the cytoplasmic translocation of a $p27^{Kip1}$-JAB1 complex should prevent the asssociation between JAB1 and AP-1, downregulating the activity of the transcription factor (Coqueret 2003).

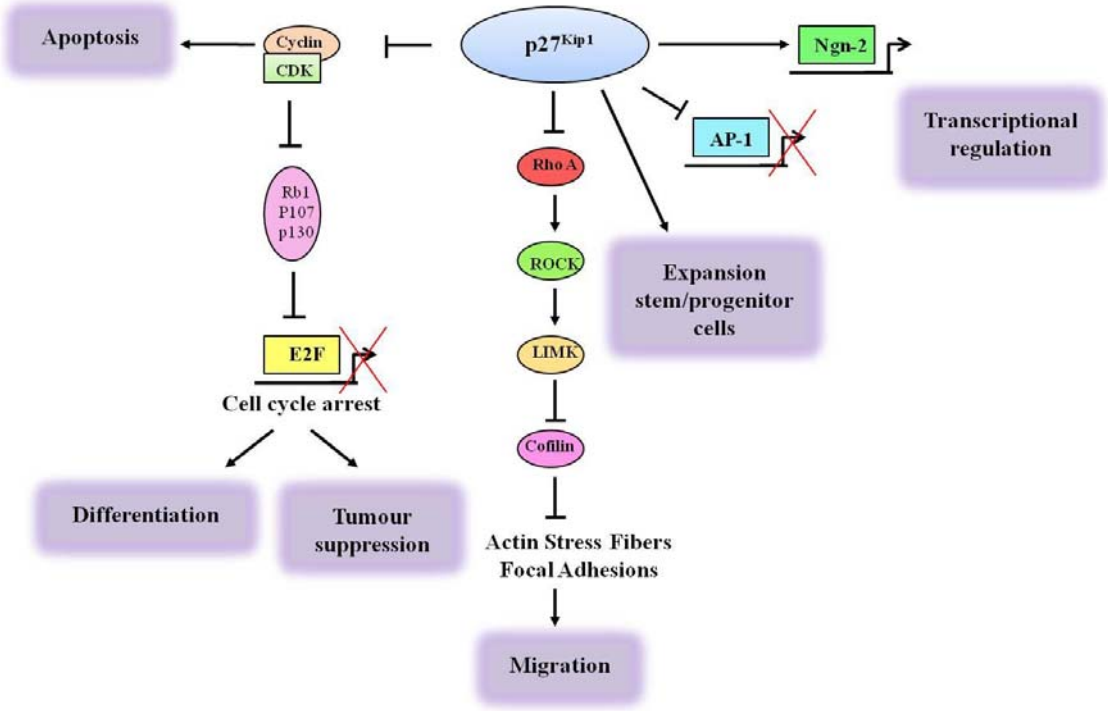

Figure 7. Diagram summarizing the diverse functions of $p27^{Kip1}$. The CKI $p27^{Kip1}$ can inhibit apoptosis and tumour growth, and promote differentiation, indirectly, via the inhibition of cyclin-CDK complexes, thereby maintaining retinoblastoma (Rb) family proteins (Rb1, p107, and p130) in a hypophosphorylated state in which they sequester E2F transcription factors and inhibit cell cycle progression. $p27^{Kip1}$ proteins also regulate transcriptions factors by direct interaction and stabilization of the transcription factor Ngn-2 promoting transcription of its target genes and, indirectly, $p27^{Kip1}$ inhibits the activity of AP-1 transcription factor through downregulation of its JAB1 cofactor. $p27^{Kip1}$ can interact with RhoA, preventing RhoA activation by interfering with RhoA binding to its GEFs, leading to decreased actin stress fibers and focal adhesion formation and resulting in several cell types in increased migration and metastasis. $p27^{Kip1}$ can function as an oncogene *in vivo* by deregulating the proliferation and/or differentiation of stem/progenitor cells in the lung and retina independently of its role as a CDK inhibitor. Ngn-2, Neurogenin-2; AP-1, Activator protein 1; JAB1, Jun activating binding protein 1; GEFs, guanine-nucleotide exchange factors; Rho A, Ras homolog gene family, member A; ROCK, Rho-associated protein kinase; LIMK, LIM domain kinase.

4. CELL CYCLE CONTROL OF EMBRYONIC STEM CELLS

Embryonic stem cells (ESC) have the remarkable capacity to divide indefinitely while retaining their potential to give rise to all cell types of the foetus. This has been shown conclusively by their complete integration into a developing embryo after being reintroduced into the blastocyst (Beddington and Robertson 1989). The capacity for unlimited proliferation relates specifically to ESC in culture, and not their embryonic counterparts which do not remain as a stable stem cell pool but differentiate into the three germ layers at gastrulation.

Embryonic stem cells have unusual proliferative properties. They are derived without the intervention of any immortalizing agent, do not undergo either crisis or senescence, and retain a normal karyotype. They proliferate without apparent limit and can readily be propagated clonally. They can multiply in the absence of serum, they are not subject to contact inhibition, and they do not quiescence on growth factor withdrawal (Burdon, Smith et al. 2002).

These unusual proliferative properties have been related to a unique cell cycle structure and mechanisms of cell cycle regulation that have been well described in mESC. Mouse embryonic stem cells use mechanisms to drive cell proliferation that are quite distinct from those observed in other somatic cell types. Only a limited amount of information is available about the cell cycle control of hESC.

4.1. CELL CYCLE CONTROL AND EARLY MOUSE EMBRYOGENESIS

Early embryonic development in lower metazoa such as *Xenopus*, *Danio*, or *Drosophila* is associated with extremely rapid cell/nuclear division cycles (White and Dalton 2005). In these situations, rapid cell division is achieved, in part at least, by structuring the cell cycle so that it lacks gap phases and consists purely of alternating rounds of DNA replication (S phase) and chromosome segregation (M phase). Similarly, the mouse embryo also grows at a rapid rate. If a critical embryonic mass is not generated at the time when gastrulation normally occurs, formation of the three embryonic germ layers will be delayed (Rands 1986; Rands 1986). Indeed, pluripotent cells of late preimplantation and early postimplantation mouse embryos have the

capacity to proliferate at unusually rapid rates. Between 4.5 and 6.0 days postcoitum (dpc), the embryonic epiblast expands from 20-25 cells to approximately 660 cells, reflecting an average generation time of 10 hours (h). Cell division rates in the embryonic epiblast are further accelerated between days 6.5 dpc and 7 dpc reaching over 4000 cells, coinciding with or just preceding gastrulation, with mean generation times estimated to be as short as 4.4 h (White and Dalton 2005). Later, during gastrulation, cell division is supressed by a prolongation of the cell cycle.

The rapid generation rates of pluripotent cells in the rodent epiblast are due to a cell cycle structure lacking fully formed G_1 and G_2 gap phases in which a high proportion of time (approximately 60%) is devoted to S phase (Stead, White et al. 2002). A similar cell cycle structure has been reported for other pluripotent cell populations including mESC (Stead, White et al. 2002), rhesus monkey ESC (Fluckiger, Marcy et al 2006), hESC (Becker, Ghule et al. 2006), murine embryonal carcinoma cells (Kranenburg, de Groot et al. 1995), and embryonal germ cells (Resnick, Bixler et al. 1992).

Cell cycle phases of mouse embryonic stem cells

Mouse embryonic stem cells divide with an unusually short generation time of approximately 8-10 h (Stead, White et al. 2002) and have an unusual cell cycle structure consisting largely of S phase cells (~65%) and a truncated G_1 phase (~15%) (Faast, White et al. 2004; Stead, White et al. 2002). The short G_1 phase lasts roughly 1.5 h (Burdon, Smith et al. 2002). Since most somatic cell types spend the majority of their time in G_1, the short G_1 phase of mESC can account for their rapid rate of cell division since the length of S phase is similar within cell types (White and Dalton 2005).

Cyclins and Cyclin Dependent Kinase expression in mouse embryonic stem cells

Mouse embryonic stem cells express very low levels of cyclins D_1 and D_3, whereas cyclin D_2 is not expressed (Burdon, Smith et al. 2002; Savatier, Lapillonne et al. 1996). The low amount of D-type cyclins in mESC reflects the situation in epiblast cells which do not express appreciable quantities of D-type cyclins until gastrulation commences (Wianny, Real et al. 1998). Moreover, cyclins E_1, A_2, and B_1 have all been described in mESC. All CDK catalytic partners have been described in mESC and, with

the exception of CDK4, appear to be assembled into active complexes with their cyclin regulatory partners (White and Dalton 2005; Faast, White et al. 2004; Stead, White et al. 2002).

Cyclin Dependent Kinase activity in mouse embryonic stem cells

Synchronization and static block experiments showed that, with the exception of the mitotic regulator cyclin B, all cyclins expressed in mESC were constitutively expressed throughout the cell cycle (Stead, White et al. 2002) (Figure 8B). This dramatically contrasts the general model of cell cycle regulation in mammalian somatic cells where cyclin levels oscillate in a strict and temporal manner (Figure 8A).

Central to the mechanisms that underpinned rapid cell division, in mESC, was the extreme activity of cyclins E/A-CDK2 complexes, all of which lacked cell cycle dependent periodicity (Stead, White et al. 2002). The only CDK activities that were under periodic control were cyclin B-CDK1 complexes, but even this CDK activity showed unusually high activity (Stead, White et al. 2002) (Figure 8). These complexes were strictly cell cycle regulated, peaking during M phase, cyclin B protein levels were also cell cycle regulated, and inhibitory phosphorylation of CDK1 was cell cycle dependent (Stead, White et al. 2002).

Subsequently, considerably amounts of cyclin D_3 were found to be associated with CDK6, but not CDK4, in mESC. Cyclin D_1 was found in complexes with CDK6, but to a lesser extent than cyclin D_3. CDK6 associated activity was high in mESC and decreased with differentiation (Faast, White et al. 2004). On the contrary, CDK4 associated kinase was virtually undetectable in mESC (Burdon, Smith et al. 2002; Savatier, Lapillonne et al. 1996).

Cyclin Dependent Kinase Inhibitors expression in mouse embryonic stem cells

Mouse embryonic stem cells exhibit little or no expression of CDK inhibitory molecules from both the INK4 family and the Cip/Kip family (Faast, White et al. 2004; Stead, White et al. 2002; Savatier, Lapillonne et al. 1996). Moreover, cyclin D_3-CDK6 complexes present in mESC are resistant to inhibition by $p16^{INK4a}$ (Faast, White et al. 2004). Therefore, mESC not only have elevated and cell cycle independent CDK

activity, they have a marked absence of CKI functions that normally perform roles in restricting cell division.

Recently, mESC-specific microRNAs have been shown to regulate some G_1 to S transition regulators to promote rapid proliferation. Specifically, miR-291a-3p, miR-294, and miR-295 rescued the G_1 accumulation phenotype of *Dgcr8* knockout mESC, which lack all canonical miRNAs, by downregulating $p21^{Cip1}$, p130, and large tumour suppressor 2 (Lats2) (Wang and Blelloch 2009; Wang, Baskerville et al. 2008).

Retinoblastoma-E2F and p53 pathways in mouse embryonic stem cells

As previously mentioned (see point 3), somatic cells undergo a period of mitogen dependence in G_1 phase, before they enter the cycle, called the Restriction point (R) where they sense the amount of available nutrients or the intensity of the mitogenic information and decide if undergo a new round of replication or exit the cell cycle to follow other cell fates. At the molecular level, R point depends on the activation of CDK activities which phosphorylate and, thus, inactivate Retinoblastoma (Rb) family members and this inactivation allows the transcription of E2F target genes. The best characterized function of E2F transcription factors is in regulating the expression of a genetic program of transcription required for the G_1 to S phase transition.

A vast body of evidence indicates that the R point is inactive in mESC (Figure 8). First, Rb and p107 are held in a hyperphosphorylated (inactive) state (Stead, White et al. 2002; Savatier, Huang et al. 1994). Second, mESC do not express p130 (Burdon, Smith et al. 2002). Third, CDK that regulate Rb family members are constitutively active, thus suppressing their activity (Stead, White et al. 2002). Fourth, Rb family members do not associate with E2F transcription factors in mESC (Stead, White et al. 2002). And, finally, E2F dependent transcription is not cell cycle regulated (White and Dalton 2005; Stead, White et al. 2002). Moreover, mESC share striking similarities in proliferative behavior with $p107^{-/-}$ $p130^{-/-}$ $Rb^{-/-}$ triple knockout (TKO) mouse embryonic fibroblasts (MEFs). Both, TKO MEFs and mESC, fail to arrest in G_1 at confluency. Both, mESC and TKO MEFs, also, escape replicative senescence and are immortal. Both, mESC and TKO MEFs fail to arrest in G_1 after DNA damage, but they do arrest at the Rb-independent G_2/M checkpoint. Therefore, mESC, like TKO MEFs, escape from contact inhibition, are immortal, and lack the G_1 checkpoint. Together, these data strongly

support the notion that mESC are not controlled by Rb in G_1 phase (Burdon, Smith et al. 2002).

The p53 checkpoint also seems to be inactive in mESC. It has been shown that p53 dependent cell cycle arrest and apoptosis are not efficient in mESC after certain types of physiological DNA damage, such as DNA double strand breaks or nucleotide depletion, although they synthesize abundant quantities of p53. It was reported that p53 protein, in mESC, was cytoplasmic and translocated inefficiently to the nucleus upon nucleotide depletion. Instead, mESC that sustained DNA damage underwent p53 independent apoptosis. The p53 dependent cell cycle arrest and apoptosis was activated again during differentiation (Aladjem, Spike et al. 1998). However, p53 seems to have a novel role involved in differentiation after DNA damage in mESC. Thus, p53 induces differentiation of mESC by suppressing *Nanog* expression. This represents an alternative pathway to maintain genetic stability, in mESC, by inducing the differentiation of ESC into other cell types that can undergo efficient p53 dependent cell cycle arrest or apoptosis (Lin, Chao et al. 2005).

4.2. CELL CYCLE CONTROL DURING DIFFERENTIATION IN MOUSE EMBRYONIC STEM CELLS

At some point during differentiation, pluripotent mESC switch their cell cycle control mechanisms from being elevated and constitutive to cell cycle regulated. The differentiation of mESC results in robust expression of D-type cyclins and appreciable CDK4 associated kinase activity (Savatier, Lapillonne et al. 1996). Besides this, the differentiation of mESC is accompanied by expression of CKI. Moreover, as mESC differentiate, CDK activity collapses and becomes cell cycle regulated (White, Stead et al. 2005; Faast, White et al. 2004). This coincides with the remodelling of the cell cycle and most notably the establishment of a fully formed G_1 phase with an increased percentage of cells in this phase (~40%). The R point control is activated as part of the developmental program as pluripotent cells differentiate, and coincides with the establishment of cell cycle regulated CDK activities and restructuring of the cell cycle (White, Stead et al. 2005).

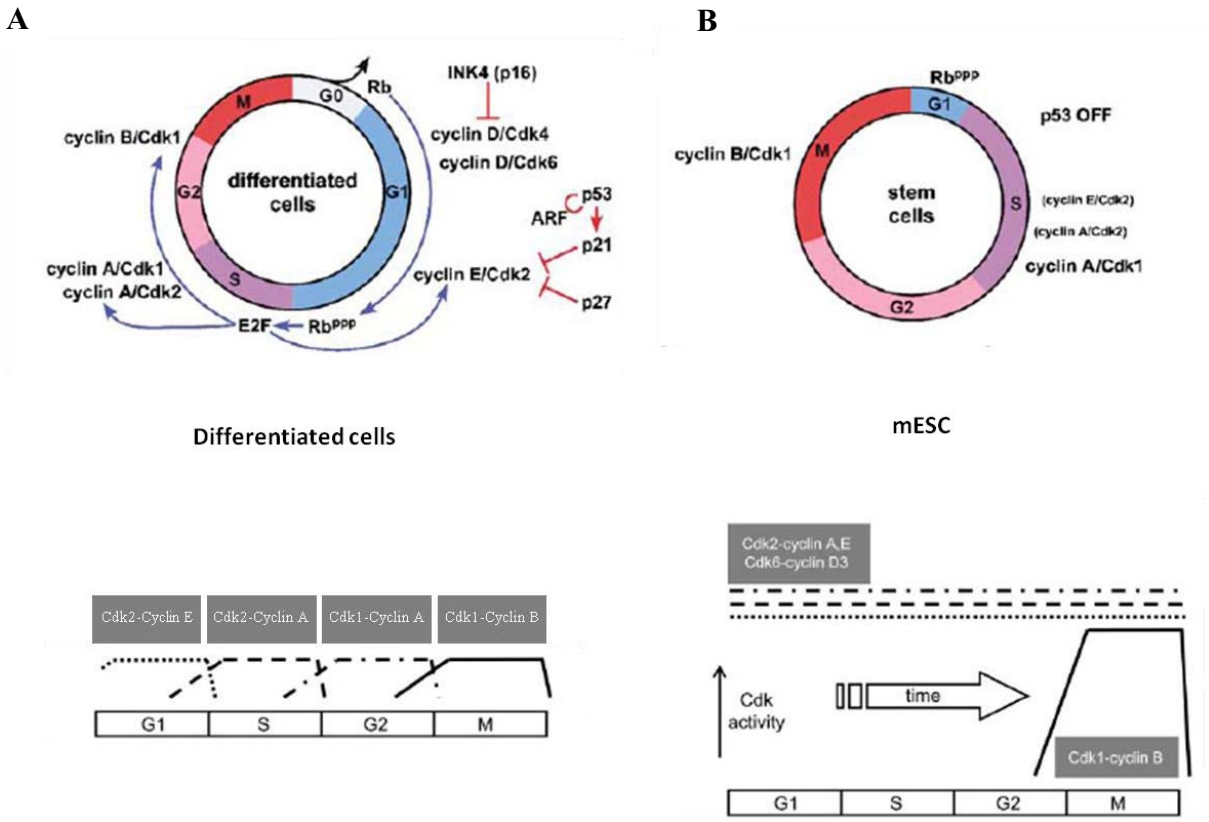

Figure 8. Models of cell cycle regulation in differentiated cells and mouse embryonic stem cells. (**A**) Proper progression through cell cycle phases in differentiated cells is controlled by the coordinated synthesis and proteolysis of cyclins E, A, and B, thus regulating cyclin dependent kinase (CDK) activity in a timely and periodic manner. Entry into S phase is controlled by the progressive phosphorylation of Rb family members for cyclin D-CDK4/6 complexes in early G_1 phase, and cyclin E-CDK2 complexes in late G_1 phase. The complete phosphorylation of Rb family proteins leads to full release of E2F transcription factors, activation of target genes, and entry into S phase. The inhibitors of cyclin dependent kinases (CKI) members of INK4 and Cip/Kip family suppress the activities of cyclin D-CDK4/6 and cyclin E-CDK2 complexes, respectively. (**B**) Mouse embryonic stem cells (mESC) have an extremely rapid cell cycle due to a reduced G_1 phase. Cyclins E and A are constitutively expressed leading to elevated and cell cycle independent CDK activities. The only obvious wave of cell cycle dependent activity is the mitotic cyclin B-CDK1. Mouse embryonic stem cells do not express CKI, Rb is constitutively phosphorylated, and p53 pathway is inactive. Adapted from (Berthet and Kaldis 2007; White and Dalton 2005).

4.3. CELL CYCLE CONTROL OF HUMAN EMBRYONIC STEM CELLS

Human embryonic stem cells (hESC) are grown under quite different conditions to mESC. They depend on bFGF for maintenance of the pluripotent state, contrary to mESC that depend on LIF. However, hESC exhibit a similar cell cycle structure to that seen in mESC, with a short proportion of cells in G_1 phase and a high proportion of cells in S phase (Becker, Ghule et al. 2006). Moreover, rhesus monkey ESC have a similar cell cycle structure to that seen in mESC with a truncated G_1 phase and a high proportion of cells in S phase (Fluckiger, Marcy et al. 2006). Upon differentiation, the cell cycle structure of hESC and rhesus monkey ESC changes dramatically such that the percentage of cells in G_1 increases and that in S phase decreases (Becker, Stein et al. 2010; Filipczyk, Laslett et al. 2007; Fluckiger, Marcy et al. 2006).

At the molecular level, rhesus monkey ESC are similar to mESC, as they also display constitutive cyclin-CDK activities, Rb is held in a hyperphosphorylated state, proliferate by mitogen-independent mechanisms, and do not growth arrest in G_1 after gamma irradiation (Fluckiger, Marcy et al. 2006). On the contrary, only a limited amount of information is available about the cell cycle molecular control in hESC and conflicting data about the cell cycle regulation of these cells is frequently encountered.

In this section, the current data on the regulation mechanisms of cell cycle of human embryonic stem cells will be reviewed highlighting differences and similarities with regulation mechanisms of cell cycle of mouse embryonic stem cells.

Cyclins and Cyclin Dependent Kinase expression and activities in human embryonic stem cells

There are some conflicting reports about the level of cyclin D expression in hESC. Meanwhile one study showed that hESC were negative for D-type cyclins expression (Filipczyk, Laslett et al. 2007), a recent report has shown that cyclin D_1 and D_3 are expressed in hESC and that upon differentiation cyclins D_2 and D_3 expression increases (Neganova, Zhang et al. 2009). On the contrary, another report has shown that cyclin D_2 is prominently expressed in pluripotent hESC, but cyclin D_1 eclipses cyclin D_2 during differentiation (Becker, Ghule et al. 2010).

Contrary to murine and rhesus monkey ESC that present an absence of cyclins E and A periodicity (Fluckiger, Marcy et al. 2006; Stead, White et al. 2002), it has been shown that only cyclin E was expressed constitutively in hESC and cyclin A showed cell cycle dependent expression (Filipczyk, Laslett et al. 2007). These results differ from other report showing cell cycle dependent expression of cyclins E, A, and B (Ghule, Becker et al. 2007). There is some evidence indicating that CDK activities display modest periodicity (2 to 3 fold fluctuations) during the cell cycle of hESC (Neganova, Zhang et al. 2009), contrary to mouse and rhesus monkey ESC that, with the exception of cyclin B-CDK1, lack cell cycle dependent CDK activities.

Cyclin Dependent Kinase Inhibitors expression in human embryonic stem cells

In the same way that mESC, the expression levels of CKI are low and, in some cases, absent in hESC. In the case of $p27^{Kip1}$, its expression is low in hESC due to a high expression of the ubiquitin ligase Skp2 that secure its ubiquitin dependent degradation (Egozi, Shapira et al. 2007). Also, and in contrast to somatic cells which have high levels of Skp2 only during S and G_2/M phases, undifferentiated hESC have also high levels of Skp2 at G_1 phase of the cell cycle (Egozi, Shapira et al. 2007).

Similarly to mESC, the embryoid bodies (EB) with low $p27^{Kip1}$ expression and high Skp2/$p27^{Kip1}$ ratio showed poorer differentiation than those with high $p27^{Kip1}$ expression (Egozi, Shapira et al. 2007; Bryja, Cajanek et al. 2005).

Retinoblastoma-E2F and p53 pathways in human embryonic stem cells

There is also a limited amount of information about the role of the different Rb-E2F complexes in hESC. It was reported that hESC presented a significantly higher proportion of cells in G_1 and retained G_1 phase specific hypophosphorylated Rb compared to mESC (Filipczyk, Laslett et al. 2007). A recent report has shown that Rb1 responsive E2F members (E2F1, E2F2, and E2F3) are expressed at lower levels than E2F4, E2F5, and E2F6, thus indicating that inhibitory E2Fs are more prominently expressed in hESC than in somatic cells. In particular, E2F5 and its cognate pocket protein Rbl2/p130 are the most abundant members of their class in hESC (Becker, Stein et al. 2007). These results are clearly different to those obtained in mESC which do not express p130 (Burdon, Smith et al. 2002). However, it should be emphasized that the

data of hESC was only taken at the transcriptional levels and it is unclear whether this is true at the protein level (Becker, Stein et al. 2007).

Also, there are contradictory data about p53 checkpoint in hESC. While, in one study, ultraviolet irradiation resulted in accumulation of p53 in apoptotic cells but it failed to activate the transcription of its target genes. This study showed that p53 induced apoptosis pathway was mediated via the mitochondrial pathway. Downregulation of p53 was also shown to result in reduction of spontaneous differentiation of hESC, whilst its accumulation could induce differentiation by suppressing *OCT4* and *NANOG* (Qin, Yu et al. 2007). Another report suggested that gamma irradiation resulted in p53 dependent transactivation of the CKI $p21^{Cip1}$, resulting in cell cycle arrest in hESC (Becker, Stein et al. 2007). Moreover, a recent report has also shown that nutlin, a selective activator of the p53 pathway *in vitro* and *in vivo* by destroying its complex with human homolog of mouse double minute 2 (HDM2), rapidly induces transcriptionally active p53 accompanied by increase of $p21^{Cip1}$ and HDM2 in hESC (Maimets, Neganova et al. 2008).

Recently, hESC-specific microRNAs have been shown to regulate some cell cycle proteins to promote rapid proliferation. Specifically, two miRNAs: miR-195 and miR-372 could partially reverse the cell cycle delay in DICER knockdown hESC. Whereas, miR-372 was shown to regulate the CKI $p21^{Cip1}$, miR-195 was shown to regulate the G_2 to M phase transition by regulating the inhibitory kinase WEE1, one of the three kinases that negatively regulate the cyclin B-CDK1 complexes in mammalian cells (Qi, Yu et al. 2009).

4.4. CELL CYCLE REGULATION AS A COMPONENT OF THE PLURIPOTENT STATE

Embryonic stem cells have an unorthodox cell cycle in which the G_1 control pathways that operate in other cell types of cells are reduced or absent. Constitutive replication is also a common aspect of early embryo development in many species. This might simply reflect the fundamental requirement of establishing sufficient cell numbers to initiate gastrulation. It is possible, however, that the uncoupling from G_1 regulation might also be involved in sustaining the undifferentiated state (Burdon, Smith et al. 2002).

G_1 phase is the phase where cells decide if continue through another round of cell division of exit the cell cycle to undergo other cell fates. Thus, a short G_1 phase should limit the "window of opportunity" during which a cell can be responsive to differentiation cues (Orford and Scadden 2008).

Active hypophosphorylated Rb forms complexes with and promotes the activity of differentiation promoting transcription factors such as MyoD, myogenin, and C/EBP (Chen, Riley et al. 1996; Gu, Schneider et al. 1993). It has been suggested that the efficient hyperphosphorylation and inactivation of Rb, and its other family members, might be important to shield pluripotent cells from activities that induce differentiation (Burdon, Smith et al. 2002). In line with this hypothesis, recent evidence has shown that some cell cycle regulators can affect transcriptional activity, independently of their roles in cell cycle exit and progression. Thus, through direct binding, $p21^{Cip1}$ inhibits the activities of E2F1, c-Myc, and STAT3 independently of the CDK function (Vigneron, Cherier et al. 2006). On the other hand, $p21^{Cip1}$ can stimulate p300/CBP transcriptional activation (Gregory, Garcia-Wilson et al. 2002). Moreover, $p57^{Kip2}$ can promote transactivation of muscle-specific genes (Reynaud, Leibovitch et al. 2000), and $p27^{Kip1}$ promotes the differentiation of mouse neuronal progenitors (Nguyen, Besson et al. 2006).

Besides CKI, D-type cyclins effectively modulate transcriptional activation. In particular, it has been shown that cyclin D_1 binds to STAT3 transcription factors to inhibit their transcriptional activity, independently of its function as a CDK regulatory subunit (Bienvenu, Gascan et al. 2001). Moreover, cyclin D_1 has been shown to bind to the transcription factor Beta2/NeuroD to inhibit its transcriptional activity, also cyclin D_1 has been reported to interact with Myb and dentin matrix acidic phosphoprotein 1 (DMP1) family of transcription factors (Coqueret 2002).

Thus, the lowering of the expression levels of CKI and/or cyclin D_1 might be important to shield pluripotent cells from activities that induce differentiation.

Another possibility is that by reducing the G_1 phase, the cell could avoid the temporal opportunity for both chromatin remodelling and the establishment of heritable transcription programs (Burdon, Smith et al. 2002). If chromatin in pluripotent cells exists in an open configuration, repressing and activating blocks of genes could require a longer remodelling period than that available during the short G_1 phase of pluripotent cells.

4.5. THE CELL CYCLE AND REPROGRAMMING

Cell types typically used to generate iPSC exhibit a significantly different cell cycle structure and, as reprogramming proceeds, a pluripotent cell cycle structure and mechanism of control is established. A mechanistic survey of the four reprogramming factors in mouse cells found that c-myc was critical for the early stages of reprogramming (Sridharan, Tchieu et al. 2009). The members of the Myc family of basic helix-loop-helix (bHLH) transcription factors have well established roles in control of cell cycle progression by regulating cell cycle proteins. Thus, elevated c-myc accelerates progression through G_1 phase by positively regulating cyclin-CDK activity (Amati, Alevizopoulos et al. 1998). This regulation occurs at multiple levels, including transcriptional and post-transcriptional control, involving the upregulation of cyclins and suppression of CKI, such as $p27^{Kip1}$ and possibly $p21^{Cip1}$ (Yang, Shen et al. 2001; Amati, Alevizopoulos et al. 1998). Also, c-myc regulates positively cyclin-CDK activity by induction of the CDK activating phosphatase Cdc25A (Amati, Alevizopoulos et al. 1998). Moreover, the regulatory subunit of telomerase reverse transcriptase (TERT) has been confirmed as an *in vivo* target of Myc in mESC (Kim, Chu et al. 2008).

Another role for cell cycle proteins in the reprogramming process has been recently shown. Thus, several studies identified p53 as a factor responsable for low efficiency of reprogramming. Supression of p53 pathway by knocking down p53 or its target gene $p21^{Cip1}$ increased reprogramming efficiency in mouse fibroblasts and human somatic cells (Kawamura, Suzuki et al. 2009). Moreover, p53 was critically involved in preventing the reprogramming of cells carrying various types of DNA damage, including short telomeres, DNA repair deficiencies, or exogenously inflicted DNA damage in both mouse and human cells (Marion, Strati et al. 2009; Hong, Takahashi et al. 2009). Moreover, we have recently reported that Rem2 GTPase, a suppressor of the p53 pathway, is an important player in the maintenance of hESC self-renewal and pluripotency, and enhances reprogramming of human somatic cells to hiPSC by suppressing the transcriptional activity of p53 and localization of cyclin D_1. Moreover, Rem2 GTPase is as efficient as c-Myc in enhancing reprogramming of human somatic cells into hiPSC (See annexe II (Edel, Menchón et al. 2010)).

These studies highlight the importance of imposing hESC specific cell cycle features in the reprogramming process.

5. EPITHELIAL TO MESENCHYMAL TRANSITION AND EARLY EMBRYOGENESIS

Gastrulation is the universal process by which the body plan is established. A fertilized egg undergoes gastrulation, generating three germ layers: ectoderm, mesoderm, and endoderm (Kalluri and Weinberg 2009).

A subset of cells from the epiblast, the single epithelial cell layer of the embryo, moves to the midline to form the primitive streak, a linear structure that bisects the embryo along the antero-posterior axis (Thiery, Acloque et al. 2009). The primitive streak is formed from a furrowed invagination in the midline of the epiblast layer that forms initially at the lower extremity of the embryo and, later on, extends in the direction of the future head. Once formed, the primitive streak, acting via ingression, generates the mesendoderm which subsequently separates to form the mesoderm and the endoderm via an epithelial to mesenchymal transition (EMT) (also known as epiblast-mesoderm transition) (Kalluri and Weinberg 2009). Those cells remaining in the epiblast become ectoderm. Thus, the embryo is transformed from a single layer to three germ layers (Thiery, Acloque et al. 2009) (Figure 9A). The embryonic mesoderm that forms between the epiblast and hypoblast eventually gives rise to primary mesenchyme associated with the axial, paraxial, intermediate, and lateral plate mesodermal layers each of which gives rise to multiple derivatives by successive mesenchymal to epithelial transitions (MET) and EMT events (Figure 9B). Endodermal derivatives can also use EMT to generate internal organs, such as the pancreas and liver, although these processes are not as well documented at the molecular level (Acloque, Adams et al. 2009).

The EMT process is a biologic process that allows a polarized epithelial cell, which normally interacts with basement membrane via its basal surface, to undergo multiple biochemical changes that enable it to assume a mesenchymal cell phenotype which includes the loss of cell-cell adhesion, the loss of cell polarity, and the acquisition of migratory and invasive properties, and an elevated resistance to apoptosis (Kalluri and Weinberg 2009). The completion of an EMT is signalled by the degradation of underlying basement membrane and the formation of a mesenchymal cell that migrate away from the epithelial layer in which it originated (Kalluri and Weinberg 2009).

The conversion of epithelial cells to mesenchymal cells is fundamental for embryonic development and the generation of tissues and organs whose precursors originate far from their final destination. Once the cells have reached their destination, they differentiate into different cell types very often involving the reverse process, a MET process (Nieto 2009).

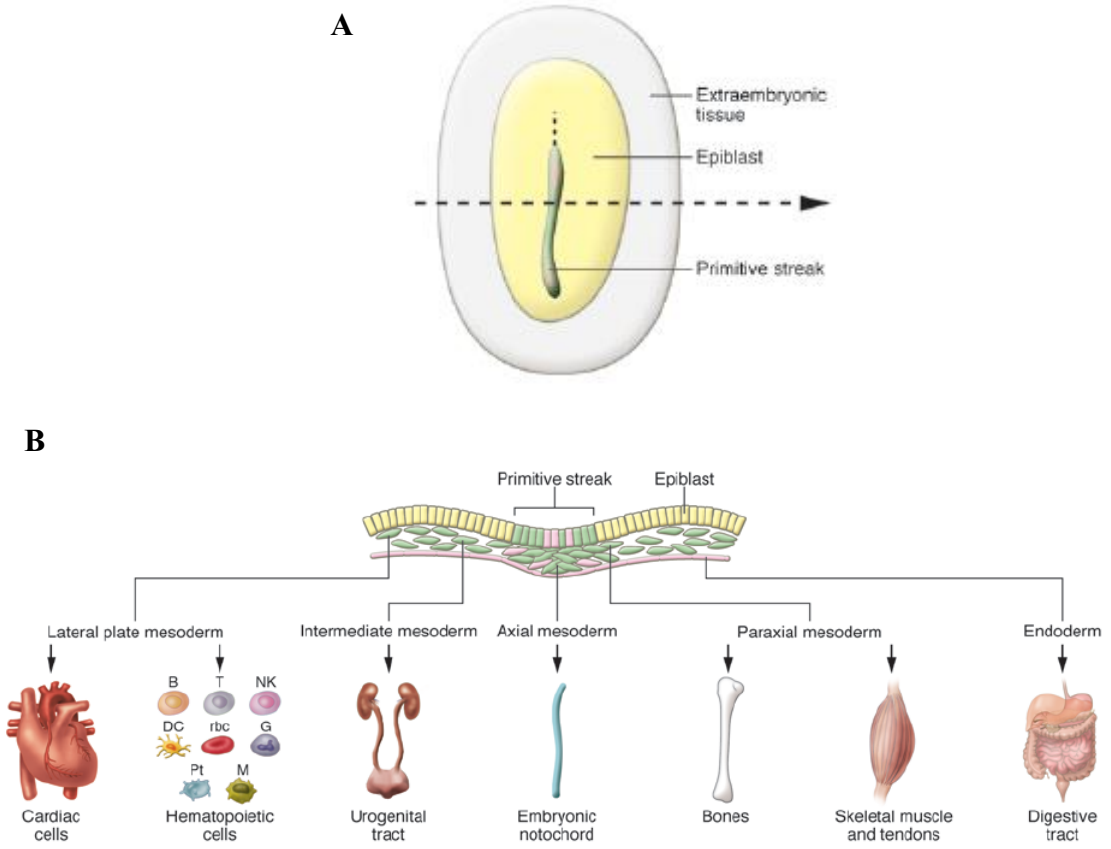

Figure 9. Formation of embryonic layers at gastrulation in vertebrates. (**A**) Dorsal view of chick embryos as representative of vertebrates. The embryonic layers are defined during gastrulation. Mesodermal (green) and endodermal cells (pink) are internalized at the primitive streak through an epithelial to mesenchymal transition process (EMT), while those cells remaining in the epiblast become ectoderm (yellow). (**B**) Transverse section taken at the level of the dotted lines. Epiblast cells that internalize at gastrulation give rise to different mesodermal and endodermal populations from which a variety of cell types form. Pt, platelets; B, T, and NK, lymphocytes; G, granulocytes; M, macrophages. Adapted from (Acloque, Adams et al. 2009).

At the biochemical level, gastrulation is iniciated by a convergence of signalling pathways at the posterior part of the embryo that leads to primitive streak formation and initiation of the mesodermal fate program, as well as, an EMT process (Thiery, Acloque et al. 2009).

Activation of Wnt signalling confers competence to the posterior part of the embryo in the formation of the primitive streak. Subsequently, members of the TGFβ superfamily, including Nodal and Vg1, induce gastrulation. Nodal signalling, together with FGF, controls the specification of the mesendoderm in all vertebrates through specific regulators and the contribution of some of the genes involved in the EMT program (Thiery, Acloque et al. 2009).

Among the crucial transcription factors that are commonly accepted as mesoderm markers, and key players in mesoderm specification and patterning are those coding for the transcription factors *Brachyury*, *Snail*, and *Twist*.

Many other genes are also important players in the formation of the inner germ layers, but this thesis will be focused on these three genes.

5.1. BRACHYURY

Brachyury (T) belongs to the T-box family, defined by a common DNA binding domain known as the T-box (T-box DNA binding sequence). The T site or T-box binding element (TBE) was first defined as the sequence with the highest affinity for Brachyury. Brachyury binds this palindromic sequence as a dimer. Depending on context, T-box proteins may homodimerize, heterodimerize, or cooperatively bind other transcription factors (Naiche, Harrelson et al. 2005).

In vertebrates, *Brachyury* is expressed in the caudal primitive streak and is responsible for posterior mesodermal development and regulates such key factors as FGF signalling and cell migration (Naiche, Harrelson et al. 2005). Mice embryos with a homozygotic defect in *Brachyury* fail to elongate along the anterior-posterior axis and they do not develop mesodermal extraembryonic tissue, which leads to death *in utero*. Brachyury therefore seems to have a dual role in mesoderm specification and axis elongation (Beddington, Rashbass et al. 1992). The role in cell migration seems to be related to a role for *Brachyury* in cell adhesion in mouse given that *in vivo* analysis of $T^{-/-}$ mutant mESC showed that they were compromised in their ability to migrate away from the primitive streak and, therefore, unable to carry out the morphogenetic movements performed by their wild-type counterparts during gastrulation, leading to their accumulation in the primitive streak (Wilson and Beddington 1997; Wilson, Manson et al. 1995; Wilson, Rashbass et al. 1993; Rashbass, Cooke et al. 1991).

Brachyury, in addition, regulates expression of target genes directly involved in mesoderm differentiation.

5.2. SNAIL

Snail is a member of the Krüppel-like subfamily of zinc finger proteins, which usually acts as a transcriptional repressor (Nieto 2002). There are two main *Snail* genes in vertebrates, *Snail1* and *Snail2* (called *SNAI1* and *SNAI2* in humans). They are induced by TGFβ superfamily members, and FGF signalling is necessary to maintain their expression and for gastrulation to proceed (Barrallo-Gimeno and Nieto 2005; Ciruna and Rossant 2001). Members of the Snail family are expressed in the primitive streak (Thiery, Acloque et al. 2009).

During *Drosophila* embryogenesis, expression of Snail is regulated by nuclear Dorsal protein and by Twist. Snail is expressed in the ventral blastoderm of *Drosophila* embryos before gastrulation in a somewhat broader domain than Twist (Leptin 1991). By repressing neuroectodermal genes, Snail favours the specification to mesoderm (Leptin 1991).

While Snail also plays a crucial role in mesoderm formation in chordates (Langeland, Tomsa et al. 1998; Fujiwara, Corbo et al. 1998; Sefton, Sanchez et al. 1998; Thisse, Thisse et al. 1995), it is also expressed in the ectoderm, in particular during the formation of the neural crest (Nieto 2002; del Barrio and Nieto 2002; Knecht and Bronner-Fraser 2002). A detailed functional, as well as, comparative analysis showed that Snail proteins act as a master regulator of the EMT (Carver, Jiang et al. 2001; Savagner 2001) as they control cell-cell adhesion, cell shape, and motility. *Snail*-deficient embryos fail to gastrulate, and “mesodermal” cells are unable to downregulate E-cadherin, and accumulate at the streak (Carver, Jiang et al. 2001; Nieto, Sargent et al. 1994). Snail proteins are not essential for mesodermal fate specification as a “mesodermal” population expressing the appropriate markers still forms in *Snail* mutant mice, although cells fail to migrate because it cannot undergo EMT (Carver, Jiang et al. 2001).

In general, Snail is expressed in cells that change their shape in such a way that they contribute to the formation of a fold or a furrow in an epithelium or that detach from an epithelium to form mesenchymal tissue (Thiery, Acloque et al. 2009).

5.3. TWIST

TWIST belongs to the large family of bHLH transcription factors. Well conserved during evolution, two *TWIST* genes exist in vertebrates, *TWIST1* and *TWIST2* (formerly Dermo-1) (Ansieau, Morel et al. 2010). The TWIST proteins act in vertebrates after specification of the mesoderm (Gitelman 1997; Chen and Behringer 1995; Wolf, Thisse et al. 1991), however it is crucially involved in mesoderm differentiation. For example, in chick embryos, this gene is expressed in the anterior head mesoderm, and also in the somites where it contributes to patterning of mesodermal tissue like muscles (Tavares, Izpisua-Belmonte et al. 2001). Interestingly, while high levels of Twist protein promote myogenesis in *Drosophila* (Baylies and Bate 1996), myogenesis in vertebrates is repressed by Twist (Spicer, Rhee et al. 1996), indicating that Twist has opposite effects in vertebrates and insects. The results support the view that in vertebrates Twist prevents premature differentiation of myogenic cells. The different function of vertebrate and insect Twist is most likely due to the heterodimer formation with E proteins, thereby competing for the binding of E proteins to the myogenic bHLH protein MyoD. Interestingly, in *in vitro* or cell culture experiments, *Drosophila* Twist behaves like the vertebrate Twist, indicating that it is the specific cellular context that is responsible for the different role *in vivo* (Technau and Scholz 2003).

The transcription factor Twist is also capable of inducing an EMT process in epithelial cells (Yang, Mani et al. 2004). Recently, it has been shown that nontumorigenic, immortalized human mammary epithelial cells (HMLEs) ectopically expressing TWIST transcription factor formed more mammospheres that did HMLEs infected with the corresponding control vector, thus demonstrating an increase of self-renewing, gland-reconstituting stem cells within the population. Moreover, this study showed that normal human breast stem like cells isolated from mammary tissue expressed markers associated with an EMT process including TWIST (Mani, Guo et al. 2008).

The EMT process also occurs during spontaneous differentiation of hESC although if any cell cycle protein is involved in this process remains unknown.

OBJECTIVES

Based on the limited amount of information available about the cell cycle regulation mechanisms of human embryonic stem cells and that to date there was no functional *in vitro* analysis for cell cycle regulators in embryonic stem cells:

This doctoral thesis has two main objectives:

1. The study of the cell cycle regulation mechanisms of human embryonic stem cells.
2. To find out if the manipulation of one single cell cycle gene could affect the pluripotency or self-renewal properties of human embryonic stem cells.

RESULTS

1. HUMAN PLURIPOTENT CELLS HAVE A COMMON BUT ATYPICAL CELL CYCLE STRUCTURE THAT CHANGES UPON DIFFERENTIATION TOGETHER WITH AN INCREASE OF $p27^{Kip1}$

The cell cycle of mouse embryonic stem cells (mESC) has been well described. Studies in mESC have demonstrated that they proliferate at extremely rapid rates that may be due to an unusual cell cycle structure consisting largely of S phase cells and a short proportion of cells in G_1 phase. Several studies have described the repertoire of cell cycle regulators expressed in mESC. Cyclins D_1, D_3, E_1, A_2, and B_1 have all been described in mESC. Cyclin D_1 and cyclin D_3 are present in low amounts in mESC, whereas cyclin D_2 is not expressed (White and Dalton 2005; Burdon, Smith et al. 2002; Savatier, Lapillonne et al. 1996).

Central to the mechanisms that underpinned rapid cell division, in mESC, was the extreme activity of cyclins E/A-CDK2 complexes, all of which lacked cell cycle dependent periodicity (Stead, White et al. 2002). The only CDK activities that were under periodic control were cyclin B-CDK1 complexes, but even this CDK activity showed unusually high activity (Stead, White et al. 2002). This elevated, cell cycle independent CDK activity may be caused by low expression of CDK inhibitors that normally perform roles in restricting cell division. Moreover, cyclin D_3-CDK6 complexes were resistant to inhibition by $p16^{Ink4a}$ (Faast, White et al. 2004). According to this high cyclin-CDK complexes activity, retinoblastoma (Rb) family members are hyperphosphorylated and constitutively inactive throughout cell cycle and E2F dependent transcription is not cell cycle dependent. When cells differentiate, mESC switch their cell cycle control mechanisms from elevated and constitutive to cell cycle regulated. This coincides with the remodelling of the cell cycle and acquisition of the Restriction point control (White, Stead et al. 2005).

In first place, we set out to confirm previous data on cell cycle in mESC, using the J1 mESC line. The percentage of pluripotent cells was analyzed by flow cytometry analysis of Oct3/4 staining. The results showed that an 87% of the population was positive for Oct3/4 pluripotency factor (Figure 10).

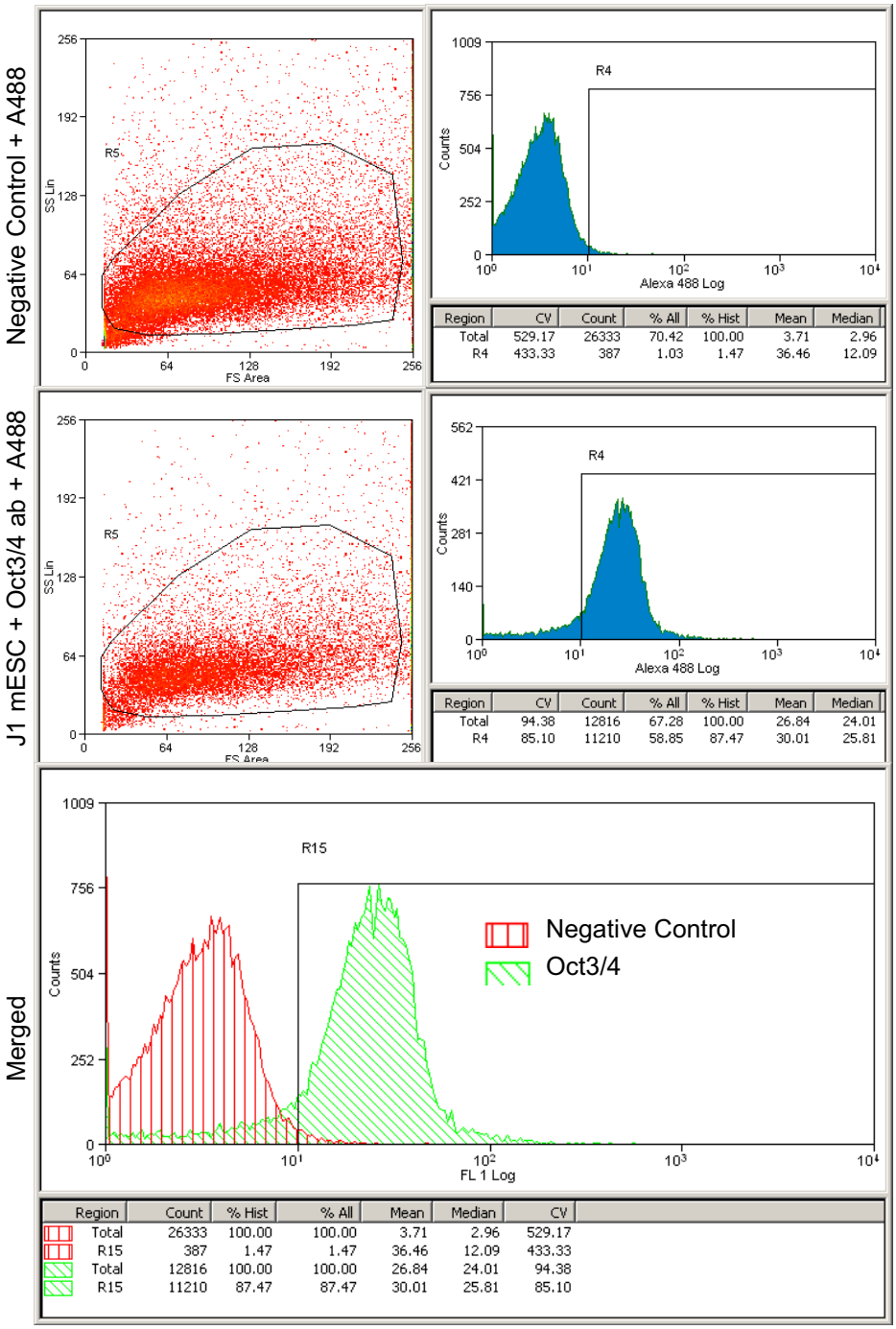

Figure 10. J1 mouse embryonic stem cells are pluripotent. Quantitative flow cytometry analysis of Oct3/4 expression shows that J1 mESC are pluripotent. For the negative control, cells were incubated with the secondary antibody Alexa 488 (A488).

We next analyzed the cell cycle structure of undifferentiated and differentiated J1 mESC by flow cytometry analysis. J1 mESC were differentiated as embryoid bodies (EB) by trypsinizating the colonies and plating them in suspension in non-adherent plates with the same mESC medium but without leukaemia inhibitory factor (LIF) for several days.

The cell cycle structures of undifferentiated cells and cells differentiated after 3, 9, and 15 days were evaluated by flow cytometry analysis of Propidium Iodide (PI)-stained cells (Figure 11).

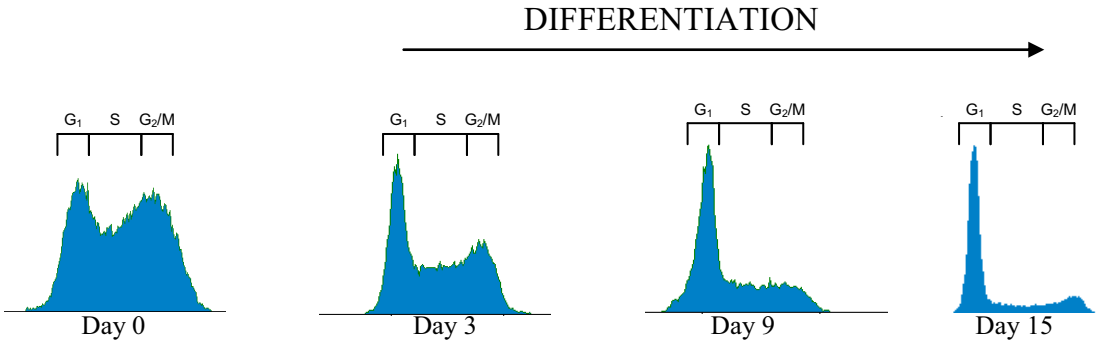

Figure 11. Cell cycle profile of mouse embryonic stem cells changes during differentiation. Flow cytometry analysis of cell cycle structure by Propidium Iodide (PI) staining of J1 mESC undifferentiated (day 0) and differentiated after several days (days 3, 9, and 15) shows that the proportion of cells in $G_0/_1$ phase increases, but that in S phase decreases as differentiation proceeds. A minimum of 10000 events were recorded.

Results showed that the proportion of cells in G_1 phase increased markedly at day 3 onwards, meanwhile, at the same time, the proportion of cells in S phase decreased. We predicted that changes in cell cycle structure during differentiation could be due to a fundamental change in the cell cycle machinery. We focused on the G_1 phase of the cell cycle due to its important role in committing cells to the cycle. To address the molecular mechanisms regulating this cell cycle structure change, the protein levels of main G_1 phase regulators were analyzed in undifferentiated cells and cells differentiated after several days, by Western blot analysis. Loss of Oct3/4 expression was used to monitor differentiation (Figure 12).

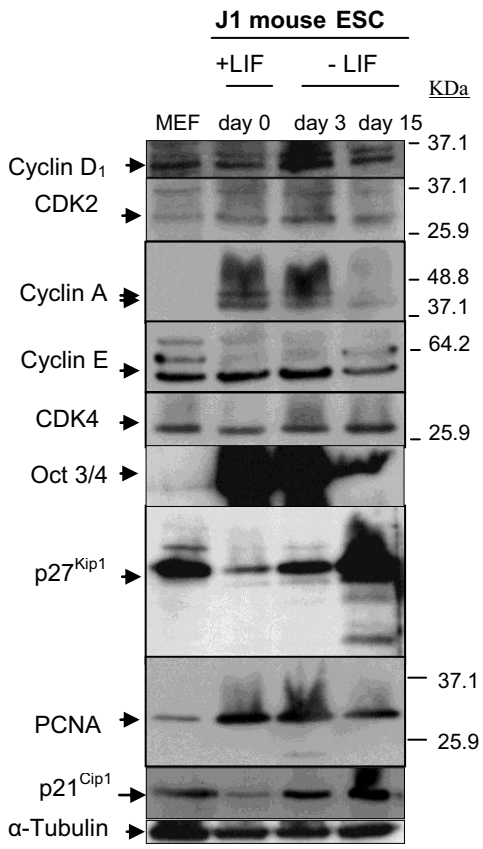

Figure 12. Cell cycle proteins profile of J1 mouse embryonic stem cells changes during differentiation. Western blot analysis of several cell cycle regulators in J1 mouse embryonic stem cells (mESC) undifferentiated (day 0) and differentiated after several days (day3 and 15) reveals that cell cycle proteins expression changes during differentiation. Twenty micrograms of protein from whole cell extracts were used. α-tubulin was used as a loading control. The position of molecular weight markers is shown in the right. KDa, Kilodaltons; LIF, leukaemia inhibitory factor; PCNA, Proliferating Cell Nuclear Antigen.

Western blot analyses showed that Oct3/4 decreased as cells differentiated. Cyclin D_1 appeared to increase with differentiation. Also, CDK4 increased slightly after 30 days of differentiation. On the contrary, cyclin E, cyclin A, and CDK2 protein expression levels decreased with the differentiation, consistent with previous work (White, Stead et al. 2005; Stead, White et al. 2002). Proliferating Cell Nuclear Antigen (PCNA), a protein important for both DNA synthesis and DNA repair, and a marker of cell proliferation decreased during differentiation. On the contrary, CDK inhibitors $p21^{Cip1}$ and $p27^{Kip1}$ protein expression levels were low in undifferentiated cells, but increased during differentiation. $p27^{Kip1}$ dramatically increased after 30 days of differentiation. These results are in agreement with the increase of G_1 phase population and reduction of S phase with differentiation, suggesting a possible role for the cell

cycle in the maintenance of the pluripotent state. Interestingly, the $p27^{Kip1}$ increase during differentiation was inversely proportional to that of Oct3/4 expression.

Very little is known about the cell cycle regulation of human embryonic stem cells (hESC). They have a rapid generation time, similar to mESC, due to a shortened G_1 phase (Becker, Ghule et al. 2006). However, hESC are grown under different conditions than mESC (they rely on basic fibroblast growth factor (bFGF) and not on LIF to maintain pluripotency). Given that only a limited amount of information about the molecular mechanisms underlying this cell cycle structure is available, we next proceeded to analyze the cell cycle structure of pluripotent hESC. We hypothesized that the atypical cell cycle structure of undifferentiated ESC was functionally important for pluripotency and self-renewal properties given the dramatic changes with differentiation. With the aim of investigating this hypothesis, we also proceeded to analyze the cell cycle profile of a recently discovered human pluripotent cell type: human induced pluripotent stem cells (hiPSC).

We proceeded to analyze, by flow cytometry analysis, the cell cycle structure of two different hESC lines derived in the CMR[B]: hES[4] and hES[6] (Raya, Rodriguez-Piza et al. 2008), and also two different hiPSC lines derived in the CMR[B]: human keratinocytes induced pluripotent stem cells (hKiPSC) and human fibroblast induced pluripotent stem cells (hFiPSC) (Aasen, Raya et al. 2008; Rodriguez-Piza, Richaud-Patin et al. 2009), respectively (Figure 13). All cell lines displayed a normal karyotype, that is a characteristic of ESC, and expressed pluripotency surface antigens SSEA-3, Tra-1-60, SSEA-4, and Tra-1-81, as well as, the pluripotency transcription factors Oct3/4, Nanog, and Sox2. Moreover, all cell lines tested readily differentiated *in vitro* into all three primary germ cell layers and expressed specific differentiation markers for ectoderm, endoderm, and mesoderm (Rodriguez-Piza, Richaud-Patin et al. 2009; Raya, Rodriguez-Piza et al. 2008; Aasen, Raya et al. 2008).

This characterization showed that these cell lines were pluripotent. We then investigated the cell cycle structure in undifferentiated cells and upon differentiation (Figure 13). General differentiation was carried out by EB generation and subsequent culture on gelatin with general differentiation medium for 30 days.

The cell cycle structure of these human pluripotent cell lines was evaluated by flow cytometry analysis of 4', 6-dimidino-2-phenylindole (DAPI)-stained cells. DAPI is a fluorescent dye that binds to DNA and allows analysis of DNA content. A modified

nucleoside: 5-ethynyl-2'-deoxyuridine (EdU) that is incorporated during DNA synthesis was used to analyze the percentage of S phase cells. In order to perform a cell cycle analysis of undifferentiated cells we selected pluripotent TRA-1-60 positive-stained cells.

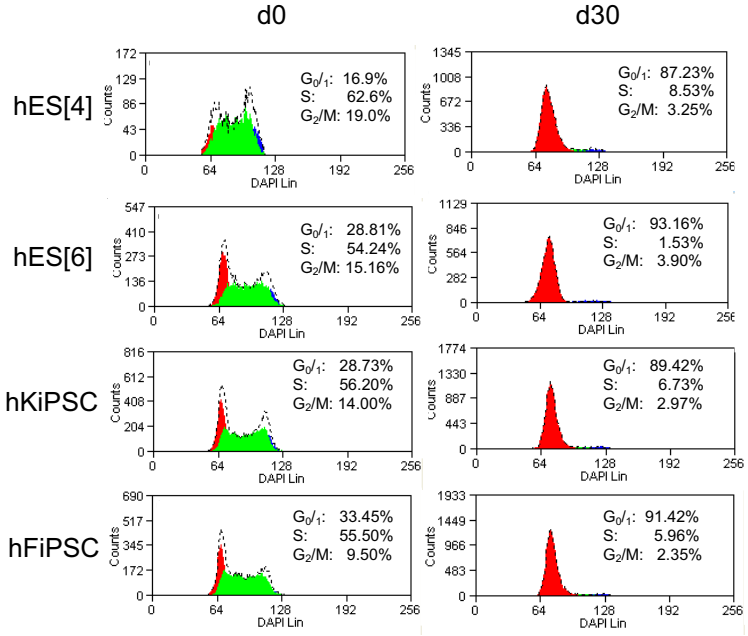

Figure 13. Human pluripotent cells share a similar cell cycle structure. Quantitative flow cytometry analysis of cell cycle by DAPI staining and EdU incorporation in two different human embryonic stem cells (hESC) lines and two different human induced pluripotent stem cells (hiPSC) lines reveals a similar cell cycle structure in undifferentiated cells, with a short percentage of cells in $G_0/_1$, and a high percentage of cells in S phase. Upon differentiation there is an increase of cells in $G_0/_1$ phase of cell cycle and a decrease of cells in S phase. Shown are the representative results obtained in two independent experiments. A minimum of 10000 events were recorded. The cell cycle profile of only TRA-1-60 positive cells was analyzed at day 0. $G_0/_1$: red; S: green; G_2/M: blue. hKiPSC, human keratinocytes induced pluripotent stem cells; hFiPSC, human fibroblast induced pluripotent stem cells.

The results showed a close resemblance between the cell cycle profile of undifferentiated hESC and hiPSC, with a high percentage (54-62%) of the population in S phase and a low proportion of cells in $G_0/_1$ phase of the cell cycle (17-33%). On differentiation, the cell cycle structure of all cell lines analyzed similary changed with a striking increase of cells in the $G_0/_1$ phase (87-93%) and a reduction of cells in the S phase (2-8%).

In conclusion, undifferentiated, pluripotent hESC and hiPSC have a similar cell cycle structure to that of mESC. These results suggest that this common, specific cell cycle structure can be functionally important in pluripotency and self-renewal properties of undifferentiated cells.

With the aim of finding out the molecular mechanisms underlying this cell cycle structure, a serie of Western blot analysis of cell cycle regulators in the hESC line ES[4] was performed, with special attention to those regulating the G_1 to S transition given that is in this stage when the cells decide if continue or exit the cell cycle (Figure 15). We chose to study the cell cycle at the protein level because many of the cell cycle proteins are regulated at post-transcriptional level (Sherr and Roberts 1995).

In order to study the cell cycle regulators expression levels upon differentiation, we performed a general differentiation protocol where differentiation into tissues representative of all three primary germ cell layers was achieved. Protein samples were collected after 15 and 30 days of differentiation (Figure 14).

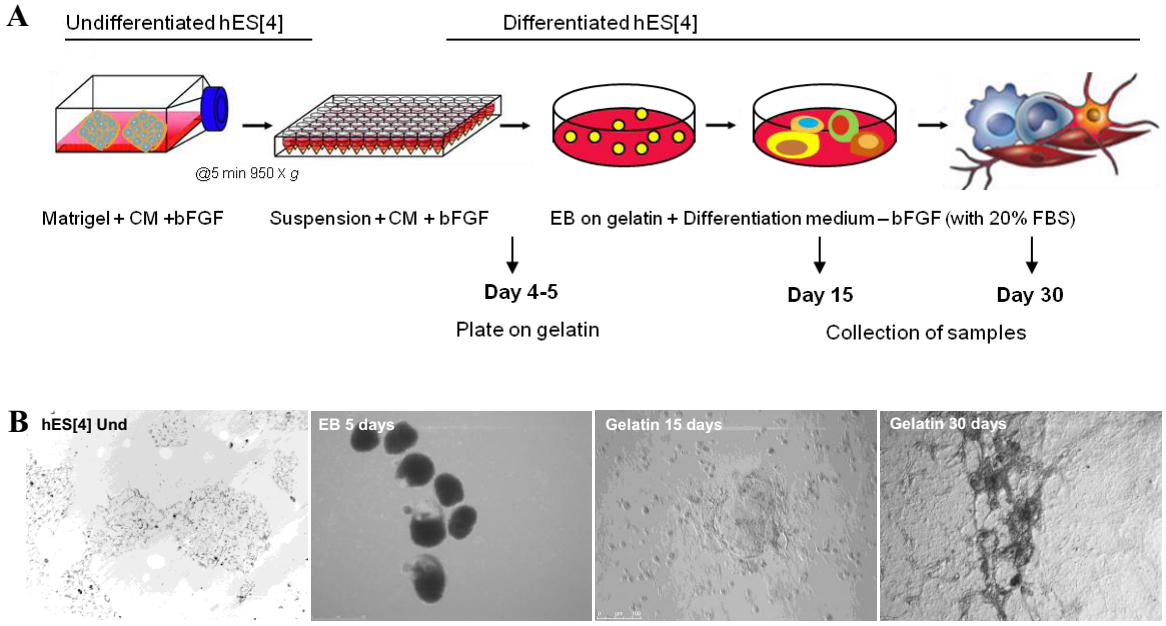

Figure 14. General differentiation protocol of human embryonic stem cells (**A**) Timeline of general differentiation protocol. Embryoid bodies (EB) were generated by trypsinizating colonies, seeding them on V-bottom non-adherent 96-well plates, and centrifuging them in order to allow aggregation. After 4-5 days in suspension with conditioned medium (CM), EB were seeded on gelatin with general differentiation medium containing 20% fetal bovine serum (FBS), without basic fibroblast growth factor (bFGF). (**B**) Representative phase contrast images of undifferentiated colonies of hESC, EB cultured in suspension, and after seeding them on gelatin. Scale bars: 100 and 500µm. (**C**) *In vitro* differentiation of hESC into all three primary germ layers: ectoderm (β-Tubulin III, red; GFAP, yellow), endoderm (α-1-Fetoprotein, red; FOXA2, yellow), and mesoderm (α-Smooth Muscle Actin, red). Nuclei were counterstained with DAPI (blue). Scale bars: 75 µm. GFAP, glial fibrillary acidic protein; FOXA2, forkhead box protein A2.

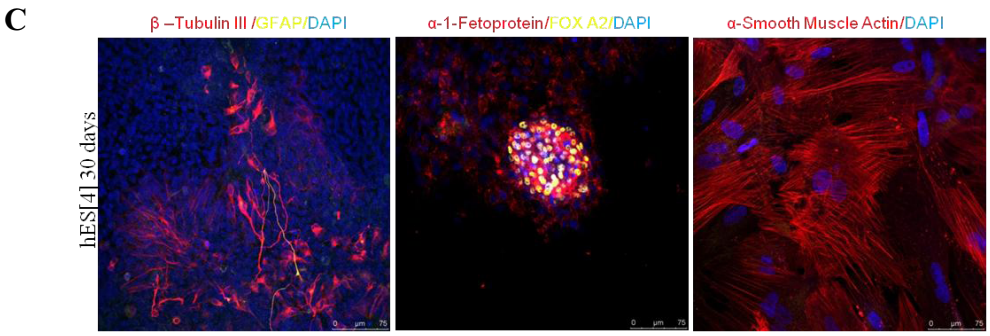

Differentiation was monitored by assessment of pluripotency factor Oct3/4 protein levels. Reduction in Oct3/4 protein levels along differentiation demonstrated that the cells were effectively differentiating.

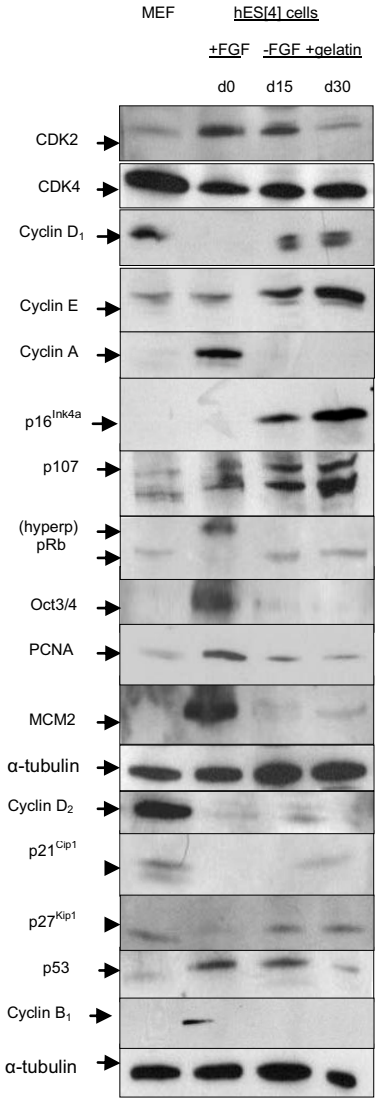

Figure 15. Cell cycle proteins profile of human embryonic stem cells changes during differentiation. Western blot analysis of several cell cycle regulators in hES[4] undifferentiated (day 0), and after differentiation for 15 and 30 days in general differentiation medium. Twenty micrograms of protein from whole cell extracts were used. α-tubulin was used as a loading control. pRb, retinoblastoma protein; hyper, hyperphosphorylated; bFGF, basic fibroblast growth factor; PCNA, proliferating cell nuclear antigen; MCM2, mini chromosome maintenance protein 2.

Western blot analyses revealed that the G_1 phase associated cyclins D_1 and D_2 were expressed at low levels in undifferentiated cells but increased during general differentiation. CDK4 protein levels, however, did not experimented substantial changes. On the contrary, S and M phase associated cyclins A and B_1, and CDK2 were expressed at high levels in undifferentiated cells but dropped as differentiation proceeded. Interestingly, cyclin E seemed to increase with differentiation. S phase related PCNA and the DNA replication licensing factor, mini chromosome maintenance protein 2 (MCM2) are proteins involved in the replication of the DNA. These proteins were expressed at high levels in undifferentiated conditions but their expression decreased during differentiation. On the contrary, the cyclin dependent kinase inhibitors (CKI), members of the Cip/Kip family, $p21^{Cip1}$ and $p27^{Kip1}$ and the member of the Ink4 family, $p16^{Ink4a}$ were expressed at low levels in undifferentiated cells but increased as differentiation proceeded. The retinoblastoma protein 1 (Rb1) was hyperphosphorylated, and thus inactive, in undifferentiated hESC, but was active again with differentiation. Interestingly, p53 was expressed at high levels in undifferentiated cells and seemed to decrease with differentiation.

All these results are in agreement with the atypical cell cycle structure observed in undifferentiated hESC, with a high percentage of cells in S phase and low in $G_0/_1$ phase that changes with differentiation. These results are also very similar to those obtained in mESC, however it is interesting to note the noticeable increases of cyclins D_1 and E during differentiation in hESC.

In summary, the cell cycle protein profile changes during differentiation. These observations made us think that maybe some of the proteins could have an effect in the properties of hESC, or this change upon differentiation was responding to the specific differentiation protocol.

With the aim of finding out if the protein changes were conserved along different differentiation protocols, or, on the contrary, there were differences in cell cycle regulators depending on the differentiation protocol used, we carried out a neuronal differentiation protocol. Protein samples were collected after 15 and 30 days of differentiation (Figures 16 and 17).

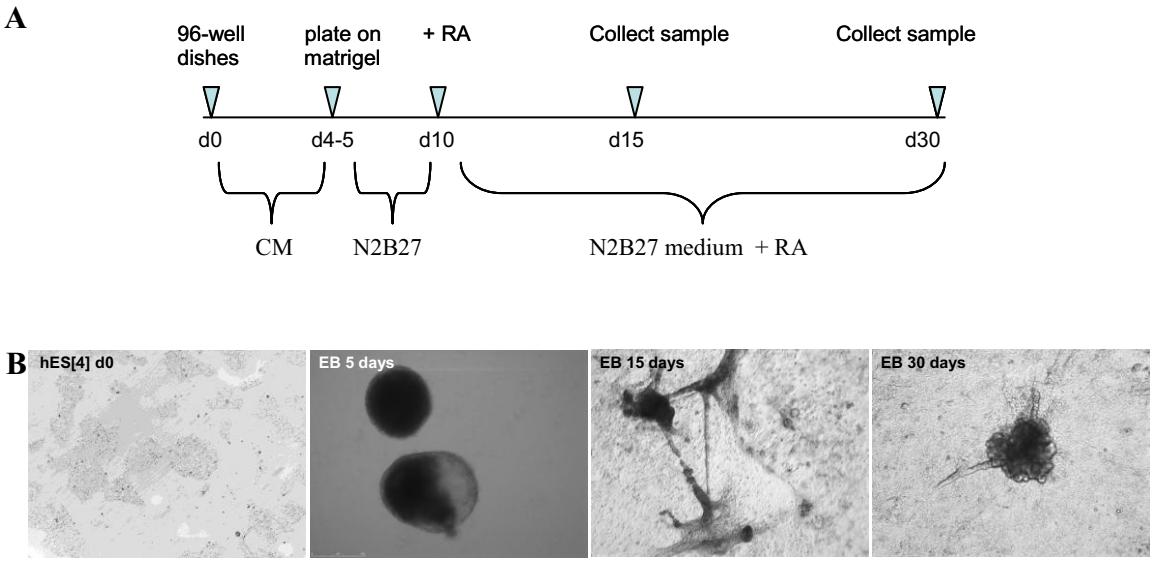

Figure 16. Neuronal differentiation protocol of human embryonic stem cells (**A**) Timeline of neuronal differentiation protocol. Embryoid bodies (EB) were generated by the same procedure as for general differentiation, but for the neuronal differentiation EB were plated on matrigel with neuronal inducing medium N2B27 for 6 days. After this time had elapsed, retinoic acid (RA) was added to the medium. CM, conditioned medium. (**B**) Representative phase contrast images of undifferentiated colonies of hESC, EB cultured in suspension, and after plating them on matrigel with neuronal medium containing RA. Scale bars: 250 and 500μm.

Differentiation was monitored by assessment of Oct3/4 protein expression levels. The reduction of this protein during differentiation confirmed that the cells were differentiated.

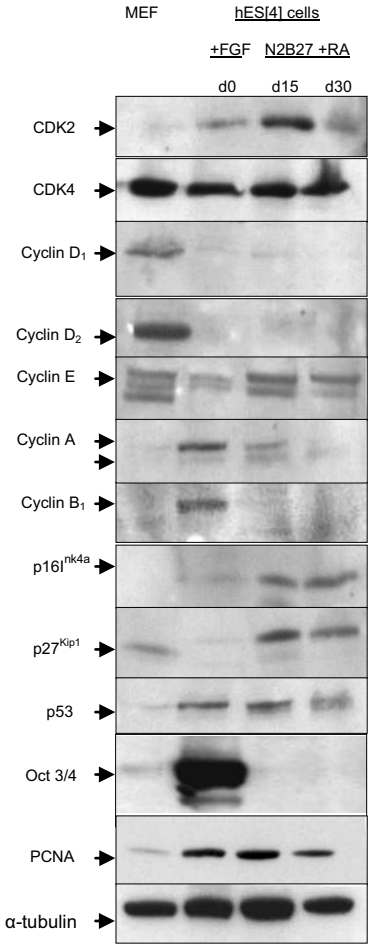

Figure 17. Cell cycle proteins profile of human embryonic stem cells changes during neuronal differentiation. Western blot analysis of several cell cycle regulators in undifferentiated hES[4] (day 0), and after guided neuronal differentiation (day 15 and 30). Twenty micrograms of protein from whole cell extracts were used. α-tubulin was used as a loading control. PCNA, proliferating cell nuclear antigen.

Protein expression analyses revealed a high level of the S and M phase cyclins A and B_1 in undifferentiated hESC that dropped as differentiation proceeded. Interestingly, cyclin E and CDK2 appeared to increase with differentiation. G_1 phase associated cyclins D_1 and D_2 were absent in pluripotent hESC, and, contrary to the general differentiation, cyclin D_1 did not increase during neuronal differentiation. CDK4, however, seemed to be constantly expressed along differentiation. PCNA decreased with differentiation. The CKI member of the Cip/Kip family $p27^{Kip1}$, and the CKI member of the Ink4 family, $p16^{Ink4a}$ were expressed at low levels in undifferentiated cells but increased during differentiation, similarly to the results obtained with the general differentiation protocol. Finally, p53 was expressed at high levels in

undifferentiated cells and experimented a slight decrease with differentiation, as previously shown for general differentiation protocol.

General differentiation

	d0	d15	d30
CDK2	++	++	+
CDK4	+++	+++	+++
Cyclin D_1	+	++	++
Cyclin D_2	+	++	++
Cyclin E	+	++	++
Cyclin A	+++	ND	ND
Cyclin B_1	+++	ND	ND
p16	ND	+	+++
$p21^{Cip1}$	ND	+	++
$p27^{Kip1}$	+	++	++
p53	+++	+++	+++/++
p107	+	+	++
pRb	++ / (hyperphospho)	+ (hypophospho)	+ (hypophospho)
Oct 4	+++	+	ND
PCNA	++	+	+
MCM2	+++	+	+

Neuronal differentiation

	d0	d15	d30
CDK2	+	+/++	+/++
CDK4	+++	+++	+++
Cyclin D_1	+	+	+
Cyclin D_2	ND	ND	ND
Cyclin E	+	+/++	+/++
Cyclin A	+++	++	+
Cyclin B_1	+++	ND	ND
$p16^{INK4a}$	+	+++	+++
$p27^{Kip1}$	+	+++	+++
p53	++	++	+
Oct3/4	+++	ND	ND
PCNA	++	++	+

\+ Low
++ Medium
+++ High
ND: Not Detectable

Table 2. Summary tables of cell cycle proteins profiles during differentiation. Summary tables of Western blot analyses for cell cycle regulators during differentiation using two different protocols in hES[4].

In summary, from these experiments we can extract interesting conclusions. Undifferentiated hESC have an atypical cell cycle structure consisting of a low proportion of cells in $G_0/_1$ phase and a high proportion of cells in S phase. This atypical cell cycle structure changes to that observed in normal somatic cells upon differentiation.

This cell cycle change is paralleled by changes in the proteins profile (Table 2). In general, the S and M phase cyclins A and B_1 are expressed at high levels in undifferentiated cells but decrease with differentiation, independently of the differentiation protocol used. On the contrary, G_1 phase associated cyclins D_1 and D_2 were absent or very low expressed in pluripotent hESC and, contrary to the general differentiation, cyclin D_1 did not increase noticeable during neuronal differentiation. This may suggest that cyclin D_1 could be involved in the differentiation of specific cell lineages according to previous work reporting that D-type cyclins are able to modulate differentiation programs (Coqueret 2002). Thus, it would appear in some kind of tissues and not in others. Interestingly, cyclin E seemed to increase with differentiation in both differentiation protocols. The CKIs $p16^{Ink4a}$ and $p27^{Kip1}$ appeared expressed at low

levels in undifferentiated cells but increased during differentiation, independently of the differentiation protocol used. It is interesting to note that the increase of $p27^{Kip1}$ during differentiation was higher in the neuronal differentiation protocol. This result could suggest that $p27^{Kip1}$ might be involved in the differentiation towards neuronal cell lineages.

Given that pluripotent cells shared a common cell cycle structure profile we hypothesized that they could be responsible for the properties of undifferentiated cells. We hypothesized that the proteins increasing during differentiation were responsible for the change in the pluripotency and self-renewal properties of ESC and, moreover, were implicated in the differentiation towards specific lineages. On the other hand, those proteins that dissapear during differentiation could be responsible for the properties of ESC, but however we could not be able to study the early differentiation towards specific lineages.

We therefore decided to study $p27^{Kip1}$ in hESC given its increase during differentiation and its well established role in cell fate decisions (Movassagh and Philpott 2008; Nguyen, Besson et al. 2006; Vernon, Movassagh et al. 2006; Vernon, Devine et al. 2003; Vernon and Philpott 2003; Galderisi, Jori et al. 2003). We predicted that a low level of $p27^{Kip1}$ was a major factor influencing pluripotent cell cycle structure. With the aim of confirming this, the level of $p27^{Kip1}$ was analyzed by Western blot analysis in several pluripotent cell lines, including two hESC and two hiPSC lines, in undifferentiated cells and after differentiation (Figure 18).

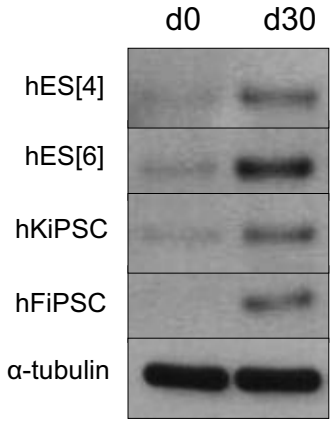

Figure 18. $p27^{Kip1}$ expression increases in human pluripotent cells upon differentiation. Western blot analysis of $p27^{Kip1}$ inhibitor in two different human embryonic stem cells (hESC) lines and two different human induced pluripotent stem cells (hiPSC) lines, in undifferentiated cells (day 0) and after differentiation (day 30), shows that its expression increases upon differentiation. Twenty micrograms of protein from whole cell extracts were used. α-tubulin was used as a loading control. hKiPSC, human keratinocytes induced pluripotent stem cells; hFiPSC, human fibroblast induced pluripotent stem cells.

Results showed that the expression of $p27^{Kip1}$ increased during differentiation in all cell lines analyzed, paralleling the changes in the cell cycle structure of an increase of G_1 phase. These results suggest that this protein may have a role in the establishment of a long G_1 phase, and consequently the induction or the maintenance of differentiation.

2. MOLECULAR REGULATION OF $p27^{Kip1}$ IN HUMAN EMBRYONIC STEM CELLS

The expression level of $p27^{Kip1}$ was low in undifferentiated conditions but increased during the differentiation in several pluripotent cell lines. This suggested that to maintain the pluripotency and self-renewal properties of undifferentiated cells, the expression levels of this protein had to be low. However, after induction of differentiation the protein levels increased, as the cell cycle structure changed. This suggested that the increase in $p27^{Kip1}$ may contribute to this change. It is not clear how the cell makes the transition from a proliferative state to the other.

With the aim of shedding light on this issue, our next question was to discover the molecular mechanisms that were regulating $p27^{Kip1}$ expression in human embryonic stem cells (hESC). In order to see if $p27^{Kip1}$ was regulated at the transcriptional level, messenger RNA (mRNA) expression levels in undifferentiated and differentiated cells were analyzed by quantitative Reverse Transcription Polymerase Chain Reaction (qRT-PCR) analysis (Figure 19A). Differentiation was carried out by embryoid bodies (EB) generation and subsequent growth on gelatin with general differentiation medium. Cell samples were taken after 30 days. The mRNA expression levels of Oct3/4 were also analyzed to monitor differentiation (Figure 19B).

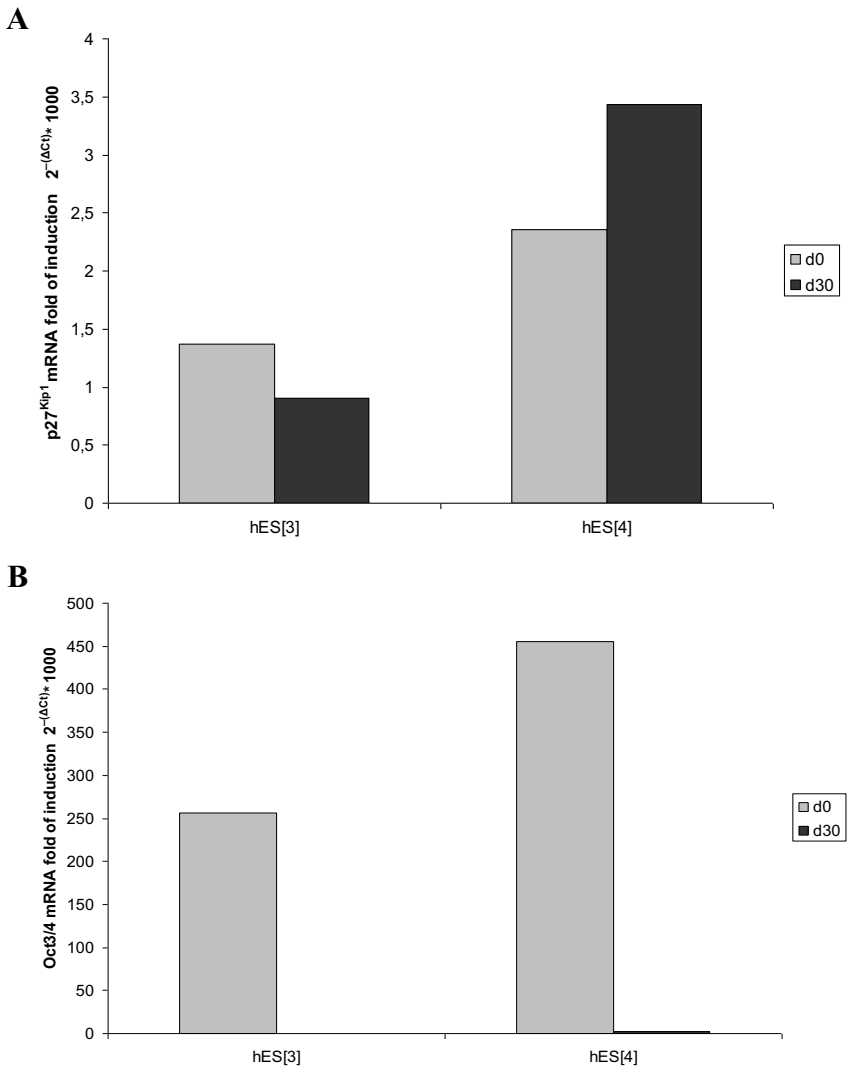

Figure 19. Expression profiles of $p27^{Kip1}$ and Oct3/4 mRNA levels upon differentiation in human embryonic stem cells. (**A**) Expression profile of $p27^{Kip1}$ mRNA upon differentiation in two human embryonic stem cells (hESC) lines: hES[3] and hES[4] was assessed by qRT-PCR analysis. Differentiation was carried out by embryoid bodies (EB) generation. After 4 days in hESC medium, EB were plated on gelatin with general differentiation medium containing 20% fetal bovine serum (FBS) without bFGF for 30 days. (**B**) Expression profile of Oct3/4 mRNA upon differentiation in hES[3] and hES[4] was assessed by qRT-PCR analysis. Relative mRNA expression levels were calculated using the comparative threshold cycle method relative to human GAPDH and multiplied by 1000 to simplify data presentation.

Results showed that $p27^{Kip1}$ mRNA expression levels did not vary significantly after differentiation, while those of Oct3/4 underwent a striking decrease. This suggested that $p27^{Kip1}$ was being regulated at the post-transcriptional level in hESC. Two types of $p27^{Kip1}$ regulation have emerged as prominent modes of post-transcriptional control involving regulation by the proteasome and by microRNAs (miRNA) (le Sage, Nagel et al. 2007). We decided to investigate if $p27^{Kip1}$ was being regulated by any of these pathways. We started to investigate the miRNA pathway in hESC given that recently different reports have identified miRNAs 221 (miR-221) and

miRNAs 222 (miR-222) as regulators of $p27^{Kip1}$ in cell lines derived from glioblastoma, melanoma, hepatocellular carcinoma, papillary thyroid carcinoma, and prostate carcinoma (Pineau, Volinia et al. 2010; Fornari, Gramantieri et al. 2008; Mercatelli, Coppola et al. 2008; le Sage, Nagel et al. 2007; Galardi, Mercatelli et al. 2007). However, other miRNAs could be involved in the regulation of $p27^{Kip1}$ given that microRNAs 181 (miR-181) have been found to regulate the translation of $p27^{Kip1}$ in human myeloid leukemia cells (Wang, Gocek et al. 2009; Cuesta, Martinez-Sanchez et al. 2009).

Potential miRNA target sites along the 3' untranslated region (UTR) of human $p27^{Kip1}$ mRNA were analyzed *in silico* using Target Scan Release 5.1 (http://www.targetscan.org) (Figure 20).

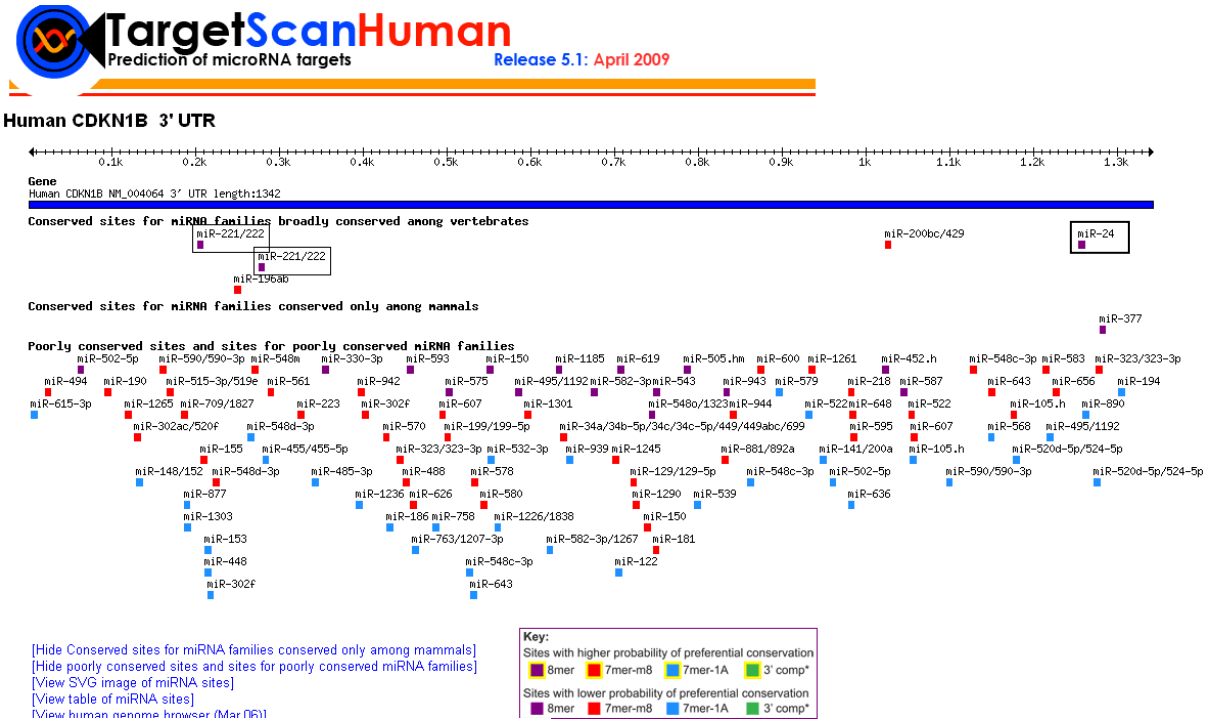

Figure 20. Analysis *in silico* of putative miRNA families targeting the 3' UTR of human $p27^{Kip1}$. Potential miRNA target sites were generated by an algorithm-based prediction method TargetScan. Sites with different probability of preferential conservation are represented by different colours. Conserved sites for miRNA families broadly conserved among vertebrates, miRNA families conserved only among mammals, and poorly conserved miRNA families are also shown.

The results showed many potential target sites for several miRNA families, but with different probabilities. We chose those that were broadly conserved among vertebrates, and among those, two families that showed higher probability of preferential conservation: miR-221/222, in agreement with previous studies, and miR-24 (Figure 21).

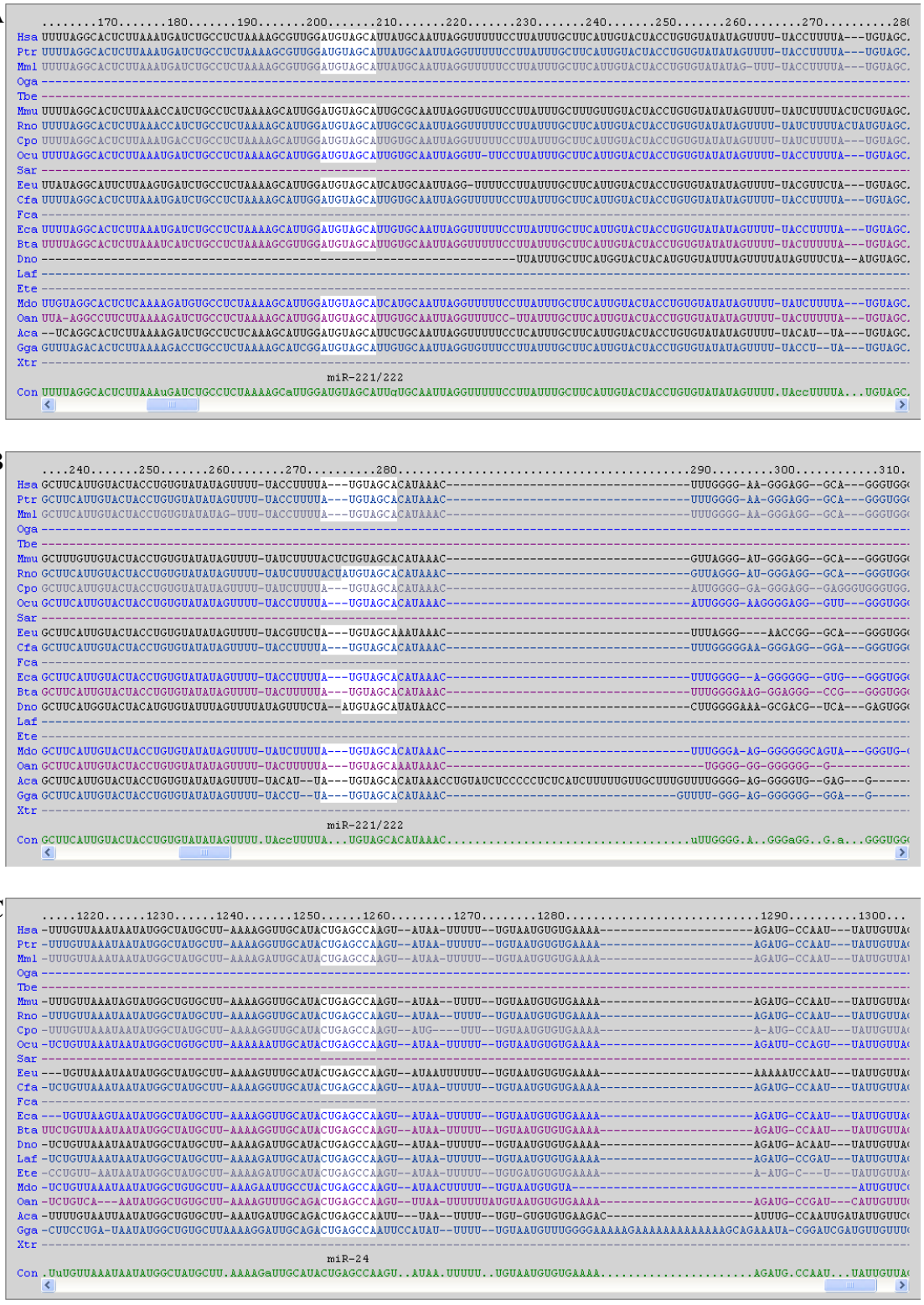

Figure 21. miR-221/222 and miR-24 families present sites with higher probability of preferential conservation in the 3' UTR of p27^{Kip1} and are broadly conserved among vertebrates. (**A**, **B**) The 3' UTR of p27^{Kip1} contain two sites expected to be recognized by both miR-221 and miR-222. (**C**) The 3' UTR of p27^{Kip1} contain one site expected to be recognized by miR-24. *Hs*, Human; *Ptr*, Chimpanzee; *Mml*, Rhesus; *Oga*, Bushbaby; *Tbe*, Treeshrew; *Mmu*, Mouse; *Rno*, Rat; *Cpo*, Guinea pig; *Ocu*, Rabbit; *Sar*, Shrew; *Eeu*, Hedgehog; *Cfa*, Dog; *Fca*, Cat; *Eca*, Horse; *Bta*, Cow; *Dno*, Armadillo; *Laf*, Elephant; *Ete*, Tenrec; *Mdo*, Opossum; *Oan*, Platypus; *Aca*, Lizard; *Gga*, Chicken; *Xtr*, Frog.

Two miR-221/222 target sites were predicted in the 3' UTR of human $p27^{Kip1}$, located at positions 202 to 208, and 275 to 281. One miR-24 target site was predicted at position 1254 to 1260 (Figure 22).

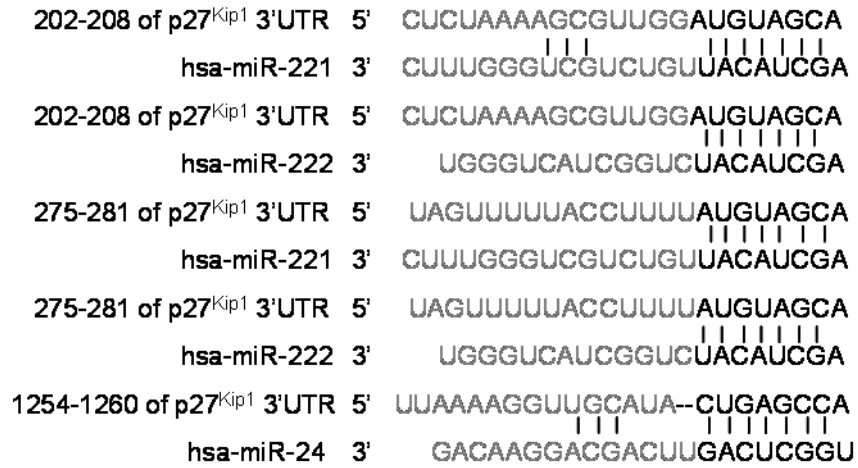

Figure 22. Schematic representation of the two miR-221 and miR-222 target sites, and the miR-24 target site located in the 3'UTR of human $p27^{Kip1}$. Numbers indicate the positions of miRNA binding sites in the 3'UTR of human $p27^{Kip1}$ mRNA. |, Watson-Crick pairing.

Based on these data, we proceeded to investigate whether any of these miRNAs were responsible for regulation of $p27^{Kip1}$ in hESC. We hypothesized that if any of these miRNAs was regulating $p27^{Kip1}$ we should see a change in their expression with differentiation. With the aim of finding this out, we proceeded to analyze the expression levels of these miRNAs during differentiation by qRT-PCR analysis.

Small RNAs were isolated using a commercial kit, *mir*Vana™ miRNA Isolation Kit (Applied Biosystems). The expression of mature miR-24, miR-221, and miR-222 was analyzed in undifferentiated hES[4] and differentiated cells after 30 days of culture in general differentiation medium, by qRT-PCR analysis, with purchased mature miRNA primers specific for human miR-24, miR-221, and miR-222 (Applied Biosystems) (Figure 23).

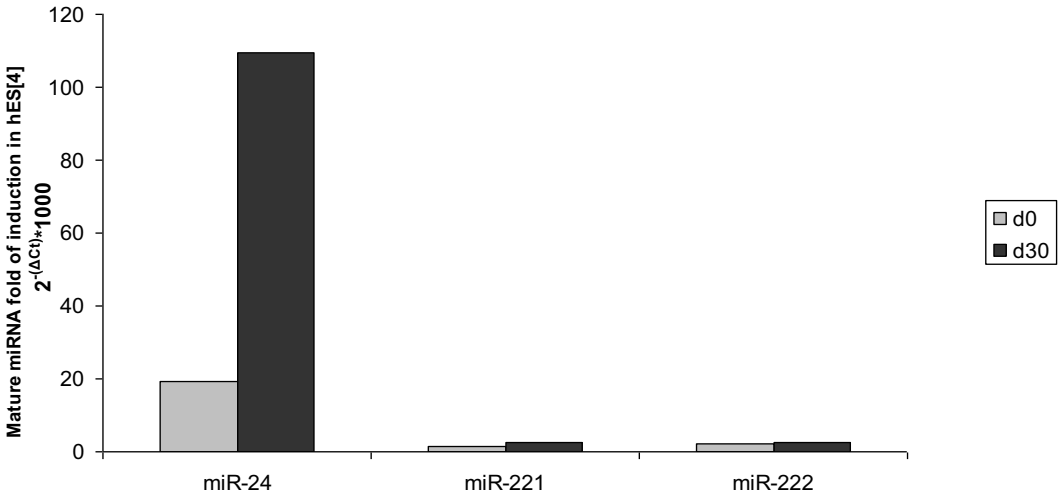

Figure 23. Expression profiles of mature human miR-24, miR-221, and miR-222 in undifferentiated hES[4] and differentiated cells after 30 days of culture in general differentiation medium. Relative miRNA expression levels were analyzed by qRT-PCR analysis, and calculated using the comparative threshold cycle method relative to human U6 snRNA and multiplied by 1000 to simplify data presentation.

Results showed a striking increase in mature miR-24 after differentiation, however we could not detect a significant change in the expression levels of mature miR-221 or miR-222 after differentiation in hESC.

Given that several miRNAs have tissue-specific expression, we repeated the same experiment but with another differentiation protocol towards neuronal cells in order to see if the expression of miRNAs changed depending on the cell type (Figure 24).

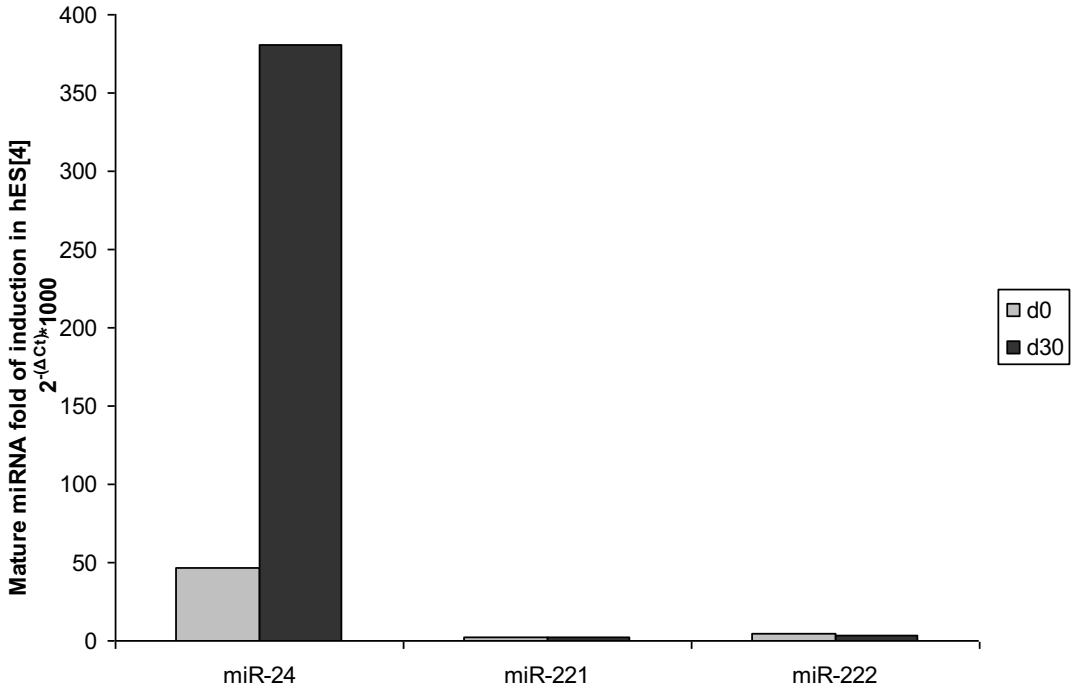

Figure 24. Expression profiles of mature human miR-24, miR-221, and miR-222 in undifferentiated hES[4] and differentiated cells after culture for 30 days in neuronal differentiation medium. Relative miRNA expression levels were analyzed by qRT-PCR analysis, and calculated using the comparative threshold cycle method relative to human U6 snRNA and multiplied by 1000 to simplify data presentation.

Results again showed a striking increase of miR-24 after 30 days of culture in neuronal differentiation medium, even higher than that observed with the general differentiation medium. miR-24 increased 8.14 times after neuronal differentiation, while with the general differentiation protocol the increase after differentiation was 5.64 times. We did not detect any change in the expression levels of human miR-221 or miR-222 after the differentiation of hESC.

Given that miR-24 increased after differentiation paralleling the increase of $p27^{Kip1}$ protein, we hypothesized that miR-24 was involved in the regulation of $p27^{Kip1}$ in hESC. miR-24 could be directly increasing the levels of $p27^{Kip1}$, or indirectly regulating a negative regulator of $p27^{Kip1}$. With the aim of confirming whether miR-24 could be regulating $p27^{Kip1}$ protein levels during differentiation, we proceeded to inhibit miR-24 expression in hESC and subsequently measure $p27^{Kip1}$ protein levels. Given that $p27^{Kip1}$ and miR-24 expression increased after differentiation, miR-24 was inhibited in differentiated cells.

RNA oligonucleotides specifically designed to bind to and inhibit endogenous miR-24 molecules, Ambion® Anti-miR™ miRNA Inhibitors were purchased from Ambion.

For the optimization of transfection conditions, commercial Cy™3 dye-labeled Anti-miR Negative Control, containing a random sequence anti-miR molecule not able to produce identifiable effects on known miRNA functions, and with a fluorescent moiety on the 5' end of the oligonucleotide, was used as a negative control. Cy3 dye-labeled Anti-miR Negative Control oligos were used for monitoring transfection efficiency during optimization of transfection conditions and were transfected with FuGENE 6 Transfection Reagent (Roche Diagnostics).

For the optimization of transfection conditions, cells were incubated in 2 mL of medium containing Cy3 dye-labeled Anti-miR Negative Control oligos at a final concentrations of 50 nM or 100 nM and mixed with different ratios of FuGENE 6 Transfection Reagent: oligo (3:1) or (6:1) (Table 3).

Condition	Ratio FuGENE:DNA	Oligo (nM)	Volume of complex (µL)	Total volume of medium (mL)
1	3:1	50	100	2
2	3:1	100	100	2
3	6:1	50	100	2
4	6:1	100	100	2

Table 3. Summary table with the conditions used for optimization of transfection of Cy3 dye-labeled Anti-miR Negative Control. Table showing the concentrations of oligo (Cy3 dye-labeled Anti-miR Negative Control) and ratios of Tranfection Reagent: oligo used in the optimization of conditions for transfection.

The percentage of transfection using the different conditions depicted in Table 3 was monitored by fluorescence microscopy images. The fluorescence intensity and the time that the Cy3 dye-labeled Anti-miR Negative Control oligos were able to remain inside the cells were also monitored by fluorescence microscopy images after 2, 5, and 14 days of transfection (Figure 25).

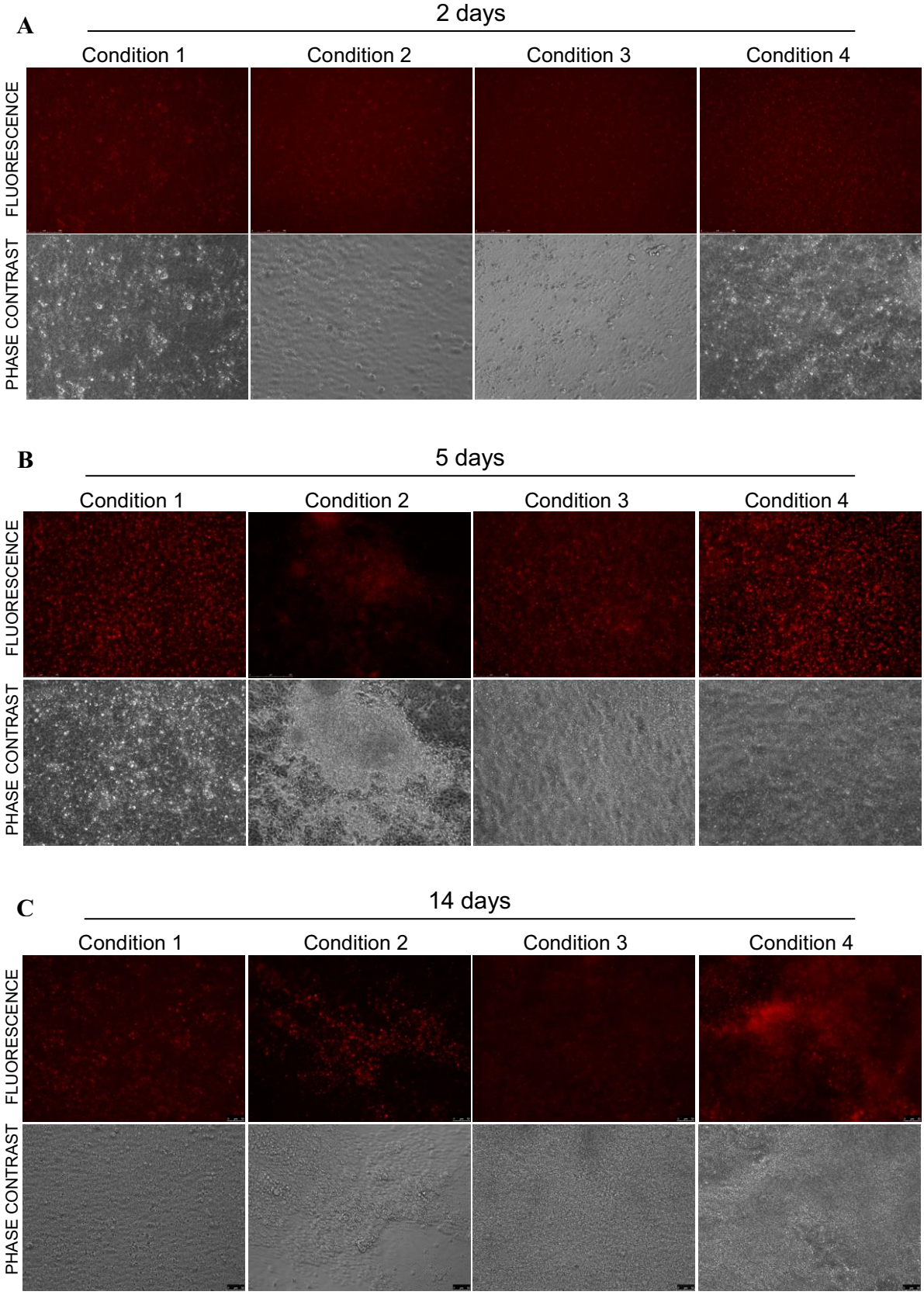

Figure 25. Optimization of transfection conditions. Transfection efficiency of Cy3 dye-labeled Anti-miR Negative Control was monitored by fluorescence microscopy images. Representative fluorescence and phase contrast microscopy images of the various transfection conditions depicted in Table 3, after (**A**) 2 days, (**B**) 5 days, and (**C**) 14 days of transfection in hES[4]. Scale bars: (**A**, **B**) 100 µm. (**C**) 50 µm.

Results showed that cells expressing fluorescence, that is to say, transfected cells were still detectable after 14 days of transfection. However, after 14 days the fluorescence intensity had decreased markedly.

We also observed that, in all cases, the condition with the highest percentage of transfection was the condition 4, when a final concentration of 100 nM of oligo and a ratio of FuGENE: oligo 6:1 were used. We then, applied the same conditions for transfecting cells with Anti-miR-24 miRNA Inhibitor.

To confirm that the cells were effectively transfected, a Z-Stack Scanning experiment was performed with a differentiated cystic EB generated from hESC (Figure 26). This EB was transfected with Cy3 dye-labeled Anti-miR Negative Control oligo at a final concentration of 100 nM and mixed with a ratio of FuGENE: oligo 6:1.

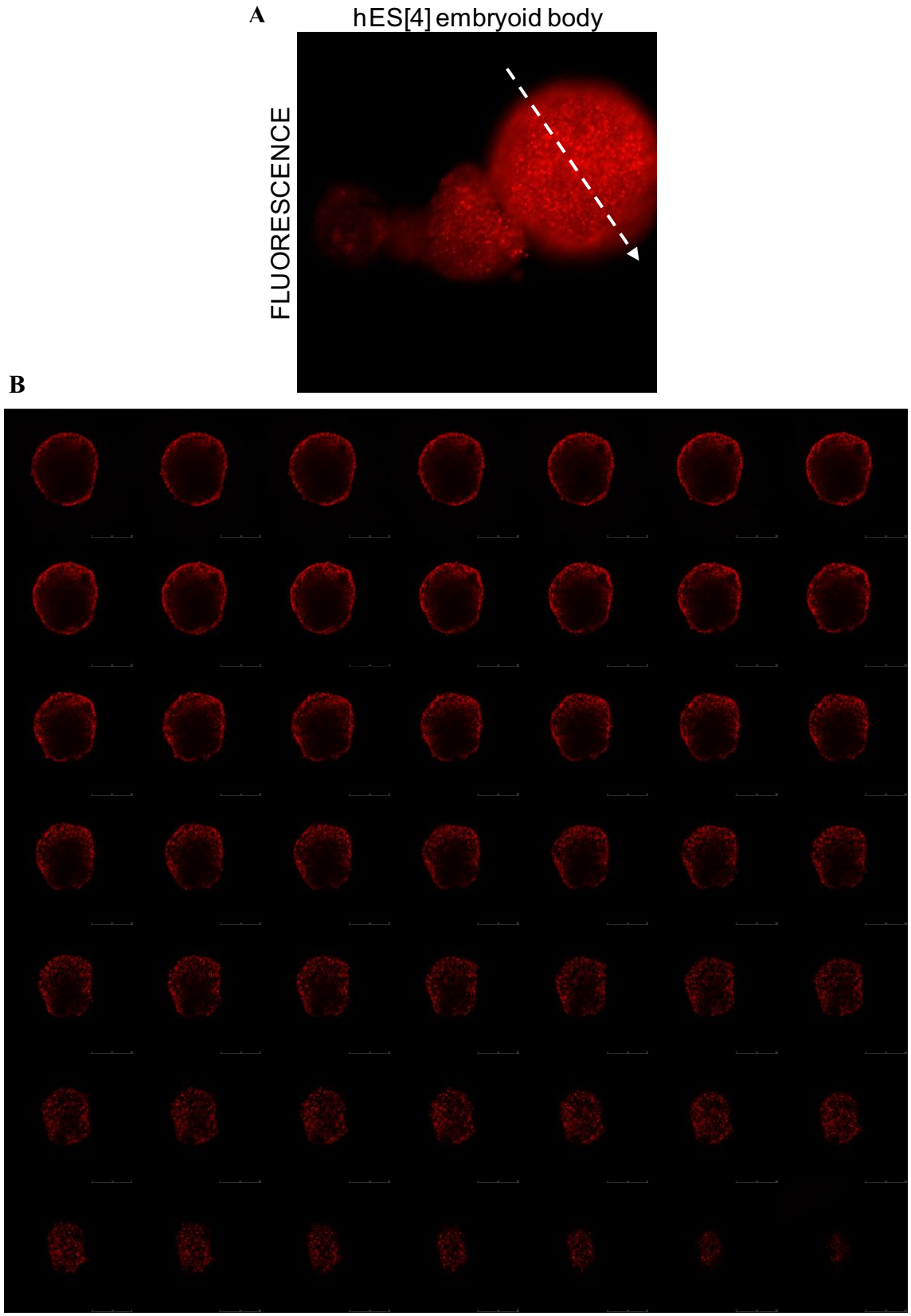

Figure 26. Z-Stack Scanning analysis. (**A**) Dorsal view of three-dimensional projection of Z-Stack Scanning fluorescence images of a cystic embryoid body (EB) transfected with Cy3 dye-labeled Anti-miR Negative Control oligos. (**B**) Fluorescence microscopy images of transverse sections taken at the level of the dotted lines of a cystic EB transfected with Cy3 dye-labeled Anti-miR Negative Control oligos. Images were taken with 1 µm of thickness. Scale bars: 250 µm.

Z-Stack Scanning analysis showed fluorescence in the different confocal planes, therefore demonstrating that these cells were successfully transfected.

After optimizating the transfection conditions, we applied these same conditions for transfecting hES[4] with Anti-miR-24 miRNA Inhibitor. To this end, we let EB generated from hES[4] to differentiate for several days. Then, we tranfected them with 100 nM of Anti-miR-24 miRNA Inhibitor oligo with a ratio of FuGENE: oligo 6:1. The same procedure, but tranfecting cells with Cy3 dye-labeled Anti-miR Negative Control oligo, was carried out as a negative control (Figure 27).

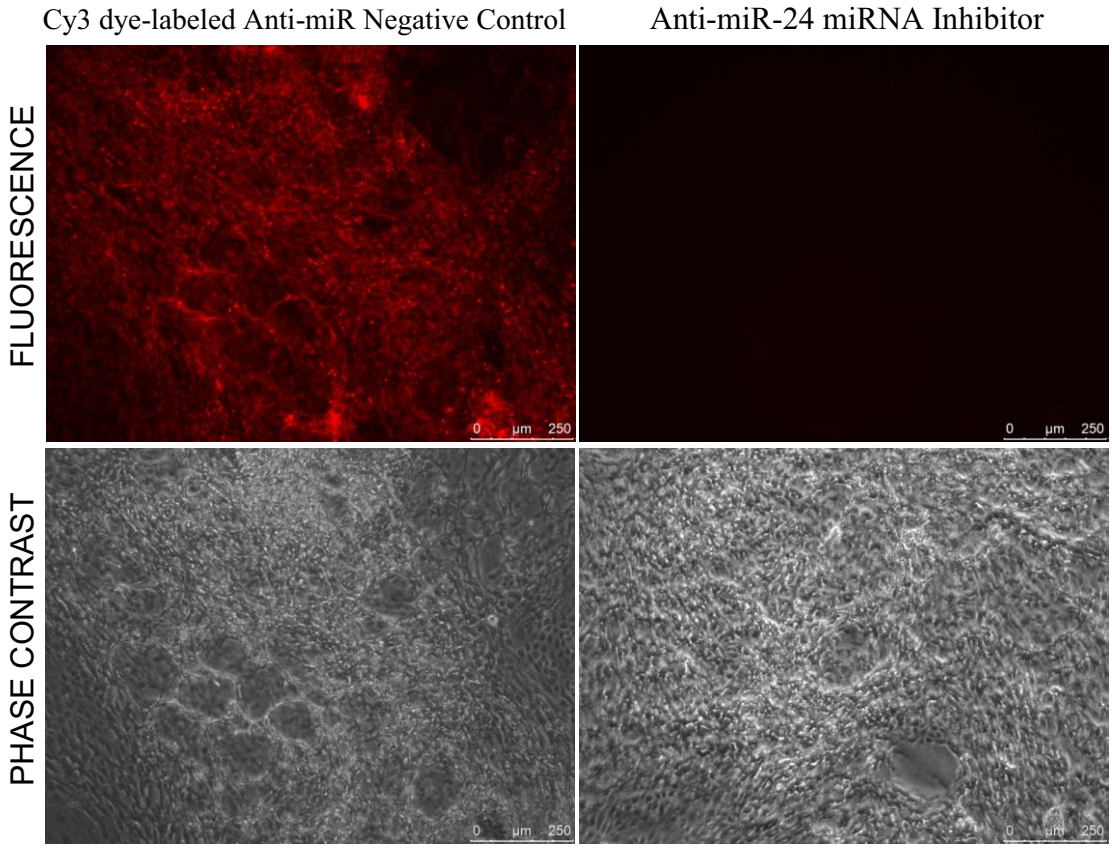

Figure 27. Morphology of differentiated human embryonic stem cells transfected with Anti-miR-24 miRNA Inhibitor or Cy3 dye-labeled Anti-miR Negative Control oligos. Representative fluorescence and phase contrast microscopy images of differentiated hES[4] three days post-transfection with Anti-miR-24 miRNA Inhibitor or Cy3 dye-labeled Anti-miR Negative Control oligos. Red fluorescence intensity in the control cells demonstrated that they were effectively transfected. Scale bars: 250 µm.

Fluorescence microscopy images of differentiated hESC transfected with Cy3 dye-labeled Anti-miR Negative Control oligos, after 3 days of transfection, revealed a high percentage of transfection demonstrating that cells were effectively transfected.

We did not observe any difference in the morphology of cells transfected with either Anti-miR-24 miRNA Inhibitor or Cy3 dye-labeled Anti-miR Negative Control oligos, but we observed an increase in the proliferation of cells transfected with Anti-miR-24 miRNA Inhibitor.

After 3 or 4 days post-transfection, we took whole cell extracts to analyze the expression levels of $p27^{Kip1}$ by Western blot analysis. As $p27^{Kip1}$ protein increased after differentiation, cells were let to differentiate for 11 and 14 days, in case $p27^{Kip1}$ would not be present in appreciable quantities at 11 days (Figure 28).

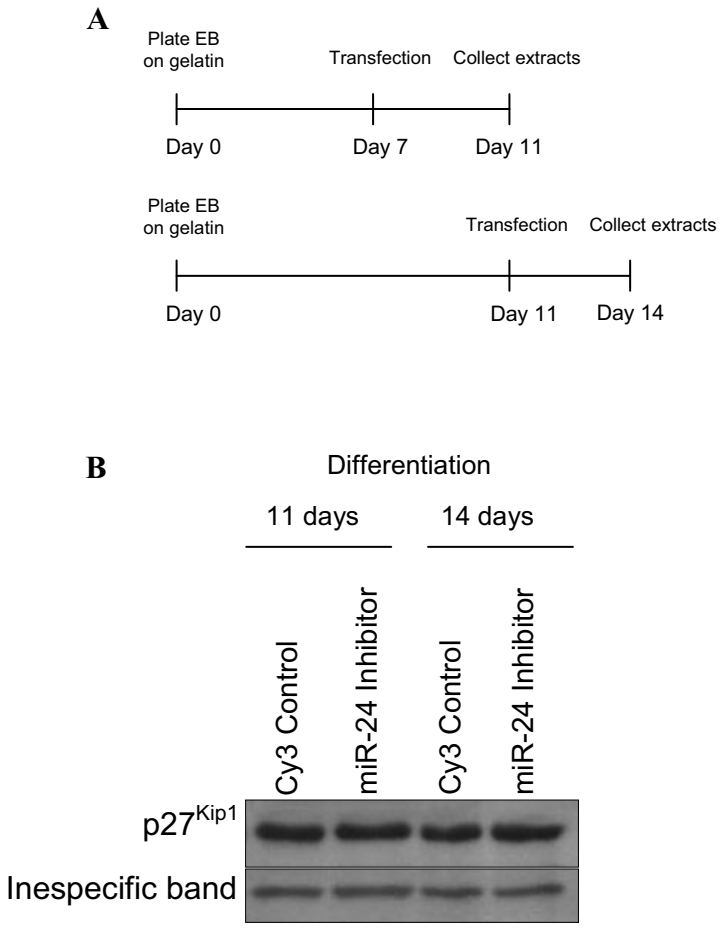

Figure 28. $p27^{Kip1}$ expression analysis after inhibition of miR-24 in human embryonic stem cells. (**A**) Timeline of miR-24 functional analysis. hES[4] were differentiated by EB generation and seeded on gelatin for seven days. After this time had elapsed, cells were tranfected with either Anti-miR-24 miRNA Inhibitor or Cy3 dye-labeled Anti-miR Negative Control oligos, and 4 days later protein lysates collected. Alternatively, hES[4] were differentiated by EB generation and seeded on gelatin hESC for eleven days. After these days, cells were transfected with either Anti-miR-24 miRNA Inhibitor or Cy3 dye-labeled Anti-miR Negative Control oligos, and three days later, protein lysates collected. (**B**) Western blot analysis of $p27^{Kip1}$ expression in differentiated hES[4] after transfection with either Anti-miR-24 miRNA Inhibitor or Cy3 dye-labeled Anti-miR Negative Control oligos following the timeline depicted in (**A**). Twenty-five micrograms of total protein from whole cell extracts were used.

Results did not show any difference in the expression levels of $p27^{Kip1}$ when miR-24 was inhibited, suggesting that $p27^{Kip1}$ was not regulated by miR-24 in hESC (Figure 28B).

Another prominent type of $p27^{Kip1}$ regulation involves the regulation by the proteasome. We next proceeded to investigate if $p27^{Kip1}$ was being regulated by the proteasome in hESC. We first, analyzed $p27^{Kip1}$ half-life by treating the cells with cycloheximide in a time-course experiment followed by Western blotting for $p27^{Kip1}$ of the cell lysates. Cycloheximide is an inhibitor of protein biosynthesis in eukaryotic organisms and can be used to determine the half-life of a protein. We cultured hESC for 1, 3, 6, or 8 hours in the presence of cycloheximide. Control cells were left untreated. We observed, after 1 hour of culture with cycloheximide, a marginal decrease of $p27^{Kip1}$ compared with the control, by Western blot analysis. However, after 3 hours of culture with cycloheximide, we observed more than a half of reduction in the expression of $p27^{Kip1}$ as compared with the control (Figure 29).

With the aim of checking if $p27^{Kip1}$ was being regulated by the proteasome we cultured hESC in the presence of cycloheximide, to inhibit completely "de novo" synthesis of $p27^{Kip1}$, in combination with non-specific proteasome activity inhibitor: MG-132 (carbobenzoxy-L-leucyl-L-leucinal) for 8 hours before harvesting. The cells were lysed and immunoblotted with an antibody against $p27^{Kip1}$ (Figure 29).

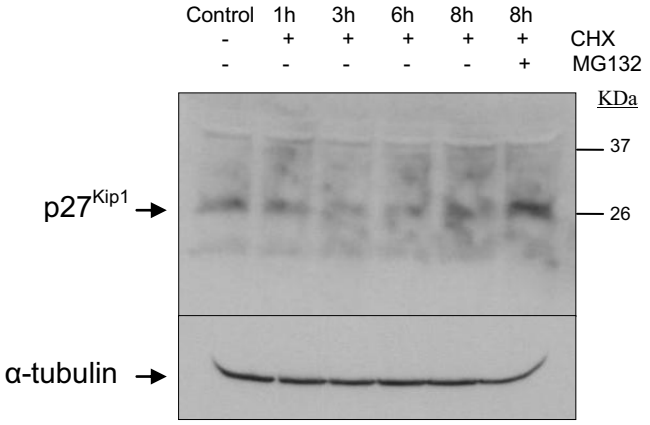

Figure 29. $p27^{Kip1}$ protein expression increases after treatment with an inhibitor of the proteasome activity: MG-132 in human embryonic stem cells. hES[4] were treated with cycloheximide (CHX), an inhibitor of protein biosynthesis for 1, 3, 6, or 8 hours for protein stability analysis. To inhibit proteasome function, cells were exposed to a non-specific proteasome activity inhibitor: MG-132 for 8 hours. The first lane corresponds to untreated hES[4], used as controls. Whole cell extracts were prepared and analyzed by immunoblot with $p27^{Kip1}$ and control α-tubulin antibodies. The position of molecular weight markers is shown in the right. KDa, Kilodaltons.

Results showed that after culture with MG-132 and cycloheximide, the expression of $p27^{Kip1}$ increased above the expression levels of control cells. This demonstrates that $p27^{Kip1}$ is being regulated by the proteasome pathway in hESC consistent with previous work reporting a role for the ubiquitin ligase Skp2 in the regulation of $p27^{Kip1}$ in hESC (Egozi, Shapira et al. 2007), although in that study they did not perform functional analysis.

Taken together these results suggest that $p27^{Kip1}$ is being regulated by the proteasome pathway in hESC. Thus, high proteasome activity in undifferentiated cells is responsible for the low $p27^{Kip1}$ levels and high proliferation rates. We have not find evidence of regulation of $p27^{Kip1}$ by miR-24, miR-221, or miR-222 in hESC. However, we have shown an important increase of miR-24 after differentiation which is even more evident with neuronal differentiation, suggesting a role for this miRNA in differentiation via other gene targets.

3. $p27^{Kip1}$ CONTROLS SELF-RENEWAL OF HUMAN EMBRYONIC STEM CELLS BY REGULATING THE CELL CYCLE AND CELL MORPHOLOGY

Our results have demonstrated that undifferentiated pluripotent cells from mouse or human share an unorthodox cell cycle structure consisting of a low proportion of cells in $G_0/_1$ phase and a high proportion of cells in S phase.

This cell cycle structure changes to that observed in normal somatic cells upon differentiation. This suggested that this atypical cell cycle structure could be responsible for the properties of undifferentiated cells. This cell cycle change, upon differentiation, is paralleled by changes in cell cycle proteins profile. Thus, the drivers of this atypical cell cycle structure in undifferentiated cells which changes upon differentiation, could be cell cycle proteins. We hypothesized that cell cycle proteins increasing during differentiation could be responsible for the restriction in the pluripotency and self-renewal properties of embryonic stem cells (ESC) upon differentiation, and maybe, could be implicated in the differentiation towards specific lineages.

The cyclin dependent kinase inhibitor (CKI) $p27^{Kip1}$ was lowly expressed in undifferentiated cells, but increased during differentiation paralleling the changes in the cell cycle structure of an increase of G_1 phase. Moreover, the low levels of this CKI in undifferentiated cells appeared to be a consequence of a high activity of the proteasome. We then hypothesized that low levels of this protein were important for maintaining the properties of undifferentiated cells, and for avoiding the differentiation. With the aim of finding this out, we proceeded to study $p27^{Kip1}$ at the functional level, and therefore to upregulate and downregulate its expression in hESC and see how could affect their properties.

To overexpress $p27^{Kip1}$ in hESC, the human $p27^{Kip1}$ coding sequence was amplified by Polymerase Chain Reaction (PCR) (Figure 30A). Subsequently, this product was sequenced to confirm that it did not present mutations, and finally it was inserted into a doxycycline TET OFF regulated lentiviral vector (pCCL TET OFF) (Figure 30B). In this system, the transcription of $p27^{Kip1}$ was minimal in presence of doxycycline and was induced by its withdrawal (Figure 30C).

A

```
>gi|17978497|ref|NM_004064.2| Homo sapiens cyclin-dependent kinase inhibitor 1B (p27, Kip1)
(CDKN1B), mRNA
Length=2422

 GENE ID: 1027 CDKN1B | cyclin-dependent kinase inhibitor 1B (p27, Kip1)
[Homo sapiens] (Over 100 PubMed links)

 Score =  648 bits (327),  Expect = 0.0
 Identities = 333/335 (99%), Gaps = 0/335 (0%)
 Strand=Plus/Plus

Query  17    CTACAGACCCCCGCGGCCCCCCAAAGGTGCCTGCAAGGTGCCGGCGCAGGAGAGCCAGGA  76
             ||||||||||||||||||||||||||||||||||||||||||||||||||||||||||||
Sbjct  729   CTACAGACCCCCGCGGCCCCCCAAAGGTGCCTGCAAGGTGCCGGCGCAGGAGAGCCAGGA  788

Query  77    AGACAGCGGGAGCCGCCCGGCGGCGCCTTTAATTGGGGCTCCGGCTAACTCTGAGGACAC  136
              | ||||||||||||||||||||||||||||||||||||||||||||||||||||||||||
Sbjct  789   TGTCAGCGGGAGCCGCCCGGCGGCGCCTTTAATTGGGGCTCCGGCTAACTCTGAGGACAC  848

Query  137   GCATTTGGTGGACCCAAAGACTGATCCGTCGGACAGCCAGACGGGGTTAGCGGAGCAATG  196
             ||||||||||||||||||||||||||||||||||||||||||||||||||||||||||||
Sbjct  849   GCATTTGGTGGACCCAAAGACTGATCCGTCGGACAGCCAGACGGGGTTAGCGGAGCAATG  908

Query  197   CGCAGGAATAAGGAAGCGACCTGCAACCGACGATTCTTCTACTCAAAACAAAAGAGCCAA  256
             ||||||||||||||||||||||||||||||||||||||||||||||||||||||||||||
Sbjct  909   CGCAGGAATAAGGAAGCGACCTGCAACCGACGATTCTTCTACTCAAAACAAAAGAGCCAA  968

Query  257   CAGAACAGAAGAAAATGTTTCAGACGGTTCCCCAAATGCCGGTTCTGTGGAGCAGACGCC  316
             ||||||||||||||||||||||||||||||||||||||||||||||||||||||||||||
Sbjct  969   CAGAACAGAAGAAAATGTTTCAGACGGTTCCCCAAATGCCGGTTCTGTGGAGCAGACGCC  1028

Query  317   CAAGAAGCCTGGCCTCAGAAGACGTCAAACGTAAA  351
             ||||||||||||||||||||||||||||||||||||
Sbjct  1029  CAAGAAGCCTGGCCTCAGAAGACGTCAAACGTAAA  1063
```

B

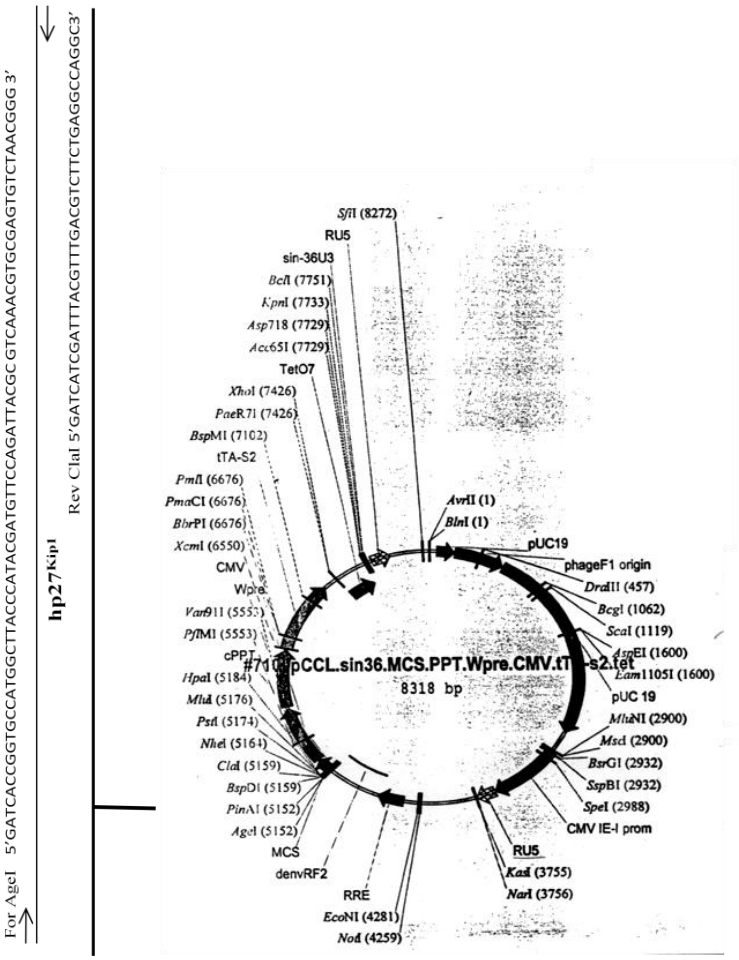

Figure 30. Doxycycline-regulated lentivirus-mediated overexpression of $p27^{Kip1}$ in human embryonic stem cells. (**A**) Nucleotide coding sequence of $p27^{Kip1}$ amplified by PCR and compared to sequence databases using the Basic Local Alignment Search Tool (BLAST) shows a complete match of the amplified $p27^{Kip1}$ with that of the databases. (**B**) Vector map of pCCL TET OFF regulated lentiviral vector showing the insertion site of p27cDNA into the restriction enzymes sites AgeI and ClaI. The primers used in the amplification of p27cDNA containing the restriction enzymes sites AgeI and ClaI are shown. (**C**) Diagram showing the TET OFF lentiviral system used to achieve doxycycline-regulated overexpression of $p27^{Kip1}$. When doxycycline is not present, the tetracycline transactivator (tTA) binds the tetR binding site ($tetO_7$) and turns on transcription of the p27cDNA. Addition of doxycycline inhibits the binding of tTA to $tetO_7$, and turns off the transcription of p27cDNA.

C

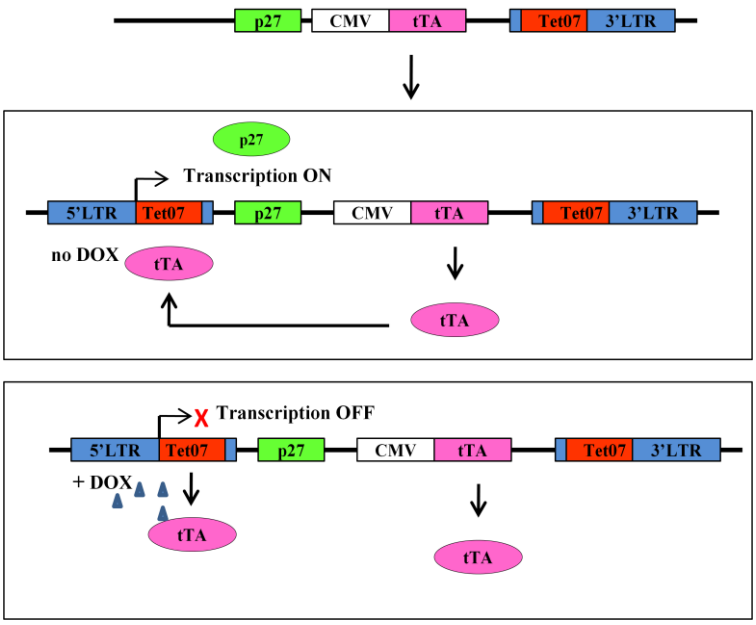

In the TET OFF lentiviral system used to achieve regulated $p27^{Kip1}$ expression, tetracycline transactivator (tTA) regulatory protein is transcribed from the CMV promoter. When doxycycline is not present, the tTA binds the tetR binding site ($tetO_7$) and turns on the transcription of $p27^{Kip1}$. Addition of doxycycline inhibits the transcription of $p27^{Kip1}$ because tTA is in its inactive conformation and does not bind $tetO_7$ (Figure 30C).

Gene delivery was performed by lentiviral transduction given that lentiviruses are one of the most efficient methods for delivering genetic information into the DNA of a host cell. Lentiviruses were independently produced by transfecting the cell line 293T with packaging and envelope vectors using a third generation approach.

In first place, the lentiviral transduction of hESC was optimized with a Green Fluorescent Protein (GFP) GFPpCCL TET OFF regulated lentiviral vector, kindly provided by Dr. L. Naldini (San Raffaele Telethon Institute for Gene Therapy-"Vita-Salute San Raffaele" University Medical School, Milano, Italy), and it was found that $2x10^5$ hESC infected with 1 mL of lentiviral supernatant for 1 hour in suspension, at 37ºC and 5% CO_2 atmosphere, resulted in nearly 80% infected cells, after 4 days post-infection, that was when we saw the GFP signal more intense (Figure 31A). Addition of doxycycline to the medium effectively repressed GFP expression (Figure 31B).

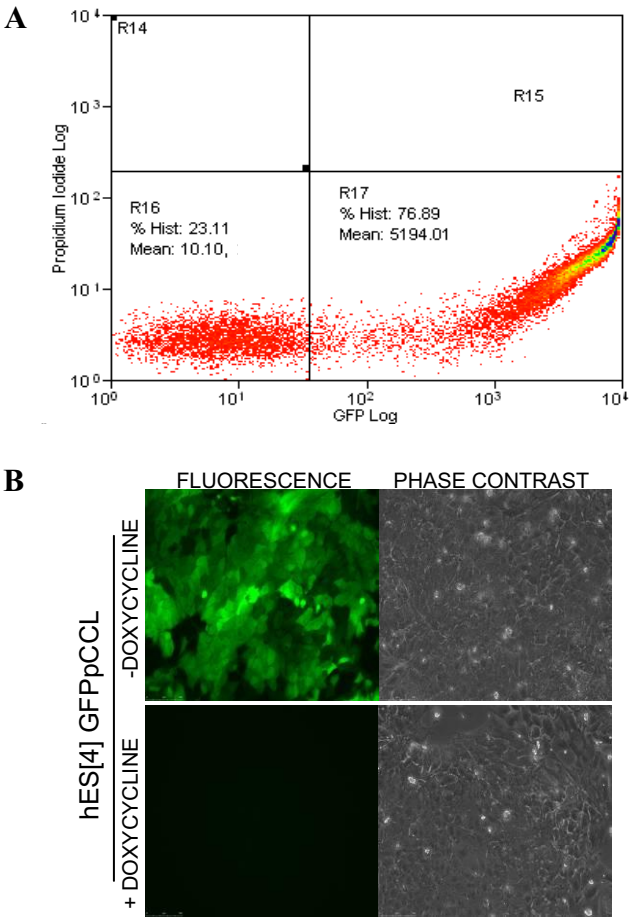

Figure 31. Optimization of transduction of human embryonic stem cells. (**A**) Quantitative flow cytometry analysis of the percentage of GFP expressing hESC after infection with GFPpCCL lentiviral vector and grown in undifferentiated conditions for four days in the absence of doxycycline showed nearly 80% transduced hESC with a high mean of intensity. Propidium Iodide staining was used to rule out dead cells. (**B**) Representative phase contrast and fluorescence microscopy images of hESC after infection with GFPpCCL lentiviral vector and grown in undifferentiated conditions for four days in the absence (-) or presence (+) of doxycycline. After culturing the cells in the absence of doxycycline, GFP expression was observed in most cells. Scale bars: 100 μm.

After this high percentage of infection, the same infection protocol was used to transduce hESC with lentiviruses encoding human $p27^{Kip1}$ coding sequence. Approximately, $2x10^5$ hESC were infected on suspension for 1 hour with 1 mL of viral supernatant at 37ºC in a 5% CO_2 atmosphere. After this time had elapsed, cells were plated in 6-well plates (Falcon) with an additional 1 mL of hESC undifferentiated medium. The next day the medium was changed, and cells were left to grow for several days.

In order to test the doxycycline-regulated expression of $p27^{Kip1}$ in hESC, its expression was measured by quantitative reverse transcription PCR (qRT-PCR)

analysis, after culturing transduced cells in the absence of doxycycline for 2, 3, or 4 days, or culturing them in the presence of doxycycline. The same procedure but using GFP infected cells was performed as a negative control (Figure 32).

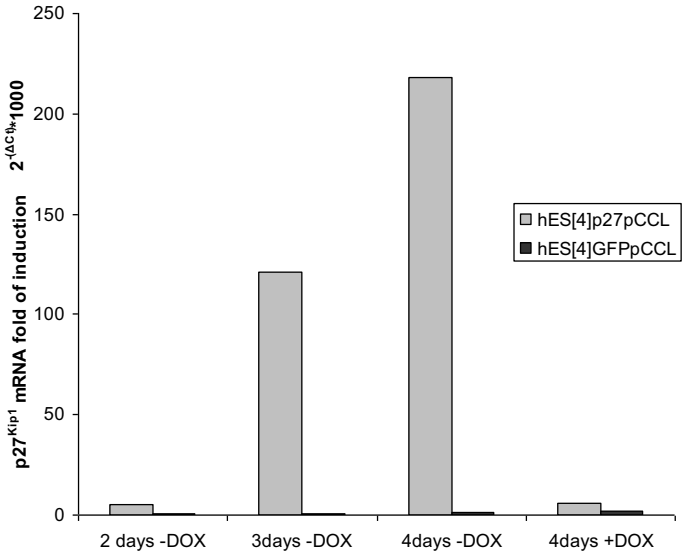

Figure 32. Doxycycline-regulated overexpression of $p27^{Kip1}$ in human embryonic stem cells. Quantitative RT-PCR analysis of $p27^{Kip1}$ expression after infection of hESC with lentiviral vectors encoding $p27^{Kip1}$ or control GFP coding sequences, and subsequently growth in the presence (+) or absence (-) of doxycycline in the culture medium. Relative mRNA expression levels were calculated using the comparative threshold cycle method relative to human GAPDH and multiplied by 1000 to simplify data presentation. Note that $p27^{Kip1}$ infected cells overexpress recombinant $p27^{Kip1}$ compared with the level of endogenous $p27^{Kip1}$ in control GFP infected cultures. DOX, doxycycline.

Results showed that whereas control GFP infected hESC expressed similar levels of endogenous $p27^{Kip1}$ in all conditions tested, lentivirally encoded $p27^{Kip1}$ expression increased gradually as doxycycline was removed from the culture medium, increasing more than 100 fold above the control levels 3 days after infection, and increasing more than 200 fold above the control levels 4 days after infection. The addition of doxycycline to the medium effectively repressed the expression of $p27^{Kip1}$ to basal expression. All the experiments were performed at 4 days post-infection, that was when the highest increase in expression was observed.

Subsequently, we proceeded to confirm the doxycycline-regulated overexpression of $p27^{Kip1}$ in hESC at the protein level by Western blot and immunofluorescence analysis (Figure 33). To this end, hESC were transduced with lentiviral vectors encoding $p27^{Kip1}$ or control GFP coding sequences, and subsequently left to grow for 4 days in the presence or absence of doxycycline in the culture medium. The same

procedure but using uninfected cells was carried out as an additional control. After this time had elapsed, samples for Western blot and immunofluorescence analysis were collected.

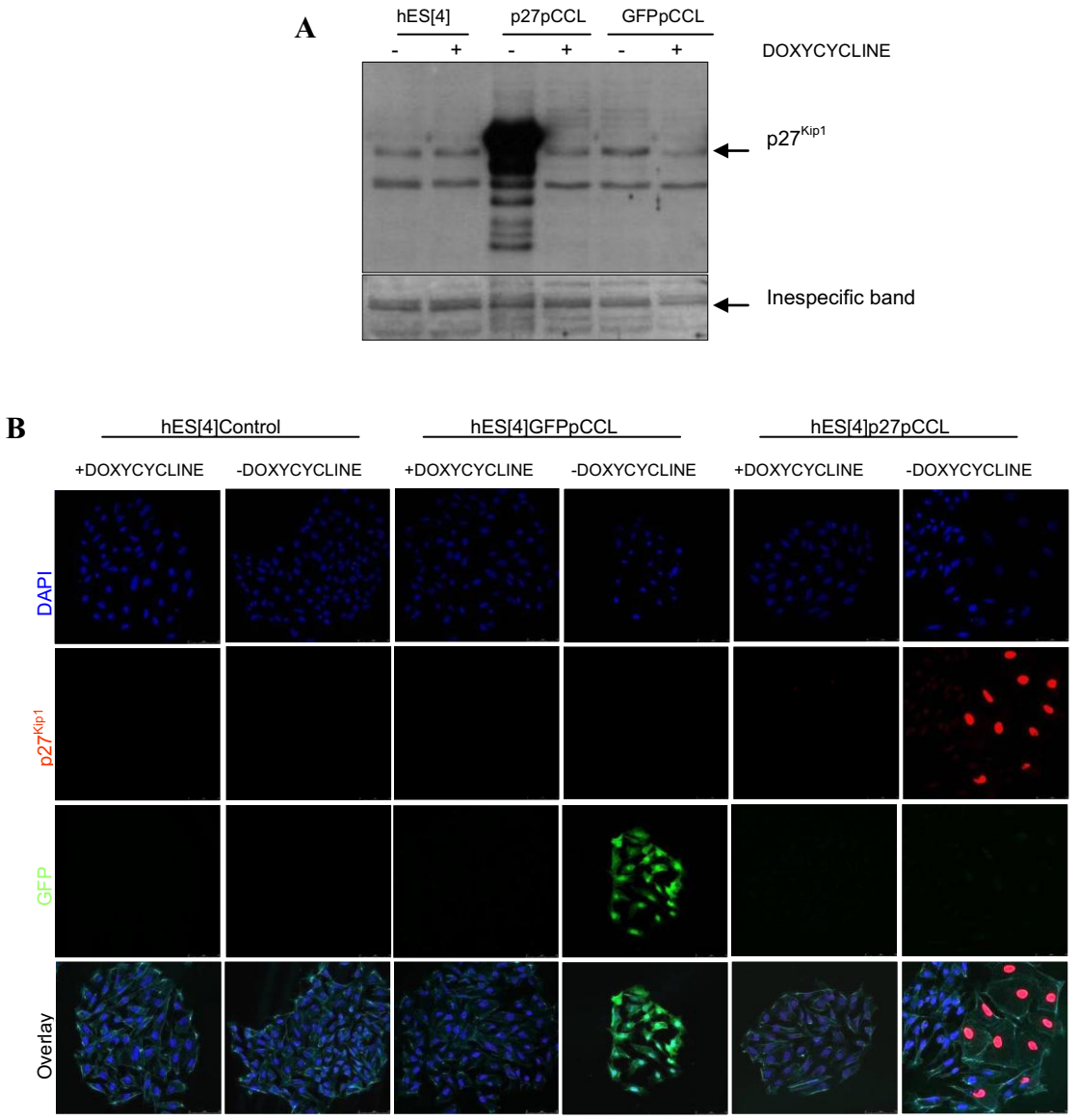

Figure 33. Doxycycline-regulated overexpression of $p27^{Kip1}$ in human embryonic stem cells resulted in a change in the morphology. (**A**) Western blot analysis of $p27^{Kip1}$ expression using 30 µg of protein from whole cell extracts of hESC transduced with lentiviral vectors encoding $p27^{Kip1}$ or control GFP coding sequences and left to grow in the presence (+) or absence (-) of doxycycline in the culture medium for 4 days. The two first lanes correspond to the same procedure but using uninfected hESC. Shown are the representative results obtained in two independent experiments. Note that lentivirally encoded $p27^{Kip1}$ was detected as a heavier band, and only in cells infected with $p27^{Kip1}$ coding sequence when doxycycline was not present in the culture medium. (**B**) Immunofluorescence analysis of $p27^{Kip1}$ expression (red) in hESC transduced with lentiviral vectors encoding $p27^{Kip1}$ or control GFP coding sequences and left grow in the presence (+) or absence (-) of doxycycline in the culture medium for 4 days, revealed a change in the morphology of $p27^{Kip1}$ overexpressing cells, with an enlarged, spread, and flattened phenotype. Shown are the representative results obtained in three independent experiments. The same procedure but using uninfected cells was carried out as an additional control. Nuclei were counterstained with DAPI (blue). Actin filaments were visualized with fluorescent phalloidin (cyan). Scale bars: 75 µm.

Results confirmed the doxycycline-regulated overexpression of $p27^{Kip1}$ in undifferentiated hESC at the protein level.

Western blot analysis showed that lentivirally encoded $p27^{Kip1}$ was detected as a heavier molecular weight band, only in cells transduced with the lentiviral vector encoding $p27^{Kip1}$ and when doxycycline was not present in the culture medium. The antibody against $p27^{Kip1}$, also detected bands of lower molecular weight most likely $p27^{Kip1}$ degradation bands. Endogenous $p27^{Kip1}$ was detected at similar levels in all conditions, demonstrating that GFP infected cells had the same $p27^{Kip1}$ levels as uninfected hESC (Figure 33A).

Immunofluorescence analysis also confirmed that $p27^{Kip1}$ overexpressing hESC were only detected in cells transduced with the lentiviral vector encoding $p27^{Kip1}$ when doxycycline was not present in the culture medium. Similarly, GFP fluorescence was detected only in cells transduced with the lentiviral vector encoding GFP when doxycycline was not present in the culture medium. The expression of lentivirally encoded proteins was effectively repressed when cells were cultured in the presence of doxycycline (Figure 33B).

Uninfected hESC generated colonies with the typical morphology of undifferentiated cells grown on matrigel, with round and tight colonies. When observed under a microscope at higher magnification, these colonies consisted of lots of cells displaying high nuclear to cytoplasmic ratio as revealed by co-staining with DAPI and phalloidin. DAPI binds to DNA while phalloidin binds to actin filaments allowing the imaging of the actin cytoskeleton of cells. However, when we looked at the morphology of $p27^{Kip1}$ overexpressing hESC, we observed a surprising phenotype that was not seen in any of the other cells. $p27^{Kip1}$ overexpressing hESC displayed an enlarged size, with big buclei, cells appeared spread and flattened. Moreover, these cells had a low nuclear to cytoplasmic ratio, just the opposite phenotype than $p27^{Kip1}$ non-overexpressing hESC (Figures 33B and 34).

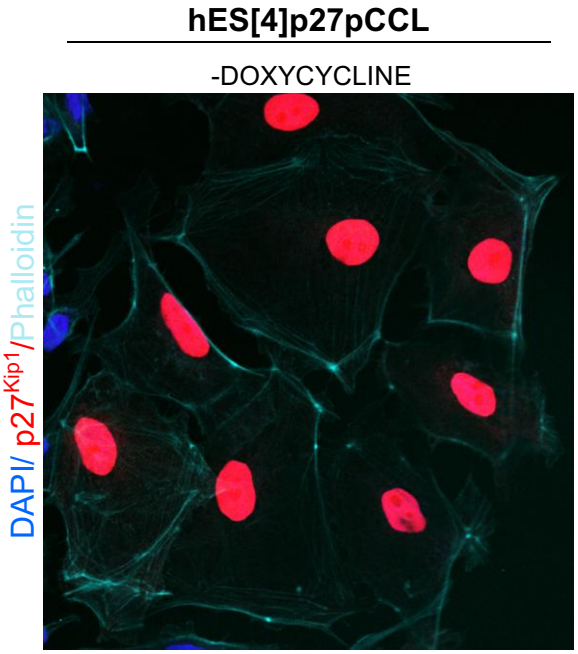

Figure 34. $p27^{Kip1}$ overexpressing human embryonic stem cells displayed a characteristic phenotype. Higher magnification image of $p27^{Kip1}$ overexpressing hESC from Figure 33B showing an enlarged size, big buclei, a spread out and flattened morphology, and a low nuclear to cytoplasmic ratio. $p27^{Kip1}$ expression is shown in red, phalloidin in cyan, and DAPI staining in blue.

Furthermore, we observed that the colonies consisting of $p27^{Kip1}$ overexpressing cells appeared to have less number of cells (Figure 35A).

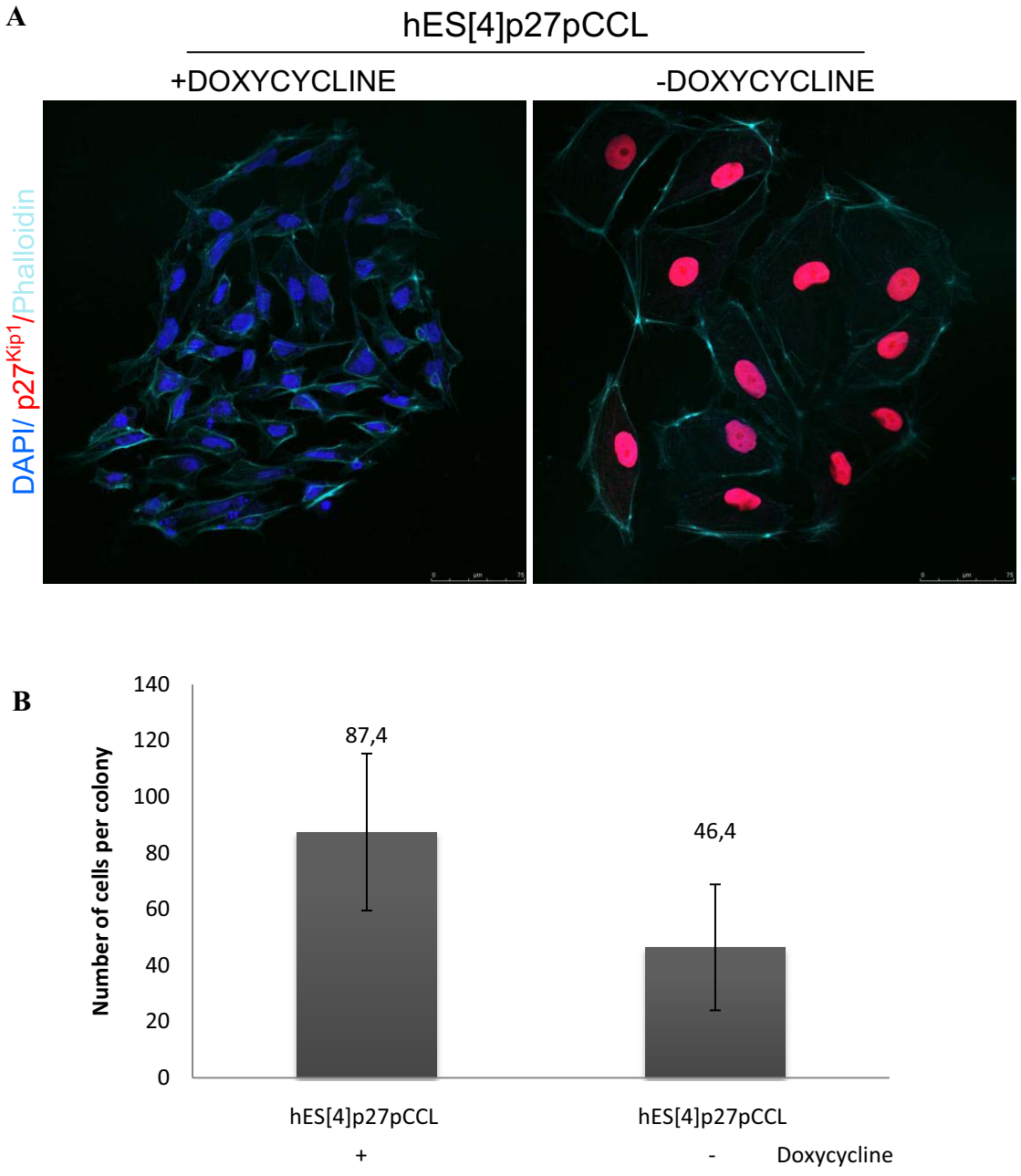

Figure 35. p27^{Kip1} overexpressing human embryonic stem cells generated colonies containing few number of cells. (**A**) Immunofluorescence analysis of p27^{Kip1} expression (red) in hESC transduced with lentiviral vectors encoding p27^{Kip1}, and left to grow with (+) or without (-) doxycycline in the culture medium for 4 days, revealed that homogeneous colonies consisting of p27^{Kip1} overexpressing cells contained less numbers of cells than colonies generated by p27^{Kip1} non-overexpressing cells. Note that both colonies have approximately the same size. Shown are the representative results obtained in three independent experiments. Nuclei were counterstained with DAPI (blue). Actin filaments were visualized with phalloidin (cyan). Scale bars: 75 µm. (**B**) The number of cells found in colonies, of approximately the same size, consisting of p27^{Kip1} overexpressing or p27^{Kip1} non-overexpressing cells were counted. Results represent the mean± Standard Deviation from three independent experiments.

With the aim of finding out if $p27^{Kip1}$ overexpressing cells generated colonies containing less number of cells, hESC were transduced with lentiviral vectors encoding the $p27^{Kip1}$ coding sequence, and subsequently left them to grow for 4 days in the presence or absence of doxycycline in the culture medium. We then looked for homogeneous colonies of approximately the same size containing either, $p27^{Kip1}$ overexpressing cells or $p27^{Kip1}$ non-overexpressing cells, and proceeded to count the number of cells that made up each colony.

The results showed that homogeneous colonies consisting of $p27^{Kip1}$ overexpressing hESC contained less number of cells than colonies of the same size but containing $p27^{Kip1}$ non-overexpressing cells, suggesting that $p27^{Kip1}$ could be impairing the cell growth (Figure 35B).

The cell growth could be impaired by arresting the cell cycle. In order to know the cell cycle status of $p27^{Kip1}$ overexpressing hESC, the cell cycle profile of these cells was analyzed by flow cytometry analysis of DAPI and EdU stained cells (Figure 36). Given that DAPI binds to DNA, it allows the analysis of DNA content, and therefore the percentage of cells in $G_0/_1$ and $G_2/_M$ phases. On the other hand, EdU is incorporated during DNA synthesis and allows the assessment of the percentage of cells in S phase.

In view of the fact that hESC transduced with lentiviral vectors encoding $p27^{Kip1}$, and subsequently grown for 4 days in the absence of doxycycline generated a heterogeneous population of cells containing either, $p27^{Kip1}$ overexpressing or $p27^{Kip1}$ non-overexpressing cells, we developed a protocol to analyze the cell cycle profile of only $p27^{Kip1}$ overexpressing cells using an antibody against $p27^{Kip1}$. In the same way, we managed to analyze the cell cycle structure of only GFP positive cells, as a control.

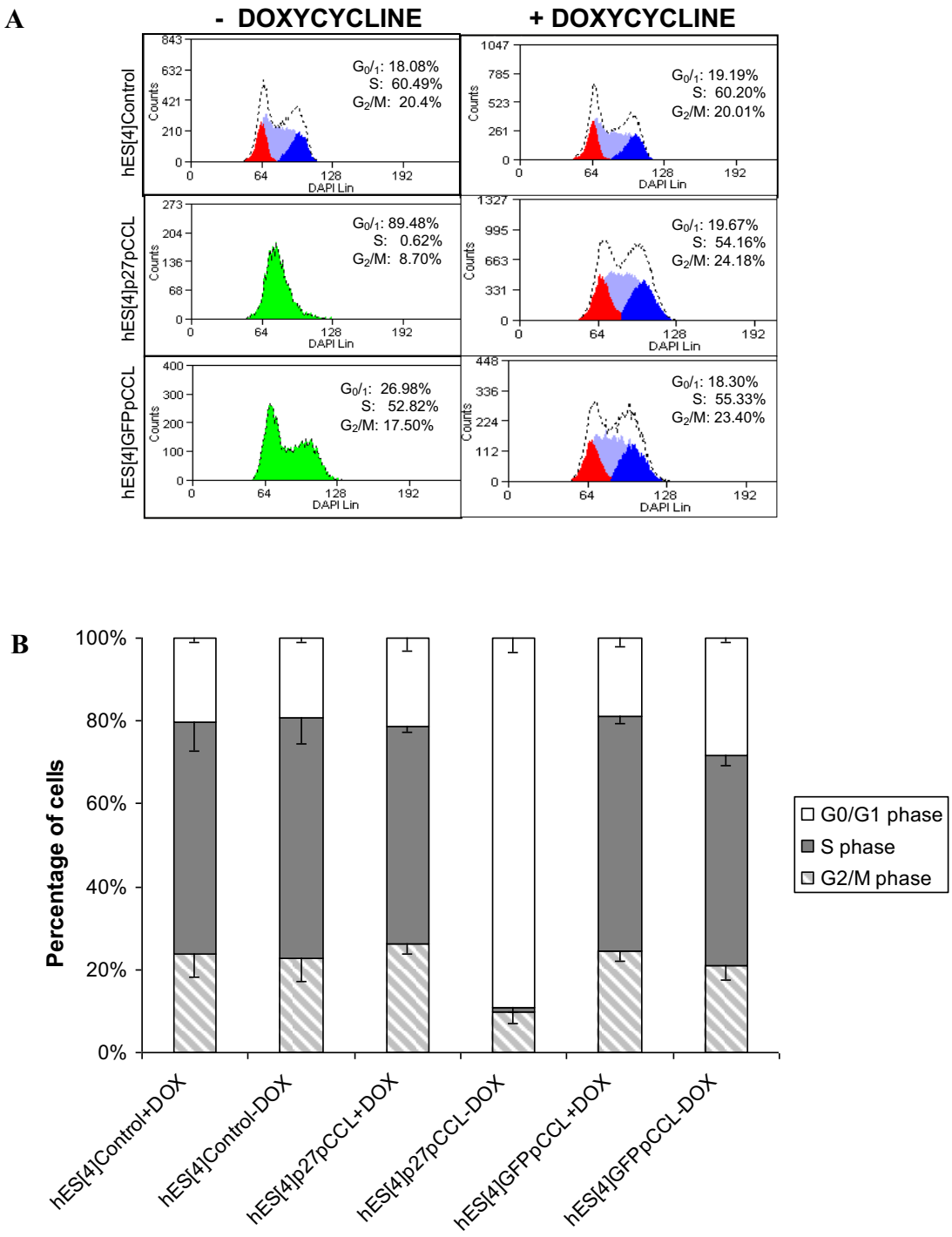

Figure 36. Overexpression of $p27^{Kip1}$ in human embryonic stem cells resulted in an arrest of the cell cycle. (**A**) Quantitative flow cytometry analysis of cell cycle profile by DAPI staining and EdU incorporation in hESC transduced with lentiviral vectors encoding $p27^{Kip1}$ or control GFP coding sequences and left to grow with (+) or without (-) doxycycline in the culture medium for 4 days. The same procedure but using uninfected hESC was carried out as an additional control. $G_0/_1$: red; S: cyan; G_2/M: blue. In green are represented the cell cycle profiles of homogeneous hESC overexpressing either $p27^{Kip1}$ or GFP fluorescence. $p27^{Kip1}$ overexpressing hESC arrested in the $G_0/_1$ phase of the cell cycle. The rest of the cells, included GFP expressing cells, presented the atypical cell cycle structure of undifferentiated hESC with a short percentage of cells in $G_0/_1$ and high percentage of cells in S phase. A minimum of 10000 events were recorded. (**B**) Results are represented in a graph to better compare the data. Results represent the mean± Standard Deviation of three independent experiments.

Results showed that overexpression of $p27^{Kip1}$ in hESC resulted in a complete arrest of the cell cycle. We did not detect any cell positive for EdU incorporation, that meant, no cell was cycling. The great majority (approximately 90%) of the population were arrested in the $G_0/_1$ phase of the cell cycle.

On the contrary, we observed that GFP expressing cells had the atypical cell cycle structure of undifferentiated hESC, that was also shared by cells uninfected or treated with doxycycline, with a low percentage (around 20-26%) of cells in $G_0/_1$ phase and a high percentage of cells (around 53- 60%) in S phase. Addition of doxycycline to the medium did not cause any effect in proliferation, demonstrated in uninfected hESC.

These results demonstrate, for the first time, that overexpression of one cell cycle protein; namely, $p27^{Kip1}$ in undifferentiated hESC inhibits the cell cycle progression by arresting the cells and consequently the cells are not able to self-renew.

We next wanted to test the complementary approach, that is, to deplete the expression of $p27^{Kip1}$ in hESC with the aim of finding out if this could affect the properties of hESC.

To this end, three short hairpin RNAs (shRNAs) targeting different regions of the $p27^{Kip1}$ gene sequence which were designed using a proprietary algorithm were purchased from Sigma-Aldrich Quimica. A shRNA is a sequence of RNA that makes a tight hairpin turn that can be used to silence gene expression via RNA interference. Short hairpin RNAs use a vector introduced into cells and utilize the U6 or H1 promoter to ensure that the shRNA is always expressed. This vector is usually passed on to daughter cells, allowing the gene silencing to be inherited. The shRNA hairpin structure is cleaved by the cellular machinery into small interfering RNA (siRNA) which is then bound to the RNA-induced silencing complex (RISC). This complex binds to and cleaves mRNAs which match the siRNA that is bound to it (Figure 37A).

Each $p27^{Kip1}$ shRNA (p27shRNA) clone was constructed within the lentivirus plasmid vector pLKO.1-puro. Puromycin sequence was removed by digestion with restriction enzymes and a GFP coding sequence was cloned instead, generating pLKO.1-GFP (see Material and Methods) (Figure 37B). Each p27shRNA construct was sequence verified to ensure a match to the $p27^{Kip1}$ gene. As a negative control, Non Target shRNA (NTshRNA) control vector was used. The short-hairpin sequence contained 5 base pair mismatches to any known human or mouse gene. This non-targeting shRNA negative control vector could activate RISC and the RNAi pathway,

but did not target any human or mouse genes. This allowed for examination of the effects of shRNA transduction on gene expression.

A

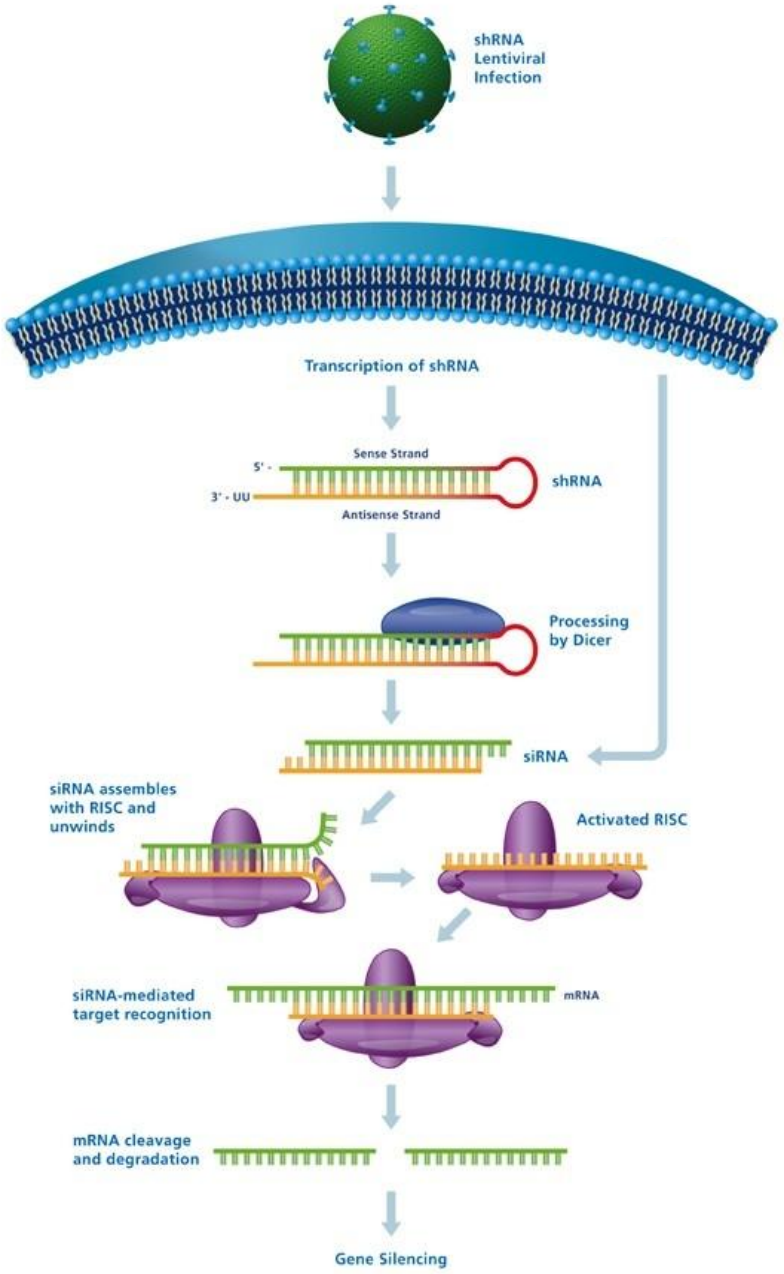

Figure 37. Schematic representation of shRNA mediated gene silencing. (**A**) Diagram depicting the shRNA mediated gene silencing pathway. Cells are transduced with shRNA lentiviral particles. Following transcription of the shRNA in the nucleus, the hairpin structure is recognized and cleaved by the RNase enzyme Dicer to form small interfering RNA (siRNA) that is subsequently taken up by the RNA-Induced Silencing Complex (RISC) which mediates cleavage of the target mRNA for gene silencing. (**B**) Vector map of pLKO.1-GFP showing the insertion site of shRNA under the U6 promoter. Shown are the 3 short hairpin sequences targeting $p27^{Kip1}$ gene that were design using a proprietary algorithm.

B

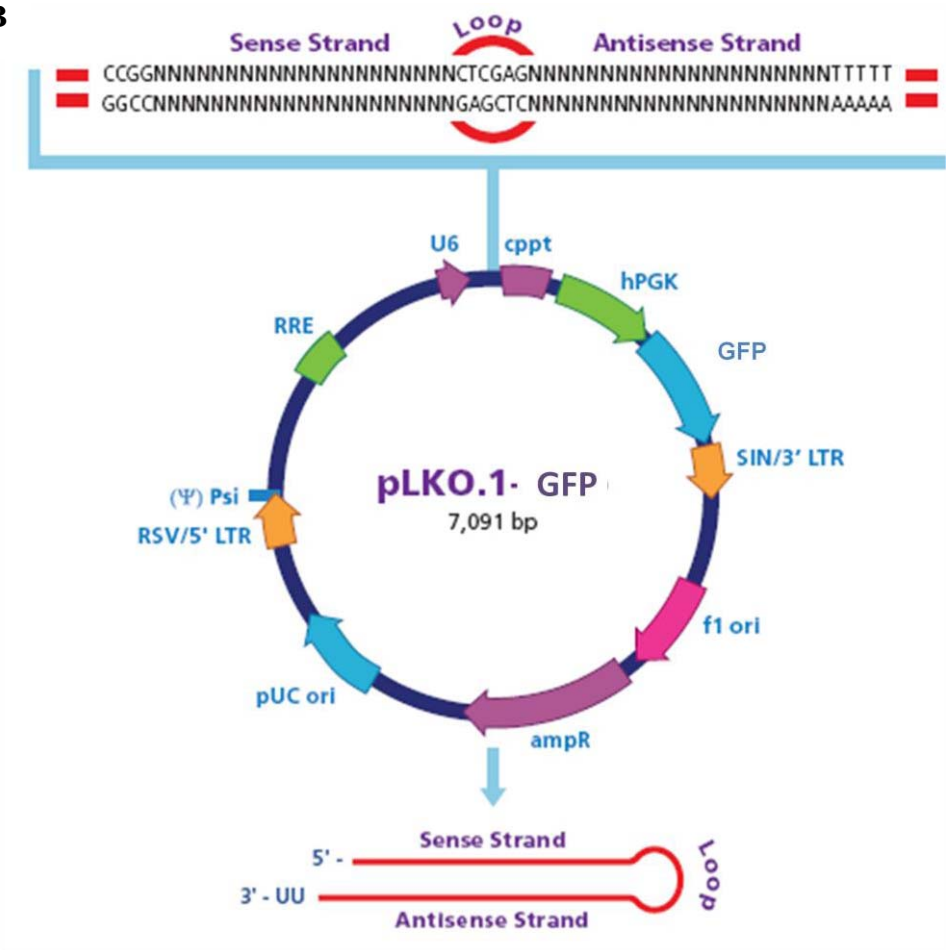

p27shRNA Hairpin sequences of individual clones		
p27shRNA#1	TRCN0000039928	**CCGGGTAGGATAAGTGAAATGGATACTCGAGTATCCATTTCACTTATCCTACTTTTTG**
p27shRNA#3	TRCN0000039930	**CCGGGCGCAAGTGGAATTTCGATTTCTCGAGAAATCGAAATTCCACTTGCGCTTTTTG**
p27shRNA#4	TRCN0000039931	**CCGGCCTCAGAAGACGTCAAACGTACTCGAGTACGTTTGACGTCTTCTGAGGTTTTTG**

Gene delivery of p27shRNA or NTshRNA constructs was performed by lentiviral transduction because lentiviruses are one of the most efficient methods for delivering genetic information into the DNA of a host cell, as mentioned before. Lentiviruses were independently produced by transfecting the packaging cell line 293T with packaging and envelope plasmids using a third generation approach.

In first place, the lentiviral transduction of hESC was optimized with NTshRNA negative control construct by flow cytometry analysis of GFP positive cells (Figure 38). Approximately, $2.5x10^5$ hES[4] were infected with different dilutions of lentivirus supernatant (1.5 µL, 2 µL, 10 µL, 100 µL, 250 µL, 500 µL, or 1000 µL) for 1 hour in suspension at 37ºC and 5% CO_2 atmosphere. Subsequently, cells were seeded in 6-well plates with an additional 1 mL of hESC medium. The next day, the medium was

changed, and cells were left to grow for 3 or 4 days. Uninfected cells were used as negative controls.

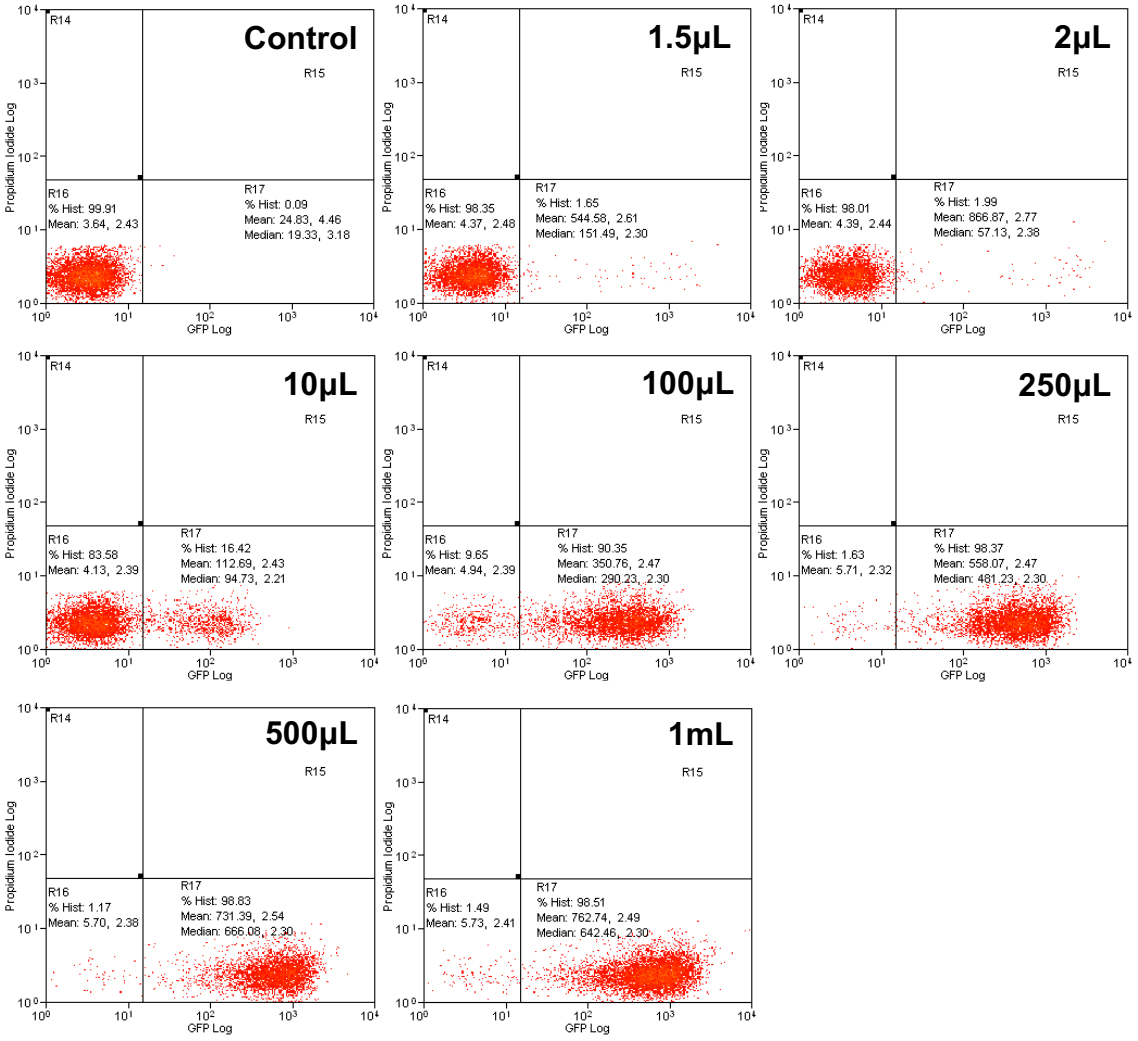

Figure 38. Optimization of NTshRNA transduction in human embryonic stem cells. Quantitative flow cytometry analysis of the percentage of GFP expressing hESC after infection with different dilutions (1.5 µL, 2 µL, 10 µL, 100 µL, 250 µL, 500 µL, or 1000 µL) of NTshRNA negative control lentivirus supernatant. Approximately, $2.5x10^5$ hES[4] were infected for 1 hour in suspension at 37ºC and 5% CO_2 atmosphere. Uninfected cells were used as a negative control. The percentage of infection was nearly 99% after infecting cells with 500 µL or 1000 µL of lentivirus supernatant. Propidium Iodide staining was used to rule out dead cells. A minimum of 10000 events were recorded.

Results showed that when hES[4] cells were infected with 1000 µL, 500 µL, or even 250 µL of NTshRNA lentiviral supernatant for 1 hour in suspension, at 37ºC and 5% CO_2 atmosphere, we obtained nearly 99% of infection. Nevertheless, the highest mean of GFP intensity signal resulted when 1000 µL of lentiviral supernatant were used.

After this excellent percentage of infection, this same infection protocol was carried out to transduce hESC with the different p27shRNA (p27shRNA#1, p27shRNA#3, or p27shRNA#4) or control NTshRNA constructs. Uninfected cells were used as additional controls (Figure 39).

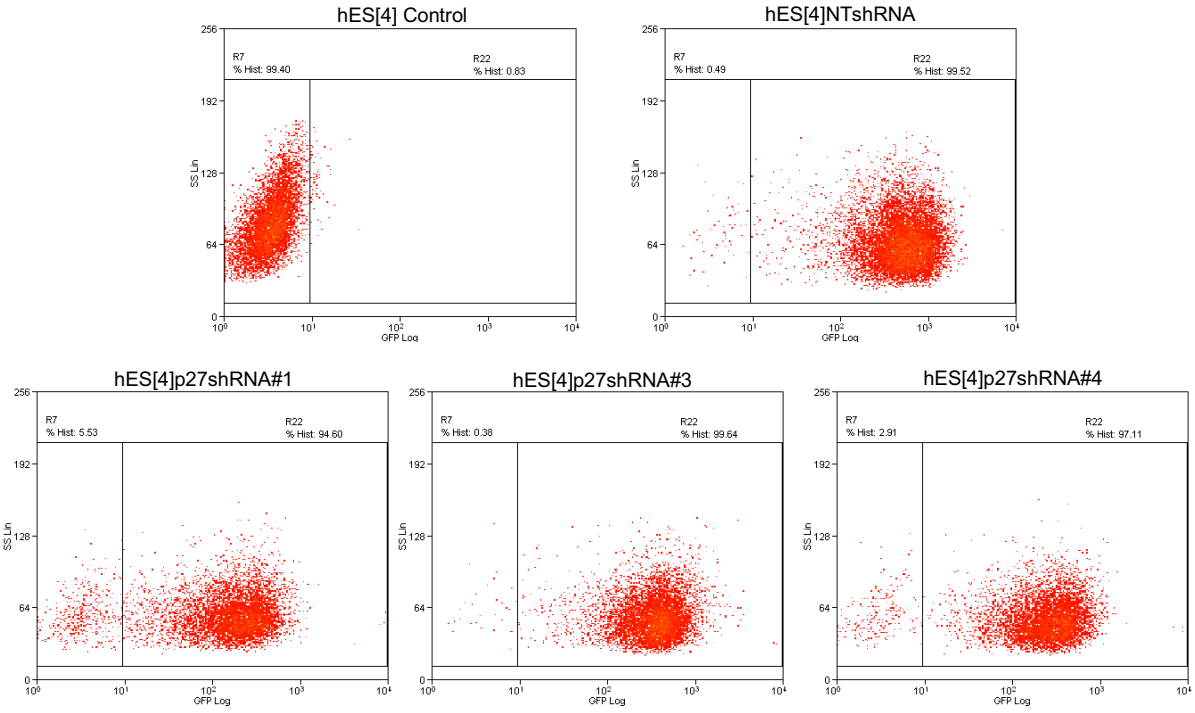

Figure 39. p27shRNA transduction in human embryonic stem cells. Quantitative flow cytometry analysis of the percentage of GFP expressing hESC after infecting $2.5x10^5$ hES[4] with 1000 µL of lentivirus supernatant carrying the different p27shRNA (p27shRNA#1, p27shRNA#3, or p27shRNA#4) or control NTshRNA constructs. Cells were infected for 1 hour in suspension at 37ºC and 5% CO_2 atmosphere. Uninfected cells were used as additional controls. The percentage of infection was more than 94% in all the conditions, reaching more than 99% in hESC transduced with NTshRNA or p27shRNA#3 constructs. A minimum of 10000 events were recorded.

Results demonstrated that hESC were successfully transduced with p27shRNA constructs, as more than 94% of the population expressed GFP fluorescence in all the conditions, by flow cytometry analysis. The percentage of infection even reached a 99% in cells transduced with NTshRNA or p27shRNA#3 constructs. As expected, uninfected hESC did not express GFP fluorescence.

These successful results had several advantages: the first one is that we had similar percentages of infection for all the conditions, thus providing a good system to detect differences in the knockdown effects of the different constructs. Secondly, we had homogeneous populations of infected cells so did not need to select them by

sorting. This could avoid the potential karyotypic abnormalities frequently detected in hESC passaged enzymatically as single cells (Mitalipova, Rao et al. 2005; Draper, Smith et al. 2004).

Moreover, to rule out any difference in the density of the infected cells by virus concentration or toxicity effects, we proceeded to take some phase contrast microscopy images of the colonies after transducing the cells with the different lentiviral vectors (Figure 40).

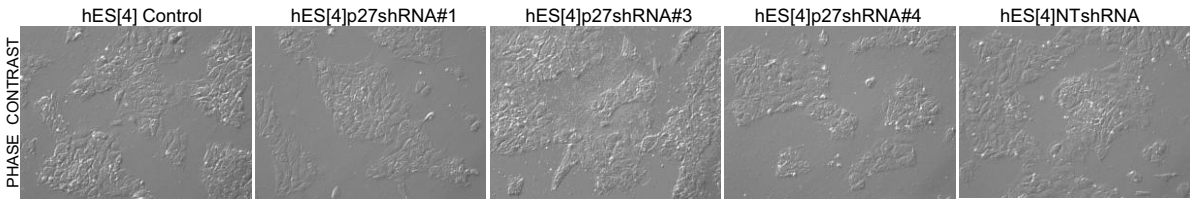

Figure 40. Cell density after p27shRNA transduction in human embryonic stem cells. Representative phase contrast microscopy images of hES[4] 24 hours post-infection with the different p27shRNA (p27shRNA#1, p27shRNA#3, or p27shRNA#4) or control NTshRNA lentiviral vectors. Uninfected cells were used as additional controls.

Results confirmed that hESC infected with the different p27shRNA or control NTshRNA lentiviral vectors presented similar number of colonies, thus the cell density was not affected by lentivirus concentration or toxicity effects.

After the optimization of the shRNA transduction conditions in hESC, and verification that the percentage of infection and the cell density was similar with the different p27shRNA constructs used, we proceeded to test the $p27^{Kip1}$ knockdown efficiency by qRT-PCR analysis. NTshRNA vector was used as a negative control for the examination of the effects of shRNA transfection on gene expression. Uninfected hESC were also used as additional controls (Figure 41).

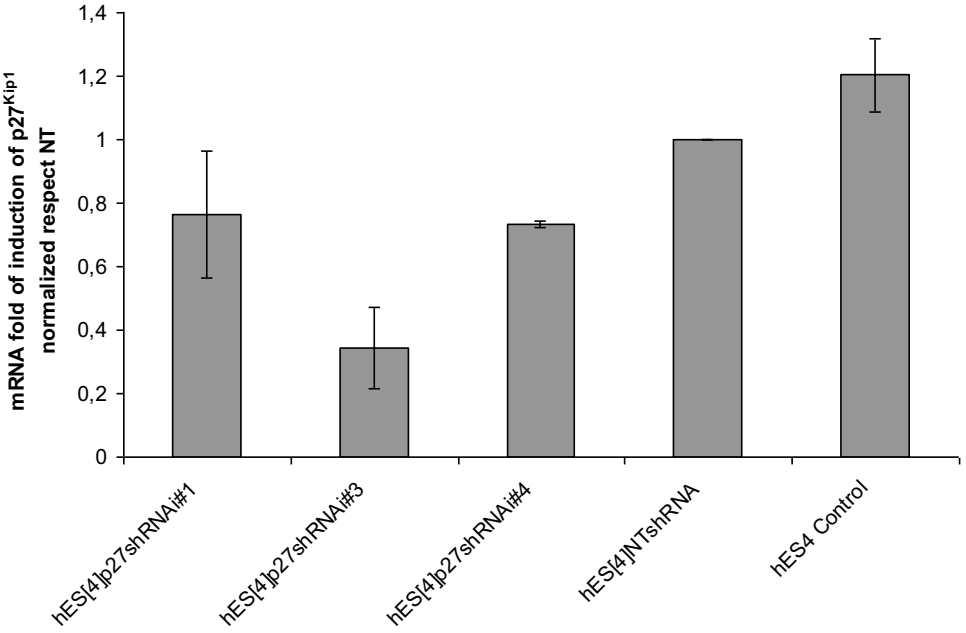

Figure 41. $p27^{Kip1}$ knockdown mediated by shRNA in human embryonic stem cells. Quantitative RT-PCR analysis of $p27^{Kip1}$ expression after transducing hES[4] with the different p27shRNA (p27shRNA#1, p27shRNA#3, or p27shRNA#4) or control NTshRNA lentiviral vectors. Approximately, $2.5x10^5$ hES[4] were infected for 1 hour in suspension at 37ºC and 5% CO_2 atmosphere. Subsequently, cells were seeded with an additional 1 mL of hESC medium. The next day the medium was changed, and cells were left to grow for three days. Uninfected cells were used as an additional negative control. Relative mRNA expression levels were calculated using the comparative threshold cycle method relative to NTshRNA control cells. Results represent the mean ± Standard Deviation of three independent experiments.

Results showed that the distinct p27shRNA constructs had different knockdown efficiencies. p27shRNA construct number 3 was the one that most effectively repressed $p27^{Kip1}$ with a reduction of approximately 70%. p27shRNA construct number 4 appeared to reduce aproximately 20% the expression of $p27^{Kip1}$. On the contrary, p27shRNA construct number 1 did not seem to significantly reduce the expression levels of $p27^{Kip1}$.

We next proceeded to confirm the knockdown of $p27^{Kip1}$ in hESC at the protein level by Western blot analysis. NTshRNA infected cells were used as a negative control. Also, uninfected hESC were used as additional controls (Figure 42).

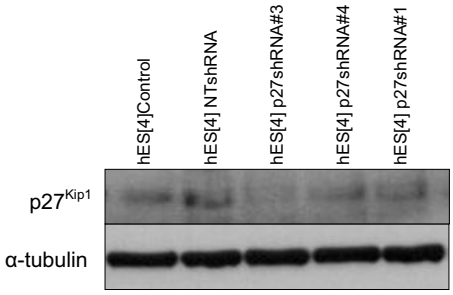

Figure 42. $p27^{Kip1}$ protein knockdown mediated by shRNA in human embryonic stem cells. Western blot analysis of $p27^{Kip1}$ expression using 20 µg of protein of whole cell extracts from hES[4] transduced with the different p27shRNA (p27shRNA#1, p27shRNA#3, or p27shRNA#4) or control NTshRNA lentiviral vectors. For the analysis, $2.5x10^5$ hES[4] were infected for 1 hour in suspension at 37ºC and 5% CO_2 atmosphere. Subsequently, cells were seeded with an additional 1 mL of hESC medium. The next day, the medium was changed, and cells were left to grow for three days. The first lane corresponds to uninfected hES[4]. α-tubulin was used as a loading control.

Results showed again that p27shRNA construct number 3 was the one that most effectively repressed $p27^{Kip1}$ protein levels, making it undetectable. Furthermore, we could conclude that the effect in the knockdown was a consequence of the construct and not of the percentage of infection given that it was similar for all the constructions (Figure 39).

We also proceeded to confirm the transduction of the different p27shRNA (p27shRNA#1, p27shRNA#3, or p27shRNA#4) or control NTshRNA lentiviral vectors by immunofluorescence analysis of GFP fluorescence. Uninfected hESC were used as negative controls (Figure 43).

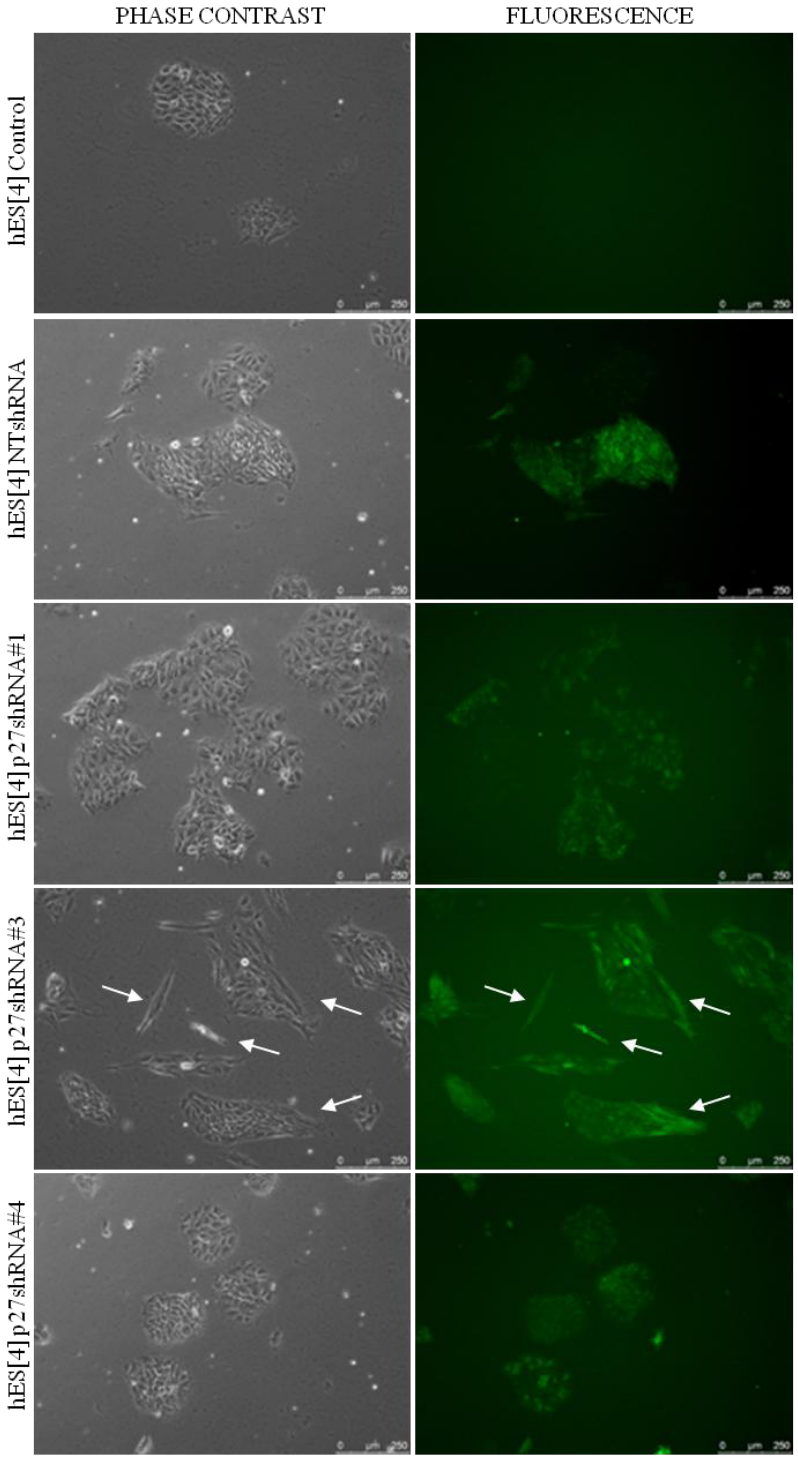

Figure 43. $p27^{Kip1}$ knockdown in human embryonic stem cells caused changes in the morphology. Representative phase contrast and fluorescence microscopy images of alive hES[4] after transduction of the different p27shRNA (p27shRNA#1, p27shRNA#3, or p27shRNA#4) or control NTshRNA lentiviral vectors. Approximately, $2.5x10^5$ hES[4] were infected for 1 hour in suspension at 37ºC and 5% CO_2 atmosphere. Subsequently, cells were seeded with an additional 1 mL of hESC medium. The next day, the medium was changed, and cells were left to grow for three days. Uninfected cells were used as controls. hES[4] infected with p27shRNA#3, the construct that reduced more than 70% the expression of $p27^{Kip1}$, showed a striking change in the morphology, with a thin and elongated phenotype (see white arrows). Shown are the representative results obtained in three independent experiments. Scale bars: 250 µm.

Results showed that most (more than 90%) of hESC infected with the different p27shRNA or NTshRNA constructs expressed GFP expression, in agreement with the flow cytometry analysis of GFP expression. As expected, uninfected hESC did not express GFP fluorescence.

Uninfected hESC generated colonies with the typical morphology of undifferentiated cells, grown on matrigel, with round and tight colonies. The same morphology was observed in cells transduced with NTshRNA, p27shRNA#1, or p27shRNA#4 constructs. p27shRNA#1 transduced hESC appeared to have less tight colonies and less well defined edges, as if these cells would have more facility to differentiate. However, hESC transduced with p27shRNA#3 construct, the one that reduced the expression of $p27^{Kip1}$ more than 70%, displayed a striking phenotype with colonies that had the edges elongated and very well defined (see white arrows of Figure 43). These edges were likely to be made up of thin, "fibroblastoid" cells that surrounded the colonies. Moreover, colonies comprised of elongated and thin cells were also observed (see white arrows of Figure 43). These cells were probably not able to spread, just the opposite phenotype than $p27^{Kip1}$ overexpression.

The next move, was to confirm these results by immunofluorescence analysis of 4% paraformaldehyde (Sigma-Aldrich Quimica) fixed cells, and subsequently immunostained with an antibody recognizing GFP, to increase the GFP signal. We focused on p27shRNA#3 transduced cells as they were the only ones with this phenotype. NTshRNA transduced cells were used as controls (Figure 44).

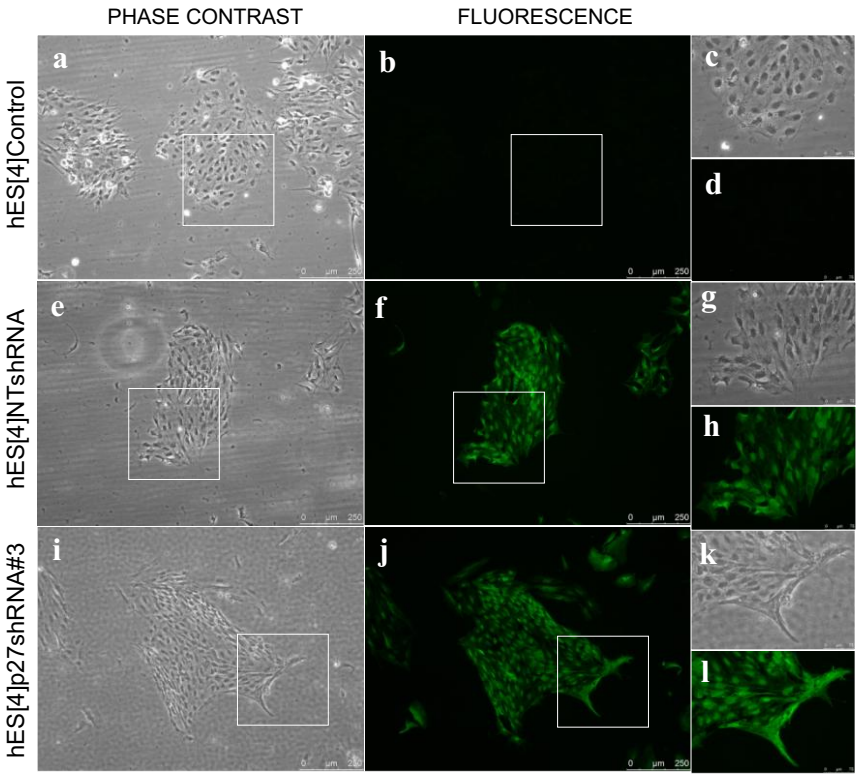

Figure 44. $p27^{Kip1}$ knockdown in human embryonic stem cells causes an elongated phenotype. Representative phase contrast and fluorescence microscopy images of uninfected hES[4] (**a**, **b**, **c**, **d**), or after transduction with control NTshRNA (**e**, **f**, **g**, and **h**) or p27shRNA#3 (**i**, **j**, **k**, and **l**) lentiviral vectors. After infection, hES[4] were fixed for 20 minutes at room temperature with 4% paraformaldehyde, and subsequently immunostained with an antibody recognizing GFP. Uninfected cells were used as additional controls. hES[4] transduced with p27shRNA#3 construct (**i**, **j**, **k**, and **l**) showed elongated cells at the edge of the colony. (**c** and **d**) represent more magnification areas of white box in (**a** and **b**), respectively; (**g** and **h**) represent more magnification areas of white boxes in (**e** and **f**), respectively; (**k** and **l**) represent more magnification areas of white boxes in (**i** and **j**), respectively. Scale bars (**a**, **b**, **e**, **f**, **i**, and **j**): 250 μm; (**c**, **d**, **g**, **h**, **k**, and **l**): 75 μm.

Results confirmed that p27shRNA#3 transduced hESC contained thin and elongated cells that mostly appeared at the edges of the colonies. Most of the colonies observed were compact and surrounded by "fibroblastoid" cells making well defined edges (Figure 45). Spontaneous differentiation often occurs in only a portion of an hESC colony, usually along the edges or as isolated spots in the center. The beginning of differentiation is noted by apparition of flattened appearance and loss of defined boundaries. In general, healthy, undifferentiated colonies are regarded as colonies with clean, well defined edges. Thus the phenotype generated by the knockdown of $p27^{Kip1}$ suggests that loss of $p27^{Kip1}$ could be affecting the "stemness" or number of cells. As expected, uninfected hESC did not express GFP fluorescence.

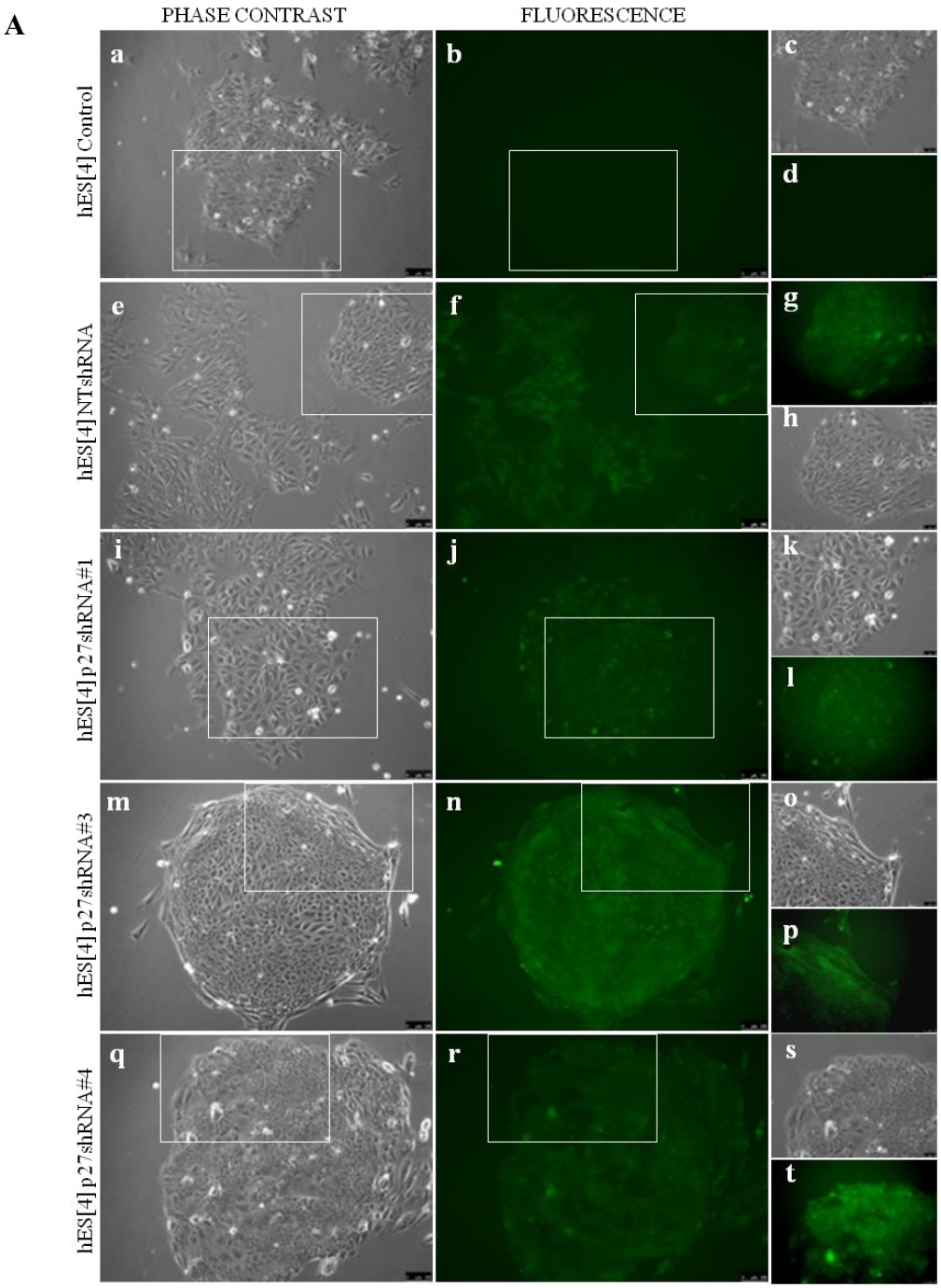

Figure 45. $p27^{Kip1}$ knockdown in human embryonic stem cells generates compact colonies with well defined edges. (**A**) Representative phase contrast and fluorescence microscopy images of uninfected hES[4] (**a**, **b**, **c**, **d**), or after transduction with control NTshRNA (**e**, **f**, **g**, and **h**), p27shRNA#1 (**i**, **j**, **k**, and **l**), p27shRNA#3 (**m**, **n**, **o**, and **p**), or p27shRNA#4 (**q**, **r**, **s**, and **t**) lentiviral vectors. Uninfected cells were used as additional controls. hES[4] transduced with p27shRNA#3 construct (**m**, **n**, **o**, and **p**) showed very well defined edges made up of elongated cells. (**c** and **d**) represent more magnification areas of white boxes in (**a** and **b**), respectively; (**g** and **h**) represent more magnification areas of white boxes in (**e** and **f**), respectively; (**k** and **l**) represent more magnification areas of white boxes in (**i** and **j**), respectively; (**o** and **p**) represent more magnification areas of white boxes in (**m** and **n**), respectively; (**s** and **t**) represent more magnification areas of white boxes in (**q** and **r**), respectively. Scale bars (**a**, **b**, **e**, **f**, **i**, **j**, **m**, **n**, **q**, and **r**): 100 µm; (**c**, **d**, **g**, **h**, **k**, **l**, **o**, **p**, **s**, and **t**): 50 µm. (**B**) Representative phase contrast images of uninfected hES[4], or after transduction with control NTshRNA, p27 shRNA#1, p27shRNA#3, or p27shRNA#4 lentiviral vectors. Note the characteristic morphology of $p27^{Kip1}$ knockdown hESC colonies.

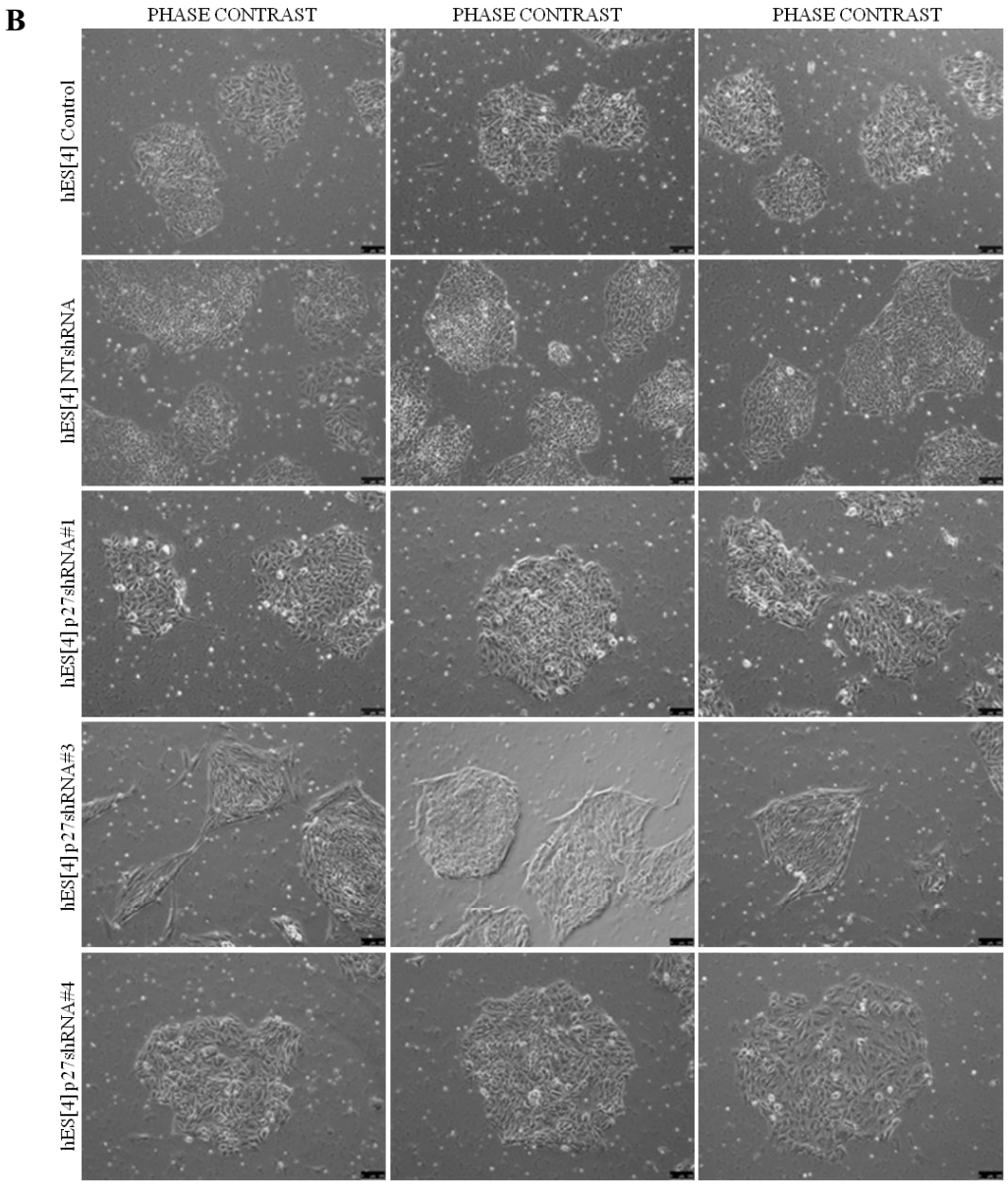

With the aim of finding out the cell cycle profile of hESC transduced with the different p27shRNA (p27shRNA#1, p27shRNA#3, or p27shRNA#4) or control NTshRNA constructs, we proceeded to analyze the cell cycle profile by flow cytometry analysis of DAPI and EdU stained cells. Uninfected hESC were used as additional controls (Figure 46).

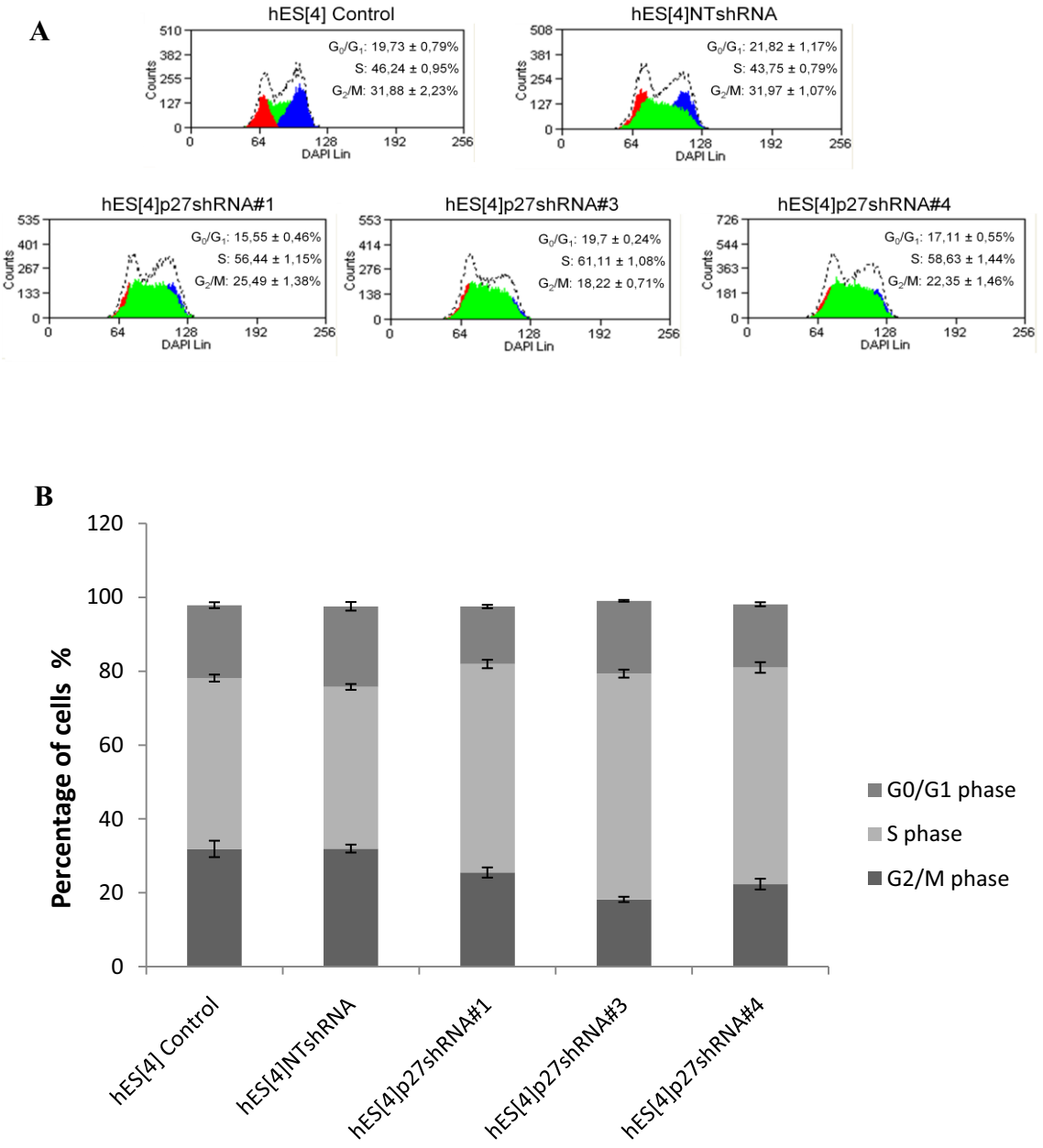

Figure 46. Cell cycle analysis of p27^{Kip1} depleted human embryonic stem cells. (**A**) Quantitative flow cytometry analysis of cell cycle profile by DAPI staining, and EdU incorporation in hES[4] transduced with the different p27shRNA (p27shRNA#1, p27shRNA#3, or p27shRNA#4) or control NTshRNA lentiviral vectors. The same procedure but using uninfected hES[4] was carried out as an additional control. $G_0/_1$: red; S: green; G_2/M: blue. hES[4] transduced with p27shRNA#3 construct, which reduced more than 70% the expression levels of p27^{Kip1}, displayed a slight increase of cells in the S phase of the cell cycle. Results represent the mean± Standard Deviation of three independent experiments. A minimum of 10000 events were recorded. (**B**) Results are represented in a graph to better compare the data. Results represent the mean± Standard Deviation of three independent experiments.

Results showed that hESC transduced with the different p27shRNA (p27shRNA#1, p27shRNA#3, or p27shRNA#4) constructs, as well as, control NTshRNA transduced or uninfected hESC presented the atypical cell cycle structure of undifferentiated hESC, with a low percentage of cells in $G_0/_1$ phase (16-22%) and a high percentage of cells in S phase (44-61%) (Figure 46A). Nevertheless, cells infected with p27shRNA constructs revealed an increase of cells in the S phase that was more evident in cells transduced with p27shRNA#3 construct which reduced more than 70% the expression of $p27^{Kip1}$. Moreover, these cells displayed a reduction in the G_2/M phase, as these cells had more facility to transit through the G_2/M phase.

In summary, these results demonstrate that the knockdown of $p27^{Kip1}$ seems to potentiate the atypical cell cycle structure of hESC, through an increase of cells in the S phase, and thus increasing the self-renewal of cells.

Taken together, these results demonstrate for the first time that expresion of one cell cycle protein; namely, $p27^{Kip1}$, in undifferentiated conditions, inhibits self-renewal of hESC by arresting the cells in $G_0/_1$ phase of the cell cycle. On the contrary, the reduction of the expression levels of $p27^{Kip1}$ appears to increase the self-renewal by increasing the proportion of cells in S phase.

Moreover, manipulation of the expression levels of $p27^{Kip1}$ induces a change in the morphology of undifferentiated hESC with an increase of the size, a decrease in the nuclear to cytoplasmic ratio, and a more spread out phenotype in $p27^{Kip1}$ overexpressing hESC, suggesting that the increase of $p27^{Kip1}$ was inducing a differentiation prone phenotype or less pluripotent. On the contrary, the reduction in the expression levels of $p27^{Kip1}$ causes a change in the phenotype, but towards more clearly defined edges, as these cells were becoming more pluripotent.

4. $p27^{Kip1}$ CONTROLS THE PLURIPOTENCY OF HUMAN EMBRYONIC STEM CELLS BY REGULATING *BRACHYURY* AND *TWIST*

We have demonstrated that $p27^{Kip1}$ controls the self-renewal property of human embryonic stem cells (hESC) by regulating the G_1 to S transition of the cell cycle. Moreover, we have shown that manipulation of the expression levels of $p27^{Kip1}$ in hESC induces changes in the morphology of undifferentiated cells. Particularly, the overexpression of $p27^{Kip1}$ in hESC caused an enlargement of the size, a decrease in the nuclear to cytoplasmic ratio, and a more spread out and flattened phenotype. On the contrary, the reduction of $p27^{Kip1}$ caused a change in the phenotype, but towards more clearly defined edges. Given the phenotypic changes observed with overexpression and knockdown of $p27^{Kip1}$ in hESC, our next question was to know if it could be affecting pluripotency since it has been reported that the high nuclear to cytoplasmic ratio is a common characteristic of undifferentiated pluripotent hESC (Thomson, Itskovitz-Eldor et al. 1998).

$p27^{Kip1}$ overexpressing hESC arrested in the $G_0/_1$ phase of the cell cycle and also displayed a reduction in the nuclear to cytoplasmic ratio compared to controls. With the objective of determining the significance of this phenotype, we evaluated the different fates that cells can follow once they have exited the cell cycle and remain in G_1 phase of the cell cycle.

Cells that withdraw from the cell cycle during G_1 phase can undergo three different fates: they can differentiate, become senescent, or go into apoptosis (Blomen and Boonstra 2007) (Figure 47). We next wanted to know if $p27^{Kip1}$ overexpressing hESC followed any of these cell fates.

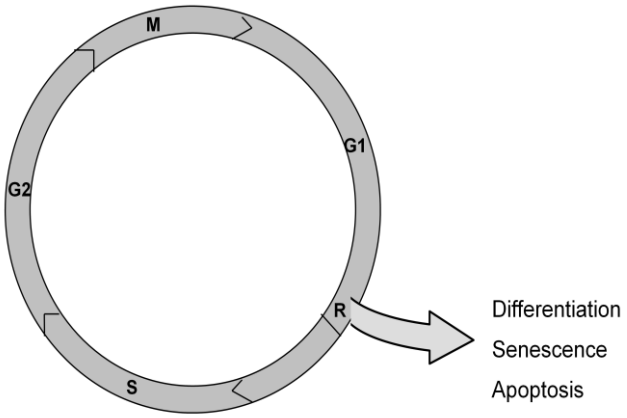

Figure 47. Diagram depicting the four phases of the cell cycle. The cell division cycle of eukaryotic cells is divided into four main phases namely Gap1 (G_1) phase where the cells grow and prepare for the Synthesis (S) phase where the chromosomes duplicate. After this process, the cells enter the Gap 2 (G_2) phase in which the cell continues to grow and prepares for Mitosis (M) phase during which the cell will actually divide. Cells undergo a period of mitogen dependence in G_1 phase before they enter the cycle. In this period, they can make different cell fate decisions. If they receive positive stimulus they proceed to progress into cell cycle. This point is called the Restriction point (R) and represents a point of no return that commits cells to a new round of cell division.

In first place, we proceeded to confirm that $p27^{Kip1}$ overexpressing hESC were larger than those that did not overexpress $p27^{Kip1}$. To this end, the cell size was analyzed by flow cytometry analysis of pulse width intensity (Figure 48A). The pulse width measurements are related to cell diameters. This method of sizing by flow cytometry was found to be independent of fluorescent or light-absorbing stain intensity, linearly related to cell diameter, and capable of resolving small diameter differences (Leary, Todd et al. 1979).

Human embryonic stem cells were transduced with lentiviral vectors encoding $p27^{Kip1}$ or control GFP coding sequences. After the infection, cells were seeded in tissue culture dishes with an additional 1 mL of hESC medium. The next day, the medium was changed, and cells were left to grow for 4 days in the presence or absence of doxycycline in the culture medium. The same procedure but using uninfected cells was carried out as an additional control.

As we knew that the cell size varied according to the cell cycle phase and, moreover, $p27^{Kip1}$ overexpressing hESC were arrested in the $G_0/_1$ phase, we managed to analyze the cell size of only cells in $G_0/_1$ phase (2N DNA content) by staining alive cells with Hoechst 33342 and excluded those in S and G_2/M phases.

A

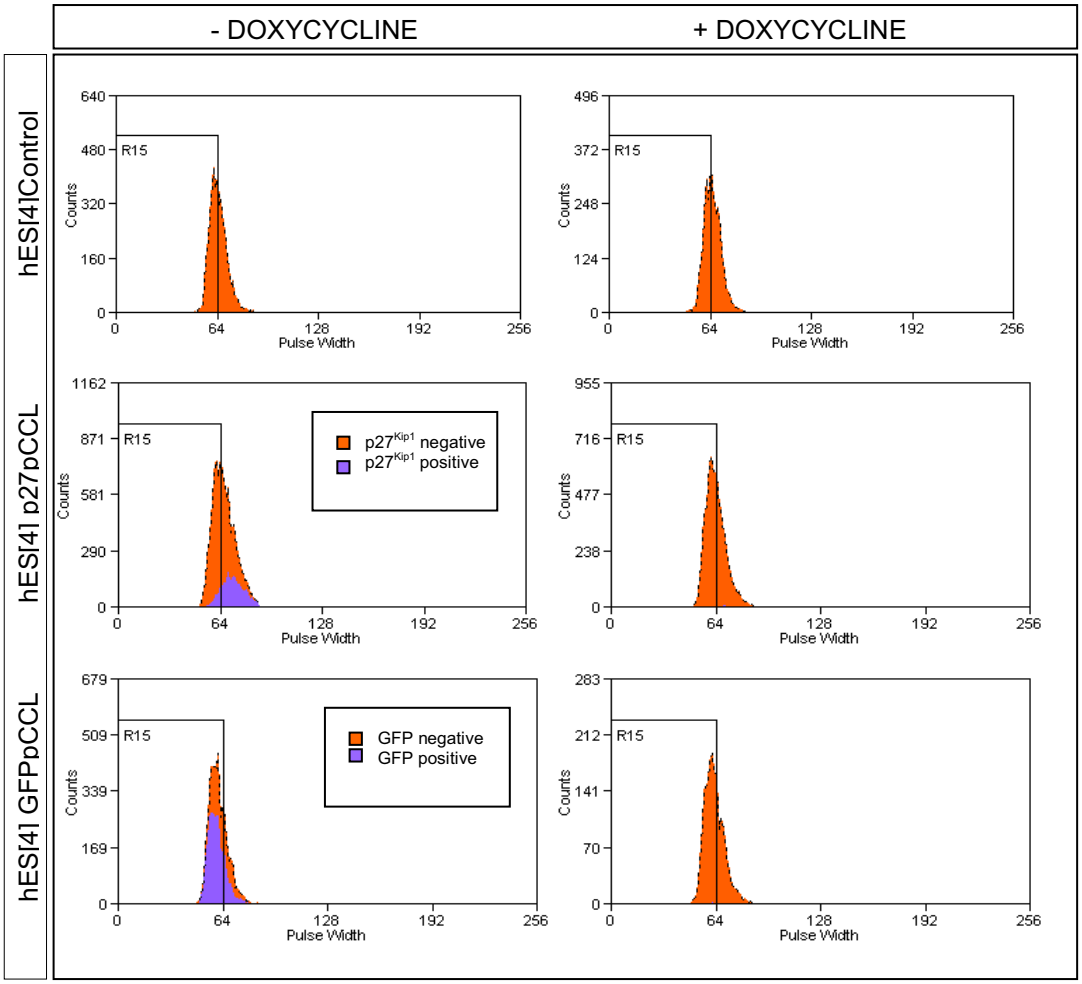

Figure 48. $p27^{Kip1}$ overexpressing human embryonic stem cells display an increase in the pulse width intensity. (**A**) Quantitative flow cytometry analysis of the pulse width intensity signal for G_0/G_1 gated hESC transduced with lentiviral vectors encoding $p27^{Kip1}$ or control GFP coding sequences and left to grow with (+) or without (-) doxycycline in the culture medium for 4 days. The same procedure but using uninfected hESC was carried out as an additional control. $G_0/_1$ phase residing cells were selected by staining alive cells with Hoechst 33342. In purple are represented hESC overexpressing either $p27^{Kip1}$ or GFP. In orange are represented the rest of the cells non-expressing the lentivirally encoded $p27^{Kip1}$ or GFP proteins. $p27^{Kip1}$ overexpressing hESC displayed an increase of the size based on the increase in the pulse width intensity mean. The rest of the cells, included GFP expressing cells, presented similar pulse width signal intensity means. Shown are the representative results of two independent experiments. A minimum of 10000 events were recorded per condition in each experiment. (**B**) Graph showing the mean ± standard deviations of the pulse width intensity values of three independent experiments. Results are expressed relative to controls (=1).

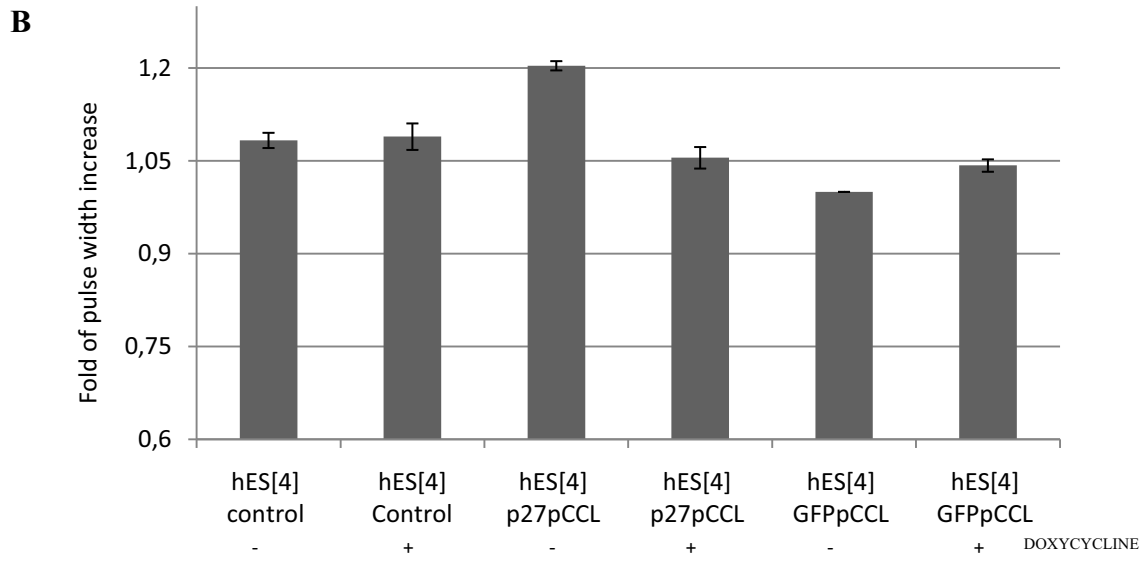

Flow cytometry analysis showed that $p27^{Kip1}$ overexpressing hESC displayed a bigger size, approximately 20% of increase compared to non-overexpressing cells. On the contrary, we observed that GFP expressing cells had a similar pulse width mean intensity signal than uninfected cells or to cells treated with doxycycline. Addition of doxycycline to the medium did not change the pulse width intensity signal, as was proven in uninfected hESC (Figure 48B).

Secondly, we wanted to know whether $p27^{Kip1}$ overexpressing hESC were apoptotic. Apoptosis can be assessed by the analysis of nuclear morphological changes indicative of apoptosis (nuclear fragmentation) after staining with DAPI and observation with a fluorescence microscope (Lai, Chien et al. 2003). We did not observe nuclear fragmentation in immunofluorescence analysis of DAPI-stained $p27^{Kip1}$ overexpressing hESC (see Figure 33B Section 3 of Results).

Moreover, and with the aim of confirming these results, we performed a time-lapse microscopy experiment of $p27^{Kip1}$ or control GFP transduced hESC after several days. To this end, hESC were transduced with lentiviral vectors encoding $p27^{Kip1}$ or control GFP coding sequences. After the infection, cells were left to grow for 7 days in the absence of doxycycline in the culture medium.

After 4 days of culture, large, spread cells could be detected in hESC transduced with the lentiviral vector encoding $p27^{Kip1}$ (Figure 49A). In the same way, GFP fluorescence could be detected in hESC transduced with the lentiviral vector encoding

GFP (Figure 49B). Individual $p27^{Kip1}$ overexpressing cells were monitored during 7 days by photographs, in order to detect any apoptotic process. The same procedure, but using GFP expressing cells, was carried out as a control.

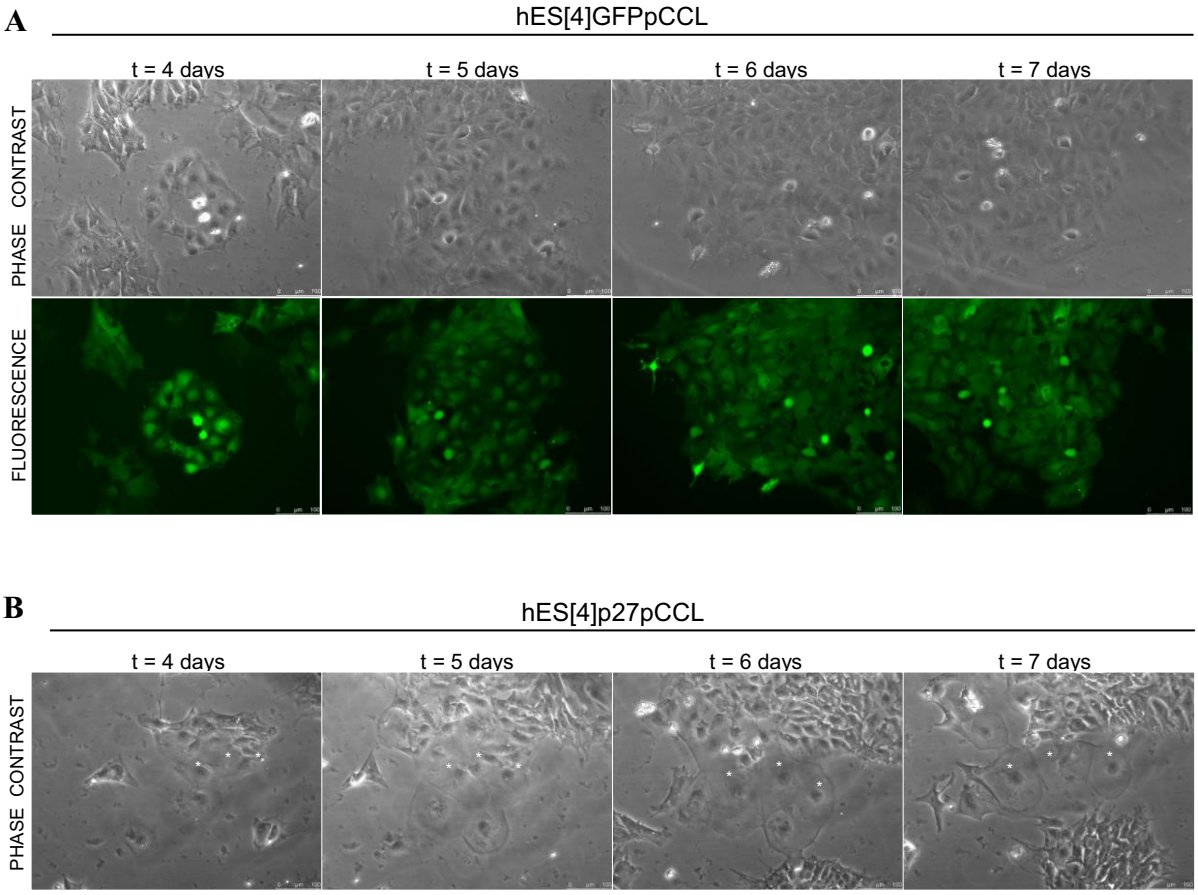

Figure 49. Time-lapse microscopy analysis of $p27^{Kip1}$ overexpressing human embryonic stem cells. Phase contrast and fluorescence microscopy images of representative GFP (**A**) and $p27^{Kip1}$ (**B**) overexpressing colonies after transducing hES[4] with GFP or $p27^{Kip1}$ lentiviral vectors, respectively. After infection, cells were left to grow for 7 days, without doxycycline in the culture medium. Note that after 4 days, enlarged and spread out cells (see white asterisks) could be seen in cells transduced with $p27^{Kip1}$ coding sequence, and could be monitored after seven days without apoptotis signals. Scale bars: 100 μm.

Results showed that hESC were effectively infected given that more than 90% of cells transduced with GFP sequence, expressed GFP fluorescence.

Enlarged, spread out cells could be detected in hESC transduced with $p27^{Kip1}$ coding sequence (white asterisks), but not in those transduced with GFP, after 4 days of culture in the absence of doxycycline, and were subsequently monitored during 7 days without observing apoptosis signals. After this time had elapsed, cells were fixed with

4% paraformaldehyde, and immunofluorescence analysis for $p27^{Kip1}$ expression and DAPI staining performed (Figure 50).

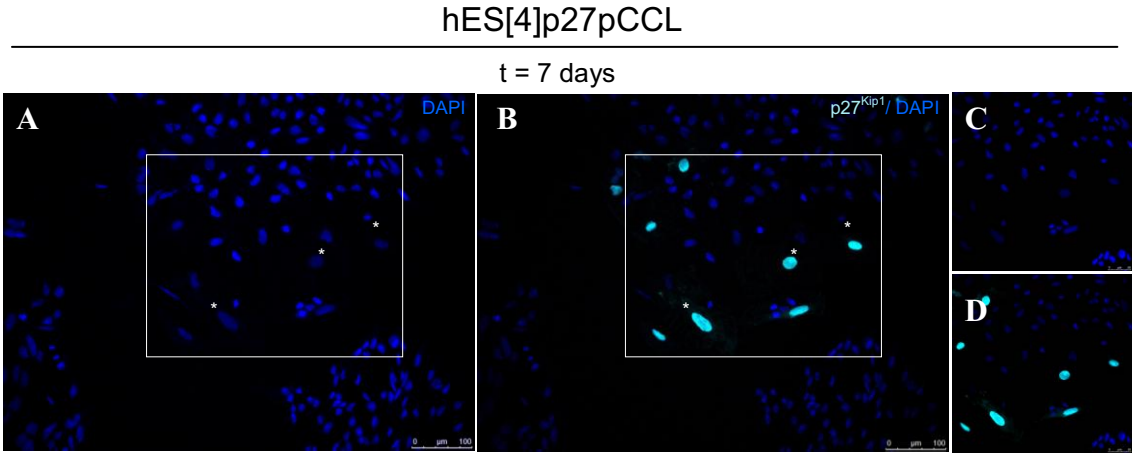

Figure 50. Nuclear morphology analysis of $p27^{Kip1}$ overexpressing human embryonic stem cells. Fluorescence microscopy images of same cells of Figure 49B after 7 days of culture in the absence of doxycycline. Cells were fixed with 4% paraformaldehyde for 20 minutes at room temperature, and stained with DAPI (blue) for visualization of the nuclei (**A**), and also immunoblotted with an antibody recognizing $p27^{Kip1}$ (cyan) for detection of $p27^{Kip1}$ overexpressing cells (**B**). Note that the enlarged and spread out cells of Figure 49B overexpressed $p27^{Kip1}$ (see white asterisks) and did not present nuclear fragmentation. (**C** and **D**) more magnification images of (**A**) and (**B**), respectively. Scale bars: (**A**, **B**): 100 µm. (**C**, **D**): 50 µm.

Results confirmed that $p27^{Kip1}$ overexpressing hESC showed no evidence of apoptosis after 7 days of culture. The nuclei appeared round, clear-edged, and uniformly stained demonstrating that these cells were not apoptotic.

Finally, apoptosis was also evaluated by quantitative flow cytometry analysis of mitochondrial membrane potential given that the abolishment of mitochondrial membrane potential is one of the earliest markers of apoptosis (Dobrosi, Toth et al. 2008). Cationic cyanine dyes have been shown to accumulate in cells in response to membrane potential (Waggoner 1979). The cyanine dye 1,1′,3,3,3′,3′-hexamethylindodicarbo-cyanine iodide ($DilC_1(5)$) penetrates the cytosol of eukaryotic cells and, at concentrations below 100 nM, accumulates primarily in mitochondria with active membrane potentials producing bright, far-red fluorescence. $DilC_1(5)$ staining intensity decreases with decreased mitochondrial membrane potential. In order to discriminate necrosis from apoptotis, Propidium Iodide staining was also used. Propidium Iodide is a nucleic acid binding dye that is impermeant to live and apoptotic

cells, but stains dead cells with red fluorescence, binding tightly to the nucleic acids in the cell.

With the combination of both dyes, alive cells would be recognized by presenting high bright $DilC_1(5)$ intensity staining and would not present Propidium Iodide staining. Apoptotic cells would present medium or low $DilC_1(5)$ staining and would not present Propidium Iodide staining. Finally, necrotic cells would not present $DilC_1(5)$ staining but would present high Propidium Iodide staining.

Then, hESC were transduced with lentiviral vectors encoding $p27^{Kip1}$ or control GFP coding sequences. After the infection, cells were left to grow for 4 days in the presence or absence of doxycycline in the culture medium. The same procedure but using uninfected cells was carried out as an additional control. Finally, the proportions of alive, apoptotic, and dead cells were analyzed by flow cytometry analysis (Figure 51).

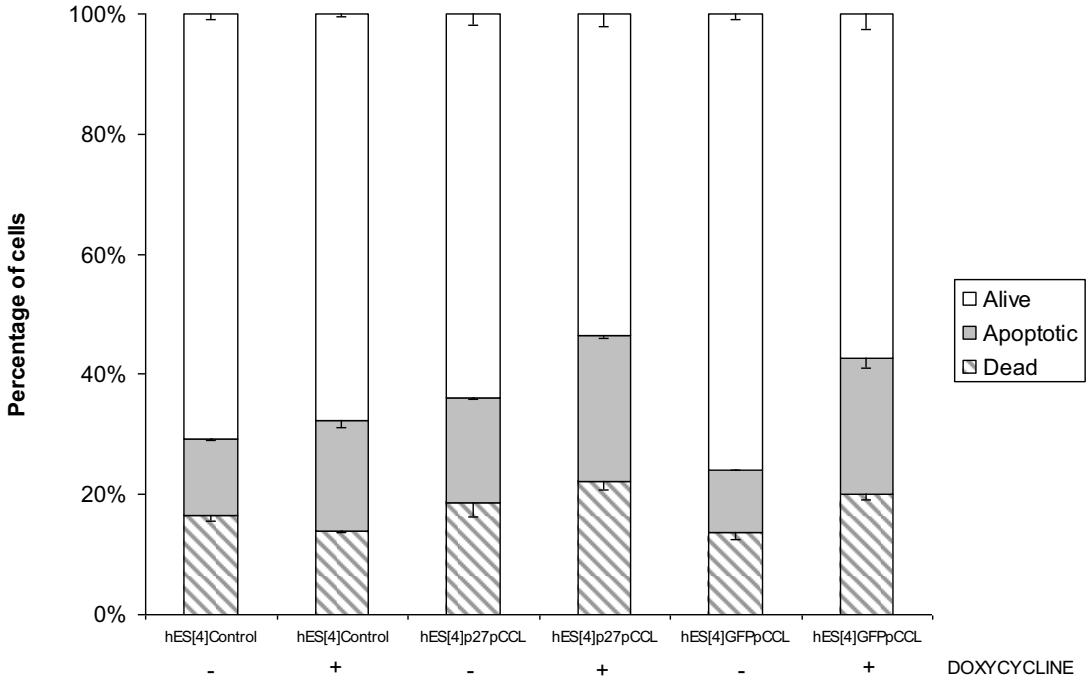

Figure 51. Overexpression of $p27^{Kip1}$ in human embryonic stem cells did not cause any effect on apoptosis. Quantitative flow cytometry analysis of percentages of alive, apoptotic, and dead hES[4] transduced with lentiviral vectors encoding $p27^{Kip1}$ or control GFP coding sequences. After the infection, cells were seeded in tissue culture dishes with an additional 1 mL of hESC medium. The next day, the medium was changed, and cells were left to grow for 4 days in the presence (+) or absence (-) of doxycycline in the culture medium. The same procedure but using uninfected hESC was carried out as an additional control. The proportions of alive cells were evaluated by $DilC_1(5)$ high intensity far-red fluorescence. Apoptotic cells presented medium or low levels of $DilC_1(5)$ staining, and dead cells did not present $DilC_1(5)$ staining but presented high Propidium Iodide red fluorescence. Results represent the mean ± standard deviations of three independent experiments. A minimum of 10000 events were recorded per condition in each experiment.

Flow cytometry apoptosis analysis did not reveal a significant increase of apoptosis in $p27^{Kip1}$ overexpressing hESC, confirming the previous results. Moreover, in this analysis we could not detect even protection from apoptosis in $p27^{Kip1}$ overexpressing hESC. Addition of doxycycline to the medium did not cause any effect in apoptosis in uninfected hESC, however a small increase in apoptosis was seen in hESC transduced with $p27^{Kip1}$ or GFP coding sequences.

We next proceeded to test the opposite approach, that is, to know if loss of $p27^{Kip1}$ could be affecting apoptosis. To this end, hESC were transduced with the different p27shRNA (p27shRNA#1, p27shRNA#3, or p27shRNA#4) or control NTshRNA constructs. The same procedure but using uninfected cells was carried out as an additional control. Finally, the proportions of alive, apoptotic, and dead cells were analyzed by flow cytometry analysis of $DilC_1(5)$ and Propidium Iodide staining (Figure 52).

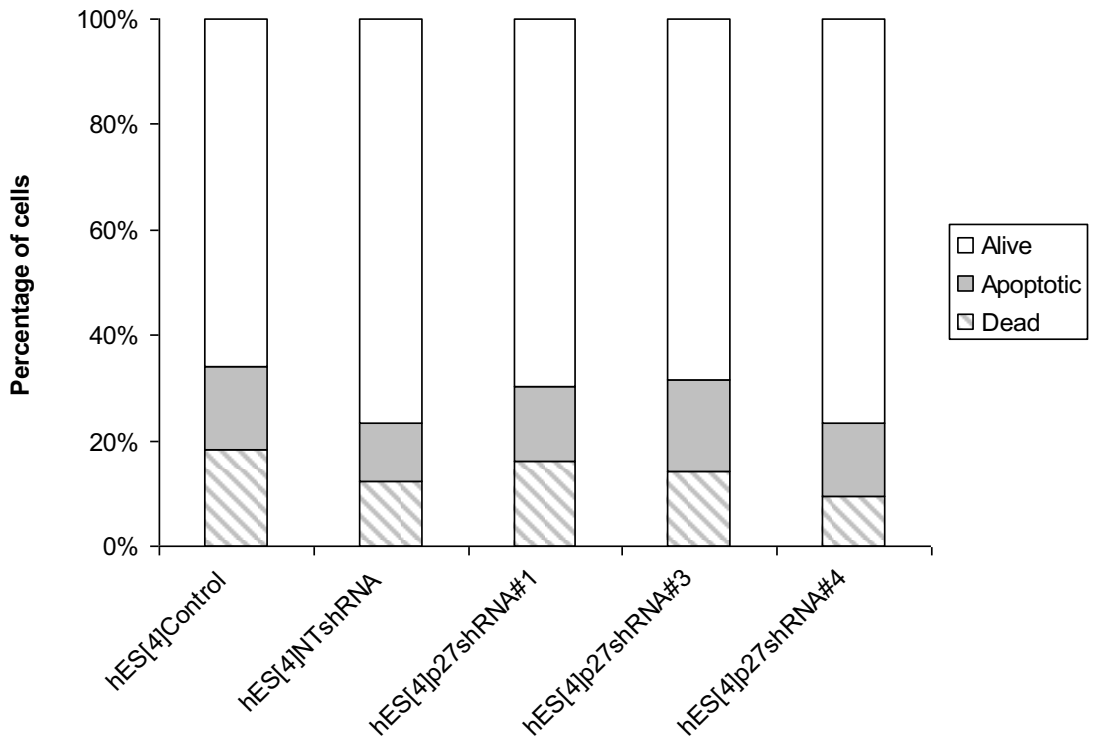

Figure 52. $p27^{Kip1}$ knockdown in human embryonic stem cells did not affect apoptosis. Quantitative flow cytometry analysis of percentages of alive, apoptotic, and dead hES[4] transduced with the different p27shRNA (p27shRNA#1, p27shRNA#3, or p27shRNA#4) or control NTshRNA constructs. Approximately, $2.5x10^5$ hES[4] were infected for 1 hour in suspension at 37ºC and 5% CO_2 atmosphere. After this time had elapsed, cells were seeded with an additional 1 mL of hESC medium. The next day, the medium was changed, and cells were left to grow for three weeks. The same procedure but using uninfected hESC was carried out as an additional control. The proportions of alive cells were evaluated by $DilC_1(5)$ high intensity far-red fluorescence. Apoptotic cells presented medium or low levels of $DilC_1(5)$ staining, and dead cells did not present $DilC_1(5)$ staining but presented high Propidium Iodide red fluorescence. A minimum of 10000 events were recorded per condition in each experiment.

Flow cytometry analysis of apoptosis did not reveal any effect on apoptosis in $p27^{Kip1}$ knockdown hESC, included cells transduced with p27shRNA#3 construct which reduced more than 70% the expression of $p27^{Kip1}$, after long term culture, despite that differences in the phenotype were evident.

In order to confirm these results, apoptosis was also checked by the analysis of nuclear morphological changes (nuclear fragmentation) after staining with DAPI and observation with a fluorescence microscope (Figure 53).

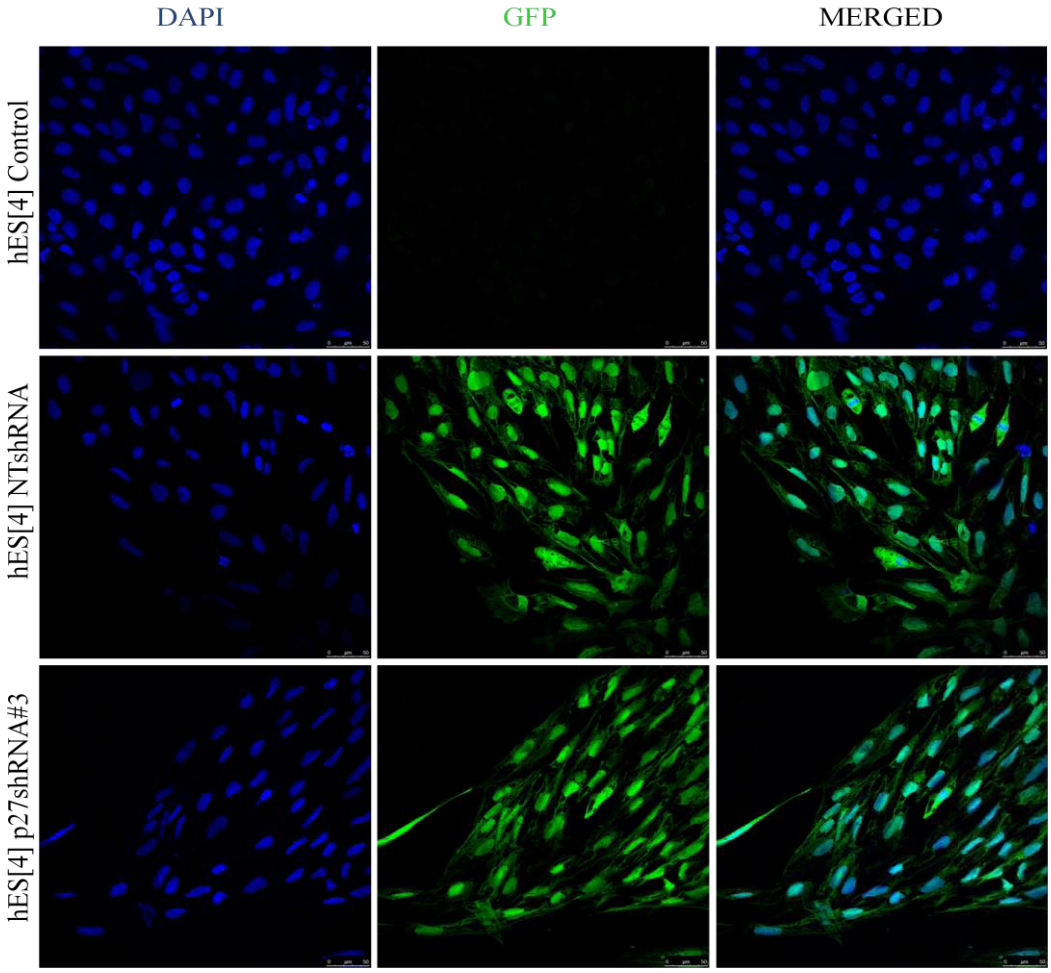

Figure 53. Analysis of nuclear morphology in $p27^{Kip1}$ knockdown human embryonic stem cells did not show evidence of apoptosis. Representative fluorescence microscopy images of hES[4] transduced with p27shRNA#3 or control NTshRNA constructs and left to grow for several days. Cells were fixed with 4% paraformaldehyde for 20 minutes at room temperature, and subsequently stained with DAPI (blue) for visualization of the nuclei. The same procedure but using uninfected hESC was carried out as an additional control. Note that $p27^{Kip1}$ knockdown hESC did not present nuclear fragmentation. Shown are the representative results obtained in three independent experiments. Scale bars: 50 μm.

In summary, taken together these results showed that $p27^{Kip1}$ did not seem to affect apoptosis in hESC, consequently we proceeded to find out if $p27^{Kip1}$ overexpressing cells followed another cell fate. As was explained above, another fate that cells can follow once they have exited the cell cycle is senescence. Senescence is highly related to cell aging (Blomen and Boonstra 2007) and is the culmination of the limited capacity to replicate of most normal somatic cells. Senescence is an arrested state in which the cell remains viable but displays altered patterns of gene and protein expression (Goldstein 1990). Senescent cells are characterized by a flattened and enlarged cell size, expression of pH dependent β-galactosidase activity (Dimri, Lee et al. 1995), and an altered pattern of gene expression (Cristofalo, Volker et al. 1998).

Human embryonic stem cell lines have an infinite proliferative life-span due to the expression of high levels of telomerase activity. Telomerase is a ribonucleoprotein that adds telomere repeats to chromosome ends and is involved in maintaining telomere length which plays an important role in replicative life-span. Diploid human somatic cells do not express telomerase, have shortened telomeres with age, and enter replicative senescence after a finite proliferative life-span in tissue culture (Thomson, Itskovitz-Eldor et al. 1998). Given the enlarged and flattened cell phenotype, we proceeded to determine if $p27^{Kip1}$ overexpressing hESC were senescent. In view of the fact that β-galactosidase activity at pH 6 is present only in senescent cells and is not found in presenescent, quiescent, or immortal cells, we proceeded to detect β-galactosidase activity at pH 6 in $p27^{Kip1}$ overexpressing hESC. To this end, hESC were transduced with $p27^{Kip1}$ or control GFP coding sequences. After the infection, cells were seeded in tissue culture dishes with an additional 1 mL of hESC medium. The next day, the medium was changed, and cells were left to grow for 4 days in the presence or absence of doxycycline in the culture medium. The same procedure but using uninfected cells was carried out as an additional control. After this time had elapsed β-galactosidase activity at pH 6 was assessed. To this end, cells were partially fixed, so as to not inactivate the β-galactosidase enzyme, at room temperature, washed extensively to remove fixative solution and allow the enzyme to function, and finally incubated at 37ºC for 48 hours in staining solution containing a chromogenic substrate: 5-bromo-4-chloro-3-indolyl-βD-galactopyranoside (X-gal).

Easily distinguished large $p27^{Kip1}$ overexpressing hESC were detected after culture in the absence of doxycycline, however when observed under a light microscope we could not see development of blue color indicative of β-galactosidase activity in these cells, thus demonstrating that $p27^{Kip1}$ overexpressing hESC were not senescent (data not shown). We did not detect β-galactosidase activity in cells transduced with control GFP coding sequence, cells treated with doxycycline, or uninfected cells either, consistent with previous reports showing that ESC have an unlimited replicative life-span.

In conclusion, these analyses demonstrated that $p27^{Kip1}$ overexpressing hESC were not senescent, consequently, and in order to clarify the significance of the phenotype of $p27^{Kip1}$ overexpressing hESC, we investigated whether $p27^{Kip1}$ overexpressing hESC were differentiating, the third fate that cells can adopt once they exit the cell cycle during G_1 phase. To this end, the expression of a focused panel of genes involved in pluripotency and differentiation of hESC was analyzed by qRT-PCR analysis. Human embryonic stem cells were transduced with $p27^{Kip1}$ or control GFP coding sequences and grown in the absence of doxycycline for 4 days. Pure population of $p27^{Kip1}$ overexpressing hESC was selected by Fluorescence Activated Cell Sorting (FACS) based on pulse width intensity signal and G_1 phase staining. The same procedure but using GFP transduced cells was carried out as a control (Figure 54).

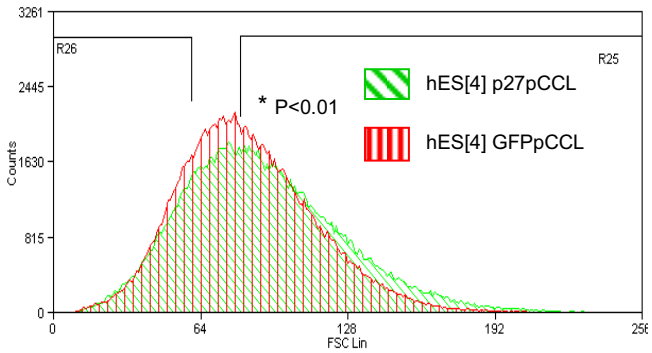

Figure 54. Cell sorting of $p27^{Kip1}$ overexpressing human embryonic stem cells based on size and cell cycle phase. Quantitative flow cytometry analysis of the pulse width intensity signal for $G_0/_1$ gated hES[4] transduced with lentiviral vectors encoding $p27^{Kip1}$ (green) or control GFP (red) coding sequences, and left to grow without doxycycline in the culture medium for 4 days. $p27^{Kip1}$ overexpressing hESC displayed a statistically significant increase in the pulse width intensity mean compared to control cells. Differences were evaluated by Student´s *t*-test. Comparisons vs. control: *P<0.01. $G_0/_1$ phase residing population was selected by staining alive cells with Hoechst 33342. Of this selected cells, largest cells from either, $p27^{Kip1}$ overexpressing or GFP expressing hESC were separated from smallest ones based on pulse width signal at comparable cell numbers (58% population). Shown are the representative results of two independent experiments.

Firstly, we checked whether cells selected by FACS overexpressed $p27^{Kip1}$. To this end, the expression levels of $p27^{Kip1}$ mRNA of cells FACS sorted were measured by qRT-PCR analysis in both $p27^{Kip1}$ and control GFP transduced hESC (Figure 55A). Fluorescence Activated Cell Sorting selection of $p27^{Kip1}$ overexpressing hESC was also validated at the protein level by Western blot analysis (Figure 55B).

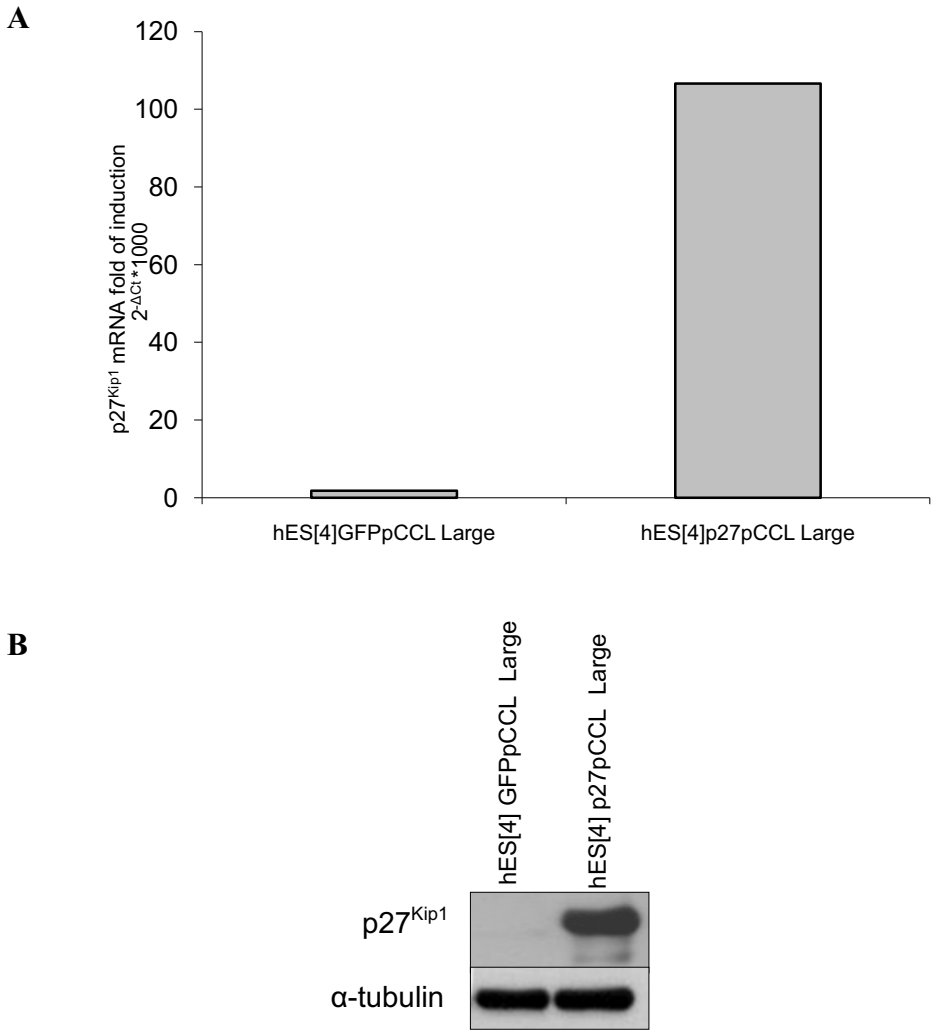

Figure 55. Fluorescence Activated Cell Sorting of $p27^{Kip1}$ overexpressing human embryonic stem cells. (**A**) Quantitative RT-PCR analysis of $p27^{Kip1}$ expression in Fluorescence Activated Cell Sorting **(**FACS) sorted cell fractions of hES[4] transduced with lentiviral vectors encoding $p27^{Kip1}$ or control GFP coding sequences and left to grow without doxycycline in the culture medium for 4 days. After this time had elapsed, cells were trypsinizated, stained with Hoechst 33342 for 30 minutes at 37ºC, and large cells, based on pulse width intensity signal, separated by FACS sorting at comparable cell numbers (58% population). Relative mRNA expression levels were calculated using the comparative threshold cycle method relative to human GAPDH and multiplied by 1000 to simplify data presentation. (**B**) Western blot analysis of $p27^{Kip1}$ expression using 10 µg of protein from FACS sorted whole cell extracts of hES[4] transduced with $p27^{Kip1}$ or control GFP coding sequences, and left to grow without doxycycline in the culture medium for 4 days. α-tubulin was used as a loading control.

Results confirmed that $p27^{Kip1}$ overexpressing hESC displayed an increase of the pulse width intensity, and moreover could be efficiently selected by FACS sorting. These cells displayed an increased expression of $p27^{Kip1}$ at the mRNA (approximately 100-fold) and protein levels compared to controls.

Then, we proceeded to analyze the transcriptional profile of 84 key genes involved in hESC maintenance and differentiation by qRT-PCR analysis. The array included hESC-specific genes that define the "stemness" of the cells and that maintain their pluripotent and self-renewal characteristics. The array also included differentiation markers that could be used to monitor the early events of hESC differentiation (Figure 56A).

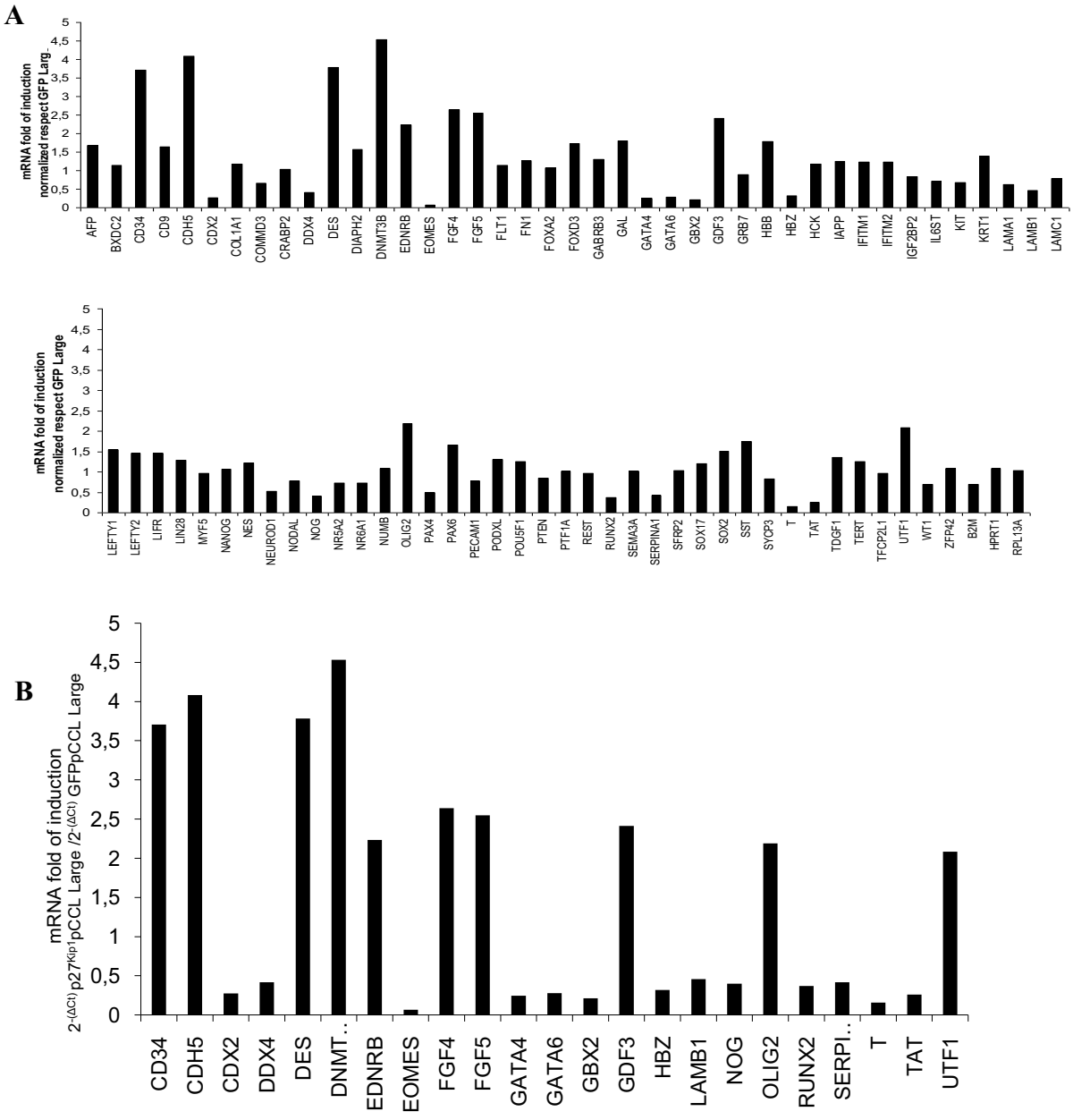

Figure 56. Analysis of human embryonic stem cells maintenance and differentiation genes in p27^{Kip1} overexpressing human embryonic stem cells. (**A**) Analysis of 84 key genes involved in maintenance of "stemness" and differentiation of hESC was performed with Human Embryonic Stem Cell RT^2 Profiler PCR Array which was purchased from SuperArray Biosciences Corporation. For the analysis, hES[4] were transduced with p27^{Kip1} or control GFP lentiviral vectors for 1 hour in suspension at 37ºC and 5% CO_2 atmosphere. After this time had elapsed, cells were seeded with additional hESC medium. The next day, the medium was changed, and cells were left to grow without doxycycline in the culture medium for 4 days. After this time had elapsed, cells were trypsinizated, stained with Hoechst 33342 for 30 minutes at 37ºC, and large cells, based on pulse width intensity signal, separated by FACS sorting at comparable cell numbers (58% population). RNA was isolated and qRT-PCR analysis performed with 500 ng of RNA. Relative mRNA expression levels were calculated using the comparative threshold cycle method and were expressed relative to control GFP (=1). (**B**) Values that were upregulated twice or more, or downregulated 50% or more were considered as significant cut offs.

Genes upregulated 2 or more times

Unigene	GeneBank	Symbol	Description
Hs.643024	NM_006892	DNMT3B	DNA (cytosine-5-)methyltransferase 3 beta
Hs.76206	NM_001795	CDH5	Cadherin 5
Hs.594952	NM_001927	DES	Desmin
Hs.374990	NM_001773	CD34	CD34 molecule
Hs.1755	NM_002007	FGF4	Fibroblast growth factor 4
Hs.37055	NM_004464	FGF5	Fibroblast growth factor 5
Hs.86232	NM_020634	GDF3	Growth differentiation factor 3
Hs.82002	NM_000115	EDNRB	Endothelin receptor type B
Hs.176977	NM_005806	OLIG2	Oligodendrocyte lineage transcription factor 2
Hs.458406	NM_003577	UTF1	Undifferentiated embryonic cell transcription factor 1

Genes downregulated 50% or more

Unigene	GeneBank	Symbol	Description
Hs.591663	NM_005442	EOMES	Eomesodermin homolog (Xenopus laevis)
Hs.389457	NM_003181	T	T,brachyury homolog (mouse)
Hs.184946	NM_001485	GBX2	Gastrulation brain homeobox 2
Hs.243987	NM_002052	GATA4	GATA binding protein 4
Hs.174249	NM_001265	CDX2	Caudal type homeobox 2
Hs.514746	NM_005257	GATA6	GATA binding protein 6
Hs.705386	NM_000353	TAT	Tyrosine aminotransferase
Hs.585357	NM_005332	HBZ	Hemoglobin, zeta
Hs.535845	NM_004348	RUNX2	Runt-related transcription factor 2
Hs.223581	NM_024415	DDX4	DEAD (Asp-Glu-Ala-Asp) box polypeptide 4, VASA
Hs.248201	NM_005450	NOG	Noggin
Hs.129706	NM_006193	PAX4	Paired box 4
Hs.270364	NM_005559	LAMA1	Laminin, alpha 1
Hs.650585	NM_002291	LAMB1	Laminin, beta 1
Hs.525557	NM_000295	SERPINA1	Serpin peptidase inhibitor, clade A, member 1
Hs.72981	NM_002500	NEUROD1	Neurogenic differentiation 1

Table 4. List of genes displaying values upregulated twice or more, or downregulated 50% or more in the Human Embryonic Stem Cell RT Profiler PCR Array for $p27^{Kip1}$ overexpresing human embryonic stem cells. Table showing symbol and description of genes from the Human Embryonic Stem Cell RT Profiler PCR Array that were upregulated twice or more, or downregulated 50% or more in $p27^{Kip1}$ overexpresing human embryonic stem cells.

Human Embryonic Stem Cell profiler array values that were upregulated twice or more, or downregulated 50% or more were considered as significant cut offs (Figure 56B and Table 4). Gene expression profiling values of this array showed that $p27^{Kip1}$ overexpression did not result in a significant change of the master pluripotency factors such as *OCT3/4*, *NANOG*, or *SOX2*. These data were further validated by qRT-PCR analysis of the above mentioned and other key pluripotency factors. Moreover, the opposite approach, that is, to check if loss of $p27^{Kip1}$ could be affecting expression of these pluripotency factors was also performed. To this end, hESC were transduced with the p27shRNA construct that more efficiently repressed $p27^{Kip1}$ expression

(p27shRNA#3) and with control NTshRNA construct. Uninfected hESC were also used as additional controls (Figure 57).

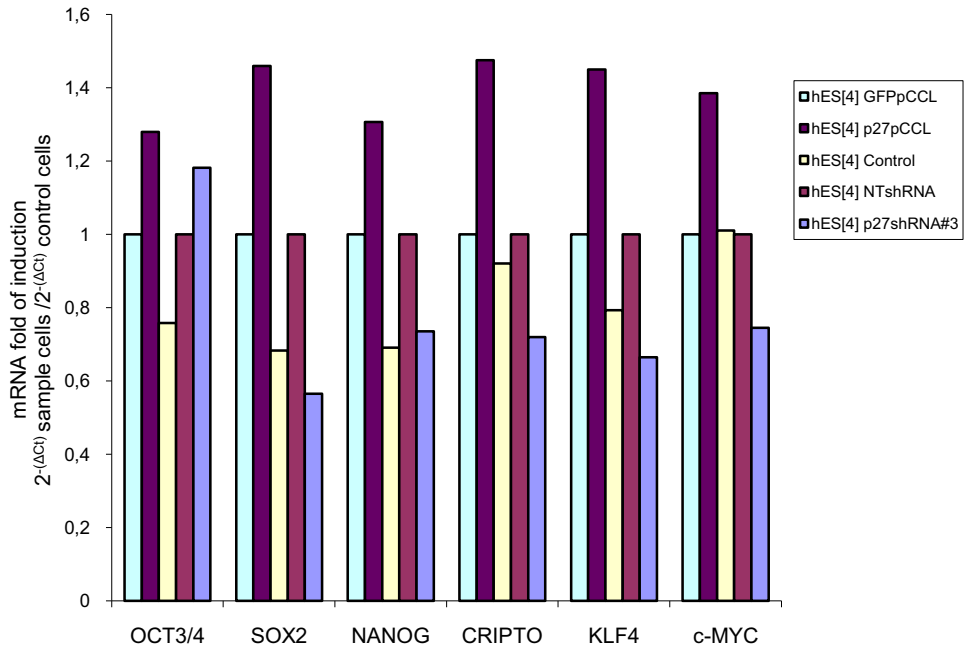

Figure 57. p27^{Kip1} did not affect expression of master pluripotency genes in human embryonic stem cells. Quantitative RT-PCR validation of master pluripotency genes in p27^{Kip1} overexpressing and p27^{Kip1} knockdown hES[4]. For the overexpression analysis, hES[4] were transduced with p27^{Kip1} or control GFP coding sequences. For the knockdown analysis, hES[4] were transduced with p27shRNA#3 or control NTshRNA constructs. Subsequently, cells were seeded with additional hESC medium. The next day, the medium was changed, and cells were left to grow without doxycycline in the culture medium. Uninfected hES[4] were used as additional controls. Relative mRNA expression levels were calculated using the comparative threshold cycle method and are expressed relative to controls (=1).

Quantitative RT-PCR analysis confirmed gene expression profiling values obtained in the array showing that p27^{Kip1} did not affect significantly the expression of key pluripotency factors in hESC in these experimental conditions. But, gene expression profiling showed that p27^{Kip1} overexpression resulted in upregulation and downregulation of specific differentiation genes. Among the more upregulated genes were *CD34*, *CADHERIN 5*, *DESMIN*, and DNA (cytosine-5-) methyltransferase 3 beta (*DNMT3B*). Among those showing more than 75% downregulation were: Gastrulation Brain Homeobox 2 (*GBX2*), GATA binding protein 6 (*GATA 6*), and early mesoderm differentiation marker, *BRACHYURY* (T) (Figure 56B and List 4).

Then, we proceeded to validate the expression of the above mentioned genes by qRT-PCR analysis in both, p27^{Kip1} overexpressing and p27^{Kip1} knockdown hESC

(Figure 58). We hypothesized that if overexpression of $p27^{Kip1}$ was affecting any gene then we should see the reverse effect in knockdown cells. GFP transduced hESC and NTshRNA transduced hESC were used as negative controls, respectively.

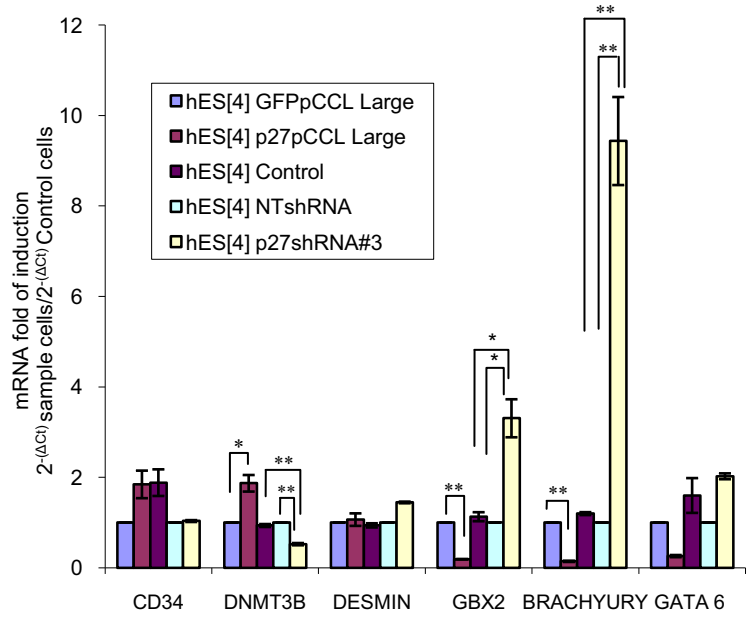

Figure 58. Analysis of human embryonic stem cells maintenance and differentiation genes reveals a novel role for $p27^{Kip1}$ in the regulation of *BRACHYURY*. Quantitative RT-PCR validation of genes showing more important expression changes in array analysis for hESC maintenance and differentiation genes (see Figure 56 and List 4). Quantitative RT-PCR analysis were performed in $p27^{Kip1}$ overexpressing and $p27^{Kip1}$ knockdown hES[4]. For the overexpression analysis, hES[4] were transduced with $p27^{Kip1}$ or control GFP coding sequences. For the knockdown analysis, hES[4] were transduced with p27shRNA#3 or control NTshRNA constructs. Uninfected hES[4] were used as additional controls. Relative mRNA expression levels were calculated using the comparative threshold cycle method and are expressed relative to controls (=1). Results represent the mean ± standard deviations of three independent experiments. Differences were evaluated by two-tailed Student´s *t*-test. Comparisons *vs*. controls:
*P < 0.05; **P < 0.01.

Quantitative RT-PCR analysis did not show a significant change in the expression levels of *CD34* and *DESMIN* with $p27^{Kip1}$ overexpression, disproving the array results. Moreover, this analysis did not show a significant change in the expression levels of *CD34* and *DESMIN* with $p27^{Kip1}$ knockdown either. However, it could be confirmed an upregulation of *DNMT3B* of approximately two times in $p27^{Kip1}$ overexpressing hESC compared to controls. Conversely, a downregulation of *DNMT3B* was observed in $p27^{Kip1}$ knockdown hESC.

The significant changes in gene expression were the downregulation of *GBX2* and *BRACHYURY* with $p27^{Kip1}$ overexpression in hESC, confirming the results obtained in

the array analysis. These values were statistically significantly different with probability values of $1.67x10^{-5}$ and 0.00011, respectively. On the contrary, expression analysis of these genes in $p27^{Kip1}$ knockdown hESC revealed the opposite results being *GBX2* and *BRACHYURY* upregulated in $p27^{Kip1}$ knockdown hESC. Again these values were statistically significantly different with probability values of 0.016 and 0.0065, respectively. Although *GATA 6* showed the same trend, that is, downregulated with $p27^{Kip1}$ overexpression and upregulated in $p27^{Kip1}$ knockdown hESC, values were not statistically significantly different.

Interestingly, *BRACHYURY* was upregulated approximately 9 times compared to controls in $p27^{Kip1}$ knockdown hESC. Conversely, the overexpression of $p27^{Kip1}$ reversed this trend producing a downregulation of *BRACHYURY* of approximately 60% (Figure 58).

These data suggested a new role for $p27^{Kip1}$ in the regulation of *BRACHYURY*. Given this important and novel effect we decided to measure BRACHYURY expression levels at the protein level in $p27^{Kip1}$ overexpressing and knockdown hESC by Western blot and immunofluorescence analyses (Figure 59).

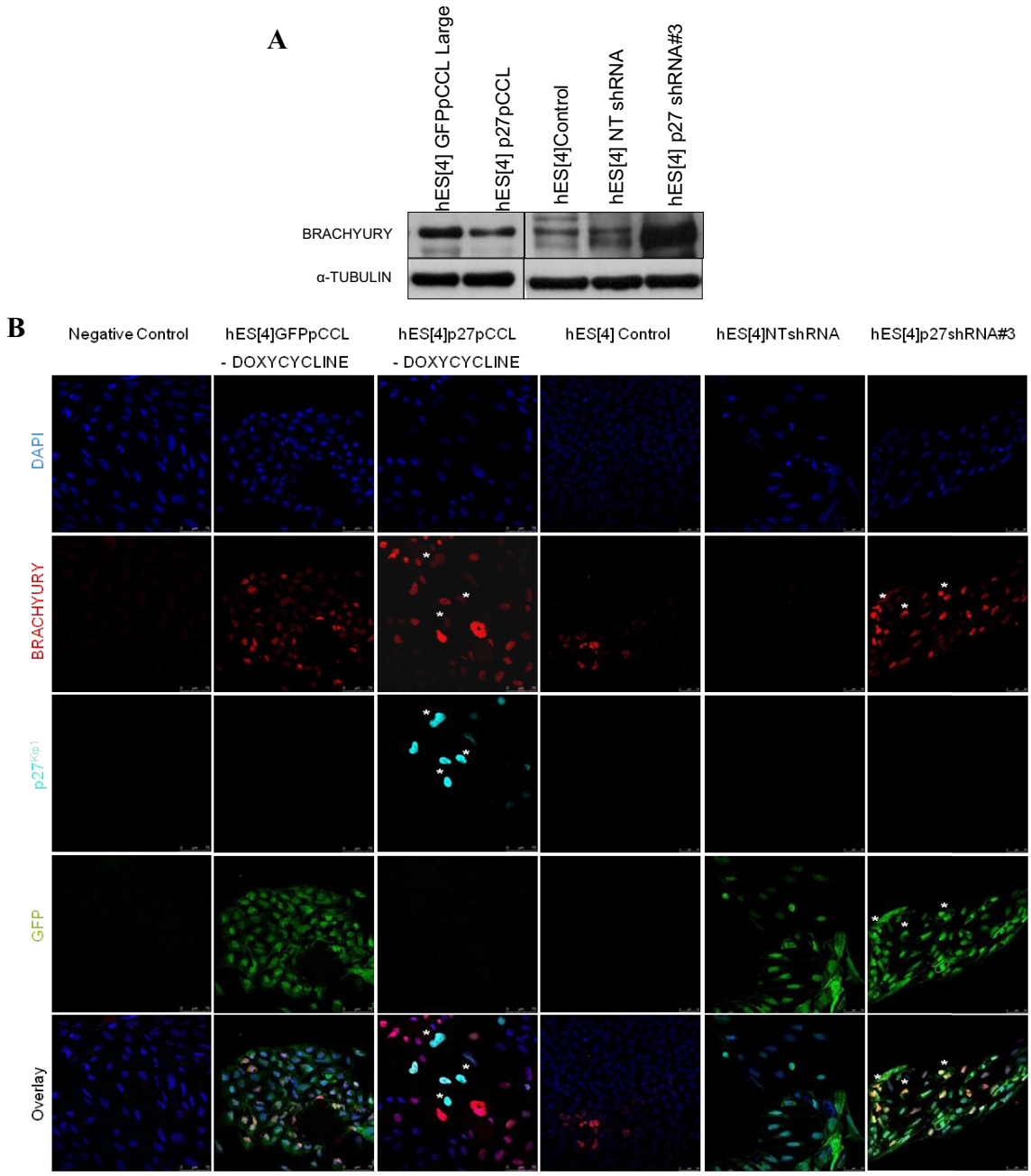

Figure 59. p27^{Kip1} is involved in the regulation of BRACHYURY levels in human embryonic stem cells. (**A**) Western blot analysis of BRACHYURY expression in p27^{Kip1} overexpressing and p27^{Kip1} knockdown hES[4] using 16 µg of protein. For the overexpression analysis, hES[4] were transduced with p27^{Kip1} or control GFP coding sequences. For the knockdown analysis, hES[4] were transduced with p27shRNA#3 or control NTshRNA constructs. Uninfected hES[4] were used as additional controls. α-TUBULIN was used as a loading control. Shown are the representative results obtained in two independent experiments. Note the notable increase of BRACHYURY in p27^{Kip1} knockdown hESC. (**B**) Immunofluorescence analysis of BRACHYURY expression (red) in p27^{Kip1} overexpressing and p27^{Kip1} knockdown hESC. The first column corresponds to immunoblot negative control cells which were only incubated with CY-conjugated secondary antibodies. p27^{Kip1} and GFP overexpression are visualized in cyan and green, respectively. Nuclei were counterstained with DAPI (blue). Shown are the representative results obtained in two independent experiments. Note that p27^{Kip1} overexpressing cells never expressed BRACHYURY (see white asterisks), just the opposite behaviour than p27^{Kip1} knockdown cells which usually presented colocalization, represented by yellow colour (see white asterisks). Scale bars: 50 and 75 µm.

Western blot analysis showed that BRACHYURY was highly upregulated in $p27^{Kip1}$ knockdown hESC, and conversely $p27^{Kip1}$ overexpression caused a downregulation of BRACHYURY compared to control cells thus confirming qRT-PCR results (Figure 59A). These results were also confirmed by immunofluorescence analysis where we never detected expression of BRACHYURY in $p27^{Kip1}$overexpressing hESC. $p27^{Kip1}$ knockdown hESC were easily recognized due to their striking and characteristic elongated shaped colonies which presented even elongated nuclei. In these colonies it was frequently observed the presence of BRACHYURY. The spatial overlap between BRACHYURY expression (red) and cells transduced with p27shRNA#3 construct (green) was evidenced by development of yellow colour (Figure 59B).

These results revealed a novel role for $p27^{Kip1}$ in the regulation of BRACHYURY. This was an unexpected result, since Brachyury has been traditionally related to the specification of mesoderm and axis elongation (Showell, Binder et al. 2004; Technau and Scholz 2003). Mesoderm formation in development involves an epithelial to mesenchymal transition (EMT) process. The EMT is a fascinating phenotypic change that is undertaken by embryonic cells in physiological conditions. It involves profound changes in the morphology, such as loss of epithelial characteristics and acquisition of a fibroblastoid phenotype, and also involves changes in the behavior of epithelial cells such as acquisition of migratory properties (Nieto 2009).

Given such effect of $p27^{Kip1}$ on BRACHYURY, we proceeded to evaluate if other key mesoderm or EMT markers were also affected by the modification of the expression levels of $p27^{Kip1}$ by qRT-PCR analysis (Figure 60).

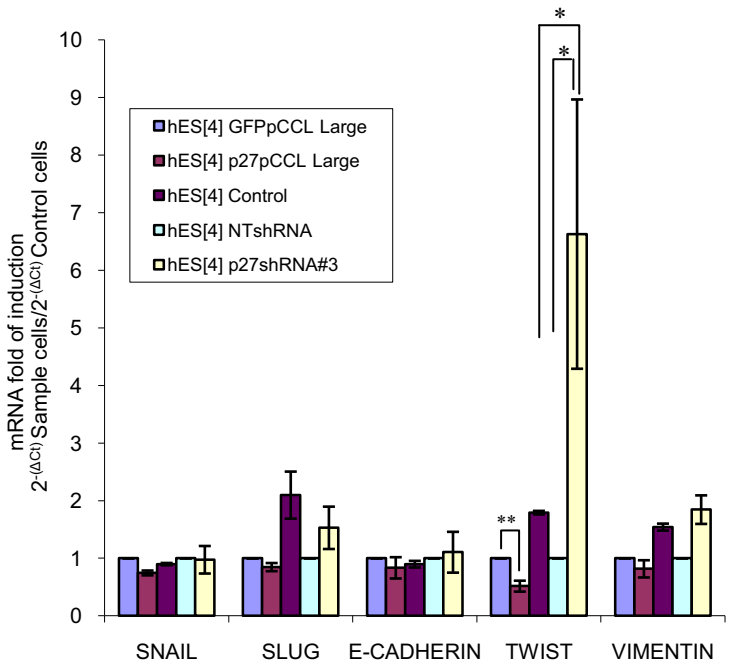

Figure 60. Analysis of key mesoderm genes reveals a novel role for p27^{Kip1} in the regulation of *TWIST* in human embryonic stem cells. Quantitative RT-PCR analysis of mesoderm genes in p27^{Kip1} overexpressing and p27^{Kip1} knockdown hES[4]. For the overexpression analysis, hES[4] were transduced with p27^{Kip1} or control GFP coding sequences. For the knockdown analysis, hES[4] were transduced with p27shRNA#3 or control NTshRNA constructs. Uninfected hES[4] were used as additional controls. Relative mRNA expression levels were calculated using the comparative threshold cycle method and are expressed relative to controls (=1). Results represent the mean ± standard deviations of two independent experiments. Differences were evaluated by ANOVA statistical analysis. Comparisons *vs*. controls: *P < 0.05; **P < 0.01.

Interestingly, this analysis revealed an upregulation of *TWIST* 6-fold with p27^{Kip1} loss of function compared to controls, and conversely a downregulation in p27^{Kip1} overexpressing hESC. We did not find statistically significantly differences in expression of the other genes in either p27^{Kip1} overexpressing or p27^{Kip1} knockdown hESC suggesting that the effect of p27^{Kip1} was specific for *TWIST*. We could not test TWIST protein levels in these cells given that were not specific antibodies for TWIST. Given that p27^{Kip1} expression was detected principally in the nuclei, we tested if p27^{Kip1} was directly affecting the transcriptional activation of the *TWIST1* promoter. To this end, we performed chromatin immunoprecipitation (ChIP) experiments (Figure 61).

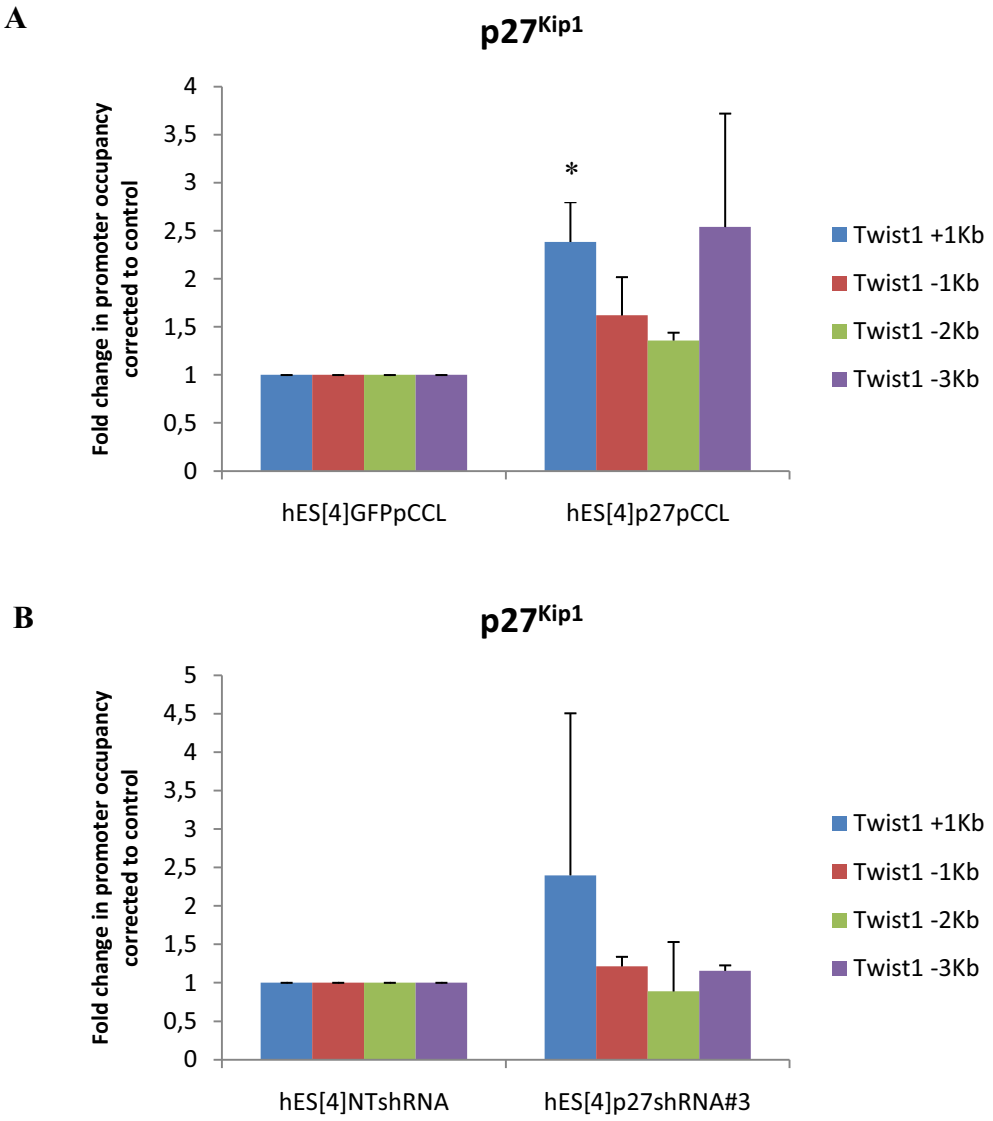

Figure 61. Chromatin immunoprecipitation experiments of p27^{Kip1} occupancy along *TWIST1* promoter in human embryonic stem cells. Soluble chromatin was prepared from asynchronously growing p27^{Kip1} overexpressing hES[4] (**A**), p27^{Kip1} knockdown hES[4] (**B**), or respective controls and immunoprecipitated with antibodies directed against p27^{Kip1}. Final DNA extractions were amplified using pairs of primers that covered 4000 Kb of *TWIST1* promoter starting from +1.0 Kb to -3.0 Kb from the ATG and were analyzed by real-time PCR. Results represent the mean ± standard deviations of two independent experiments and are expressed relative to controls (=1). Differences were evaluated by two-tailed Student´s *t*-test. Comparisons *vs*. controls: *P < 0.05.

We searched for p27^{Kip1} occupancy along 4000 Kb of *TWIST1* promoter starting from +1.0 Kb to -3.0 Kb from the ATG. We found that p27^{Kip1} protein was recruited to +1.0 Kb site of *TWIST1* promoter in p27^{Kip1} overexpressing hESC based on a statistically significant two-fold increase compared to control cells (Figure 61A). We did not detect significant differences for p27^{Kip1} on *TWIST1* promoter occupancy in p27^{Kip1} knockdown cells where p27^{Kip1} protein levels had been reduced by short hairpin

RNAs (Figure 61B). The significant increase in +1.0 Kb site promoter occupancy suggested that $p27^{Kip1}$ had a direct role in the regulation of *TWIST1* gene expression in hESC, but if this was by direct or indirect binding to the promoter of *TWIST1* remains unknown.

Mesoderm differentiation involves an EMT process and dissociated adherence junctions. Regulation of E–Cadherin is a hallmark of the EMT process and for this reason we investigated further if the protein levels were affected in the characteristic elongated shaped phenotype of $p27^{Kip1}$ knockdown hESC by immunofluorescence analysis (Figure 62).

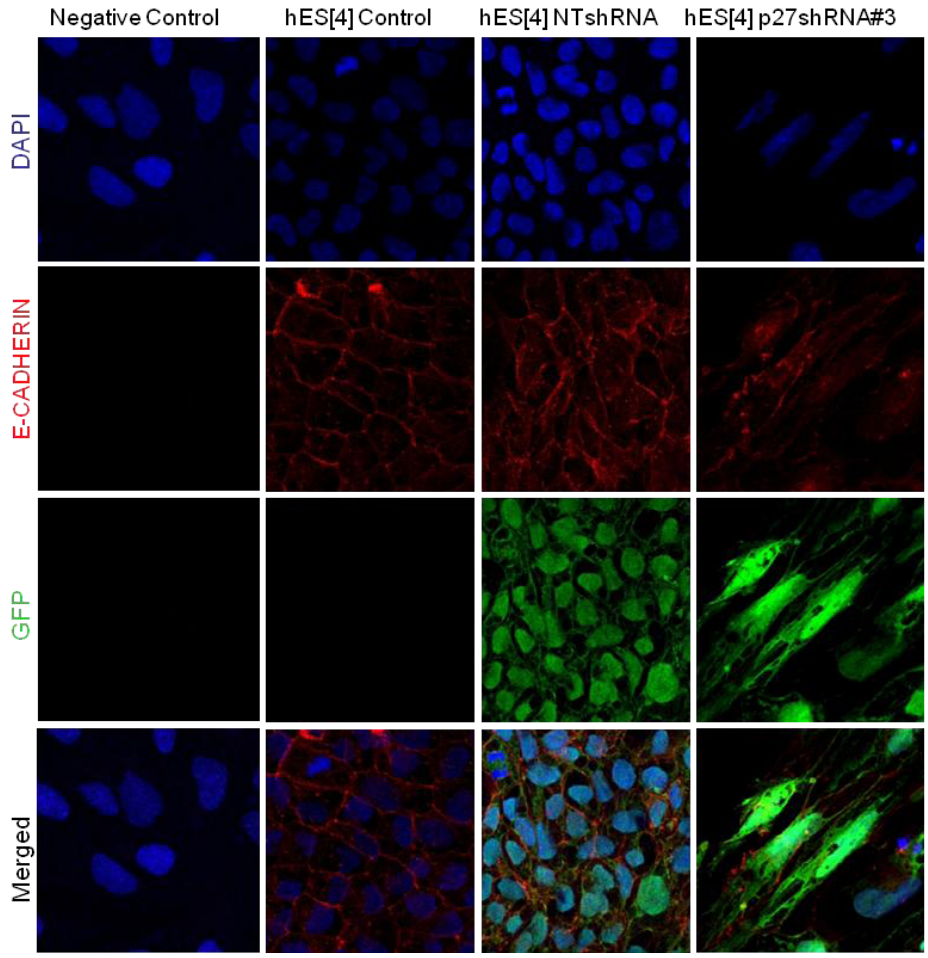

Figure 62. Analysis of E-CADHERIN expression in $p27^{Kip1}$ depleted human embryonic stem cells. Immunofluorescence analysis of E-CADHERIN expression (red) in $p27^{Kip1}$ knockdown hES[4]. For the generation of $p27^{Kip1}$ knockdown cells, hES[4] were transduced with p27shRNA#3 or control NTshRNA constructs. After infection, cells were seeded with additional hESC medium. The next day, the medium was changed and cells were left to grow for several days until appearance of characteristic phenotype. The same procedure but using uninfected cells was carried out as an additional control. The first column corresponds to immunoblotting negative control cells which were only incubated with CY-conjugated secondary antibodies. Nuclei were counterstained with DAPI (blue). Scale bars: 50 µm.

Preliminary studies of E-CADHERIN expression showed that $p27^{Kip1}$ knockdown hESC appeared to have less E-CADHERIN in the plasma membrane compared to controls. The lack of regulation of *E-CADHERIN* at gene level suggested that $p27^{Kip1}$ could be involved in the regulation of E-CADHERIN at a post-transcriptional level. Further experiments are required to clarify if this effect of $p27^{Kip1}$ on E-CADHERIN is direct or indirect.

Given that pluripotency is the capacity to give rise to all cell types of the foetus, we tested pluripotency in hESC as their ability to produce a range of well differentiated progeny representative of the three primary germ layers (ectoderm, mesoderm, and endoderm) *in vitro*.

To determine if the regulation of mesoderm markers by $p27^{Kip1}$ affected the differentiation capacity of hESC, we performed some preliminary experiments of differentiation in $p27^{Kip1}$ depleted hESC. To this end, hESC were transduced with p27shRNA#3 or control NTshRNA constructs. After infection, cells were seeded in tissue culture dishes with additional hESC medium. The next day the medium was changed and cells were left to grow for several days until compact colonies appeared. Cells were then differentiated by embryoid body (EB) generation. The same procedure but using uninfected cells was carried out as an additional control (Figure 63).

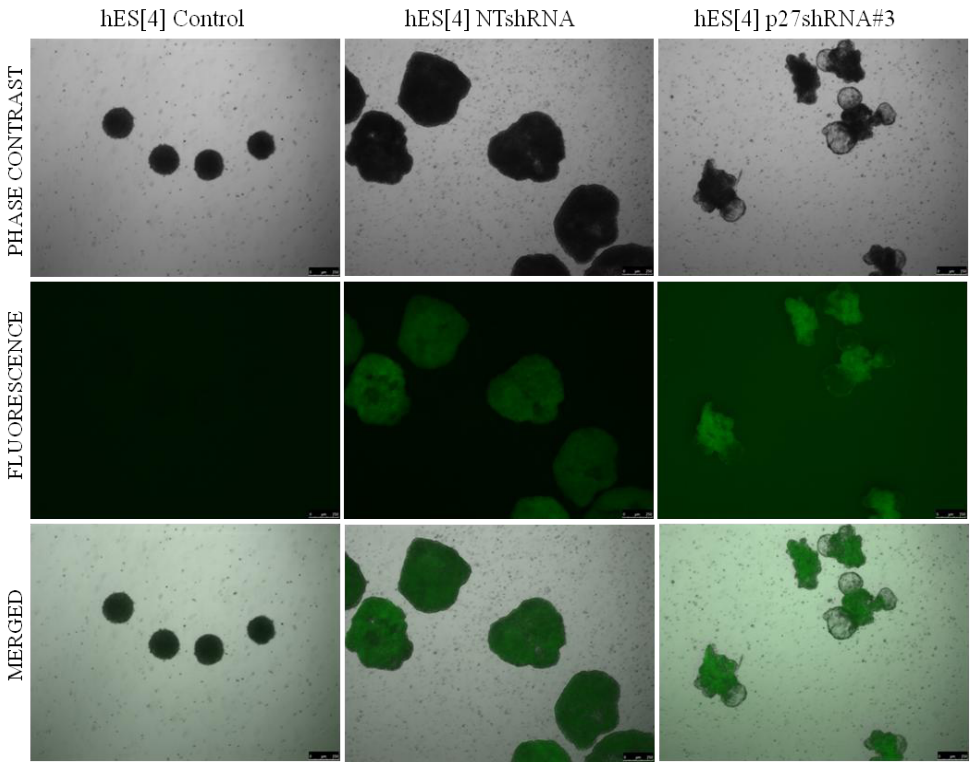

Figure 63. Differentiation analysis of p27^{Kip1} depleted human embryonic stem cells. Representative phase contrast and fluorescence microscopy images of embryoid bodies (EB) generated from hES[4] transduced with p27shRNA#3 or control NTshRNA constructs. After infection, cells were left to grow for several days until compact colonies appeared. Cells were then trypsinized for single cell suspension, seeded in wells of 96-well v-bottom low attachment plates, and subsequently centrifuged to allow aggregation of the cells. Embryoid bodies were cultured in suspension for 3-4 days. The same procedure but using uninfected cells was carried out as an additional control. Scale bars: 250 μm.

Results showed that hESC were effectively transduced given that almost 100% of cells transduced with p27shRNA#3 or control NT shRNA constructs expressed GFP fluorescence. Uninfected cells and control NTshRNA transduced cells generated round and compact EB after 3-4 days of culture in suspension. On the contrary, p27^{Kip1} knockdown hESC generated irregular, cystic EB suggesting that these cells were unable or had an impaired capacity to differentiate. Cavitations of EB are the result of programmed cell death, and this first wave of cell death is considered indispensable for morphogenesis (Joza, Susin et al. 2001). The fact that p27^{Kip1} knockdown hESC had premature cavitations compared to controls suggested that it was impairing survival or increasing apoptosis. Another possibility is that it could be affecting specific differentiation lineages. Given that recently it has been shown that p27^{Kip1} deficient mESC have an impairment of normal differentiation after treatment with Retinoic Acid (Bryja, Pachernik et al. 2004), and given the fact that Retinoic Acid is an inducer of

neuronal differentiation and hence ectoderm lineage, we differentiated $p27^{Kip1}$ depleted hESC towards neuroectoderm and mesoderm lineages. To this end, hESC were transduced with p27shRNA#3 or control NTshRNA constructs. After infection, cells were left to grow for several days and subsequently differentiated through EB generation. Embryoid bodies were further cultured in mesoderm or neuroectoderm specific differentiation culture mediums for 30 days. The same procedure but using uninfected cells was carried out as an additional control.

Firstly, the percentage of $p27^{Kip1}$ knockdown in differentiated hESC was measured by qRT-PCR analysis (Figure 64).

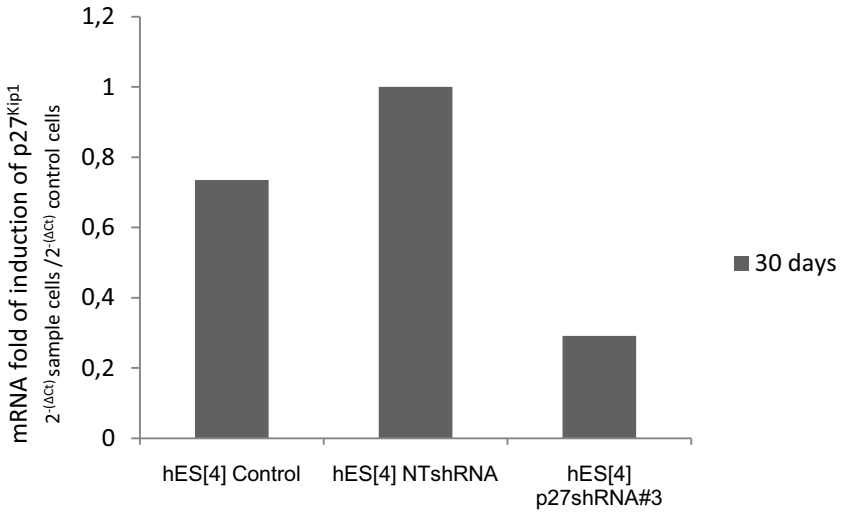

Figure 64. $p27^{Kip1}$ shRNA mediated knockdown in differentiated human embryonic stem cells. Quantitative RT-PCR analysis of $p27^{Kip1}$ expression in hES[4] transduced with p27shRNA#3 or control NT shRNA constructs and subsequently differentiated by embryoid body (EB) generation. Embryoid bodies were cultured in suspension with neuroectoderm inducing medium for 6 days. After this time had elapsed, EB were seeded onto matrigel-coated plates with the same media plus 10^{-6} M Retinoic Acid for 30 days. The medium was changed every day. Uninfected hES[4] were used as additional controls. Relative mRNA expression levels were calculated using the comparative threshold cycle method and are expressed relative to control (=1).

These results confirmed a decrease in $p27^{Kip1}$ expression levels, of approximately 70%, in cells transduced with p27shRNA#3 construct compared to control NTshRNA transduced cells.

Then, cells cultured in mesoderm or neuroectoderm specific differentiation mediums for 30 days were immunostained with lineage-specific antibodies for mesoderm (α-Smooth Muscle Actin) or neuroectoderm (Nestin and β-Tubulin III) germ layers, respectively (Figure 65).

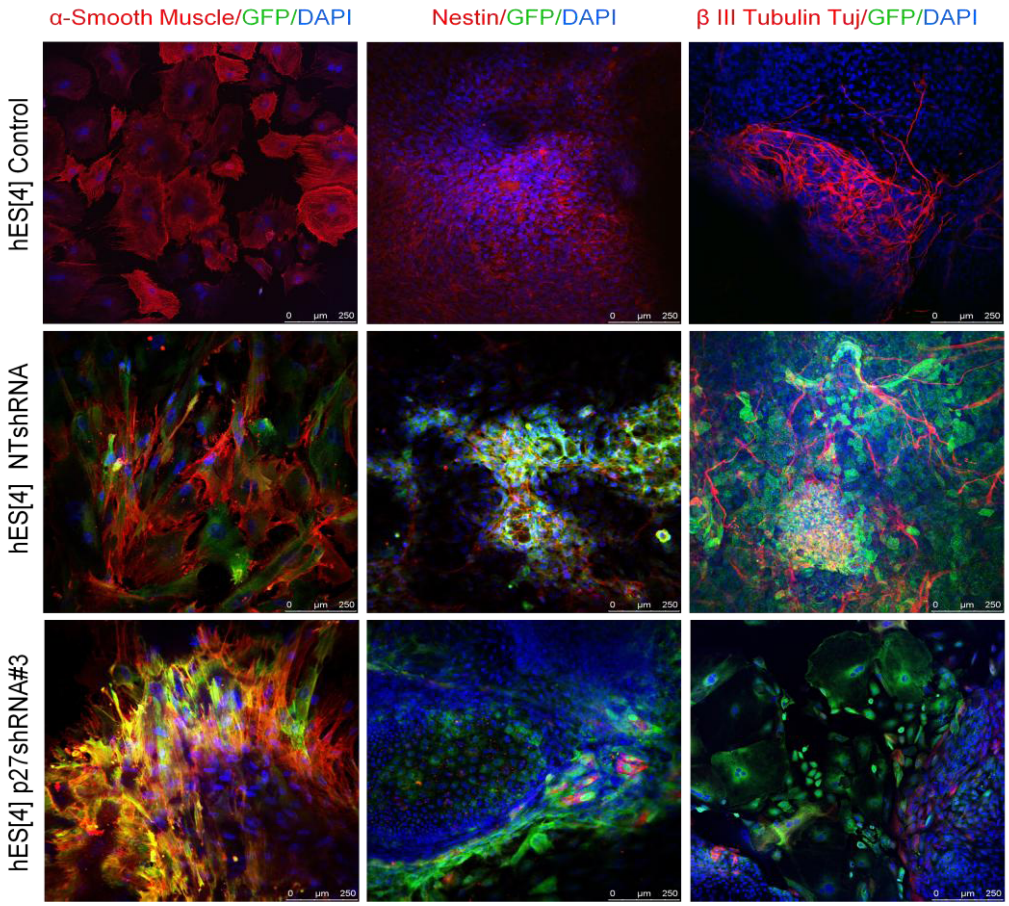

Figure 65. Immunofluorescence analysis reveals an impairment of $p27^{Kip1}$ depleted human embryonic stem cells to differentiate into neuroectoderm. Representative immunofluorescence images of $p27^{Kip1}$ knockdown hES[4] differentiated towards neuroectoderm or mesoderm lineages. For the analysis, hES[4] were transduced with p27shRNA#3 or control NTshRNA constructs for 1 hour in suspension at 37ºC and 5% CO_2 atmosphere. After this time had elapsed, cells were seeded with additional hESC medium. The next day, the medium was changed, and cells were left to grow for several days until compact colonies appeared. Cells were then trypsinized for single cell suspension, seeded in wells of 96-well v-bottom low attachment plates, and subsequently centrifuged to allow aggregation of the cells. For neuroectoderm differentiation, EB were cultured in suspension with neuroectoderm inducing medium for 6 days. After this time had elapsed, EB were seeded onto matrigel-coated chamber-slide flasks with the same media plus 10^{-6} M Retinoic Acid for 30 days. After this time had elapsed, cells were immunostained with Nestin (red) or β-Tubulin III (Tuj 1) (red) antibodies. For mesoderm differentiation, EB were seeded onto gelatin-coated chamber-slide flasks, and subsequently cultured with general differentiation medium supplemented with 100 µM Ascorbic Acid for 30 days. After this time had elapsed, cells were immunostained with α-Smooth Muscle Actin (red) antibodies. The same procedures but using uninfected cells were carried out as additional controls. Nuclei were counterstained with DAPI (blue). Scale bars: 250 µm.

These results showed that uninfected cells and control NTshRNA transduced cells effectively differentiated into neuroectoderm and mesoderm lineages judging by the high expression of specific differentiation markers. Moreover, NTshRNA transduced GFP cells effectively colocalized with specific differentiation markers as was evident by the development of yellow colour. Surprisingly, and in contrast to control cells we observed that loss of $p27^{Kip1}$ impaired proper differentiation of neuroectoderm judging by a striking reduction in the expression of Nestin and β-Tubulin III (Tuj1) immunostained positive cells. Moreover, in these cells we did not detect the typical axonal morphology observed in Nestin or β-Tubulin III-stained control cells, suggesting that these cells had an impaired capacity to differentiate into neuroectoderm. If this effect was due to a specific impairment of differentiation or to an increase of apoptosis of these cell types remains to be investigated.

Taken together, these data suggest that $p27^{Kip1}$ does not affect master pluripotency factors such as *OCT3/4*, *SOX2*, or *NANOG* in hESC, but regulates the mesoderm markers *BRACHYURY* and *TWIST* in undifferentiated conditions. These results suggest that $p27^{Kip1}$ has to be tightly regulated for the maintenance of the self-renewal and pluripotency properties of hESC through its regulation of these important differentiation genes. Changes in the balance of $p27^{Kip1}$ define the lineage commitment of hESC towards mesoderm, using undifferentiated conditions.

DISCUSSION

Regulation of the cell cycle in human embryonic stem cells

A considerable effort has been devoted to unravel the differentiation pathways towards specific cell types but less attention has been paid to the unusual proliferative properties of embryonic stem cells (ESC) and even less to those of human embryonic stem cells (hESC). The fact that ESC can give rise to tumours comprising the three embryonic germ layers when grafted into an adult host is believed to be due to the presence of undifferentiated cells and their unusual proliferative properties. This fact makes hESC cannot be used currently in clinical applications. A better understanding of the cell cycle is needed if hESC are going to be used in therapy. Thus, many basic questions about the biology of these cells and especially the study of the unusual proliferative properties of hESC need to be addressed if their potential is to be realized. Moreover, such studies will shed light on the mechanisms underlying proliferation and acquisition of malignant properties, such as undifferentiation, of tumour cells.

The unusual proliferative properties of ESC have been related to a unique cell cycle structure and mechanisms of cell cycle regulation that have been well described in mouse embryonic stem cells (mESC). Mouse embryonic stem cells use mechanisms to drive cell proliferation that are quite distinct from those in other somatic cell types (White and Dalton 2005; White, Stead et al. 2005; Faast, White et al. 2004; Burdon, Smith et al. 2002; Stead, White et al. 2002; Savatier, Lapillonne et al. 1996).

Firstly, we proceeded to confirm these data and we chose the J1 mESC line. To this end, we characterized the cell cycle profile of undifferentiated cells, by flow cytometry analysis, and confirmed that they had a low proportion of cells in $G_0/_1$ phase but a high proportion of cells in S phase. Upon differentiation, the proportion of cells in $G_0/_1$ phase increased progressively as differentiation proceeded, while that in S phase decreased. These results demonstrated that during differentiation the structure of the cell cycle of mESC changed and correlated with long generation times, consistent with previous studies (White, Stead et al. 2005; Stead, White et al. 2002).

We predicted that changes in cell cycle structure during differentiation could be accounted for a fundamental change in the cell cycle machinery. Moreover, we predicted that to self-renew, ESC had to choose continually enter the S phase and to avoid exit the cell cycle. The decisions to progress into the cell cycle or exit the cell cycle to follow other fates are made in the G_1 phase (Blomen and Boonstra 2007), and

for this reason we speculated that regulators of the G_1 to S transition had to develop an important role in the change of the cell cycle structure during differentiation.

With the aim of finding out the molecular mechanisms regulating this cell cycle structure change, we analyzed the protein levels of main G_1 to S phase regulators by Western blot in undifferentiated and differentiated mESC (see Figure 12, page 64). Western blot analyses showed that master pluripotency factor Oct3/4 decreased as cells differentiated, validating our differentiation protocol. Early G_1 phase cyclin D_1 and CDK4 appeared to increase with differentiation. On the contrary, late G_1 and S phase cyclins E and A, and CDK2 decreased with differentiation. On the other hand, cyclin dependent kinase inhibitors (CKIs) $p21^{Cip1}$ and $p27^{Kip1}$ were low expressed in undifferentiated cells, but they increased during differentiation. Interestingly, $p27^{Kip1}$ underwent a huge increase after 30 days of differentiation. Finally, Proliferating Cell Nuclear Antigen (PCNA), a protein important for both, DNA synthesis and DNA repair, and a marker of cell proliferation decreased during differentiation. These results coincide with previous work (White, Stead et al. 2005; Burdon, Smith et al. 2002; Stead, White et al. 2002; Savatier, Lapillonne et al. 1996), and are in agreement with the increase of G_1 phase and reduction of S phase with differentiation, suggesting a possible role for the cell cycle in the maintenance of the properties of ESC. Interestingly, the increase of $p27^{Kip1}$ during differentiation was inversely proportional to master pluripotency factor Oct3/4 suggesting a possible link between $p27^{Kip1}$ and maintenance of pluripotency.

Although during recent years there have been studies describing the cell cycle of mESC, only a limited amount of information is available about the cell cycle regulation of hESC. For this reason, one of the main aims of this thesis was the study of the cell cycle regulation of hESC. This was addressed **in Section 1 of Results**.

Similarly than mESC, hESC have a rapid generation time too due to a shortened G_1 phase (Becker, Ghule et al. 2006). However, hESC are grown under different conditions to mESC (they rely on basic fibroblast growth factor (bFGF) and not on leukaemia inhibitory factor (LIF) to maintain pluripotency). We hypothesized that basic cell cycle control mechanisms might be conserved between mouse and human pluripotent cells. With the aim of finding this out we proceeded to analyze the cell cycle profile of pluripotent hESC, and also of a recently discovered human pluripotent cell

type: human induced pluripotent stem cells (hiPSC) derived from fibroblasts (hFiPSC) (Rodriguez-Piza, Richaud-Patin et al. 2009) and keratinocytes (hKiPSC) (Aasen, Raya et al. 2008).

The results showed a strong resemblance between the cell cycle profile of undifferentiated hESC and hiPSC, with a high percentage (54-62%) of the population in S phase and a low proportion of cells in $G_0/_1$ phase of the cell cycle (17-33%). On differentiation, the cell cycle structure for all cell lines analyzed similarly changed with a striking increase of cells in the $G_0/_1$ phase (87-93%) and a reduction of cells in the S phase (2-8%) (see Figure 13, page 66).

In conclusion, undifferentiated hESC, hiPSC, and mESC share a common and atypical cell cycle structure suggesting that the cell cycle properties of ESC are functionally important for pluripotency and self-renewal properties. Indeed it has been suggested that a short G_1 phase should limit the "window of opportunity" during which a cell can be responsive to differentiation cues (Orford and Scadden 2008).

With the aim of finding out the molecular mechanisms underlying this cell cycle structure, we performed a serie of Western blot analyses of G_1 to S phase transition regulators in undifferentiated and differentiated hESC. With the aim of finding out conserved protein profiles along differentiation, and to rule out specific differentiation effects, we carried out two different differentiation protocols: a general and a neuronal differentiation protocol (see Figure 15, page 68 and Figure 17, page 71).

This is the first time that cell cycle proteins profiles of ESC are compared using two distinct differentiation protocols. From these experiments we can extract interesting conclusions. The cell cycle change of hESC during differentiation is paralleled by changes in the proteins profile. In general, the S and M phase cyclins A and B_1 were highly expressed in undifferentiated cells but decreased with differentiation, independently of the differentiation protocol used. These results are also observed in mESC (see Figure 12, page 64). On the other hand, the early G_1 proteins cyclins D_1 and D_2 were very low expressed in undifferentiated cells but they increased during general differentiation, according to previous results in hESC (Filipczyk, Laslett et al. 2007). These results were also observed in mESC (Burdon, Smith et al. 2002; Savatier, Lapillonne et al. 1996). On the contrary, cyclin D_1 did not increase noticeably when cells were differentiated towards neuronal cells. These results are in accordance with tissue specific expression of D-type cyclins (Wianny, Real et al. 1998). In support of

this, concomitant ablation of the three D-type cyclins results in haematopoietic defects (Kozar, Ciemerych et al. 2004), and ablation of the genes encoding individual D-type cyclins leads to specific developmental defects, most probably owing to their differential patterns of expression. This suggests that cyclin D_1 could be involved in the differentiation of specific cell lineages according to previous work reporting that D-type cyclins are able to modulate differentiation programs (Coqueret 2002). These observations suggest that early G_1 cyclins are involved in cell type specific regulation of the cell cycle, and may explain why conflicting data is frequently encountered in expression of D-type cyclins in hESC (Becker, Ghule et al. 2010; Neganova, Zhang et al. 2009). They may contain distinct populations representative of different developmental stages.

CDK4 seemed to be constantly expressed along differentiation, independently of the differentiation protocol used. Interestingly, cyclin E appeared to increase with differentiation using both protocols (see Figure 15, page 68 and Figure 17, page 71). These results clearly differ from those obtained in mESC where cyclin E expression decreased with differentiation (see Figure 12, page 64 and (White, Stead et al. 2005; White and Dalton 2005)). These results suggest that in hESC cell cycle progression is mainly driven by cyclins A and B_1. One speculative explanation may be hESC and mESC represent different developmental stages, or contain distinct populations representative of different developmental stages.

As expected, proteins involved in the replication of DNA, such as PCNA and DNA replication licensing factor, Mini Chromosome Maintenance Protein 2 (MCM2) were highly expressed in undifferentiated conditions but their expression decreased during differentiation, independently of the differentiation protocol used. On the contrary, CKI members of the Cip/Kip family $p21^{Cip1}$ and $p27^{Kip1}$, and the member of the Ink4 family, $p16^{Ink4a}$ were expressed at low levels in undifferentiated cells but they increased as differentiation proceeded in both differentiation models. These results are identical to those shown in mESC (see Figure 12, page 64 and (Savatier, Lapillonne et al. 1996)). However, the increase of $p27^{Kip1}$ was higher with the neuronal differentiation protocol than with the general differentiation protocol suggesting a potential role for $p27^{Kip1}$ in the cell fate of hESC.

The retinoblastoma protein (Rb) was hyperphosphorylated and thus, inactive in undifferentiated hESC but was hypophosphorylated again with differentiation, in

agreement with previous studies in mESC (Burdon, Smith et al. 2002; Savatier, Huang et al. 1994). Interestingly, p53 was expressed at high levels in undifferentiated cells and underwent a slight decrease with differentiation, independently of the differentiation protocol used. This fact could be related to the high proportion of dead cells in cultures of undifferentiated hESC.

In summary, despite differences in the expression of D-type cyclins along distinct differentiation protocols, we observed a similar proteins profile along the two different differentiation protocols in hESC (Figure 66). In general, the expression of G_1 cyclins and CKI increased during differentiation, and on the contrary S and M phase associated cyclins A and B_1 as well as proteins involved in the replication of DNA decreased during differentiation. Moreover, Rb was hyperphosphorylated in undifferentiated hESC but was hypophosphorylated again with differentiation. These results are in accordance with a reduced G_1 phase and lack of restriction (R) point mechanisms of control in undifferentiated cells, and acquisition of a longer G_1 phase with differentiation. These results are also very similar to those obtained in mESC. Nevertheless, there are some differences between hESC and mESC mainly at the G_1 phase components level such as cyclin E and CDK2.

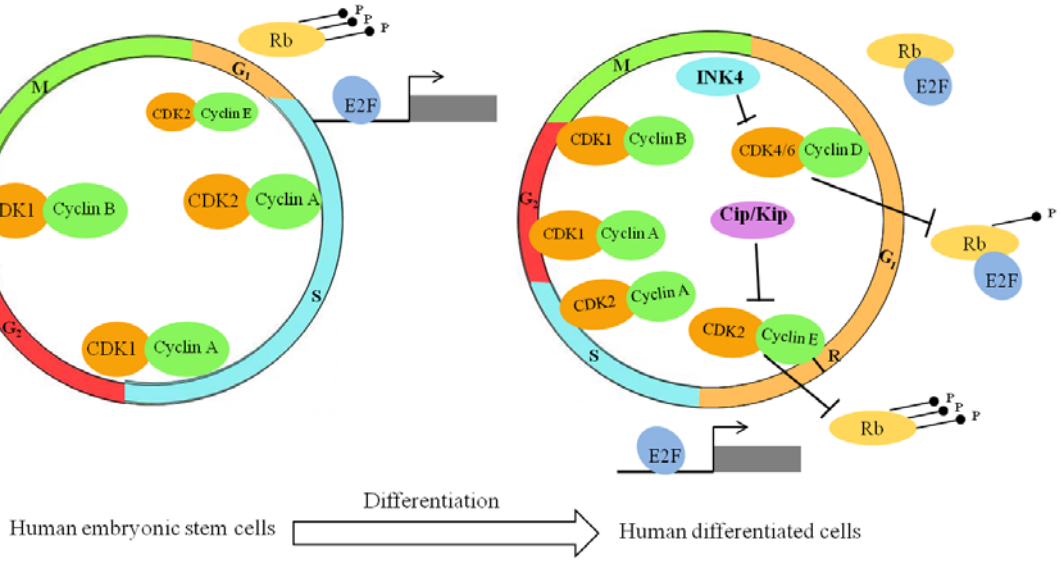

Figure 66. Comparison of cell cycle regulation in human embryonic stem cells and differentiated cells. The proportion of cells in G_1 phase is reduced in human embryonic stem cells and increases during differentiation. Cyclins A and B and their associated CDK seem to be the major regulators of the cell cycle in human embryonic stem cells. Retinoblastoma proteins (Rb) are constitutively hyperphosphorylated. During differentiation, the cells proliferate under the control of multiple cyclin-CDK complexes and their inhibitors. Restriction point (R) is activated during differentiation. CDK, Cyclin Dependent Kinase; G_1, Gap1; S, Synthesis; G_2, Gap 2; M, Mitosis.

Given that basic cell cycle proteins profiles were conserved between pluripotent mESC and hESC, we hypothesized that maybe some of these proteins were responsible for the self-renewal or pluripotency properties of hESC.

We hypothesized that the proteins increasing during differentiation could be responsible for the switch from undifferentiation to differentiation states. Moreover, these proteins could be implicated in the differentiation towards specific lineages. On the other hand, those proteins that dissapeared during differentiation could be responsible for the maintenance of ESC properties. In support of this, genetic studies in mouse models have shown widespread compensation among the mammalian CDK and among cyclins as well. However, cyclins A_2 and B_1 emerged as the most nonredundant cyclin and were essential for embryonic development (Satyanarayana and Kaldis 2009). Also, it has been reported that cyclin A function was essential for cell cycle progression of ESC but not for fibroblasts where it was redundant (Kalaszczynska, Geng et al. 2009).

On the other hand, a vast body of Literature has reported a role for $p27^{Kip1}$ in differentiation associated with a cell cycle arrest (Li, Jia et al. 2006; Munoz-Alonso, Acosta et al. 2005; Galderisi, Jori et al. 2003). However, very recently new functions for $p27^{Kip1}$ independent of the cell cycle have been discovered, reporting a role for $p27^{Kip1}$ in migration (Besson, Gurian-West et al. 2004), differentiation (Movassagh and Philpott 2008; Nguyen, Besson et al. 2006; Vernon, Movassagh et al. 2006; Vernon and Philpott 2003; Vernon, Devine et al. 2003), and stem cell expansion (Besson, Hwang et al. 2007).

Taken together, the data presents a strong argument for a direct role of cell cycle proteins in maintenance of hESC pluripotency and self-renewal properties.

We decided to focus on those proteins that increased during differentiation. We hypothesized that low levels of these proteins were important for maintenance of ESC properties. Given its increase during differentiation and its well established role in cell fate decisions we decided to study $p27^{Kip1}$ in hESC. We found that $p27^{Kip1}$ increased as the length of G_1 phase increased during differentiation (see Figure 15, page 68 and Figure 17, page 71). During G_1 phase a cell decides to progress into the cell cycle or to exit the cell cycle to follow other cell fates. For these reasons we hypothesized that $p27^{Kip1}$ could be responsible for the switch from undifferentiation to differentiation states being low levels the major factors influencing the pluripotent cell cycle structure.

With the aim of finding this out, we analyzed its expression levels in several pluripotent human cells, including two hESC lines and two hiPSC lines. In all cell lines analyzed, the expression level of $p27^{Kip1}$ was low in undifferentiated conditions but it increased during differentiation, paralleling the changes in the cell cycle structure (see Figure 18, page 74). This suggested that low levels of $p27^{Kip1}$ were functionally important for self-renewal and pluripotency properties of hESC and that this protein may have a role in the establishment of a long G_1 phase and consequently the induction or the maintenance of differentiation.

It is not clear how the cell makes the transition from a proliferative state to the other. With the aim of shedding light on this issue, **in Section 2 of Results** we proceeded to investigate the molecular mechanisms that were regulating $p27^{Kip1}$ in hESC. Quantitative Reverse Transcription Polymerase Chain Reaction (qRT-PCR) analysis showed that $p27^{Kip1}$ was not regulated at the transcriptional level in hESC, given that mRNA levels did not vary significantly after differentiation, meanwhile *OCT3/4* expression decreased. This suggested that $p27^{Kip1}$ was being regulated at post-transcriptional level.

Between the distinct modes of post-transcriptional regulation of $p27^{Kip1}$, two types have emerged as prominent modes of regulation involving regulation by microRNA (miRNA) and by the proteasome pathway (le Sage, Nagel et al. 2007). We decided to study these pathways in hESC and started by the miRNA pathway. We looked for potential miRNA target sites along the 3' untranslated region (UTR) of human $p27^{Kip1}$ mRNA, *in silico*. The results showed two families with higher probability of preferential conservation among vertebrates: miR-221/222 and miR-24. Then, we analyzed its expression levels in undifferentiated and differentiated hESC by qRT-PCR analysis using two distinct differentiation protocols: a general and a neuronal specific differentiation protocol to rule out differentiation specific effects given the fact that some miRNA are cell type specific. Unexpectedly, we did not detect a significant change in the expression levels of mature miR-221 or miR-222 in hESC in any differentiation protocol, but we observed a striking increase of mature miR-24 after differentiation in both differentiation models (see Figure 23, page 80 and Figure 24, page 81).

These results suggest that $p27^{Kip1}$ is not regulated by miR-221 or miR-222 in hESC, contrary to some carcinoma cell lines where high miR-221 and miR-222

maintain low levels of $p27^{Kip1}$ allowing a fast cell cycle (Fornari, Gramantieri et al. 2008; Galardi, Mercatelli et al. 2007; Gillies and Lorimer 2007; le Sage, Nagel et al. 2007; Visone, Russo et al. 2007). Given that miR-221 and miR-222 are expressed in carcinoma cell lines but not embryonic stem cells, a therapy targeting miR-221 or miR-222 might be highly selective in shutting off selectively the proliferation of carcinoma cells and not the normal cells.

Given the fact that miR-24 increased after differentiation paralleling the increase of $p27^{Kip1}$ protein, we hypothesized that miR-24 could be involved in the regulation of $p27^{Kip1}$ in hESC. This regulation could be direct by increasing the levels of $p27^{Kip1}$ or indirect by repressing a negative regulator of $p27^{Kip1}$. With the aim of answering this question we proceeded to inhibit miR-24 expression in hESC by means of RNA oligonucleotides specifically designed to bind to and inhibit endogenous miR-24 molecules, and subsequently to measure $p27^{Kip1}$ protein levels. We did not detect any difference in the expression levels of $p27^{Kip1}$ when miR-24 was inhibited in our experimental conditions suggesting that $p27^{Kip1}$ was not regulated by miR-24 in hESC (see Figure 28, page 87). Alternatively, miR-24 could be acting downstream of $p27^{Kip1}$. It would be interesting to inhibit $p27^{Kip1}$ in differentiated cells and look at the expression levels of miR-24.

These results suggest that similarly than other miRNAs that are broadly expressed across differentiated tissues, and directly influence critical gene regulatory networks controlled by pluripotency factors, miR-24 may contribute to the restricted expression of pluripotency factors during hESC differentiation. It could be interesting to overexpress or downregulate miR-24 and look at the expression levels of key pluripotency factors.

Given that $p27^{Kip1}$ expression appeared not to be regulated by these miRNAs, we investigated whether $p27^{Kip1}$ was regulated by the proteasome in hESC. To this end, we cultured the cells in the presence of cycloheximide, to inhibit *de novo* synthesis of $p27^{Kip1}$, in combination with a non-specific proteasome activity inhibitor: MG-132 (carbobenzoxy-L-leucyl-L-leucinal), and observed that the expression of $p27^{Kip1}$ increased above the expression levels of control cells (see Figure 29, page 88). This demonstrated that $p27^{Kip1}$ was being regulated by the proteasome pathway in hESC, according to previous work reporting a role for the ubiquitin ligase Skp2 in the regulation of $p27^{Kip1}$ in hESC (Egozi, Shapira et al. 2007). Moreover, in contrast to

somatic cells which had high levels of Skp2 only during S and G_2/M phases, undifferentiated hESC had also high levels of Skp2 at G_1 phase of the cell cycle (Egozi, Shapira et al. 2007). It should be noted that in this study the authors did not perform any functional analysis of Skp2.

Taken together these results functionally showed that $p27^{Kip1}$ was regulated by the proteasome pathway in hESC. Thus, the low expression levels of $p27^{Kip1}$ protein were a consequence of proteasome activity and could explain the high proliferation rates in undifferentiated cells. Future work is required to functionally study the proteasome activity in differentiated cells to find out if it is differently regulated during differentiation.

The cell cycle inhibitor $p27^{Kip1}$ controls self-renewal and pluripotency of human embryonic stem cells by regulating the cell cycle, *BRACHYURY* and *TWIST*

Undifferentiated pluripotent cells shared a common and atypical cell cycle structure that changed upon differentiation. Moreover, conserved cell cycle proteins profiles were underlying these changes, suggesting that cell cycle properties of ESC were functionally important for pluripotency and self-renewal properties. We hypothesized that alteration of the balance of cell cycle proteins in hESC could affect their properties. An approach to test this hypothesis was to perform a functional analysis of cell cycle proteins involved in the maintenance of ESC cell cycle structure using a gain and loss of gene function strategy. To date there were no *in vitro* reports showing functional analysis for cell cycle proteins in either mESC or hESC.

We hypothesized that low levels of the CKI $p27^{Kip1}$ were the major factors influencing pluripotent cell cycle structure given that: 1) $p27^{Kip1}$ appeared lowly expressed in several undifferentiated pluripotent cell lines, but increased during differentiation paralleling the increase of G_1 phase during differentiation. 2) Mitogen stimulated pathways involved in degradation of $p27^{Kip1}$, such as Ras, PI3K, and/or tyrosine kinases pathways are also important for the maintenance of ESC properties.

For these reasons the second main objective of this thesis was to know if alteration of the balance of $p27^{Kip1}$ expression levels affected the pluripotency and/or self-renewal properties of hESC. This objective **was addressed in sections 3 and 4 of Results.**

Firstly, we proceeded to overexpress human $p27^{Kip1}$ coding sequence in hESC by lentiviral transduction of a doxycycline TET OFF regulated vector. Gene delivery was performed by lentiviral transduction given that lentiviruses are one of the most efficient methods for delivering genetic information into the DNA of a host cell. In this system, the transcription of $p27^{Kip1}$ was minimal in presence of doxycycline and was induced by its withdrawal.

Control hESC generated colonies with the typical morphology of undifferentiated cells grown on matrigel, with round and tight colonies. When observed under a microscope at higher magnification, these colonies consisted of lots of small cells displaying high nuclear to cytoplasmic ratio. Surprisingly, $p27^{Kip1}$ overexpression in

hESC resulted in a change in the morphology that was not seen in control cells (see Figure 33B, page 96 and Figure 34, page 98). $p27^{Kip1}$ overexpressing hESC displayed a striking phenotype with an enlarged size, a spread out, and flattened phenotype. Moreover, these cells presented a low nuclear to cytoplasmic ratio, just the opposite phenotype than undifferentiated control cells. Furthermore, $p27^{Kip1}$ overexpressing hESC generated colonies containing less number of cells than colonies of the same size but containing control cells, suggesting that $p27^{Kip1}$ could be impairing the cell growth.

Cell growth can be impaired by arresting the cell cycle. In order to know the cell cycle status of $p27^{Kip1}$ overexpressing hESC we proceeded to analyze the cell cycle profile by flow cytometry analysis, and we showed that overexpression of $p27^{Kip1}$ in hESC resulted in a complete arrest of the cell cycle (see Figure 36, page 101). We did not detect any cell incorporating a modified nucleoside: 5-ethynyl-2'-deoxyuridine (EdU) which is incorporated during DNA synthesis. These results support further that hESC were not cycling. The great majority of the population was arrested in the $G_0/_1$ phase of the cell cycle. On the contrary, control cells displayed the atypical cell cycle structure of undifferentiated hESC with a low percentage (approximately 20-26%) of cells in $G_0/_1$ phase and a high percentage of cells (approximately 53- 60%) in S phase.

These results demonstrate for the first time that overexpression of one cell cycle protein; namely $p27^{Kip1}$, in undifferentiated hESC inhibits the cell cycle progression by arresting the cells and consequently the cells are not able to self-renew.

The overexpression of $p27^{Kip1}$ in human somatic cells also causes an arrest of the cell cycle in $G_0/_1$. Thus these results show a similarity between the cell cycle of human somatic cells and hESC. Moreover, the fact that overexpression of $p27^{Kip1}$ in hESC caused an arrest in $G_0/_1$ phase suggested that despite its ability to inhibit the mitotic cyclin B-CDK1 complexes, it acted mainly by inhibiting cyclin E/A-CDK2 complexes. Contrary to mESC where cyclin D_3-CDK6 complexes are resistant to inhibition by $p16^{INK4a}$ and are not growth-arrested by overexpression of $p16^{INK4a}$ (Faast, White et al. 2004; Savatier, Lapillonne et al. 1996), cyclin E/A-CDK2 complexes are not resistant to inhibition by $p27^{Kip1}$ in hESC.

As the effect of $p27^{Kip1}$ was to arrest the cell cycle in $G_0/_1$ phase of the cell cycle which is the phase where cells can follow different cell fates such as senescence, apoptosis, or differentiation this suggested that the increase of this protein could be necessary for the cell to change from a proliferating undifferentiated state to a

differentiating state. Moreover, the function of this protein might be linked to any or more of the above mentioned cell fate decisions.

The reduction of $p27^{Kip1}$ expression levels in hESC, by short hairpin RNAs (shRNAs), also caused a striking change in the morphology of the colonies (see Figure 43, page 110 and Figure 45, page 113). Whereas control hESC generated colonies with the typical morphology of undifferentiated cells grown on matrigel with round and tight colonies, $p27^{Kip1}$ knockdown caused a striking phenotype with compact colonies that had the edges elongated and very well defined. These edges were likely to be made up of thin, "fibroblastoid" cells that surrounded the colonies. Moreover, we observed colonies just comprised of elongated and thin cells. These cells were probably not able to spread out, just the opposite phenotype than $p27^{Kip1}$ overexpression. This curious phenotype was not seen in hESC control cells.

Spontaneous differentiation often occurs in only a portion of a hESC colony, usually along the edges or as isolated spots in the center of the colony. The beginning of differentiation is noted by apparition of flattened appearance and loss of defined boundaries. In general, healthy, undifferentiated colonies are regarded as colonies with clean, well defined edges. Thus the phenotype generated by the knockdown of $p27^{Kip1}$ suggested that these colonies were becoming more undifferentiated or having a "stemness" phenotype.

With the aim of finding out if a change in the cell cycle was underlying this phenotype, we proceeded to analyze the cell cycle profile of $p27^{Kip1}$ knockdown hESC by flow cytometry analysis. Results showed that control hESC presented the atypical cell cycle structure of undifferentiated cells, with a low percentage of cells in $G_0/_1$ phase and a high percentage of cells in S phase. However, cells transduced with p27shRNA constructs displayed a slight increase of cells in the S phase which was more evident in the cells transduced with the construct presenting the highest knockdown efficiency (see Figure 46, page 115).

These results reveal that the knockdown of $p27^{Kip1}$ increases the cell cycling of hESC through an increase of the transit from the G_1 to S phase, while maintaining an undifferentiated phenotype. Consequently it potentiates the atypical cell cycle structure of pluripotent cells and thus self-renewal. Alternatively, the loss of $p27^{Kip1}$ could be increasing the undifferentiated state by inhibiting the exit from the cell cycle and thus impairing the acquisition of other cell fates, such as differentiation.

Taken together, these interesting results demonstrate for the first time that overexpression of one cell cycle protein; namely $p27^{Kip1}$, in undifferentiated conditions, inhibits self-renewal of hESC by arresting the cells in $G_0/_1$ phase of the cell cycle. Moreover, it causes a change in the morphology of cells with an increase of the size, a decrease in the nuclear to cytoplasmic ratio, and a more spread out and flattened phenotype.

As the beginning of differentiation is characterized by the appearance of a flattened morphology and since it has been reported that a high nuclear to cytoplasmic ratio is a common characteristic of undifferentiated pluripotent hESC (Thomson, Itskovitz-Eldor et al. 1998), these results suggested that the increase of $p27^{Kip1}$ was inducing a less pluripotent or more differentiation prone phenotype.

On the contrary, the knockdown of $p27^{Kip1}$ appeared to potentiate the self-renewal of hESC by increasing the proportion of cells in S phase probably through an increase of the transit from the G_1 to S phase. Also, the reduction of $p27^{Kip1}$ expression levels caused a striking phenotype with colonies that had very well defined and elongated edges consisting of thin, “fibroblastoid” cells. This change in the phenotype towards more clearly defined edges suggested these colonies were turning into a more undifferentiated phenotype.

These revealing results single out $p27^{Kip1}$ as a key protein in the switch from a pluripotent and self-renewing state to a differentiation prone state.

These results may have several applications. The overexpression of $p27^{Kip1}$ could stop the development of tumours when hESC or hiPSC are transplanted into adult animal models by arresting the cell cycle. The use of chemical compounds that increase $p27^{Kip1}$ expression could avoid the potential risk of using virus to transduce cells, and thus may be better for safer use in clinical applications. It would be of interest to slow down the cell cycle of hESC and see if the capacity to develop tumours when they are injected into adult animal models is reduced. On the other hand it should be important to find out if the slowing down of the cell cycle could affect the differentiation towards the three germ layers.

The reduction of $p27^{Kip1}$ expression levels in somatic cells would increase the efficiency of generation of hiPSC by facilitating the transition towards a more self-renewing and possibly pluripotent state. Efficiency of generation of hiPSC is very low when oncogenes, such as c-myc, are eliminated from the initial cocktail of transcription

factors, however the development of tumours is reduced (Nakagawa, Koyanagi et al. 2008). Recently, we and others have reported the increase of efficiency of generation of hiPSC by inhibiting p53 or $p21^{Cip1}$ (see Annexe II (Edel, Menchón et al. 2010)) (Kawamura, Suzuki et al. 2009; Marion, Strati et al. 2009) in the absence of c-myc. However, as p53 and $p21^{Cip1}$ are involved in DNA-damage-induced cell cycle arrest or apoptosis, the inhibition of these proteins generates hiPSC carrying persistent DNA damage and chromosomal aberrations (Marion, Strati et al. 2009) which induces tumour formation. As $p27^{Kip1}$ is not involved in DNA damage pathways, but in cell fate decisions through cell cycle arrest mediated by anti-proliferative signals, it may constitute a better target to increase the efficiency of generation of hiPSC without the risk of having genetic or chromosomal alterations.

As the alteration in the expression levels of $p27^{Kip1}$ caused phenotypic changes in hESC, we next proceeded to study this in depth. This question was addressed in **section 4 of Results.** $p27^{Kip1}$ overexpressing hESC arrested in $G_0/_1$ phase of the cell cycle and, among other morphology changes, displayed an evident reduction in the nuclear to cytoplasmic ratio compared to controls. We also confirmed that they presented an increase of the cell size by flow cytometry analysis of pulse width intensity. In order to explain this phenotype, we evaluated the different fates that cells can undergo once have exited the cell cycle and remain in G_1 phase of the cell cycle, as was the case of $p27^{Kip1}$ overexpressing hESC. Cells that withdraw from the cell cycle during G_1 phase can undergo three different fates: they can go into apoptosis, become senescent, or differentiate (Blomen and Boonstra 2007). We then proceeded to evaluate each one of these cell fates.

We started by assessing if $p27^{Kip1}$ overexpressing hESC were apoptotic. Apoptosis was assessed by two different methodologies: the analysis of nuclear morphological changes indicative of apoptosis (nuclear fragmentation) after staining with DAPI and observation with a fluorescence microscope (Lai, Chien et al. 2003), and by quantitative flow cytometry analysis of mitochondrial membrane potential, because the abolishment of mitochondrial membrane potential is one of the earliest markers of apoptosis (Dobrosi, Toth et al. 2008). Moreover, in flow cytometry analysis, Propidium Iodide staining was also used for staining dead cells and consequently discriminate necrosis from apoptotis. We did not detect a significant increase of apoptosis in $p27^{Kip1}$

overexpressing hESC with any of the above mentioned methodologies (see Figure 50, page 122 and Figure 51, page 123). Moreover, flow cytometry analysis did not reveal even protection from apoptosis in $p27^{Kip1}$ overexpressing hESC. Moreover, and with the aim of confirming these results, we performed a time-lapse microscopy experiment in which we monitored individual $p27^{Kip1}$ overexpressing cells during seven days of cell culture by photographs. After these days had elapsed, we could still detect enlarged and spread out $p27^{Kip1}$ overexpressing cells without observing apoptotis signals. Analysis of nuclear morphological changes revealed round, clear-edged, and uniformly stained nuclei confirming that $p27^{Kip1}$ overexpressing hESC were not apoptotic after seven days of culture (see Figure 49B, page 121 and Figure 50, page 122).

On the other hand, we tested the complementary approach, that is, we checked if loss of $p27^{Kip1}$ using short hairpin RNAs could be affecting apoptosis. Apoptosis was also measured by two different methodologies: by the analysis of nuclear morphological changes (nuclear fragmentation) after staining with DAPI and by quantitative flow cytometry analysis of mitochondrial membrane potential. We did not detect any significant change in apoptosis in $p27^{Kip1}$ knockdown hESC judging by the normal appearance of round, clear-edged, and uniformly DAPI- stained nuclei (see Figure 53, page 125). These results were also confirmed by flow cytometry analysis in which we could not appreciate any significant change in apoptosis after long term culture, despite the phenotype of $p27^{Kip1}$ knockdown hESC was evident (Figure 52, page 124).

Taken together these results showed that $p27^{Kip1}$ did not affect apoptosis in hESC. At present there are conflicting data in Literature about regulation of apoptosis by $p27^{Kip1}$. Different apoptosis responses, either inhibition or promotion, have been reported in various cell types by manipulating $p27^{Kip1}$ levels. For instance, numerous reports have suggested proapoptotic roles for $p27^{Kip1}$ by overexpression in cancer cell lines (Wang, Gorospe et al. 1997). However in these studies $p27^{Kip1}$ was overexpressed using adenoviral vectors and their relevance to physiological conditions is uncertain. On the contrary, other studies have reported a function for $p27^{Kip1}$ in protection from apoptosis. Thus, $p27^{Kip1}$ has been reported to play a protective role in safeguarding normal tissues from excessive apoptosis during inflamatory injury (Ophascharoensuk, Fero et al. 1998). This ability of $p27^{Kip1}$ to limit or prevent apoptosis is also particularly relevant in cancer therapies, and induction of $p27^{Kip1}$ has been associated with resistance to apoptosis induced by cytotoxic drugs or irradiation (Eymin and Brambilla 2004). One

way by which Cip/Kip proteins protect against apoptosis is via their CDK inhibitory activity. This was first shown in endothelial cells where caspase-mediated cleavage of $p21^{Cip1}$ and $p27^{Kip1}$ upregulated CDK2 activity, thereby enhancing the apoptotic program (Levkau, Koyama et al. 1998). However, in a study with mESC in which it was shown increased apoptosis in differentiating $p27^{Kip1}$ deficient mESC neither CDK2 nor CDK4 associated kinase activities were altered in the absence of $p27^{Kip1}$. Although this study inferred that caspase independent apoptotic pathways were responsible for the massive cell death of differentiating $p27^{Kip1}$ deficient mESC, they did not provide a specific molecular mechanism or pathway by which $p27^{Kip1}$ protected mESC from differentiation associated apoptosis (Bryja, Pachernik et al. 2004). It should be noted that these experiments were carried out in differentiating $p27^{Kip1}$-deficient mESC, contrary to our studies performed in undifferentiated $p27^{Kip1}$-deficient hESC, suggesting that the effect of $p27^{Kip1}$ in apoptosis could vary depending on the cellular context.

Therefore we proceeded to know if $p27^{Kip1}$ overexpressing cells underwent another cell fate. As explained above, another fate that cells can undergo once they have exited the cell cycle during $G_0/_1$ is senescence. In view of the fact that β-galactosidase activity at pH 6 is present only in senescent cells and is not found in presenescent, quiescent, or immortal cells and that it has been widely used as a biomarker of senescence (Kurz, Decary et al. 2000), we proceeded to measure β-galactosidase activity at pH 6 in $p27^{Kip1}$ overexpressing hESC. Easily distinguished large, spread out, and flattened $p27^{Kip1}$ overexpressing hESC were detected after 4 days of culture in the absence of doxycycline, however when observed under a light microscope we did not detect β-galactosidase activity in these cells, demonstrating that $p27^{Kip1}$ overexpressing hESC were not senescent (data not shown). As expected, we did not detect β-galactosidase activity in control cells either, consistent with previous reports showing that undifferentiated hESC have an unlimited proliferation *in vitro* in part due to the high expression of telomerase activity (Thomson, Itskovitz-Eldor et al. 1998).

Taken together the data demonstrated that $p27^{Kip1}$ overexpressing hESC were not senescent. Consequently in order to clarify the phenotype of $p27^{Kip1}$ overexpressing hESC, we investigated whether $p27^{Kip1}$ overexpressing hESC were differentiating. To answer this question, we analyzed the transcriptional profile of 84 key genes involved in hESC maintenance and differentiation by qRT-PCR analysis. The array included hESC-specific genes that define the "stemness" of the cells and that are involved in the

maintenance of their pluripotent and self-renewal properties. The array also included differentiation markers that can be used to monitor the early events of hESC differentiation. Gene expression profiling values of this array showed that $p27^{Kip1}$ overexpression did not result in a significant change of master pluripotency factors such as *OCT3/4*, *NANOG*, or *SOX2* after 4 days of culture (see Figure 56, page 130). These data were further validated by qRT-PCR analysis of the above mentioned and other key pluripotency factors. Moreover, the loss of $p27^{Kip1}$ did not significantly affect the expression of key pluripotency genes either (see Figure 57, page 132).

However, gene expression profiling showed that $p27^{Kip1}$ overexpression resulted in upregulation and downregulation of specific differentiation genes (see Figure 56, page 130). We then proceeded to validate those genes showing the most important changes by qRT-PCR analysis in both $p27^{Kip1}$ overexpressing and also in $p27^{Kip1}$ knockdown hESC. We hypothesized that if overexpression of $p27^{Kip1}$ was affecting any gene then we should see the reverse effect in knockdown cells. Validation of the genes showing the most important changes in the array values revealed a potential novel role for $p27^{Kip1}$ in the regulation of *BRACHYURY* in hESC. Overexpression of $p27^{Kip1}$ in hESC produced an important downregulation of *BRACHYURY* of approximately 60%. Interestingly, the knockdown of $p27^{Kip1}$ reversed this trend producing a statistically significant upregulation of approximately 9 times compared to controls (see Figure 58, page 133). This is the first time a role for $p27^{Kip1}$ in the regulation of *BRACHYURY* gene expression has been shown. *BRACHYURY* is an important gene involved in early mesoderm specification (Technau and Scholz 2003).

Given this important and novel effect we decided to also measure BRACHYURY levels at the protein level in $p27^{Kip1}$ overexpressing and knockdown hESC, by Western blot and immunofluorescence analyses, confirming the mRNA results (see Figure 59, page 135). These data revealed BRACHYURY as a novel target of $p27^{Kip1}$.

Brachyury has been traditionally related to the specification of mesoderm and axis elongation (Showell, Binder et al. 2004; Technau and Scholz 2003). Mesoderm formation in development involves an epithelial to mesenchymal transition (EMT) process (Acloque, Adams et al. 2009). The EMT is a fascinating phenotypic change that is undertaken by embryonic cells in physiological conditions. It involves profound changes in the morphology, such as loss of epithelial characteristics, acquisition of a fibroblastoid phenotype, and also changes in the behavior of epithelial cells such as

acquisition of migratory properties (Nieto 2009). However, this physiological program can also be activated in pathological processes such as metastasis (Nieto 2009). Given such effect of $p27^{Kip1}$ on BRACHYURY, we evaluated if other key mesoderm specification or EMT markers were also affected by the modification of the expression levels of $p27^{Kip1}$ by qRT-PCR analysis. The testing of a battery of mesoderm and EMT gene markers revealed a statistically significant upregulation of *TWIST* 6-fold with $p27^{Kip1}$ loss of function compared to controls and conversely, a statistically significant downregulation in $p27^{Kip1}$ overexpressing hESC (see Figure 60, page 137). We did not find statistically significantly differences in expression of the other genes in either $p27^{Kip1}$ overexpressing or $p27^{Kip1}$ knockdown hESC, suggesting that the effect of $p27^{Kip1}$ was specific for *TWIST* gene expression. Although we were not able to measure TWIST protein levels in these cells given that were no specific antibodies for TWIST, these results are very promising given the important functions of TWIST. For example, TWIST1 remains essential in mesoderm differentiation including muscle, cartilage, and osteogenic cell lineages (Ansieau, Morel et al. 2010). In vertebrates, TWIST1 is initially expressed throughout the somatic mesoderm at high levels before differentiation and is subsequently silenced in the forming myotome (Wolf, Thisse et al. 1991). TWIST1 is also likely to be important for maintaining the immature phenotype of several cell types such as chondrocytes and osteoblasts through inactivation of specific transcription factors such as MyoD, Myocyte Enhancer Factor-2 (MEF2), Runt-related transcription factor (RUNX) family members RUNX1 and RUNX2, Peroxisome proliferator-activated receptor gamma coactivator 1-alpha (PGC1-α), p53, and nuclear factor kappa-light-chain-enhancer of activated B cells (NF-κβ) (Ansieau, Morel et al. 2010). Moreover, TWIST1 is capable of inducing an EMT process and was found to be overexpressed in a large set of human tumours (Ansieau, Morel et al. 2010).

This is not the first time that $p27^{Kip1}$ and the other members of the Cip/Kip family have been reported as having a role in transcriptional regulation. Cip/Kip proteins can repress transcription indirectly by inhibiting cyclin-CDK complexes, in turn preventing the phosphorylation of Rb family proteins (Rb1, p107, and p130). In their hypophosphorylated state, Rb-related proteins sequester E2F family members, thereby repressing their transcriptional targets (Sherr and Roberts 1999). In addition, Cip/Kip proteins have been recently found to modulate the activity of transcription factors through direct binding to transcription factors. In this way, the N-terminal cyclin-CDK

binding region of $p57^{Kip2}$ can interact with MyoD, protecting MyoD from degradation and thus promoting transactivation of muscle-specific genes (Reynaud, Leibovitch et al. 2000). A similar mechanism is observed between $p27^{Kip1}$ and Neurogenin-2, and $p27^{Kip1}$-mediated stabilization of Neurogenin-2 promotes the differentiation of mouse neuronal progenitors in the cortex (Nguyen, Besson et al. 2006), independently of its role in cell cycle regulation. The inhibitor $p21^{Cip1}$ is also a potent regulator of several transcription factors such as E2F1, c-Myc, Cdc25A, and STAT3 through direct binding (Vigneron, Cherier et al. 2006; Coqueret 2003).

Given that $p27^{Kip1}$ expression was detected principally in the nuclei, we examined if $p27^{Kip1}$ was directly affecting the transcriptional activation of *TWIST1* promoter. To this end, we performed chromatin immunoprecipitation experiments of $p27^{Kip1}$ occupancy along 4000 Kb of *TWIST1* promoter starting from +1.0 Kb to -3.0 Kb from the ATG in asynchronously growing $p27^{Kip1}$ overexpressing or $p27^{Kip1}$ knockdown hESC (see Figure 61, page 138). We found that $p27^{Kip1}$ protein was recruited to +1.0 Kb site of *TWIST1* promoter in $p27^{Kip1}$ overexpressing hESC based on a statistically significant two-fold increase compared to control cells. We did not detect the presence of $p27^{Kip1}$ on *TWIST1* promoter in control cells or $p27^{Kip1}$ knockdown cells where $p27^{Kip1}$ protein expression levels had been reduced by short hairpin RNAs.

The increase in *TWIST1* promoter occupancy suggested that $p27^{Kip1}$ functioned as a transcriptional repressor of *TWIST1* gene in hESC in undifferentiating culture conditions (Figure 67). In agreement with these results, a similar role has been shown for another similar CKI, $p21^{Cip1}$ which was found to bind the *myc* and *cdc25A* promoters upon DNA damage by means of chromatin immunoprecipitation experiments inducing transcriptional repression (Vigneron, Cherier et al. 2006), further supporting the novel discovery that cell cycle inhibitor proteins may have additional roles to their kinase inhibitor functions by binding chromatin, most probably indirectly as a complex, to regulate gene expression. A previous report showed that ectopic expression of $p27^{Kip1}$ blocked the induction of *Twist* in chicken skeletal muscle satellite cells (a type of stem cells) (Leshem, Spicer et al. 2000). We show for the first time direct evidence of the regulation of *TWIST1* promoter by $p27^{Kip1}$ in mammalian hESC associated with gene expression levels showing a novel role for $p27^{Kip1}$ in Cell Biology. If $p27^{Kip1}$ regulates *TWIST1* directly or indirectly as part of a repressor complex via other chromatin modelling proteins during gene regulation remains to be defined.

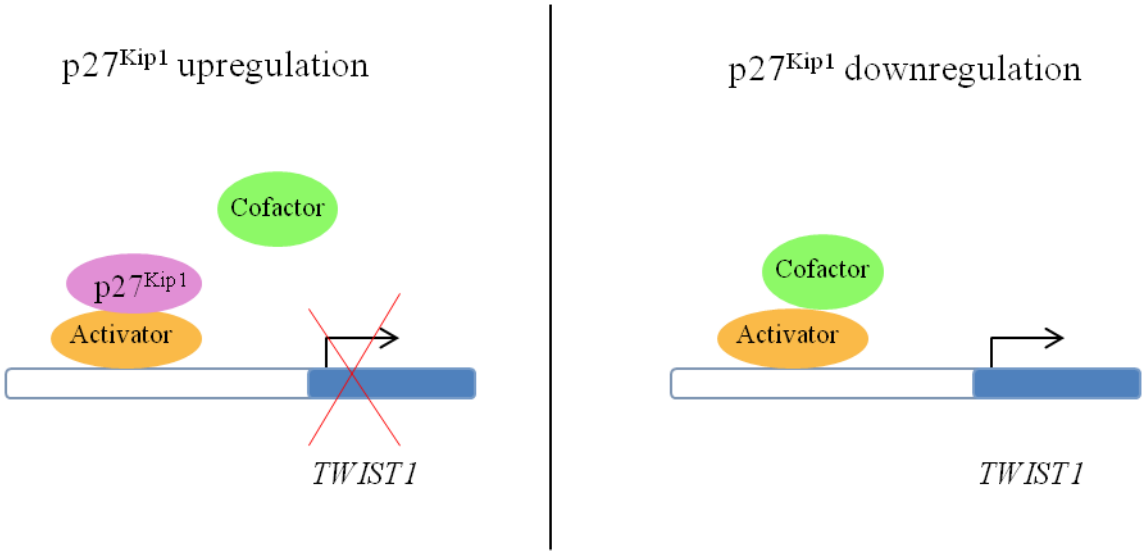

Figure 67. Proposed model for the p27^{Kip1} mediated transcriptional regulation of *TWIST1* promoter in human embryonic stem cells. When p27^{Kip1} is overexpressed in human embryonic stem cells is recruited to the promoter of *TWIST1* and induces transcriptional repression.

The discovery that a change in the balance of p27^{Kip1} levels in undifferentiated hESC affects expression of *BRACHYURY* and *TWIST* mesoderm markers has interesting implications in Cell Biology for a number of reasons. First, these results are in agreement with previous studies showing that p27^{Kip1} is involved in the maintenance of differentiation (Movassagh and Philpott 2008; Nguyen, Besson et al. 2006; Li, Jia et al. 2006; Munoz-Alonso, Acosta et al. 2005; Vernon, Devine et al. 2003; Galderisi, Jori et al. 2003). Second, Twist induces an EMT to facilitate tumour metastasis (Yang, Mani et al. 2004), and it is upregulated in several types of cancers (Ansieau, Morel et al. 2010).

Mesoderm differentiation involves an EMT process and dissociated adherence junctions. Regulation of E–CADHERIN is a hallmark of the EMT process and for this reason we performed preliminary studies of E-CADHERIN expression to determine if the protein levels were affected in the characteristic elongated shaped phenotype of p27^{Kip1} knockdown hESC. Immunofluorescence analysis of E-CADHERIN expression showed that p27^{Kip1} knockdown hESC appeared to have less E-CADHERIN in the plasma membrane compared to controls. The lack of regulation of *E-CADHERIN* at the gene level suggested that p27^{Kip1} could be involved in the regulation of E-CADHERIN at a post-transcriptional level. These results suggested that a mesoderm differentiation

program could be starting in $p27^{Kip1}$ knockdown hESC. However, and given the fact that both BRACHYURY and TWIST transcription factors can homodimerize or heterodimerize depending on context and have distinct activities depending on the balance of these complexes (Ansieau, Morel et al. 2010; Naiche, Harrelson et al. 2005), we cannot rule out context-specific activities of these factors in undifferentiated hESC. In support of this, recent work in mESC has shown that *Nanog* expression is up-regulated by the binding of Brachyury and STAT3 to an enhancer element in the mouse *Nanog* gene. In turn, Nanog downregulates Brachyury expression and leads to the maintenance of a pluripotent population (Suzuki, Raya et al. 2006; Suzuki, Raya et al. 2006). In line with this, a recent report has shown that ectopic expression of TWIST in nontumorigenic, immortalized human mammary epithelial cells (HMLEs) resulted in induction of EMT and the expression of antigenic markers associated with stem cells and also a gain in mammosphere-forming ability which is relationed with the presence of self-renewing stem cells. However the specific mechanisms by which this was achieved are not known. Moreover, stem cells naturally present in normal human mammary epithelial cells expressed, between other EMT genes, a considerably increase of TWIST expression respect non stem cells (Mani, Guo et al. 2008).

The commitment of hESC towards mesoderm fate would involve the loss of pluripotency and consequently the loss of the capacity to give rise to all cell types of the foetus. To determine if the regulation of mesoderm markers by $p27^{Kip1}$ was affecting the differentiation capacity of hESC, we performed preliminary experiments of differentiation in $p27^{Kip1}$ depleted hESC. These cells were differentiated by embryoid bodies (EB) generation. Results showed that control hESC generated round and compact EB after 3-4 days of culture in suspension. On the contrary, $p27^{Kip1}$ knockdown hESC generated irregular, cystic EB suggesting that these cells were unable or had an impaired capacity to differentiate (see Figure 63, page 141). Cavitations of EB are the result of programmed cell death and this first wave of cell death is considered indispensable for morphogenesis (Joza, Susin et al. 2001). The fact that $p27^{Kip1}$ knockdown hESC had premature cavitations compared to controls, suggests that it was impairing survival or increasing apoptosis. Another possibility is that it could be affecting specific differentiation lineages. Given that it has been recently shown that $p27^{Kip1}$ deficient mESC have an impairment of normal differentiation after treatment

with Retinoic Acid (Bryja, Pachernik et al. 2004) and given the fact that Retinoic Acid is an inducer of neuronal differentiation and hence neuroectoderm lineage, we proceeded to differentiate $p27^{Kip1}$ depleted hESC towards neuroectoderm and mesoderm lineages. To this end, hESC were differentiated through EB generation, cultured in mesoderm or neuroectoderm specific differentiation culture mediums for 30 days, and subsequently immunostained with lineage-specific antibodies for mesoderm (α-Smooth Muscle Actin) or neuroectoderm (Nestin, and β-tubulin III) lineages, respectively.

Immunofluorescence analyses showed that control hESC effectively differentiated into neuroectoderm and mesoderm lineages judging by the high expression of specific differentiation markers. Surprisingly and in contrast to control cells, we observed that loss of $p27^{Kip1}$ impaired proper differentiation of neuroectoderm judging by a striking reduction in the expression of Nestin and β-Tubulin III (Tuj1) immunostained positive cells (see Figure 65, page 143). Moreover, in these cells we did not detect the typical axonal morphology observed in Nestin or β-Tubulin III-stained control cells, suggesting that these cells had an impaired capacity to differentiate into neuroectoderm. These results are in accordance with a recent report showing an impairment of normal differentiation in $p27^{Kip1}$ deficient mESC after treatment with Retinoic Acid (Bryja, Pachernik et al. 2004). Given the fact that Retinoic Acid is an inducer of neuronal differentiation, these results suggest that $p27^{Kip1}$ is necessary for neuronal differentiation. Moreover, these results are also in agreement with the role of $p27^{Kip1}$ in the promotion of differentiation of neuronal progenitors in the cortex of mice (Nguyen, Besson et al. 2006).

These results demonstrate that in the absence of $p27^{Kip1}$ the ability of hESC to produce a range of differentiated progeny representative of the three primary germ layers is affected, thus demonstrating that $p27^{Kip1}$ is essential for the maintenance of the pluripotency of hESC. The idea that the cell cycle regulates pluripotency has been previously discussed joining a growing body of scientific data supporting a link between the cell cycle and pluripotency (see Annexes II (Edel, Menchón et al. 2010) and III (Edel, Boue et al. 2010))(Burdon, Smith et al. 2002).

In summary, in this thesis we sought to understand if changes in the balance of a cell cycle gene could regulate self-renewal or pluripotency properties of undifferentiated hESC. We focused on $p27^{Kip1}$ given the low levels of expression in undifferentiated pluripotent cells and its well established role in cell fate decisions. We used a gain and loss of function strategy to define the functional role of the cell cycle in self-renewal or pluripotency by manipulating the expression levels of $p27^{Kip1}$ in hESC.

The results presented in this thesis have uncovered a new role for $p27^{Kip1}$ in the self-renewal of hESC by regulating the G_1 to S transition and cell morphology. Moreover, we have shown that in undifferentiating conditions $p27^{Kip1}$ regulates the mesoderm markers *BRACHYURY* and *TWIST* to maintain pluripotency and self-renewal properties, however under differentiating conditions which involves removal of bFGF, we found that $p27^{Kip1}$ regulates neuronal cell fate. This demonstrates that $p27^{Kip1}$ is essential for the maintenance of a true pluripotent state. These discoveries have been made possible thanks to the ESC model of early embryogenesis and suggest that $p27^{Kip1}$ undertakes a role dependent on extracellular signalling with differentiation signals. This mechanism may allow hESC to selectively respond to environmental cues by specifically upregulating a particular component of the cell cycle engine, and to undergo self-renewal or cell differentiation.

Taken together, using either undifferentiating or guided differentiating conditions, these results show that $p27^{Kip1}$ regulates the pluripotent state of hESC, and that it has to be tightly regulated for the maintenance of the self-renewal and pluripotency properties of hESC. In light of these results, we propose that $p27^{Kip1}$ simultaneously targets CDK and transcriptional regulators to coordinate self-renewal and lineage commitment (Figure 68). These results are a proof of principle that proteins regulating the cell cycle play a critical role in self-renewal of hESC and also with making cell fate decisions.

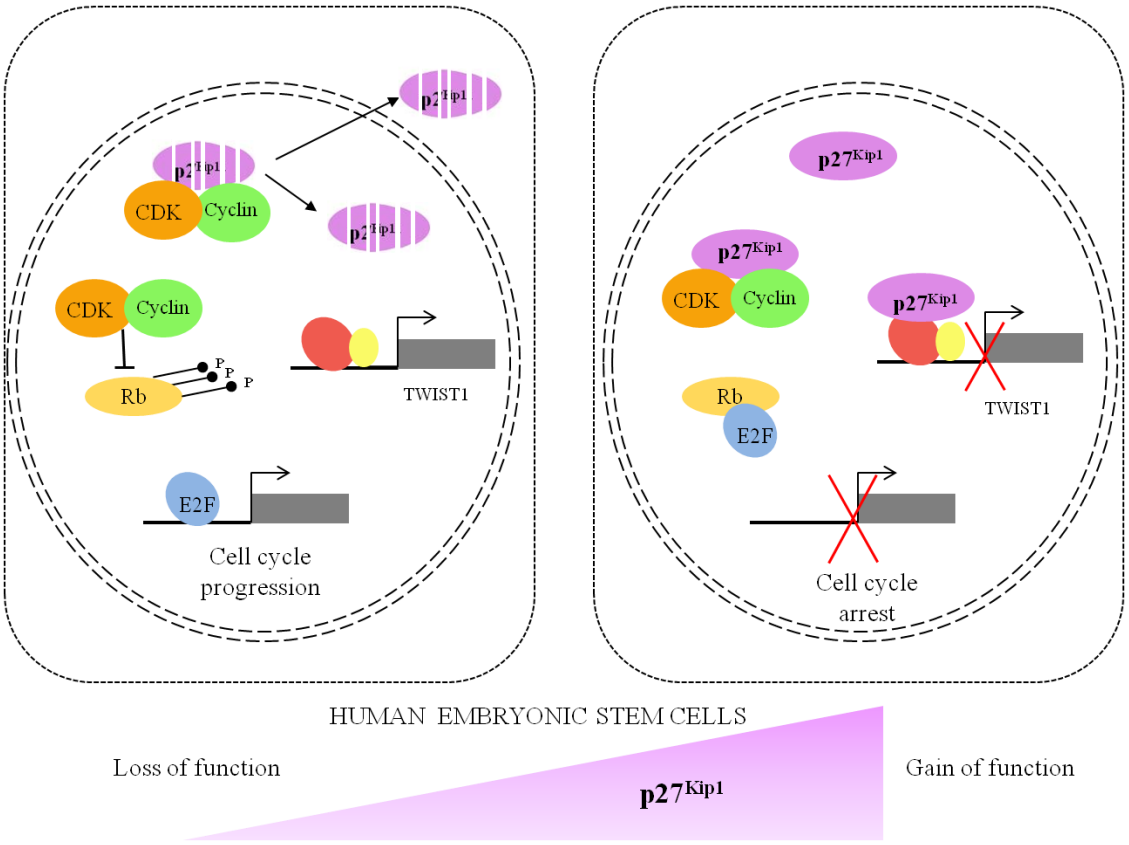

Figure 68. Proposed model for p27^{Kip1} function in human embryonic stem cells. p27^{Kip1} simultaneously targets CDK and transcriptional regulators to coordinate self-renewal and lineage commitment. The loss of function of p27^{Kip1} in undifferentiated human embryonic stem cells increases the proportion of cells in S phase due to an increase of cyclin-CDK complexes activity, consequently retinoblastoma proteins (Rb) are hyperphosphorylated (inactive) and cell cycle progression constitutively on. The loss of function of p27^{Kip1} in undifferentiated human embryonic stem cells induces the transcription of *TWIST1*. The gain of function of p27^{Kip1} in human embryonic stem cells prevents cell cycle progression through a G_1 to S phase arrest through inhibition of cyclin-CDK complexes. The gain of function of p27^{Kip1} in human embryonic stem cells represses the transcription of *TWIST1* and it is associated with the presence of p27^{Kip1} protein in the *TWIST1* gene promoter.

CONCLUSIONS

1. Undifferentiated pluripotent human embryonic stem cells (hESC), human induced pluripotent stem cells (hiPSC), and mouse embryonic stem cells (mESC) share an atypical cell cycle structure consisting of a low proportion of cells in $G_0/_1$ phase and a high proportion of cells in S phase. On differentiation, the cell cycle structure for all cell lines changes with a striking increase of cells in the $G_0/_1$ phase and a reduction of cells in the S phase.

2. The cell cycle structure change during differentiation is underlain by conserved changes in the protein profiles of pluripotent human and mouse embryonic stem cells. The expression of G_1 cyclins and cyclin dependent kinase inhibitors increased during differentiation, and on the contrary S and M phase associated cyclins A and B_1 as well as proteins involved in the replication of DNA decreased during differentiation.

3. The cyclin dependent kinase inhibitor $p27^{Kip1}$ appeared expressed in low levels in undifferentiated pluripotent human and mouse cell lines, but its expression increased during differentiation paralleling the changes in the cell cycle structure.

4. The expression levels of $p27^{Kip1}$ are regulated by the proteasome pathway in undifferentiated human embryonic stem cells.

5. The cell cycle inhibitor $p27^{Kip1}$ controls the self-renewal of human embryonic stem cells by regulating the G_1 to S transition and cell morphology.

6. The cell cycle inhibitor $p27^{Kip1}$ has an important role in the proper pluripotency of human embryonic stem cells via its effect in regulating the mesoderm markers *BRACHYURY* and *TWIST* in undifferentiating conditions, and under guided differentiating conditions of human embryonic stem cells towards mesoderm or ectoderm, loss of $p27^{Kip1}$ caused loss of ectoderm markers.

7. The cell cycle inhibitor $p27^{Kip1}$ is recruited to the *TWIST1* gene promoter and it is associated with gene expression levels in human embryonic stem cells.

MATERIAL AND METHODS

Cell culture

Human embryonic stem cells (hESC), human keratinocytes induced pluripotent stem cells (hKiPS), and human fibroblast induced pluripotent stem cells (hFiPS) were derived and characterized at the CMR[B] (Rodriguez-Piza, Richaud-Patin et al. 2009; Aasen, Raya et al. 2008; Raya, Rodriguez-Piza et al. 2008). All these cells were cultured on top of mitotically inactivated human fibroblasts and picked mechanically, or cultured over Matrigel (BD Biosciences) coated plates with hESC conditioned medium and passaged by trypsinization with 0.05% trypsin-EDTA (Invitrogen) (Raya, Rodriguez-Piza et al. 2008). The culture medium of hESC consisted of Knockout Dulbecco´s Modified Eagle´s Medium (DMEM) supplemented with 20% Knockout Serum Replacement (KSR), 1% non-essential amino acids, 50 µM of 2-Mercaptoethanol, 100 U/mL penicillin, 100 µg/mL streptomycin, 2 mM GlutaMAX (all Invitrogen), and 10 ng/mL basic fibroblast growth factor (bFGF) (Peprotech). The conditioned medium was prepared from irradiated mouse embryonic fibroblasts (MEFs) grown for seven days in hESC medium. Cell supernatants were collected, filter sterilized, and then stored at 4ºC for up to two weeks.

Cultures were maintained at 37ºC, 5% CO_2 atmosphere, with medium changes daily. Feeder cells used were: human foreskin fibroblasts (HFF-1, ATCC), and mouse embryonic fibroblasts (MEFs) established from dissociated C57BL/6 mouse embryos (13.5 d gestation). Both, HFF-1 and MEFs, were mitotically inactivated by gamma irradiation (55 Gy) and grown in DMEM medium supplemented with 10% Fetal Bovine Serum (FBS), 100 U/mL penicillin, 100 µg/mL streptomycin, and 2 mM GlutaMAX (all Invitrogen).

293T cells (CRL-12103 ATCC number, Rockville, MD, USA) were cultured in DMEM medium supplemented with 10% FBS, 100 U/mL penicillin, 100 µg/mL streptomycin, and 2 mM GlutaMAX (all Invitrogen).

Mouse embryonic stem cells (mESC) were grown over MEFs feeder layer and the cell culture medium consisted of Knockout DMEM, 15 % FBS (HyClone), 1% non-essential amino acids, 50 µM of 2-Mercaptoethanol, 100 U/mL penicillin, 100 µg/mL streptomycin, 2 mM GlutaMAX, and 1000 U/mL recombinant leukaemia inhibitory factor (LIF) (ESGRO).

Karyotype analysis

Karyotype analyses were carried out routinely and a normal karyotype was observed in all pluripotent cell lines used in this thesis.

Samples of hESC and human induced pluripotent stem cells (hiPSC) were treated with colcemid (KaryoMax^{TM}; Invitrogen). Colcemid is a methylated derivative of colchicine which blocks microtubule assembly by binding to the tubuline heterodimer blocking mitosis at the metaphase stage. For the treatments, 2 µL of colcemid 10 µg/mL were added to 1 mL of hESC medium and incubated 45 minutes at 37ºC in a CO_2 incubator. After this time had elapsed, the medium containing colcemid was removed and cells were washed twice with Phosphate-buffered saline (PBS) consisting of 137 mM NaCl, 2.7 mM KCl, 10 mM sodium phosphate dibasic, 2 mM potassium phosphate monobasic, pH 7.4. After washing, the cells were incubated in 0.05% trypsin-EDTA solution for 5 minutes in the incubator. After this time had elapsed, trypsin was inactivated by adding hESC medium and cells were harvested by centrifugation (1200 rpm for 5 minutes at room temperature). Supernatant was aspirated and cells were washed with PBS. Cells were, again, collected by centrifugation (1200 rpm for 5 minutes at room temperature). Supernatant was aspirated and pellet was loosen by tapping the tube and resuspended in a hypotonic solution (KaryoMax KCl 0.075M; Invitrogen). Cells were incubated in 10 mL of hypotonic solution for 10 minutes at 37ºC. After this time had elapsed, 1 mL of cold Carnoy fixative (Methanol:Acetic Acid 3:1) (Sigma-Aldrich Quimica) (-20ºC) was added to the cells. Pellet was collected by centrifugation (1800 rpm for 10 minutes at room temperature) and pellet resuspended in cold (-20ºC) Carnoy fixative. Metaphase chromosomes were analyzed under a microscope.

***In vitro* differentiation**

For general differentiation of mechanically picked cells, colonies of undifferentiated cells were detached from the feeder layer using a modified glass pipette and transferred to low attachment plates 60mm x 15mm (Corning, NY 14831) in hESC medium for 3-4 days. After 3-4 days, the embryoid bodies (EB) were transferred to 0.1% gelatin (Chemicon) coated plates and cultured with general differentiation medium consisting of Knockout DMEM (Invitrogen) supplemented with 20% FBS (HyClone), non-essential aminoacids, 100 U/mL penicillin, 100 µg/mL streptomycin, 2 mM GlutaMAX, and 50 µM 2-Mercaptoethanol (all Invitrogen) for 30 days. The medium was changed every two days (Figure 69A).

For general differentiation of hESC passaged by trypsinization, 0.05% trypsin-EDTA (Invitrogen) was used for single cell suspension and 35000-40000 hESC, in a final volume of 200 µL of conditioned medium, were seeded in each well of 96-well v-bottom low attachment plates (NUNC), and subsequently centrifuged at 950 x *g* for 10 minutes to aggregate the cells. After 3-4 days, EB were transferred to 0.1% gelatin coated plates and cultured with general differentiation medium. Cell samples for Western blot and Flow cytometry analysis were taken after 15 and/or 30 days. The medium was changed every two days.

For neuroectoderm differentiation, EB were cultured with DMEM/F12 and Neurobasal media in 1:1 proportions supplemented with N2 and B27 supplements, 100 U/mL penicillin, 100 µg/mL streptomycin, and 2 mM GlutaMAX (all Invitrogen) in suspension for 6 days, subsequently they were seeded onto Matrigel-coated plates or Matrigel-coated chamber-slide flasks (NUNC) with the same media plus 10^{-6} M Retinoic Acid (Sigma-Aldrich Quimica). Cell samples for Western blot and immunofluorescence analysis were taken after 15 and/or 30 days. The medium was changed every day.

For mesoderm differentiation, EB were seeded onto gelatin-coated chamber-slide flasks and cultured with general differentiation medium supplemented with 100 µM Ascorbic Acid (Sigma-Aldrich Quimica) for 30 days. The medium was changed every day.

For differentiation of mESC into EB, cells were harvested by trypsinization and seeded into 10 cm. bacteriological dishes (Nirco) in 10 mL of mESC medium without LIF (Figure 69B).

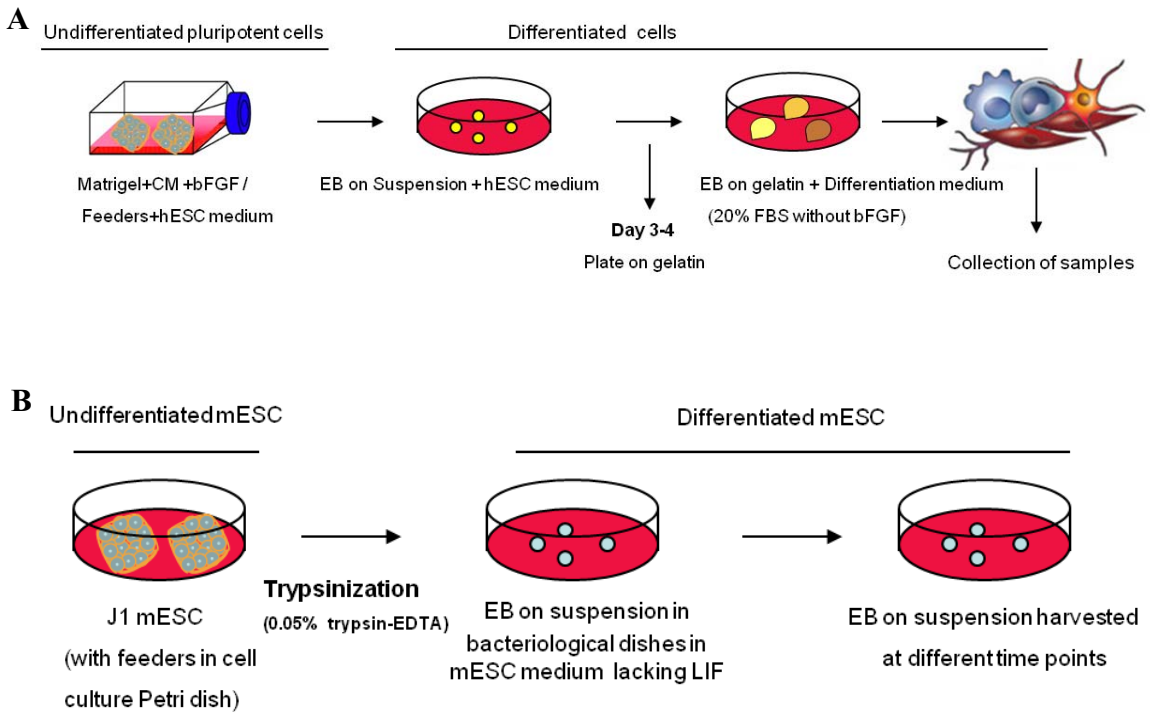

Figure 69. General differentiation protocols of human and mouse pluripotent cells. (**A**) General differentiation protocol of pluripotent human embryonic stem cells (hESC) or human induced pluripotent stem cells (hiPSC) was carried out by embryoid body (EB) generation using a modified glass pipette (for mechanically picked cells) or trypsinization (for cells passaged by trypsinization) and subsequent growth on gelation with differentiation medium containing 20% fetal bovine serum (FBS) and lacking basic fibroblast growth factor (bFGF). (**B**) Differentiation protocol of mouse embryonic stem cells (mESC) was carried out by EB generation, via trypsinization, and subsequent growth in suspension in non-adherent bacteriological dishes with mESC medium lacking leukaemia inhibitory factor (LIF).

Flow cytometry analysis

For measuring apoptosis, the commercial kit "MitoProbe $DilC_1(5)$ Assay Kit" (Invitrogen) was used. Briefly, cells were washed with warm PBS and trypsinizated with 0.05% trypsin-EDTA solution. After this time had elapsed, trypsin was inactivated with hESC medium and cells collected by centrifugation (2000 rpm, 3 minutes). Cells were suspended in 1 mL of warm PBS containing 1% bovine serum albumin (BSA) (PBS-1% BSA) at approximately $1x10^6$ cells/mL. Five µL of 10 µM $DilC_1(5)$ solution were added to the cells and left to incubate at 37ºC in 5% CO_2 atmosphere for 15 to 30 minutes. Cells were washed once with warm PBS-1% BSA and harvested by centrifugation (2000 rpm, 3 minutes). Cells were resuspended in 500 µL of warm PBS-1% BSA, and 100 µL of Propidium Iodide (P4170, Sigma-Aldrich) solution (0.5 mg/mL in PBS with 0.1% sodium azide, pH 7.4) were added to the 500 µL and left to

incubate at 37ºC for 15 minutes. Finally, $DilC_1(5)$ fluorescence was analyzed on a MoFlo cell sorter (DakoCytomation) with 633 nm excitation and far red emission (658 nm). Propidium Iodide was analyzed with a blue-green excitation (493 nm) and red emission (630 nm). A minimum of 10000 events were collected for analysis with Summit software.

For the cell cycle analyses, the commercial kit "Click-iT EdU AlexaFluor647 Flow Cytometry Assay kit" (Invitrogen) was used. For the analysis, 2 µL of 10 mM EdU solution was added to 2 mL of culture medium containing cells for 1 hour, cells were then trypsinizated with 0.05% trypsin and resuspended in 100 µL of PBS-1% BSA. Subsequently, 100 µL of Click-iT fixative solution were added to the cells, mixed for 5 seconds and left to incubate at room temperature for 15 minutes. Cells were washed with 3 mL of PBS-1% BSA and collected by centrifugation (2000 rpm, 3 minutes). Subsequently, 100 µL of 1X saponin-based permeabilization and wash buffer were added to the cell pellet and left to incubate with either mouse antibody against human Tra-1-60-FITC (BD) or rabbit polyclonal antibody against human $p27^{Kip1}$ (M-197, Santa Cruz Biotechnology) 1:20 for 30 minutes at room temperature. After this time had elapsed, cells were washed with PBS-1% BSA, collected by centrifugation (2000 rpm, 3 minutes), and those incubated with antibodies against $p27^{Kip1}$ were incubated with alexa fluor 488-conjugated anti-rabbit IgG (Invitrogen) 1:50 for 15 minutes at room temperature. Subsequently, cells were washed with 3 mL of the 1X saponin-based permeabilization and wash buffer, and collected by centrifugation (2000 rpm, 3 minutes). Then, 500 µl of Click-iT reaction cocktail containing 1X Click-iT EdU buffer additive, $CuS0_4$, and Alexa Fluor 647 were added to the cells and left to incubate for 30 minutes at room temperature. After this time had elapsed, cells were washed with saponin 1X buffer, collected by centrifugation, and resuspended in 500 µL of saponin 1X buffer. DNA content was assessed by staining cells with the addition of 4', 6-dimidino-2-phenylindole (DAPI) solution consisting of 0.1M Tris Base pH 7.4; 0.9% or 150 mM NaCl; 1mM $CaCl_2$; 0.5mM $MgCl_2$; 0.2% BSA; 0.1% Nonidet P40 (all from Sigma-Aldrich Quimica), and 10 mg/mL DAPI (Invitrogen) for 2 hours at room temperature or overnight at 4ºC. Finally, cells were analyzed on a MoFlo cell sorter (DakoCytomation) with Summit software. A total of 10000 events were collected for the cell cycle analysis.

For cell sorting of alive cells based on size and cell cycle phase, cells residing in G_1 phase of the cell cycle were selected after staining with 2 µg/mL of Hoechst 33342 for 30 minutes at 37ºC. Hoechst 33342 was detected by using ultraviolet light excitation. Of this selected G_1 phase residing cells, the biggest cells from either $p27^{Kip1}$ overexpressing or GFP expressing hESC were separated from the smallest ones based on pulse-width signal at comparable cell numbers (58% population).

Western blot analysis

Cells were washed twice with cold PBS, then harvested by scraping cells in ice-cold lysis buffer (150 µL for 10 cm Petri dishes) consisting of Tris-HCl pH 7.4 (Roche), 250 mM NaCl, 1% Triton X100, 1 mM EDTA, 1 mM EGTA, 0.2 mM PMSF (all Sigma-Aldrich Quimica), 1X protease inhibitor cocktail (Roche), and 1X phosphatase inhibitor cocktail (Sigma-Aldrich Quimica). Lysates were passaged through a 1 mL syringe (Rubilabor) and a 25 G needle (Terumo) and left to incubate on ice for 30 minutes. Lysates were clarified by centrifugation at 10000 rpm for 10 minutes at 4ºC and protein concentrations determined by Bradford assay (Bio-Rad Laboratories GmbH). This assay involves the addition of an acidic dye to protein solution and subsequent measurement at 595 nm with a spectrophotometer. One part of Dye Reagent Concentrate was diluted with 4 parts of distilled, deionized water. Then, 5 µL of sample were added to 1 mL of Dye Reagent diluted, mixed, and transferred to polystyrene cuvettes. The absorbance was measured at 595 nm with a spectrophotometer. Equal quantities of protein were mixed with 4X of a commercial loading buffer containing 20 % 2-mercaptoethanol (Sigma-Aldrich Quimica), heated at 100ºC for 5 minutes, and resolved on 8% or 12% SDS polyacrilamide electrophoresis gels. After electrophoresis, proteins were transferred to a nitrocellulose membrane (Bio-Rad Laboratories) using a submerged transfer apparatus (BioRad), filled with 25 mM Tris Base (Roche), 200 mM glycine (Sigma-Aldrich Quimica), and 20% methanol (Merck). Non-specific binding was blocked with PBS containing 0.1% Tween-20 (Sigma-Aldrich Quimica) (PBST) and 5% milk powder (Sigma-Aldrich Quimica) for 1 hour at room temperature. Membranes were incubated with primary antibodies in PBST supplemented with 2% milk powder for 2 hours at room temperature or overnight at 4ºC. Primary antibodies were raised against $p27^{Kip1}$ (M-197), E2F4 (A-20), $p16^{Ink4a}$ (H-156), $p21^{Cip1}$(F-5), p107 (C-18), CDK2 (H- 298), CDK4 (H-22), Cyclin A (C-19), Cyclin D_1 (H-295), Cyclin D_2

(M-20), Cyclin E (M-20), PCNA (PC10), Rb (C-15), MCM2 (N-19), Cyclin B_1 (GNS1), p53 (FL-393) (all Santa Cruz Biotechnology); Oct3/4 (ab19857) (Abcam); Cyclin D_1 (Ab-2), Cyclin D_2 (Ab-2), and Cyclin D_3 (Ab-2) (all from Neomarkers) all primary antibodies were used as a 1:1000 dilution. Brachyury (AF2085, R&D Systems, Inc) and E-cadherin (BD, Transduction Laboratories) were used as a 1:500 dilution. α-tubulin (T6074, Sigma-Aldrich) was used as a 1:8000 dilution. Membranes were washed four times at room temperature for 5 minutes in PBST, then incubated for 1 hour at room temperature with horseradish peroxidase (HRP)-conjugated secondary anti-rabbit, anti-mouse, or anti-goat antibodies, whichever applies (Amersham Biosciences) 1:10000 in PBST 2% milk powder. Horseradish peroxidase activity was detected using ECL Plus detection kit (GE Healthcare Europe GmbH). Membranes were incubated with 2 mL of a mix Solution A:Solution B (1:40) for 5 minutes. After this time had elapsed, they were dried and exposed on Amersham ECL Hyperfilm (VWR international Eurolab) and, finally, films were scanned by means of a document scanner.

Protein stability analysis

Undifferentiated hESC were treated with an inhibitor of protein biosynthesis: cycloheximide (Sigma-Aldrich Quimica) and harvested after 1, 3, 6, or 8 hous of culture. To inhibit proteasome function, cells were exposed to a non-specific proteasome activity inhibitor: MG-132 (carbobenzoxy-L-leucyl-L-leucinal) (Sigma-Aldrich Quimica) for 8 hours before harvesting. Subsequently, the cells were lysed and immunoblotted with an antibody against $p27^{Kip1}$ (Santa Cruz Biotechnology) 1:1000. An α-tubulin antibody (T6074, Sigma-Aldrich) 1:8000 was used as a loading control.

Immunofluorescence

Cells were grown on plastic cover slide chambers (170920, NUNC), fixed with 4% paraformaldehyde (Sigma-Aldrich Quimica) for 20 minutes at room temperature or fixed with cold methanol for 5 minutes. After fixation, cells were washed 3 times with Tris-buffered saline (TBS) and blocked in TBS containing 0.5% Triton X-100 (Sigma-Aldrich Quimica) and 6% donkey serum (S-30; Chemicon) for 30 minutes at room temperature. After this time had elapsed, cell samples were incubated overnight at 4ºC with the following antibodies in TBS containing 0.1% Triton X-100 (TBST) and 6% donkey serum: $p27^{Kip1}$ (M-197, Santa Cruz Biotechnology) 1:200, Brachyury (AF2085,

R&D Systems, Inc) 1:25, E-Cadherin (BD, Transduction Laboratories) 1:100, GFP (GFP-1020, AVES) 1:250, Actin-α Smooth Muscle (A5228, Sigma) 1:400, β-Tubulin III TUJ1 (MMS-435P, Covance) 1:500, or Nestin (AB5922, Chemicon) 1:100. After primary antibody incubation, samples were washed three times with TBST containing 6% donkey serum and incubated with CY-conjugated secondary anti-rabbit, anti-mouse, anti-goat (all 1:200), or anti-chicken antibodies (1:50), whichever applies (all from Jackson) and Phalloidin (1:400) when needed, for two hours at 37ºC. Samples were washed three times in TBS buffer at room temperature for 5 minutes, and subsequently they were counterstained with DAPI (Invitrogen, 21490) 1:10000 for 10 minutes at room temperature in the dark. Samples were covered with mounting medium and a 24 x 40 mm coverslip (Knittel Glass) on top. Images were taken using Leica SP5 confocal microscope and Leica AF6000 software.

Time-lapse microscopy analysis

Approximately, $2x10^5$ hES[4] were infected with lentiviruses encoding p27pCCL or GFPpCCL constructs in suspension at 37ºC and 5% CO_2 atmosphere for one hour, and then plated in chamber slide flasks with an additional 1 mL of hESC conditioned medium. Cells were left to grow in a 5% CO_2 atmosphere at 37°C, and images of individual cells were taken after 4, 5, 6, and 7 days using Leica DMI4000B inverted microscope equipped with a Leica DFC320 digital fluorescence camera and Leica AF6000 software. After this time had elapsed, cultures were fixed with 4% Paraformaldehyde for 20 minutes at room temperature and immunofluorescence analyses performed for detection of $p27^{Kip1}$ expression. Cells were counterstained with DAPI 1:10000 for 10 minutes to allow the identification of nuclei.

Isolation of RNA and quantitative Reverse Transcription Polymerase Chain Reaction analysis

Total RNA was isolated using TRIzol reagent (Invitrogen). For the isolation of total RNA, 1 mL of TRIzol was added to each well of a 6-well plate and cell lysates were passed several times through a syringe. Lysates were transferred to Eppendorf tubes (Sarstedt) and 0.2 mL of Chloroform (Sigma-Aldrich Quimica) were added, samples were incubated at room temperature for 2 to 3 minutes, and then centrifuged at 12000 rpm for 15 minutes at 4ºC. The upper aqueous phase was transferred to a new

tube, and RNA was precipitated by mixing with 0.5 mL of isopropyl alcohol (Sigma-Aldrich Quimica). Samples were then incubated for 10 minutes at room temperature, and subsequently centrifuged at 12000 rpm for 10 minutes at 4ºC. Supernatants were removed and RNA pellet washed once with 1 mL of 75% of Ethanol (Panreac). Supernatants were removed after centrifugation at 7500 rpm for 5 minutes at 4ºC. RNA pellet was air-dried for 5 to 10 minutes, and subsequently dissolved in RNase-free water.

For the quantitative Reverse Transcription Polymerase Chain Reaction (qRT-PCR) analysis, 500 ng of total RNA were used to synthesize complementary DNA (cDNA) using Cloned AMV First-strand cDNA synthesis kit (Invitrogen). Complementary DNA was synthesized by combining 500 ng of total RNA, 50 pmoles of oligo $(dT)_{20}$ primer, 10 mM of dNTP mix, 0.1 M DTT, 40 units of RNaseOUT^{TM}, 15 units of Cloned AMV reverse transcriptase plus its reaction buffer in a final volume of 20 μL, followed by 1 hour incubation at 50ºC and 5 minutes inactivation at 85ºC. One μL of the reaction was mixed with SYBR GreenER quantitative Polymerase Chain Reaction (qPCR) superMix for ABI PRISM (Invitrogen) and corresponding primers for the reaction of qRT-PCR. Each reaction was done per triplicate and run in an ABI Prism 7000 thermocycler (Applied Biosystems).

Quantitative RT-PCR conditions consisted of 50ºC for 2 minutes hold, 95ºC for 10 minutes hold followed by 40 cycles consisting of 95ºC for 15 seconds and 60ºC for 60 seconds. Relative mRNA expression levels were determined using the comparative threshold cycle method (Livak and Schmittgen 2001). The graphics represent $[2^{-CT\ (target)}/2^{-CT\ (housekeeping)}]$ cell line/$[2^{-CT\ (target)}/2^{-CT\ (housekeeping)}]$ control cells. The sequences of the oligonucleotides used for qRT-PCR analyses were designed with the Primer Express® software v2.0 (Applied Biosystems) and are shown in the table 5.

Gene	Forward primer (5'→ 3')	Reverse primer (5'→ 3')
$hp27^{Kip1}$	CCTGCAACCGACGATTCTTC	TCCACAGAACCGGCATTTG
CD34	AGGTATGCTCCCTGCTCCTT	GAATAGCTCTGGTGGCTTGC
DNMT3B	CAAGACTCGAAGACGCACAG	GGCAACATCTGAAGCCATTT
DESMIN	CTACACCTGCGAGATTGACG	TGTTGTCCTGGTAGCCACTG
GBX2	GGCGGTAACTTCGACAAGG	GGTCGTCTTCCACCTTTGAC
GATA 6	GGCTCTACAGCAAGATGAACG	CTGCGCCATAAGGTGGTAGT
BRACHYURY	GCTTCAAGGAGCTCACCAAT	GAAGGAGTACATGGCGTTGG
SNAIL 1	ACCCCAATCGGAAGCCTAAC	TGGTCGTAGGGCTGCTGGAA
SLUG	CAGCGAACTGGACACACATACA	AGGATCTCTGGTTGTGGTATGACA
CADHERIN E	GAACGCATTGCCACATACAC	ATTCGGGCTTGTTGTCATTC
TWIST	CCGGAGACCTAGATGTCATTGTT	TTTTAGTTATCCAGCTCCAGAGTCTCT
VIMENTIN	CCTCCGGGAGAAATTGCA	GCATTGTCAACATCCTGTCTGAA
GAPDH	GCACCGTCAAGGCTGAGAAC	AGGGATCTCGCTCCTGGAA
OCT3/4	GGAGGAAGCTGACAACAATGAAA	GGCCTGCACGAGGGTTT
SOX2	TGCGAGCGCTGCACAT	TCATGAGCGTCTTGGTTTTCC
NANOG	ACAACTGGCCGAAGAATAGCA	GGTTCCCAGTCGGGTTCAC
CRIPTO	CGGAACTGTGAGCACGATGT	GGGCAGCCAGGTGTCATG
KLF4	CGAACCCACACAGGTGAGAA	GAGCGGGCGAATTTCCAT
c-MYC	AGGGTCAAGTTGGACAGTGTCA	TGGTGCATTTTCGGTTGTTG

Table 5. Sequences of the oligonucleotides used for quantitative Reverse Transcription Polymerase Chain Reaction analysis.

For the expression analysis of stem cell related genes, Human Stem Cell RT2 profiler PCR array (SuperArray Bioscences Corporation) was purchased, and 500 ng of RNA isolated with RNeasy Mini Kit (Qiagen) were used for the analysis, following the manufacturer's directions. Briefly, cell samples were firstly lysed and homogenized in the presence of a highly denaturing guanidine-thiocyanate–containing buffer which inactivated RNases to ensure purification of intact RNA. One volume of 70% ethanol was added to the lysates, creating conditions that promoted selective binding of RNA to the RNeasy silica-based membrane. The sample was then transferred to the RNeasy

Mini spin column, placed in a 2 mL collection tube, and centrifuged for 15 seconds at 10000 rpm. Total RNA bound to the membrane and the flow-through was discarded. Contaminants were efficiently washed away and high-quality RNA was eluted in 30-50 µL of RNase-free water after centrifugation for 1 minute at 10000 rpm.

Relative mRNA expression levels were determined using the comparative threshold cycle method. The graphics represent [$2^{-CT(target)}/2^{-CT(housekeeping)}$] cell line/[$2^{-CT\ (target)}/2^{-CT\ (housekeeping)}$] control cells. Values that were upregulated twice or more or downregulated 50% or more were considered as significant changes.

MicroRNA expression and functional analysis

Small RNAs were isolated using *mir*Vana™ miRNA Isolation Kit (Applied Biosystems) following the manufacturer's directions. Briefly, cells were firstly washed with PBS and placed on ice. Cells were then disrupted in 600 µL of a denaturing lysis/binding buffer which stabilized RNA and inactivated RNases. Then, 1/10 volume (60 µL) of microRNA (miRNA) Homogenate additive was added to the cell lysate, mixed, and incubated on ice for 10 minutes. The lysate was then extracted once with 600 µL of Acid-Phenol:Chloroform which removed most of the other cellular components, leaving a semi-pure RNA sample after centrifugation for 5 minutes at 10000 rpm at room temperature. The aqueous phase was transferred to a new tube, and 1/3 volume of 100% ethanol was added and mixed by vortexing the tube. This lysate/ethanol mixture was then passed through a glass-fiber filter and centrifuged for 15 seconds at 10000 rpm. Large RNAs were immobilized while the small RNA species were collected in the filtrate. The ethanol concentration of the filtrate was increased by adding 2/3 volumes of room temperature 100% ethanol. After mixing, the sample was passed through a second glass-fiber filter, where the small RNAs became immobilized, after centrifugation for 15 seconds at 10000 rpm. This second filter was then washed a few times, and the small-RNA enriched sample was eluted in a low ionic strength solution after centrifugation for 30 seconds at 10000 rpm.

The analysis of potential miRNA target sites in 3' untranslated region (UTR) of human $p27^{Kip1}$ were performed *in silico* using Target Scan Release 5.1 (http://www.targetscan.org).

Mature miRNA expression of human miR-221, miR-222, and miR-24 was detected by qRT-PCR analysis using *mir*Vana™ qRT-PCR miRNA detection Kit

(Applied Biosystems). mirVana qRT-PCR Primer Sets specifics for hsa-miR-221 (AM 30115), hsa-miR-222 (AM 30116), or hsa-miR-24 (AM 30121) were purchased from (Applied Biosystems). Each qRT-PCR Primer Set included a primer for reverse transcription and a PCR primer pair for detection by qPCR analysis. MicroRNA expression assays of human U6 small nuclear RNA (snRNA) (AM 30303) were used to normalize the relative abundance of miRNA. Reverse transcription (RT) reactions containing 2 μL of *mir*Vana 5X RT Buffer, 1 μL of 1X *mir*Vana RT primer, 0.4 μL of ArrayScript Enzyme Mix, and 50 ng of RNA was prepared until a final volume of 10 μL. These RT reactions were incubated in a thermal cycler for 30 minutes at 37ºC, and then incubated for 10 minutes at 95ºC to inactivate the ArrayScript. Subsequently, qPCR was performed by combining 4.5 μL of the RT reaction mixed with 1X SYBR GreenER qPCR superMix for ABI PRISM and corresponding primers for the reactions of qPCR.

Each reaction was done per triplicate and run in an ABI Prism 7000 thermocycler. Relative miRNA expression levels were calculated using the comparative threshold cycle method relative to human U6 snRNA and multiplied by 1000 to simplify data presentation.

For the functional analysis, RNA oligonucleotides designed to specifically bind to, and inhibit endogenous miR-24 molecules: Ambion® Anti-miR™ miRNA Inhibitors, were purchased from (Ambion) (AM 17000). Cy™3 dye-labeled Anti-miR Negative Control (AM 17011), containing a random sequence anti-miR molecule not able to produce identifiable effects on known miRNA functions, and with a fluorescent moiety on the 5' end of the oligonucleotide, was used for monitoring transfection efficiency during optimization of transfection conditions and was purchased from (Ambion).

Approximately, 10-12 EB of hES[4] passage 22 were seeded in each well of 6-well plates (Falcon) with differentiation medium and left to grow for 11 or 14 days. Cy™3 dye-labeled Anti-miR Negative Control oligos were transfected by Fugene 6 Transfection Reagent (Roche Diagnostics). For the optimization of transfection conditions, differentiated cells were incubated in 2 mL of medium containing Cy™3 dye-labeled Anti-miR Negative Control oligos at a final concentrations of 50 nM or 100 nM, and mixed with different ratios of Fugene: oligo (3:1), or (6:1). The percentages of transfection were monitored by fluorescence microscopy using Leica DMI4000B inverted microscope with a tetramethyl rhodamine (TRITC) filter.

The condition that gave the highest percentage of transfection was when a final concentration of 100 nM of oligo and a ratio of Fugene: oligo 6:1 were used. The same conditions were then applied for transfecting cells with Anti-miR-24 miRNA Inhibitor. Cell samples were collected after 3-4 days of tranfection, and $p27^{Kip1}$ protein levels analyzed by Western blot analysis.

Z-Stack Scanning analysis of an EB transfected with Cy™3 dye-labeled Anti-miR Negative Control oligos were performed with a Leica SP5 confocal microscope, and showed fluorescence in different confocal planes therefore demonstrating that these cells were successfully transfected.

Constructs and plasmid purification

Human *p27Kip1* coding sequence was amplified by Polymerase Chain Reaction (PCR) using a forward primer containing an AgeI restriction enzyme site and a reverse primer containing a ClaI restriction enzyme site. Primer sequences were as follows:
Forward, 5'GATCACCGGTGCCATGGCTTACCCATACGATGTTCCAGATTACGC GTCAAACGTGCGAGTGTCTAACGGG 3'
Reverse, 5'GATCATCGATTTACGTTTGACGTCTTCTGAGGCCAGGC3'

This PCR reaction amplified a fragment of 650 base pairs, and it was obtained after 20 cycles of amplification with an annealing temperature of 60ºC. The *p27Kip1* coding sequence was subcloned into the pcRII vector (Invitrogen), following the manufacturer´s directions, to give pcRII-p27 and subsequently sequenced to confirm its correct sequence.

Sequencing amplification was performed by combining 150-300 ng of plasmid, 2.5 µL of sequence kit (BIG*Dye*™, Applied Biosystems), 2.5 µL of sequencing buffer (200 mM Tris-HCl pH=9, and 5 mM $MgCl_2$) plus 25 µM of primer in a final volume of 10 µL followed by incubation at 96ºC for 2 minutes and 35 cycles consisting of 96ºC for 10 seconds, 50ºC for 5 seconds, and 60ºC for 4 minutes in a Thermal cycler GeneAmp PCR 2400 (Applied Biosystems). DNA was precipitated and sequenced in the Genomic Service of the Barcelona Biomedical Research Park (PRBB).

The pcRII-p27 vector was digested using AgeI/ClaI restriction enzymes (NEB) and run on low-melt 0.5% agarose (Sigma-Aldrich Quimica) gel in Tris-Acetate/EDTA (TAE) buffer. The *p27Kip1* coding sequence was gel purified using "QIAquick Gel Extraction Kit" (Qiagen) following the manufacturer's instructions. Briefly, DNA

fragment was excised from the agarose gel with a sharp scalpel. Three volumes of buffer QG were added to one volumen of gel. Buffer QG contains high concentration of chaotropic salts and a pH ≤7.5 which solubilizes the agarose gel slice and provides the correct salt concentration and pH for adsorption of DNA to the silica QIAquick membrane. The sample was applied to the QIAquick column and centrifuged for 1 minute at 13000 rpm and room temperature to allow binding of DNA to the membrane. The flow-through was discarded and 0.75 mL of Buffer PE containing ethanol were added to the QIAquick column to wash away salts and rest of impurities. Any residual Buffer PE, which might interfere with subsequent analysis, was removed by an additional centrifugation step for 1 minute at 13000 rpm and room temperature. Pure DNA was eluted under basic conditions and low salt concentrations with 30-50 µL of Buffer EB (10 mM Tris-Cl, pH 8.5) after centrifugation for 1 minute at 13000 rpm and room temperature.

The *p27^{Kip1}* coding sequence was then subcloned into AgeI and ClaI sites of pCCL TET OFF inducible lentiviral vector. pCCL TET OFF and GFPpCCL TET OFF inducible lentiviral vectors were kindly provided by L. Naldini (San Raffaele Telethon Institute for Gene Therapy-'Vita-Salute San Raffaele' University Medical School, Milano, Italy).

Short hairpin RNAs (shRNAs) targeting different regions of the p27^{Kip1} gene sequence (p27shRNA) which were designed using a proprietary algorithm and were sequence verified to ensure a match to the p27^{Kip1} gene, and negative control Non Target shRNA constructs (NTshRNA) containing 5 base pair mismatches to any known human or mouse gene were purchased from Sigma-Aldrich Quimica. Puromycin sequence was removed by digestion with Bam H1 (New England Biolabs) and Asp 718 (Roche) restriction enzymes and a GFP sequence, containing Bam H1 and Kpn I cloning sites, was cloned instead. GFP cDNA was amplified by PCR using a forward primer containing a Bam H1 restriction enzyme site and a reverse primer containing a Kpn I restriction enzyme site. Primer sequences were as follows:

Forward, 5'GATCGGATCCATGGTGAGCAAGGGC 3'

Reverse, 5' GATCGGTACCTTACTTGTACAGC 3'

PCR products amplifying GFP cDNA were obtained after 30 cycles of amplification with an annealing temperature of 58ºC. PCR products were then cloned into pGEM-T easy vector (Promega Biotech Iberica) which was digested with Bam H1

and Asp 718 restriction enzymes. Digestion products were then run on low-melt 0.5% agarose gel in TAE buffer, and GFP cDNA was gel purified and cloned into Bam H1 and Asp 718 sites of p27 shRNA and Non Target shRNA vectors.

Subsequently, constructs were amplified after transformation into competent *E. coli* (Invitrogen). Briefly, one µL of each construct was added to a vial containing 50 µL of One Shot TOP10 Chemically Competent *E. coli* (Invitrogen) and mixed by tapping. The vials were incubated on ice for 30 minutes followed for a 30 seconds incubation in a 42ºC water bath. After this time had elapsed, the vials were placed again on ice and 250 µL of pre-warmed Super Optimal broth with Catabolite Repression (S.O.C.) medium was added to bacteria. The vials were shaked at 37ºC for one hour at 225 rpm in a shaking incubator. After this time had elapsed, 200 µL from each transformation were spreaded on separate Luria Bertani (LB) agar plates containing the appropriate selective antibiotic, inverted, and incubated overnight at 37ºC. The next day, a single bacterial colony was picked from a selective plate and inoculated into a starter culture of 2-5 mL of LB medium containing the appropriate selective antibiotic, and left to grow for approximately 8 hours at 37ºC with vigourous shaking (approximately 300 rpm). The starter culture was diluted 1:1000 into selective LB medium and left to grow at 37ºC for 12-16 hours with vigourous shaking (approximately 300 rpm). Then, the bacterial cells were harvested by centrifugation at 6000 x *g* for 15 minutes at 4ºC.

Plasmids were purificated using the EndoFree Plasmid Maxi Kit (Qiagen) following the manufacturer's instructions. Briefly, the bacterial pellets were resuspended in 10 mL of Buffer P1 containing 50 mM Tris-HCl, pH 8.0, 10 mM EDTA, and 100 µg/mL RNasa. Subsequently, bacterial pellets were lysed by addition of 10 mL of alkaline lysis P2 buffer containing 200 mM NaOH, 1% SDS (w/v), mixed by inverting the tube, and incubated at room temperature for 5 minutes. After this time had elapsed, 10 mL of chilled neutralization P3 buffer (3 M potassium acetate, pH 5.5) were added to the lysates causing the precipitation of genomic DNA, proteins, and cell debris. Clearing of neutralized bacterial lysates were carried out without centrifugation by pushing the liquid through a QIAfilter Cartridge. Filtered lysates were incubated on ice for 30 minutes with 2.5 mL of a specific endotoxin removal buffer (Buffer ER). The filtered lysates were subsequently applied to a QIAGEN Anion-Exchange Resin under appropriate low-salt and pH conditions and allowed them to enter the resin by gravity

flow. The endotoxin removal buffer prevents lipopolysaccharides (LPS) molecules from binding to the resin in the QIAGEN-tips. Plasmids DNA bound to QIAGEN Anion-Exchange Resin, while RNA, proteins, dyes, and low molecular weight impurities were removed by a medium-salt wash containing 1 M NaCl, 50 mM MOPS, pH 7.0, and 15% isopropanol (v/v). Plasmids DNA were subsequently eluted with 15 mL of a high salt buffer (QN) containing 1.6 M NaCl, 50 mM MOPS, pH 7.0, and 15% isopropanol (v/v). DNA was precipitated and desalted by adding 10.5 mL of room temperature isopropanol to the eluted DNA and centrifugated at ≥15000 x *g* for 30 minutes at 4ºC. Supernatant was removed and DNA was washed with 5 mL of endotoxin-free room temperature 70% ethanol. Supernatants were removed after centrifugation at ≥15000 rpm for 10 minutes, and the pellets air-dried for 5 to 10 minutes and redissolved in alkaline TE buffer (10 mM Tris-HCl, pH 8.0; 1 mM EDTA).

Lentiviral production

Lentiviruses were independently produced by transfecting the cell line 293T with packaging and envelope vectors: pMDLg-pRRE (6.5 μg), pMD2.VSV.G (4 μg), pRSV-Rev (2.5 μg) kindly provided by L. Naldini (San Raffaele Telethon Institute for Gene Therapy-'Vita-Salute San Raffaele' University Medical School, Milano, Italy), and lentiviral constructs (10 μg) using 50 μL of Lipofectamine 2000 (Invitrogen) according to the manufacturer's instructions. After 16 hours, transfecting medium was replaced with 6 mL of hESC conditioned medium, and cells were incubated at 37ºC in a 5% CO_2 atmosphere. Viral supernatants were harvested after 24 and 48 hours, filtered, and stored at -80ºC in 1 mL aliquots. Virus titer was tested using a HIV-1 p24 ELISA kit (Perkin Elmer). Approximately, $2x10^5$ hESC were infected in suspension with 1 mL of viral supernatant at 37ºC in a 5% CO_2 atmosphere for one hour and then seeded in a well of 6-well plates with an additional 1 mL of hESC conditioned medium. The next day the medium was changed.

Senescence-associated β-galactosidase staining

Approximately, $2x10^5$ hESC were infected with p27pCCL or GFPpCCL lentiviral supernatants in suspension at 37ºC in a 5% CO_2 atmosphere, for one hour, and then seeded in a well of 6-well plates with an additional 1 mL of hESC conditioned medium. The next day the medium was changed. Cells were left to grow for 5-6 days.

Senescence-associated β-galactosidase activity was determined using the Senescence β-Galactosidase Staining Kit (Cell Signaling Technology™). The kit is designed to histochemically detect β-galactosidase activity at pH 6, a known characteristic of senescent cells. Briefly, cells were washed once with 2 mL of PBS, fixed for 10 minutes at room temperature with 1 mL of 2% formaldehyde/ 0.2% glutaraldehyde (vol/vol), and subsequently washed twice with 2 mL of PBS. Cells were subsequently incubated with 1 mL of freshly prepared staining solution containing 1 mg/mL of 5-bromo-4-chloro-3-indolyl-βD-galactopyranoside (X-gal), 40 mM citric acid/ sodium phosphate pH 6, 5 mM potassium ferrocyanide, 5 mM potassium ferricyanide, 150 mM NaCl, and 2 mM $MgCl_2$ overnight at 37ºC without CO_2. Cells were checked under a microscope (200 x total magnification) for development of color.

Alternatively, senescence-associated β-galactosidase activity was detected using another procedure. Cells were washed in PBS and partially fixed, so as to not inactivate the β-galactosidase enzyme, for 5 to 10 minutes at room temperature in β-galactosidase freshly prepared fixative solution containing: 0.2% (v/v) glutaraldehyde, 1.5% (v/v) formaldehyde, 5 mM EGTA, 2 mM $MgCl_2$, and 100 mM sodium phosphate buffer, pH 8.0. In order to remove fixative solution, cells were washed three times in β-galactosidase wash buffer containing: 2 mM $MgCl_2$, 0.01% (w/v) sodium deoxycholate, 0.02% (v/v) Nonidet P-40, and 100 mM phosphate buffer, pH 8.0 for washes of 15 minutes, each time, at room temperature. Cells were subsequently incubated overnight at 37ºC without CO_2 in β-galactosidase staining solution prepared from 25 mg/mL X-gal, 100 mM potassium ferrocyanide in 100 mM sodium phosphate buffer, pH 8.0, and 100 mM potassium ferricyanide in 100 mM sodium phosphate buffer, pH 8.0 stock solutions diluted in β-galactosidase wash buffer to yield the following final concentrations: 1 mg/mL X-gal, 5 mM potassium ferrocyanide, and 5 mM potassium ferricyanide. Finally, cells were washed three times in PBS and observed under a microscope.

Chromatin Immunoprecipitation Analysis

Chromatin Immunoprecipitation (ChIP) assays were performed using the commercial kit "ChampionChIP™ One-Day Kit" (SABiosciences) following the manufacturer's directions. Briefly, approximately 4 to 6 million hES[4] transduced with p27pCCL or p27shRNA constructs asynchronously growing were washed and cross-

linked with 1% formaldehyde at 37ºC for 10 minutes. Cells were then washed twice with ice-cold PBS, harvested by scraping cells with a silicone cell scraper, centrifuged at 800 x *g* for 10 minutes at 4ºC, and resuspended in 0.5 mL of ice-cold lysis buffer and sonicated four times for 10 seconds each at the maximum setting. Supernatants were then recovered by centrifugation at 14000 x *g* for 10 minutes at 4 °C, diluted in dilution buffer, and subjected to one round of immunoclearing for 1 hour at 4 °C with 25 µL of protein A-Sepharose. Immunoprecipitation was performed overnight on rotator with specific antibodies, and then 40 µL of protein A-Sepharose were further added and incubated on a rotator for 3 hours at 4 °C. Immunoprecipitates were washed sequentially for 4 minutes each in Wash Buffer I (0.1% SDS, 1% Triton X-100, 2 mM EDTA, 20 mM Tris-HCl, pH 8.1, 150 mM NaCl), Wash Buffer II (0.1% SDS, 1% Triton X-100, 2 mM EDTA, 20 mM Tris-HCl, pH 8.1, 500 mM NaCl), and Wash Buffer III (0.25 M LiCl, 1% Nonidet P-40, 1% deoxycholate, 1 mM EDTA, 10 mM Tris-HCl, pH 8.1). Bead precipitates were then washed twice with TE buffer (10 mM Tris-HCl, pH 8.0, 1 mM EDTA), and histone complexes were eluted twice from the antibodies with 1% SDS, 0.1 M $NaHCO_3$, vortexed, and rotated 20 minutes at room temperature. Eluates were pooled, and 8 µL of 5 M NaCl were added to the combined eluates and heated for 6 hours at 65°C in a water bath to reverse the protein/histone-DNA cross-links. After this time had elapsed, 0.5 µL of RNase A (20 µg/µL) were added to the samples and incubated for 30 minutes at 37ºC. Subsequently, 4 µL of 0.5 M EDTA, 8 µL of 1 M Tris-HCl pH 6.5, and 1 µL of Proteinase K (20 mg/mL) were added to the samples and incubated at 45ºC for 1-2 hours. After this time had elapsed, DNA was recovered using the commercial "QIAquick PCR Purification Kit" (Qiagen), following the manufacturer's instructions. DNA was eluted in 50 µL, and 2 µL were used for each quantitative PCR reaction.

Quantification of ChIP was performed by quantitative PCR using ABI Prism 7000 thermocycler (Applied Biosystems) using the comparative threshold cycle method (Livak and Schmittgen 2001). The results were calculated as % Input with the equation $2^{-(Ct\ [ChIP] - (Ct\ [Input] - Log2\ (Input\ Dilution\ Factor)))}$ cell line/ $2^{-(Ct\ [ChIP] - (Ct\ [Input] - Log2\ (Input\ Dilution\ Factor)))}$ control cells. The primers for the quantitative PCR reactions for *TWIST1* gene from +1.0 Kb to -3.0 Kb at 1000 base pairs intervals were purchased from SABiosciences.

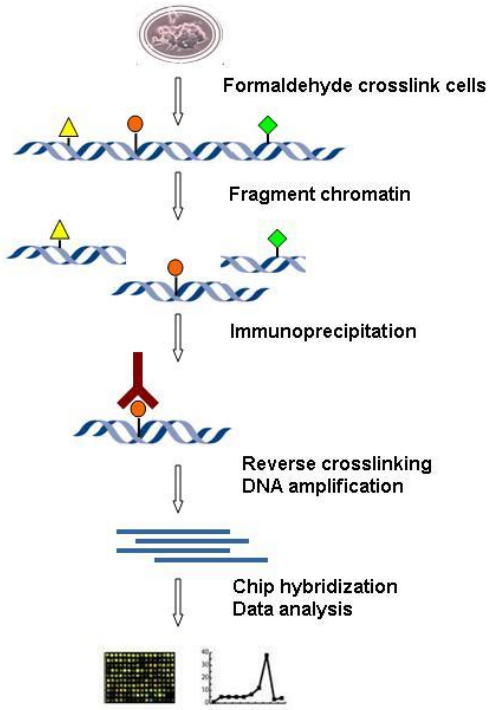

Figure 70. Schematic representation of Chromatin Immunoprecipitation (ChIP) assay.

Statistical Analysis

Data were expressed as means ± standard deviations and were analyzed applying two-tailed Student´s *t*-test or analysis of variance (ANOVA) statistic analysis. Probability values that were less than 0,05 were considered as statistically significant.

REFERENCES

Aasen, T., A. Raya, et al. (2008). "Efficient and rapid generation of induced pluripotent stem cells from human keratinocytes." *Nat Biotechnol* **26**(11): 1276-84.

Acloque, H., M. S. Adams, et al. (2009). "Epithelial-mesenchymal transitions: the importance of changing cell state in development and disease." *J Clin Invest* **119**(6): 1438-49.

Aladjem, M. I., B. T. Spike, et al. (1998). "ES cells do not activate p53-dependent stress responses and undergo p53-independent apoptosis in response to DNA damage." *Curr Biol* **8**(3): 145-55.

Alessandrini, A., D. S. Chiaur, et al. (1997). "Regulation of the cyclin-dependent kinase inhibitor p27 by degradation and phosphorylation." *Leukemia* **11**(3): 342-5.

Amati, B., K. Alevizopoulos, et al. (1998). "Myc and the cell cycle." *Front Biosci* **3**: d250-68.

Amit, M., M. K. Carpenter, et al. (2000). "Clonally derived human embryonic stem cell lines maintain pluripotency and proliferative potential for prolonged periods of culture." *Dev Biol* **227**(2): 271-8.

Andres, V., J. Urena, et al. (2001). "Role of Sp1 in the induction of p27 gene expression in vascular smooth muscle cells in vitro and after balloon angioplasty." *Arterioscler Thromb Vasc Biol* **21**(3): 342-7.

Ansieau, S., A. P. Morel, et al. (2010). "TWISTing an embryonic transcription factor into an oncoprotein." *Oncogene* **29**(22): 3173-84.

Aoi, T., K. Yae, et al. (2008). "Generation of pluripotent stem cells from adult mouse liver and stomach cells." *Science* **321**(5889): 699-702.

Asada, M., T. Yamada, et al. (1999). "Apoptosis inhibitory activity of cytoplasmic p21(Cip1/WAF1) in monocytic differentiation." *Embo J* **18**(5): 1223-34.

Avilion, A. A., S. K. Nicolis, et al. (2003). "Multipotent cell lineages in early mouse development depend on SOX2 function." *Genes Dev* **17**(1): 126-40.

Baldassarre, G., A. Boccia, et al. (2000). "Retinoic acid induces neuronal differentiation of embryonal carcinoma cells by reducing proteasome-dependent proteolysis of the cyclin-dependent inhibitor p27." *Cell Growth Differ* **11**(10): 517-26.

Baldassarre, G., B. Belletti, et al. (2005). "p27(Kip1)-stathmin interaction influences sarcoma cell migration and invasion." *Cancer Cell* **7**(1): 51-63.

Barrallo-Gimeno, A. and M. A. Nieto (2005). "The Snail genes as inducers of cell movement and survival: implications in development and cancer." *Development* **132**(14): 3151-61.

Bartek, J. and J. Lukas (2001). "Pathways governing G1/S transition and their response to DNA damage." *FEBS Lett* **490**(3): 117-22.

Baylies, M. K. and M. Bate (1996). "twist: a myogenic switch in Drosophila." *Science* **272**(5267): 1481-4.

Becker, K. A., J. L. Stein, et al. (2010). "Human embryonic stem cells are pre-mitotically committed to self-renewal and acquire a lengthened G1 phase upon lineage programming." *J Cell Physiol* **222**(1): 103-10.

Becker, K. A., J. L. Stein, et al. (2007). "Establishment of histone gene regulation and cell cycle checkpoint control in human embryonic stem cells." *J Cell Physiol* **210**(2): 517-26.

Becker, K. A., P. N. Ghule, et al. (2010). "Cyclin D2 and the CDK substrate p220(NPAT) are required for self-renewal of human embryonic stem cells." J Cell Physiol **222**(2): 456-64.

Becker, K. A., P. N. Ghule, et al. (2006). "Self-renewal of human embryonic stem cells is supported by a shortened G1 cell cycle phase." *J Cell Physiol* **209**(3): 883-93.

Beddington, R. S. and E. J. Robertson (1989). "An assessment of the developmental potential of embryonic stem cells in the midgestation mouse embryo." *Development* **105**(4): 733-7.

Beddington, R. S., P. Rashbass, et al. (1992). "Brachyury--a gene affecting mouse gastrulation and early organogenesis." *Dev Suppl*: 157-65.

Berthet, C. and P. Kaldis (2007). "Cell-specific responses to loss of cyclin-dependent kinases." *Oncogene* **26**(31): 4469-77.

Besson, A., H. C. Hwang, et al. (2007). "Discovery of an oncogenic activity in p27Kip1 that causes stem cell expansion and a multiple tumor phenotype." *Genes Dev* **21**(14): 1731-46.

Besson, A., M. Gurian-West, et al. (2004). "p27Kip1 modulates cell migration through the regulation of RhoA activation." *Genes Dev* **18**(8): 862-76.

Besson, A., R. K. Assoian, et al. (2004). "Regulation of the cytoskeleton: an oncogenic function for CDK inhibitors?" *Nat Rev Cancer* **4**(12): 948-55.

Besson, A., S. F. Dowdy, et al. (2008). "CDK inhibitors: cell cycle regulators and beyond." *Dev Cell* **14**(2): 159-69.

Bibikova, M., L. C. Laurent, et al. (2008). "Unraveling epigenetic regulation in embryonic stem cells." *Cell Stem Cell* **2**(2): 123-34.

Bienvenu, F., H. Gascan, et al. (2001). "Cyclin D1 represses STAT3 activation through a Cdk4-independent mechanism." *J Biol Chem* **276**(20): 16840-7.

Blomen, V. A. and J. Boonstra (2007). "Cell fate determination during G1 phase progression." *Cell Mol Life Sci* **64**(23): 3084-104.

Boehm, M., T. Yoshimoto, et al. (2002). "A growth factor-dependent nuclear kinase phosphorylates p27(Kip1) and regulates cell cycle progression." *Embo J* **21**(13): 3390-401.

Borchert, G. M., W. Lanier, et al. (2006). "RNA polymerase III transcribes human microRNAs." *Nat Struct Mol Biol* **13**(12): 1097-101.

Borriello, A., V. Cucciolla, et al. (2007). "p27Kip1 metabolism: a fascinating labyrinth." *Cell Cycle* **6**(9): 1053-61.

Bouchard, C., K. Thieke, et al. (1999). "Direct induction of cyclin D2 by Myc contributes to cell cycle progression and sequestration of p27." *Embo J* **18**(19): 5321-33.

Boyer, L. A., T. I. Lee, et al. (2005). "Core transcriptional regulatory circuitry in human embryonic stem cells." *Cell* **122**(6): 947-56.

Brownawell, A. M., G. J. Kops, et al. (2001). "Inhibition of nuclear import by protein kinase B (Akt) regulates the subcellular distribution and activity of the forkhead transcription factor AFX." *Mol Cell Biol* **21**(10): 3534-46.

Brunet, A., A. Bonni, et al. (1999). "Akt promotes cell survival by phosphorylating and inhibiting a Forkhead transcription factor." *Cell* **96**(6): 857-68.

Bryja, V., J. Pachernik, et al. (2004). "Increased apoptosis in differentiating p27-deficient mouse embryonic stem cells." *Cell Mol Life Sci* **61**(11): 1384-400.

Bryja, V., L. Cajanek, et al. (2005). "Abnormal development of mouse embryoid bodies lacking p27Kip1 cell cycle regulator." *Stem Cells* **23**(7): 965-74.

Burdon, T., A. Smith, et al. (2002). "Signalling, cell cycle and pluripotency in embryonic stem cells." *Trends Cell Biol* **12**(9): 432-8.

Burdon, T., C. Stracey, et al. (1999). "Suppression of SHP-2 and ERK signalling promotes self-renewal of mouse embryonic stem cells." *Dev Biol* **210**(1): 30-43.

Carrano, A. C., E. Eytan, et al. (1999). "SKP2 is required for ubiquitin-mediated degradation of the CDK inhibitor p27." *Nat Cell Biol* **1**(4): 193-9.

Carver, E. A., R. Jiang, et al. (2001). "The mouse snail gene encodes a key regulator of the epithelial-mesenchymal transition." *Mol Cell Biol* **21**(23): 8184-8.

Chambers, I., D. Colby, et al. (2003). "Functional expression cloning of Nanog, a pluripotency sustaining factor in embryonic stem cells." *Cell* **113**(5): 643-55.

Chambers, I., J. Silva, et al. (2007). "Nanog safeguards pluripotency and mediates germline development." *Nature* **450**(7173): 1230-4.

Chandramohan, V., S. Jeay, et al. (2004). "Reciprocal control of Forkhead box O 3a and c-Myc via the phosphatidylinositol 3-kinase pathway coordinately regulates p27Kip1 levels." *J Immunol* **172**(9): 5522-7.

Chen, P. L., D. J. Riley, et al. (1996). "Retinoblastoma protein positively regulates terminal adipocyte differentiation through direct interaction with C/EBPs." *Genes Dev* **10**(21): 2794-804.

Chen, Z. F. and R. R. Behringer (1995). "twist is required in head mesenchyme for cranial neural tube morphogenesis." *Genes Dev* **9**(6): 686-99.

Cheng, M., P. Olivier, et al. (1999). "The p21(Cip1) and p27(Kip1) CDK 'inhibitors' are essential activators of cyclin D-dependent kinases in murine fibroblasts." *Embo J* **18**(6): 1571-83.

Chu, I. M., L. Hengst, et al. (2008). "The Cdk inhibitor p27 in human cancer: prognostic potential and relevance to anticancer therapy." *Nat Rev Cancer* **8**(4): 253-67.

Chu, I., J. Sun, et al. (2007). "p27 phosphorylation by Src regulates inhibition of cyclin E-Cdk2." *Cell* **128**(2): 281-94.

Ciruna, B. and J. Rossant (2001). "FGF signaling regulates mesoderm cell fate specification and morphogenetic movement at the primitive streak." *Dev Cell* **1**(1): 37-49.

Connor, M. K., R. Kotchetkov, et al. (2003). "CRM1/Ran-mediated nuclear export of p27(Kip1) involves a nuclear export signal and links p27 export and proteolysis." Mol Biol Cell **14**(1): 201-13.

Coqueret, O. (2002). Linking cyclins to transcriptional control. *Gene*. **299:** 35-55.

Coqueret, O. (2003). "New roles for p21 and p27 cell-cycle inhibitors: a function for each cell compartment?" *Trends Cell Biol* **13**(2): 65-70.

Cristofalo, V. J., C. Volker, et al. (1998). "Age-dependent modifications of gene expression in human fibroblasts." *Crit Rev Eukaryot Gene Expr* **8**(1): 43-80.

Cross, D. A., D. R. Alessi, et al. (1995). "Inhibition of glycogen synthase kinase-3 by insulin mediated by protein kinase B." *Nature* **378**(6559): 785-9.

Cuesta, R., A. Martinez-Sanchez, et al. (2009). "miR-181a regulates cap-dependent translation of p27(kip1) mRNA in myeloid cells." *Mol Cell Biol* **29**(10): 2841-51.

del Barrio, M. G. and M. A. Nieto (2002). "Overexpression of Snail family members highlights their ability to promote chick neural crest formation." *Development* **129**(7): 1583-93.

Deng, C., P. Zhang, et al. (1995). "Mice lacking p21CIP1/WAF1 undergo normal development, but are defective in G1 checkpoint control." *Cell* **82**(4): 675-84.

Denicourt, C., C. C. Saenz, et al. (2007). "Relocalized p27Kip1 tumor suppressor functions as a cytoplasmic metastatic oncogene in melanoma." *Cancer Res* **67**(19): 9238-43.

Diehl, J. A., M. Cheng, et al. (1998). "Glycogen synthase kinase-3beta regulates cyclin D1 proteolysis and subcellular localization." *Genes Dev* **12**(22): 3499-511.

Dijkers, P. F., R. H. Medema, et al. (2000). "Forkhead transcription factor FKHR-L1 modulates cytokine-dependent transcriptional regulation of p27(KIP1)." *Mol Cell Biol* **20**(24): 9138-48.

Dimri, G. P., X. Lee, et al. (1995). "A biomarker that identifies senescent human cells in culture and in aging skin in vivo." *Proc Natl Acad Sci U S A* **92**(20): 9363-7.

Dobrosi, N., B. I. Toth, et al. (2008). "Endocannabinoids enhance lipid synthesis and apoptosis of human sebocytes via cannabinoid receptor-2-mediated signaling." *Faseb J* **22**(10): 3685-95.

Draper, J. S., K. Smith, et al. (2004). "Recurrent gain of chromosomes 17q and 12 in cultured human embryonic stem cells." *Nat Biotechnol* **22**(1): 53-4.

Dravid, G., Z. Ye, et al. (2005). "Defining the role of Wnt/beta-catenin signaling in the survival, proliferation, and self-renewal of human embryonic stem cells." *Stem Cells* **23**(10): 1489-501.

Durand, B., F. B. Gao, et al. (1997). "Accumulation of the cyclin-dependent kinase inhibitor p27/Kip1 and the timing of oligodendrocyte differentiation." *Embo J* **16**(2): 306-17.

Edel, M. J., C. Menchón, et al. (2010). "Rem2 GTPase maintains survival of human embryonic stem cells as well as enhancing reprogramming by regulating p53 and cyclin D1." *Genes Dev* **24**(6): 561-73.

Edel, M. J., S. Boue, et al. (2010). "Rem2 GTPase controls proliferation and apoptosis of neurons during embryo development." *Cell Cycle* **9**(17).

Egozi, D., M. Shapira, et al. (2007). "Regulation of the cell cycle inhibitor p27 and its ubiquitin ligase Skp2 in differentiation of human embryonic stem cells." *Faseb J* **21**(11): 2807-17.

el-Deiry, W. S., T. Tokino, et al. (1993). "WAF1, a potential mediator of p53 tumor suppression." *Cell* **75**(4): 817-25.

Evans, M. J. and M. H. Kaufman (1981). "Establishment in culture of pluripotential cells from mouse embryos." *Nature* **292**(5819): 154-6.

Eymin, B. and E. Brambilla (2004). "The yin and the yang of p27Kip1 as a target for cancer therapy." *Eur Respir J* **23**(5): 663-4.

Faast, R., J. White, et al. (2004). "Cdk6-cyclin D3 activity in murine ES cells is resistant to inhibition by p16(INK4a)." *Oncogene* **23**(2): 491-502.

Felicetti, F., M. C. Errico, et al. (2008). "The promyelocytic leukemia zinc finger-microRNA-221/-222 pathway controls melanoma progression through multiple oncogenic mechanisms." *Cancer Res* **68**(8): 2745-54.

Feng, G. S. (2007). "Shp2-mediated molecular signaling in control of embryonic stem cell self-renewal and differentiation." *Cell Res* **17**(1): 37-41.

Fero, M. L., E. Randel, et al. (1998). "The murine gene p27Kip1 is haplo-insufficient for tumour suppression." *Nature* **396**(6707): 177-80.

Fero, M. L., M. Rivkin, et al. (1996). "A syndrome of multiorgan hyperplasia with features of gigantism, tumorigenesis, and female sterility in p27(Kip1)-deficient mice." *Cell* **85**(5): 733-44.

Filipczyk, A. A., A. L. Laslett, et al. (2007). "Differentiation is coupled to changes in the cell cycle regulatory apparatus of human embryonic stem cells." *Stem Cell Res* **1**(1): 45-60.

Fluckiger, A.C., G. Marcy, et al. (2006). "Cell cycle features of primate embryonic stem cells." *Stem Cells* **24**(3): 547-56.

Fong, H., K. A. Hohenstein, et al. (2008). "Regulation of self-renewal and pluripotency by Sox2 in human embryonic stem cells." *Stem Cells* **26**(8): 1931-8.

Fornari, F., L. Gramantieri, et al. (2008). "MiR-221 controls CDKN1C/p57 and CDKN1B/p27 expression in human hepatocellular carcinoma." *Oncogene* **27**(43): 5651-61.

Fujita, N., S. Sato, et al. (2002). "Akt-dependent phosphorylation of p27Kip1 promotes binding to 14-3-3 and cytoplasmic localization." *J Biol Chem* **277**(32): 28706-13.

Fujiwara, S., J. C. Corbo, et al. (1998). "The snail repressor establishes a muscle/notochord boundary in the Ciona embryo." *Development* **125**(13): 2511-20.

Funk, J. O. and D. A. Galloway (1998). "Inhibiting CDK inhibitors: new lessons from DNA tumor viruses." *Trends Biochem Sci* **23**(9): 337-41.

Galardi, S., N. Mercatelli, et al. (2007). "miR-221 and miR-222 expression affects the proliferation potential of human prostate carcinoma cell lines by targeting p27Kip1." *J Biol Chem* **282**(32): 23716-24.

Galderisi, U., F. P. Jori, et al. (2003). "Cell cycle regulation and neural differentiation." *Oncogene* **22**(33): 5208-19.

Gangaraju, V. K. and H. Lin (2009). "MicroRNAs: key regulators of stem cells." *Nat Rev Mol Cell Biol* **10**(2): 116-25.

Ghule, P. N., K. A. Becker, et al. (2007). "Cell cycle dependent phosphorylation and subnuclear organization of the histone gene regulator p220(NPAT) in human embryonic stem cells." *J Cell Physiol* **213**(1): 9-17.

Gillies, J. K. and I. A. Lorimer (2007). "Regulation of p27Kip1 by miRNA 221/222 in glioblastoma." *Cell Cycle* **6**(16): 2005-9.

Gitelman, I. (1997). "Twist protein in mouse embryogenesis." *Dev Biol* **189**(2): 205-14.

Goldstein, S. (1990). "Replicative senescence: the human fibroblast comes of age." *Science* **249**(4973): 1129-33.

Gregory, D. J., E. Garcia-Wilson, et al. (2002). "Induction of transcription through the p300 CRD1 motif by p21WAF1/CIP1 is core promoter specific and cyclin dependent kinase independent." *Cell Cycle* **1**(5): 343-50.

Grimmler, M., Y. Wang, et al. (2007). "Cdk-inhibitory activity and stability of p27Kip1 are directly regulated by oncogenic tyrosine kinases." *Cell* **128**(2): 269-80.

Gu, W., J. W. Schneider, et al. (1993). "Interaction of myogenic factors and the retinoblastoma protein mediates muscle cell commitment and differentiation." *Cell* **72**(3): 309-24.

Gu, Y., C. W. Turck, et al. (1993). "Inhibition of CDK2 activity in vivo by an associated 20K regulatory subunit." *Nature* **366**(6456): 707-10.

Hanna, J., S. Markoulaki, et al. (2008). "Direct reprogramming of terminally differentiated mature B lymphocytes to pluripotency." *Cell* **133**(2): 250-64.

Harbour, J. W. and D. C. Dean (2000). "The Rb/E2F pathway: expanding roles and emerging paradigms." *Genes Dev* **14**(19): 2393-409.

Hatfield, S. D., H. R. Shcherbata, et al. (2005). "Stem cell division is regulated by the microRNA pathway." *Nature* **435**(7044): 974-8.

Hemberger, M., W. Dean, et al. (2009). "Epigenetic dynamics of stem cells and cell lineage commitment: digging Waddington's canal." *Nat Rev Mol Cell Biol* **10**(8): 526-37.

Hochegger, H., S. Takeda, et al. (2008). "Cyclin-dependent kinases and cell-cycle transitions: does one fit all?" *Nat Rev Mol Cell Biol* **9**(11): 910-6.

Hong, H., K. Takahashi, et al. (2009). "Suppression of induced pluripotent stem cell generation by the p53-p21 pathway." *Nature* **460**(7259): 1132-5.

Huangfu, D., R. Maehr, et al. (2008). "Induction of pluripotent stem cells by defined factors is greatly improved by small-molecule compounds." *Nat Biotechnol* **26**(7): 795-7.

Ishida, N., M. Kitagawa, et al. (2000). "Phosphorylation at serine 10, a major phosphorylation site of p27(Kip1), increases its protein stability." *J Biol Chem* **275**(33): 25146-54.

Ishida, N., T. Hara, et al. (2002). "Phosphorylation of p27Kip1 on serine 10 is required for its binding to CRM1 and nuclear export." *J Biol Chem* **277**(17): 14355-8.

Itoh, Y., N. Masuyama, et al. (2007). "The cyclin-dependent kinase inhibitors p57 and p27 regulate neuronal migration in the developing mouse neocortex." *J Biol Chem* **282**(1): 390-6.

Ivey, K. N., A. Muth, et al. (2008). "MicroRNA regulation of cell lineages in mouse and human embryonic stem cells." *Cell Stem Cell* **2**(3): 219-29.

Jaenisch, R. and R. Young (2008). "Stem cells, the molecular circuitry of pluripotency and nuclear reprogramming." *Cell* **132**(4): 567-82.

James, D., A. J. Levine, et al. (2005). "TGFbeta/activin/nodal signaling is necessary for the maintenance of pluripotency in human embryonic stem cells." *Development* **132**(6): 1273-82.

Joza, N., S. A. Susin, et al. (2001). "Essential role of the mitochondrial apoptosis-inducing factor in programmed cell death." *Nature* **410**(6828): 549-54.

Kalaszczynska, I., Y. Geng, et al. (2009). "Cyclin A is redundant in fibroblasts but essential in hematopoietic and embryonic stem cells." *Cell* **138**(2): 352-65.

Kalluri, R. and R. A. Weinberg (2009). "The basics of epithelial-mesenchymal transition." *J Clin Invest* **119**(6): 1420-8.

Kamura, T., T. Hara, et al. (2004). "Cytoplasmic ubiquitin ligase KPC regulates proteolysis of p27(Kip1) at G1 phase." *Nat Cell Biol* **6**(12): 1229-35.

Kang, H. B., J. S. Kim, et al. (2005). "Basic fibroblast growth factor activates ERK and induces c-fos in human embryonic stem cell line MizhES1." *Stem Cells Dev* **14**(4): 395-401.

Karnik, S. K., C. M. Hughes, et al. (2005). "Menin regulates pancreatic islet growth by promoting histone methylation and expression of genes encoding p27Kip1 and p18INK4c." *Proc Natl Acad Sci U S A* **102**(41): 14659-64.

Kawamura, T., J. Suzuki, et al. (2009). "Linking the p53 tumour suppressor pathway to somatic cell reprogramming." *Nature* **460**(7259): 1140-4.

Kim, J. B., H. Zaehres, et al. (2008). "Pluripotent stem cells induced from adult neural stem cells by reprogramming with two factors." *Nature* **454**(7204): 646-50.

Kim, J., J. Chu, et al. (2008). "An extended transcriptional network for pluripotency of embryonic stem cells." *Cell* **132**(6): 1049-61.

Knecht, A. K. and M. Bronner-Fraser (2002). "Induction of the neural crest: a multigene process." *Nat Rev Genet* **3**(6): 453-61.

Kozar, K., M. A. Ciemerych, et al. (2004). "Mouse development and cell proliferation in the absence of D-cyclins." *Cell* **118**(4): 477-91.

Kranenburg, O., R. P. de Groot, et al. (1995). "Differentiation of P19 EC cells leads to differential modulation of cyclin-dependent kinase activities and to changes in the cell cycle profile." *Oncogene* **10**(1): 87-95.

Kunath, T., M. K. Saba-El-Leil, et al. (2007). "FGF stimulation of the Erk1/2 signalling cascade triggers transition of pluripotent embryonic stem cells from self-renewal to lineage commitment." *Development* **134**(16): 2895-902.

Kurz, D. J., S. Decary, et al. (2000). "Senescence-associated (beta)-galactosidase reflects an increase in lysosomal mass during replicative ageing of human endothelial cells." *J Cell Sci* **113 (Pt 20)**: 3613-22.

Lacy, E. R., I. Filippov, et al. (2004). "p27 binds cyclin-CDK complexes through a sequential mechanism involving binding-induced protein folding." *Nat Struct Mol Biol* **11**(4): 358-64.

Lai, J., J. Chien, et al. (2003). "Loss of HSulf-1 up-regulates heparin-binding growth factor signaling in cancer." *J Biol Chem* **278**(25): 23107-17.

Langeland, J. A., J. M. Tomsa, et al. (1998). "An amphioxus snail gene: expression in paraxial mesoderm and neural plate suggests a conserved role in patterning the chordate embryo." *Dev Genes Evol* **208**(10): 569-77.

Lapenna, S. and A. Giordano (2009). "Cell cycle kinases as therapeutic targets for cancer." *Nat Rev Drug Discov* **8**(7): 547-66.

le Sage, C., R. Nagel, et al. (2007). "Diverse ways to control p27Kip1 function: miRNAs come into play." *Cell Cycle* **6**(22): 2742-9.

le Sage, C., R. Nagel, et al. (2007). "Regulation of the p27(Kip1) tumor suppressor by miR-221 and miR-222 promotes cancer cell proliferation." *Embo J* **26**(15): 3699-708.

Leary, J. F., P. Todd, et al. (1979). "Laser flow cytometric light scatter and fluorescence pulse width and pulse rise-time sizing of mammalian cells." *J Histochem Cytochem* **27**(1): 315-20.

Lee, M. H., I. Reynisdottir, et al. (1995). "Cloning of p57KIP2, a cyclin-dependent kinase inhibitor with unique domain structure and tissue distribution." *Genes Dev* **9**(6): 639-49.

Lee, M. H., M. Nikolic, et al. (1996). "The brain-specific activator p35 allows Cdk5 to escape inhibition by p27Kip1 in neurons." *Proc Natl Acad Sci U S A* **93**(8): 3259-63.

Lee, Y., M. Kim, et al. (2004). "MicroRNA genes are transcribed by RNA polymerase II." *Embo J* **23**(20): 4051-60.

Leptin, M. (1991). "twist and snail as positive and negative regulators during Drosophila mesoderm development." *Genes Dev* **5**(9): 1568-76.

Leshem, Y., D. B. Spicer, et al. (2000). "Hepatocyte growth factor (HGF) inhibits skeletal muscle cell differentiation: a role for the bHLH protein twist and the cdk inhibitor p27." *J Cell Physiol* **184**(1): 101-9.

Levkau, B., H. Koyama, et al. (1998). "Cleavage of p21Cip1/Waf1 and p27Kip1 mediates apoptosis in endothelial cells through activation of Cdk2: role of a caspase cascade." *Mol Cell* **1**(4): 553-63.

Li, B., N. Jia, et al. (2006). "Cul4A targets p27 for degradation and regulates proliferation, cell cycle exit, and differentiation during erythropoiesis." *Blood* **107**(11): 4291-9.

Li, J., G. Wang, et al. (2007). "MEK/ERK signaling contributes to the maintenance of human embryonic stem cell self-renewal." *Differentiation* **75**(4): 299-307.

Lin T., C. Chao, et al. (2005). "p53 induces differentiation of mouse embryonic stem cells by suppressing Nanog expression." *Nat Cell Biol* **7**(2): 165-71.

Livak, K. J. and T. D. Schmittgen (2001). "Analysis of relative gene expression data using real-time quantitative PCR and the 2(-Delta Delta C(T)) Method." *Methods* **25**(4): 402-8.

Loh, Y. H., S. Agarwal, et al. (2009). "Generation of induced pluripotent stem cells from human blood." *Blood* **113**(22): 5476-9.

Luo, Y., J. Hurwitz, et al. (1995). "Cell-cycle inhibition by independent CDK and PCNA binding domains in p21Cip1." *Nature* **375**(6527): 159-61.

Maimets, T., I. Neganova, et al. (2008). "Activation of p53 by nutlin leads to rapid differentiation of human embryonic stem cells." *Oncogene* **27**(40): 5277-87.

Malumbres, M. and M. Barbacid (2009). "Cell cycle, CDKs and cancer: a changing paradigm." *Nat Rev Cancer* **9**(3): 153-66.

Mani, S. A., W. Guo, et al. (2008). "The epithelial-mesenchymal transition generates cells with properties of stem cells." *Cell* **133**(4): 704-15.

Marion, R. M., K. Strati, et al. (2009). "A p53-mediated DNA damage response limits reprogramming to ensure iPS cell genomic integrity." *Nature* **460**(7259): 1149-53.

Marson, A., S. S. Levine, et al. (2008). "Connecting microRNA genes to the core transcriptional regulatory circuitry of embryonic stem cells." *Cell* **134**(3): 521-33.

Martin, G. R. (1981). "Isolation of a pluripotent cell line from early mouse embryos cultured in medium conditioned by teratocarcinoma stem cells." *Proc Natl Acad Sci U S A* **78**(12): 7634-8.

Matsuda, T., T. Nakamura, et al. (1999). "STAT3 activation is sufficient to maintain an undifferentiated state of mouse embryonic stem cells." *Embo J* **18**(15): 4261-9.

Matsuoka, S., M. C. Edwards, et al. (1995). "p57KIP2, a structurally distinct member of the p21CIP1 Cdk inhibitor family, is a candidate tumor suppressor gene." *Genes Dev* **9**(6): 650-62.

McAllister, S. S., M. Becker-Hapak, et al. (2003). "Novel p27(kip1) C-terminal scatter domain mediates Rac-dependent cell migration independent of cell cycle arrest functions." *Mol Cell Biol* **23**(1): 216-28.

McLean, A. B., K. A. D'Amour, et al. (2007). "Activin a efficiently specifies definitive endoderm from human embryonic stem cells only when phosphatidylinositol 3-kinase signaling is suppressed." *Stem Cells* **25**(1): 29-38.

Medema, R. H., G. J. Kops, et al. (2000). "AFX-like Forkhead transcription factors mediate cell-cycle regulation by Ras and PKB through p27kip1." *Nature* **404**(6779): 782-7.

Melton, C., R. L. Judson, et al. "Opposing microRNA families regulate self-renewal in mouse embryonic stem cells." *Nature* **463**(7281): 621-6.

Mercatelli, N., V. Coppola, et al. (2008). "The inhibition of the highly expressed miR-221 and miR-222 impairs the growth of prostate carcinoma xenografts in mice." *PLoS One* **3**(12): e4029.

Misumi, S., T. S. Kim, et al. (2008). "Enhanced neurogenesis from neural progenitor cells with G1/S-phase cell cycle arrest is mediated by transforming growth factor beta1." *Eur J Neurosci* **28**(6): 1049-59.

Mitalipova, M. M., R. R. Rao, et al. (2005). "Preserving the genetic integrity of human embryonic stem cells." *Nat Biotechnol* **23**(1): 19-20.

Miyabayashi, T., J. L. Teo, et al. (2007). "Wnt/beta-catenin/CBP signaling maintains long-term murine embryonic stem cell pluripotency." *Proc Natl Acad Sci U S A* **104**(13): 5668-73.

Miyazawa, K., T. Himi, et al. (2000). "A role for p27/Kip1 in the control of cerebellar granule cell precursor proliferation." *J Neurosci* **20**(15): 5756-63.

Movassagh, M. and A. Philpott (2008). "Cardiac differentiation in Xenopus requires the cyclin-dependent kinase inhibitor, p27Xic1." *Cardiovasc Res* **79**(3): 436-47.

Munoz-Alonso, M. J., J. C. Acosta, et al. (2005). "p21Cip1 and p27Kip1 induce distinct cell cycle effects and differentiation programs in myeloid leukemia cells." *J Biol Chem* **280**(18): 18120-9.

Nagahara, H., A. M. Vocero-Akbani, et al. (1998). "Transduction of full-length TAT fusion proteins into mammalian cells: TAT-p27Kip1 induces cell migration." *Nat Med* **4**(12): 1449-52.

Naiche, L. A., Z. Harrelson, et al. (2005). "T-box genes in vertebrate development." *Annu Rev Genet* **39**: 219-39.

Nakagawa, M., M. Koyanagi, et al. (2008). "Generation of induced pluripotent stem cells without Myc from mouse and human fibroblasts." *Nat Biotechnol* **26**(1): 101-6.

Nakayama, K., N. Ishida, et al. (1996). "Mice lacking p27(Kip1) display increased body size, multiple organ hyperplasia, retinal dysplasia, and pituitary tumors." *Cell* **85**(5): 707-20.

Nallamshetty, S., M. Crook, et al. (2005). "The cell cycle regulator p27Kip1 interacts with MCM7, a DNA replication licensing factor, to inhibit initiation of DNA replication." *FEBS Lett* **579**(29): 6529-36.

Navarro, A. and M. Monzo (2010) "MicroRNAs in human embryonic and cancer stem cells." *Yonsei Med J* **51**(5): 622-32.

Neganova, I., X. Zhang, et al. (2009). "Expression and functional analysis of G1 to S regulatory components reveals an important role for CDK2 in cell cycle regulation in human embryonic stem cells." *Oncogene* **28**(1): 20-30.

Nguyen, L., A. Besson, et al. (2006). "Coupling cell cycle exit, neuronal differentiation and migration in cortical neurogenesis." *Cell Cycle* **5**(20): 2314-8.

Nguyen, L., A. Besson, et al. (2006). "p27kip1 independently promotes neuronal differentiation and migration in the cerebral cortex." *Genes Dev* **20**(11): 1511-24.

Nieto, M. A. (2002). "The snail superfamily of zinc-finger transcription factors." *Nat Rev Mol Cell Biol* **3**(3): 155-66.

Nieto, M. A. (2009). "Epithelial-Mesenchymal Transitions in development and disease: old views and new perspectives." *Int J Dev Biol* **53**(8-10): 1541-7.

Nieto, M. A., M. G. Sargent, et al. (1994). "Control of cell behavior during vertebrate development by Slug, a zinc finger gene." *Science* **264**(5160): 835-9.

Niwa, H. (2007). "How is pluripotency determined and maintained?" *Development* **134**(4): 635-46.

Niwa, H., J. Miyazaki, et al. (2000). "Quantitative expression of Oct-3/4 defines differentiation, dedifferentiation or self-renewal of ES cells." *Nat Genet* **24**(4): 372-6.

Niwa, H., T. Burdon, et al. (1998). "Self-renewal of pluripotent embryonic stem cells is mediated via activation of STAT3." *Genes Dev* **12**(13): 2048-60.

Ohtsuka, S. and S. Dalton (2008). "Molecular and biological properties of pluripotent embryonic stem cells." *Gene Ther* **15**(2): 74-81.

Ophascharoensuk, V., M. L. Fero, et al. (1998). "The cyclin-dependent kinase inhibitor p27Kip1 safeguards against inflammatory injury." *Nat Med* **4**(5): 575-80.

Orford, K. W. and D. T. Scadden (2008). "Deconstructing stem cell self-renewal: genetic insights into cell-cycle regulation." *Nat Rev Genet* **9**(2): 115-28.

Pagano, M., S. W. Tam, et al. (1995). "Role of the ubiquitin-proteasome pathway in regulating abundance of the cyclin-dependent kinase inhibitor p27." *Science* **269**(5224): 682-5.

Paling, N. R., H. Wheadon, et al. (2004). "Regulation of embryonic stem cell self-renewal by phosphoinositide 3-kinase-dependent signaling." *J Biol Chem* **279**(46): 48063-70.

Pan, G. and J. A. Thomson (2007). "Nanog and transcriptional networks in embryonic stem cell pluripotency." *Cell Res* **17**(1): 42-9.

Pan, G., J. Li, et al. (2006). "A negative feedback loop of transcription factors that controls stem cell pluripotency and self-renewal." *Faseb J* **20**(10): 1730-2.

Park, I. H., R. Zhao, et al. (2008). "Reprogramming of human somatic cells to pluripotency with defined factors." *Nature* **451**(7175): 141-6.

Pera, M. F. and P. P. Tam (2010). "Extrinsic regulation of pluripotent stem cells." *Nature* **465**(7299): 713-20.

Perez-Juste, G. and A. Aranda (1999). "Differentiation of neuroblastoma cells by phorbol esters and insulin-like growth factor 1 is associated with induction of retinoic acid receptor beta gene expression." *Oncogene* **18**(39): 5393-402.

Perez-Roger, I., S. H. Kim, et al. (1999). "Cyclins D1 and D2 mediate myc-induced proliferation via sequestration of p27(Kip1) and p21(Cip1)." *Embo J* **18**(19): 5310-20.

Pieper, U., N. Eswar, et al. (2009). "MODBASE, a database of annotated comparative protein structure models and associated resources." *Nucleic Acids Res* **37**(Database issue): D347-54.

Pineau, P., S. Volinia, et al. (2010). "miR-221 overexpression contributes to liver tumorigenesis." *Proc Natl Acad Sci U S A* **107**(1): 264-9.

Polyak, K., J. Y. Kato, et al. (1994). "p27Kip1, a cyclin-Cdk inhibitor, links transforming growth factor-beta and contact inhibition to cell cycle arrest." *Genes Dev* **8**(1): 9-22.

Polyak, K., M. H. Lee, et al. (1994). "Cloning of p27Kip1, a cyclin-dependent kinase inhibitor and a potential mediator of extracellular antimitogenic signals." *Cell* **78**(1): 59-66.

Ponce-Castaneda, M. V., M. H. Lee, et al. (1995). "p27Kip1: chromosomal mapping to 12p12-12p13.1 and absence of mutations in human tumors." *Cancer Res* **55**(6): 1211-4.

Qi, J., J. Y. Yu, et al. (2009). "microRNAs regulate human embryonic stem cell division." *Cell Cycle* **8**(22): 3729-41.

Qi, X., T. G. Li, et al. (2004). "BMP4 supports self-renewal of embryonic stem cells by inhibiting mitogen-activated protein kinase pathways." *Proc Natl Acad Sci U S A* **101**(16): 6027-32.

Qin, H., T. Yu, et al. (2007). "Regulation of apoptosis and differentiation by p53 in human embryonic stem cells." *J Biol Chem* **282**(8): 5842-52.

Rands, G. F. (1986). "Size regulation in the mouse embryo. I. The development of quadruple aggregates." *J Embryol Exp Morphol* **94**: 139-48.

Rashbass, P., L. A. Cooke, et al. (1991). "A cell autonomous function of Brachyury in T/T embryonic stem cell chimaeras." *Nature* **353**(6342): 348-51.

Raya, A., I. Rodriguez-Piza, et al. (2008). "Generation of cardiomyocytes from new human embryonic stem cell lines derived from poor-quality blastocysts." *Cold Spring Harb Symp Quant Biol* **73**: 127-35.

Raz, R., C. K. Lee, et al. (1999). "Essential role of STAT3 for embryonic stem cell pluripotency." *Proc Natl Acad Sci U S A* **96**(6): 2846-51.

Reed, S. I. (2002). "Keeping p27(Kip1) in the cytoplasm: a second front in cancer's war on p27." *Cell Cycle* **1**(6): 389-90.

Resnick, J. L., L. S. Bixler, et al. (1992). "Long-term proliferation of mouse primordial germ cells in culture." *Nature* **359**(6395): 550-1.

Reynaud, E. G., M. P. Leibovitch, et al. (2000). "Stabilization of MyoD by direct binding to p57(Kip2)." *J Biol Chem* **275**(25): 18767-76.

Ridley, A. J., M. A. Schwartz, et al. (2003). "Cell migration: integrating signals from front to back." *Science* **302**(5651): 1704-9.

Rodriguez-Piza, I., Y. Richaud-Patin, et al. (2009). "Reprogramming of Human Fibroblasts to Induced Pluripotent Stem Cells under Xeno-free Conditions." *Stem Cells* **28**(1): 36-44.

Russo, A. A., P. D. Jeffrey, et al. (1996). "Structural basis of cyclin-dependent kinase activation by phosphorylation." *Nat Struct Biol* **3**(8): 696-700.

Satyanarayana, A. and P. Kaldis (2009). "Mammalian cell-cycle regulation: several Cdks, numerous cyclins and diverse compensatory mechanisms." *Oncogene* **28**(33): 2925-39.

Savagner, P. (2001). "Leaving the neighborhood: molecular mechanisms involved during epithelial-mesenchymal transition." *Bioessays* **23**(10): 912-23.

Savatier, P., H. Lapillonne, et al. (1996). "Withdrawal of differentiation inhibitory activity/leukemia inhibitory factor up-regulates D-type cyclins and cyclin-dependent kinase inhibitors in mouse embryonic stem cells." *Oncogene* **12**(2): 309-22.

Savatier, P., S. Huang, et al. (1994). "Contrasting patterns of retinoblastoma protein expression in mouse embryonic stem cells and embryonic fibroblasts." *Oncogene* **9**(3): 809-18.

Sefton, M., S. Sanchez, et al. (1998). "Conserved and divergent roles for members of the Snail family of transcription factors in the chick and mouse embryo." *Development* **125**(16): 3111-21.

Sekimoto, T., M. Fukumoto, et al. (2004). "14-3-3 suppresses the nuclear localization of threonine 157-phosphorylated p27(Kip1)." *Embo J* **23**(9): 1934-42.

Sheaff, R. J., M. Groudine, et al. (1997). "Cyclin E-CDK2 is a regulator of p27Kip1." *Genes Dev* **11**(11): 1464-78.

Shen, M. M. (2007). "Nodal signaling: developmental roles and regulation." *Development* **134**(6): 1023-34.

Sherr, C. J. and J. M. Roberts (1995). "Inhibitors of mammalian G1 cyclin-dependent kinases." *Genes Dev* **9**(10): 1149-63.

Sherr, C. J. and J. M. Roberts (1999). "CDK inhibitors: positive and negative regulators of G1-phase progression." *Genes Dev* **13**(12): 1501-12.

Shi, Y., C. Desponts, et al. (2008). "Induction of pluripotent stem cells from mouse embryonic fibroblasts by Oct4 and Klf4 with small-molecule compounds." *Cell Stem Cell* **3**(5): 568-74.

Shim, J., H. Lee, et al. (1996). "A non-enzymatic p21 protein inhibitor of stress-activated protein kinases." *Nature* **381**(6585): 804-6.

Shimada, M. and M. Nakanishi (2006). "DNA damage checkpoints and cancer." *J Mol Histol* **37**(5-7): 253-60.

Shin, I., F. M. Yakes, et al. (2002). "PKB/Akt mediates cell-cycle progression by phosphorylation of p27(Kip1) at threonine 157 and modulation of its cellular localization." *Nat Med* **8**(10): 1145-52.

Shirane, M., Y. Harumiya, et al. (1999). "Down-regulation of p27(Kip1) by two mechanisms, ubiquitin-mediated degradation and proteolytic processing." *J Biol Chem* **274**(20): 13886-93.

Showell, C., O. Binder, et al. (2004). "T-box genes in early embryogenesis." *Dev Dyn* **229**(1): 201-18.

Silva, J., O. Barrandon, et al. (2008). "Promotion of reprogramming to ground state pluripotency by signal inhibition." *PLoS Biol* **6**(10): e253.

Snowden, A. W., L. A. Anderson, et al. (2000). "A novel transcriptional repression domain mediates p21(WAF1/CIP1) induction of p300 transactivation." *Mol Cell Biol* **20**(8): 2676-86.

Spicer, D. B., J. Rhee, et al. (1996). "Inhibition of myogenic bHLH and MEF2 transcription factors by the bHLH protein Twist." *Science* **272**(5267): 1476-80.

Sridharan, R., J. Tchieu, et al. (2009). "Role of the murine reprogramming factors in the induction of pluripotency." *Cell* **136**(2): 364-77.

Stadtfeld, M., K. Brennand, et al. (2008). "Reprogramming of pancreatic beta cells into induced pluripotent stem cells." *Curr Biol* **18**(12): 890-4.

Stahl, M., P. F. Dijkers, et al. (2002). "The forkhead transcription factor FoxO regulates transcription of p27Kip1 and Bim in response to IL-2." *J Immunol* **168**(10): 5024-31.

Stead, E., J. White, et al. (2002). "Pluripotent cell division cycles are driven by ectopic Cdk2, cyclin A/E and E2F activities." *Oncogene* **21**(54): 8320-33.

Storm, M. P., H. K. Bone, et al. (2007). "Regulation of Nanog expression by phosphoinositide 3-kinase-dependent signaling in murine embryonic stem cells." *J Biol Chem* **282**(9): 6265-73.

Sugiyama, Y., K. Tomoda, et al. (2001). "Direct binding of the signal-transducing adaptor Grb2 facilitates down-regulation of the cyclin-dependent kinase inhibitor p27Kip1." *J Biol Chem* **276**(15): 12084-90.

Suzuki, A., A. Raya, et al. (2006). "Maintenance of embryonic stem cell pluripotency by Nanog-mediated reversal of mesoderm specification." *Nat Clin Pract Cardiovasc Med* **3 Suppl 1**: S114-22.

Suzuki, A., A. Raya, et al. (2006). "Nanog binds to Smad1 and blocks bone morphogenetic protein-induced differentiation of embryonic stem cells." *Proc Natl Acad Sci U S A* **103**(27): 10294-9.

Suzuki, A., Y. Tsutomi, et al. (1998). "Resistance to Fas-mediated apoptosis: activation of caspase 3 is regulated by cell cycle regulator p21WAF1 and IAP gene family ILP." *Oncogene* **17**(8): 931-9.

Takahashi, K. and S. Yamanaka (2006). "Induction of pluripotent stem cells from mouse embryonic and adult fibroblast cultures by defined factors." *Cell* **126**(4): 663-76.

Takahashi, K., K. Tanabe, et al. (2007). "Induction of pluripotent stem cells from adult human fibroblasts by defined factors." *Cell* **131**(5): 861-72.

Tavares, A. T., J. C. Izpisuja-Belmonte, et al. (2001). "Developmental expression of chick twist and its regulation during limb patterning." *Int J Dev Biol* **45**(5-6): 707-13.

Tay, Y. M., W. L. Tam, et al. (2008). "MicroRNA-134 modulates the differentiation of mouse embryonic stem cells, where it causes post-transcriptional attenuation of Nanog and LRH1." *Stem Cells* **26**(1): 17-29.

Tay, Y., J. Zhang, et al. (2008). "MicroRNAs to Nanog, Oct4 and Sox2 coding regions modulate embryonic stem cell differentiation." *Nature* **455**(7216): 1124-8.

Technau, U. and C. B. Scholz (2003). "Origin and evolution of endoderm and mesoderm." *Int J Dev Biol* **47**(7-8): 531-9.

Thiery, J. P., H. Acloque, et al. (2009). "Epithelial-mesenchymal transitions in development and disease." *Cell* **139**(5): 871-90.

Thisse, C., B. Thisse, et al. (1995). "Expression of snail2, a second member of the zebrafish snail family, in cephalic mesendoderm and presumptive neural crest of wild-type and spadetail mutant embryos." *Dev Biol* **172**(1): 86-99.

Thomson, J. A., J. Itskovitz-Eldor, et al. (1998). "Embryonic stem cell lines derived from human blastocysts." *Science* **282**(5391): 1145-7.

Toyoshima, H. and T. Hunter (1994). "p27, a novel inhibitor of G1 cyclin-Cdk protein kinase activity, is related to p21." *Cell* **78**(1): 67-74.

Tsvetkov, L. M., K. H. Yeh, et al. (1999). "p27(Kip1) ubiquitination and degradation is regulated by the SCF(Skp2) complex through phosphorylated Thr187 in p27." *Curr Biol* **9**(12): 661-4.

Vallier, L., M. Alexander, et al. (2005). "Activin/Nodal and FGF pathways cooperate to maintain pluripotency of human embryonic stem cells." *J Cell Sci* **118**(Pt 19): 4495-509.

Vernon, A. E. and A. Philpott (2003). "A single cdk inhibitor, p27Xic1, functions beyond cell cycle regulation to promote muscle differentiation in Xenopus." *Development* **130**(1): 71-83.

Vernon, A. E., C. Devine, et al. (2003). "The cdk inhibitor p27Xic1 is required for differentiation of primary neurones in Xenopus." *Development* **130**(1): 85-92.

Vernon, A. E., M. Movassagh, et al. (2006). "Notch targets the Cdk inhibitor Xic1 to regulate differentiation but not the cell cycle in neurons." *EMBO Rep* **7**(6): 643-8.

Viglietto, G., M. L. Motti, et al. (2002). "Cytoplasmic relocalization and inhibition of the cyclin-dependent kinase inhibitor p27(Kip1) by PKB/Akt-mediated phosphorylation in breast cancer." *Nat Med* **8**(10): 1136-44.

Vigneron, A., J. Cherier, et al. (2006). "The cell cycle inhibitor p21waf1 binds to the myc and cdc25A promoters upon DNA damage and induces transcriptional repression." *J Biol Chem* **281**(46): 34742-50.

Visone, R., L. Russo, et al. (2007). "MicroRNAs (miR)-221 and miR-222, both overexpressed in human thyroid papillary carcinomas, regulate p27Kip1 protein levels and cell cycle." *Endocr Relat Cancer* **14**(3): 791-8.

Viswanathan, S. R., G. Q. Daley, et al. (2008). "Selective blockade of microRNA processing by Lin28." *Science* **320**(5872): 97-100.

Waggoner, A. S. (1979). "The use of cyanine dyes for the determination of membrane potentials in cells, organelles, and vesicles." *Methods Enzymol* **55**: 689-95.

Wang, C., X. Hou, et al. (2005). "Activation of p27Kip1 Expression by E2F1. A negative feedback mechanism." *J Biol Chem* **280**(13): 12339-43.

Wang, G., H. Zhang, et al. (2005). "Noggin and bFGF cooperate to maintain the pluripotency of human embryonic stem cells in the absence of feeder layers." *Biochem Biophys Res Commun* **330**(3): 934-42.

Wang, X., E. Gocek, et al. (2009). "MicroRNAs181 regulate the expression of p27Kip1 in human myeloid leukemia cells induced to differentiate by 1,25-dihydroxyvitamin D3." *Cell Cycle* **8**(5): 736-41.

Wang, X., M. Gorospe, et al. (1997). "p27Kip1 overexpression causes apoptotic death of mammalian cells." *Oncogene* **15**(24): 2991-7.

Wang, Y. and R. Blelloch (2009). "Cell cycle regulation by MicroRNAs in embryonic stem cells." *Cancer Res* **69**(10): 4093-6.

Wang, Y., S. Baskerville, et al. (2008). "Embryonic stem cell-specific microRNAs regulate the G1-S transition and promote rapid proliferation." *Nat Genet* **40**(12): 1478-83.

Wellner, U., J. Schubert, et al. (2009). "The EMT-activator ZEB1 promotes tumorigenicity by repressing stemness-inhibiting microRNAs." *Nat Cell Biol* **11**(12): 1487-95.

White, J. and S. Dalton (2005). "Cell cycle control of embryonic stem cells." *Stem Cell Rev* **1**(2): 131-8.

White, J., E. Stead, et al. (2005). "Developmental activation of the Rb-E2F pathway and establishment of cell cycle-regulated cyclin-dependent kinase activity during embryonic stem cell differentiation." *Mol Biol Cell* **16**(4): 2018-27.

Wianny, F., F. X. Real, et al. (1998). "G1-phase regulators, cyclin D1, cyclin D2, and cyclin D3: up-regulation at gastrulation and dynamic expression during neurulation." *Dev Dyn* **212**(1): 49-62.

Wilson, V. and R. Beddington (1997). "Expression of T protein in the primitive streak is necessary and sufficient for posterior mesoderm movement and somite differentiation." *Dev Biol* **192**(1): 45-58.

Wilson, V., L. Manson, et al. (1995). "The T gene is necessary for normal mesodermal morphogenetic cell movements during gastrulation." *Development* **121**(3): 877-86.

Wilson, V., P. Rashbass, et al. (1993). "Chimeric analysis of T (Brachyury) gene function." *Development* **117**(4): 1321-31.

Wolf, C., C. Thisse, et al. (1991). "The M-twist gene of Mus is expressed in subsets of mesodermal cells and is closely related to the Xenopus X-twi and the Drosophila twist genes." *Dev Biol* **143**(2): 363-73.

Wright, P. E. and H. J. Dyson (1999). "Intrinsically unstructured proteins: re-assessing the protein structure-function paradigm." *J Mol Biol* **293**(2): 321-31.

Xiong, Y., G. J. Hannon, et al. (1993). "p21 is a universal inhibitor of cyclin kinases." *Nature* **366**(6456): 701-4.

Xu, N., T. Papagiannakopoulos, et al. (2009). "MicroRNA-145 regulates OCT4, SOX2, and KLF4 and represses pluripotency in human embryonic stem cells." *Cell* **137**(4): 647-58.

Xu, R. H., X. Chen, et al. (2002). "BMP4 initiates human embryonic stem cell differentiation to trophoblast." *Nat Biotechnol* **20**(12): 1261-4.

Yamanaka, S. (2008). "Pluripotency and nuclear reprogramming." *Philos Trans R Soc Lond B Biol Sci* **363**(1500): 2079-87.

Yang, J., S. A. Mani, et al. (2004). "Twist, a master regulator of morphogenesis, plays an essential role in tumor metastasis." *Cell* **117**(7): 927-39.

Yang, W., J. Shen, et al. (2001). "Repression of transcription of the p27(Kip1) cyclin-dependent kinase inhibitor gene by c-Myc." *Oncogene* **20**(14): 1688-702.

Ying, Q. L., J. Nichols, et al. (2003). "BMP induction of Id proteins suppresses differentiation and sustains embryonic stem cell self-renewal in collaboration with STAT3." *Cell* **115**(3): 281-92.

Yu, J. and J. A. Thomson (2008). "Pluripotent stem cell lines." *Genes Dev* **22**(15): 1987-97.

Yu, J., M. A. Vodyanik, et al. (2007). "Induced pluripotent stem cell lines derived from human somatic cells." *Science* **318**(5858): 1917-20.

Yuan, H., N. Corbi, et al. (1995). "Developmental-specific activity of the FGF-4 enhancer requires the synergistic action of Sox2 and Oct-3." *Genes Dev* **9**(21): 2635-45.

Zeng, Y., K. Hirano, et al. (2000). "Minimal requirements for the nuclear localization of p27(Kip1), a cyclin-dependent kinase inhibitor." *Biochem Biophys Res Commun* **274**(1): 37-42.

Zhao, R. and G. Q. Daley (2008). "From fibroblasts to iPS cells: induced pluripotency by defined factors." *J Cell Biochem* **105**(4): 949-55.

RESUMEN DE LA TESIS DOCTORAL

INTRODUCCIÓN

El descubrimiento de las células madre embrionarias (conocidas como ESC por sus siglas en inglés de *embryonic stem cells*) ha hecho posible un gran avance en el campo de la Embriología (Evans and Kaufman 1981). Sobre todo la derivación de las células madre embrionarias humanas (conocidas como hESC por sus siglas en inglés de *human embryonic stem cells*) ha permitido estudiar los mecanismos moleculares de la embriogénesis humana, los cuales han sido muy escasos hasta recientemente debido a cuestiones éticas (Thomson, Itskovitz-Eldor et al. 1998).

Las células madre embrionarias son las células equivalentes *in vitro* de una población *in vivo* conocida como epiblasto específicas del embrión temprano. Estas células poseen dos propiedades importantes: pluripotencia y auto-renovación. Pluripotencia es la capacidad para generar todos los tipos celulares de un embrión. La auto-renovación es la capacidad de dividirse indefinidamente reteniendo al mismo tiempo el amplio potencial de diferenciación. Esta propiedad, sin embargo, es propia de las células madre embrionarias en cultivo y no de sus equivalentes embrionarias, las cuales no permanecen como una población estable de células madre sino que se diferencian hacia las tres capas germinales (ectodermo, mesodermo y endodermo) en la gastrulación. Las células madre embrionarias son derivadas sin la intervención de ningún agente inmortalizador, no experimentan crisis o senescencia y retienen un cariotipo normal. Estas células proliferan sin ningún límite aparente y pueden multiplicarse en la ausencia de suero (Burdon, Smith et al. 2002).

Estas propiedades han hecho de las células madre embrionarias un excelente modelo para el estudio de procesos embrionarios tempranos, particularmente, los asociados con la proliferación celular en el desarrollo pre-implantacional tardío y post-implantacional temprano, así como, para el estudio de los procesos embrionarios tempranos asociados con la formación y diferenciación de las tres capas germinales.

Las células madre embrionarias humanas permiten el estudio de las condiciones requeridas para la diferenciación hacia lineajes específicos y, consecuentemente, la posibilidad de trasplantar tipos celulares específicos en tejidos dañados creando así las bases de la Medicina Regenerativa. Sin embargo, antes de que la aplicación de las células madre embrionarias humanas pueda hacerse realidad se necesitan resolver ciertos problemas. En primer lugar, las cuestiones éticas del uso de células procedentes de embriones humanos, en segundo lugar, el trasplante alogénico de las células madre

embrionarias puede resultar en rechazo y, finalmente, si estas células no son diferenciadas correctamente pueden dar lugar a la formación de tumores formados por tejidos procedentes de las tres capas germinales cuando son trasplantadas en un modelo animal adulto.

Recientemente, los problemas éticos y de rechazo de trasplantes han sido resueltos fácilmente con el descubrimiento de las células madre pluripotentes inducidas (iPSC por sus siglas en inglés de *induced pluripotent stem cells*). En 2006, un estudio pionero reportó la reversión de células diferenciadas somáticas hacia un estado pluripotente similar al de las células madre embrionarias mediante la transducción por retrovirus de cuatro genes codificando los factores de transcripción: c-Myc, Klf4, Oct4 y Sox2 (Takahashi and Yamanaka 2006). A este proceso se le denominó reprogramación celular (en inglés *reprogramming*).

Siguiendo este descubrimiento, a finales de 2007, se reportó el aislamiento de células madre pluripotentes inducidas a partir de fibroblastos embrionarios y adultos humanos (Park, Zhao et al. 2008; Takahashi, Tanabe et al. 2007; Yu, Vodyanik et al. 2007). Además de fibroblastos, las células madre pluripotentes inducidas humanas han sido generadas a partir de keratinocitos (Aasen, Raya et al. 2008) y células progenitoras sanguíneas (Loh, Agarwal et al. 2009).

La tecnología de la reprogramación celular ofrece la posibilidad de derivar células madre pluripotentes inducidas específicas de pacientes, las cuales pueden ser diferenciadas en el tipo celular dañado, manipuladas para expresar una molécula específica que no esté presente en la enfermedad, y ser trasplantadas en el receptor. De esta manera se resuelven dos problemas importantes asociados a las células madre embrionarias, como son, el rechazo inmune y los problemas éticos del uso de embriones humanos. No obstante, los mecanismos de la reprogramación celular son procesos complejos y largamente desconocidos y en los que será necesaria más investigación antes de que las células madre pluripotentes inducidas puedan utilizarse en aplicaciones clínicas. Además, los vectores utilizados en el proceso de reprogramación celular pueden causar mutaciones insercionales debido a la integración de provirus en áreas críticas del genoma del hospedador causando de este modo una transformación maligna. Se ha intentado resolver este problema mediante la reprogramación celular utilizando proteínas o pequeñas moléculas evitando así el uso de virus en el proceso (Huangfu, Maehr et al. 2008; Shi, Desponts et al. 2008). Sin embargo, incluso si las células madre

pluripotentes inducidas no mostraran integración transgénica, el cultivo a largo término requerido para la reprogramación celular podría generar anormalidades genéticas y cromosómicas, así como, inestabilidad epigénetica, las cuales podrían inducir la formación de tumores (Zhao and Daley 2008).

Por el contrario, las células madre embrionarias constituyen un modelo mejor estudiado. Son derivadas sin la intervención de ningún agente inmortalizador y no necesitan cultivo a largo término. Sin embargo, si no son correctamente diferenciadas, estas células pueden dar lugar a tumores formados por tejidos procedentes de las tres capas germinales cuando son trasplantadas en un receptor adulto. Se cree que la causa de este problema es debida a la presencia de células indiferenciadas, las cuales poseen propiedades proliferativas inusuales. Este hecho hace que las células madre embrionarias humanas no puedan aplicarse en terapias clínicas actualmente.

Se ha dedicado un esfuerzo considerable en aclarar las vías de diferenciación hacia tipos celulares específicos, sin embargo, se ha prestado menos atención a las propiedades proliferativas inusuales de las células madre embrionarias y menos aún a las humanas. Por lo tanto, un mejor conocimiento del ciclo celular de las células madre embrionarias humanas es necesario si estas células van a ser utilizadas en terapias clínicas. Así pues, para que la aplicación terapéutica de estas células pueda hacerse realidad se necesitan resolver cuestiones básicas acerca de la Biología de estas células y, especialmente, se necesitan estudiar sus propiedades proliferativas. Por otro lado, el estudio de estas células permitirá avanzar en el conocimiento de los mecanismos moleculares de la proliferación y adquisición de propiedades malignas, como la indiferenciación, de las células tumorales.

Las inusuales propiedades proliferativas de las células madre embrionarias han sido adscritas a una estructura atípica y mecanismos de regulación del ciclo celular que han sido bien descritos en las células madre embrionarias murinas. Estas células utilizan mecanismos para controlar el ciclo celular que son bastante distintos a los mecanismos de control de las células somáticas (Savatier, Lapillonne et al. 1996; Burdon, Smith et al. 2002).

El ciclo celular de las células eucariotas somáticas se divide en cuatro fases: la fase G_1 donde las células crecen y se preparan para la fase de síntesis (abreviada como fase S) donde los cromosomas se duplican. Tras la fase S, las células entran en la fase

G_2 en la cual continúan creciendo y se preparan para la fase de mitosis (abreviada como fase M) durante la cual la célula se divide propiamente.

La transición de una fase del ciclo celular a la siguiente es llevada a cabo por las quinasas dependientes de ciclina (conocidas como CDK por sus siglas en inglés de *cyclin dependent kinase*). La actividad de las quinasas dependientes de ciclina requiere la unión de subunidades reguladoras conocidas como ciclinas. Las ciclinas son sintetizadas y destruidas periódicamente durante el ciclo celular, regulando así la actividad kinasa en una manera periódica y dependiente del tiempo. Las kinasas son completamente inactivas sin las ciclinas, pero para que las kinasas sean activadas además de la unión de ciclinas requieren la fosforilación activadora de un residuo clave de la kinasa (Hochegger, Takeda et al. 2008). Las kinasas pueden ser inactivadas mediante diferentes maneras, por ejemplo, las ciclinas pueden ser degradadas por proteólisis altamente específica, además, los complejos formados por las quinasas dependientes de ciclinas y sus subunidades reguladoras las ciclinas pueden ser sometidos a fosforilaciones inhibidoras y, finalmente, estos complejos pueden unirse a proteínas inhibidoras, muy potentes, denominadas inhibidores de las quinasas dependientes de ciclinas (conocidos como CKI por sus siglas en inglés de *cyclin dependent kinase inhibitor*) (Sherr and Roberts 1995).

De acuerdo al modelo clásico del ciclo celular de las células somáticas de mamífero, determinados complejos formados por quinasas dependientes de ciclinas y sus subunidades reguladoras las ciclinas son responsables de dirigir los diversos eventos que tienen lugar durante el ciclo celular en una manera ordenada y secuencial. De esta manera, en la fase G_1 temprana, señales mitogénicas son procesadas, primeramente, por la expresión de ciclinas tipo D (D_1, D_2 y D_3) que se unen y activan preferentemente las quinasas dependientes de ciclinas: CDK4 y CDK6. La activación de los complejos: ciclina D-CDK4 y ciclina D-CDK6 inicia la fosforilación de la proteína de retinoblastoma (Rb) y, posiblemente, la del resto de miembros de la familia: p107 y p130. La familia del Rb es un componente esencial en la transición de la fase G_1 a la fase S del ciclo celular. La actividad de Rb está regulada por fosforilación: Rb hipofosforilado (activo) inhibe la expresión de genes que son requeridos para entrar en la fase S secuestrando miembros de la familia de factores de transcripción E2F (Sherr and Roberts 1999). La inactivación de Rb por la fosforilación, mediada por los complejos ciclina D-CDK4 y ciclina D-CDK6, induce una liberación parcial de factores

de transcripción E2F que resulta en la activación y la transcripción de genes requeridos para la progresión del ciclo celular como *ciclinas tipo E* y *cdc25A*. La fosfatasa cdc25A elimina fosfatos inhibitorios de quinasas dependientes de ciclinas 2 (CDK2) y los complejos resultantes: ciclina E-CDK2 completan la fosforilación de Rb llevando a una liberación completa de los factores de transcripción E2F, la activación de genes diana y la entrada en la fase S del ciclo celular (Harbour and Dean 2000).

Los supresores tumorales pertenecientes a las familias de inhibidores de quinasas dependientes de ciclina: INK4 y Cip/Kip inhiben la actividad de los complejos: ciclina D-CDK4/6 y ciclina E-CDK2, respectivamente.

Por su parte, los complejos ciclina E-CDK2 fosforilan a $p27^{Kip1}$, inhibidor de estos complejos perteneciente a la familia de Cip/Kip inhibidores, marcándolo para la proteólisis y de esta manera reforzar la inactivación de las proteínas de Rb (Sheaff, Groudine et al. 1997).

Una vez que la célula ha entrado en fase S, CDK2 es activada posteriormente por ciclinas tipo A. Las ciclinas tipo A son sintetizadas en el comienzo de la fase S y junto a CDK2 fosforilan proteínas implicadas en la replicación de DNA para dirigir la transición de la fase S a la fase G_2. Finalmente, CDK1 es activada por ciclinas tipo A para facilitar el inicio de la mitosis. Siguiendo la ruptura de la envoltura nuclear, las ciclinas tipo A son degradadas facilitando la formación de los complejos ciclina B-CDK1 que son responsables de llevar a la célula a través de la mitosis (Satyanarayana and Kaldis 2009; Malumbres and Barbacid 2009).

Estudios en células madre embrionarias de ratón han demostrado que proliferan a un ritmo extremadamente rápido debido a una estructura del ciclo celular poco ortodoxa consistiendo principalmente por células en fase S del ciclo celular y una baja proporción de células en fase G_1 (Burdon, Smith et al. 2002; Stead, White et al. 2002). Varios estudios han descrito el repertorio de reguladores del ciclo celular presentes en las células madre embrionarias murinas. Las ciclinas D_1, D_3, E_1, A_2 y B_1 han sido descritas en células madre embrionarias de ratón. Sin embargo, las ciclinas D_1 y D_3 están presentes en muy bajos niveles mientras que la ciclina D_2 no está presente (Faast, White et al. 2004; Burdon, Smith et al. 2002; Savatier, Lapillonne et al. 1996).

Central a los mecanismos que sostienen la rápida división celular de las células madre embrionarias murinas, es la actividad extremadamente alta de las quinasas

dependientes de ciclinas: CDK2 y sus subunidades reguladoras: las ciclinas E/A (Stead, White et al. 2002). Además de una actividad extremadamente alta, todos los complejos carecen de periodicidad dependiente del ciclo celular. Los únicos complejos exhibiendo actividad regulada periódicamente son los complejos ciclina B-CDK1, pero incluso estos complejos exhiben una actividad inusualmente alta (Stead, White et al. 2002).

La actividad elevada e independiente del ciclo celular de las quinasas dependientes de ciclinas puede ser causada por la baja expresión de sus inhibidores (conocidos como CKI por sus siglas en inglés de *cyclin dependent kinase inhibitor*), los cuales desempeñan normalmente funciones de inhibición de la división celular. Asimismo, los complejos de ciclinas D_3-CDK6 son resistentes a la inhibición por $p16^{Ink4a}$ (inhibidor perteneciente a la familia INK4) (Faast, White et al. 2004). De acuerdo con la alta actividad de los complejos de ciclinas y quinasas dependientes de ciclinas, los miembros de la familia del Retinoblastoma (Rb) están hiperfosforilados y constitutivamente inactivos a lo largo del ciclo celular, y la transcripción mediada por los factores de transcripción E2F no es dependiente del ciclo celular.

Cuando las células madre embrionarias de ratón se diferencian, sus mecanismos de control del ciclo celular pasan de ser elevados y constitutivos a ser regulados a lo largo del ciclo celular. Este hecho coincide con la remodelación de la estructura del ciclo celular y la adquisición del punto de Restricción (R) de la fase G_1 (White, Stead et al. 2005).

A pesar de que los mecanismos de regulación del ciclo celular de las células madre embrionarias de ratón han sido bien descritos, disponemos de muy poca información acerca de los mecanismos de regulación del ciclo celular de las células madre embrionarias humanas y los pocos datos encontrados en la Literatura son a menudo contradictorios.

OBJETIVOS

En base a la información tan limitada de los mecanismos de regulación del ciclo celular de las células madre embrionarias humanas y que hasta la fecha no se había realizado ningún estudio funcional *in vitro* de los reguladores del ciclo celular en las células madre embrionarias:

Esta tesis doctoral tiene dos objetivos principales:

1. El estudio de los mecanismos de control del ciclo celular de las células madre embrionarias humanas.
2. Averiguar si la manipulación de una única proteína de la maquinaria del ciclo celular pudiera afectar las propiedades de auto-renovación o pluripotencia de las células madre embrionarias humanas.

RESULTADOS Y DISCUSIÓN

Regulación del ciclo celular en células madre embrionarias humanas

En primer lugar, procedimos a confirmar los datos descritos para las células madre embrionarias de ratón y, para ello, elegimos la línea celular murina J1 ESC. Para este fin caracterizamos el perfil del ciclo celular de células indiferenciadas por medio de análisis de citometría de flujo y confirmamos que estas células poseen una baja proporción de células en fase $G_0/_1$ pero una alta proporción de células en fase S. Cuando estas células fueron sometidas a diferenciación, la proporción de células en fase $G_0/_1$ aumentó progresivamente al mismo tiempo que la proporción de células en fase S disminuyó.

Estos resultados confirmaron que la estructura del ciclo celular de las células madre embrionarias murinas cambia durante la diferenciación celular y se corresponde con tiempos de generación más largos, de acuerdo con estudios previos (White, Stead et al. 2005; Stead, White et al. 2002).

Hipotetizamos que los cambios en la estructura del ciclo celular durante la diferenciación podrían ser debidos a un fundamental cambio en la maquinaria del ciclo celular. Además, hipotetizamos que para la auto-renovación, las células madre embrionarias debían elegir continuamente progresar a través del ciclo celular y evitar salir del mismo. Las decisiones de progresar a través del ciclo celular o salir del mismo para seguir otros destinos como senescencia, apoptosis o diferenciación, son tomadas en la fase G_1 (Blomen and Boonstra 2007) y, por esta razón, pensamos que los reguladores de la transición de la fase G_1 a la fase S tenían que desarrollar un papel importante en el cambio de la estructura del ciclo celular durante la diferenciación.

Con el objetivo de averiguar los mecanismos moleculares responsables del cambio de la estructura del ciclo celular, procedimos a analizar los niveles de expresión de los principales reguladores de la transición de la fase G_1 a S, mediante análisis por Western blot en la línea celular murina J1 ESC (ver Figura 12, pág.64). Elegimos estudiar el ciclo celular a nivel de proteínas dado que la mayoría de reguladores del ciclo celular están regulados a nivel post-transcripcional (Sherr and Roberts 1995). También analizamos el marcador de pluripotencia Oct3/4 para comprobar que las células estaban diferenciadas.

Estos análisis demostraron que la expresión del factor de transcripción Oct3/4 disminuyó durante la diferenciación validando nuestro protocolo de diferenciación. La expresión de proteínas específicas de la fase G_1 temprana: ciclina D_1 y CDK4 aumentó con la diferenciación. Por el contrario, la expresión de proteínas específicas de la fases G_1 tardía y S: ciclinas E y A y CDK2 disminuyó con la diferenciación. Por otro lado, la expresión de los inhibidores de las quinasas dependientes de ciclinas: $p21^{Cip1}$ y $p27^{Kip1}$ era baja en células indiferenciadas pero aumentó durante la diferenciación. A destacar fue el espectacular aumento del inhibidor $p27^{Kip1}$ tras 30 días de diferenciación. Finalmente, el antígeno nuclear de células en proliferación (conocido como PCNA por sus siglas en inglés de *Proliferating Cell Nuclear Antigen*), una proteína importante para la síntesis y reparación del DNA así como un marcador de proliferación celular, disminuyó durante la diferenciación. Estos resultados concuerdan con el aumento de la proporción celular en fase G_1 y la reducción celular en fase S durante la diferenciación, sugiriendo una posible función del ciclo celular en el mantenimiento de las propiedades de las células madre embrionarias. De manera interesante, el aumento de la $p27^{Kip1}$ durante la diferenciación fue inversamente proporcional al experimentado por el factor de pluripotencia Oct3/4, sugiriendo un posible nexo entre la expresión de $p27^{Kip1}$ y el mantenimiento de la pluripotencia.

Contrariamente a las células madre embrionarias de ratón, las células madre embrionarias humanas han sido menos estudiadas y disponemos de muy poca o nula información acerca de la regulación del ciclo celular de estas células. Por esta razón uno de los principales objetivos de esta tesis doctoral fue el estudio de la regulación del ciclo celular de las células madre embrionarias humanas.

Con el objetivo de averiguar si los mecanismos del control del ciclo celular de células madre embrionarias murinas y humanas pudieran estar conservados, procedimos a analizar el perfil de ciclo celular de las células madre embrionarias humanas y, también, el de otro tipo de células humanas pluripotentes descubiertas recientemente: células madre pluripotentes inducidas humanas (conocidas como hiPSC por sus siglas en inglés de *human induced pluripotent stem cells*) derivadas de fibroblastos humanos (hFiPSC) (Rodriguez-Piza, Richaud-Patin et al. 2009) y keratinocitos humanos (hKiPSC) (Aasen, Raya et al. 2008). Los resultados mostraron que los perfiles de ciclo celular de diferentes líneas pluripotentes humanas eran muy similares entre sí, con una

alta proporción de células en fase S (54-62%) y una baja proporción de células en fase $G_0/_1$ (17-33%). Estos atípicos perfiles de ciclo celular cambiaron durante la diferenciación similarmente, en todas las líneas celulares analizadas, aumentando espectacularmente la proporción de células en fase $G_0/_1$ (87-93%) y disminuyendo la proporción de células en fase S (2-8%) (ver Figura 13, pág. 66).

En conclusión, las células pluripotentes indiferenciadas humanas y murinas comparten un perfil de ciclo celular atípico que cambia durante la diferenciación sugiriendo que las propiedades del ciclo celular son funcionalmente importantes para mantener las propiedades de auto-renovación y pluripotencia. Así pues la reducción de la fase G_1 podría limitar temporalmente la fase donde las células son receptivas a los estímulos de diferenciación (Orford and Scadden 2008).

Dado que las células madre embrionarias humanas son cultivadas bajo condiciones de cultivo diferentes a las murinas, quisimos averiguar si este hecho podría influir en los mecanismos moleculares subyacentes a esta estructura del ciclo celular y, para ello, procedimos a realizar una serie de Western blots para reguladores de la transición de fase G_1 a S en células madre embrionarias humanas indiferenciadas y diferenciadas. Con el objetivo de encontrar perfiles de proteínas conservados a lo largo de la diferenciación y evitar efectos específicos de determinados linajes llevamos a cabo dos protocolos de diferenciación diferentes: uno general y uno para diferenciar hacia neuronas. Esta es la primera vez que se comparan perfiles de ciclo celular en células madre embrionarias usando dos protocolos distintos de diferenciación y de estos experimentos extrajimos conclusiones interesantes (ver Figura 15, pág. 68 y Figura 17, pág. 71).

El cambio en el perfil de la estructura del ciclo celular en las células madre embrionarias humanas se corresponde con cambios en el perfil de proteínas de reguladores del ciclo celular. En general, las ciclinas de las fases S y M: ciclinas A y B_1 estaban expresadas abundantemente en células indiferenciadas pero disminuyeron con la diferenciación, independientemente del protocolo de diferenciación usado. Estos resultados también fueron observados en células murinas. Por otra parte, las ciclinas de la fase G_1 temprana: ciclinas D_1 y D_2, eran inexistentes o estaban expresadas en niveles muy bajos en células indiferenciadas pero aumentaron durante la diferenciación general. Este patrón de expresión también fue observado en células murinas (Burdon, Smith et al. 2002; Savatier, Lapillonne et al. 1996). Por el contrario, la expresión de ciclina D_1 no

aumentó cuando las células fueron diferenciadas hacia neuronas. Estos resultados concuerdan con la expresión específica tisular de las ciclinas D (Wianny, Real et al. 1998) y explican por qué la abolición de las ciclinas D_1, D_2 o D_3 resulta en defectos en tejidos específicos (Kozar, Ciemerych et al. 2004).

La expresión de CDK4 fue constante a lo largo de la diferenciación, independientemente del protocolo de diferenciación utilizado. La expresión de ciclina E siguió un patrón interesante, aumentando con la diferenciación en ambos protocolos de diferenciación. Estos resultados difieren claramente de los obtenidos en ratón, donde la expresión de ciclina E disminuyó con la diferenciación (White, Stead et al. 2005; White and Dalton 2005). Estos resultados sugieren que en las células madre embrionarias humanas la progresión del ciclo celular está dirigida principalmente por las ciclinas A y B_1. Una explicación a estos hallazgos podría ser que las células madre embrionarias humanas y murinas representan estadíos del desarrollo diferentes o que contienen poblaciones celulares representativas de deferentes estadíos.

Las proteínas implicadas en la replicación del DNA, como PCNA y proteínas de la familia de mantenimiento de mini-cromosomas (MCM) estaban expresadas abundantemente en células indiferenciadas pero disminuyeron durante la diferenciación, independientemente del protocolo de diferenciación utilizado. Estos resultados concuerdan con los obtenidos en células de ratón. Por otro lado, los inhibidores de quinasas dependientes de ciclinas $p21^{Cip1}$, $p27^{Kip1}$ y $p16^{Ink4a}$ fueron expresados en niveles bajos en células indiferenciadas y aumentaron durante la diferenciación en ambos protocolos de diferenciación, siendo el inhibidor $p27^{Kip1}$ la proteína que más espectacularmente aumentó. Estos resultados fueron similares a los obtenidos con células murinas (Savatier, Lapillonne et al. 1996).

La proteína del retinoblastoma fue detectada como hiperfosforilada y, de esta manera, inactiva en células indiferenciadas mientras que pasó a ser hipofosforilada con la diferenciación, de acuerdo con estudios previos en ratón (Burdon, Smith et al. 2002; Savatier, Huang et al. 1994). Los niveles de expresión del factor de transcripción p53 fueron altos en células indiferenciadas pero experimentaron un descenso con la diferenciación.

En resumen, estos resultados demuestran que en las células madre embrionarias humanas, a pesar de diferencias en la expresión de ciclinas tipo D durante protocolos de diferenciación distintos, se observa un perfil de proteínas similar a lo largo de la

diferenciación utilizando dos protocolos de diferenciación distintos. En general, la expresión de ciclinas de fase G_1 e inhibidores de quinasas dependientes de ciclinas aumentó durante la diferenciación. Por el contrario, la expresión de ciclinas asociadas a las fases S y M, como ciclinas A y B_1, y también proteínas implicadas en la replicación del DNA disminuyó durante la diferenciación. Además, Rb se encontró hiperfosforilada en células indiferenciadas pero se encontró hipofosforilada en células diferenciadas. Estos resultados concuerdan con la reducción de la fase G_1 y falta del punto de Restricción en células indiferenciadas. Estos resultados son muy similares a los obtenidos en células madre embrionarias murinas.

Dado que los perfiles de proteínas del ciclo celular estaban conservados en las células madre embrionarias murinas y humanas, a pesar de ser cultivadas bajo condiciones diferentes (las humanas dependen del Factor Básico de Crecimiento de Fibroblastos, bFGF por sus siglas en inglés de *basic Fibroblast Growth Factor* y las murinas del factor inhibidor de leucemia, LIF por sus siglas en inglés de *Leukaemia Inhibitory Factor*), hipotetizamos que algunas de estas proteínas tendrían una función importante en las propiedades de auto-renovación y/o pluripotencia de las células madre embrionarias. Particularmente, pensamos que aquellas proteínas aumentando durante la diferenciación serían responsables para el cambio de un estado de indiferenciación al de diferenciación. Además, hipotetizamos que estas proteínas podrían estar implicadas en la diferenciación hacia linajes específicos. Asimismo, pensamos que aquellos reguladores del ciclo celular que desaparecen durante la diferenciación podrían ser responsables del mantenimiento de las propiedades de indiferenciación. A favor de esta hipótesis, estudios genéticos en modelo de ratón han revelado que las ciclinas A_2 y B_1 son esenciales para el desarrollo embrionario (Satyanarayana and Kaldis 2009). También se ha descrito que la función de la ciclina A es esencial para la progresión del ciclo celular de las células madre embrionarias pero no en fibroblastos donde es redundante (Kalaszczynska, Geng et al. 2009).

Por otro lado, una gran cantidad de Literatura ha descrito una función para la molécula $p27^{Kip1}$ en la diferenciación asociada con un arresto del ciclo celular (Li, Jia et al. 2006; Munoz-Alonso, Acosta et al. 2005; Galderisi, Jori et al. 2003). $p27^{Kip1}$ fue primeramente identificada como un inhibidor del ciclo celular mediando señales de crecimiento inhibidoras durante el desarrollo, la diferenciación y en respuesta a estreses celulares (Polyak, Lee et al. 1994; Polyak, Kato et al. 1994; Toyoshima and Hunter

1994). Sin embargo, recientemente, se ha descubierto que $p27^{Kip1}$ posee funciones independientes de la regulación del ciclo celular implicadas en migración (Besson, Gurian-West et al. 2004), diferenciación (Movassagh and Philpott 2008; Nguyen, Besson et al. 2006; Vernon, Movassagh et al. 2006; Vernon, Devine et al. 2003; Vernon and Philpott 2003) y expansión de células madre (Besson, Hwang et al. 2007). Estas funciones son esenciales para el mantenimiento de la homeostasis celular y tisular en procesos tan diversos como el desarrollo embrionario y la supresión tumoral.

En conjunto, estos datos presentan una gran evidencia de una función directa de las proteínas del ciclo celular en el mantenimiento de las propiedades de auto-renovación y pluripotencia de las células madre embrionarias humanas.

Dado este hecho, decidimos centrarnos en aquellas proteínas aumentando durante la diferenciación. Hipotetizamos que bajos niveles de expresión de estas proteínas serían importantes para el mantenimiento de las propiedades de las células madre embrionarias. Dado su espectacular aumento durante la diferenciación y su función bien establecida en las decisiones acerca del destino celular, decidimos estudiar $p27^{Kip1}$ en las células madre embrionarias humanas. Descubrimos que la expresión de $p27^{Kip1}$ aumentó de manera paralela al aumento de la fase G_1 durante la diferenciación. Durante la fase G_1 una célula decide si continuar dividiéndose o salir del ciclo celular para seguir otros destinos celulares. Por estas razones hipotetizamos que $p27^{Kip1}$ podría ser responsable del cambio de un estado de indiferenciación al de diferenciación siendo los bajos niveles de expresión los factores principales influyendo la estructura pluripotente del ciclo celular. Con el objetivo de averiguar esto procedimos a analizar sus niveles de expresión en diversas líneas celulares pluripotentes humanas incluyendo dos líneas de células madre embrionarias humanas y dos líneas de células madre pluripotentes inducidas humanas. En todas las líneas celulares analizadas demostramos que los niveles de expresión de $p27^{Kip1}$ en células indiferenciadas eran bajos pero aumentaron durante la diferenciación, paralelamente, al cambio experimentado en la estructura del ciclo celular (ver Figura 18, pág. 74). Estos resultados nos sugirieron que los bajos niveles de expresión de la $p27^{Kip1}$ serían funcionalmente importantes para las propiedades de las células pluripotentes y, además, que esta proteína podría tener un papel importante en el establecimiento de una fase G_1 más larga y, por consiguiente, la inducción o el mantenimiento de la diferenciación.

No está claro cómo una célula hace la transición de un estado proliferativo al otro. Con el objetivo de arrojar luz en este proceso, procedimos a investigar los mecanismos moleculares que estaban regulando los niveles de $p27^{Kip1}$ en las células madre embrionarias humanas. Mediante análisis de transcripción reversa y reacción en cadena de la polimerasa a tiempo real (técnica conocida como qRT-PCR por sus siglas en inglés de *quantitative Reverse Transcription Polymerase Chain Reaction*) demostramos que el inhibidor $p27^{Kip1}$ no estaba regulado a nivel transcripcional en las células madre embrionarias humanas dado que los niveles de RNA mensajero (mRNA) no cambiaron significativamente tras la diferenciación, al contrario que el factor de transcripción Oct3/4 el cual experimentó una gran disminución. Estos resultados sugirieron que el inhibidor $p27^{Kip1}$ estaba regulado a nivel post-transcripcional. Entre los distintos modos de regulación post-transcripcional de $p27^{Kip1}$, dos tipos han emergido como prominentes modos de regulación de $p27^{Kip1}$: la vía de los microRNAs (miRNAs) y la vía del proteosoma (le Sage, Nagel et al. 2007). Decidimos estudiar estas vías en las células madre embrionarias humanas y empezamos por la vía de los miRNAs. Para ello buscamos sitios potenciales de unión de miRNAs a lo largo de la región 3' no traducida (conocida como 3' UTR por sus siglas en inglés de *untranslated region*) del mRNA de $p27^{Kip1}$ mediante análisis informáticos. Estos análisis revelaron dos familias de miRNAs potencialmente reguladoras de $p27^{Kip1}$: miR-221/222 y miRNA-24. Tras estos resultados procedimos a analizar los niveles de expresión de estos miRNAs en células madre embrionarias humanas indiferenciadas y diferenciadas mediante análisis de reacción en cadena de la polimerasa a tiempo real. Puesto que algunas familias de miRNA muestran expresión específica de tejidos, llevamos a cabo dos protocolos de diferenciación distintos: uno general y uno específico de diferenciación neuronal. Estos análisis no revelaron ningún cambio en la expresión de miR-221 ni miRNA-222 con la diferenciación en las células madre embrionarias humanas. Sin embargo, sí detectamos un gran aumento en la expresión de miR-24 tras la diferenciación en ambos modelos de diferenciación (ver Figura 23, pág. 80 y Figura 24, pág. 81). Con el fin de averiguar si miR-24 estaba implicado en la regulación de $p27^{Kip1}$ en las células madre embrionarias humanas, procedimos a inhibir la expresión de miR-24 mediante oligonucleótidos de RNA especialmente diseñados para unirse e inhibir moléculas endógenas de miR-24 y posteriormente procedimos a medir la expresión proteica de $p27^{Kip1}$. Estos análisis no revelaron ninguna diferencia significativa en los niveles de expresión de $p27^{Kip1}$

sugiriendo que $p27^{Kip1}$ no estaba siendo regulado por miR-24 en las células madre embrionarias humanas (ver Figura 28, pág. 87).

Dado que la expresión de $p27^{Kip1}$ no parecía estar regulada por estos miRNAs, procedimos a averiguar si $p27^{Kip1}$ pudiera estar regulado por la vía del proteosoma en las células madre embrionarias humanas. Para este fin procedimos a cultivar las células madre en presencia de cicloheximida, un inhibidor de la síntesis proteica, en combinación con un inhibidor no específico de la actividad del proteosoma: MG-132. Como células control utilizamos células no tratadas. Los resultados demostraron que los niveles de expresión de $p27^{Kip1}$ aumentaron por encima de los niveles de expresión de $p27^{Kip1}$ en las células control, demostrando funcionalmente que $p27^{Kip1}$ estaba siendo regulado por la vía del proteosoma en las células madre embrionarias humanas (ver Figura 29, pág. 88). Por lo tanto, los niveles de expresión bajos de $p27^{Kip1}$ en las células madre embrionarias indiferenciadas son una consecuencia de la actividad del proteosoma y podrían explicar las tasas tan altas de proliferación en las células indiferenciadas.

El inhibidor del ciclo celular $p27^{Kip1}$ controla la auto-renovación y pluripotencia de las células madre embrionarias humanas por medio de la regulación del ciclo celular, *BRACHYURY* y *TWIST*

Los resultados de esta tesis han demostrado que las células pluripotentes indiferenciadas comparten una estructura del ciclo celular atípica que cambia durante la diferenciación. Además hemos demostrado que perfiles conservados de proteínas del ciclo celular se encuentran subyacentes a este cambio en la estructura del ciclo celular, sugiriendo que las propiedades del ciclo celular de las células madre embrionarias son importantes para las propiedades de auto-renovación y pluripotencia. Por esta razón hipotetizamos que la alteración del balance de proteínas del ciclo celular de las células madre embrionarias humanas podría afectar sus propiedades. Una aproximación para averiguar esta hipótesis sería realizar análisis funcionales de proteínas del ciclo celular implicadas en el mantenimiento de la estructura del ciclo celular. Hasta la fecha, no se había llevado a cabo ningún estudio funcional *in vitro* de las proteínas del ciclo celular en las células madre embrionarias.

Dados los datos obtenidos en esta tesis hipotetizamos que uno de los principales factores responsables de la estructura del ciclo celular de las células pluripotentes eran los niveles bajos del inhibidor $p27^{Kip1}$ dado que: 1) $p27^{Kip1}$ apareció poco expresado en diversas líneas celulares pluripotentes indiferenciadas pero su expresión aumentó considerablemente durante la diferenciación paralelamente al aumento de la fase G_1 durante la diferenciación, y 2) vías de señalización implicadas en la degradación de $p27^{Kip1}$ como Ras, fosfatidilinositol-3-OH-quinasa (conocida como PI3K por sus siglas en inglés), y vías mediadas por tirosinas quinasas, están implicadas en el mantenimiento de las propiedades de las células madre embrionarias.

Por todas estas razones, el segundo objetivo principal de esta tesis fue investigar si la alteración del balance de los niveles de expresión de $p27^{Kip1}$ podría afectar las propiedades de auto-renovación y/o pluripotencia de las células madre embrionarias humanas. Para ello, procedimos a estudiar funcionalmente el inhibidor $p27^{Kip1}$ mediante análisis de ganancia o pérdida de función.

En primer lugar, procedimos a sobreexpresar la secuencia codificadora de $p27^{Kip1}$ en las células madre embrionarias mediante transducción lentiviral de un vector TET OFF regulado por doxiciclina. En este sistema, la transcripción de $p27^{Kip1}$ es mínima en presencia de doxiciclina y es inducida en ausencia de doxiciclina. Las células madre embrionarias humanas control generaron colonias con la morfología típica de las células indiferenciadas crecidas sobre matrigel, generando colonias redondas y compactas. Cuando fueron observadas bajo un microscopio a más aumentos, se observó que estas colonias estaban formadas por una gran cantidad de células muy pequeñas y apretadas entre sí, y presentando un ratio núcleo *vs* citoplasma elevado. Sorprendentemente, la sobreexpresión de $p27^{Kip1}$ en las células madre embrionarias humanas resultó en un cambio en la morfología celular, generando células de gran tamaño, extendidas y aplanadas (ver Figura 33B, pág. 96 y Figura 34, pág. 98). Además, estas células presentaron un ratio núcleo *vs* citoplasma bajo, justamente el fenotipo opuesto al de las células control, y generaron colonias conteniendo muy pocas células, sugiriendo que la sobreexpresión de $p27^{Kip1}$ en las células madre emrbionarias humanas podría estar perjudicando el crecimiento celular.

El crecimiento celular puede ser impedido por un arresto del ciclo celular. Con el fin de averiguar el estado del ciclo celular, procedimos a analizar el perfil del ciclo celular de las células madre embrionarias humanas sobreexpresando $p27^{Kip1}$ mediante

análisis de citometría de flujo. Los resultados mostraron que la sobreexpresión de $p27^{Kip1}$ en las células madre embrionarias humanas resultó en un completo arresto del ciclo celular (ver Figura 36, pág. 101). No detectamos ninguna célula positiva para el nucleósido EdU, el cual es incorporado durante la síntesis de DNA, lo que significaba que ninguna célula se estaba dividiendo. La gran mayoría de la población estaba arrestada en la fase $G_0/_1$ del ciclo celular (aproximadamente 90%). Por el contrario, las células control presentaron la atípica estructura del ciclo celular de las células madre embrionarias humanas presentando un porcentaje bajo de células en fase $G_0/_1$ (aproximadamente 20-26%), y un porcentaje muy alto de células (aproximadamente 53-60%) en fase S.

Estos resultados demuestran por primera vez que la sobreexpresión de una única proteína del ciclo celular: $p27^{Kip1}$ en las células madre embrionarias humanas inhibe la progresión del ciclo celular impidiendo la transición de la fase G_1 a S y, por consiguiente, las células no pueden auto-renovarse.

Como el efecto de $p27^{Kip1}$ fue arrestar las células madre embrionarias humanas en la fase $G_0/_1$, que es la fase del ciclo celular donde las células pueden decidir salir del ciclo celular y seguir destinos celulares diferentes como senescencia, apoptosis o diferenciación, este hecho sugirió que el aumento de esta proteína podría ser necesario para el cambio del estado proliferativo e indiferenciado de una célula madre embrionaria al estado de diferenciación, y también sugirió que la función de esta proteína podría estar unida a alguno o varios de los anteriormente mencionados destinos celulares. El hecho de que la sobreexpresión de $p27^{Kip1}$ en las células madre embrionarias humanas causara un arresto en la fase $G_0/_1$ sugirió que a pesar de la habilidad de $p27^{Kip1}$ para inhibir los complejos mitóticos ciclina B-CDK1, actuó principalmente inhibiendo los complejos de ciclinas E/A-CDK2. También, estos resultados revelaron que los complejos de ciclinas E/A-CDK2 no son resistentes a la inhibición por $p27^{Kip1}$ en las células madre embrionarias humanas, al contrario que los complejos de ciclina D_3-CDK6 en las células madre embrionarias murinas que son resistentes a la inhibición por $p16^{INK4a}$ y no paran el crecimiento cuando $p16^{INK4a}$ es sobreexpresada (Faast, White et al. 2004; Savatier, Lapillonne et al. 1996).

La reducción de los niveles de expresión de $p27^{Kip1}$ fue llevada a cabo mediante fragmentos pequeños de RNA de interferencia (conocidos como siRNA por sus siglas en inglés de *small interfering RNA*). El RNA pequeño de interferencia es un tipo de

ARN interferente con una longitud de 20 a 25 nucleótidos que es altamente específico para la secuencia de nucleótidos de su ARN mensajero diana, interfiriendo por ello con la expresión del gen respectivo. Los RNA pequeño de interferencia se ensamblan en el complejo de silenciamiento inducido por RNA (conocido como RISC por sus siglas en inglés de *RNA-induced silencing complex*). Estos complejos se unen y destruyen los RNA mensajeros complementarios a la secuencia de RNAs pequeños de interferencia que están unidos a estos complejos.

La reducción de los niveles de expresión de $p27^{Kip1}$, mediante RNAs pequeños de interferencia, también causó un cambio llamativo en la morfología de las colonias de las células madre embrionarias humanas (ver Figura 43, pág. 110 y Figura 45, pág. 113). Mientras que las células control generaron colonias con la típica morfología de células madre embrionarias indiferenciadas, es decir, colonias redondas y compactas, la pérdida de función de la $p27^{Kip1}$ ocasionó un fenotipo llamativo con colonias muy compactas con unos bordes alargados y muy bien definidos. Estos bordes parecieron estar formados por células finas y con una morfología "fibroblastoide" que aparecieron envolviendo las colonias. También observamos colonias formadas únicamente por células alargadas y finas que parecían incapaces de extenderse, justamente, el fenotipo opuesto a las células sobreexpresando $p27^{Kip1}$.

La diferenciación espontánea de las células madre embrionarias ocurre con frecuencia, en sólo una porción de las colonias, normalmente, a lo largo de los bordes o como puntos aislados en el centro de las colonias. El comienzo de la diferenciación es detectado por la aparición de una apariencia aplanada y pérdida de definición de los bordes. En general, las colonias sanas e indiferenciadas de las células madre embrionarias humanas son consideradas como colonias con los bordes limpios, compactos y bien definidos. Así pues el fenotipo ocasionado por la pérdida de función de $p27^{Kip1}$ sugirió que estas colonias se estaban volviéndo más indiferenciadas.

Con el objetivo de averiguar si un cambio en el ciclo celular yacía tras este fenotipo, procedimos a analizar el perfil del ciclo celular de estas células mediante análisis de citometría de flujo. Estos resultados demostraron que las células madre embrionarias humanas control presentaron la estructura del ciclo celular atípica de las células indiferenciadas presentando un porcentaje bajo de células en fase $G_0/_1$ pero un porcentaje alto de células en fase S. Sin embargo, las células transducidas con las construcciones codificando para RNA pequeño de interferencia para el RNA mensajero

de $p27^{Kip1}$ presentaron un aumento leve de células en la fase S del ciclo celular que se hizo más evidente en las células presentando mejor eficiencia de reducción de $p27^{Kip1}$ (ver Figura 46, pág. 115).

Estos resultados revelan que la pérdida de función de $p27^{Kip1}$ parece aumentar la tasa de división de las células madre embrionarias humanas aumentando el tránsito de la fase G_1 a S manteniendo, al mismo tiempo, un fenotipo indiferenciado, esto es, potenciando la auto-renovación.

En conjunto, estos resultados demuestran por primera vez que la sobreexpresión de una proteína del ciclo celular: $p27^{Kip1}$, en condiciones de indiferenciación, inhibe la auto-renovación de las células madre embrionarias humanas mediante un arresto de las células en la fase $G_0/_1$ del ciclo celular. Además causa un cambio en la morfología de las células produciendo un aumento del tamaño, una disminución del ratio núcleo *vs* citoplasma y un fenotipo más extendido y aplanado. Como el comienzo de la diferenciación es detectado por la aparición de una morfología aplanada y desde que se ha descrito que un ratio núcleo *vs* citoplasma alto es una característica común de las células madre embrionarias humanas indiferenciadas (Thomson, Itskovitz-Eldor et al. 1998), estos resultados nos sugirieron que el aumento de $p27^{Kip1}$ estaba induciendo un fenotipo menos pluripotente o más propenso a la diferenciación.

Por el contrario, la reducción de los niveles de expresión de $p27^{Kip1}$ apareció potenciar la auto-renovación de las células madre embrionarias humanas aumentando la proporción de células en fase S, probablemente, facilitando el tránsito de la fase G_1 a la fase S del ciclo celular. Además, la reducción de los niveles de expresión de $p27^{Kip1}$ causó un cambio llamativo en la morfología generando colonias con bordes muy bien definidos y alargados consistiendo de células finas y "fibroblastoides". Este cambio en la morfología hacia un fenotipo con bordes más compactos y definidos sugirió que estas colonias se estaban volviendo más indiferenciadas.

Estos resultados tan reveladores señalan a $p27^{Kip1}$ como una proteína clave en el cambio de un estado de pluripotencia y auto-renovación hacia un estado propenso a la diferenciación.

Estos resultados podrían tener varias aplicaciones. Por un lado, la sobreexpresión de $p27^{Kip1}$ podría parar el desarrollo de tumores cuando las células madre embrionarias o las células madre pluripotentes inducidas humanas son trasplantadas en animales adultos, a través de un arresto del ciclo celular. El empleo de compuestos químicos que

aumentasen la expresión de $p27^{Kip1}$ constituiría un método seguro para su uso con fines terapéuticos puesto que evitaría el riesgo potencial de usar virus para transducir las células.

Por otro lado, la reducción de los niveles de expresión de $p27^{Kip1}$ en células somáticas incrementaría la eficiencia de generación de células madre pluripotentes inducidas humanas facilitando la transición hacia un estado más auto-renovable y, posiblemente, más pluripotente. La eficiencia de generación de las células madre pluripotentes inducidas humanas es muy baja cuando oncogenes, como c-myc, son eliminados del cocktail inicial de factores de transcripción, sin embargo, el desarrollo de tumores es reducido considerablemente (Nakagawa, Koyanagi et al. 2008). Recientemente, nosotros y otros hemos revelado el aumento de la eficiencia de generación de células madre pluripotentes inducidas humanas inhibiendo p53 o el inhibidor $p21^{Cip1}$ (ver Anexo II (Edel, Menchón et al. 2010)) (Kawamura, Suzuki et al. 2009; Marion, Strati et al. 2009) en ausencia de c-myc. Sin embargo, como las proteínas p53 y $p21^{Cip1}$ están implicadas en el arresto del ciclo celular o apoptosis inducidos por daño en el DNA, la inhibición de estas proteínas genera células madre pluripotentes inducidas humanas teniendo daños en el DNA y aberraciones cromosómicas persistentes (Marion, Strati et al. 2009) lo que provoca la formación de tumores. Como el inhibidor $p27^{Kip1}$ no está implicado en vías de señalización de daño en el DNA, sino en decisiones sobre el destino celular a través de un arresto del ciclo celular mediado por señales anti-proliferativas, constituiría una diana mejor para aumentar la eficiencia de generación de células madre pluripotentes inducidas humanas sin el riesgo de tener alteraciones genéticas o cromosómicas.

Como la alteración de los niveles de expresión de $p27^{Kip1}$ ocasionó cambios en el fenotipo de las células madre embrionarias humanas, procedimos a investigarlos en profundidad.

Las células madre embrionarias humanas que sobreexpresaron $p27^{Kip1}$ experimentaron un arresto en la fase $G_0/_1$ del ciclo celular y mostraron, entre otros cambios morfológicos, una reducción evidente en el ratio núcleo *vs* citoplasma en comparación con las células control. Además, confirmamos que presentaron un aumento del tamaño celular mediante análisis de la intensidad de anchura de pulso por citometría de flujo. Con el objetivo de investigar este fenotipo, procedimos a evaluar los diferentes destinos que las células pueden llevar a cabo una vez que han salido del ciclo celular y

permanecen en la fase G_1 del ciclo celular, como era el caso de las células madre embrionarias humanas que sobreexpresaron $p27^{Kip1}$. Las células que salen del ciclo celular durante la fase G_1 pueden sufrir tres destinos diferentes: apoptosis, senescencia o diferenciación (Blomen and Boonstra 2007), por lo tanto procedimos a evaluar si las células que estaban sobreexpresando $p27^{Kip1}$ siguieron alguno de estos destinos celulares.

En primer lugar, procedimos a evaluar si las células que sobreexpresaron $p27^{Kip1}$ estaban sufriendo apoptosis. La apoptosis (proceso conocido también como muerte celular programada) fue analizada mediante dos metodologías diferentes: el análisis de cambios morfológicos nucleares indicativos de apoptosis, esto es, fragmentación nuclear tras tinción con DAPI (el cual se une al DNA) y observación con un microscopio de fluorescencia (Lai, Chien et al. 2003), y mediante análisis cuantitativos por citometría de flujo del potencial de membrana mitocondrial, dado que la abolición del potencial de membrana mitocondrial es uno de los marcadores más tempranos de apoptosis (Dobrosi, Toth et al. 2008). En los análisis de citometría de flujo, también se utilizó la tinción con Ioduro de Propidio para teñir las células muertas y, por consiguiente, discriminar necrosis de apoptosis. Los resultados no mostraron ningún aumento significativo de la apoptosis en las células madre embrionarias humanas sobreexpresando $p27^{Kip1}$ con ninguna de las metodologías mencionadas anteriormente (ver Figura 50, pág. 122 y Figura 51, pág 123). Además, los análisis de citometría de flujo tampoco revelaron protección de la apoptosis en las células madre embrionarias humanas que sobreexpresaron $p27^{Kip1}$. Adicionalmente, y con el objetivo de confirmar estos resultados, realizamos un experimento de microscopía *time-lapse*, en el que fotografiamos células madre embrionarias humanas individuales sobreexpresando $p27^{Kip1}$, a intervalos regulares de tiempo durante siete días. Cuando este tiempo hubo pasado, las células grandes y extendidas sobreexpresando $p27^{Kip1}$ aún persistían en el cultivo sin mostrar señales de apoptosis. El análisis de la morfología nuclear de estas células reveló que poseían núcleos redondos, bien delimitados y uniformemente teñidos confirmando que las células madre emrbionarias humanas sobreexpresando $p27^{Kip1}$ no eran apoptóticas tras siete días de cultivo (ver Figura 49B, pág 121 y Figura 50, pág. 122).

Por otro lado, también comprobamos la aproximación complementaria, esto es, si la pérdida de expresión de $p27^{Kip1}$ en las células madre embrionarias humanas podría

estar afectando la apoptosis. La apoptosis también fue analizada mediante el análisis de la morfología nuclear (fragmentación nuclear) tras tinción con DAPI, y mediante análisis cuantitativos del potencial de membrana mitocondrial por citometría de flujo. Los resultados tampoco mostraron un cambio significativo en la apoptosis con ninguna de las dos metodologías tras un cultivo a largo término a pesar de que el fenotipo de pérdida de función de $p27^{Kip1}$ en las células madre embrionarias humanas era evidente (ver Figura 52, pág. 124 y Figura 53, pág. 125).

En conjunto, estos resultados demostraron que la manipulación de los niveles de expresión de $p27^{Kip1}$ en las células madre embrionarias humanas indiferenciadas no afectó la apoptosis. Por lo tanto, nuestro siguiente paso fue investigar si las células madre embrionarias humanas sobreexpresando $p27^{Kip1}$ experimentaron otro destino celular. Como fue explicado más arriba, otro destino que las células pueden llevar a cabo una vez que han salido del ciclo celular durante la fase $G_0/_1$ es senescencia. En base al hecho de que la actividad de la β-galactosidasa a pH=6 está presente, únicamente, en células senescentes y no en células pre-senescentes, quiescentes o inmortales, y que ha sido utilizada comúnmente como un biomarcador de senescencia (Kurz, Decary et al. 2000), procedimos a medir la actividad de la β-galactosidasa a pH=6 en las células madre embrionarias humanas sobreexpresando $p27^{Kip1}$. Los resultados demostraron que células grandes, extendidas y aplanadas sobreexpresando $p27^{Kip1}$ fueron distinguidas fácilmente del resto de células que no sobreexpresaban $p27^{Kip1}$ tras cuatro días de cultivo en ausencia de doxiciclina. Sin embargo, cuando estas células fueron observadas bajo un microscopio de luz, no detectamos actividad de la β-galactosidasa en ellas, demostrando que las células madre embrionarias humanas sobreexpresando $p27^{Kip1}$ no eran senescentes. Como era de esperar, tampoco detectamos actividad de la β-galactosidasa a pH=6 en las células control, de acuerdo a publicaciones previas mostrando que las células madre embrionarias humanas indiferenciadas experimentan una proliferación ilimitada *in vitro*, debido en parte a la expresión elevada de la actividad de la telomerasa (Thomson, Itskovitz-Eldor et al. 1998). La telomerasa es una ribonucleoproteína que está implicada en el mantenimiento de la longitud de los cromosomas mediante la adición de repeticiones de telómero a los extremos de los cromosomas, lo cual desempeña un papel importante en el período de vida replicativo de la célula. Las células diploides somáticas humanas no expresan telomerasa, por lo tanto, los telómeros se acortan con el tiempo y entran en senescencia

replicativa tras un período de vida replicativo limitado en cultivo (Thomson, Itskovitz-Eldor et al. 1998).

En conjunto, estos resultados demostraron que las células madre embrionarias humanas sobreexpresando $p27^{Kip1}$ no eran senescentes. Por lo tanto, y con el objetivo de clarificar cuál podría ser el fenotipo de estas células, procedimos a investigar si se estaban diferenciado. Para ello, procedimos a analizar el perfil transcripcional de 84 genes clave implicados en el mantenimiento y la diferenciación temprana de las células madre embrionarias humanas, mediante transcripción reversa y reacción en cadena de la polimerasa a tiempo real. Entre esta selección de genes, estaban incluidos genes específicos de las células madre embrionarias humanas implicados en el mantenimiento de las propiedades de auto-renovación y pluripotencia. También estaban incluidos, marcadores de diferenciación que pueden ser utilizados para controlar los procesos de diferenciación temprana de las células madre embrionarias humanas.

El análisis de los valores de expresión de esta matriz de genes mostró que la sobreexpresión de $p27^{Kip1}$ en las células madre embrionarias humanas no resultó en un cambio significativo de los factores de pluripotencia por excelencia como *OCT3/4*, *NANOG* o *SOX2* después de cuatro días de cultivo celular (ver Figura 56, pág. 130). Estos datos fueron validados posteriormente mediante transcripción reversa y reacción en cadena de la polimerasa a tiempo real de los factores mencionados anteriormente y otros factores de pluripotencia clave. Asimismo, la pérdida de $p27^{Kip1}$ tampoco afectó la expresión de estos factores de pluripotencia clave (ver Figura 57, pág. 132).

Sin embargo, el análisis de los valores de expresión de esta matriz de genes reveló que la sobreexpresión de $p27^{Kip1}$ en las células madre embrionarias humanas resultó en el aumento y disminución de genes específicos de la diferenciación (ver Figura 56, pág. 130). Por lo tanto, procedimos a validar aquellos genes que mostraron los cambios más importantes en células sobreexpresando $p27^{Kip1}$ y también en células sin expresión de $p27^{Kip1}$ mediado por RNAs pequeños de interferencia, puesto que si la sobreexpresión de $p27^{Kip1}$ estaba afectando la expresión de algún gen deberíamos ver el efecto contrario en las células con pérdida de función de $p27^{Kip1}$.

La validación de los genes mostrando los cambios más importantes de expresión reveló una nueva función potencial de $p27^{Kip1}$ en la regulación de *BRACHYURY* en las células madre embrionarias humanas. La sobreexpresión de $p27^{Kip1}$ en las células madre embrionarias humanas produjo una disminución significativa de *BRACHYURY* de

aproximadamente un 60%. De manera interesante, la pérdida de función de $p27^{Kip1}$ resultó en un aumento estadísticamente significativo de aproximadamente nueve veces en comparación con los controles (ver Figura 58, pág. 133). Esta es la primera vez que se muestra un rol para $p27^{Kip1}$ en la regulación de *BRACHYURY*. *BRACHYURY* es un gen importante implicado en la especificación temprana de mesodermo (Technau and Scholz 2003). Dado este descubrimiento importante y novel, procedimos a medir los niveles proteicos de BRACHYURY mediante análisis de Western blot e immunofluorescencia, confirmando los resultados de mRNA (ver Figura 59, pág. 135).

Brachyury ha sido relacionado tradicionalmente con la especificación de mesodermo y la elongación del eje embrionario (Showell, Binder et al. 2004; Technau and Scholz 2003). La formación de mesodermo en el desarrollo embrionario conlleva un proceso de transición de epitelio a mesénquima (Acloque, Adams et al. 2009) (proceso conocido como EMT por sus siglas en inglés de *epithelial to mesenchymal transition*). La transición de epitelio a mesénquima es un cambio fenotípico fascinante que es llevado a cabo por las células del embrión en condiciones fisiológicas. Este proceso conlleva cambios profundos en la morfología, como la pérdida de las características epiteliales, la adquisición de un fenotipo "fibroblastoide", y cambios en el comportamiento de las células epiteliales como la adquisición de propiedades migratorias (Nieto 2009). Sin embargo, este programa fisiológico puede reactivarse en procesos patológicos como las metástasis (Nieto 2009). Dado este efecto de $p27^{Kip1}$ en la regulación de BRACHYURY, procedimos a evaluar si también otros especificadores de mesodermo y/o marcadores de transición de epitelio a mesénquima clave pudieran estar afectados por $p27^{Kip1}$ mediante análisis de transcripción reversa y reacción en cadena de la polimerasa a tiempo real. El ensayo de una batería de genes especificadores de mesodermo y/o marcadores de transición de epitelio a mesénquima reveló un aumento estadísticamente significativo de *TWIST* (aproximadamente 6 veces) con la pérdida de función de $p27^{Kip1}$ e, inversamente, una disminución estadísticamente significativa de *TWIST* con la ganancia de función de $p27^{Kip1}$ en las células madre embrionarias humanas (ver Figura 60, pág. 137). No encontramos diferencias estadísticamente significativas en la expresión de otros genes como *SNAIL1*, *SNAIL2* (también conocido como *SLUG*), *CADHERINA E*, o *VIMENTINA*, ni con la ganancia ni con la pérdida de función de $p27^{Kip1}$ sugiriendo que el efecto de $p27^{Kip1}$ era específico para *TWIST*. Aunque no pudimos evaluar la expresión proteica de TWIST en estas

células dado que no hay anticuerpos específicos para TWIST que funcionen, estos resultados son muy prometedores dado las funciones tan importantes en las que TWIST está implicado. Por ejemplo, en vertebrados TWIST1 es expresado inicialmente a lo largo del mesodermo somático en grandes niveles antes de la diferenciación (Wolf, Thisse et al. 1991), y además de ser esencial en la diferenciación de linajes derivados de mesodermo, incluyendo músculo, cartílago y linajes osteogénicos (Ansieau, Morel et al. 2010), TWIST1 es capaz de inducir el proceso de transición de epitelio a mesénquima y se encuentra sobreexpresado en una gran variedad de tumores humanos (Ansieau, Morel et al. 2010).

Estos resultados concuerdan con la función de los inhibidores de la familia Cip/Kip ($p27^{Kip1}$, $p21^{Cip1}$ y $p57^{Kip2}$) en la modulación de la actividad de factores de transcripción específicos mediante su unión directa y aumento de la estabilidad de estos factores independientemente de la regulación del ciclo celular (Nguyen, Besson et al. 2006; Coqueret 2003; Reynaud, Leibovitch et al. 2000).

Dado que la expresión de $p27^{Kip1}$ fue detectada principalmente en los núcleos celulares, procedimos a averiguar si $p27^{Kip1}$ estaba afectando directamente la activación transcripcional del promotor de *TWIST1*. Para ello, procedimos a realizar experimentos de inmunoprecipitación de cromatina buscando sitios de ocupación de $p27^{Kip1}$ a lo largo de 4000 Kilobases (Kb) del promotor de *TWIST1* empezando en la región +1.0 Kb hasta -3.0 Kb desde la ATG en células madre embrionarias humanas sobreexpresando $p27^{Kip1}$ o sin expresar $p27^{Kip1}$. Los resultados revelaron que la proteína $p27^{Kip1}$ estaba siendo reclutada en la región +1.0 Kb del promotor de *TWIST1* en las células que sobreexpresaban $p27^{Kip1}$ (ver Figura 61, pág. 138). El aumento en la ocupación del promotor de *TWIST1* sugirió que la $p27^{Kip1}$ funcionaba como un represor transcripcional de *TWIST1* en las células madre embrionarias humanas bajo condiciones de cultivo indiferenciado. De acuerdo con estos resultados, una función similar se ha descrito para otro inhibidor del ciclo celular, perteneciente a la família Cip/Kip: $p21^{Cip1}$ el cual se une a los promotores de *myc* y *cdc25A* analizado mediante experimentos de inmunoprecipitación de cromatina induciendo represión transcripcional (Vigneron, Cherier et al. 2006), reforzando el descubrimiento novedoso de que los inhibidores del ciclo celular pertenecientes a la familia Cip/Kip poseen funciones adicionales a su función como inhibidores de quinasas, uniéndose a cromatina para regular la expresión génica. Un trabajo previo mostró que la expresión ectópica de $p27^{Kip1}$ bloqueó la

inducción de Twist en células satélite del músculo (un tipo de células madre) en pollo (Leshem, Spicer et al. 2000). Los resultados de esta tesis muestran por primera vez evidencia directa de la regulación del promotor de *TWIST1* por $p27^{Kip1}$ en las células madre embrionarias humanas asociado con los niveles de expresión génica, revelando una nueva función para $p27^{Kip1}$ en la Biología Celular. Si $p27^{Kip1}$ regula el promotor de *TWIST1* directamente o indirectamente como parte de un complejo represor vía unión a otras proteínas presentes en la cromatina permanece por ser investigado.

En conjunto, estos resultados han demostrado que un cambio en el balance de los niveles de $p27^{Kip1}$ en las células madre embrionarias humanas indiferenciadas afecta la expresión de los reguladores de mesodermo: *BRACHYURY* y *TWIST*. El compromiso de las células madre embrionarias humanas hacia mesodermo implicaría la pérdida de pluripotencia y, por consiguiente, la pérdida de la capacidad para generar todos los tipos celulares de un embrión. Con el objetivo de determinar si la regulación de marcadores de mesodermo por $p27^{Kip1}$ estaba afectando la capacidad de diferenciación de las células madre embrionarias humanas llevamos a cabo algunos experimentos preliminares de diferenciación en células madre embrionarias humanas carentes de $p27^{Kip1}$. Para lograr este objetivo, las células fueron diferenciadas mediante la generación de cuerpos "embrioides" (EB por sus siglas en inglés de *embryoid bodies*). Los cuerpos "embrioides" son agregados de células que se forman una vez que las células madre embrionarias son despegadas de la matriz a la cual se adhieren para formar las típicas colonias. Una vez que se agregan, las células comienzan a diferenciarse recapitulando hasta un cierto límite el desarrollo embrionario.

Los resultados mostraron que las células madre embrionarias humanas control generaron cuerpos "embrioides" típicos, compactos y redondos después de tres o cuatro días de cultivo celular en suspensión. Por el contrario, las células madre embrionarias humanas carentes de $p27^{Kip1}$ generaron cuerpos "embrioides" irregulares y quísticos sugiriendo que estas células eran incapaces o tenían una capacidad de diferenciación deficiente (ver Figura 63, pág. 141). Las cavitaciones de los cuerpos "embrioides" son el resultado de la muerte celular programada o apoptosis y esta primera oleada de muerte celular se considera indispensable para la morfogénesis (Joza, Susin et al. 2001). El hecho de que la pérdida de función de la $p27^{Kip1}$ en las células madre embrionarias humanas ocasionara cavitaciones prematuras comparado con los controles, sugirió que

estaba impidiendo la supervivencia o aumentando la apoptosis. Otra posibilidad es que podría estar afectando la diferenciación de linajes específicos.

Dado que se ha demostrado recientemente que las células madre embrionarias de ratón deficientes en $p27^{Kip1}$ llevan a cabo una diferenciación defectuosa tras tratamiento con ácido retinoico (Bryja, Pachernik et al. 2004), y dado el hecho de que el ácido retinoico induce la diferenciación neuronal y, así pues, el destino hacia neuroectodermo, procedimos a diferenciar las células madre embrionarias humanas deficientes en $p27^{Kip1}$ hacia neuroectodermo y mesodermo. Para este fin, las células fueron diferenciadas mediante la generación de cuerpos "embrioides", cultivadas en medios de diferenciación específicos para mesodermo o neuroectodermo durante treinta días y, posteriormente, sometidas a análisis de inmunofluorescencia con anticuerpos específicos para marcadores de mesodermo (α-actina de músculo liso) o neuroectodermo (nestina y β-tubulina clase III), respectivamente. Los resultados de estos análisis revelaron que las células madre embrionarias humanas control se diferenciaron hacia neuroectodermo y mesodermo eficazmente juzgando por la expresión elevada de los marcadores de diferenciación específicos. Sorprendentemente, y al contrario que las células control, observamos que la pérdida de función de la $p27^{Kip1}$ impidió la correcta diferenciación hacia neuroectodermo juzgando por la reducción evidente de la expresión de nestina y β-tubulina clase III (ver Figura 65, pág. 143). Además, en estas células no observamos la morfología típica axonal observada en las células control positivas para la expresión de nestina o β-tubulina clase III, sugiriendo que las células madre embrionarias humanas deficientes en $p27^{Kip1}$ no podían diferenciarse hacia neuroectodermo. Estos resultados concuerdan con un trabajo reciente mostrando una incapacidad para la diferenciación de las células madre embrionarias de ratón deficientes en $p27^{Kip1}$ tras tratamiento con ácido retinoico (Bryja, Pachernik et al. 2004). Dado el hecho de que el ácido retinoico es un inductor de la diferenciación neuronal, estos resultados sugieren que $p27^{Kip1}$ es necesaria para la diferenciación neuronal. Además, estos resultados concuerdan con la función de $p27^{Kip1}$ en el fomento de la diferenciación de los progenitores neuronales en el cortex de ratón (Nguyen, Besson et al. 2006).

Estos resultados demuestran que en la ausencia de $p27^{Kip1}$, la habilidad de las células madre embrionarias humanas para producir un rango de progenie diferenciada representativa de las tres capas germinales primarias está afectada, demostrando que

$p27^{Kip1}$ es esencial para el mantenimiento de la pluripotencia en células madre emrbionarias humanas.

En resumen, en esta tesis doctoral pretendimos comprender si cambios en el balance de un regulador del ciclo celular podrían afectar las propiedades de auto-renovación o pluripotencia de las células madre embrionarias humanas indiferenciadas. Nos centramos en el inhibidor $p27^{Kip1}$ dado sus niveles de expresión bajos en células pluripotentes indiferenciadas y su función bien establecida en las decisiones sobre el destino celular. Para definir el papel funcional del ciclo celular en la auto-renovación o pluripotencia, manipulamos los niveles de expresión de $p27^{Kip1}$ en las células madre embrionarias humanas utilizando una estrategia de ganancia y pérdida de función.

Los resultados presentados en esta tesis doctoral han revelado una nueva función para $p27^{Kip1}$ en la auto-renovación de las células madre embrionarias humanas mediante la regulación de la transición de la fase G_1 a la fase S del ciclo celular y la regulación de la morfología celular. También hemos demostrado que en condiciones de indiferenciación $p27^{Kip1}$ regula los marcadores de mesodermo *BRACHYURY* y *TWIST* para mantener las propiedades de pluripotencia y auto-renovación, sin embargo bajo condiciones de diferenciación las cuales implican la eliminación de bFGF, encontramos que $p27^{Kip1}$ regula el destino celular neuronal. Estos resultados demuestran que $p27^{Kip1}$ es esencial para el mantenimiento de un estado pluripotente apropiado. Estos descubrimientos han sido posibles gracias al modelo de embriogénesis temprana de las células madre embrionarias y sugieren que $p27^{Kip1}$ adapta sus funciones dependiendo de señales extracelulares con señales de diferenciación. Este mecanismo puede permitir a las células madre embrionarias humanas responder selectivamente a señales presentes en el medio mediante el aumento específico de algún componente particular de la maquinaria del ciclo celular y de esta manera continuar con la auto-renovación o diferenciación.

En conjunto utilizando tanto condiciones de indiferenciación como diferenciación dirigida, estos resultados muestran que $p27^{Kip1}$ regula el estado pluripotente de las células madre embrionarias humanas y tiene que ser regulado estrechamente para el mantenimiento de las propiedades de estas células. A la luz de estos resulados, proponemos que $p27^{Kip1}$ regula simultáneamente quinasas dependientes de ciclinas y reguladores transcripcionales para coordinar la auto-renovación y especificación de linajes celulares.

CONCLUSIONES

1. Las células madre embrionarias humanas y murinas, así como, las células madre pluripotentes inducidas humanas comparten una estructura del ciclo celular atípica consistiendo de una baja proporción de células en fase $G_0/_1$ y una alta proporción de células en fase S. La estructura del ciclo celular cambia dramáticamente durante la diferenciación aumentando el porcentaje de células en fase $G_0/_1$ y disminuyendo el porcentaje de células en fase S.
2. Cambios conservados en los perfiles de proteínas del ciclo celular subyacen al cambio de la estructura del ciclo celular, durante la diferenciación, en las células madre embrionarias humanas y murinas. La expresión de ciclinas asociadas a la fase G_1 e inhibidores de quinasas dependientes de ciclinas aumentó durante la diferenciación. Por el contrario, la expresión de proteínas asociadas a las fases S y M: ciclinas A y B_1, así como, la expresión de proteínas implicadas en la replicación del DNA disminuyó durante la diferenciación.

3. El inhibidor de quinasas dependientes de ciclinas: $p27^{Kip1}$ fue expresado en niveles muy bajos en líneas celulares indiferenciadas pluripotentes, tanto humanas como murinas, pero su expresión aumentó durante la diferenciación paralelamente a los cambios en la estructura del ciclo celular.

4. Los niveles de expresión de $p27^{Kip1}$ están regulados por la vía del proteasoma en las células madre embrionarias humanas indiferenciadas.

5. El inhibidor del ciclo celular $p27^{Kip1}$ controla la auto-renovación de la células madre embrionarias humanas por medio de la regulación de la transición de la fase G_1 a S y la morfología celular.

6. El inhibidor del ciclo celular $p27^{Kip1}$ posee una función importante en el mantenimiento de la pluripotencia de las células madre embrionarias humanas mediante la regulación de los marcadores de mesodermo *BRACHYURY* y *TWIST* en condiciones de indiferenciación, y en condiciones de diferenciación dirigida hacia mesodermo o ectodermo la pérdida de $p27^{Kip1}$ causó la pérdida de marcadores de ectodermo.
7. El inhibidor del ciclo celular $p27^{Kip1}$ es reclutado en el promotor de *TWIST1* y está asociado a sus niveles de expresión.

ANNEXES

The work developed during my PhD Thesis period has given rise to four publications:

1. **Annexe I**: **Cristina Menchón**, Michael J. Edel, and Juan Carlos Izpisúa Belmonte. The cell cycle inhibitor $p27^{Kip1}$ controls self-renewal and pluripotency of human embryonic stem cells by regulating the cell cycle, *BRACHYURY*, and *TWIST*. *Cell Cycle*. 2011 May 1; **10**(9)

2. **Annexe II**: Edel M.J., **Menchón C.**, Menéndez S., Consiglio A., Raya A., and Izpisúa Belmonte J.C. Rem2 GTPase maintains survival of human embryonic stem cells as well as enhancing reprogramming by regulating p53 and cyclin D_1. *Genes Dev*. 2010 Mar 15; **24**(6): 561-73.

3. **Annexe III**: Edel M.J., Boué S., **Menchón C.**, Sánchez-Danés A., and Izpisúa Belmonte J.C. Rem2 GTPase controls proliferation and apoptosis of neurons during embryo development. *Cell Cycle*. 2010 Sep; **9**(17): 3414-22.

4. **Annexe IV**: Michael J. Edel, **Cristina Menchón**, José Miguel Andrés Vaquero, and Juan Carlos Izpisúa Belmonte. A protocol to assess cell cycle and apoptosis in human and mouse pluripotent cells. *Cell Commun Signal*. 2011 Apr 11; **9**(1):8.

REPORT

Cell Cycle 10:9, 1-13; May 1, 2011; © 2011 Landes Bioscience

The cell cycle inhibitor p27^{Kip1} controls self-renewal and pluripotency of human embryonic stem cells by regulating the cell cycle, Brachyury and Twist

Cristina Menchón,[1,†,‡] Michael J. Edel[1,†] and Juan Carlos Izpisua Belmonte[1,2,*]

[1]Center of Regenerative Medicine in Barcelona; Barcelona, Spain; [2]Gene Expression Laborator; Salk Institute for Biological Studies; La Jolla, CA USA

[†]Current Address: Vall d' Hebron Research Institute; Banc de Sang i Teixits; Barcelona, Spain

[‡]These authors contributed equally to this work.

Key words: cell cycle, embryonic stem cell, induced pluripotent stem cell, self renewal, pluripotency, differentiation

The continued turn over of human embryonic stem cells (hESC) while maintaining an undifferentiated state is dependent on the regulation of the cell cycle. Here we asked the question if a single cell cycle gene could regulate the self-renewal or pluripotency properties of hESC. We identified that the protein expression of the p27^{Kip1} cell cycle inhibitor is low in hESC cells and increased with differentiation. By adopting a gain and loss of function strategy we forced or reduced its expression in undifferentiating conditions to define its functional role in self-renewal and pluripotency. Using undifferentiation conditions, overexpression of p27^{Kip1} in hESC lead to a G_1 phase arrest with an enlarged and flattened hESC morphology and consequent loss of self-renewal ability. Loss of p27^{Kip1} caused an elongated/scatter cell-like phenotype involving upregulation of Brachyury and Twist gene expression. We demonstrate the novel finding that p27^{Kip1} protein occupies the Twist1 gene promoter and manipulation of p27^{Kip1} by gain and loss of function is associated with Twist gene expression changes. These results define p27^{Kip1} expression levels as critical for self-renewal and pluripotency in hESC and suggest a role for p27^{Kip1} in controlling an epithelial to mesenchymal transition (EMT) in hESC.

This manuscript has been published online, prior to printing. Once the issue is complete and page numbers have been assigned, the citation will change accordingly.

Introduction

Embryonic stem cells are derived from the inner cell mass (ICM) of the blastocyst and have the capacity for unlimited proliferation while retaining their potential to differentiate into a wide variety of cell types when cultured in vitro.[1,2] Recently, it has been shown that a combination of three or four factors, such as, Oct4, Sox2, KLf4 and c-Myc can reprogram somatic cells to generate induced pluripotent stem cells or iPSC that have similar characteristics to ESC.[3-7] For mouse ESC and to a lesser extent, primate and human ESC, the cell cycle profile has been well described characterized by a short G_1 phase and a high proportion of cells in S-phase resulting in an average cell cycle of 9 hours (for mouse ESC).[8-10] Mouse ESC have been found to express very low levels of CDK inhibitory protein levels such as the Ink family (p16^{INK4a}), Cip/Kip family (p21^{Cip1}, p27^{Kip1}) and are specifically dependent on cyclin A expression for pluripotency.[11,12] When ESC differentiate, their cell cycle structure changes dramatically so as to incorporate a significantly longer G_1 phase and their mechanism of cell cycle regulation changes to that typically seen in other mammalian somatic cells.[10]

Recently, new roles for p27^{Kip1} independent from its function on cell cycle have been described in promoting differentiation suggesting that expression of p27^{Kip1} is a key protein for cell cycle to differentiation switches during development.[13-20] Here we describe a gain and loss of function study to define the functional role of a single cell cycle gene, namely p27^{Kip1}, in self-renewal and pluripotency of human embryonic stem cells.

Results

We evaluated the cell cycle structure of two hESC and two hiPSC lines in undifferentiated conditions, and after differentiation, by flow cytometry analysis of 4',6-dimidino-2-phenylindole (DAPI)-stained cells (**Fig. 1A**). An analog of BrdU, namely EdU, was used to analyze the percentage of cells in S phase. In order to perform a cell cycle analysis of undifferentiated cells we selected pluripotent TRA-1-60 positive-stained cells. We observed a strong resemblance between the cell cycle profile of undifferentiated hESC and hiPSC, where 54–62% of the population was in S phase and a low proportion of cells in $G_0/_1$ phase of the cell

*Correspondence to: Izpisua Belmonte; Email: belmonte@salk.edu or izpisua@cmrb.eu
Submitted: 01/13/11; Revised: 03/03/11; Accepted: 03/09/11
DOI:

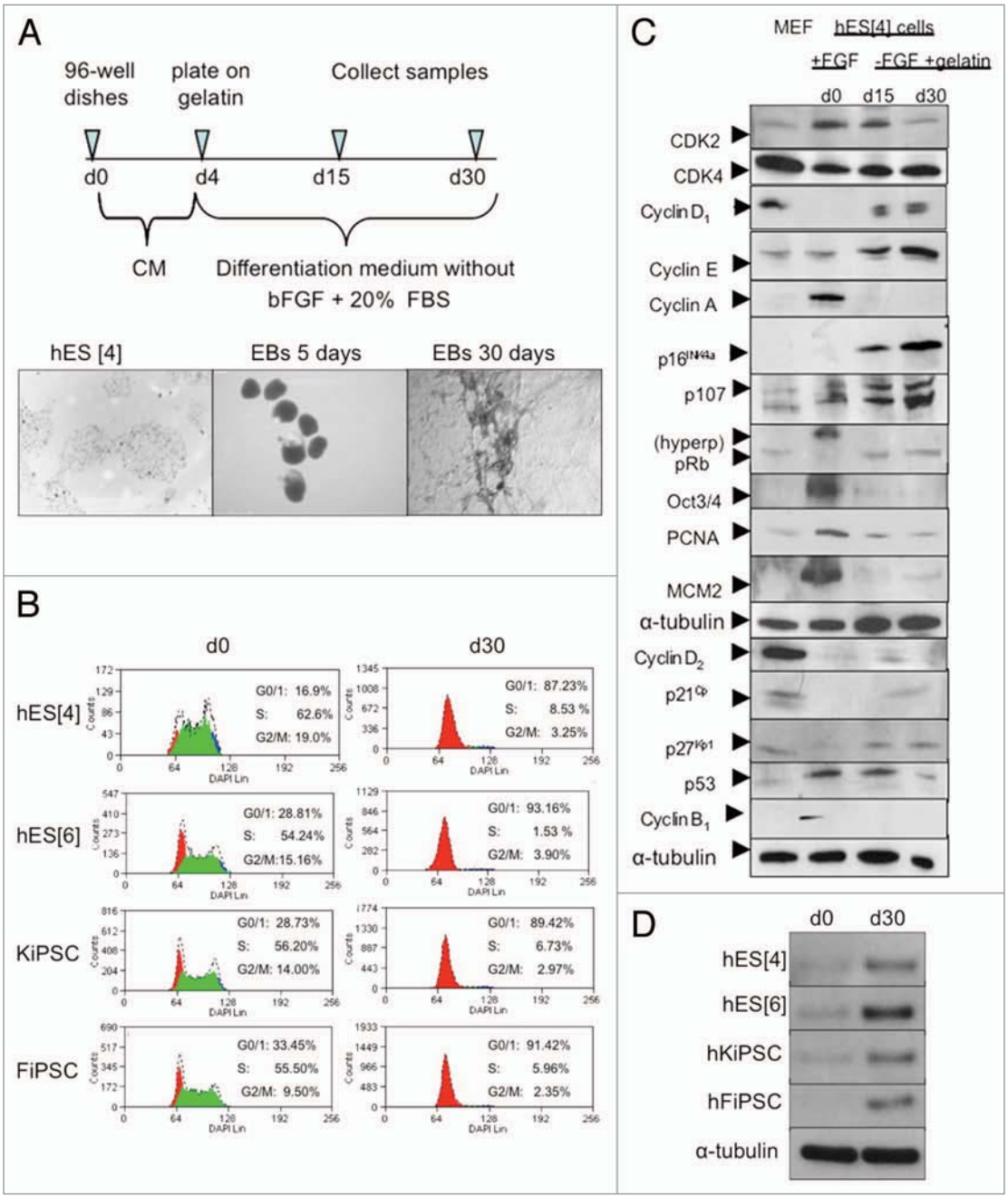

Figure 1. Pluripotent hESC and hiPSC share a conserved cell cycle structure that changes upon differentiation paralleled by an increase of $p27^{Kip1}$. (A) Timeline of general differentiation protocol and representative phase contrast images of hESC in undifferentiated conditions and during general differentiation. Scale bars 500 μm. (B) Quantitative flow cytometry analysis of cell cycle in two different hESC lines and two different iPSC lines reveals a cell cycle structure change along differentiation with a high percentage of cells in S phase and low in $G_{0/1}$ phase of cell cycle in undifferentiated cells, and a reduction of cells in S phase and increase of cells in $G_{0/1}$ phase of cell cycle when cells are differentiated. Shown are the representative results obtained in two independent experiments. (C) Western blot of main cell cycle proteins in undifferentiated conditions and during general differentiation in hESC reveals changes in the expression of some cell cycle proteins along differentiation. MEFs were used as a control. (D) Western blot of human $p27^{Kip1}$ in two different hESC lines and two different iPSC reveals low levels in undifferentiated conditions and high levels in differentiated conditions.

cycle (17–33%) (**Fig. 1B**). On differentiation, the cell cycle structure for all cell lines analyzed, similarly changed with a striking increase of cells in the $G_{0/1}$ phase (87–93%) and a reduction of cells in the S phase (2–8%) (**Fig. 1B**). We confirmed these results in mESC (**Sup. Fig. 1**). Taken together, the results showed no differences in the cell cycle profile of hESC, hiPSC or mESC suggesting a conserved cell cycle structure for the pluripotent cells.

Next, we decided to study the cell cycle, in more detail, at the protein level because many of the cell cycle proteins are regulated at the post-transcriptional level.[23] We performed comprehensive series of western blot analysis for the cell cycle proteins regulating

the G_1 phase in mESC and hESC because the G_1 phase is when the cell commits to go into cell cycle. We analyzed the cell cycle protein profile in undifferentiatiated conditions and compared to ESC under general differentiation conditions (**Fig. 1C and Sup. Fig. 1** for mouse ESC). Among the changes in protein levels during differentiation we found the cell cycle inhibitor $p27^{Kip1}$. Interestingly, with differentiation, $p27^{Kip1}$ protein levels increased over time, suggesting that low levels of $p27^{Kip1}$ were important for the typical cell cycle structure of pluripotent cells (**Fig. 1C and Sup. Fig. 1** for mouse ESC). Reduction in Oct3/4 protein levels was used to monitor differentiation (**Fig. 1C**). Given this important increase in both mESC, as well as, hESC and because, previously, has been shown to have critical functions in determining cell fate we decided to investigate $p27^{Kip1}$ in other hESC and hiPSC lines.[13-20] In all human pluripotent cell lines analyzed, the expression of $p27^{Kip1}$ was low in undifferentiated conditions and increased during differentiation suggesting that low levels of $p27^{Kip1}$ were important for maintaining hESC self-renewal and pluripotency (**Fig. 1D**). We also confirmed these results with another differentiation protocol towards neuronal cells using hESC (**Sup. Fig. 2**).

We sought to investigate whether overexpression of $p27^{Kip1}$ could affect pluripotency or self-renewal properties. To this end, we overexpressed $p27^{Kip1}$ in hESC using a doxycycline tet-off regulated lentiviral pCCL vector (kindly provided by the group of Dr. Naldini). We optimized the lentiviral transduction of hESC with a GFPpCCL vector to achieve over 76% of cells infected (**Sup. Fig. 3**). Next, we used this infection conditions to transduce hESC with a p27pCCL vector. In this system, the expression of $p27^{Kip1}$ was minimal in presence of doxycycline, and was induced by its withdrawal progressively after 4 days of infection, at both the mRNA and protein level (**Fig. 2A**). Based on these results we performed all the experiments at 4 days post-infection. To perform loss of function assays, we used RNAi hairpins against $p27^{Kip1}$ sequence cloned into a pLKO lentiviral vector and found that construct number three gave 70% knockdown (**Fig. 2B**). With the aim to know the subcellular localization within the cell, we overexpressed $p27^{Kip1}$ in hESC and performed immunofluorescence analysis after 4 days in the presence or absence of doxycycline (**Fig. 2C and S4**). Surprisingly, we observed that $p27^{Kip1}$ overexpressing hESC displayed a characteristic phenotype, with a large and spread cell morphology after staining with phalloidin (**Fig. 2C**). Moreover, monitorization of $p27^{Kip1}$ or GPF infected cells for 7 days, by time-lapse microscope photographs, demonstrated that large, spread $p27^{Kip1}$ overexpressing cells could be observed after 4 days onwards (**Sup. Fig. 5**). These results are consistent with previous work showing that overexpression of $p27^{Kip1}$ in murine fibroblasts NIH-3T3 produces a flat phenotype and an augmented cell size.[24] Conversely, with loss of function of $p27^{Kip1}$, we observed a elongated/scatter cell phenotype, whereby the cells elongated away from the hESC colony (**Fig. 2C and S6**). This data demonstrates that maintaining $p27^{Kip1}$ at a certain level of expression is essential for normal hESC morphology.

In order to first explain the enlarged and flattened cell phenotype caused by $p27^{Kip1}$ overexpression, we investigated a number of possible explanations: (1) cell cycle kinetics, (2) apoptosis, (3) induction of senescence and (4) differentiation. To analyze the cell cycle kinetics, we performed flow cytometry analysis of the cell cycle with DAPI and EdU substrate, for stain cells in S phase, of hESC immuno-stained for $p27^{Kip1}$ expression. Control cells had low levels of $p27^{Kip1}$ protein and had a normal hESC profile; however, with hESC overexpressing $p27^{Kip1}$, 90% of the population arrested in G_1 phase of the cell cycle (**Fig. 3A**). On the contrary, with the $p27^{Kip1}$ knockdown a slight increase in the proportion of cells in S phase and a decrease in the G_1 phase could be observed. These results are proof of principle that a single cell cycle protein; namely, $p27^{Kip1}$, inhibits self-renewal of hESC by arresting hESC in the G_1 phase of the cell cycle.

Next, we checked if $p27^{Kip1}$ overexpressing hESCs were apoptotic. We first, analyzed the nuclear morphology by DAPI staining of DNA. Results showed that the nuclei appeared round, clear-edged and uniformly stained further demonstrating that the cells were not apoptotic (**Sup. Fig. 4 and 5B**). We, also, determined the apoptosis by flow cytometry analysis of the mitochondrial membrane potential, by DiLC incorporation, using both, gain and loss of $p27^{Kip1}$ function in hESC (**Fig. 3B**). No significant changes were detected in apoptosis with either gain or loss of $p27^{Kip1}$ function in undifferentiation conditions (**Fig. 3B**). Next, we determined if $p27^{Kip1}$ overexpressing cells could be senescent by performing β-galactosidase activity at pH 6. We did not detect β-galactosidase activity at pH 6 in $p27^{Kip1}$ overexpressing hESC, suggesting that these cells were not senescent (data not shown).

To investigate in more detail the effect of $p27^{Kip1}$on pluripotency of hESC, we compared the transcriptional profiles for 84 genes related to embryonic stem cell pluripotency and differentiation (**Fig. 4 and Sup. Fig. 7**). We had observed from flow cytometry analysis of the cell size that $p27^{Kip1}$ overexpressing hESC were larger than controls and displayed an increase of the mean of intensity of the pulse width signal (**Fig. 4A**). Based on these results and, with the aim to obtain a homogeneous population of $p27^{Kip1}$ overexpressing cells, we FACS sorted cells in G_1 phase by staining with Hoechst 33342 and displaying a higher mean of intensity of the pulse width signal (**Fig. 4A**). We confirmed a 25-fold increase of $p27^{Kip1}$ mRNA expression, by qRT-PCR analysis, in $p27^{Kip1}$ large cells FACS sorted compared to GFP large cells as controls (**Fig. 4B**). This was confirmed by western blot analysis (**Fig. 4B**). We, then, performed the superarray for embryonic stem cell pluripotency and differentiation genes (**Sup. Fig. 7**). Values that were 2 times upregulated or 50% downregulated were considered as significant cut offs (**Fig. 4C**). We found that functional manipulation of $p27^{Kip1}$ gene expression affected mainly genes regulating differentiation than pluripotency (**Fig. 4C**). To confirm this we assessed the effect on pluripotency genes in undifferentiated conditions (**Fig. 4D**). Gene expression profiling of this array values, showed that $p27^{Kip1}$ overexpression did not result in a significant change of the master pluripotency factors such as Oct3/4, Nanog and Sox2 (**Fig. 4D**). Moreover, with $p27^{Kip1}$ loss of function we did not observe a significant change in any of these pluripotent genes (**Fig. 4D**).

Next, we validated the expression of those genes that were more than 2-times upregulated or 50% downregulated, by

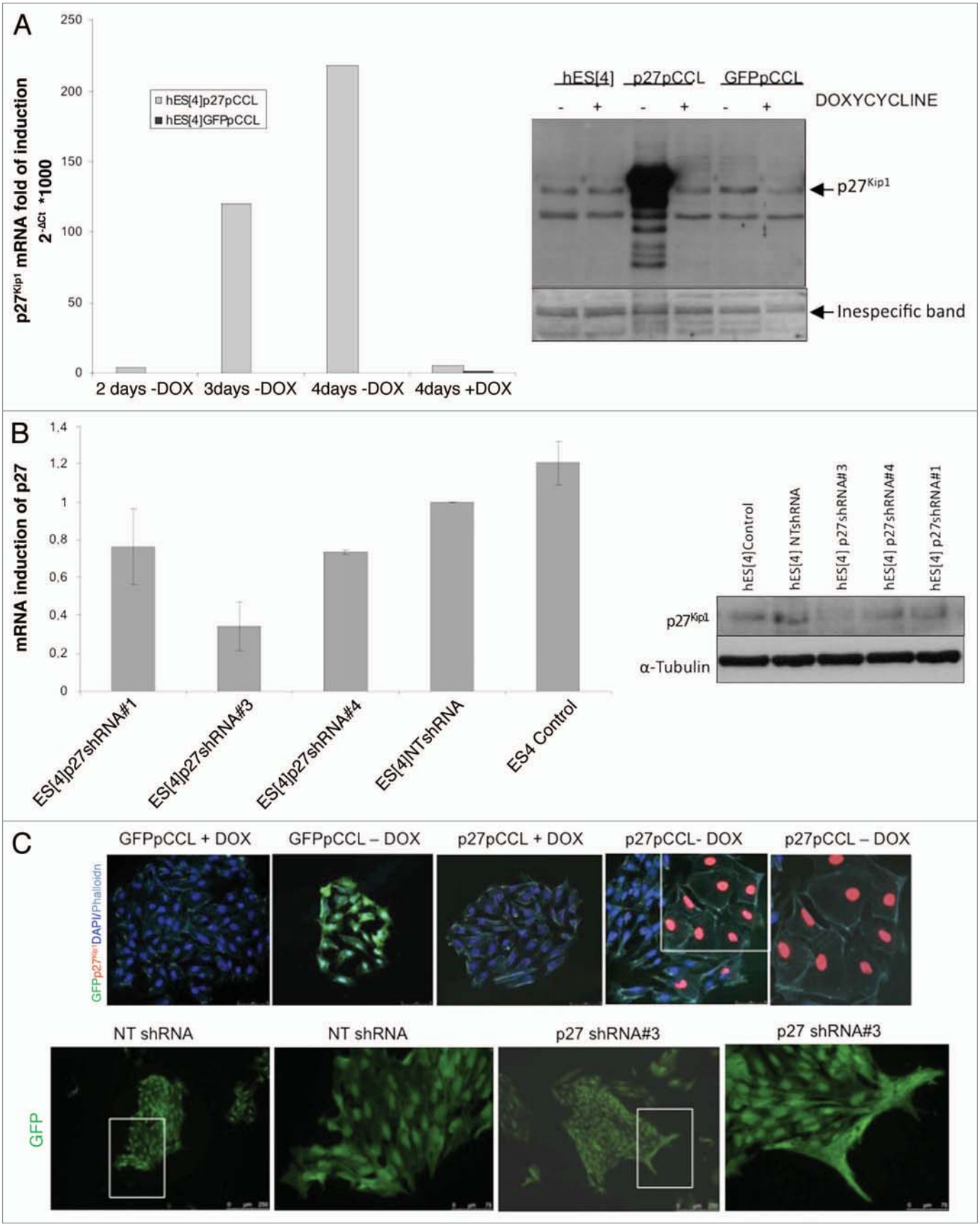

Figure 2. For figure legend, see page 5.

Figure 2 (See opposite page). Gain and loss of function of $p27^{Kip1}$ in hESC. (A) Quantitative RT-PCR analysis of $p27^{Kip1}$ expression in hESC infected with lentiviral tet-off inducible vector encoding for human $p27^{Kip1}$ shows a gradual increase in the levels of $p27^{Kip1}$ mRNA after removing doxycycline and a repression when doxycycline is added to the medium. Western blot analysis of the level of $p27^{Kip1}$ protein in hESC infected with lentiviral tet-off inducible vector encoding for human $p27^{Kip1}$ cultured in the presence or absence of doxycycline confirmed qRT-PCR results. Uninfected hESC were used for control of endogenous $p27^{Kip1}$. (B) Quantitative RT-PCR analysis of $p27^{Kip1}$ expression in hESC infected with 3 different lentivirus-derived GFP plasmids. These plasmids generated short hairpin RNA (shRNA) with different percentages of efficiency. The construct number 3 reached ~70% of knockdown. A Non-Target shRNA lentivirus GFP plasmid vector (NT shRNA) that does not target human genes was used as a control. Western blot analysis confirmed qRT-PCR results. (C) Immunofluorescence analysis of hESC after overexpression and knockdown of $p27^{Kip1}$, in undifferentiated conditions, reveals an enlarged phenotype in cells overexpressing $p27^{Kip1}$ and a fibroblastoid scatter-cell phenotype in knockdown cells. Scale bars 250 μm for lower magnification and 75 μm for higher magnification.

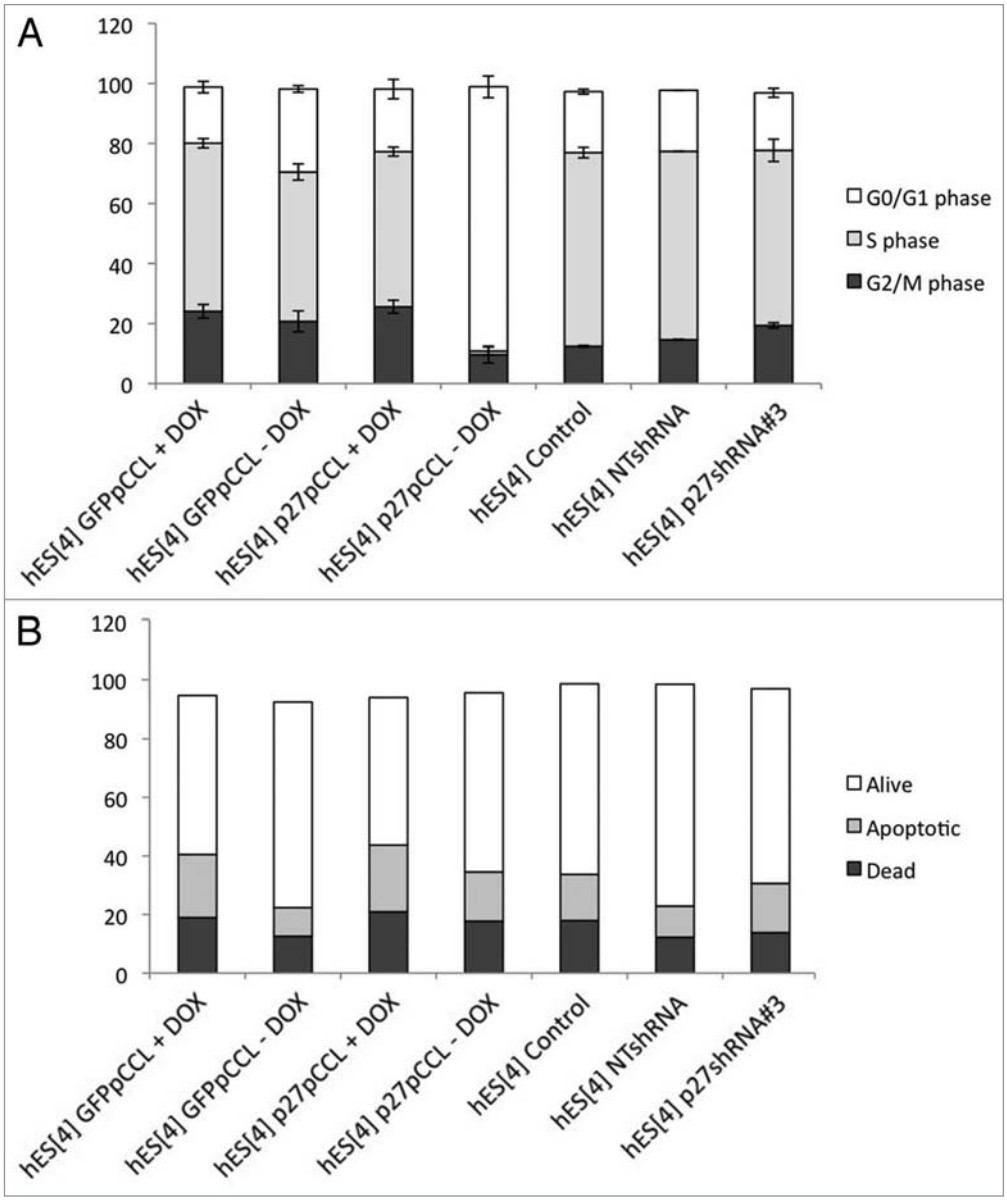

Figure 3. Analysis of Cell cycle and Apoptosis in hESC. (A) Quantitative flow cytometry analysis of the cell cycle in $p27^{Kip1}$ overexpressing and knockdown hESC. Overexpression of $p27^{Kip1}$ induces an arrest in G_1 phase of cell cycle in undifferentiated conditions. Representative results obtained in three independent experiments. (B) Quantitative flow cytometry analysis of apoptosis in $p27^{Kip1}$ overexpressing and knockdown hESC in undifferentiated conditions.

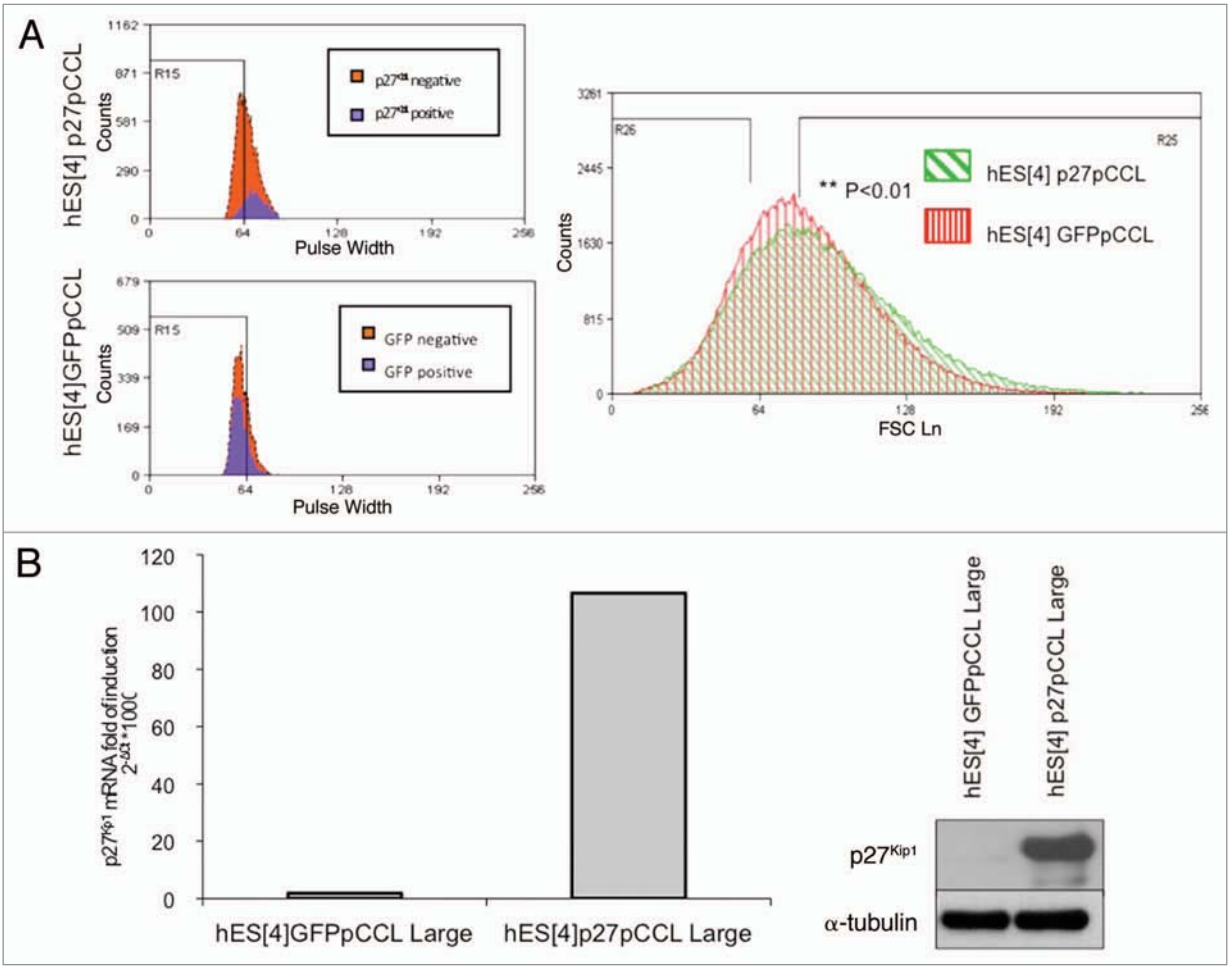

Figure 4A and B. Super Array Real Time PCR of pluripotency and differentiation genes in p27^{Kip1} overexpressing hESC. (A) Quantitative flow cytometry analysis of the cell size of the G_1 phase residing population in p27^{Kip1} overexpressing cells and GFP expressing cells. Shown are the representative results obtained in three independent experiments. p27^{Kip1} overexpressing cells present a significative increase in the mean of the pulse width signal. Student t test **p < 0.01. The cells presenting the highest pulse width signal were separated from the ones presenting the lowest pulse width signal. (B) Quantitative RT-PCR and western blot analysis of p27^{Kip1} expression confirmed that the large cells selected by FACS were overexpressing p27^{Kip1}.

qRT-PCR, in p27^{Kip1} overexpressing, p27^{Kip1} depleted cells and respective controls (**Fig. 5**). These data revealed a decrease of early mesoderm differentiation marker Brachyury, Gbx2 and GATA 6 with gain of function and, conversely, loss of function of p27^{Kip1} reverted this trend (**Fig. 5A**). We decided to investigate Brachyury given that p27^{Kip1} had the largest effect on it compared to the other genes and due to its important role in differentiation. We confirmed by western blot that with loss of p27^{Kip1}, Brachyury was induced, as seen with the real time PCR data, and conversely, with p27^{Kip1} gain of function, Brachyury was repressed (**Fig. 5B**). The regulation of Brachyury was, also, seen by immunofluorescence analysis, in which, p27^{Kip1} overexpressing hESC had reduced levels of expression (**Fig. 5B** and see asterisk). Conversely, with p27^{Kip1} shRNA infected hESC, we observed that a high number of colonies, containing elongated shape cells, expressed Brachyury (**Fig. 5B**).

Given that we had observed the major effect of p27^{Kip1} on a mesodermal marker, namely Brachyury, and that loss of p27^{Kip1} by shRNA lead to an elongated/scatter cell type resembling an EMT phenotype, we proceeded to analyze if other EMT markers could be regulated by p27^{Kip1}. We analyzed a battery of EMT genes, by qRT-PCR, in both p27^{Kip1} overexpressing and shRNA infected hESC (**Fig. 5C**). This analysis revealed an upregulation of Twist mRNA 6-fold compared to controls with loss of function. We did not detect any change in Vimentin, Snail1 or Snail2 genes, or E-Cadherin gene expression, suggesting that the effect of p27^{Kip1} was specific for Twist. Because we had detected p27^{Kip1} nuclear with overexpression in hESC, we performed ChIP analysis on the TWIST1 promoter for p27^{Kip1} and methylation changes using antibodies against p27^{Kip1}. We searched for p27^{Kip1} along 4,000 Kb of Twist1 promoter starting from +1.0 Kb to -3.0 Kb from the ATG. We found that p27^{Kip1} protein occupies the +1.0 Kb sites of the Twist1 promoter with overexpression of p27^{Kip1} in hESC but not seen in controls (based on 2-fold increases compared to control cells) (**Fig. 5D**). This data suggests that p27^{Kip1} is a repressor of Twist1 gene expression in hESC by either binding directly or indirectly the promoter of Twist1.

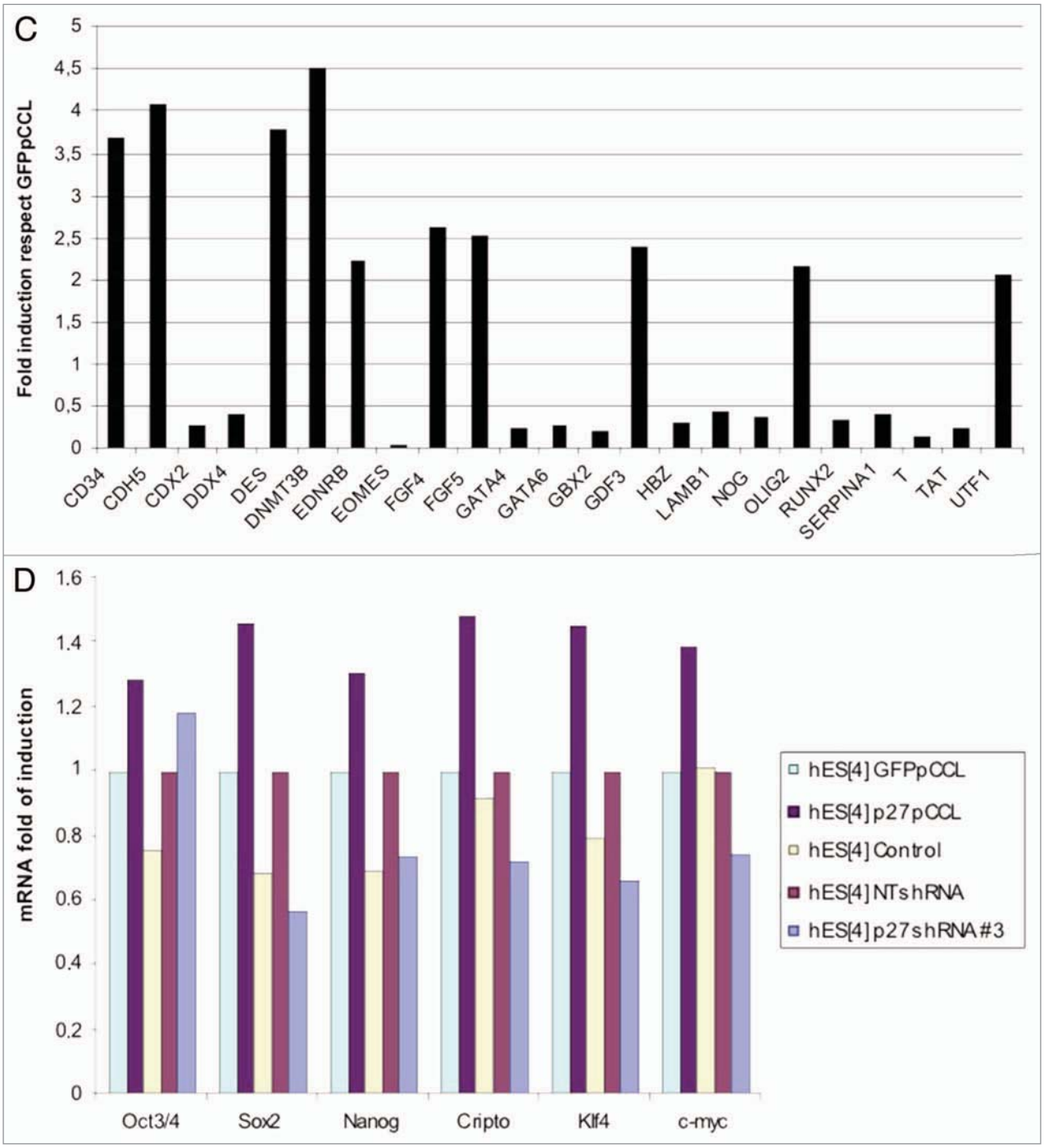

Figure 4C and D. Super Array Real Time PCR of pluripotency and differentiation genes in $p27^{Kip1}$ overexpressing hESC. (C) Graph summarizing genes that were upregulated two fold or more or downregulated 50% or less were considered significant changes. (D) Quantitative RT-PCR of pluripotency markers in $p27^{Kip1}$ overexpressing and knockdown hESC.

Discussion

To date, most studies of the cell cycle in hESC have been descriptive, lacking functional studies that reveal the mechanisms of how the cell cycle maintains pluripotency and self-renewal of hESC.[7] In this study we sought to understand if overexpression or knockdown of a cell cycle gene, could regulate self-renewal or pluripotency of undifferentiated hESC. We focused on $p27^{Kip1}$, given the low levels of expression in undifferentiated ESC and the critical role in cell fate decisions.[13-20] We used a gain and loss of function strategy to define the functional role of the cell cycle in self-renewal or pluripotency by manipulating the expression of $p27^{Kip1}$ in hESC.

The results demonstrate that a single cell cycle protein; namely, $p27^{Kip1}$, inhibits self-renewal of hESC by arresting hESC in the

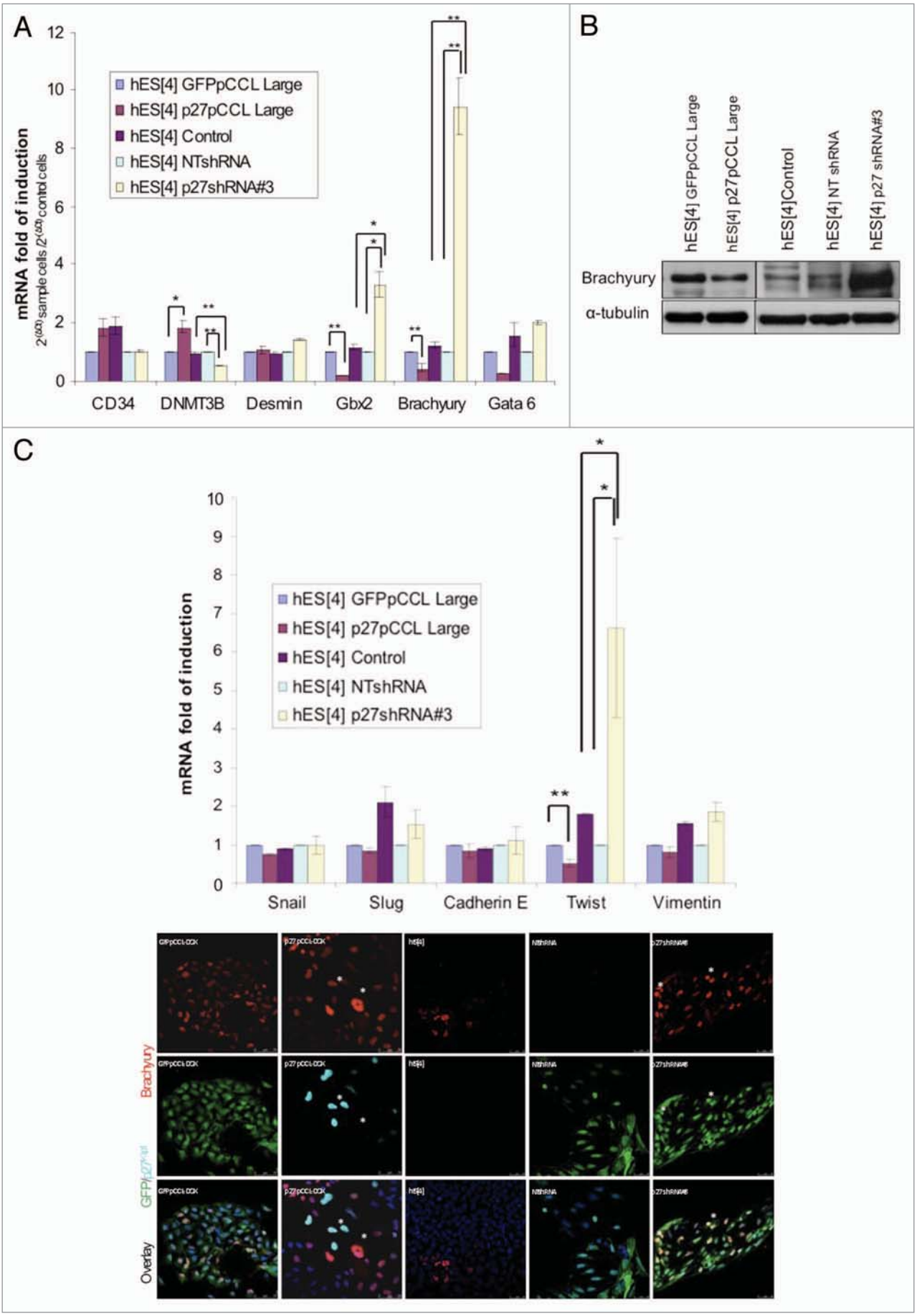
A
mRNA fold of induction
2^(ΔΔ) sample cells /2^(ΔΔ) control cells
hES[4] GFPpCCL Large
hES[4] p27pCCL Large
hES[4] Control
hES[4] NTshRNA
hES[4] p27shRNA#3
CD34
DNMT3B
Desmin
Gbx2
Brachyury
Gata 6
B
hES[4] GFPpCCL Large
hES[4] p27pCCL Large
hES[4]Control
hES[4] NT shRNA
hES[4] p27 shRNA#3
Brachyury
α-tubulin
C
mRNA fold of induction
hES[4] GFPpCCL Large
hES[4] p27pCCL Large
hES[4] Control
hES[4] NTshRNA
hES[4] p27shRNA#3
Snail
Slug
Cadherin E
Twist
Vimentin
Brachyury
GFP/p27
Overlay

Figure 5A–C (See opposite page). Manipulation of p27^{Kip1} expression in hESC affects pluripotency by regulating expression of Brachyury and Twist. (A) Quantitative RT-PCR validation of the markers presenting the most significant changes in p27^{Kip1} overexpressing hESC, p27^{Kip1} knockdown hESC and controls, reveals Brachyury repressed in p27^{Kip1} overexpressing cells and upregulated in p27^{Kip1} knockdown cells. Results represent the mean ± Standard Deviation of two independent experiments performed per duplicate. ANOVA test *p < 0.05, **p < 0.01. (B) Western blot and immunofluorescence analysis for Brachyury expression in p27^{Kip1} overexpressing and knockdown hESC confirmed qRT-PCR results. Note the decrease of Brachyury expression in cells overexpressing p27^{Kip1} by immunofluorescence (denoted by an asterisk *) and the elongated morphology of p27^{Kip1} knockdown cells. These elongated cells were positive for Brachyury expression. Nuclei were counterstained with DAPI. Scale bars 75 μm. (C) qRT-PCR analysis for selected EMT markers in p27^{Kip1} overexpressing and knockdown hESC revealed a significant increase of Twist gene in p27^{Kip1} overexpressing hESC compared to controls in undifferentiated conditions. Results represent the mean ± Standard Deviation of two independent experiments performed per duplicate. ANOVA Test, p < 0.05.

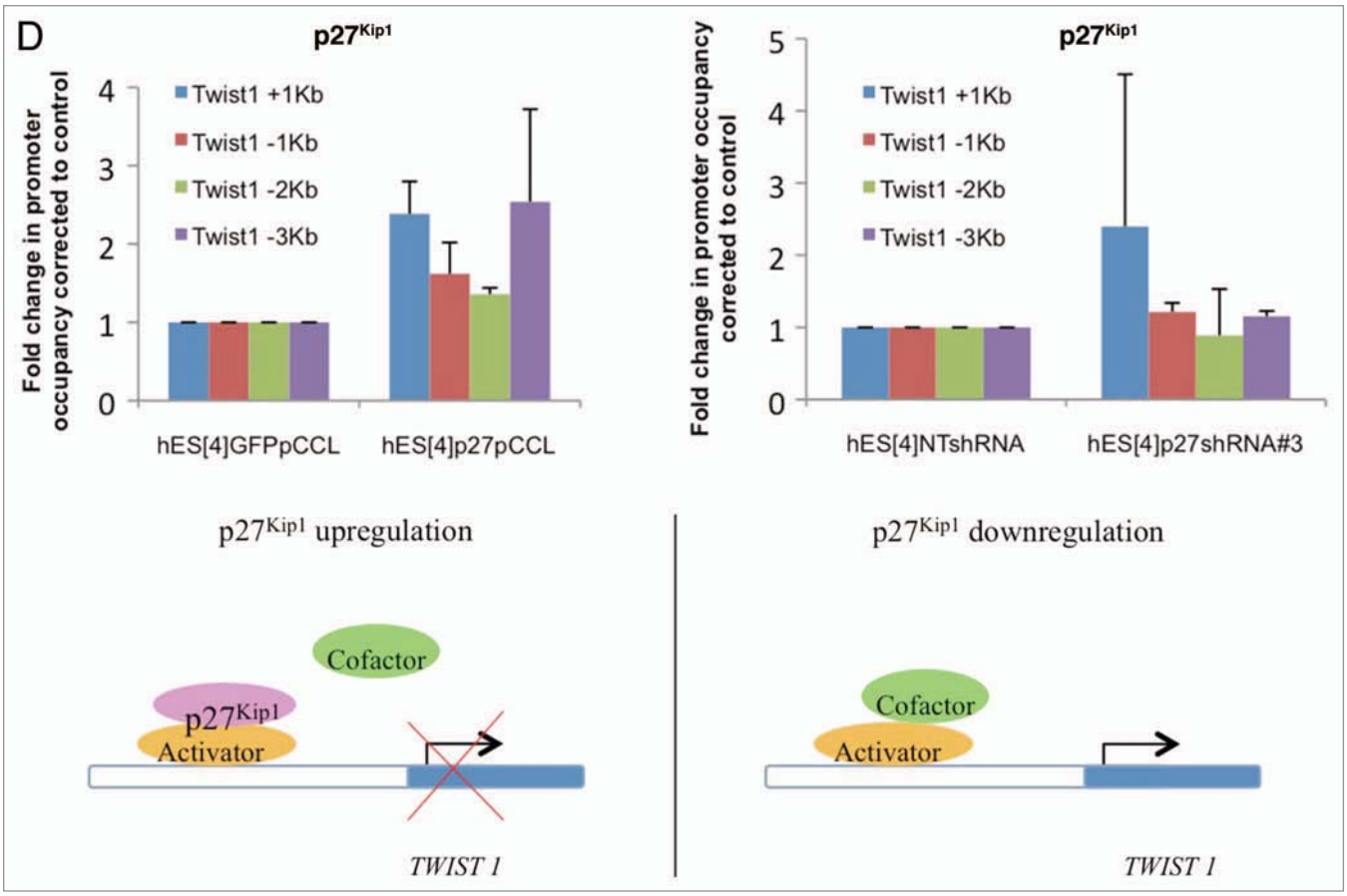

Figure 5D. Manipulation of p27^{Kip1} expression in hESC affects pluripotency by regulating expression of Brachyury and Twist. (D) ChIP assay for p27^{Kip1} in hESC treated with p27^{Kip1} RNAi (loss of function) or p27^{Kip1} cDNA (gain of function) on the Twist1 gene promoter (+1 Kb to -3 Kb). Schematic model suggesting that p27^{Kip1} binds the Twist1 gene promoter as part of a repressor complex in undifferentiated cell culture conditions of human embryonic stem cells.

G_1 phase of the cell cycle. Moreover, we observe that p27^{Kip1} has an important role in the proper pluripotency of hESC (**Fig.** 4), supporting previous work in mESC showing an impairment of normal differentiation in p27^{Kip1} deficient cells after treatment with Retinoic Acid.[25] Under undifferentiating conditions the data demonstrates that p27^{Kip1} regulates proper pluripotency of hESC most likely via its effect in regulating Brachyury and Twist expression. WE did not find that overexpression of p27^{Kip1} cuased senescence in hESC.

The idea that the cell cycle regulates pluripotency has been previously discussed joining a growing body of scientific data supporting a link between the cell cycle and pluripotency.[7,26] Interestingly, loss of p27^{Kip1} initiates an elongated/scatter cell phenotype suggesting a possible regulation of the EMT phenotype. The discovery that loss of p27^{Kip1} initiates an elongated/scatter cell phenotype in hESC in undifferentiated cell conditions by regulating Twist and Brachyury has interesting implications in cell biology for a number of reasons. First, these results are in agreement with previous studies showing that overexpression of p27^{Kip1} promotes the maintenance of differentiation.[13-20] Second, Twist induces an epithelial-mesenchymal transition to facilitate tumor metastasis[27,28] and is upregulated in several types of epithelial cancers.[29] The novel discovery that p27^{Kip1} is present on the Twist1 gene promoter associated with gene expression levels

suggests other functions of $p27^{Kip1}$ in cell biology. A previous role for $p27^{Kip1}$ in suppressing Twist in chicken muscle satellite cells (a type of stem cell) has been described, supporting further our own finding that $p27^{Kip1}$ is an important and novel regulator of Twist in hESC.[30] A previous role for another similar cell cycle kinase inhibitor (CKI), $p21^{waf1}$, has also been found to bind chromatin to regulate gene expression supporting the novel discovery that cell cycle inhibitor proteins may have additional roles to their kinase inhibitor functions by binding chromatin, most probably indirectly as a complex, to regulate gene expression.[31] If $p27^{Kip1}$ regulates Twist1 as part of a repressor complex indirectly via other chromatic modeling proteins during gene regulation remains to be defined. Moreover, how $p27^{Kip1}$ is regulating Brachyury at a gene level remains to be defined. These results are a proof of principle that proteins regulating the cell cycle play a critical role in self-renewal of hESC and also with making cell fate decisions that have far reaching implications for cell biology.

Previous work has shown that overexpression of cyclin D_1, which we observed increases during differentiation, can induce senescence when the cell cycle is blocked.[32] Furthermore, pS6, a marker of mTOR activity is low in quiescent cells and this remains to be determined in hESC.[32]

Materials and Methods

Cell culture. Human embryonic stem cells (hESC), human keratinocytes induced pluripotent stem cells (hKiPS) and human fibroblast induced pluripotent stem cells (hFiPS) were derived and characterized at the CMR[B].[4-6] hESC, hKiPS and hFiPS were cultured on top of mitotically inactivated human fibroblasts and picked mechanically, or over Matrigel (BD Biosciences) coated plates with hESC conditioned medium from irradiated MEFs and passaged by trypsinization (0.05%).[21] hESC medium consisted of Knockout DMEM supplemented with 20% Knockout Serum Replacement, non-essential amino acids, 50 μM of 2-Mercaptoethanol, 100 U/ml penicillin, 100 μg/ml streptomycin, 2 mM GlutaMAX (all Invitrogen) and 10 ng/ml bFGF (Peprotech). Cultures were maintained at 37°C, 5% CO_2 atmosphere, with medium changes daily. Feeder cells used were HFF-1: human foreskin fibroblasts, ATCC. MEFs were established from dissociated C57BL/6 mouse embryos (13.5 d gestation). Both HFF-1 and MEFs were mitotically inactivated by gamma irradiation (55 Gy) and grown in DMEM medium supplemented with 10% FBS, 100 U/ml penicillin, 100 μg/ml streptomycin and 2 mM GlutaMAX (all Invitrogen). Karyotypic analysis were carried out routinely and in all cases normal karyotype was observed.

293T cells (CRL-12103 ATCC number, Rockville, MD USA) were cultured in DMEM medium supplemented with 10% FBS, 100 U/ml penicillin, 100 μg/ml streptomycin and 2 mM GlutaMAX (all Invitrogen). mESC were grown over MEFs feeder layer and the cell culture medium consisted of Knockout DMEM, 15% FBS (HyClone), 1% non-essential amino acids, 50 μM of 2-Mercaptoethanol, 100 U/ml penicillin, 100 μg/ml streptomycin, 2 mM GlutaMAX and 1,000 U/ml recombinant leukemia inhibitory factor (LIF) (ESGRO).

In vitro differentiation. For mechanically picked cells, colonies of undifferentiated cells were detached from the feeder layer using a modified glass pipette and transferred to low attachment plates 60 mm x 15 mm (Corning, NY 14831) in hESC medium for 3–4 days. After 3–4 days the embryoid bodies were transferred to 0.1% gelatin (Chemicon) coated plates and cultured in general differentiation medium: Knockout DMEM (Invitrogen) supplemented with 20% Fetal Bovine Serum (HyClone), nonessential aminoacids, 100 U/ml penicillin, 100 μg/ml streptomycin, 2 mM GlutaMAX and 50 μM 2-Mercaptoethanol (all Invitrogen) for 30 days. Cell samples for western blot and FACs analysis were taken after 15 and 30 days. The medium was changed every other day.

For hESC cells passaged by trypsinization, 0.05% trypsin-EDTA (Invitrogen) was used for single cell suspension and 35,000–40,000 hESC were seeded in 200 μl of conditioned medium in each well of 96-well v-bottom low attachment plates (NUNC) and centrifuged at 950 g for 10 minutes to aggregate the cells. After 3–4 days embryoid bodies were transferred to 0.1% gelatin coated plates and cultured in general differentiation medium. Cell samples for western blot and FACs analysis were taken after 15 and 30 days. The medium was changed every other day.

For ectoderm differentiation: embryoid bodies were cultured in DMEM/F12 (Invitrogen), N2 and B27 supplements (Invitrogen), 1 mM l-glutamine, 1% nonessential aminoacids, 0.1 mM beta-mercaptoethanol for 6 days, after which they were seeded onto matrigel chamber-slides with the same media plus 10-6 M Retinoic Acid (Sigma-Aldrich Quimica). Media was changed every two days. For mesoderm differentiation, embryoid bodies were replated onto gelatin-coated chambers-slide. Cultures were maintained in general differentiation medium supplemented with 100 μM Ascorbic Acid (Sigma-Aldrich Quimica). Media was changed every two days.

Flow cytometry analysis. For measuring apoptosis and proliferation we used the commercial kits "MitoProbe DilC1(5) Assay Kit" and "Click-iT EdU AlexaFluor647 Flow Cytometry Assay kit" respectively (both from Invitrogen) following the manufacturer's instructions. Briefly, for the proliferation assay, 2 μl of 10 mM EdU solution was added to 2 ml of culture medium containing cells for 1 hour, cells were then trypsinized with 0.05% trypsin and resuspended in 100 μl of PBS supplemented with 1% BSA, 100 μl of Click-iT fixative solution was added to the cells, mixed for 5 seconds and left at room temperature for 15 minutes. Cells were washed with 3 ml of PBS-1% BSA and collected by centrifugation (2,000 rpm, 3 min). 100 μl of 1x saponin-based permeabilization and wash buffer were added to the cell pellet and incubated with rabbit polyclonal antibodies against rabbit $p27^{Kip1}$ (M-197, Santa Cruz Biotechnology) 1:20, and mouse Tra-1-60-FITC (BD) for 30 minutes at room temperature. Cells were then washed in PBS-1% BSA, collected by centrifugation and cells incubated with antibodies against $p27^{Kip1}$, were incubated with alexa fluor 488-conjugated anti-rabbit IgG 1:50 for 15 minutes at room temperature. Cells were washed with 3 ml of the 1x saponin-based permeabilization and wash buffer and collected by centrifugation. 500 μl of Click-iT reaction cocktail containing 1x Click-iT EdU buffer additive, $CuSO_4$ and Alexa

Fluor 647 were added to the cells and left for 30 minutes at room temperature. After this time, cells were washed with saponin 1x buffer, collected by centrifugation and resuspended in 500 μl of saponin 1x buffer. Cells were stained by the addition of DAPI solution (0.1 M Tris Base pH 7.4; 0.9% or 150 mM NaCl; 1 mM $CaCl_2$; 0.5 mM $MgCl_2$; 0.2% BSA; 0.1% Nonidet P40; 10 mg/ml DAPI) (Invitrogen) for 2 hours at room temperature or overnight at 4°C. Finally cells were analysed on a MoFlo cell sorter (DakoCytomation) with Summit software. A total of 10,000 events were collected for the cell cycle analysis.

For cell sorting of alive cells based on size, we selected the cells residing in G_1 phase of the cell cycle by staining with 2 μg/ml of Hoechst 33342 for 30 minutes at 37°C. Hoechst 33342 was detected by using UV light excitation. Of this selected G_1 phase residing cells, the biggest cells were separated from the smallest ones based on pulse-width signal at comparable cell numbers (58% population).

Western blot analysis. Cells were washed twice with cold PBS then harvested by scraping cells in ice-cold lysis buffer (150 μl for 10 cm petri dishes) consisting of Tris-HCl pH 7.4 (Roche), 250 mM NaCl, 1% Triton X100, 1 mM EDTA, 1 mM EGTA, 0.2 mM PMSF (all Sigma-Aldrich Quimica), 1x protease inhibitor cocktail (Roche) and 1x phosphatase inhibitor cocktail (Sigma-Aldrich Quimica). Lysates were passaged through a 1 ml syringe (Rubilabor) and a 25G needle (Terumo) and left for 30 minutes on ice. Lysates were clarified by centrifugation at 10,000 rpm for 10 minutes at 4°C and protein concentrations determined by Bradford assay (Bio-Rad Laboratories GmbH). 20 μg of protein were mixed with 4x of a commercial loading buffer containing 20% 2-mercaptoethanol (Sigma-Aldrich Quimica), boiled at 100°C for 5 minutes and resolved on 8–12% SDS polyacrilamide electrophoresis gels. After electrophoresis, proteins were transferred to a nitrocellulose membrane using a submerged transfer apparatus (BioRad), filled with 25 mM Tris Base (Roche), 200 mM glycine (Sigma-Aldrich Quimica) and 20% methanol (Merck). Membranes were blocked in PBS containing 0.1% Tween-20 (PBST) (Sigma-Aldrich Quimica) and 5% milk powder (Sigma-Aldrich Quimica) for 1 hour at room temperature. Membranes were incubated with primary antibody in PBST supplemented with 2% milk powder for 2 hours at room temperature or overnight at 4°C. Primary antibodies were raised against $p27^{Kip1}$ (M-197), E2F4 (A-20), p16 (H-156), $p21^{Cip1}$ (F-5), p107 (C-18), Cdk2 (H-298), Cdk4 (H-22), Cyclin A (C-19), Cyclin D1 (H-295), Cyclin D2 (M-20), Cyclin E (M-20), PCNA (PC10), Rb (C-15), MCM2 (N-19), Cyclin B1 (GNS1), p53 (FL-393) (all Santa Cruz Biotechnology); Oct3/4 (ab19857) (Abcam); Cyclin D1 (Ab-2), Cyclin D2 (Ab-2) and Cyclin D3 (Ab-2) (all from Neomarkers) all primary antibodies were used as a 1: 1,000 dilution. Brachyury (AF2085, R&D Systems, Inc.,) and E-cadherin (BD, Transduction Laboratories) were used as a 1:500 dilution. Alfa-tubulin (T6074, Sigma-Aldrich) was used as a 1:8,000. All antibodies were used according to the manufacturer's specifications. Membranes were washed four times at room temperature for 5 minutes in PBST, then incubated for 1 hour at room temperature with horseradish peroxidase (HRP)-conjugated secondary anti-rabbit, anti-mouse or anti-goat antibodies (Amersham Biosciences; 1:10,000) in PBST 2% milk powder. HRP activity was detected using ECL Plus detection kit (Pierce) following manufacturer's instructions on Amersham ECL Hyperfilm (GE Healthcare, Limited).

Immunofluorescence. Cells were grown on plastic cover slide chambers (170920, NUNC), fixed with 4% paraformaldehyde (Sigma-Aldrich Quimica) for 20 minutes at room temperature or fixed with cold methanol for 5 minutes. After fixation cells were washed 3 times with TBS and blocked in TBS containing 0.5% Triton X-100 plus 6% donkey serum (S-30; Chemicon) for 30 minutes at room temperature. The following antibodies in TBS containing 0.1% Triton X-100 plus 6% donkey serum were used: $p27^{Kip1}$ (M-197, Santa Cruz Biotechnology) 1:200, Brachyury (AF2085, R&D Systems, Inc.,) 1:25, E-Cadherin (BD, Transduction Laboratories) 1:100, GFP (GFP-1020, AVES) 1:250, Actin-α Smooth Muscle (A5228, Sigma) 1:400, β-Tubulin III TUJ1 (MMS-435P, Covance) 1:500 and Nestin (AB5922, Chemicon) 1:100.

After overnight primary antibody incubation, samples were washed 3 times with TBS 0.1% Triton X-100 plus 6% donkey serum and incubated with CY-conjugated secondary anti-rabbit, anti-mouse, anti-goat or anti-chicken antibodies (Jackson) for 2 hours at 37°C. Samples were washed three times in TBS buffer at room temperature for 5 minutes and were counterstained with DAPI (Invitrogen, 21490, 1:10,000) for 10 minutes at room temperature in the dark. Samples were covered with mounting medium. Images were taken using Leica SP5 confocal microscope.

Time-lapse microscopy analysis. 2 x 10^5 hESC were infected with lenti-p27pCCL or GFPpCCL control vector for one hour and then plated in chamber slide flasks with a further 1 ml of hESC conditioned medium. Cells were left grow in a 5% CO_2 atmosphere at 37°C and photographs of individual cells were taken after 4, 5, 6 and 7 days using Leica DMI4000B inverted microscope equipped with a Leica DFC320 digital fluorescence camera and Leica AF6000 software. After this time, cultures were fixed with 4% Paraformaldehyde for 20 minutes at room temperature and immunofluorescence analysis performed for detection of $p27^{Kip1}$ expression. Cells were counterstained with DAPI 1:10,000 for 10 minutes to allow the identification of nuclei.

Isolation of RNA and quantitative RT-PCR analysis. Total RNA was isolated using TRIzol reagent (Invitrogen) as recommended by the manufacturer and 500 ng of mRNA were used to synthesize cDNA using Cloned AMV First-strand cDNA synthesis kit (Invitrogen). One μl of the reaction was mixed with SYBR GreenER qPCR superMix for ABI PRISM (Invitrogen) and corresponding primers. Each reaction was done per duplicate and run in an ABI Prism 7000 thermocycler (Applied Biosystems). Relative mRNA expression levels were determined using the comparative threshold cycle method (Lu et al. 2001). The graphics represent $[2^{-CT\ (target)}/2^{-CT\ (housekeeping)}]$ cell line/$[2^{-CT\ (target)}/2^{-CT\ (housekeeping)}]$ control cells. The sequences of the oligonucleotides used for the quantitative RT-PCR are shown in (**Sup. Table 1**).

For the expression analysis of stem cell related genes, we used the Human Stem Cell RT2 profiler PCR array (SuperArray Bioscences Corporation) with 500 ng of RNA isolated with

Qiagen RNA easy mini kit following the manufacturer's directions. Relative mRNA expression levels were determined using the comparative threshold cycle method. The graphics represent $[2^{-CT\ (target)}/2^{-CT\ (housekeeping)}]$ cell line/$[2^{-CT\ (target)}/2^{-CT\ (housekeeping)}]$ control cells. Values that were not 2 times upregulated or 50% downregulated were not considered as significant changes.

Constructs and lentiviral production. Human *p27* cDNA was amplified by PCR using a forward primer containing an Age I restriction enzyme site and a reverse primer containing a Cla I restriction enzyme site. Primer sequences were as follows:

Forward, 5'-GAT CAC CGG TGC CAT GGC TTA CCC ATA CGA TGT TCC AGA TTA CGC GTC AAA CGT GCG AGT GTC TAA CGG G-3'

Reverse, 5'-GAT CAT CGA TTT ACG TTT GAC GTC TTC TGA GGC CAG GC-3' (amplified a fragment of 650 bp). PCR products were obtained after 20 cycles of amplification with an annealing temperature of 60°C. PCR products were cloned into pcRII (Invitrogen) to give pcRII-p27. The fragment was digested using Age I/Cla I restriction enzymes (NEB) and cloned into Age I and Cla I sites of pCCL TET OFF inducible lentiviral vector. GFP pCCL TET OFF inducible lentiviral vector was kindly provided by Dr. Antonella Consiglio.

p27 shRNA and non target shRNA constructs were cloned into pLK0.1 puromycin lentiviral vector and were purchased from Sigma-Aldrich. Puromycin sequence was removed by digestion with Bam H1 (New England Biolabs) and Asp 718 (Roche) restriction enzymes and a GFP sequence containing Bam H1 and Kpn I cloning sites was cloned instead. GFP cDNA was amplified by PCR using a forward primer containing a Bam H1 restriction enzyme site and a reverse primer containing a Kpn I restriction enzyme site. Primer sequences were as follows:

Forward, 5'-GAT CGG ATC CAT GGT GAG CAA GGG C-3'

Reverse, 5'-GAT CGG TAC CTT ACT TGT ACA GC-3'

PCR products were obtained after 30 cycles of amplification with an annealing temperature of 58°C. PCR products were cloned into pGEM-T easy vector (Promega Biotech Iberica) and digested with Bam H1 and Asp 718 restriction enzymes. The fragment was cloned into Bam H1 and Asp 718 sites of p27 shRNA and non target shRNA.

Lentiviruses were independently produced by transfecting the cell line 293T with packaging and envelope vectors: pMDLg-pRRE (6.5 μg), pMD2.VSV.G (4 μg), pRSV-Rev (2.5 μg) kindly provided by L. Naldini (San Raffaele Telethon Institute for Gene Therapy-'Vita-Salute San Raffaele' University Medical School, Milano, Italy) and lentiviral constructs (10 μg) using Lipofectamine 2000 (Invitrogen) according to the manufacturer's instructions. After 16 hours medium was replaced with 6 ml of hESC conditioned medium, and cells incubated at 37°C in a 5% CO_2 atmosphere. Viral supernatant was harvested after 24 and 48 hours, filtered and stored at -80°C in ml aliquots. Virus titer was tested using a HIV-1 p24 ELISA kit (Perkin Elmer). 2,00,000 human ESC were infected in suspension with 1 ml of viral supernatant at 37°C in a 5% CO_2 atmosphere for one hour and then plated in a well of 6-well plates with a further 1 ml of hESC conditioned medium. The next day the medium was changed.

Chromatin immunoprecipitation assays. ChIP assays were performed as described in reference 22, by using chromatin from the human embryonic stem cells cultured and treated as described above. The antibodies used for ChIPs assays are listed in Figures. Quantification of ChIP was performed by real-time PCR using Roche Lightcycler (Roche). The change in promoter occupancy in the immunoprecipitated (IP) compared to input (Ref) fractions was calculated using the comparative Ct (the number of cycles required to reach a threshold concentration) method with the equation 2Ct(IP) - Ct(Ref). Real Time PCR primers for the human Twist 1 gene from +1.0 Kb to -3.0 Kb at 1,000 bp intervals were bought from SA biosciences. Oct4 primers were used as a positive technical control to ensure the ChIP had worked.

Statistical analysis. All data were analyzed applying ANOVA or Student t-test statistic analysis. Probability values that were less than 0.05 were considered statistically significant.

Conclusion

In conclusion, we have proven using functional genetic approach that a cell cycle inhibitor, $p27^{Kip1}$, controls self-renewal and pluripotency of hESC in undifferentiated conditions, by imposing a G_1 arrest and controlling the expression of the specific differentiation genes Brachyury and Twist. This suggests that $p27^{Kip}$ levels must be maintained at a critical level in undifferentiated hESC in order to maintain low levels of mesenchymal markers and that alteration of expression either way unbalances the pluripotent state towards differentiation and cell cycle slowing.

Acknowledgements

The authors are indebted to José Miguel Andrés Vaquero for assistance with flow cytometry, Meritxell Carrió for expert assistance with cell culture techniques, Mercé Martí Gaudes, Lola Mulero Pérez and Esther Melo for bioimaging assistance. Dr. Naldini for providing pCCL vector. Federico González for helpful expertise with the cloning. Members of the laboratory for helpful discussion. María José Barrero for assistance with the ChIP assay. Cristina Menchón is partly supported by a pre-doctoral grant from the Spanish Ministry (AP-2004-3523). This work was partially supported by grants from the Fondo de Investigaciones Sanitarias (P1071209), MICINN, Fundacion Cellex and Sanofi-Aventis.

Author Contributions

Cristina Menchón: Collection and assembly of data, Data analysis and interpretation, Manuscript writing.

Michael J. Edel: Conception and design, Financial support, Collection and assembly of data, Data analysis and interpretation, Manuscript writing, Final approval of manuscript.

Juan Carlos Izpisúa Belmonte: Financial support, Administrative support, Final approval of manuscript, Provision of study material or patients.

Note

Supplemental materials can be found at:
www.landesbioscience.com/journals/cc/article/15421

References

1. Evans MJ, Kaufman MH. Establishment in culture of pluripotential cells from mouse embryos. Nature 1981; 292:154-6.
2. Thomson JA, Itskovitz-Eldor J, Shapiro SS, Waknitz MA, Swiergiel JJ, Marshall VS, et al. Embryonic stem cell lines derived from human blastocysts. Science 1998; 282:1145-7.
3. Takahashi K, Yamanaka S. Induction of pluripotent stem cells from mouse embryonic and adult fibroblast cultures by defined factors. Cell 2006; 126:663-76.
4. Aasen T, Raya A, Barrero MJ, Garreta E, Consiglio A, Gonzalez F, et al. Efficient and rapid generation of induced pluripotent stem cells from human keratinocytes. Nat Biotechnol 2008; 26:1276-84.
5. Gonzalez F, Barragan Monasterio M, Tiscornia G, Montserrat Pulido N, Vassena R, Batlle Morera L, et al. Generation of mouse-induced pluripotent stem cells by transient expression of a single nonviral polycistronic vector. Proc Natl Acad Sci USA 2009; 106:8918-22.
6. Raya A, Rodriguez-Piza I, Guenechea G, Vassena R, Navarro S, Barrero MJ, et al. Disease-corrected haematopoietic progenitors from Fanconi anaemia induced pluripotent stem cells. Nature 2009; 460:53-9.
7. Edel MJ, Menchon C, Menendez S, Consiglio A, Raya A, Izpisua Belmonte JC. Rem2 GTPase maintains survival of human embryonic stem cells as well as enhancing reprogramming by regulating p53 and cyclin D1. Genes Dev 2010; 24:561-73.
8. Becker KA, Ghule PN, Therrien JA, Lian JB, Stein JL, van Wijnen AJ, et al. Self-renewal of human embryonic stem cells is supported by a shortened G_1 cell cycle phase. J Cell Physiol 2006; 209:883-93.
9. Fluckiger AC, Marcy G, Marchand M, Negre D, Cosset FL, Mitalipov S, et al. Cell cycle features of primate embryonic stem cells. Stem Cells 2006; 24:547-56.
10. White J, Dalton S. Cell cycle control of embryonic stem cells. Stem Cell Rev 2005; 1:131-8.
11. Kalaszczynska I, Geng Y, Iino T, Mizuno S, Choi Y, Kondratiuk I, et al. Cyclin A is redundant in fibroblasts but essential in hematopoietic and embryonic stem cells. Cell 2009; 138:352-65.
12. Savatier P, Lapillonne H, van Grunsven LA, Rudkin BB, Samarut J. Withdrawal of differentiation inhibitory activity/leukemia inhibitory factor upregulates D-type cyclins and cyclin-dependent kinase inhibitors in mouse embryonic stem cells. Oncogene 1996; 12:309-22.
13. Buttitta LA, Edgar BA. Mechanisms controlling cell cycle exit upon terminal differentiation. Curr Opin Cell Biol 2007; 19:697-704.
14. Nguyen L, Besson A, Heng JI, Schuurmans C, Teboul L, Parras C, et al. $p27^{kip1}$ independently promotes neuronal differentiation and migration in the cerebral cortex. Genes & development 2006; 20:1511-24.
15. Vernon AE, Devine C, Philpott A. The cdk inhibitor $p27^{Xic1}$ is required for differentiation of primary neurones in Xenopus. Development 2003; 130:85-92.
16. Vernon AE, Movassagh M, Horan I, Wise H, Ohnuma S, Philpott A. Notch targets the Cdk inhibitor Xic1 to regulate differentiation but not the cell cycle in neurons. EMBO Rep 2006; 7:643-8.
17. Messina G, Blasi C, La Rocca SA, Pompili M, Calconi A, Grossi M. $p27^{Kip1}$ acts downstream of N-cadherin-mediated cell adhesion to promote myogenesis beyond cell cycle regulation. Mol Biol Cell 2005; 16:1469-80.
18. Vernon AE, Philpott A. A single cdk inhibitor, $p27^{Xic1}$, functions beyond cell cycle regulation to promote muscle differentiation in Xenopus. Development 2003; 130:71-83.
19. Movassagh M, Philpott A. Cardiac differentiation in Xenopus requires the cyclin-dependent kinase inhibitor, $p27^{Xic1}$. Cardiovasc Res 2008; 79:436-47.
20. Deschenes C, Vezina A, Beaulieu JF, Rivard N. Role of p27(Kip1) in human intestinal cell differentiation. Gastroenterology 2001; 120:423-38.
21. Raya A, Rodriguez-Piza I, Aran B, Consiglio A, Barri PN, Veiga A, et al. Generation of cardiomyocytes from new human embryonic stem cell lines derived from poor-quality blastocysts. Cold Spring Harb Symp Quant Biol 2008; 73:127-35.
22. Strutt H, Paro R. Mapping DNA target sites of chromatin proteins in vivo by formaldehyde crosslinking. Methods Mol Biol 1999; 119:455-67.
23. Sherr CJ, Roberts JM. Inhibitors of mammalian G_1 cyclin-dependent kinases. Genes Dev 1995; 9:1149-63.
24. Diez-Juan A, Andres V. Coordinate control of proliferation and migration by the $p27^{Kip1}$/cyclin-dependent kinase/retinoblastoma pathway in vascular smooth muscle cells and fibroblasts. Circ Res 2003; 92:402-10.
25. Bryja V, Pachernik J, Soucek K, Horvath V, Dvorak P, Hampl A. Increased apoptosis in differentiating p27-deficient mouse embryonic stem cells. Cell Mol Life Sci 2004; 61:1384-400.
26. Edel MJ, Belmonte JC. The cell cycle and pluripotency: Is there a direct link? Cell Cycle 2010; 9:2694-5.
27. Yang J, Mani SA, Donaher JL, Ramaswamy S, Itzykson RA, Come C, et al. Twist, a master regulator of morphogenesis, plays an essential role in tumor metastasis. Cell 2004; 117:927-39.
28. Karreth F, Tuveson DA. Twist induces an epithelial-mesenchymal transition to facilitate tumor metastasis. Cancer Biol Ther 2004; 3:1058-9.
29. Puisieux A, Valsesia-Wittmann S, Ansieau S. A twist for survival and cancer progression. Br J Cancer 2006; 94:13-7.
30. Leshem Y, Spicer DB, Gal-Levi R, Halevy O. Hepatocyte growth factor (HGF) inhibits skeletal muscle cell differentiation: a role for the bHLH protein twist and the cdk inhibitor p27. J Cell Physiol 2000; 184:101-9.
31. Vigneron A, Cherier J, Barre B, Gamelin E, Coqueret O. The cell cycle inhibitor $p21^{waf1}$ binds to the myc and cdc25A promoters upon DNA damage and induces transcriptional repression. J Biol Chem 2006; 281:34742-50.
32. Demidenko ZN, Blagosklonny MV. Growth stimulation leads to cellular senescence when the cell cycle is blocked. Cell Cycle 2008; 7:3355-61.

A

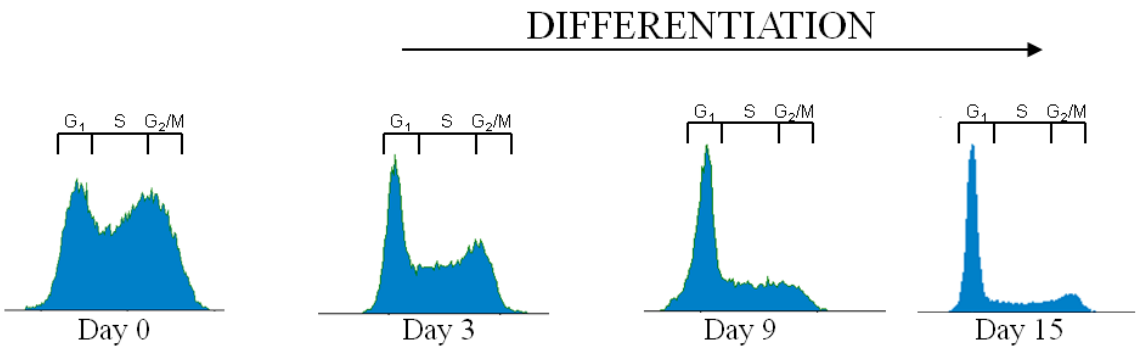

B

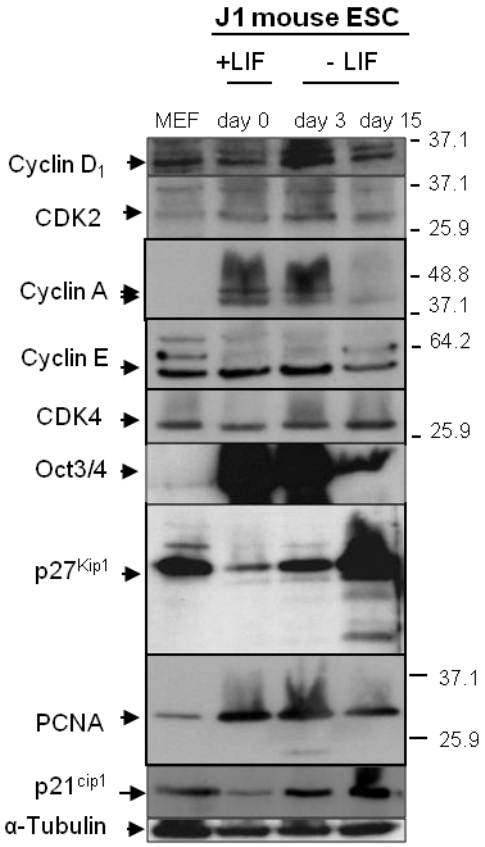

Supplementary Figure 1. Structure and molecular analysis of the cell cycle in J1 mouse embryonic stem cell line. (**A**) Flow cytometry analysis of the cell cycle structure during differentiation reveals a progressive change in the cell cycle structure with an increase of the $G_0/_1$ population and a decrease of the S phase during differentiation. (**B**) Western blot expression analysis of main cell cycle regulators in the J1 mouse ESC line in undifferentiated conditions and along differentiation.

A

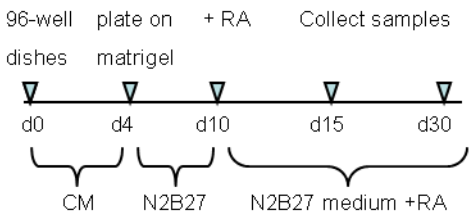

B

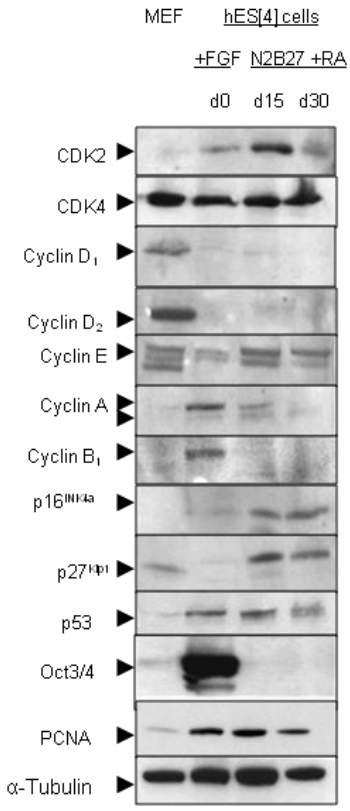

Supplementary Figure 2. Molecular analysis of the cell cycle during neuronal differentiation in human embryonic stem cells. (**A**) Timeline of neuronal differentiation protocol. (**B**) Western blot analysis of main cell cycle proteins in undifferentiated conditions and during neuronal differentiation in hESC reveals similar changes in the expression of cell cycle proteins along differentiation as with the general differentiation protocol. MEFs were used as a control.

A

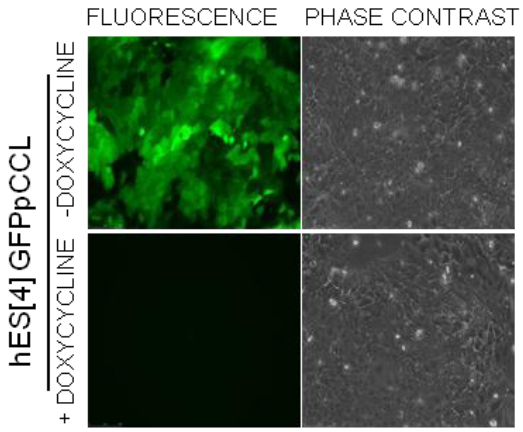

B

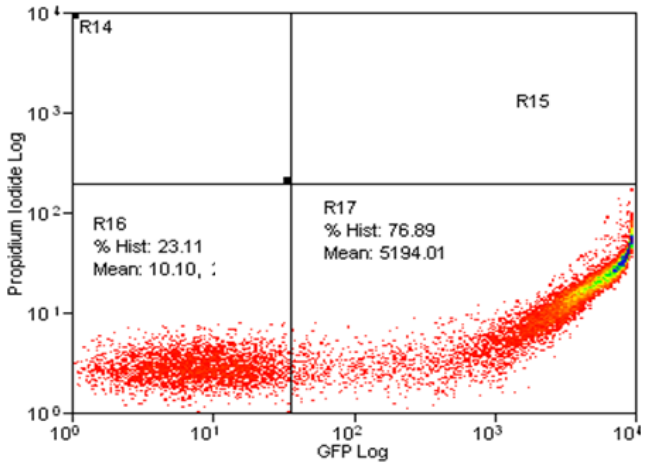

Supplementary Figure 3. Immunofluorescence and flow cytometry analysis of GFP expression. (**A**) Immunofluorescence analysis of GFP expression in hESC infected with a GFP doxycycline tet-off regulated lentiviral construct cultured in the presence or absence of doxycycline for four days. Scale bars: 100 μm. (**B**) Quantitative flow cytometry analysis of GFP positive population in hESC infected with a GFP doxycycline tet-off regulated lentiviral construct cultured in the absence of doxycycline for four days revealed approximately 77% infected cells.

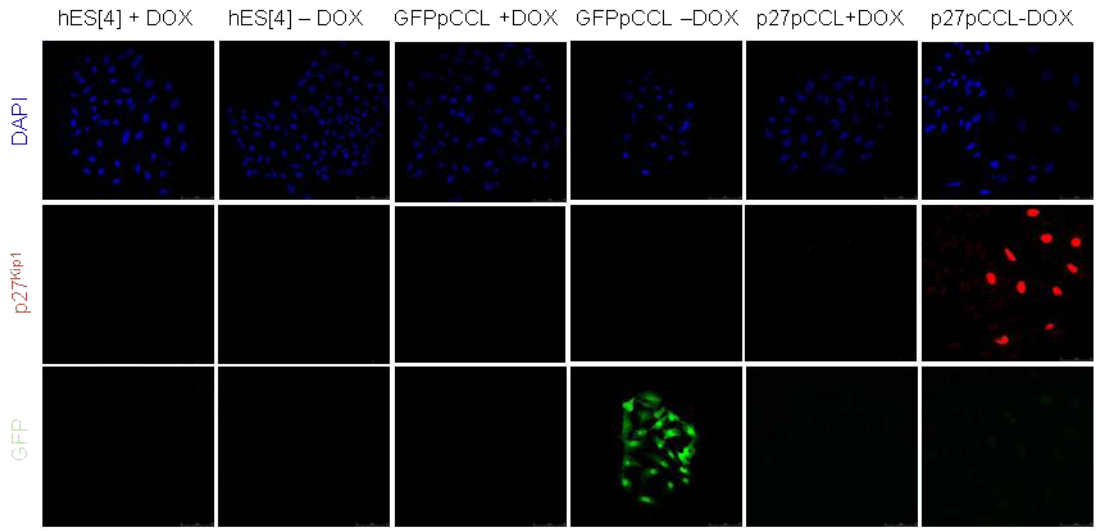

Supplementary Figure 4. Analysis of p27^{Kip1} overexpression in human embryonic stem cells. Immunofluorescence analysis of hESC infected with lentiviral tet- off inducible vector encoding for human p27^{Kip1} shows an increase in the expression levels of p27^{Kip1} protein after culturing the cells 4 days in the absence of doxycycline. hESC infected with lentiviral tet- off inducible vector encoding for GFP shows expression of GFP after culturing the cells for 4 days without doxycycline. Nuclei were counterstained with DAPI. Scale bars 75 μm. DOX, doxycycline.

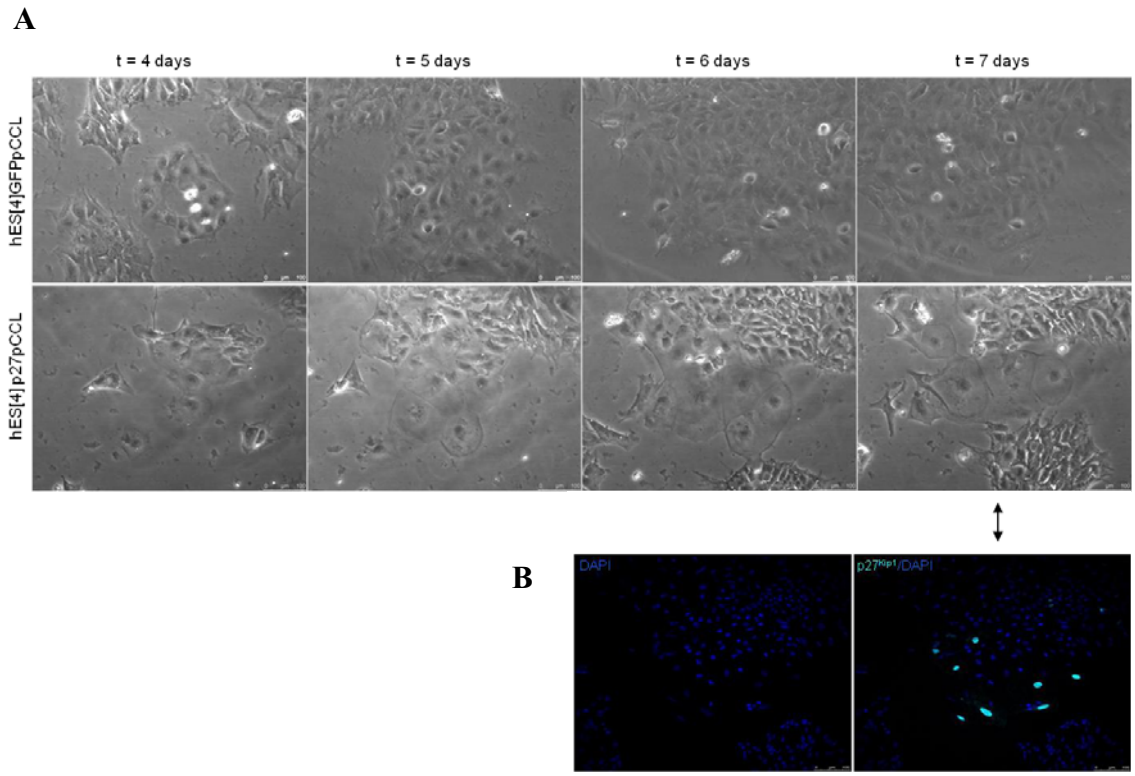

Supplementary Figure 5. Time lapse images of $p27^{Kip1}$ and GFP infected hESC. (**A**) Phase contrast images of hESC infected with $p27^{Kip1}$ and GFP doxycycline tet-off regulated lentiviral constructs cultured in the absence of doxycycline for different days, revealed a clear enlarged and spread morphology in $p27^{Kip1}$ overexpressing hESC in undifferentiated conditions. Scale bars 100 µm. (**B**) Immunofluorescence analysis of these cells revealed they were positive for $p27^{Kip1}$ (cyan). Nuclei were counterstained with DAPI (blue).

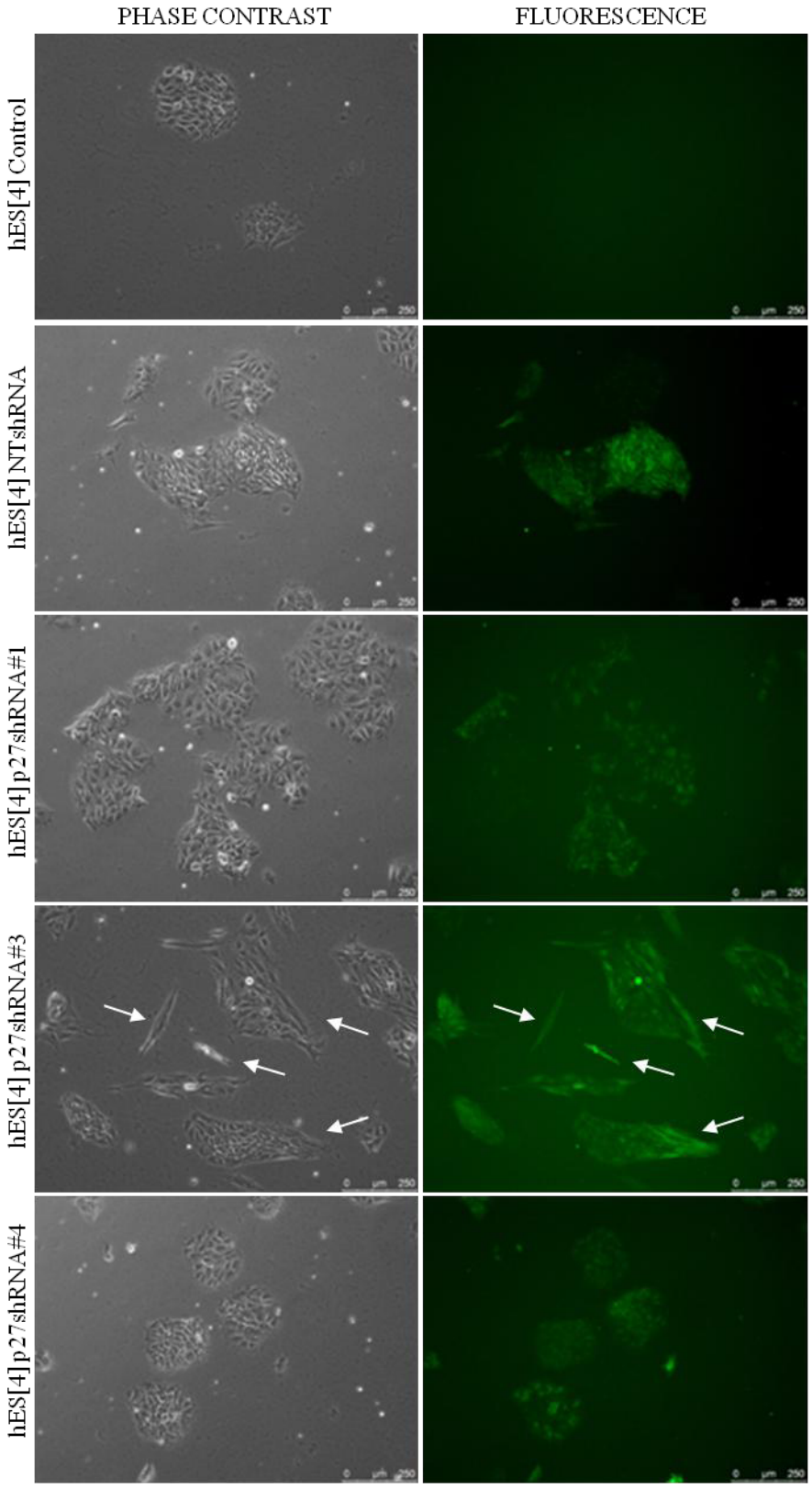

Supplementary Figure 6. Morphology of p27^{Kip1} knockdown in human embryonic stem cells. Phase contrast and fluorescence microscopy images of hESC infected with the 3 different p27 ^{Kip1} shRNA lentiviral GFP vectors clearly revealed an elongated morphology in the cells infected with the construct (p27shRNA#3) that reached more percentage of knockdown.

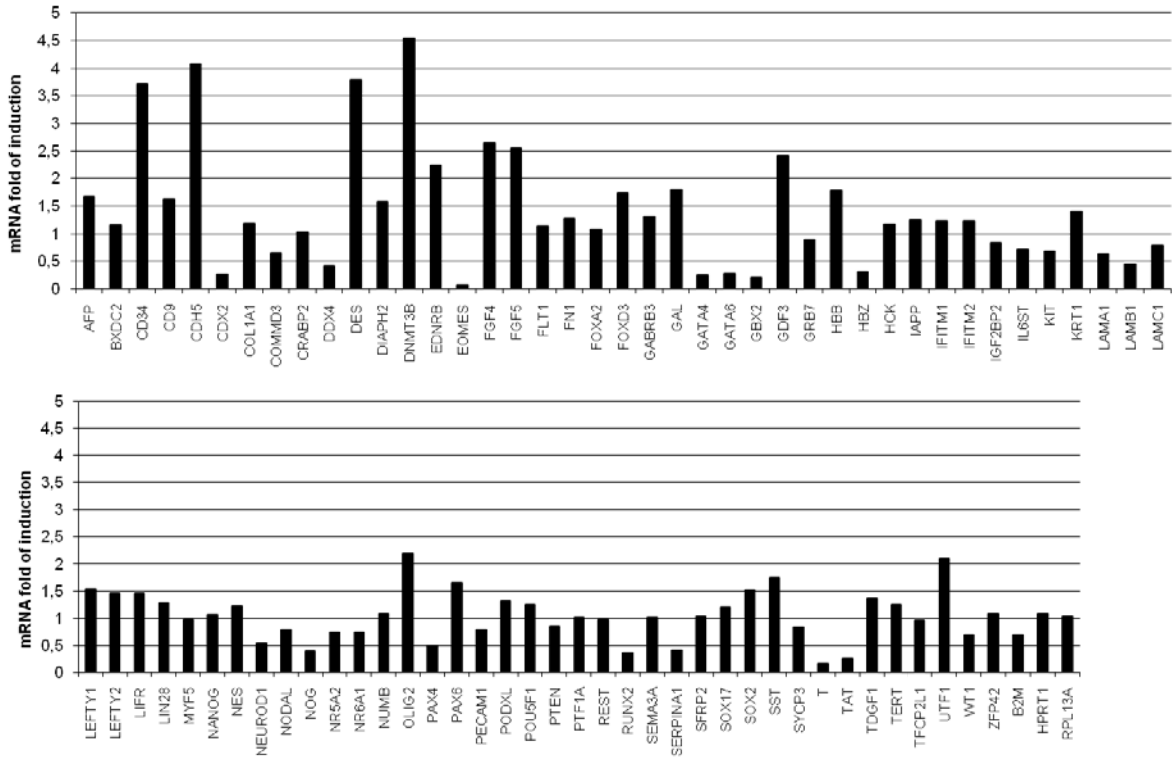

Supplementary Figure 7. Superarray of pluripotency and differentiation genes in large p27^{Kip1} overexpressing human embryonic stem cells *versus* large GFP expressing human embryonic stem cells. Quantitative RT-PCR analysis of 84 genes related to embryonic stem cell pluripotency and differentiation in p27^{Kip1} overexpressing cells. The gene expression levels of large p27^{Kip1} overexpressing hESC are expressed relative to control large GFP expressing cells (=1).

Downloaded from genesdev.cshlp.org on July 8, 2010 - Published by Cold Spring Harbor Laboratory Press

Rem2 GTPase maintains survival of human embryonic stem cells as well as enhancing reprogramming by regulating p53 and cyclin D_1

Michael J. Edel,[1] Cristina Menchon,[1] Sergio Menendez,[1] Antonella Consiglio,[1,5] Angel Raya,[1,2,3,6] and Juan Carlos Izpisua Belmonte[1,3,4,7]

[1]Center of Regenerative Medicine in Barcelona, 08003 Barcelona, Spain; [2]Institució Catalana de Recerca i Estudis Avançats (ICREA), 08010 Barcelona, Spain; [3]Networking Center of Biomedical Research in Bioengineering, Biomaterials and Nanomedicine (CIBER-BBN), 08003 Barcelona, Spain; [4]Gene Expression Laboratory, Salk Institute for Biological Studies, La Jolla, California 92037, USA

Human pluripotent stem cells, such as embryonic stem cells (hESCs) and induced pluripotent stem cells (iPSCs), have the unique abilities of differentiation into any cell type of the organism (pluripotency) and indefinite self-renewal. Here, we show that the Rem2 GTPase, a suppressor of the p53 pathway, is up-regulated in hESCs and, by loss- and gain-of-function studies, that it is a major player in the maintenance of hESC self-renewal and pluripotency. We show that Rem2 mediates the fibroblastic growth factor 2 (FGF2) signaling pathway to maintain proliferation of hESCs. We demonstrate that Rem2 effects are mediated by suppressing the transcriptional activity of p53 and cyclin D_1 to maintain survival of hESCs. Importantly, Rem2 does this by preventing protein degradation during DNA damage. Given that Rem2 maintains hESCs, we also show that it is as efficient as c-Myc by enhancing reprogramming of human somatic cells into iPSCs eightfold. Rem2 does this by accelerating the cell cycle and protecting from apoptosis via its effects on cyclin D_1 expression/localization and suppression of p53 transcription. We show that the effects of Rem2 on cyclin D_1 are independent of p53 function. These results define the cell cycle and apoptosis as a rate-limiting step during the reprogramming phenomena. Our studies highlight the possibility of reprogramming somatic cells by imposing hESC-specific cell cycle features for making safer iPSCs for cell therapy use.

[*Keywords*: Rem2; cyclin D1; p53; reprogramming; self-renewal]

Supplemental material is available at http://www.genesdev.org.

Received October 20, 2009; revised version accepted February 3, 2010.

In recent years, the field of pluripotent human embryonic stem cells (hESCs), including the discovery of induced pluripotent stem cells (iPSCs), has moved rapidly in the direction of finding a safe application for clinical use, such as cell replacement therapy and modeling for drug discovery. However, relatively little has been done to advance our mechanistic insights into the properties of self-renewing hESCs, and even less is known about the mechanisms governing iPSC formation. A better understanding of the molecular mechanisms controlling pluripotency and self-renewal would be essential for the clinical translation of hESCs and iPSCs.

Present addresses: [5]Institute of Biomedicine of the University of Barcelona (IBUB), Baldiri Reixac 15, 08028 Barcelona, Spain; [6]Control of Stem Cell Potency Group, Institute for Bioengineering of Catalonia (IBEC), Baldiri Reixac 15, 08028 Barcelona, Spain.
[7]Corresponding author.
E-MAIL belmonte@salk.edu and izpisua@cmrb.eu; FAX (858) 453-2573.
Article is online at http://www.genesdev.org/cgi/doi/10.1101/gad.1876710.

hESCs were first derived from the pluripotent cells of the blastocyst inner cell mass and can be maintained in vitro indefinitely with the addition of fibroblastic growth factor 2 (FGF2) and other unknown factors secreted from feeder cell layers (Thomson et al. 1998). The pluripotency of hESCs is regulated by a set of unique transcription factors including Oct4, Sox2, and Nanog (Chambers and Smith 2004). It has been shown that a combination of three or four factors of Oct4, Sox2, and KLf4, with or without Myc, can reprogram somatic cells to generate iPSCs (Takahashi and Yamanaka 2006; Takahashi et al. 2007). Analysis of partially reprogrammed iPSCs reveals temporal and separable contributions of the four factors and indicates that ectopic c-Myc acts earlier than the pluripotency regulators (Sridharan et al. 2009). Indeed, overexpression of Myc is known to regulate cyclin D_1, promoting cell cycle progression, although it remains unknown if the cell cycle function of c-Myc plays a separate role to the pluripotency genes (Oct4/sox2/Klf4) in

Downloaded from genesdev.cshlp.org on July 8, 2010 - Published by Cold Spring Harbor Laboratory Press

the reprogramming process (Daksis et al. 1994). Recently, it has been shown that loss of p53 function can enhance the efficiency of reprogramming, suggesting that the cell cycle is a rate-limiting step in the reprogramming process (Zhao et al. 2008; Hong et al. 2009; Kawamura et al. 2009; Li et al. 2009; Utikal et al. 2009). Regulators of p53 transcriptional activity in hESC survival or the reprogramming process remain to be defined.

The cell cycle of mouse ESCs and, to a lesser extent, hESCs has been well described; however, defined functional data are lacking (Savatier et al. 2002; Stead et al. 2002; White and Dalton 2005). The core cell cycle regulatory machinery of ESCs—namely, Cyclins A, E, D, and B, and their kinases CDK2, CDK4, and CDK6—are not regulated in a cyclic fashion, with the exception of cyclin B (Savatier et al. 2002; Stead et al. 2002). Cyclin D_1 is a unique cyclin in having a destruction box that responds to cellular stress leading to its degradation and cell cycle arrest (Agami and Bernards 2000). Of the core machinery, cyclins A/E/CDK2 are regarded as constitutively on in mouse ESCs, driving an almost nonexistent G1 phase into S phase in which 60%–70% of ESCs are present. Consequently, the rate of ESC proliferation is much faster, with an average cycle lasting just 12 h compared with somatic cells (White and Dalton 2005; Becker et al. 2006). A recent study functionally demonstrated that Cyclin A regulates pluripotency, albeit in mouse ESCs, but is redundant in fibroblasts (Kalaszczynska et al. 2009). In addition to these differences, many of the peripheral genes that control cell cycle, such as $p16^{INK4a}$, are thought to be inactive, resulting in a different regulation of cell cycle in mouse ESCs (Faast et al. 2004). Given such differences between somatic and pluripotent cells, little is known about the role of the cell cycle in maintaining hESCs or iPSCs in culture. Much less is known about control of apoptosis in hESCs or iPSCs. Recently, the use of a Rho kinase inhibitor has been shown to protect hESCs from apoptosis, and is now used with in vitro culture of hESCs (Watanabe et al. 2007).

We sought to understand the role of the cell cycle and apoptosis in hESCs and formation of iPSCs by investigating the Rem2 GTPase. Rem2 is a recently identified member of the Rem/Rad/Gem/Kir (RGK) family of Ras-related GTPases, which were first described as overexpressed in muscle cells of patients with type II diabetes mediating signal transduction (Reynet and Kahn 1993; Maguire et al. 1994). Recently, Rem2 was identified from a functional genetic screen to bypass a p53-induced senescence to immortalize somatic cells, demonstrating a fundamental role for cell cycle control (Bierings et al. 2008). Here we hypothesize that the immortalization of cells is a feature very similar to self-renewal of hESCs, suggesting a role for Rem2 in self-renewal.

Results

Rem2 GTPase is expressed in hESCs, and is essential for self-renewal and pluripotency

We found that Rem2 GTPase is highly expressed in six independent hESC lines derived, compared with human fibroblasts. Protein expression was found to be located predominantly in the cell membrane; however, when Rem2 was forced, overexpressed protein expression was observed in the cytoplasm and nucleus as well (Fig. 1A). We next tested the expression levels during hESC differentiation and found that Rem2 is down-regulated under general differentiation conditions (Fig. 1B). This suggests that high levels of Rem2 expression are important for maintaining a self-renewing undifferentiated state in hESCs. Given this, we knocked down Rem2 in hESCs using stably expressed shRNAs and found that loss of Rem2 caused loss of hESC self-renewal, as evidenced in colony-formation assays (CFAs) (Fig. 1C). With gain of Rem2 function in hESCs, the differences compared with controls suggested an overgrowth of colony formation, which was overgrown deliberately to show the effect of the Rem2 RNAi (Fig. 1C). Shorter-term CFAs also suggested an increase in growth with Rem2 overexpression (data not shown). To rule out any effects of the virus titer or effect of the virus on the adherence of hESCs to the culture plates following infection, we tested the virus titer and took time-lapse photos following plating and did not observe any significant effect (Supplemental Figs. 1, 2). The karyotype of hESC lines following infection and passaging was found to be normal (Supplemental Fig. 3).

The main molecular markers of pluripotency—such as Oct4, Sox2, Nanog, and Klf4—in hESCs did not appear to be affected by Rem2 knockdown or overexpression, including c-Myc, even though the hESCs were dying (Fig. 1D). However, molecular markers of differentiation were affected in undifferentiating in vitro conditions (Fig. 1D). To investigate the role of Rem2 in pluripotency further, we overexpressed Rem2 in hESCs and differentiated them under general conditions (20% fetal calf serum [FCS] on gelatin-coated flasks). We were unable to do the same with loss of function of Rem2 due to the rapid loss of hESC survival (Fig. 1E). Forced expression of Rem2 under general differentiating conditions in vitro pushed ESC fate toward an ectodermal lineage at the expense of mesoderm (Fig. 1E), demonstrating that Rem2 plays a critical role in maintaining a true pluripotent state.

In order to further describe the importance of Rem2 in hESC biology, we tested a panel of established chemical inhibitors known to affect signaling pathways essential for maintenance of hESCs in vitro. We found that chemical inhibition of FGF receptors caused down-regulation of *Rem2*, and inhibition of the Rho pathway caused up-regulation of Rem2 (Fig. 2A). However, inhibition of the c-Jun N-terminal kinase (JNK) or transforming growth factor (TGF) pathways had no effect on *Rem2* expression, suggesting a specific pathway of *Rem2* regulation via FGF or Rho pathways (Fig. 2A). To define the role of Rem2 in these pathways further, we overexpressed Rem2 in hESCs and were able to rescue the FGFr inhibitor effects of slowing hESC growth as assessed by CFA (Fig. 2B). We used a dox-regulated lentiviral vector (a kind gift of Professor L. Naldini); the addition of DOX to cell culture reduced expression of *Rem2* in 2 d (data not shown). To determine if FGF2 regulated *Rem2* further, we added FGF2 to the culture medium of human fibroblasts that

Downloaded from genesdev.cshlp.org on July 8, 2010 - Published by Cold Spring Harbor Laboratory Press

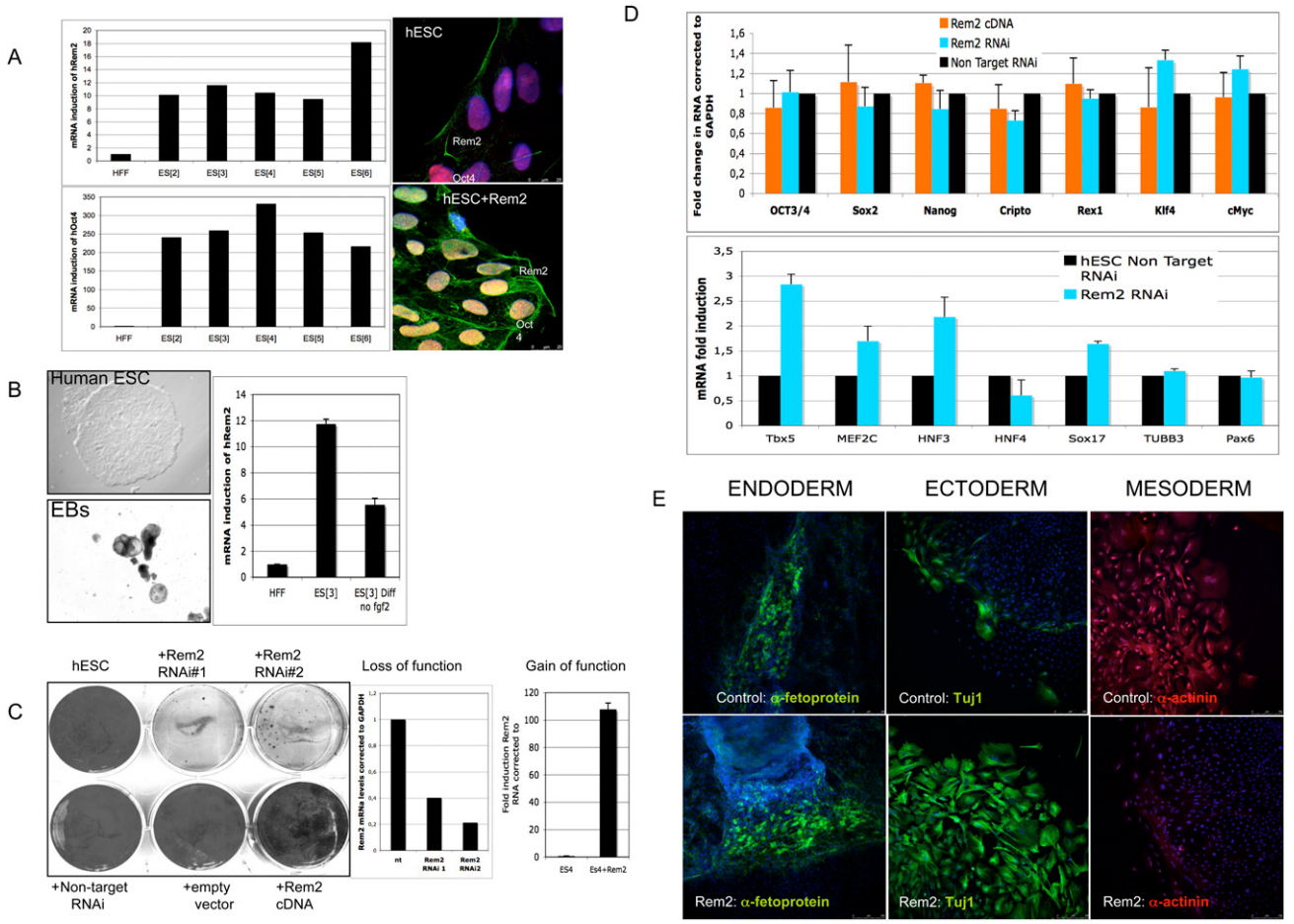

Figure 1. Rem2 GTPase is expressed in hESCs and is essential for self-renewal. (*A*, *left* panels) Real-time PCR of *Rem2* and *Oct4* RNA levels in hESC lines and endogenous Rem2 or ectopic Rem2 localization by immunostaining. (*B*, *left* panels) Photographs of differentiation of hESCs into EBs using general conditions on gelatin (×100). (*Right* panel) Real-time PCR levels of *Rem2* mRNA. (*C*, *left* panel) CFA with gain (cDNA) and loss (RNAi) of function of Rem2 in hESCs in undifferentiating conditions. (*Middle right* panels) Graphs of real-time PCR levels of *Rem2* mRNA levels following treatment with two independent *Rem2* RNAi hairpins or nontarget RNAi controls and *Rem2* cDNA in hESCs. (*D*, *top* graph) Graph of real-time PCR of mRNA levels of pluripotency genes with gain and loss of function of Rem2. (*Bottom* graph) Graph of real-time PCR of mRNA levels of differentiation genes with loss of function of Rem2. (*E*) Photos of immunohistochemical markers of the three germ layers after 20 d with general in vitro differentiation conditions of hESCs, with or without ectopic Rem2.

express relatively low levels of *Rem2* and saw a 10-fold induction of *Rem2* RNA with 25 ng/mL (Fig. 2B). Moreover, we removed FGF2 from hESC culture medium and saw a reduction of *Rem2* levels over 5 d (Fig. 2B), further supporting that FGF2 regulates Rem2 expression. We also chose to investigate the effects of the Rho inhibitor further, as it has been shown previously to control survival of hESCs (Watanabe et al. 2007). Indeed, loss of Rem2 function by RNAi prevented the ability of the Rho inhibitor to promote survival of hESCs, suggesting that Rem2 antagonizes Rho signaling in hESCs to control survival (Fig. 2C). A role of Rem2 family members in antagonizing Rho signaling has been shown before (Olson 2002). Furthermore, the effects of the Rho inhibitor were to increase the cell cycle of hESCs grown on Matrigel rather than protection against apoptosis, which is in contrast to what has been reported previously (Fig. 2C; Watanabe et al. 2007). Together, these data demonstrate that Rem2 is overexpressed in hESCs compared with fibroblasts, controls self-renewal as well as pluripotency of hESCs, and is regulated by and mediates signaling pathways essential for maintaining hESCs in vitro.

Rem2 GTPase cell cycle and apoptosis by regulating cyclin D_1 expression and localization in hESCs

We next sought to understand the mechanisms by which Rem2 regulates hESC self-renewal using the same gain (cDNA) and loss (RNAi) of gene function strategies described above. We first analyzed the effects of Rem2 on the cell cycle of hESCs because we showed previously that Rem2 regulates the cell cycle of endothelial cells via the p53 pathway to immortalize cells (Bierings et al. 2008). Given this, we first examined the effects of Rem2 on $p14^{ARF}$ in hESCs, but did not find any effect (Supplemental Fig. 4). This is not surprising, given that many cell

Downloaded from genesdev.cshlp.org on July 8, 2010 - Published by Cold Spring Harbor Laboratory Press

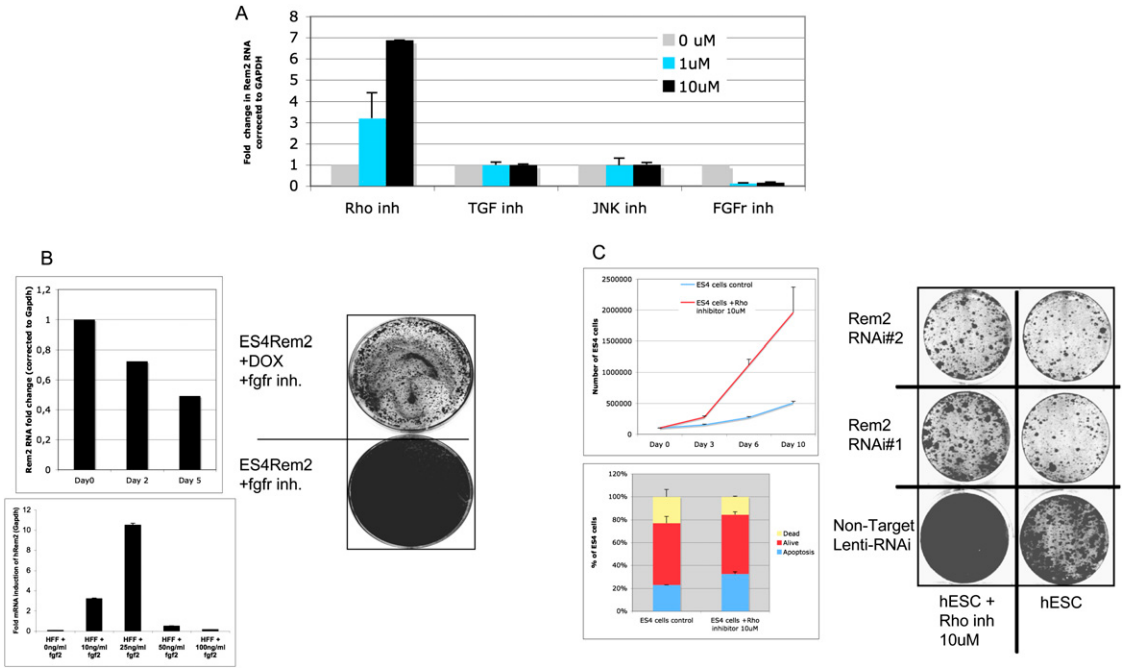

Figure 2. Rem2 is regulated and mediates FGF2/Rho signaling. (*A*) Graph of real-time PCR of *Rem2* RNA levels in hESCs treated with chemical inhibitors of signaling pathways known to be important in hESC survival: FGFr (SU5402), JNK (SP600125), TGF-b-R1 Kinase-Alk5 (Inhibitor II), and Rho-kinase (Y-27632). (*B*, *top left* panel) Graph showing hESCs cultured without FGF2 in the media and *Rem2* expression levels measured by real-time PCR. (*Bottom left* panel) Real-time PCR of *Rem2* expression in human fibroblasts treated with different concentrations of FGF2 growth factor. (*Right* panel) Rescue of effects of FGFr inhibitor (SU5402) by ectopic Rem2. CFA of Rem2-overexpressing hESC growth on Matrigel with and without DOX plus FGFr inhibitor SU5402. (*C*, *top left* panel) Graph of effect of Rho kinase inhibitor on hESC proliferation. (*Bottom left* panel) Graph representing FACs analysis of apoptosis using DilC in hESCs treated with Rho inhibitor. Note that Rho inhibitor does not protect hESCs from apoptosis, but rather increases proliferation of hESCs cultured on Matrigel. (*Right* panel) Rescue of Rho inhibitor effects on proliferation by *Rem2* RNAi in hESCs by CFA.

cycle pathways such as $p16^{INK4a}$–cyclin D are not functional in ESCs (Faast et al. 2004). In ESCs, we found that loss of Rem2 caused a decrease of cells in S phase and an increase in G2/M phase in a short-term experiment (Fig. 3A; Supplemental Figs. 5, 6). With long-term passaging of the cells, we saw that, after 5–7 d, most of the RNAi-treated cells were arrested or dead. Conversely, gain of Rem2 function caused an increase in proliferation of hESCs over time, demonstrating that Rem2 is necessary and sufficient for maintaining the rapid cell cycle of hESCs (Fig. 3A). This supports the initial observation using CFA methodology that overexpression of Rem2 increases growth of hESCs (Fig. 1C).

To understand further how loss of Rem2 could be regulating proliferation, we performed a real-time PCR superarray for all cell cycle- and apoptosis-related genes. We found that there were little significant differences of gene expression on the core machinery of cell cycle kinases with loss of Rem2 in hESCs (Fig. 3A). To our surprise, the only exception was up-regulation of cyclin D_1/CDK6, which normally promotes cell cycle progression—the opposite of what we observed with hESCs treated with Rem2 RNAi (Figs. 1, 3A). We show that the up-regulation of cyclin D_1 with loss of Rem2 is partially cytoplasmic in undifferentiated conditions, and suggests that expression of Rem2 expression regulates cyclin D_1 localization to maintain cell cycle and survival of hESCs (Fig. 3A). We also observed a deregulation of DNA damage-controlling genes such as BRCA2 by Rem2, which we validated by Western blot analysis, suggesting further a role for protection of apoptosis pathways (Fig. 3A). The apparent specific regulation of DNA damage-controlling genes by Rem2 suggests a more specific regulation than that known for c-Myc.

Given that loss of Rem2 caused hESC death in vitro, we assessed apoptosis using three approaches. With all three approaches—FACs analysis for DilC, DAPI staining, and Western blot for cleaved caspase 3—an increase in apoptosis with loss of Rem2 was observed (Fig. 3B; Supplemental Fig. 7). Overexpression of Rem2 did not reveal a significant change by FACs; however, by Western blot analysis, we observed a decrease in cleaved caspase 3 with Rem2 cDNA in hESCs (Fig. 3B), suggesting that they were protected from apoptosis with overexpression of Rem2 even under nonstress conditions. To test if overexpression of Rem2 protected hESCs from apoptosis, we treated the hESCs with mitomycin C, an activator of the DNA damage p53/apoptosis pathway. We observed that the hESCs were protected from apoptosis with eightfold more alive cells in Rem2/mitomycin C-treated hESCs compared with controls (Fig. 3C). To dissect the mechanism further, Western blot analyses showed that MDM2 levels, an indirect readout for the transcriptional activity of p53, were not induced in hESC cells with ectopic Rem2

Downloaded from genesdev.cshlp.org on July 8, 2010 - Published by Cold Spring Harbor Laboratory Press

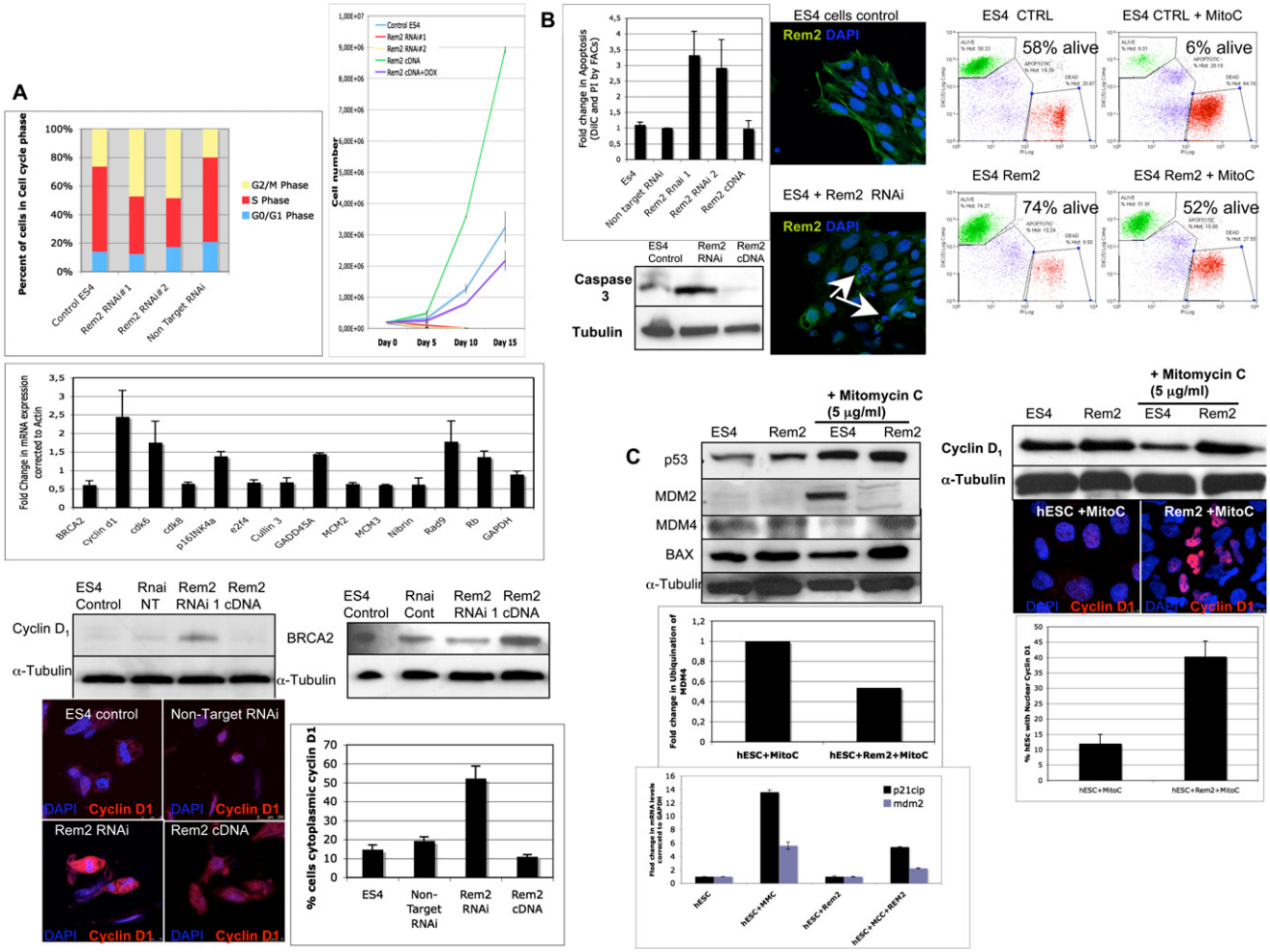

Figure 3. Rem2 GTPase controls cell cycle and apoptosis by regulating cyclin D_1 and p53. (*A*, *top left* panel) Graph of FACs analysis of cell cycle profile of hESCs with loss of function of Rem2. (*Top right* panel) Proliferation curve of hESCs with loss and gain of Rem2 function. (*Middle left* panel) Real-time PCR superarray of cell cycle genes (summary of most significant changes) with loss of Rem2 function compared with nontarget RNAi controls in hESCs. (*Bottom left* panel) Validation of array using Western blot of cyclin D_1 protein levels with loss and gain of Rem2 function in hESCs. (*Bottom right* panel) Validation of array by Western blot of BRCA2 protein levels with loss and gain of Rem2 function in hESCs. (*Far bottom* panel) Photographs of immunostaining with cyclin D_1 with loss and gain of Rem2 function in hESCs. The graph shows quantification of the percent of cells expressing high levels of cyclin D_1 in the cytoplasm. (*B*, *top left* panel) Graph of FACs analysis of apoptosis using DilC and PI staining of hESCs with loss and gain of Rem2 function. (*Top middle* panels) Photographs of DAPI/Rem2 immunostaining of hESCs with no infection control or with *Rem2* RNAi demonstrating apoptotic nuclei with loss of Rem2 function in undifferentiating conditions. (*Top right* panels) FACs histograms of apoptosis (assessed by DilC) with and without Rem2 gain of function in hESCs treated with or without 5 μg/mL Mitomycin C. (*Bottom left* panel) Western blot of activated caspase 3 levels with loss and gain of Rem2 function in hESCs. (*C*, *top left* panel) Western blot analysis of p53 pathway with and without Rem2 gain of function in hESCs treated with or without 5 μg/mL Mitomycin C. (*Top right* panel) Western blot of cyclin D_1 protein localization and level of expression with and without Rem2 gain of function in hESCs treated with or without 5 μg/mL Mitomycin C. The graph indicates quantification of the percent of hESCs with cyclin D_1 protein localization. (*Middle left* panel) Quantification of ubiquitination assay for MDM4 with or without Rem2 and with or without Mitomycin C treatment demonstrates reduced ubiquitination of MDM4 with Rem2 overexpression in hESCs treated with Mitomycin C compared with input controls (MDM4). Note: A photo of the blot can be seen in Supplemental Figure 8. (*Bottom left* panel) Graph of real-time PCR of p53 transcriptional targets *MDM2* and $p21^{CIP}$ mRNA levels treated with 5 μg/mL Mitomycin C and with or without Rem2 in hESCs, clearly showing that Rem2 regulates the transcriptional activity of p53 under stressful conditions.

following mitomycin C treatment as compared with the clear p53 transcriptional activation observed in the control, suggesting a role for Rem2 in suppressing p53 activation (Fig. 3C). Moreover, MDM4 protein, which is known to bind directly to p53 to inhibit its activity and needs to be degraded in response to stress to allow for p53 activation, was not degraded with mitomycin C treatment in Rem2 hESCs, further supporting a role for Rem2 in suppression of the p53 pathway (Fig. 3C). We show that Rem2 prevents the ubiquitination and degradation of MDM4 upon stress, suggesting that Rem2 is a novel and active component in the DNA damage–ubiquitination

Downloaded from genesdev.cshlp.org on July 8, 2010 - Published by Cold Spring Harbor Laboratory Press

signaling pathway in response to stress (Fig. 3C). To further establish and define that Rem2 suppresses p53 transcriptional activity, we demonstrate that ectopic Rem2 blocks the induction of MDM2 and $p21^{CIP}$ mRNA, two transcriptional targets of p53 observed in control cells in the presence of stress, and that a p53 luciferase reporter construct is suppressed following treatment with mitomycin C with ectopic Rem2 (Fig. 3C; Supplemental Fig. 8). Although the fold activation of the p53 luciferase reporter construct by mitomycin C in controls is small, the obvious suppression by Rem2 in the presence of mitomycin C below basal levels (<1) demonstrates clearly the ability of Rem2 to suppress p53 transcriptional activity under stress (Supplemental Fig. 8).

We observed that the FGF2 inhibitor (SU5402) inhibits *Rem2* expression and consequently increases *Cyclin D_1* mRNA expression levels, consistent with the Rem2 RNAi data (Fig. 3A), implicating the FGF2 pathway in regulation of Cyclin D_1 in hESCs (Supplemental Fig. 9). Moreover, Cyclin D_1 has been shown previously to be a target of the DNA damage pathway (Agami and Bernards 2000). Given this, we also examined if Rem2 controlled cyclin D_1 protein level when hESCs were placed under stress with mitomycin treatment. Whereas cyclin D_1 normally is degraded in response to cell stress, which we observed in hESCs by Western blot methodology, we show that ectopic Rem2 protected the degradation of cyclin D_1 under stress conditions in hESCs (Fig. 3C). Moreover we observed that stress of Rem2-overexpressing hESCs causes a nuclear localization of cyclin D_1, which would enable faster proliferation and survival (Fig. 3C). Therefore, under normal culturing conditions of hESCs, Rem2 maintains cyclin D_1 expression and localization, whereas under stressful conditions such as DNA damage, Rem2 maintains cyclin D_1 nuclear to promote hESC survival. Taken together, these data define Rem2 as a critical mediator of proliferation and apoptosis in hESCs by suppressing the ability of p53 to transcriptionally induce its targets, as well as the expression/location of cyclin D_1 to promote survival and therefore self-renewal of hESCs in vitro.

Rem2 GTPase controls efficiency of reprogramming into iPSCs

Recent work has demonstrated that ectopic Rem2 regulates the p53 pathway to immortalize primary cultured cells, indicating a possible role with instating self-renewal-like properties in somatic cells (Bierings et al. 2008). Moreover, it has been shown that loss of p53 can enhance reprogramming, although regulators of p53 remain to be defined (Zhao et al. 2008; Hong et al. 2009; Kawamura et al. 2009; Li et al. 2009; Utikal et al. 2009). Given that we showed that Rem2 maintains self-renewal and pluripotency in hESCs, we next asked if Rem2 could enhance reprogramming of somatic cells into iPSCs. To answer these questions, we reprogrammed somatic cells with three factors alone (Oct4/sox2/Klf4) or with either Myc, cyclin D_1, or Rem2 (Supplemental Fig. 10).

We first observed that endogenous Rem2 levels increase in reprogrammed iPSCs, similar to levels of Rem2 in hESCs (Fig. 4A). We also found that cyclin D_1 protein levels were highly expressed in iPSCs compared with ESCs (Supplemental Fig. 11). Consequently, we investigated if Rem2 could increase the number of pluripotent cells reprogramming with just three factors by staining for the early pluripotency marker SSEA4 (Fig. 4B). The increase in proliferation that we observed was correlated to an eightfold increase in SSEA4-positive cells expressing three factors plus Rem2, which was more than that observed from three factors plus c-Myc (Fig. 4B; Supplemental Fig. 12). Next, we asked if Rem2 expression is essential for the reprogramming process by stably knocking down Rem2 using a lentiviral system to deliver shRNAi in human keratinocytes infected with four factors—Oct4, Sox2, Klf4, and c-Myc. We achieved a 50% knockdown of *Rem2* mRNA in human keratinocytes (data not shown), and observed a 60% loss of alkaline phosphatase (AP)-positive-stained colonies (Fig. 4C). This demonstrates that Rem2 expression is an essential component of the reprogramming phenomena of somatic cells to iPSCs. The trend of an increase in SSEA4-positive cells with three factors plus Rem2 correlates to the AP staining, thus validating AP staining as a reliable tool for assessment of reprogramming efficiency. We observed no effect of Rem2 on $p14^{ARF}$ levels in keratinocytes or mouse embryonic fibroblasts (MEFs), ruling out regulation of this pathway during iPSC formation (Supplemental Fig. 4). Finally, we overexpressed Rem2 with just three factors—Oct4, Sox2, and Klf4—to determine if gain of Rem2 function could enhance reprogramming and replace c-Myc. We saw an eightfold increase in efficiency of reprogramming with three factors plus Rem2, which was as efficient as using four factors (Fig. 4C,D).

To check that we had made iPSCs, we overexpressed Rem2 with three or four factors and picked colonies for characterization. Rem2 iPSC colonies have been named RiPs (Rem2-induced pluripotent stem cells) and were picked between days 12 and 18 for expansion. We observed that RiPs were threefold more likely to survive picking and expansion than other iPSCs, and that four factor plus Rem2 colonies were more prone to differentiation during expansion than three factors plus Rem2 (data not shown). Further characterization of the RiPs revealed protein expression of ESC markers OCT4, Sox2, Nanog, Tra1-81, Tra1-60, SSEA3, and SSEA4 (Fig. 5A, panels a–l). To determine if RiPs were able to differentiate into the three germ layers, a hallmark of true ESC function, embryoid bodies (EBs) were made using general differentiation conditions, and we show that they were rapidly able to form all three germ cell layers, demonstrating that real iPSCs were made (Fig. 5B, panels m–u). Real-time PCR analysis of the endogenous and transgene expression of the four factors demonstrates that endogenous factors are up-regulated in RiPs and the transgenes are almost all totally silenced (Fig. 5C). We found consistently that the Oct4 transgene shows some residual expression in other studies where we made fully characterized human iPSCs (Aasen et al. 2008). These data demonstrate that Rem2 is able to reprogram human somatic cells into iPSCs with

Downloaded from genesdev.cshlp.org on July 8, 2010 - Published by Cold Spring Harbor Laboratory Press

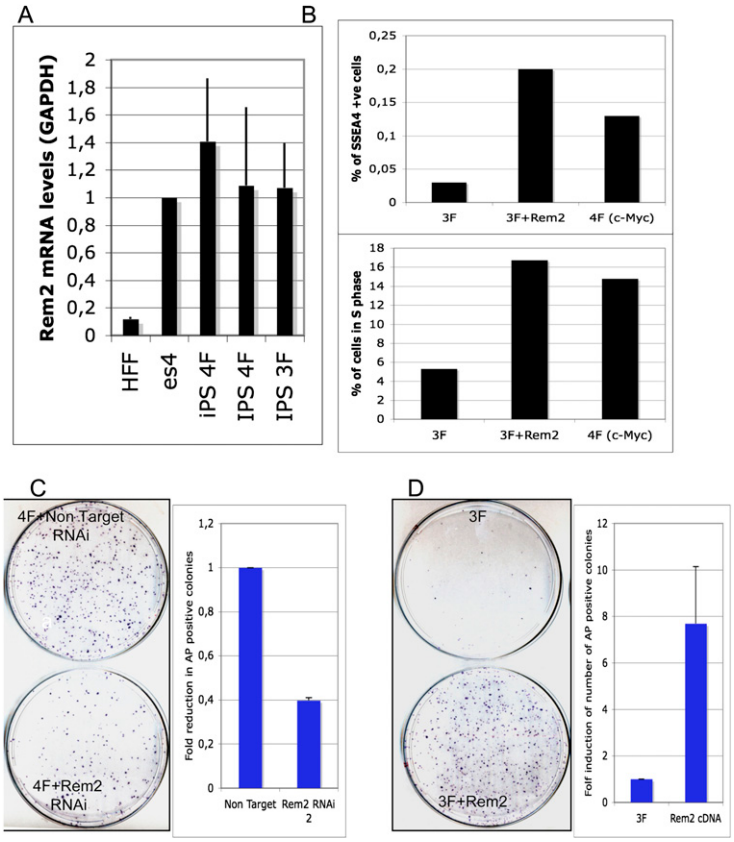

Figure 4. Rem2 GTPase controls efficiency of reprogramming into iPSCs. (*A*) Graph of real-time PCR of *Rem2* levels in fibroblasts compared with iPSCs and hESCs. (*B*, *top* panel) Graph of SSEA4 staining of early reprogramming cells (day 12) as analyzed by FACs. The trend of an increase in SSEA4-positive cells with 3F plus Rem2 correlates to the AP staining, thus validating AP staining as a reliable tool for assessment of reprogramming efficiency. (*Bottom* panel) Graph of FACs analysis of the same cells analyzed for SSEA4 and GFP (a polycistronic Oct4/Sox2/Klf4/Myc or Rem2 GFP-tagged expression vector was used for these reprogramming experiments) for percent of early reprogramming cells in S phase (measured by EDU and DAPI). (*C*, *left* panel) Photo of colony formation assay of reprogramming with four factors with *Rem2* RNAi or nontarget RNAi stained with AP. (*Right* panel) Graph of quantification of number of AP-positive colonies with four factors with *Rem2* RNAi or nontarget RNAi. (*D*, *left* panel) Photo of CFA of reprogramming with three (no c-Myc) factors with *Rem2* cDNA or controls stained with AP. (*Right* panel) Graph of quantification of number of AP-positive colonies with three factors with Rem2 cDNA or controls stained with AP.

just three factors and is as efficient as c-Myc in reprogramming.

Rem2 is dependent on p53 and regulates cyclin D_1 localization to enhance reprogramming

We gleaned from the work in hESCs that Rem2 regulates cyclin D_1 expression and localization. Cyclin D_1 is a main regulator of the cell cycle and is a target of c-Myc, suggesting further that a change in the cell cycle is required to attain pluripotency during reprogramming. We sought then to understand if the regulation/localization of cyclin D_1 is responsible for reprogramming human somatic cells toward iPSCs. We overexpressed wild-type cyclin D_1 and a cytoplasmic-expressed cyclin D_1 mutant in an attempt to mimic the effects of Rem2 on cyclin D_1 regulation and localization in hESCs (Fig. 4A,B). We overexpressed these cyclin D_1 constructs with only three factors—Oct4/sox2/Klf4—as Myc is known to regulate cyclin D_1 (Daksis et al. 1994). We found that overexpression of wild-type cyclin D_1 (a target of c-Myc) increased the efficiency of reprogramming more than threefold, by increasing the number of cells in S phase of the cell cycle ($P = 0.009$), demonstrating that cyclin D_1 up-regulation is sufficient for enhancing reprogramming (Fig. 4C,D). However, the converse was true with overexpression of the cytoplasmic cyclin D_1 mutant, which caused apoptosis, loss of S-phase cycling cells ($P = 0.05$), and loss of reprogramming capacity (Fig. 4C,D). We observed in hESCs that overexpression of Rem2 under stress conditions in vitro protected hESCs to increase survival by maintaining high levels of cyclin D_1 protein (Fig. 2). Because reprogramming is thought to evoke high levels of cellular stress, we measured Cyclin D_1 protein levels and location by immunostaining in early reprogramming colonies (at 12 d) that were made with three factors alone (Oct4/Sox2/Klf4) with either Rem2 or c-Myc as well. We show that cyclin D_1 is mainly cytoplasmic, where it is inactive, when reprogramming with three factors, which may explain why it is so inefficient compared with four factors. However, there is a clear up-regulation of cyclin D_1 protein levels and a shift to the nucleus with three factors plus Rem2, where it is active to phosphorylate Retinoblastoma Protein (pRb) and promote cell cycle progression (Fig. 4E). This was also the case for three factors plus c-Myc, where most early reprogramming cells have nuclear-located cyclin D_1 expression (Fig. 4E). Next, we asked whether localization of cyclin D_1 was independent of p53, and found that, in early developing human iPSCs (RNAi for p53) or mouse iPSCs (using p53-null MEFs), loss of p53 did not affect the localization of cyclin D_1 by Rem2 or c-Myc, suggesting that it is independent of p53 (Fig. 4E). Taken together, the data demonstrate that the Rem2 control of the localization of cyclin D_1 is critical to the reprogramming phenomena.

We next asked if the role of Rem2 was independent of the p53 pathway during reprogramming, and if their effects during reprogramming are via proliferation and/or apoptosis pathways. We infected human keratinocytes

Downloaded from genesdev.cshlp.org on July 8, 2010 - Published by Cold Spring Harbor Laboratory Press

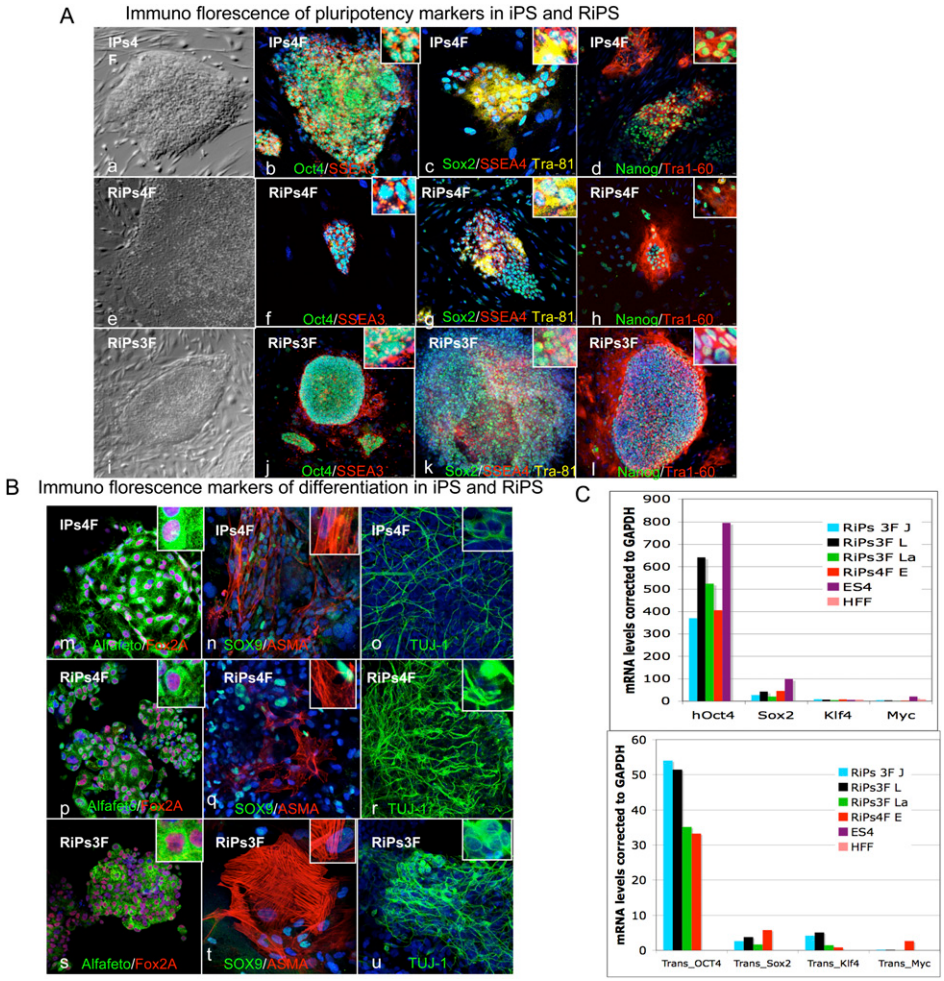

Figure 5. Characterization of RiPs. (*A*, panels *a–l*) Phase contrast and immunostaining of iPSCs (one clone) and RiPs (two clones) for pluripotency markers Oct4, SSEA3, Sox2, SSEA4, Tra-81, Nanog, and Tra-60. (*B*, panels *m–u*) Immunostaining of differentiation markers following 3 wk of general differentiation of iPSC and RiP clones (gelatin with 20% FCS medium) for Alfafeto protein, Fox2A, Sox9, Alfa smooth muscle (ASMA), and TUJ1. (*C*) Real-time PCR of transgenes and pluripotency marker expression in RiPs compared with hESCs and somatic cells.

with Rem2, with and without a p53 dominant-negative construct (p53dd), a p53 RNAi construct we published previously (Kawamura et al. 2009), and expression was checked by Western blot analysis (Supplemental Fig. 12). Infected cells were split into CFAs to assess efficiency (on feeder layers) or into slide flasks for assessment of apoptosis (tunnel) and proliferation (phospho-H3) of early reprogramming colonies (day 12) by selecting only SSEA3-positive colonies (Supplemental Fig. 11). We found that loss of p53 with three factors increased efficiency of reprogramming eightfold compared with three factors alone, and this was due to reducing apoptosis and increasing the number of proliferating cells, suggesting that both the apoptotic and cell cycle functions of p53 are critical for the reprogramming process (Fig. 4F,G). In the absence of an active p53, overexpression of Rem2 enhanced reprogramming to ~10-fold; similar to three factors with p53dd alone, demonstrating that Rem2 cannot enhance reprogramming in the absence of an active p53 (Fig. 4F,G). Overexpression of Rem2 or cyclin D_1 caused a large increase in the number of SSEA3-positive proliferating cells in early reprogramming colonies, demonstrating that control of cell cycle during reprogramming is essential for the process (Fig. 4H). Taken together, these data demonstrate that a cell cycle element is essential for the early reprogramming process, and that Rem2 increases efficiency of early reprogramming events by accelerating proliferation and protection of cells via its regulation of cyclin D_1 localization and suppression of p53 (Fig. 4).

Discussion

In order to develop further our understanding of human pluripotent ESCs, we investigated the role of Rem2 GTPase because it is known to regulate p53 to immortalize somatic cells, a feature similar to self-renewal of both hESCs and hiPSCs. This study identified Rem2 GTPase as a gene highly expressed in hESCs and iPSCs compared with fibroblasts to promote survival and therefore

Downloaded from genesdev.cshlp.org on July 8, 2010 - Published by Cold Spring Harbor Laboratory Press

self-renewal of hESCs in vitro. Furthermore, we make the novel discovery that Rem2 regulates the ability of hESCs to differentiate into all three germ layers, suggesting a role in pluripotency. By manipulating the expressed levels of Rem2, we can force hESCs toward an ectodermal lineage under general differentiating conditions. Rem2 has been identified in neuronal developments such as control neuron synapse formation (Paradis et al. 2007) and has enriched expression in the central extended amygdala (Becker et al. 2008). Recently, two microarray-based experiments identified Rem2 as overexpressed in the formation of two different adult stem cells: those making pancreas, and those making dopamine neurons (Lee et al. 2006; Treff et al. 2006). Further work to define the role of Rem2 and its cell cycle targets toward a specific cell fate is warranted.

The control of apoptosis and cell cycle are two essential functions for ESCs to maintain their self-renewal capacity. In hESCs we show that Rem2 regulates cyclin D_1 expression and p53 transcriptional activation controlling cell cycle and apoptosis of hESCs. The regulation of DNA damage genes such as p53 and the cell cycle kinase cyclin D_1 suggests that Rem2 is an important regulator of apoptosis and maintaining an ESC-like cell cycle profile. The ability of Rem2 to regulate the localization of cyclin D_1 and to suppress p53 transcriptional activity during stress underscores a pivotal functional role for Rem2 to maintain survival and a rapid rate of cell cycle, and therefore self-renewal of hESCs. Indeed, assessment of SSEA4-, SSEA3-, and TRA1-60-positive cells with three factors (Oct4/Sox2/Klf4) plus Rem2 during reprogramming reveals that Rem2 can increase the number of pluripotent cells during the early reprogramming process (Fig. 6H). By using either p53RNAi or p53dd cells for reprogramming, and FACs sorting for SSEA3- or TRA1-60-positive cells, Rem2 cannot enhance reprogramming. This suggests that Rem2's main mechanism of action is via the p53 pathway (Fig. 6F,H). We also showed that overexpression of cyclin D_1, which is also a target of c-Myc, increases the number of SSEA4-positive cells in S phase (Fig. 4B), demonstrating for the first time that the cell cycle functions of c-Myc plays an important role in the efficiency of reprogramming. Taken together, the data clearly define that the core machinery of the cell cycle—namely, cyclin D_1—is a rate-determining step in the reprogramming phenomena. We propose that imposing a hESC-like cell cycle profile in somatic cells with Rem2 or cyclin D_1, in addition to the pluripotency module (Oct4/Sox2/Klf4), may be a safer and more efficient way to make iPSCs. It remains to be defined if other cell cycle genes overlap with pluripotency or not, which future gain- and loss-of-function studies of other cell cycle genes would reveal.

When we stressed hESCs with a DNA-damaging agent, we observed that cyclin D_1 is degraded, as expected. With overexpression of Rem2 in the presence of stress, cyclin D_1 is not degraded in hESCs and moves nuclear, relative to hESCs without Rem2 but equally stressed, suggesting that localization of cyclin D_1 is critical for maintaining self-renewal and pluripotency. Indeed, overexpression of Rem2 during the early reprogramming stages up-regulates and maintains cyclin D_1 exclusively nuclear, further supporting that cyclin D_1 localization is an important rate-determining step during acquisition of pluripotency (Fig. 6E). Moreover, overexpression of a mutant cyclin D_1 that is cytoplasmically expressed (to mimic the effects of loss of Rem2 on cyclin D_1 in hESCs) caused an increase in apoptosis of somatic cells and loss of reprogramming efficiency, consistent with the idea that maintenance of proper cyclin D_1 location in human pluripotent cells is essential for self-renewal and pluripotency. This critical function of Rem2 to regulate Cyclin D_1 under stressful conditions (which reprogramming presents to a cell), and to maintain it nuclear during early reprogramming, increases the efficiency of reprogramming by accelerating the cell cycle. The phosphorylation of Rb has been described as a ground state of the hESC cell cycle profile, suggesting that Rem2 can instate a hESC cell cycle profile during reprogramming. The novel discovery that the localization and overexpression of cyclin D_1 controls reprogramming defines a critical role for the cell cycle during the reprogramming process. How Rem2 controls cyclin D_1 localization during reprogramming to achieve pluripotency remains to be defined, although modification of the ubiquitination and protein transport pathways seem likely pathways involved. Rem2 GTPase is a unique GTPase in having an extended N-terminal protein tail with many signal transduction-binding sites, and we did not rule out the GTPase activity of Rem2 in regulating cell survival decisions.

Indeed, the process of reprogramming is thought to evoke huge cellular stresses caused by the introduction of the four factors and the viral or transfection procedures themselves. It follows then that the introduction of genes such as Rem2 in somatic cells, which can control the effects of cellular stresses, increases survival and therefore the efficiency of reprogramming. Here we show that Rem2 GTPase can enhance the reprogramming efficiency of somatic cells into iPSCs eightfold (Fig. 4). This supports the hypothesis that loss of p53 signaling is an important step in making reprogramming more efficient, and suggests that signaling proteins upstream of p53 are important contributors to reprogramming by monitoring cellular stress levels.

In conclusion, the identification of Rem2 function in hESCs and reprogramming will help with understanding the molecular mechanisms of survival and proliferation that are essential for self-renewal and pluripotency of hESCs. Our studies highlight the possibility of reprogramming somatic cells by imposing hESC-specific cell cycle features—rather than relying on oncogenes such as c-Myc—for making safer iPSCs for cell therapy use.

Materials and methods

Culture of hESCs

hESCs were derived and fully characterized at the CMR[B] (Raya et al. 2008). They were maintained on either human feeder layers or on Matrigel-coated plates with HUES medium, consisting of

Downloaded from genesdev.cshlp.org on July 8, 2010 - Published by Cold Spring Harbor Laboratory Press

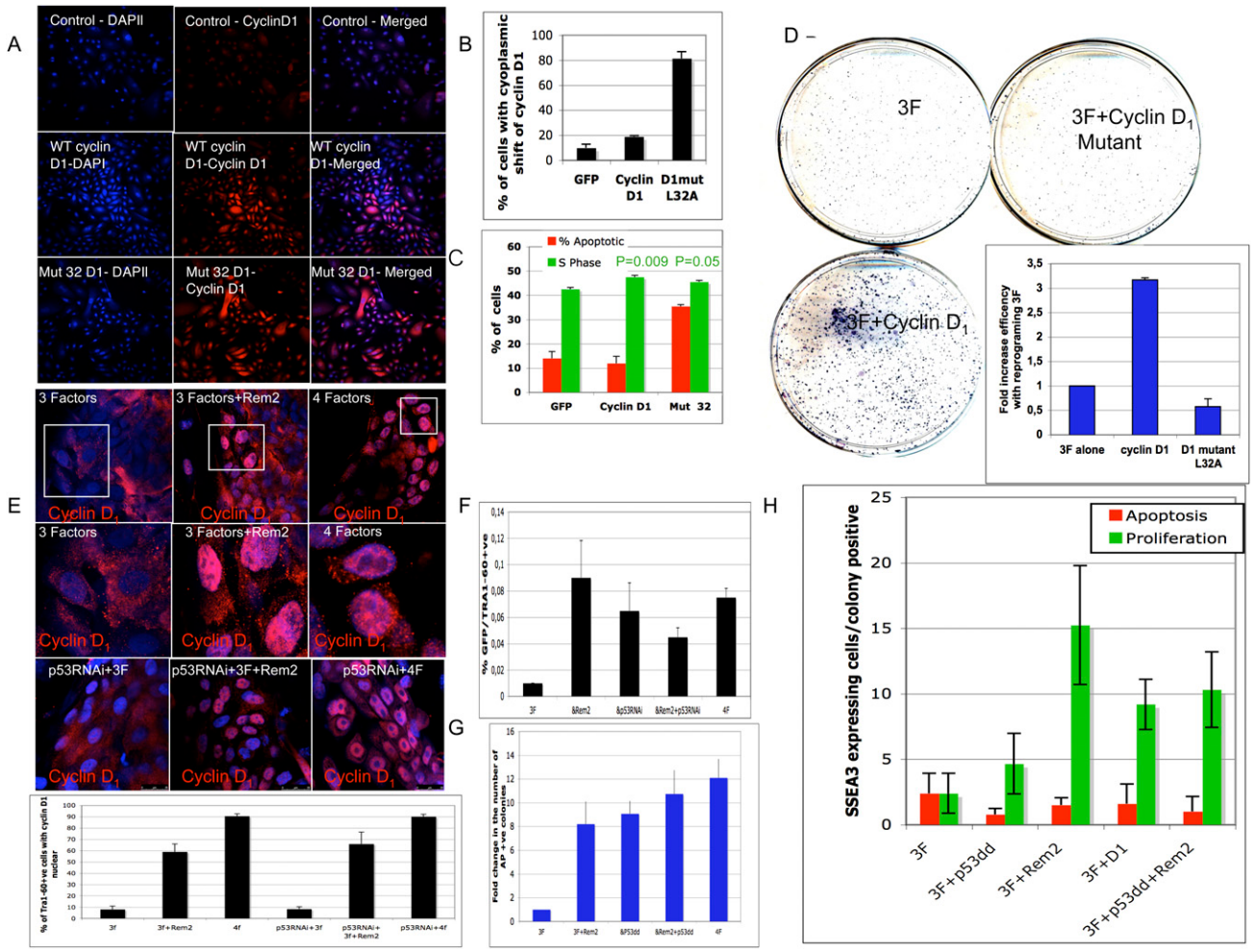

Figure 6. Rem2 is dependent on p53 and regulates cyclin D_1 localization to enhance reprogramming. (*A*) Photographs of immunostaining with cyclin D_1 in somatic cells before reprogramming, overexpressing GFP (control), cyclin D_1, and cyclin D_1 mutant (L32A). Magnification, 200× . (*B*) Graph of the quantification of the number of somatic cells before reprogramming expressing cyclin D_1 in the cytoplasm, demonstrating that the expression of the mutant cyclin D_1 is more cytoplasmic. (*C*) Graph summarizing FACs analysis of the percent of cells in S phase or apoptotic cells by DilC plus PI staining for overexpressing GFP (control), cyclin D_1, and cyclin D_1 mutant (L32A) in somatic cells before reprogramming, demonstrating that the mutant causes apoptosis and reduced proliferation. *P*-values given by a Student's *t*-test. (*D*) Photo of CFA of reprogramming colonies at day 21with three factors, three factors plus cyclin D_1, or three factors plus cyclin D_1 mutant (L32A) stained with AP. (*Insert*) The number of colonies was quantified by image analysis software and is presented as a graph, demonstrating loss of reprogramming efficiency with expression of mutant cyclin D_1. (*E*) Photos of localization of cyclin D_1 during early reprogramming (at day 12), demonstrating a nuclear localization with ectopic Rem2 plus three factors (Oct4/Sox2/Klf4) and three factors plus c-Myc (four factors). P53 RNAi-treated cells were also reprogrammed, and demonstrate nuclear localization of cyclin D_1. (*E*) Graph of quantification of percent of cells with nuclear-located cyclin D_1. (*F*) Assessment of Tra1-60-positive cells in early reprogramming colonies with p53 RNAi-treated cells, Rem2 and c-Myc (4F) assessed by FACs analysis. (*G*) Assessment of AP-positive colonies in early reprogramming colonies with p53dd-treated cells. The number of colonies was quantified by image analysis software and is presented as a graph. (*H*) Quantification of proliferation and apoptosis in early developing reprogramming colonies with three factors (Oct4/Sox2/Klf4) plus Rem2 or cyclin D_1 or p53dd at day 12 by immunostaining for tunnel (red bars), phospho-H3 (green bars), and SSEA3 (to assess specific reprogramming colonies) for different gene treatments as described in the figure.

KO-DMEM (Invitrogen) supplemented with 10% KO-Serum Replacement (Invitrogen), 0.5% human albumin (Grifols), 2 mM Glutamax (Invitrogen), 50 μM 2-mercaptoethanol (Invitrogen), nonessential amino acids (Cambrex), and 10 ng/mL bFGF (Peprotech). Cultures were maintained at 37°C, 5% CO_2, with media changes every other day. hESCs were routinely tested for normal karyotype. For hESC lines adapted to Matrigel-coated plates, HUES-conditioned medium from irradiated MEFs was used instead. MEFs were cultured using 10% FCS with Dulbecco's modified Eagle's medium (DMEM).

Constructs and lentivirus production

Rem2 cDNA made from RNA extracted from hESCs was cloned into the pCCL TET-off-inducible lenti-vector. *Rem2* RNAi constructs and nontarget RNAi controls were purchased from

Downloaded from genesdev.cshlp.org on July 8, 2010 - Published by Cold Spring Harbor Laboratory Press

RZPD and were cloned into the pLKO.1puro lenti-vector (Sigma-Aldrich). All lentiviruses were made using a third-generation approach. Briefly, *MDL* (6.5 μg), *VSV* (4 μg), *REV* (2.5 μg), and lentiviral constructs (10 μg) were transfected into 293T cells using Lipofectamine2000 overnight. 293T cells (American Type Culture Collection no. CRL-12103) were used for the production of lentiviruses. These cell lines were grown in DMEM (GIBCO) supplemented with 10% fetal bovine serum (FBS; Biowhitaker). The next day, medium was refreshed, and the following day virus was harvested, tested for titer using an HIV-1 p24 ELISA kit (Perkin Elmer), and stored at −80°C in 1-mL aliquots. hESCs (200,000) were infected in suspension with 1 mL of viral supernatant for 1 h at 37°C and then plated in six-well Matrigel-coated plates with a further 1 mL of conditioned media. The next day, media was changed, cells were allowed to recover, and experiments were performed. For proliferation curves, equal cells were plated and then counted every 5 d.

Constructs and retroviral production

Cyclin D_1 pBabe puro cDNA constructs were a kind gift from Reuven Agami (Agami and Bernards 2000). cDNAs for *Rem2*, *Oct4*, and *Sox2* were amplified from ES[4] total RNA by RT–PCR. *Klf-4* was amplified from IMAGE clone 5111134. *c-Myc* T58A mutant cDNA was amplified from DNA kindly provided by Dr. Luciano DiCroce. The amplified cDNAs were cloned into the EcoRI/ClaI sites of a modified pMSCVpuro vector, which allows the expression of N-terminal Flag-tagged proteins. The single polycistronic vector containing three factors (Oct4, Sox2, and Klf4) or four factors plus a GFP tag has been described elsewhere (Gonzalez et al. 2009). Retroviruses for the four factors were produced independently after transfecting the cell line Phoenix Amphotropic using Fugene 6 reagent (Roche) according to the manufacturer's directions. After 24 h, the DMEM was replaced, cells were incubated at 32°C, and the viral supernatant was harvested after 24 h and 48 h.

Generation of iPSCs

The generation of iPSCs using human primary keratinocytes has been described before (Aasen et al. 2008). Briefly, cells were isolated from juvenile foreskins (2–16 yr old) using dispase to remove the dermis from the epidermis followed by trypsinization and culture in serum-free low-calcium medium (Epilife; Invitrogen) at 37°C, 5% CO_2, 5% O_2, and used between two and four passages. For reprogramming experiments, ~50,000 or 100,000 cells were seeded per well of a six-well plate and infected with a virus from a polycistronic vector (Oct4, Sox2, and Klf4 plus Rem2) or with a 1:1:1:1 mix of retroviral supernatants of Flag-tagged Rem2, OCT4, SOX2, KLF4, and c-MYCT58A in the presence of 1 mg/mL polybrene. Infection consisted of a 45-min spinfection at 750*g*, washed with PBS and with keratinocyte medium replaced. Two rounds of infections on consecutive days were performed. Two days after beginning the last round of infection, cells were trypsinized and seeded onto feeder layers of irradiated MEFs in the same culture medium. The medium was changed upon plating to hESC medium, consisting of KO-DMEM (Invitrogen) supplemented with 10% KO-Serum Replacement (Invitrogen), 0.5% human albumin (Grifols), 2 mM Glutamax (Invitrogen), 50 μM 2-mercaptoethanol (Invitrogen), nonessential amino acids (Cambrex), and 10 ng/mL bFGF (Peprotech). Cultures were maintained at 37°C, 5% CO_2, with media changes every other day. IPSCs were picked, expanded, and characterized. For CFA experiments, plates were fixed with 50% methanol/10% acetic acid/40% water for 5 min, stained with 0.1% Coomassie blue for 5 min, and washed with water, and an electronically scanned photo was produced.

Immunofluorescence and AP analysis

Cells were grown on plastic coverslide chambers and fixed with 4% paraformaldehyde (PFA). The antibodies used have been described before (Aasen et al. 2008). Rem2 antibody has been described before (Bierings et al. 2008). Cyclin D_1 was used at 1:100 (Santa Cruz Biotechnologies). The secondary antibodies used were all the Alexa Fluor series from Invitrogen (all 1:500). Images were taken using a Leica SP5 confocal microscope. Direct AP activity was analyzed using an Alkaline Phosphatase Blue/Red Membrane Substrate solution kit according to the manufacturer's guidelines (Sigma).

Chemical inhibitors

Inhibitors were used at the concentration and time described in Figure 2 or with vehicle alone. FGFr (SU5402), JNK (SP600125), TGF-b-R1 Kinase-Alk5 (Inhibitor II), and Rho-kinase (Y-27632) were all purchased from Calbiochem.

In vitro differentiation

Differentiation toward endoderm, mesoderm, and neuroectoderm was carried out by plating EBs on gelatin and DMEM medium with 20% FCS changed every second day for 2–3 wk. Cells were then stained for appropriate markers as described in the figures.

Flow cytometry analyses

All analyses were performed on a MoFlo cell sorter (DakoCytomation) running Summit software. For measuring apoptosis and proliferation, we used the commercial kits from Invitrogen—the "MitoProbe DilC1(5) Assay kit" and the "Click-iT EdU AlexaFluor647 Flow Cytometry Assay kit," respectively—following the manufacturer's instructions. For the proliferation assay using the click-IT kit, instead of using the supplied DNA dyes, we used a homemade DNA DAPI-staining solution (0.1 M Tris Base at pH 7.4, 0.9% or 150 mM NaCl, 1 mM $CaCl_2$, 0.5 mM $MgCl_2$, 0.2% BSA, 0.1% Nonidet NP-40, 10 mg/mL DAPI) at 0.5 mL per test (2 h at room temperature or overnight at 4°C).

Western blot

Western blot analyses were performed as described previously, using extracts of cells collected by centrifugation, washed twice in PBS, lysed in 1× lysis buffer (50 nM Tris-HCl, 70 mM 2-mercaptoethanol, 2% sodium dodecylsulfate [SDS]), then boiled for 5 min and subjected to 12% polyacrylamide SDS gel electrophoresis. After electrophoresis, proteins were transferred to a nitrocellulose membrane using a submerged transfer apparatus (Bio-Rad) filled with 25 mM Tris Base, 200 mM glycine, and 20% methanol. After blocking with 5% nonfat dried milk in TBS-T (50 mM Tris-HCl at pH 8.0, 150 mM NaCl, 0.1% Tween 20), the membrane was incubated with the primary antibodies diluted in TBS-T and washed extensively. Primary antibodies were anti-Flag (Sigma), BRCA-1 (Santa Cruz Biotechnologies), p53 (Santa Cruz Biotechnologies, D01), MDM2 (4B2) (Chen et al. 1993), MDM4 (Affinity, bioreagents PA1-24307), Bax (Santa Cruz Biotechnologies), tubulin, and cleaved Caspase 3 (Cell Signaling, 5A1). The membrane was washed three times with TBS-T and then incubated with the appropriate horseradish peroxidase-linked secondary antibody (Amersham). The detection was

Downloaded from genesdev.cshlp.org on July 8, 2010 - Published by Cold Spring Harbor Laboratory Press

performed with the Western Breeze Immunodetection kit (Invitrogen). The concentration of protein was measured by the Bradford assay. For the ubiquitination assay for MDM4, we used a previously described protocol (Xirodimas et al. 2001). Briefly, hESCs were infected with ubiquitin lentivirus, and stably expressed Ub-hESCs were then infected again with Rem2. Cells were then treated with Mitomycin C, and the ubiquitination assay for MDM4 was performed.

Real-time PCR

Total mRNA was isolated using Trizol and 1 μg was used to synthesize cDNA using the Invitrogen Cloned AMV First-Strand cDNA synthesis kit. One microliter to 2 μL of the reaction were used to quantify gene expression by quantitative PCR for transgenes, endogenous pluripotent genes, as described previously (Aasen et al. 2008). For analysis of cell cycle and apoptosis-related genes, we used a real-time PCR superarray for human cell cycle genes. For *Rem2*, *MDM2*, and *cyclin D_1*, we used the following primers: *hRem2*: FOR, AGATGCCACGCTACTAAA GAAG, and REV, GCCCAAGGAGTCAGACGAGCCA; *hCyclin D_1*: FOR, GATCAAGTGTGACCCGGACT, and REV, TCCTC CTCCTCTTCCTCCTC; *hMDM2*: FOR, TGTTGGTGCACAA AAAGACA, and REV, CACGCCAAACAAATCTCCTA; *p21*: FOR, ACCTGTCACTGTCTTGTACCCTTGT, and REV, GTTT GGAGTGGTAGAAATCTGTCATG.

Real-time PCR superarrays for cell cycle genes were purchased, and the manufacturer's instructions were followed (SA Biosciences).

Quantification using computer-aided analysis software

Analysis of the number of colonies in CFAs was done using computer-assisted video analysis using Metamorph software. Briefly, a region of interest was set in a photograph of the CFA, a threshold for color was set (blue), and the number of colonies was exported directly to Excel for analysis. All data were analyzed using Excel spreadsheet software for mean, standard deviation, and Student's *t*-test.

Acknowledgments

We are indebted to José Miguel Andrés Vaquero for assistance with flow cytometry; Meritxell Carrió for expert assistance with cell culture techniques; Esther Melo, Lola Mulero Pérez, and Mercé Gaudes Martí for bioimaging assistance; and Reuven Agami for the cyclin D_1 constructs. Cristina Menchon is partly supported by a predoctoral grant from MICINN. This work was supported by grants from the Fondo de Investigaciones Sanitarias, MICINN, RETICS, CIBER, Fundacion Cellex, and The G. Harold and Leila Y. Mathers Charitable Foundation.

References

Aasen T, Raya A, Barrero MJ, Garreta E, Consiglio A, Gonzalez F, Vassena R, Bilic J, Pekarik V, Tiscornia G, et al. 2008. Efficient and rapid generation of induced pluripotent stem cells from human keratinocytes. *Nat Biotechnol* **26:** 1276–1284.

Agami R, Bernards R. 2000. Distinct initiation and maintenance mechanisms cooperate to induce G1 cell cycle arrest in response to DNA damage. *Cell* **102:** 55–66.

Becker KA, Ghule PN, Therrien JA, Lian JB, Stein JL, van Wijnen AJ, Stein GS. 2006. Self-renewal of human embryonic stem cells is supported by a shortened G1 cell cycle phase. *J Cell Physiol* **209:** 883–893.

Becker JA, Befort K, Blad C, Filliol D, Ghate A, Dembele D, Thibault C, Koch M, Muller J, Lardenois A, et al. 2008. Transcriptome analysis identifies genes with enriched expression in the mouse central extended amygdala. *Neuroscience* **156:** 950–965.

Bierings R, Beato M, Edel MJ. 2008. An endothelial cell genetic screen identifies the GTPase Rem2 as a suppressor of $p19^{ARF}$ expression that promotes endothelial cell proliferation and angiogenesis. *J Biol Chem* **283:** 4408–4416.

Chambers I, Smith A. 2004. Self-renewal of teratocarcinoma and embryonic stem cells. *Oncogene* **23:** 7150–7160.

Chen J, Marechal V, Levine AJ. 1993. Mapping of the p53 and mdm-2 interaction domains. *Mol Cell Biol* **13:** 4107–4114.

Daksis JI, Lu RY, Facchini LM, Marhin WW, Penn LJ. 1994. Myc induces cyclin D1 expression in the absence of de novo protein synthesis and links mitogen-stimulated signal transduction to the cell cycle. *Oncogene* **9:** 3635–3645.

Faast R, White J, Cartwright P, Crocker L, Sarcevic B, Dalton S. 2004. Cdk6-cyclin D3 activity in murine ES cells is resistant to inhibition by p16(INK4a). *Oncogene* **23:** 491–502.

Gonzalez F, Barragan Monasterio M, Tiscornia G, Montserrat Pulido N, Vassena R, Batlle Morera L, Rodriguez Piza I, Izpisua Belmonte JC. 2009. Generation of mouse-induced pluripotent stem cells by transient expression of a single nonviral polycistronic vector. *Proc Natl Acad Sci* **106:** 8918–8922.

Hong H, Takahashi K, Ichisaka T, Aoi T, Kanagawa O, Nakagawa M, Okita K, Yamanaka S. 2009. Suppression of induced pluripotent stem cell generation by the p53–p21 pathway. *Nature* **460:** 1132–1135.

Kalaszczynska I, Geng Y, Iino T, Mizuno S, Choi Y, Kondratiuk I, Silver DP, Wolgemuth DJ, Akashi K, Sicinski P. 2009. Cyclin A is redundant in fibroblasts but essential in hematopoietic and embryonic stem cells. *Cell* **138:** 352–365.

Kawamura T, Suzuki J, Wang YV, Menendez S, Morera LB, Raya A, Wahl GM, Belmonte JC. 2009. Linking the p53 tumour suppressor pathway to somatic cell reprogramming. *Nature* **460:** 1140–1144.

Lee MS, Jun DH, Hwang CI, Park SS, Kang JJ, Park HS, Kim J, Kim JH, Seo JS, Park WY. 2006. Selection of neural differentiation-specific genes by comparing profiles of random differentiation. *Stem Cells* **24:** 1946–1955.

Li H, Collado M, Villasante A, Strati K, Ortega S, Canamero M, Blasco MA, Serrano M. 2009. The Ink4/Arf locus is a barrier for iPS cell reprogramming. *Nature* **460:** 1136–1139.

Maguire J, Santoro T, Jensen P, Siebenlist U, Yewdell J, Kelly K. 1994. Gem: An induced, immediate early protein belonging to the Ras family. *Science* **265:** 241–244.

Olson MF. 2002. Gem GTPase: Between a ROCK and a hard place. *Curr Biol* **12:** R496–R498. doi: 10.1016/S0960-9822(02)00968-5.

Paradis S, Harrar DB, Lin Y, Koon AC, Hauser JL, Griffith EC, Zhu L, Brass LF, Chen C, Greenberg ME. 2007. An RNAi-based approach identifies molecules required for glutamatergic and GABAergic synapse development. *Neuron* **53:** 217–232.

Raya A, Rodriguez-Piza I, Aran B, Consiglio A, Barri PN, Veiga A, Izpisua Belmonte JC. 2008. Generation of cardiomyocytes from new human embryonic stem cell lines derived from poor-quality blastocysts. *Cold Spring Harb Symp Quant Biol* **73:** 127–135.

Reynet C, Kahn CR. 1993. Rad: A member of the Ras family overexpressed in muscle of type II diabetic humans. *Science* **262:** 1441–1444.

Savatier P, Lapillonne H, Jirmanova L, Vitelli L, Samarut J. 2002. Analysis of the cell cycle in mouse embryonic stem cells. *Methods Mol Biol* **185:** 27–33.

Downloaded from genesdev.cshlp.org on July 8, 2010 - Published by Cold Spring Harbor Laboratory Press

Sridharan R, Tchieu J, Mason MJ, Yachechko R, Kuoy E, Horvath S, Zhou Q, Plath K. 2009. Role of the murine reprogramming factors in the induction of pluripotency. *Cell* **136:** 364–377.

Stead E, White J, Faast R, Conn S, Goldstone S, Rathjen J, Dhingra U, Rathjen P, Walker D, Dalton S. 2002. Pluripotent cell division cycles are driven by ectopic Cdk2, cyclin A/E and E2F activities. *Oncogene* **21:** 8320–8333.

Takahashi K, Yamanaka S. 2006. Induction of pluripotent stem cells from mouse embryonic and adult fibroblast cultures by defined factors. *Cell* **126:** 663–676.

Takahashi K, Tanabe K, Ohnuki M, Narita M, Ichisaka T, Tomoda K, Yamanaka S. 2007. Induction of pluripotent stem cells from adult human fibroblasts by defined factors. *Cell* **131:** 861–872.

Thomson JA, Itskovitz-Eldor J, Shapiro SS, Waknitz MA, Swiergiel JJ, Marshall VS, Jones JM. 1998. Embryonic stem cell lines derived from human blastocysts. *Science* **282:** 1145–1147.

Treff NR, Vincent RK, Budde ML, Browning VL, Magliocca JF, Kapur V, Odorico JS. 2006. Differentiation of embryonic stem cells conditionally expressing neurogenin 3. *Stem Cells* **24:** 2529–2537.

Utikal J, Polo JM, Stadtfeld M, Maherali N, Kulalert W, Walsh RM, Khalil A, Rheinwald JG, Hochedlinger K. 2009. Immortalization eliminates a roadblock during cellular reprogramming into iPS cells. *Nature* **460:** 1145–1148.

Watanabe K, Ueno M, Kamiya D, Nishiyama A, Matsumura M, Wataya T, Takahashi JB, Nishikawa S, Nishikawa S, Muguruma K, et al. 2007. A ROCK inhibitor permits survival of dissociated human embryonic stem cells. *Nat Biotechnol* **25:** 681–686.

White J, Dalton S. 2005. Cell cycle control of embryonic stem cells. *Stem Cell Rev* **1:** 131–138.

Xirodimas D, Saville MK, Edling C, Lane DP, Lain S. 2001. Different effects of $p14^{ARF}$ on the levels of ubiquitinated p53 and Mdm2 in vivo. *Oncogene* **20:** 4972–4983.

Zhao Y, Yin X, Qin H, Zhu F, Liu H, Yang W, Zhang Q, Xiang C, Hou P, Song Z, et al. 2008. Two supporting factors greatly improve the efficiency of human iPSC generation. *Cell Stem Cell* **3:** 475–479.

Edel, MJ et al: Supplementary Fig 1: HIV-1 p24 ELISA test of lentivirus titre shows no difference between Constructs or batches over time.

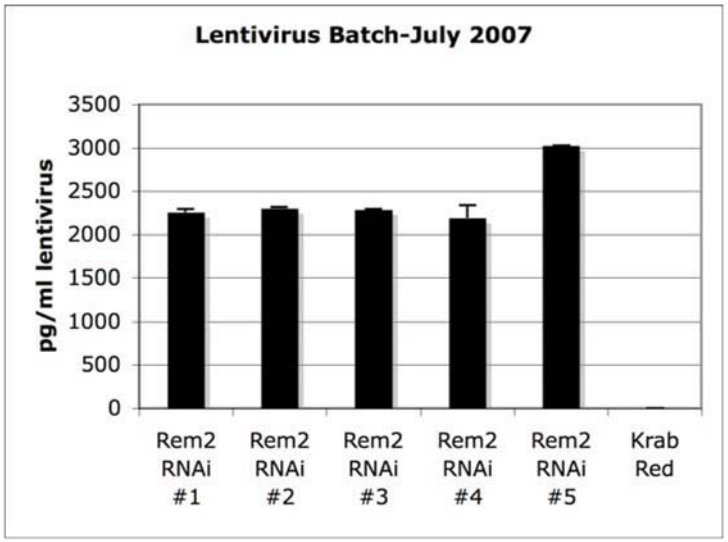

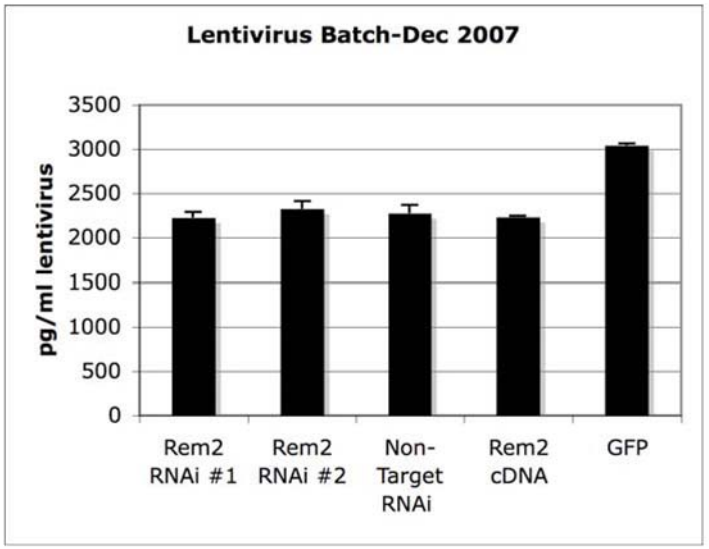

Edel, MJ et al: Supplementary Fig 2: Primitive time-lapse photography reveals that infection with Rem2 RNAi or cDNA virus does not effect adherence of cell numbers to the plate after 24 hrs.

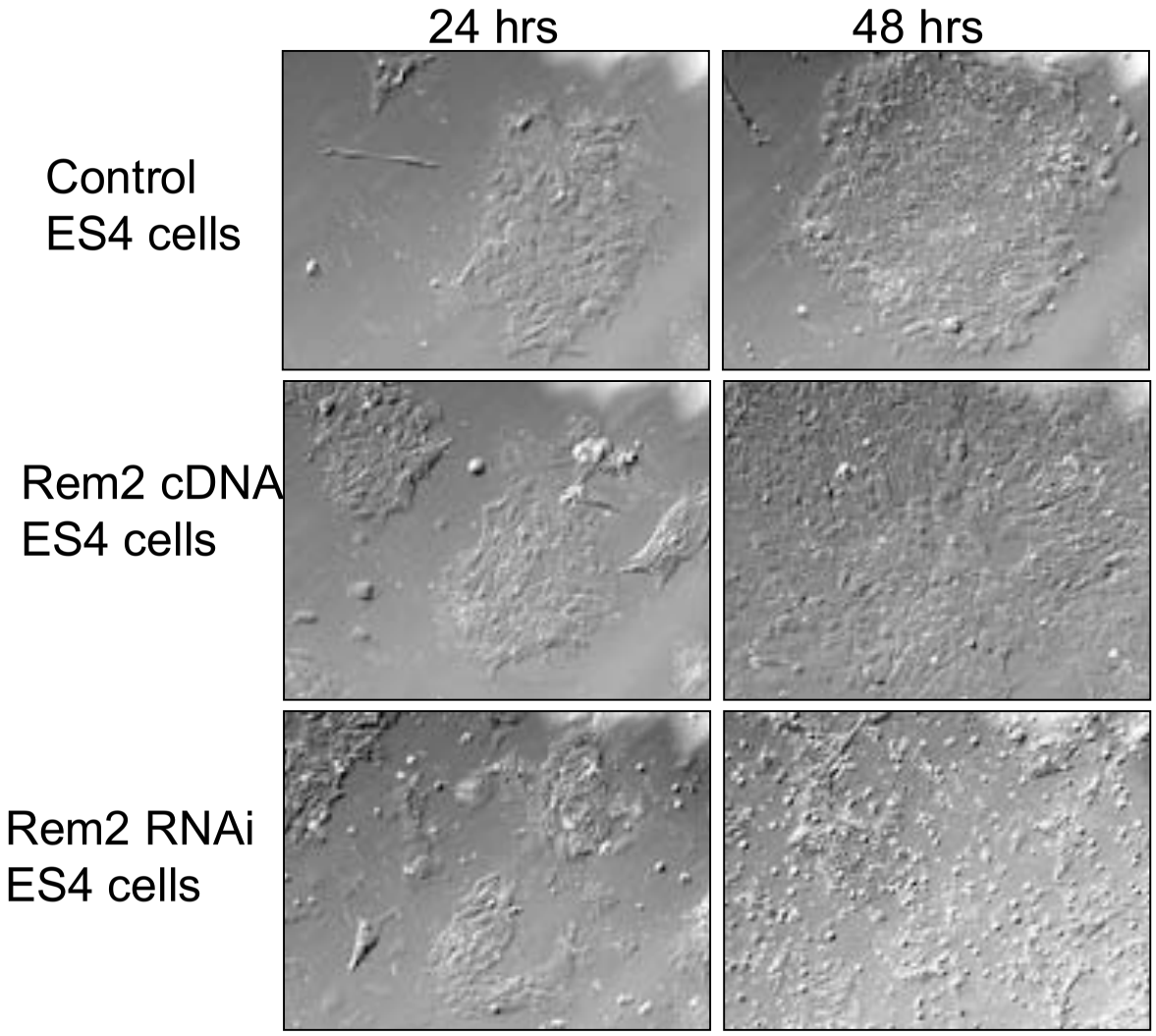

Edel MJ et al: Supplementary Fig 3: Karyotype of human ES cells and ES4 cells infected with Rem2 over expression.

Human ES4 cells

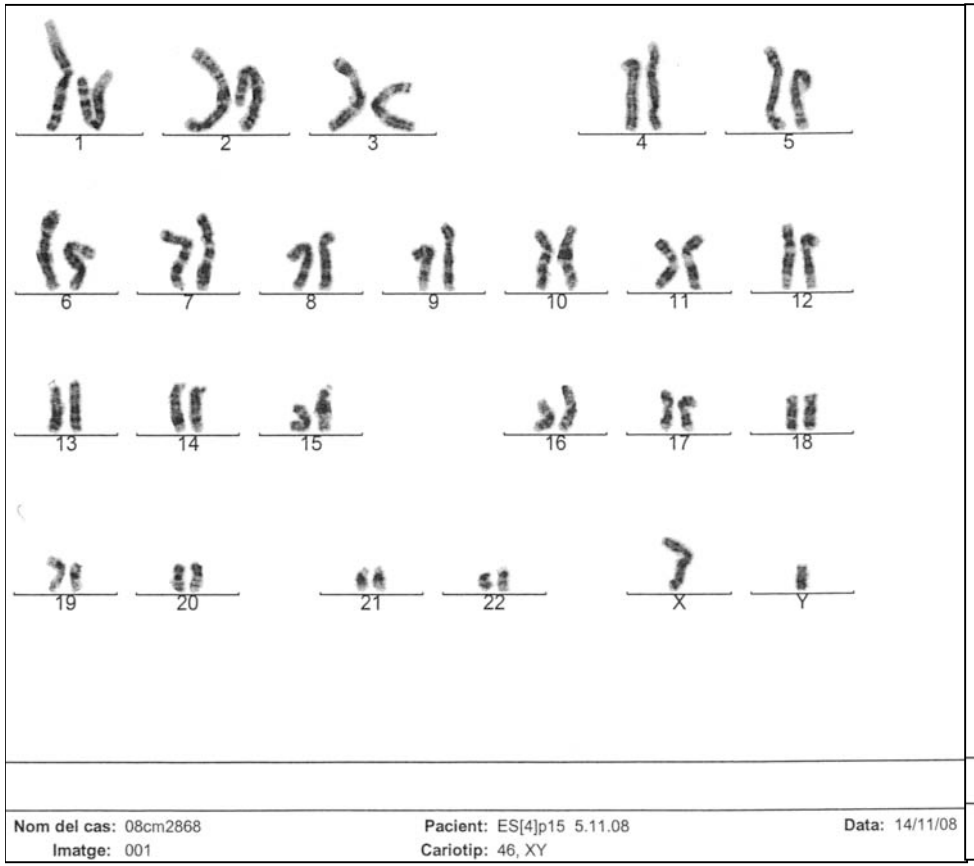

Human ES4 cells with Rem2 overexpression

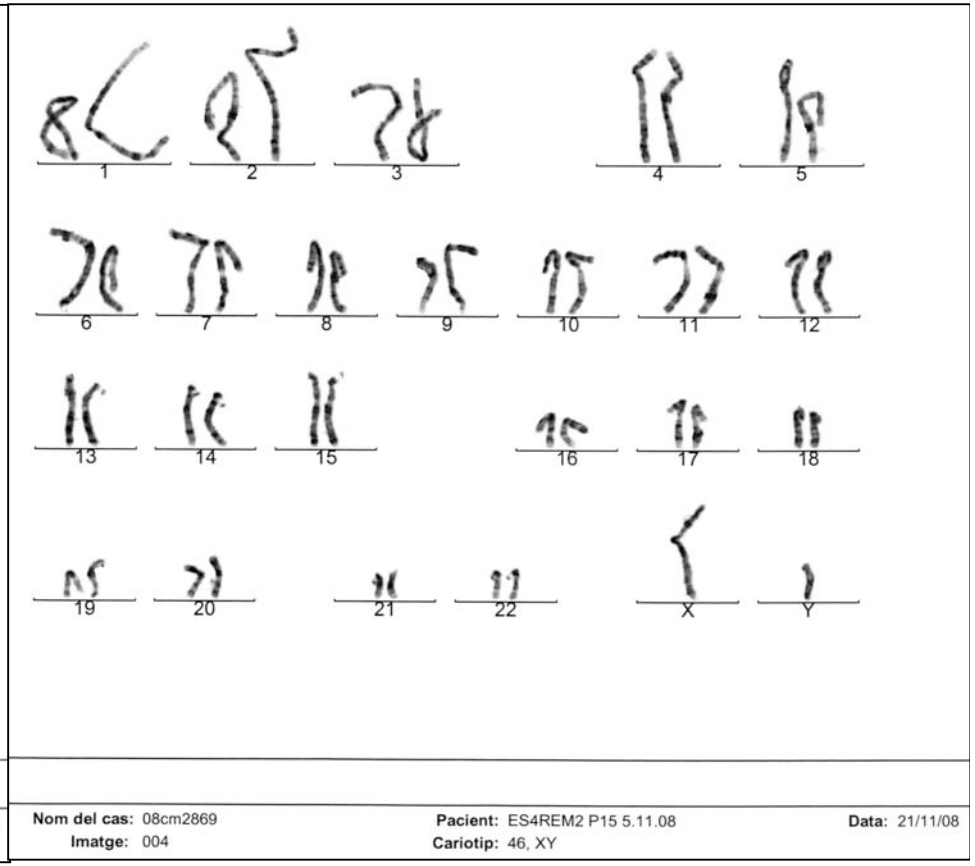

Edel, MJ et al: Supplementary Fig 4: Analysis of $p14^{ARF}$ or $p19^{ARF}$ mRNA levels in hESC, Keratinocytes and MEFs demonstrates that it is not regulated by Rem2 in these specific cell types or conditions.

Human ES cells + fgfr inhibitor

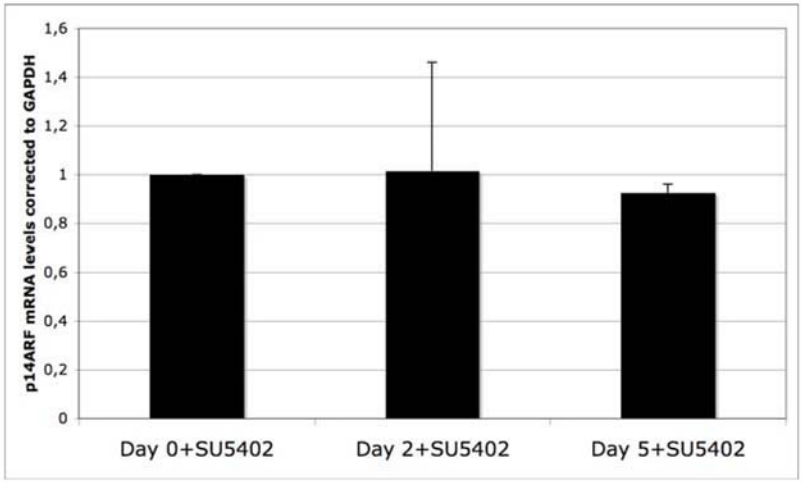

Human ES cells + Rem2 cDNA

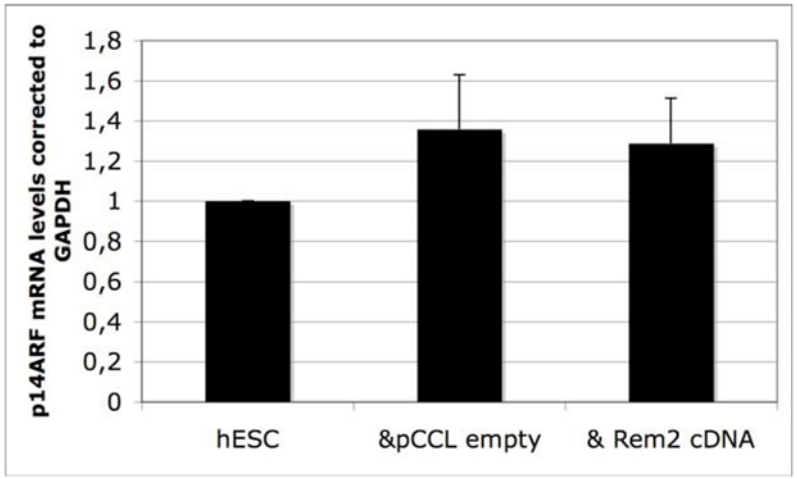

Human Keratinocytes or MEFs

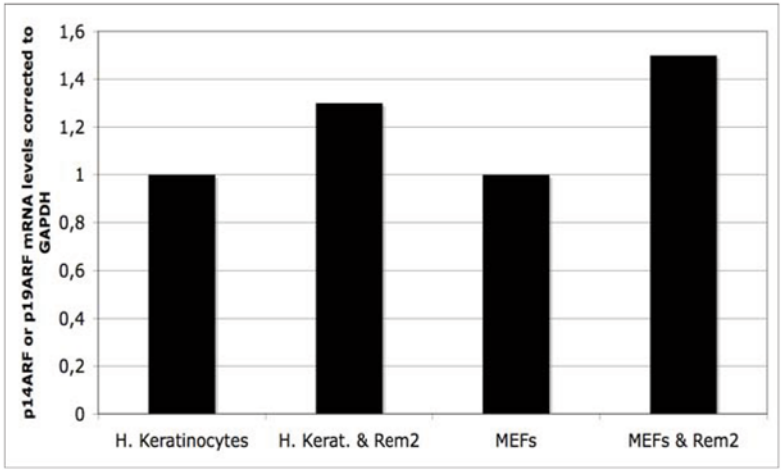

Edel, MJ et al: Supplementary Fig 5: EDU pulse time and effect of human ES cell density.

Time pulse to determine best time for EDU staining

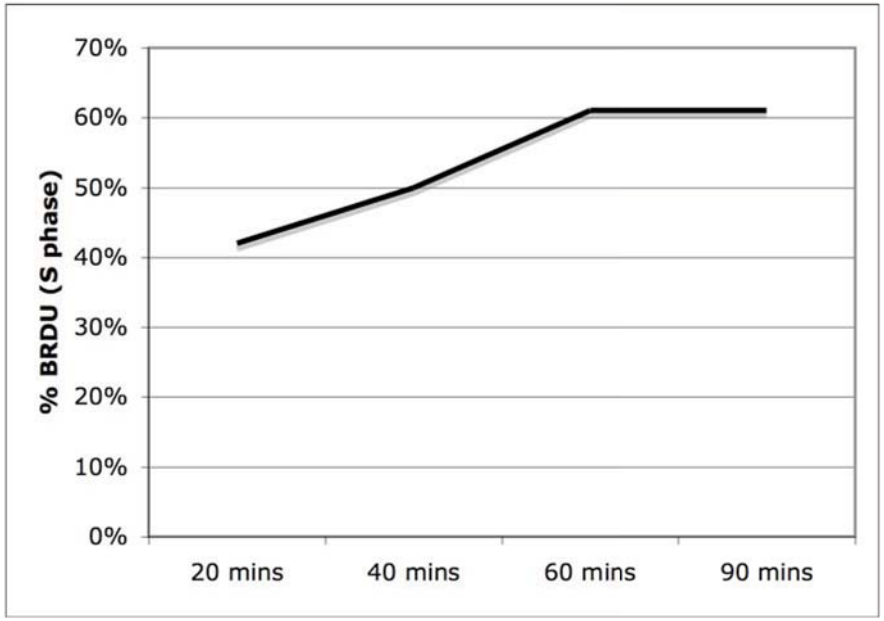

Effect of ES4 cell density on Cell cycle by PI and EDU staining.

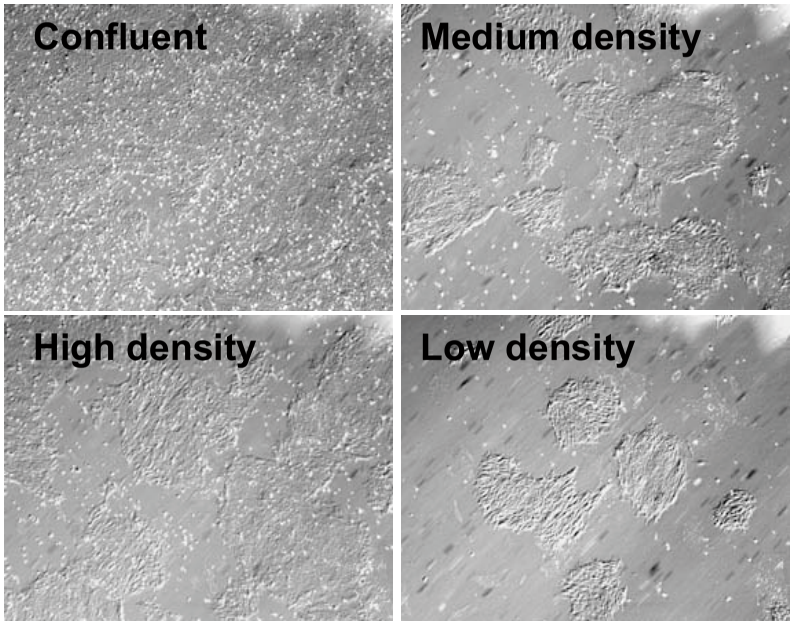

G0/G1	G2/M	EDU % S PHASE
Low*13%*	Low *29%*	Low54%
Medium16%	Medium22%	Medium54%
High16%	High 22%	High53%
Confl.18%	Confl. 20%	Confl.53%

Edel, MJ et al: Supplementary Fig 6: FACs histogram for EDU staining of human ES cells with Rem2 cDNA and RNAi.

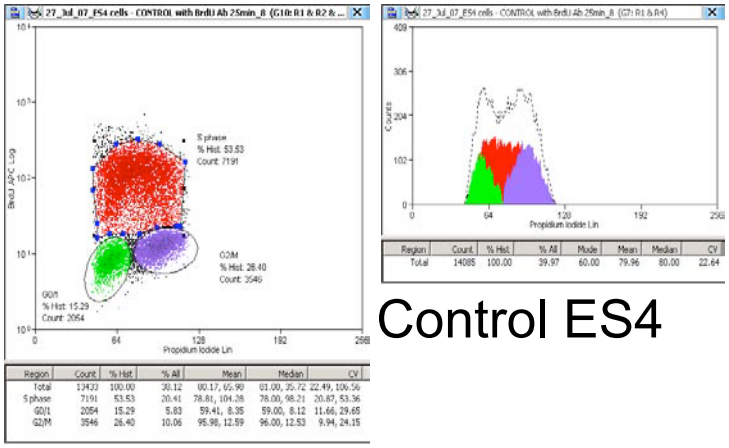

Control ES4

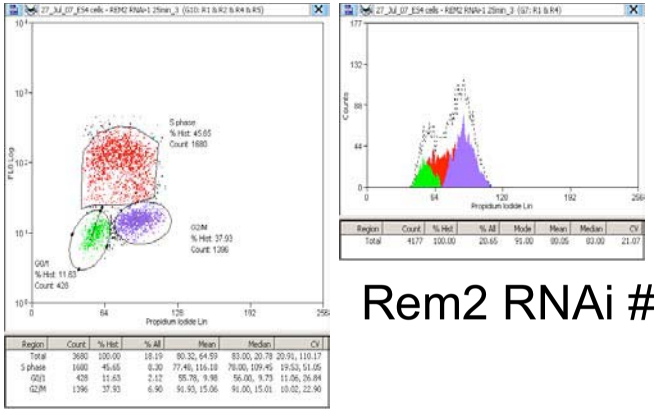

Rem2 RNAi #1

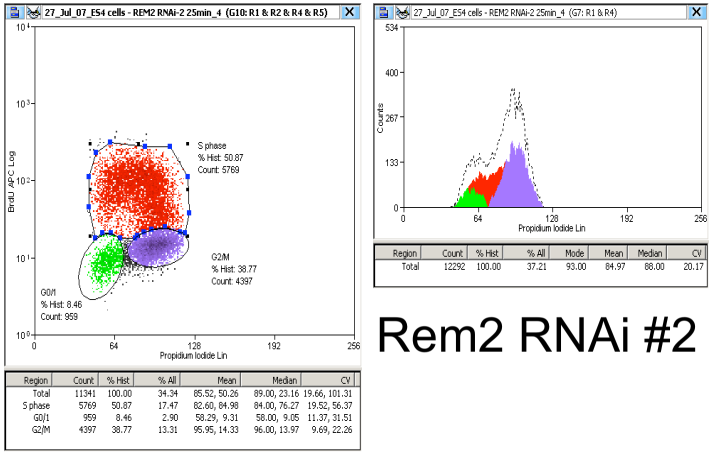

Rem2 RNAi #2

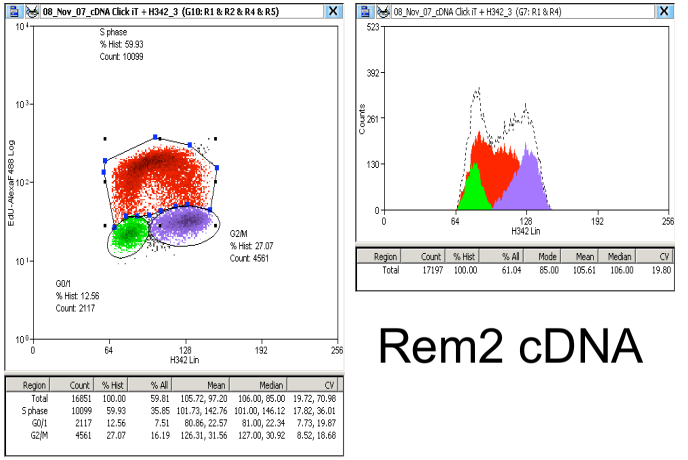

Rem2 cDNA

Edel, MJ et al: Supplementary Fig 7: FACs histogram for DiLC staining of human ES cells with Rem2 cDNA and RNAi. Control staining for CCCP shift, demonstrating that the DilC method is working in human ES cells.

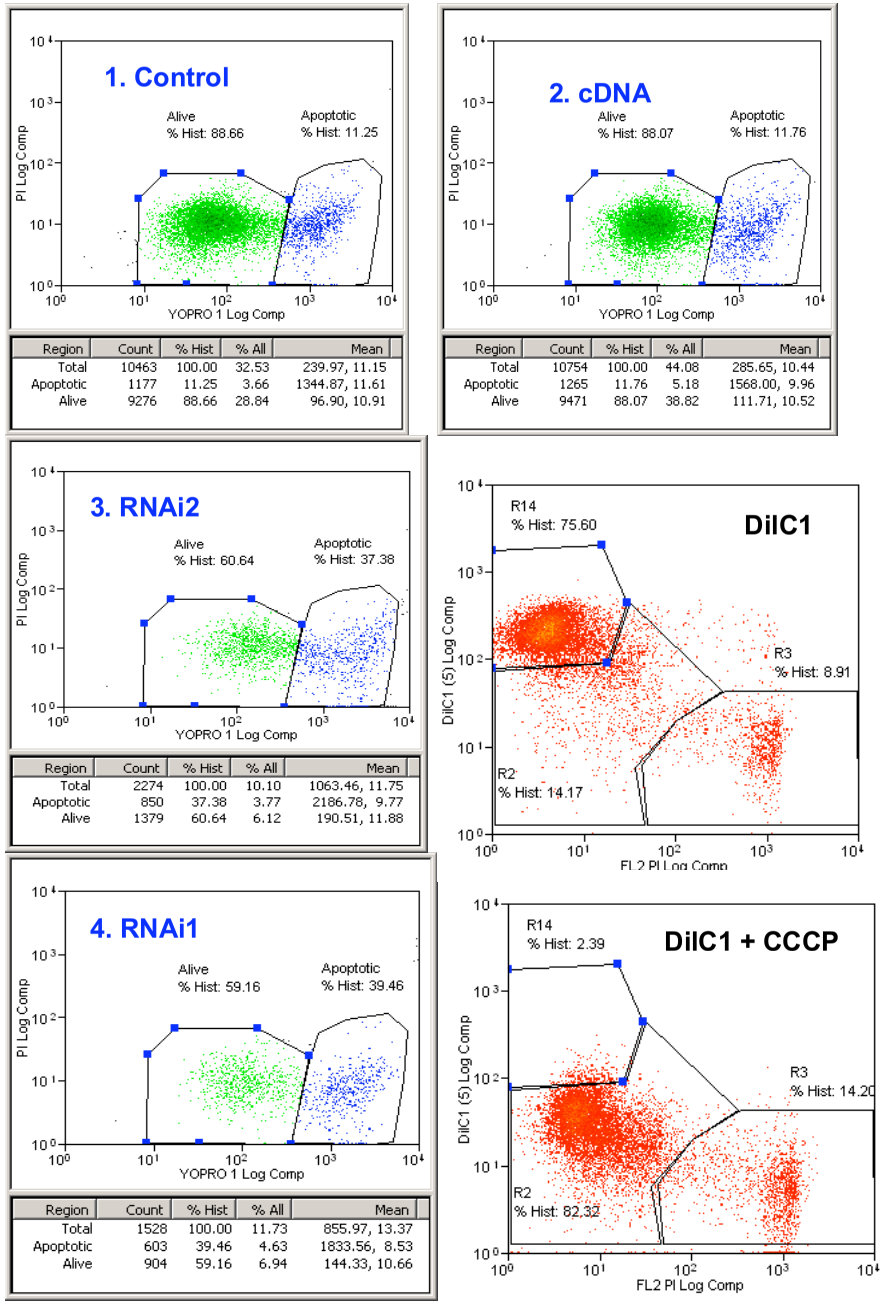

Edel MJ et al: Supplementary Fig 8 *Top panel:* Graph of p53 binding site luciferase reporter treated with 5 μg/ml Mitomycin C and with or without Rem2 in hESC. Results expressed as fold change from control with no treatment. *Bottom Panel:* Photo of Ubiquination blot of MDM4 in hESC with and without Rem2 treated with Mitomycin C. Ubiquination bands are marked with an asterix and quantified in Figure 2 of main figures.

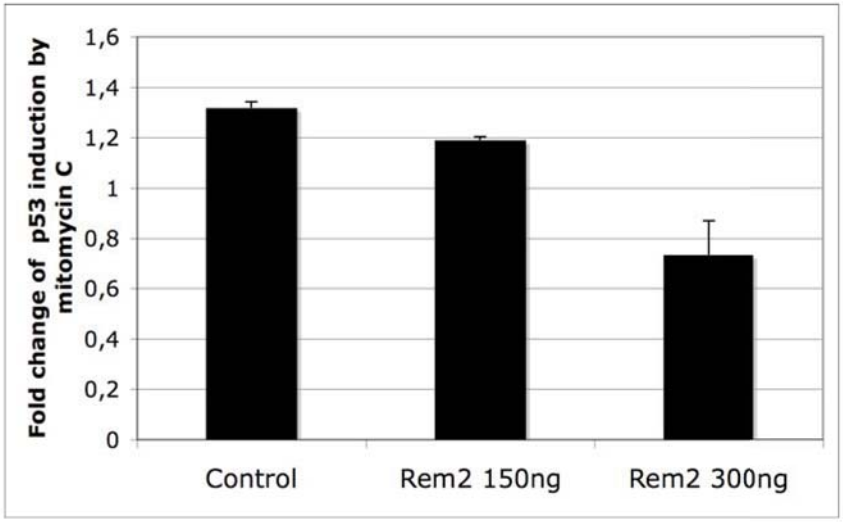

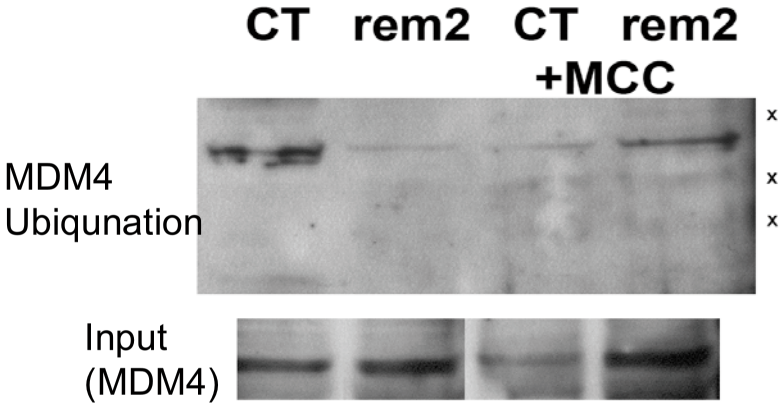

Edel MJ et al: Supplementary Fig 9: Real time PCR analysis of cyclin D_1 levels in hESC with FGFr inhibitor SU5402. Inhibition of FGFr signalling results in reduction of Rem2 (see Fig 1) and consequent upregulation of cyclin D_1 mRNA expression levels. This is in agreement with the Rem2 RNAi data in Figure 2 showing that loss of Rem2 results in an increase in cyclin D_1 mRNA expression levels, suggesting that FGF signaling regulates cyclin D_1 expression in hESC.

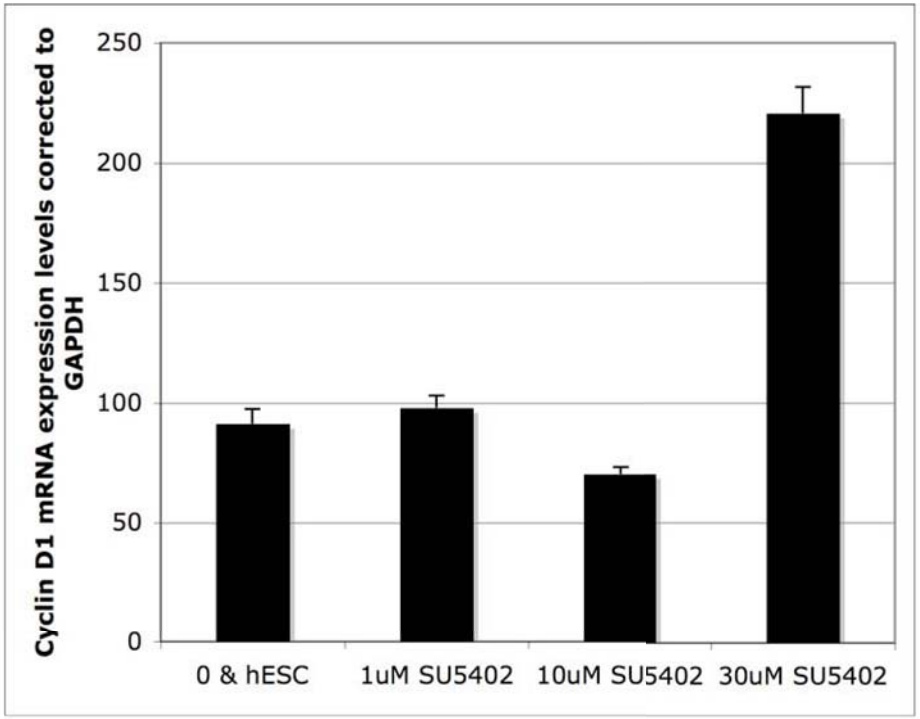

Edel MJ et al: Supplementary Fig 10: Western blot of expression of factors 4 days post-infection.

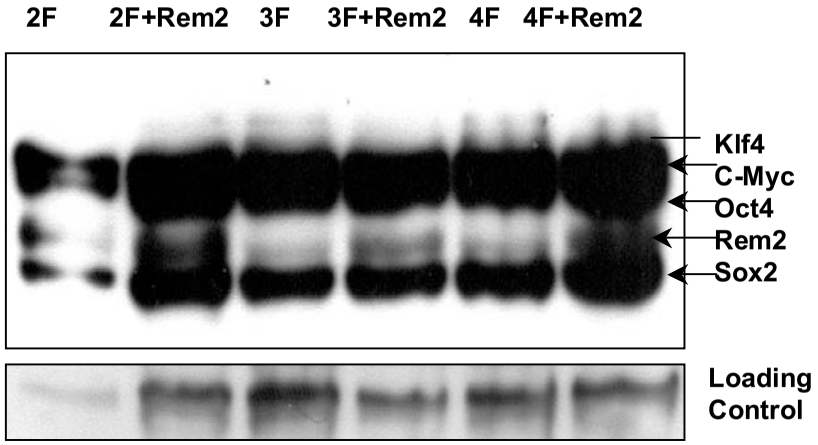

Edel MJ et al: Supplementary Fig11: Western blot of Cyclin D1 protein levels in iPS cells compared to embryonic stem cells, demonstrates high levels of expression in iPS clones.

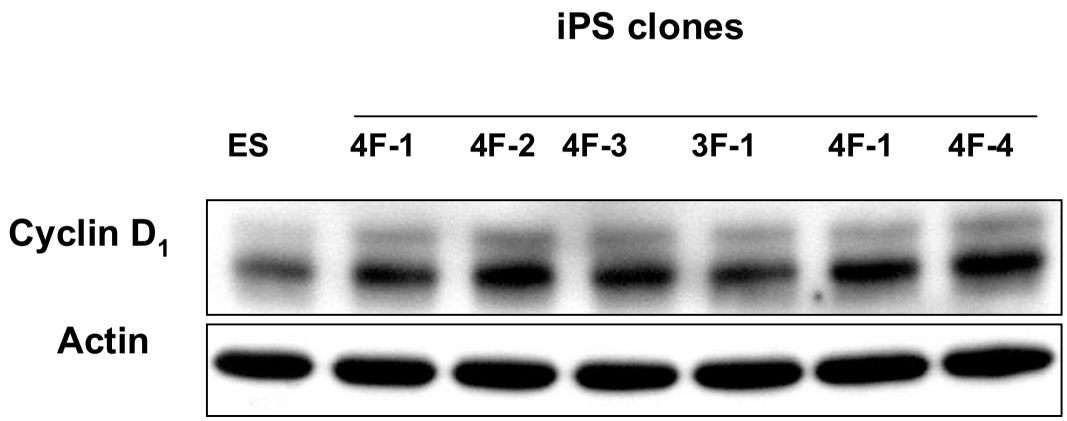

Edel MJ et al: Supplementary Fig 12: Western blot of expression of 3 factors plus either p53dd, cyclin D1 or Rem2, 4 days post-infection.

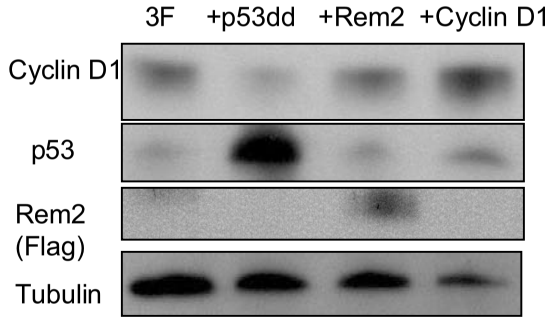

Edel MJ et al: Supplementary Fig 13: Immunoflorescence of cyclin D_1 protein localisation in p53 null MEFs during early reprogramming (day 10), shows that the nuclear localisation associated with Rem2 overexpression is not dependent on p53.

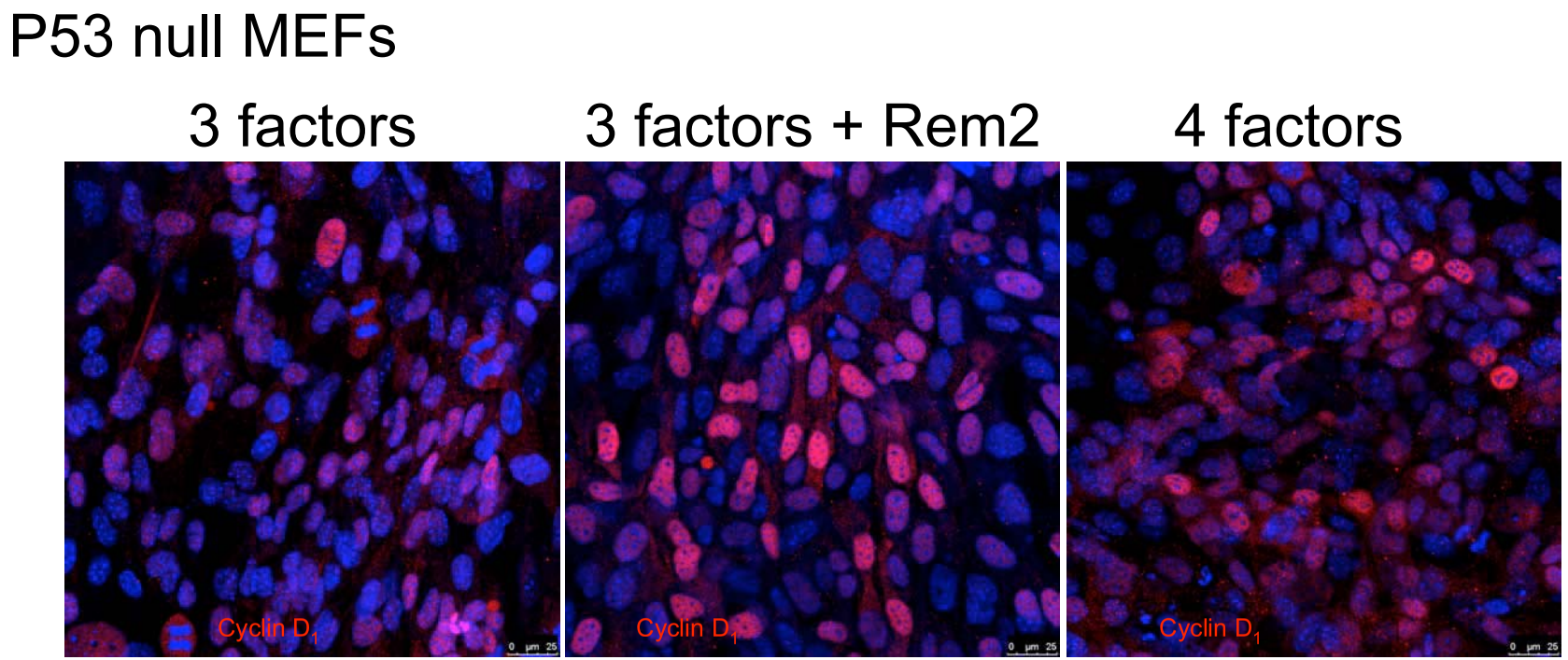

Edel MJ et al: Supplementary Fig 14: Photos of Immuno-florescence staining of early reprogramming colonies (day12) with tunnel (apoptosis), Phospho-H3 (proliferation) and SSEA3 (Pluripotent) treated with dominant negative p53 (p53dd), cyclin D_1 and Rem2 as described in the figure below (x200). This figure has been quantified in Figure 4H.

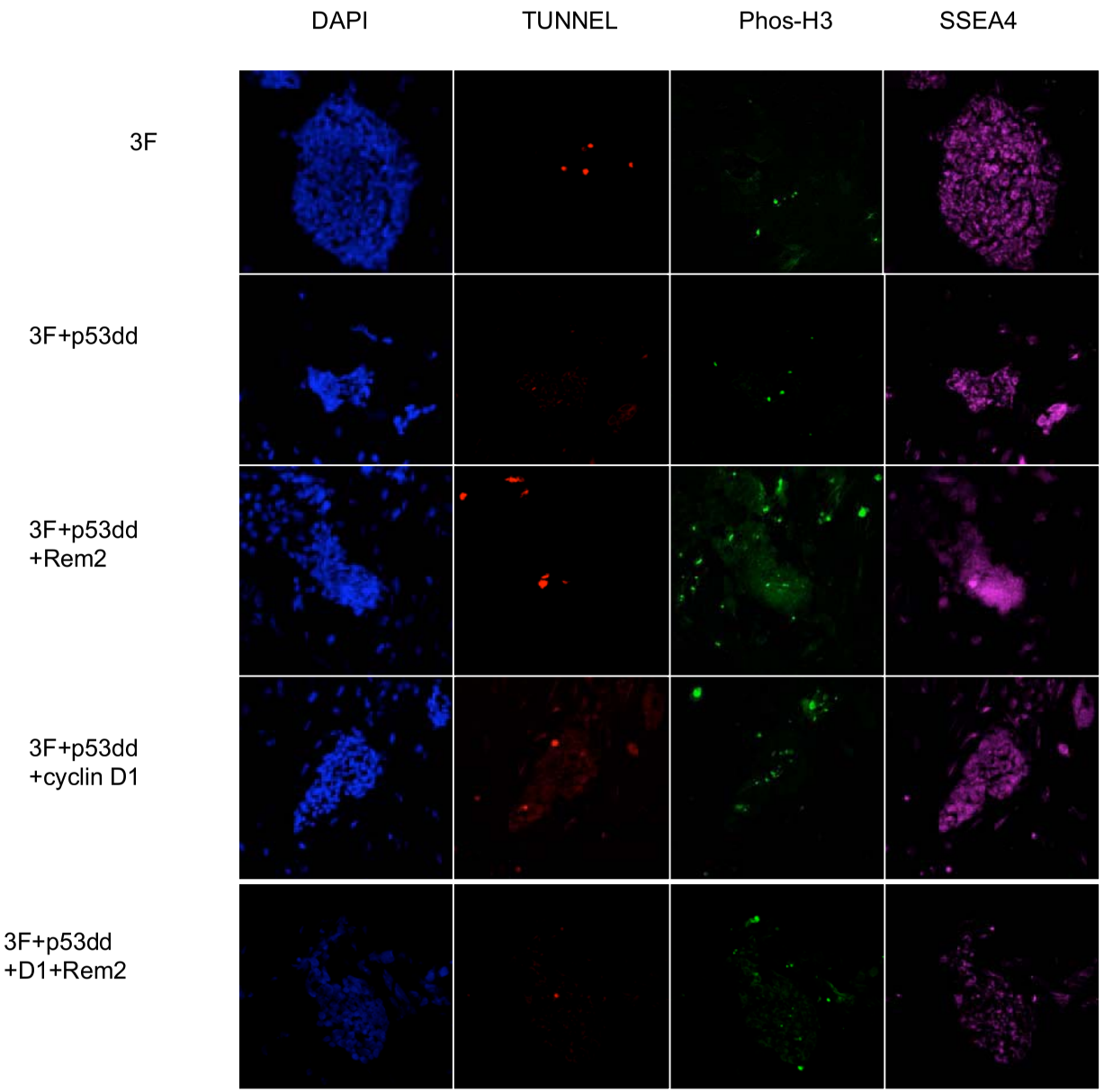

Cell Cycle 9:17, 3414-3422; September 1, 2010; © 2010 Landes Bioscience

Rem2 GTPase controls proliferation and apoptosis of neurons during embryo development

Michael J. Edel,[1] Stéphanie Boué,[1] Cristina Menchon,[1] Adriana Sánchez-Danés[1,†] and Juan Carlos Izpisua Belmonte[1,2,*]

[1]Center of Regenerative Medicine in Barcelona; Barcelona, Spain; [2]Gene Expression Laboratory; Salk Institute for Biological Studies; La Jolla, California USA

[†]Current Address: Institute of Biomedicine of the University of Barcelona (IBUB); Barcelona, Spain

We have recently found that Rem2 GTPase, highly expressed in human embryonic stem cells (hESC), maintains the cell cycle and controls proper differentiation towards ectoderm, suggesting a role in neuronal development. We describe here the use of the zebrafish (*Danio rerio*) model to determine the physiological significance of Rem2 during embryogenesis. We show that *Rem2* RNA is highly expressed in zebrafish embryos up to 2 hours of development followed by a decrease in expression until 48 hours when afterwards *Rem2* is switched on again until 5 days. In situ expression analysis reveals that *Rem2* is expressed exclusively in the tectum of the brain and eye of the zebrafish. Rem2 morpholino demonstrates impaired embryo development resulting in loss of neural tissue. We show that the mechanism of action of Rem2 is to control apoptosis and proliferation, peaking at 36 hours of development. Rem2 is down-regulated under general differentiation conditions of hESC and is lower expressed in most differentiated cells; however, it is upregulated with neuronal development. This suggests that Rem2 is critical for neuronal development during embryogenesis by regulating proliferation and apoptosis. We propose a model in which Rem2 GTPase is a key regulator maintaining pluripotency during early stages of embryogenesis and survival of neurons during later embryonic development.

Key words: cell cycle, embryogenesis, pluripotency, apoptosis, zebrafish, embryonic stem cells, differentiation, neurons

Submitted: 05/20/10

Accepted: 06/11/10

Previously published online: www.landesbioscience.com/journals/cc/article/12719

DOI: 10.4161/cc.9.17.12719

*Correspondence to: Juan Carlos Izpisua Belmonte; Email: belmonte@salk.edu and izpisua@cmrb.eu

Introduction

Genes involved in switching between pluripotency and differentiation into specific cell lineages are critical to the proper development of embryos. Recent work by our own group has revealed that Rem2 GTPase is an important regulator of human embryonic stem cell (hESC) survival although the in vivo significance remains to be defined.[1] Rem2 is a recently identified member of the Rem/Rad/Gem/Kir (RGK) family of Ras-related GTPases, which were first described as overexpressed in muscle cells of patients with type II diabetes mediating signal transduction.[2,3] Recently, Rem2 was identified from a functional genetic screen to by-pass a p53 induced senescence to immortalize somatic cells demonstrating a fundamental role for cell cycle control.[4]

Interestingly, we have shown that forced expression of Rem2 under general differentiation of hESC causes improper differentiation to form ectoderm at the expense of mesoderm.[1] The Rem2 GTPase has been identified in neuronal development such as control neuron synapse formation and has enriched expression in the central extended amygdala.[5,6] Recently two microarray-based experiments identified Rem2 as upregulated during the formation of two different adult stem cells, those making pancreas and those making dopaminergic neurons.[7,8] This prompted us to investigate further the physiological role of Rem2 during embryonic development and we chose the *Danio rerio* model because it is a powerful model organism in the field of comparative genomics.[9]

Results

Annotation of Rem2 in Zebrafish and expression kinetics during embryogenesis.

To annotate the Rem2 gene in zebrafish we used a bioinformatics approach described in the material and methods section. In summary, we identified the zebrafish Rem2 gene from the EST sequence with the accession number gi 114118945 in the NCBI database (**Fig. 1A**). Indeed, this sequence located on the zebrafish chromosome 2 hits best the human Rem2 gene by a Blast analysis, and is different from the other family members of the RGK GTPases in Zebrafish (data not shown). A multiple alignment of the protein sequences reveals the conservation of Rem2 across many species (**Fig. 1A**). The hypothetical protein sequence can been seen in the **Supplementary Section** (**Fig. S1**). A phylogenetic tree of the RGK family confirms that the hypothetical protein is indeed the zebrafish Rem2 (**Fig. 1B**).

Analysis of Rem2 mRNA expression levels by real time PCR of whole zebrafish embryos reveals that ***Rem2*** is highly expressed at less than 2 hours (64 cells) of development and then decreases until 48 hours of development, following very closely the expression pattern of the pluripotency gene Oct3/4 (**Fig. 1A**). At 48 to 72 hours of development ***Rem2*** mRNA expression levels increase again to similar levels of expression seen at 2 hours, while Oct3/4 levels continue to decrease (**Fig. 1A**). This suggests that Rem2 has a biphasic response during embryo development where it is needed during the 2-cell to 64-cell stage as a pluripotency factor and then its expression level decreases until the long-pec stage, where its expression level increases again in response to the differentiating embryo (**Fig. 1**).

Rem2 is expressed in the brain of zebrafish embryos starting at 24 hours. Next we set out to investigate in more detail where Rem2 is expressed during embryo development. We performed whole embryo in situ analysis of ***Rem2*** expression from the 24 hour stage to 5 days (**Fig. 2**). We find that ***Rem2*** is lowly expressed at 24 hours and increases towards 5 days of development where Rem2 expression increases dramatically in the neural tissue of the tectum of the zebrafish brain as well as to the eyes.

Rem2 morpholino causes impaired development of mid-brain of zebrafish. In order to judge whether Rem2 is essential during embryo development we performed a loss of Rem2 function experiment in vivo using Rem2 morpholino. Compared to morpholino controls, Rem2 morpholino demonstrates a loss of midbrain development at 36 hours (**Fig. 3**). From the side view a clear indentation near the midbrain of the zebrafish is to be seen, suggesting loss of tissue (**Fig. 3**). This is made clearer in the top view at 36–48 hours of development where phase contrast microscopy reveals that the 5 segments seen in controls are malformed and general head size is smaller (**Fig. 3**). This suggested that loss of Rem2 causes loss of neural tissue during embryonic development.

Rem2 controls proliferation and apoptosis of neurons during embryo development. In order to define if loss of Rem2 function during zebrafish development regulates proliferation and apoptosis, we performed tunnnel and proliferation assay at the same time in whole fish embryos using antibodies against phosphorylated histone H3 respectively (**Fig. 4**). At 36 hours of development a clear increase in apoptosis (Red) signal can be seen concomitant with loss of Rem2 function. A decrease in proliferation (Green) signal compared to morpholino controls and non-injected embryos are also observed (**Fig. 4**). Quantification of apoptosis/proliferation ratios by image analysis software reveals that during embryo development the ratio of apoptosis increases more than 3.5 fold with loss of Rem2 at 36 hours of development. This demonstrates that Rem2 expression is critical at the 36 hour to 48-hour time point to maintain survival by regulating proliferation and apoptosis during development. Regulation of apoptosis by Rem2 was also assessed by another technique, Acridine Orange. This approach demonstrated with the Rem2 morpholino an increase in cell death in the eye and brain of the zebrafish in agreement with the Tunnel assays (**Fig. S2**).

Importantly, the increase in signal intensity around the brain and eye regions of the embryo, correlates well with the Rem2 in situ analysis (**Fig. 2**). This suggests that the cell type most affected by Rem2 expression are neural cells. To investigate this further and because a role for dopamine neuron development had been previously suggested in a microarray experiment,[8] we analyzed TH (tyrosine hydroxylase) expression in Rem2 morpholino. Indeed we find that loss of Rem2 function during zebrafish embryo development results in loss of the number of TH positive neurons, supporting that Rem2 is an important regulator of neurons during development of the embryo (**Fig. 5**).

Model of Rem2 function in pluripotency and differentiation. We present the model that Rem2 is highly expressed in early embryo development during the formation of the inner cell mass and therefore likely plays a role in the pluripotency of the embryo. In agreement, we found that Rem2 maintains pluripotency and self-renewal of ES cells by controlling the cell cycle and apoptosis to maintain survival of human embryonic stem cells (hESC).[1] During further differentiation of the embryo, different environmental conditions presented to the cells may regulate Rem2 expression. Assessment of Rem2 mRNA levels in hESC that have been differentiated towards neuronal linage demonstrates a 15-fold increase in Rem2 expression compared to controls suggesting a role for Rem2 in neuronal development (**Fig. 5**). We propose that those cells that maintain high level of Rem2 GTPase expression are then destined to become neurons whereas most of other cells that have low levels differentiate into other lineages (**Fig. 5**). Indeed Rem2 is not highly expressed in most tissues of the human or mouse (Novartis tissue arrays), further suggesting a specific expression in the brain.

Discussion

We have recently found that Rem2 GTPase is highly expressed in human embryonic stem cells (hESC) maintaining the cell cycle and apoptosis levels and controlling proper differentiation towards ectoderm, suggesting a role in neuronal development.[1] We have used the zebrafish (*Danio rerio*) model to determine the physiological significance of Rem2 during embryogenesis.

We show that Rem2 is expressed in the embryonic neural tissue of the developing zebrafish embryo. This is in general keeping

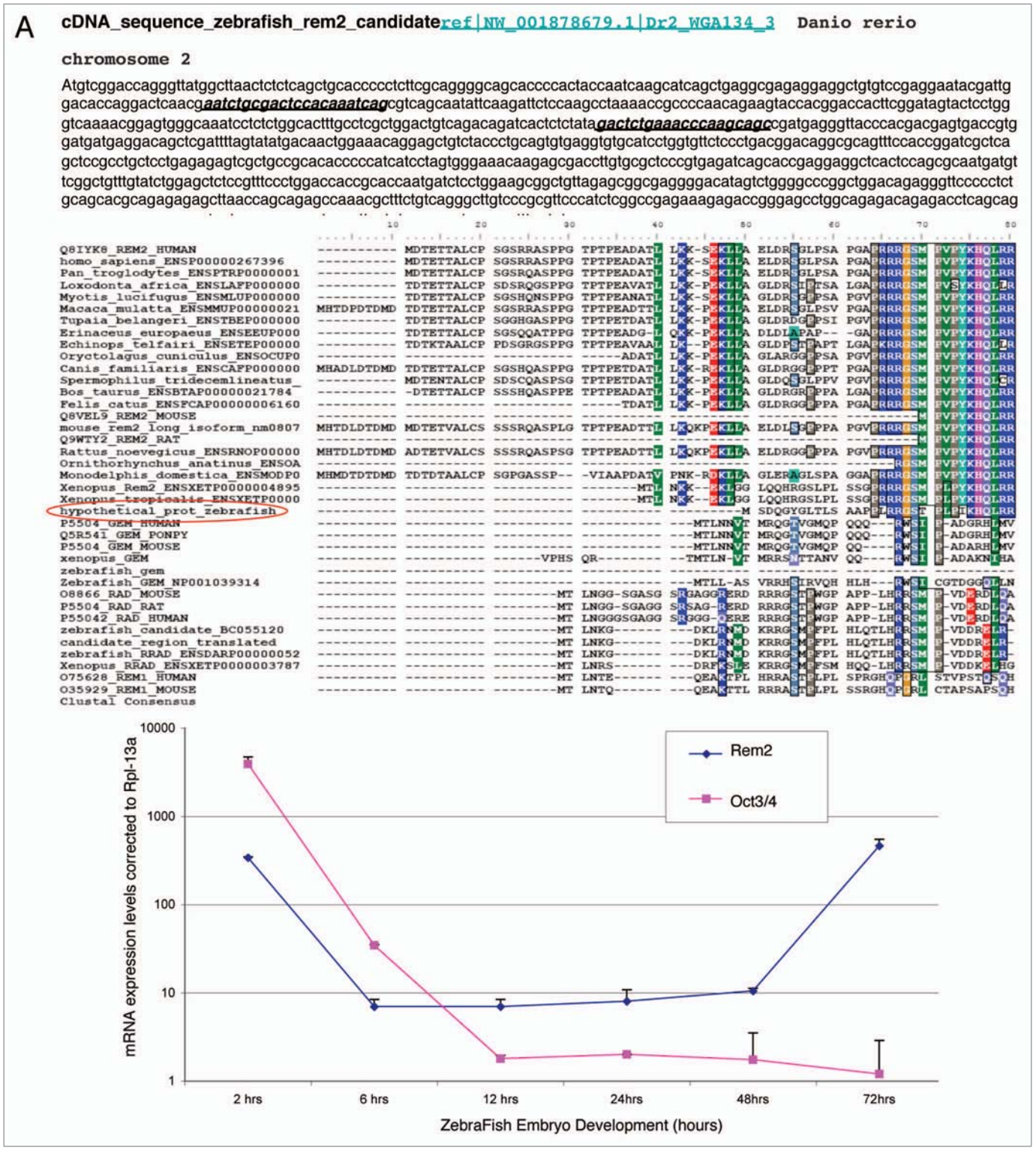

Figure 1. (A) Bioinformatics annotate Rem2 GTPase in zebrafish and reveal expression kinetics during embryogenesis. Top part: cDNA sequence of *Danio rerio* Rem2 GTPase identified by a bioinformatics approach. Underlined area primers used for real time PCR analysis of expression in zebrafish embryos. Middle part: Protein alignment of *Danio rerio* Rem2 GTPase reveals very good homology to Rem2 conserved across many species. Rem2 is circled in red. Bottom part: Real time PCR analysis of Rem2 mRNA expression in the developing *Danio rerio* embryo over time from 2 hours to 72 hours.

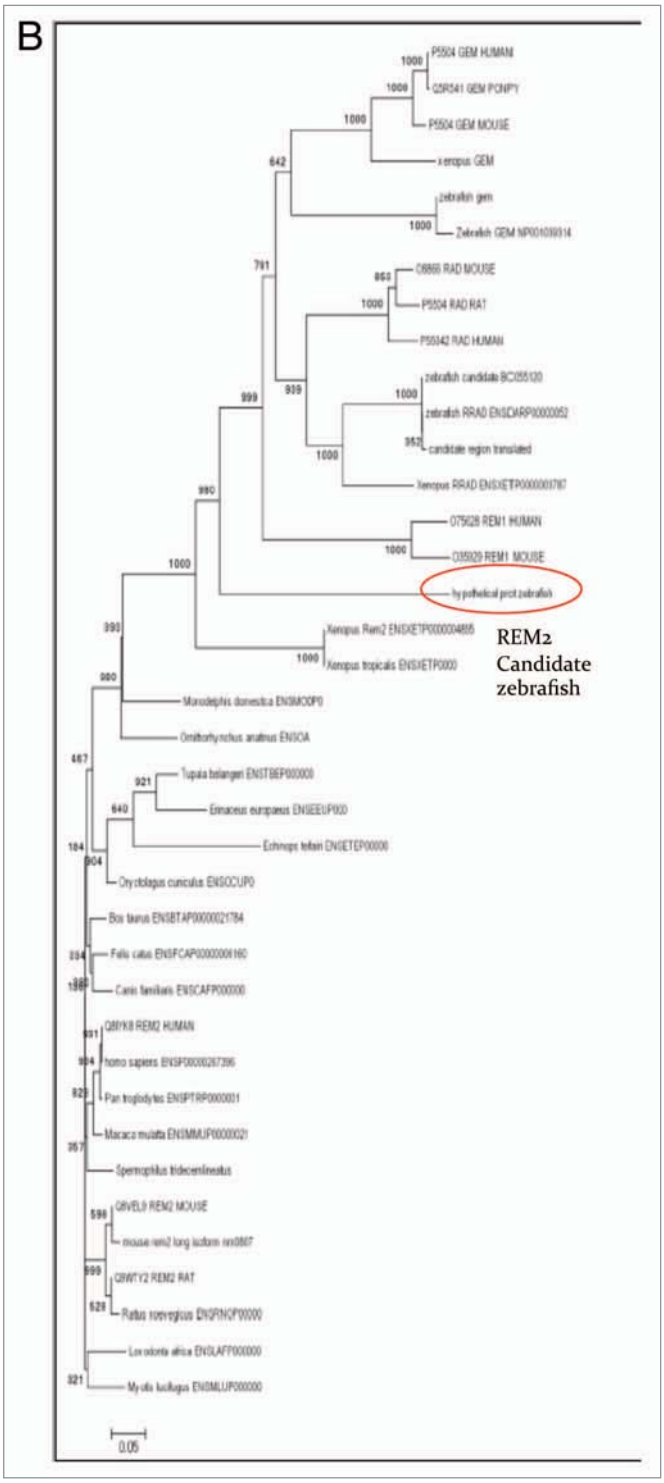

Figure 1. (B) Bioinformatics annotate Rem2 GTPase in zebrafish and reveal expression kinetics during embryogenesis. Phylogenetic tree analysis of Danio Rerio Rem2 GTPase. Rem2 is circled in red.

with location of expression of other RGK family members Rem1 and Rad, which are also expressed in the neural tissue albeit with a different localisation and expression pattern (http://zfin.org). Interestingly, we show that Rem2 is highly expressed in early embryo development by real time PCR (less than 2 hours of development), which is the same stage as the inner cell mass development from which embryonic stem cells are derived from. Following a reduction in expression levels of ***Rem2*** mRNA, it is again switched on to high levels towards the 48 hour time point and is expressed exclusively in the tectum of the fish brain. The real time PCR data correlates very well with the Rem2 in situ hybridisation reults in which we see little expression of ***Rem2*** mRNA at 24 hours and a specific signal developing in the neural tissue by 48 hours of development (**Figs. 1 and 2**). Loss of Rem2 in the developing zebrafish embryo results in an increase of apoptosis/decrease in proliferation of embryonic neural tissue and a correlative loss of TH positive dopaminergic neurons by day 5 of development (**Figs. 4 and 5**). The exclusive expression of Rem2 GTPase during neuronal development has been described before, such as control neuron synapse formation and enriched expression in the central extended amygdala of the mouse.[5,6]

Although we have previously demonstrated an essential role of Rem2 in the survival hESC in vitro, the survival of zebrafish embryos at the early stages (ICM formation) following loss of Rem2 expression is not contradictory to what we have seen in human ESCs, because of the rapid development of the zebrafish (before the morpholino can take effect). Moreover, there exits many other examples of embryonic development that are not affected by loss of ESC self-renewal factors such as Eras, Zfx or Tbx3.[10-12] Interestingly, both TBX3 and Rem2 have been shown to regulate the p53 pathway by similar mechanisms.[4] The data suggest that Rem2 has a critical role in promoting the survival and proliferation and therefore self-renewal of ESC cells in vitro.[1] Given that Rem2 can promote survival of dopamine neurons, further studies to determine the role of Rem2 for the development of dopamine neurons as well as cell replacement therapy for Parkinson's disease is warranted.

In conclusion, we present the model that Rem2 GTPase is a key regulator maintaining pluripotency during early stages of embryogenesis and survival of neurons during later embryonic development.

Methods

Zebrafish culture. Wild-type zebrafish of the Tubingen strain were maintained at

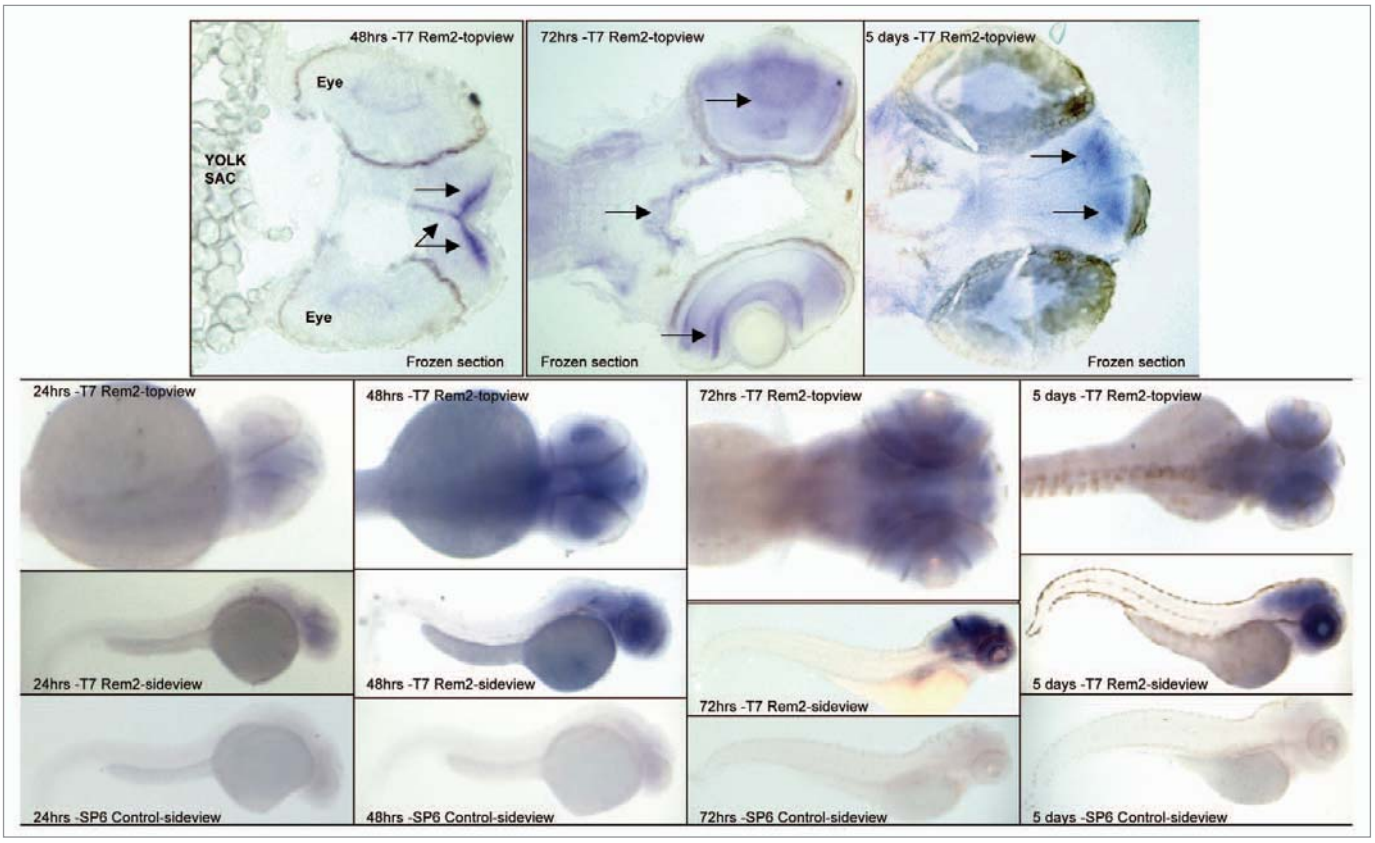

Figure 2. Rem2 is expressed in the brain of zebrafish embryos starting at 24 hours. Top parts: In situ hybridisation of Rem2 GTPase in early embryo development from 24 hours to 5 days with T7 and SP6 full length Rem2 probes. Frozen sections of Rem2 GTPase in situ hybridisation in whole embryos clearly showing expression of Rem2 in the brain and eye (arrows) at different stages of development. Bottom three parts: In situ hybridisation of Rem2 in early embryo development from 24 hours to 5 days showing expression exclusively in the brain and eye increasing at 5 days of development.

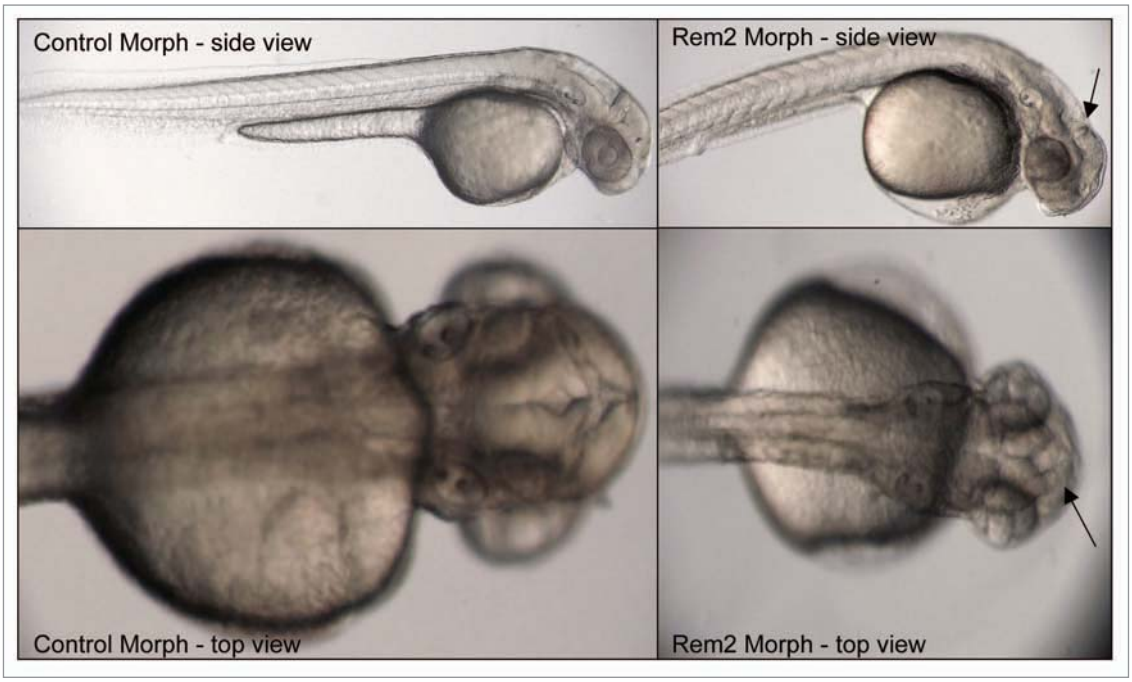

Figure 3. Rem2 morpholino causes impaired development of mid-brain of zebrafish. Phase contrast photographs of control morpholino compared to Rem2 morpholino at 48 hours development. A clear phenotype is demonstrated with smaller heads and loss of midbrain development (see arrows).

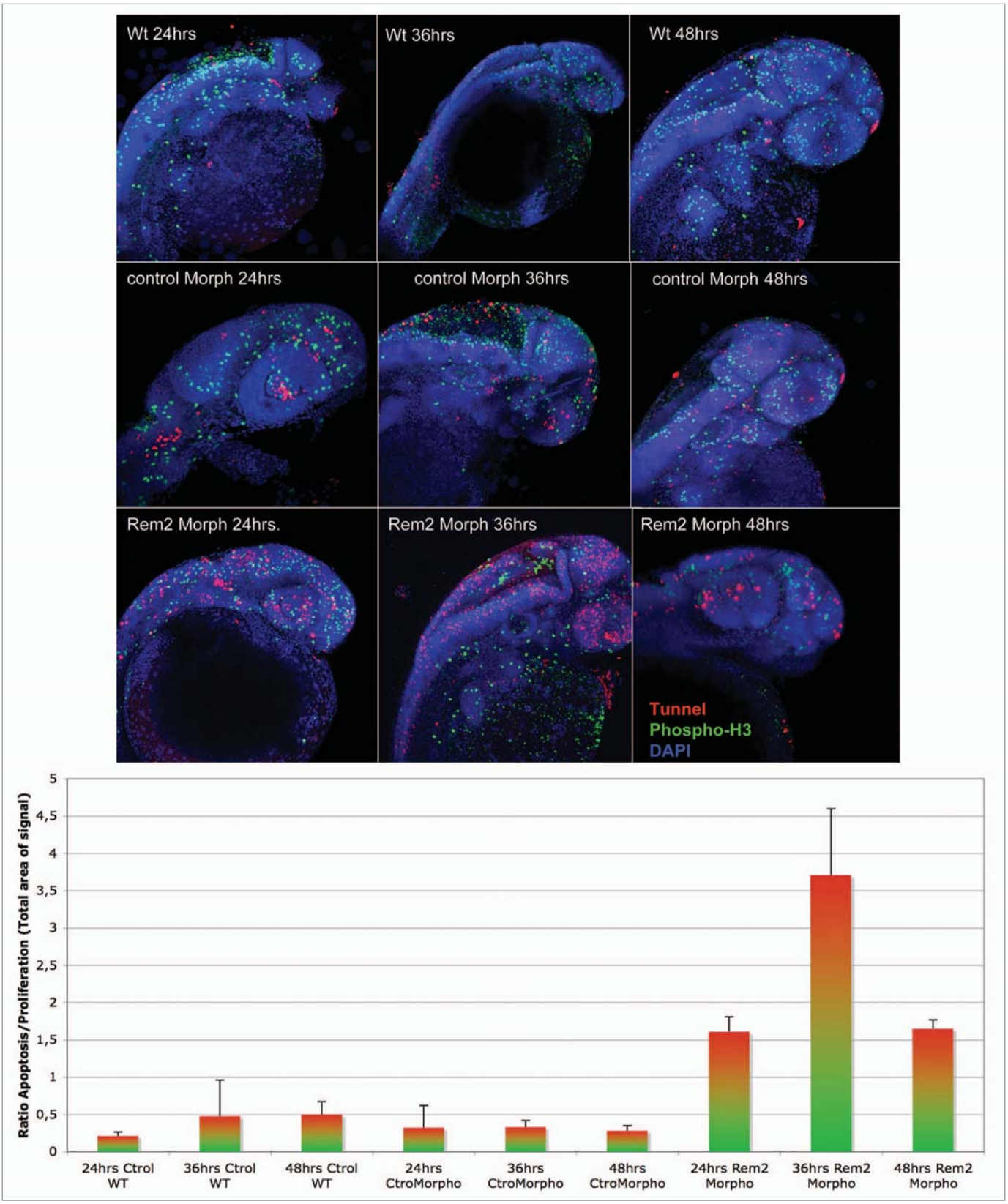

Figure 4. Rem2 controls proliferation and apoptosis of neurons during embryo development. Top parts: Confocal photographs of double staining for Tunnel (red) and phospho-H3 antibody for proliferation (green) in whole wild type, morpholino control and Rem2 morpholino from 24 hours to 48 hours zebrafish embryo development. Note the increase in apoptosis with Rem2 morpholino at 36 hours. Lower part: quantification of the amount of apoptosis and proliferation expressed as a ratio of apoptosis to proliferation. Note a 3.5 fold increase with Rem2 morpholino at 36 hours.

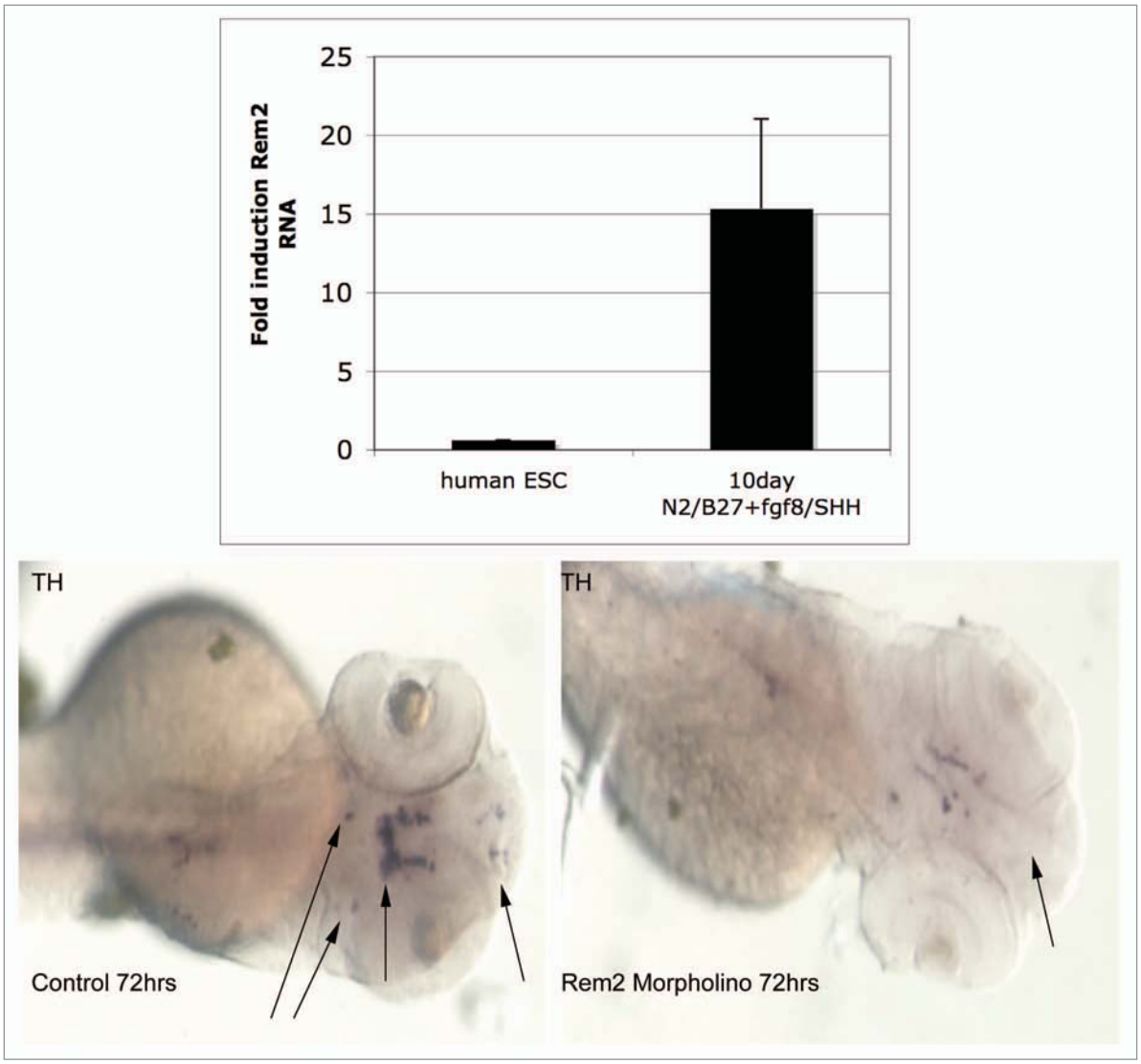

Figure 5. Model of Rem2 function in pluripotency and differentiation. Top Part: Graph of real time PCR of Rem2 mRNA expression levels in hESc and after 10 days differentiation towards neuronal cells. Bottom Parts: Photos of in situ analysis of the dopamine neuron marker TH in control morpholino compared to Rem2 morpholino at 72 hours development. Note the clear decrease in TH signal with Rem2 morpholino and complete absence of signal in the anterior part of the brain (arrows).

27°C in a recirculating aquaculture system equipped with carbon filtration, ultraviolet light sterilizers and biofiltration (Aquatic Habitats). Fertilized eggs obtained from mating pairs of adult zebrafish were cultured in Holtfreter's solution (60 mM NaCl, 2.4 mM sodium bicarbonate, 0.8 mM calcium chloride, 0.67 mM potassium chloride) containing streptomycin and penicillin. Phenylthiourea (PTU, Sigma-Aldrich) was added for a final concentration of 0.003% to prevent pigmentation of embryos (up to 3 dpf) and larvae (>3 dpf).

Bioinformatics analysis to identify *Danio rerio* Rem2 gene. To identify the zebrafish ortholog of the human Rem2, we started with blating (http://genome.ucsc.edu/blat) the human Rem2 protein sequence, as well as other RGK family members, in order to identify the genomic location of a potential Rem2 by excluding from the hit list the genomic sequence of other members of the RGK family. There were two hits on chromosome 2 (one on the negative strand, and one on the positive one), which when extended and blasted against the NR protein database at NCBI hit a putative transposase, as well as an unannotated zebrafish protein (XP_001333620) and human Rem2. The gene structure (location of the exon-exon boundaries) of this hypothetical protein matches the structure of the human Rem2 gene. Moreover, when blated back to the human genome, the best hit for this protein is the human Rem2 genomic location on chromosome 16. We integrated this protein sequence, which we identify as the Rem2 zebrafish homolog into the multiple alignment of the RGK family, and drew a tree using MEGA3,[13] with a bootstrap of 1,000. We found a mRNA clone corresponding to this protein sequence in the databases with the accession number gi 114118945.

Cloning *Danio rerio* Rem2. The zebrafish Rem2 gene was cloned from zebrafish RNA using primers designed at the 3

prime and 5 prime ends of the annotated sequence described in **Figure 1**. (FOR: GAG CTG ATG AAC TGA GGA ACG. REV: CGG TGG TCT CTC TCA TCT CC). A PCR product was produced using Taqman high fidelity kit following manufacturers instructions and cloned into PCR 2.1 vector using the poly A hangover. The resulting plasmid was sequenced to verify the correct DNA sequence and used in subsequent experiments. For whole embryo in situ analysis, full-length wild type Rem2 or a shorter 330 bp probe were used as probes and data presented in this paper are from the full-length probe. In situ hybridisation was performed as previously described.

Real time PCR and whole embryo in situ hybridisation. Total mRNA was isolated using TRIZOL and 1 ug was used to synthesize cDNA using the Invitrogen Cloned AMV First-Strand cDNA synthesis kit. For Rem2 and Oct3/4 we used the following primers:

ZF Rem2. FOR: AAT CTG CGA CTC CAC AAA TCA G

REV: GAC TCT GAA ACC CAA GCA GC

ZF Oct3/4 (Pou5f1). FOR: GGT TCG GAA GCC CAG GAT T

REV: TGA GCT GAG GGA ATG TTT TGC

House keeping gene. Rpl 13A

FOR: GTC TGA AAC CCA CAC GCA AA

REV: GCC AAC TTC ATG GGC CAA T.

RNA probes were prepared using digoxygenin-UTP. In situ hybridization was performed essentially as described by.[14] Two probes were made, a full length, which photos in **Figure 2** are presented and a N-terminal probe.

Full Length:

FOR: GAG CTG ATG AAC TGA GGA ACG; REV: CGG TGG TCT CTC TCA TCT CC.

N-Terminal:

FOR: GAG CTG ATG AAC TGA GGA ACG; REV:CGA AGT GGT CCG TGG TAC TT.

The TH probe was a kind gift of Amy Rubinstein.[15] Briefly, larvae were hybridized with probe overnight at 70°C in 50% formamide buffer. After several washes, larvae were incubated overnight with an antibody to digoxygenin conjugated to alkaline phosphatase (Roche Molecular Biochemicals). After several additional washes, larvae were developed in an alkaline solution containing nitro blue tetrazolium (NBT) and 5 bromo-4-chloro-3-indolyl phosphate (BCIP). Larvae were dehydrated in methanol and impregnated with methyl salicylate prior to mounting on glass slides.

Rem2 morpholino. A morpholino (purchased from Gene Tools) was designed to hybridize to the 5 prime untranslated region of the Rem2 gene. The Rem2 morpholino (0.25 mM) was injected into embryos at the 1- to 4-cell stage. Primers were designed from zebrafish genomic sequence generated by the Sanger Institute (http://www.ensembl.org). Morphonlino sequences were as follows:

Rem2 morpholino:

(5-3): CGT GAA AGC GAA GAT TTT ACC TGG T

Control morpholino:

(5-3): CGT cAA AGg cAA GAT TTT AgC TcG T.

Apoptosis and proliferation assay. Apoptosis was measured in whole embryos using tunnel kit following manufactures instructions (Roche). Proliferation was measured in whole embryos using antibodies to phospho-H3 as a dual stain with tunnel. Briefly, embryos were blocked and photpho-H3 antibody applied over night at 4°C. The next day secondary anti rabbit Cy3 conjugated antibody was applied for 2 hours 37°C, washed 3 times in TBS, stained with DAPI (1:10,000) for 10 minutes and then fixed in 4% PFA for 50 minutes at R/T. Next, the TUNNEL kit from Roche was used following manufacturers instructions including an amplification step with anti-Rhodamine biotinylated for 2 hours R/T, overnight 4°c and then for a further 2 hours R/T. Embryos were then washed, incubated with Steptavidin Alexa 568 (red) at 1:400 for 1 hour at 37°C, washed again and mounted in mounting medium. Photographs of whole embryos were taken using confocal microscopy.

Culture of human embryonic stem cells (hESC). hESC were derived and fully characterized at the CMR[B].[16] They were maintained on either human feeder layers or on matrigel coated plates with HUES medium, consisting of KO-DMEM (Invitrogen) supplemented with 10% KO-Serum Replacement (Invitrogen), 0.5% human albumin (Grifols, Barcelona, Spain), 2 mM Glutamax (Invitrogen), 50 μM 2-mercaptoethanol (Invitrogen), non-essential aminoacids (Cambrex) and 10 ng/ml bFGF (Peprotech). Cultures were maintained at 37°C, 5% CO_2, with media changes every other day. hESC were routinely tested for normal karyotype. For hESC lines adapted to matrigel coated plates, HUES conditioned media from irradiated MEFs was used instead. MEFs were cultured using 10% FCS with DMEM. Differentiation towards endoderm, mesoderm and neuroectoderm was carried out by plating EBs on gelatin and DMEM medium with 20% FCS changed every second day for 2–3 weeks. Cells were then stained for appropriate markers described in the figures. Guided differentiation of EBs towards neurons was performed using FGF2/FGF8/SHH supplemented media.

Quantification using computer aided analysis software. Analysis of signal in whole embryos was done using computer assisted video analysis using Metamorph software. Briefly, a region of interest was set in a photograph of the whole embryo, a threshold for color set and exported directly to Excel for analysis. All data was analyzed using excel spreadsheet software for mean and standard deviation.

Acknowledgements

The authors are indebted to Marina Raya, Chris Jopling and Fabregat Maria Carme for the zebrafish work. Amy Rubinstein for the TH probe. Esther Melo, Lola Mulero Pérez and Mercé Martí Gaudes for bioimaging assistance. This work was partially supported by grants from CIBER, TERCEL, Marato and the Fondo de Investigaciones Sanitarias (P1071209). Cristina Menchon is partly supported by a pre-doctoral grant from the Spanish Ministry (AP-2004-3523).

Notes

Supplementary materials can be found at: www.landesbioscience.com/supplement/EdelCC9-17-sup.pdf

References

1. Edel MJ, Menchon C, Menendez S, Consiglio A, Raya A, Izpisua Belmonte JC. Rem2 GTPase maintains survival of human embryonic stem cells as well as enhancing reprogramming by regulating p53 and cyclin D1. Genes & development 2010; 24:561-73.

2. Maguire J, Santoro T, Jensen P, Siebenlist U, Yewdell J, Kelly K. Gem: an induced, immediate early protein belonging to the Ras family. Science New York, NY 1994; 265:241-4.
3. Reynet C, Kahn CR. Rad: a member of the Ras family overexpressed in muscle of type II diabetic humans. Science New York, NY 1993; 262:1441-4.
4. Bierings R, Beato M, Edel MJ. An endothelial cell genetic screen identifies the GTPase Rem2 as a suppressor of $p19^{ARF}$ expression that promotes endothelial cell proliferation and angiogenesis. The Journal of biological chemistry 2008; 283:4408-16.
5. Paradis S, Harrar DB, Lin Y, Koon AC, Hauser JL, Griffith EC, et al. An RNAi-based approach identifies molecules required for glutamatergic and GABAergic synapse development. Neuron 2007; 53:217-32.
6. Becker JA, Befort K, Blad C, Filliol D, Ghate A, Dembele D, et al. Transcriptome analysis identifies genes with enriched expression in the mouse central extended amygdala. Neuroscience 2008; 156:950-65.
7. Lee MS, Jun DH, Hwang CI, Park SS, Kang JJ, Park HS, et al. Selection of neural differentiation-specific genes by comparing profiles of random differentiation. Stem cells (Dayton, Ohio) 2006; 24:1946-55.
8. Treff NR, Vincent RK, Budde ML, Browning VL, Magliocca JF, Kapur V, et al. Differentiation of embryonic stem cells conditionally expressing neurogenin 3. Stem cells (Dayton, Ohio) 2006; 24:2529-37.
9. Lamason RL, Mohideen MA, Mest JR, Wong AC, Norton HL, Aros MC, et al. SLC24A5, a putative cation exchanger, affects pigmentation in zebrafish and humans. Science (New York, NY) 2005; 310:1782-6.
10. Takahashi K, Mitsui K, Yamanaka S. Role of ERas in promoting tumour-like properties in mouse embryonic stem cells. Nature 2003; 423:541-5.
11. Ivanova N, Dobrin R, Lu R, Kotenko I, Levorse J, DeCoste C, et al. Dissecting self-renewal in stem cells with RNA interference. Nature 2006; 442:533-8.
12. Galan-Caridad JM, Harel S, Arenzana TL, Hou ZE, Doetsch FK, Mirny LA, et al. Zfx controls the self-renewal of embryonic and hematopoietic stem cells. Cell 2007; 129:345-57.
13. Kumar S, Tamura K, Nei M. MEGA3: Integrated software for Molecular Evolutionary Genetics Analysis and sequence alignment. Briefings in bioinformatics 2004; 5:150-63.
14. Thisse C, Thisse B. High-resolution in situ hybridization to whole-mount zebrafish embryos. Nature protocols 2008; 3:59-69.
15. McKinley ET, Baranowski TC, Blavo DO, Cato C, Doan TN, Rubinstein AL. Neuroprotection of MPTP-induced toxicity in zebrafish dopaminergic neurons. Brain research 2005; 141:128-37.
16. Raya A, Rodriguez-Piza I, Aran B, Consiglio A, Barri PN, Veiga A, et al. Generation of Cardiomyocytes from New Human Embryonic Stem Cell Lines Derived from Poor-quality Blastocysts. Cold Spring Harbor symposia on quantitative biology 2008.

Edel et al: Supl Fig 1: Gene structure of this hypothetical protein for Rem2 for Zebrafish.

Alignment of hypothetical_prot_zebrafish and chr2:35536667-35586289

Click on links in the frame to the left to navigate through the alignment. Matching bases are colored blue and capitali

hypothetical_prot_zebrafish

```
msdQGYGLTL SAAPPLRRGS TPLPIKHQLR REEAVSEEYD WTPGLNESAT PQISVtNIQD   60
SPSLKPPQQK YHGPLRIVLL GQNGVGKSSL ALCLAGLSDR SLSIDSETQA ADEGYPRRVT  120
VDDEDSSILV YDNWKQELST LQCEVCILVF SLTDRRSFHR IAQLRLLLRE SLPHTPIILV  180
GNKSDLVRSR EISTEEAHSS AMMFGCLYLE LSVSLDHRTN DLLEAAVRAA RGHSLGPGWT  240
EGSPSAARRE SLTSRAKRFL SGLVPRSHLG RERDREPGRD RDLSRHRGSR MLRQKSRSCH  300
DLSALM
```

Edel et al: Supl Fig 2: Acridine Orange assessment of Apoptosis at 48 hours with Rem2 Morpholino.

WT embryos, Rem2-MO1 injection (0.25mM), 48hpf

WT embryos, non-injected 48hpf

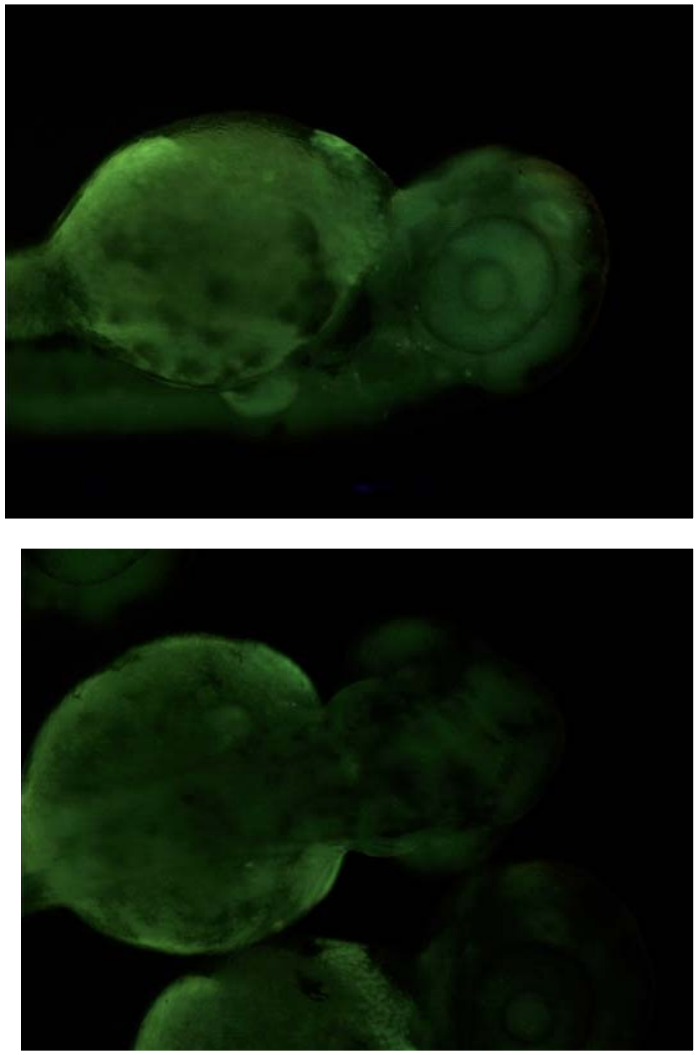

A protocol to assess cell cycle and apoptosis in human and mouse pluripotent cells

Michael J. Edel [1,2,3], Cristina Menchon[1], Jose Miguel Andres Vaquero[1] and Juan Carlos Izpisua Belmonte[1,4 *].

1. Center of Regenerative Medicine in Barcelona, Dr. Aiguader 88, 08003 Barcelona, Spain.

2. Current address: Vall d' Hebron Research Institute, Xcelia and Banc de Sang i Teixits, Passeig Vall d'Hebron, 119 – 129, 08035 Barcelona, Spain.

3. Affiliation with Victor Chang Cardiac Research Institute, Lowy Packer Building 405 Liverpool St, Darlinghurst New South Wales 2010, Australia.

4. Gene Expression Laboratory, Salk Institute for Biological Studies, 10010 North Torrey Pines Rd., La Jolla, California 92037, USA

* Corresponding author: belmonte@salk.edu; izpisua@cmrb.eu

ABSTRACT

Embryonic stem cells (ESC) and induced pluripotent stem cells (iPSCs) present a great opportunity to treat and model human disease as a cell replacement therapy. There is a growing pressure to understand better the signal transduction pathways regulating pluripotency and self-renewal of these special cells in order to deliver a safe and reliable cell based therapy in the near future. Many signal transduction pathways converge on two major cell functions associated with self-renewal and pluripotency: control of the cell cycle and apoptosis, although a standard method is lacking across the field. Here we present a detailed protocol to assess the cell cycle and apoptosis of ESC and iPSCs as a single reference point offering an easy to use standard approach across the field.

INTRODUCTION

Human embryonic stem cells (hESC) have been derived from the inner cell mass of blastocytes and can be maintained *in vitro* indefinitely with the addition of fibroblastic growth factor 2 (FGF2) [1]. It has been shown that a combination of three or four pluripotency transcription factors; Oct4, Sox2 and KLf4, with or without Myc can reprogram somatic cells to generate induced pluripotent stem cells (iPSC) [2]; [3]. Recently, it has been shown that loss of p53 function can enhance the efficiency of reprogramming, suggesting that the cell cycle is a rate limiting step in the reprogramming process [4]; [5]; [6]; [7]; [8]; [9]; [10]. Given the important role of the cell cycle and apoptosis in pluripotent cells, a detailed protocol that standardises the technique of measuring cell cycle and apoptosis in pluripotent cells across the field is called for.

The cell cycle of mouse ESCs and to a lesser extent hESCs has been well described [11-13]. The cell cycle regulatory machinery of ESC including the Cyclin families A, E, D, and B and their kinases CDK2, 4 and 6, are not regulated in a cyclic fashion, with the exception of cyclin B [11, 12]. Of the core machinery, cyclin A/E/CDK2 are regarded as constitutively on in mouse ESC driving an almost non-existent G_1 phase into S phase, in which 60-70% of ESC are present. Consequently, the rate of ESC proliferation is much faster with an average cycle lasting just twelve hours compared to somatic cells [13, 14]. A recent study functionally demonstrated that Cyclin A regulates pluripotency but is redundant in fibroblasts suggesting it is a pluripotent associated cell cycle kinase [15]. Many of the peripheral genes that control cell cycle such as $p16^{INK4a}$ are thought to be inactive, resulting in a different regulation of cell cycle in mouse ESC [16]. It is evident that there are many differences between somatic and pluripotent cells; however, little is known about the role of the cell cycle in maintaining ESC or iPSC in culture. Much less is known about control of apoptosis in ESC or iPSC while under *in vitro* conditions.

Here we describe a protocol how to measure cell cycle and apoptosis in pluripotent stem cells (hESC and iPS cells) that could be used, for example, following infection with a lentivirus to manipulate cell cycle function of ESC or iPSC *in vitro*. Detailed protocols how to make lentivirus have been published previously [17], [18], [19]. We describe a standard method to measure cell cycle profile by FACs in hESC and iPS cells using EdU substrate; and apoptosis using DilC mitochondrial membrane method in the same sample concurrently. The use of DNA dyes and EdU staining (an advance on BRDU staining) has been discussed extensively by Cappella et al and Hamelik et al [20];[21]. In addition we describe a list of working antibodies for cell cycle and apoptosis proteins

by western blot methodology. The protocol described here is applicable to any human or animal pluripotent stem cell and enables “getting the most” from your cell cycle and apoptosis analyses, offering an easy to reference, comprehensive standardised protocol across the field of pluripotent stem cells.

MATERIALS

For detailed methods on how to make iPSCs as well as how to infect such cells using concentrated lentiviruses and supernatant retroviruses including reagents, equipment and set up please refer to recently published work [17], [18], [19].

REAGENTS

- Human and mouse embryonic stem cells (ESC)

CAUTION: Check ethic issues with your specific institute for use of hESC.

- Human or mouse induced pluripotent stem cells (iPSC)
- Mitotically inactivated mouse embryonic fibroblasts (irMEFs)
- Mitotically inactivated human foreskin fibroblasts (irHFFs) (ATCC, cat. no. CRL-2429)
- 0.1% (wt/vol) Gelatin solution (Millipore, cat. no. ES-006-B)
- Matrigel (Mg, BD Biosciences, cat. no. 356234)
- Dulbecco's PBS, without Ca2+ or Mg2+ (PAA laboratories GmbH, cat. no. H15-002)
- DMEM (Invitrogen, cat. no. 21969-035)
- KO-DMEM (Knockout DMEM, Invitrogen, cat. no. 10829-018)
- Fetal calf serum (FCS, Perbio, Hyclone, cat. no. CH30160.03)

- Heat-inactivated fetal bovine serum (FBS, Invitrogen, cat. no. 10270-106)
- Knockout Serum Replacement (KO-SR, Invitrogen, cat. no. 10828-028)
- Trypan Blue stain (Invitrogen, cat. no. 15250-061)
- 20% (wt/vol) Human serum albumin (HSA, Instituto Grifols SA, cat. no. 670612)
- GlutaMAX (Invitrogen, cat. no. 35050-038)
- Minimum essential medium Eagle's nonessential amino acids, 100× (Lonza, cat. no. BE13-114E)
- Nucleosides, 100× (Millipore, cat. no. ES-008-D)
- Penicillin/streptomycin (Invitrogen, cat. no. 15140-163)
- Lipofectamine 2000 (Invitrogen)
- 50 mM 2-mercaptoethanol (Invitrogen, cat. no. 31350-010)
- Basic fibroblast growth factor (Peprotech cat. no. 100-18B) (see REAGENT SETUP)
- 0.25% (wt/vol) Trypsin/EDTA (Invitrogen, cat. no. 25200-056)
- 0.05% (wt/vol) Trypsin/EDTA (Invitrogen, cat. no. 25300-054)
- Polybrene (10 mg ml−1, Millipore, cat. no. TR-1003-G)
- FuGENE 6 transfection reagent (Roche Applied Science, cat. no. 11 988 387 001)
- DMSO (Sigma, cat. no. D4540)
- MitoProbe DilC assay kit for flow cytometry (M34151)
- Invitrogen Click iT Edu cell proliferation assay kit for flow cytometry (A10202).

EQUIPMENT

- DakoCytomation MoFlo High-performance cell sorter equipped with 3 lasers, an Innova 90C UV laser from Coherent, a red diode 635nm and a Lytcyt200s 488nm solid-state laser. The PMT detectors used are Hamamatsu -15.
- Leica SP5 AOBS confocal microscope

- Water Bath set to 37°C.
- Class-II cabinet with aspirator for tissue culture (Telstar Bio-II-A)
- Class-II cabinet with space for stereomicroscope (Telstar Bio-II-A/G)
- Aspirator tube assembly (Sigma, cat. no. A5177)
- Stereomicroscope (Olympus SZX12, Olympus)
- Low-end color video camera (JVC TKC1481BEG)
- Low-end 8-inch LCD display (BOMAN TV304)
- Inverted tissue culture microscope with phase contrast and epifluorescence, with ×5, ×10, ×20 and ×40 objectives (Leica DMIL, Leica)
- Thermostatized tissue culture centrifuge and swinging rotor with adapters for 15-ml and 50-ml tubes and microplates (Beckman Coulter Allegra X-12R centrifuge with SX4750A rotor, Beckman Coulter)
- High-speed centrifuge and swinging rotor (Beckman Coulter Avanti J-30I centrifuge with JS-24.38 rotor, Beckman Coulter)
- Cell culture incubator set at 37 °C, 5% CO2 (REVCO, cat. no. RCO3000D-9-VBC)
- Cell culture incubator set at 32 °C, 5% CO2 (REVCO, cat. no. RCO3000D-9-VBC)
- Cell culture incubator set at 37 °C, 5% CO2 and 5% O2 (REVCO, cat. no. RTG5000D-9-VBC)
- Microcentrifuge (Eppendorf 5424, Eppendorf)
- Tissue culture dish, 100 and 150 mm
- Tissue culture flasks, T75 and T150
- Tissue culture plates, six-well
- Conical tubes, 15 and 50 ml
- Screw-cap microcentrifuge tubes (Sarstedt, cat. no. 72.692.005)
- Polyallomer centrifuge tubes, 13 × 51 mm (Beckman, cat. no. 326819)

- Cover slips
- Stripper micropipette (Mid Atlantic, cat. no. MXL3-STR)
- Stripper tips, 150 uM (REF MXL3-150) ORIGIO mid-atlantic devices.
- Cryo 1 °C Freezing Container, 'Mr. Frosty' (Nalgene, cat. no. 5100-0001)
- Slide flask (Nunc, cat. no. 170920)
- Bottle-top filter system 0.22 μm, 500 ml (Millipore, cat. no. SCGPU05RE)
- Filter, Mille-HV PVDF (polyvinylidene fluoride) (0.45 μm, Millipore, cat. no. SLHV033RS)
- Invitrogen western blot and transfer equipment.

REAGENT SETUP

Basic fibroblast growth factor (bFGF)

After spinning briefly, resuspend the contents of the vial with 10 ml of 0.2% (wt/vol) HSA in PBS. The final concentration of bFGF is 100 μg/ml. Prepare 50 μl and 100 μl aliquots in screw-cap microcentrifuge tubes and store at minus 20 °C for up to 6 months. Avoid more than three freeze thaw cycles.

10mM EdU solution

Add 4ml of DMSO to EdU substrate, mix well and aliquot into 50ul batches and store at -20C.

Saponin based wash buffer

Add 1ml of Saponin from Click iT kit to 9 mls of PBS for working buffer.

DAPI solution.

CAUTION: DAPI is a known mutagen and should be handled with care. The dye must be disposed of safely and in accordance with applicable local regulations.

0,1M Tris Base pH7,4 (from Sigma ref. T1503; MW=121.14)

0,9% or 150mM NaCl (from Sigma ref. S3014; MW=58.44)

1mM CaCl2 (from Sigma ref. C2661; MW=110.986)

0.5mM MgCl2 (from Merk ref. 1.05833.1000; MW=203.30) – 6H2O

0.2% BSA (from Sigma ref. A4503)

0.1% Nonidet P40 (from Sigma ref. I8896) – Igepal

10µg/mL DAPI (from Invitrogen ref. D21490)

Propidium Iodide (P4170, Sigma-Aldrich) solution

(0.5 mg/ml in PBS with 0.1% sodium azide, pH approximately 7.4)

BOX 1

HES media (for culture of hESc and hIPSC on ir MEF or irHFF feeder layers)

-Knockout DMEM (Gibco #10829-018) (4ºC).

-Knockout Serum Replacement (KSR) (Gibco #10828-028) (-20ºC).

- Non-Essetial Amino Acids 100X (Gibco) (4ºC).

-2-Mercaptoethanol 50mM (Gibco #31350-010) (4ºC).

-Penicillin (10.000U/ml)/Streptomycin (10.000µg/ml) (100X).

(Gibco #15140-122) (-20ºC).

-GlutaMAX 200mM (100X) (Gibco #35050-038) (-20ºC).

- basic Fibroblastic Growth factor 100µg/ml (Peprotech) (-20ºC).

	250ml
-Knock-Out DMEM	193,5 ml
-20% Knock-Out serum replacement	50 ml
-1x Non-Essetial Amino Acids	2,5 ml
-50 U/ml-50µg/ml Penicillin/Streptomycin (P/S)	1,25 ml
-1x GlutaMAX	2,5 ml
-50 µM 2-Mercaptoethanol	250 µl
-8 ng/ml basic Fibroblastic Growth factor	20 µl

HUES media (for culture of hESC or hiPSC independent of feeder layers on matrigel)

-Knockout DMEM (Gibco #10829-018) (4ºC).

-Knockout Serum Replacement (KSR) (Gibco #10828-028) (-20ºC).

- Non-Essetial Amino Acids 100x (Gibco) (4ºC).

-2-Mercaptoethanol 50mM (Gibco #31350-010) (4ºC).

-Penicillin (10.000U/ml)/Streptomycin (10.000ug/ml)(100X)

(Gibco #15140-122) (-20ºC).

-GlutaMAX 200mM (100X) (Gibco #35050-038) (-20ºC).

- basic Fibroblastic Growth factor 100µg/ml (Peprotech) (-20ºC).

-Human albumin 20% (Grifols) (RT).

	300 ml
- Knockout DMEM	250ml
-10% Knockout Serum Replacement	30 ml
-1x Non-Essetial Amino Acids	3 ml
-50µM 2-Mercaptoethanol	0,3 ml
-1x penicillin/Streptomycin (100U/ml, 100µg/ml)	3 ml

-1x GlutaMAX 200mM	3 ml
-10 ng/ml basic Fibroblastic Growth factor	30 µl
-Human albumin 20%	7.5 ml

The use of conditioned media for hESC or hiPSC on matrigel is essential. To make conditioned media, simply add HEUS media to irMEFS over night and the next day fliter through a millipore 0.45uM filter onto cells.

BOX 2

Plating irHFF or irMEF cells

The day before plating ES[4] cells seed irradiated feeders HFF (ATCC) on gelatinized plates. For a 100mm plate:

1. Gelatinize by adding 5ml/dish 0.1% gelatin in water (Chemicon). Incubate at least 30min at 37°C (you can also leave the plate with gelatin overnight at 37°C). Aspirate the gelatin solution and let the plate dry under the hood. **2.** Plate $4x10^6$ cells /100mm plate in DMEM +10%FBS, 1x Glutamax, 1x Pen/Strep.

Plating hESC or hiPSC by trypsinization on matrigel coated plates

When the colonies get big enough and start to touch other colonies is time to passage them. Coating of plates using 1:15 diluted Growth Factor Reduced (GFR) matrigel (from BD) in Knockout DMEM is done the day before at 4°C and has been described previously [19]**.**

- Aspirate media and wash cells with PBS.
- Add 1ml of 0,05% trypsine-EDTA and incubate at 37°C for 2-5 minutes.
- Add 9ml of HUES media and resuspend the cells:

- If you want a single cell suspension: perform a complete trypsinization and pipette up and down several times before plating.
- Plate the cells at the desired dilution, usually 1:6 dilution.
- Don't change the media the following 48 hours after plating.
- Change the media daily. Warm up just the needed media each time.

PROCEDURE

Maintaining ESC and iPSC in culture using matrigel or feeder layers.

For hESC or iPSC on feeder layers, pluripotent cells can be trypsinized and then separated during analysis based on Forward Scatter (FSC). To maintain the line, cells must be passaged using a scrapper via a video screen linked to a stereomicroscope. Pluripotent cell colonies are scrapped off the feeder layer, collected and split into waiting feeder layers no more than 1:3 (for ES cells) and 1:10 (for iPS cells). For hESC or hiPSC maintained on matrigel trypsinization is used (**see box 2**).

CRITICAL STEP: Proper cultivation of pluripotent stem cells to keep cells healthy is essential because it can affect growth rates dramatically, which can be seen by some cell cycle analyses.

Assessment of cell cycle profile and apoptosis by Flow Cytometry from the same sample.

TIMING 3 hours.

We use the Invitrogen Click IT EdU kit for detection of S phase with a modified protocol to give quicker and easier to achieve results. We have tested many DNA dyes and DAPI has been found best DNA staining for pluripotent cells, especially when samples are left overnight at 4°C (**Figure 1**). For assessment of apoptosis we use the

MitoProbe DiLC assay kit (M34151). Pluripotent cells can be split after EdU treatment into two tubes, one for EdU assessment of cell cycle profile and the other for assessment of apoptosis by DiLC (Mitochondrial membrane potential). In that way both measures can be made from the same sample.

BOX 3: Getting the most out of your cell cycle flow cytometry analysis.

In addition to information about the percent of cells in each of the phases of the cell cycle from EdU/DAPI staining, extra information about the proliferative state of the cells can be gleaned from the analysis.

(A). To the right of the percentages of each phase in Flow Cytometry analysis histograms there are two values (**figure 2).** The first is the mean intensity of signal from DAPI and the second is the intensity of signal for EdU. The value for EdU is an indication of how fast the cells are proliferating because the faster they proliferate the more EdU they will absorb. Therefore this number can act as a guide to the S phase percentages when assessing how fast they are proliferating. Be careful to ensure to use the same concentration of EdU (10uM) for the same time period (45 minutes exposure to cells) with the same density of pluripotent cells for all experiments. **(B).** A second piece of information that can be taken from the cell cycle Flow Cytometry analysis is a clear separation of the 3 phases; G1, S and G2/M phases (**Figure 2).** A clear separation is desirable with the S phase high above the other phases. If this is not the case it means that the EdU staining did not work or the pluripotent cells are not healthy and not proliferating normally (they could be quiescent. Ensure to check that the pluripotent cells are healthy before experiments.

Assessment of cell cycle profile by flow cytometry.

CRITICAL STEP Make sure pluripotent cells are between 40-60% confluent in all experiments because cell density affects the final results (**Figure 2**).

1. Label the cells with EdU substrate by adding 10ul of 10mM EdU solution to 10mls of culture medium in 10cm plate of cells (a 1:1000 dilution) to make a 10uM final working concentration and incubate for 45 minutes at 37°C 5% CO2. **See Table 1.**

2. We have found that for pluripotent cells leaving the EdU for 45 minutes is optimal[4].

3. Wash cells once with PBS and harvest cells by trypsinization for pluripotent cells cultured on matrigel or by scrapping the cells off the feeder layer to get pure pluripotent cell population. Timing 10 minutes.

4. Wash the cells again in PBS and transfer cells to Flow Cytometry tubes. Spin down at 1500rpm for 2 minutes to form pellet. Remove PBS simply by turning tube upside down into a waste container with one quick movement, drying the edges on paper to remove drops at edge of tube. This leaves approximately 50ul of PBS in the FACS tube.

CRITICAL STEP: Tapping the tube only once upside is essential otherwise the cells will slide out.

CAUTION: EdU cocktail breaks down GFP signal that may be expressed in genetically modified pluripotent cells being used, but not the Alexa fluor dyes. Therefore consider

adding an anti-GFP AlexaFluor-488 conjugated antibody step to cells before labelling with EdU cocktail to retrieve the GFP signal.

5. Add 100µl of Click IT fixative for 15 minutes R/T and mix well by vortex.

6. Wash once 3mls of PBS and pellet cells again at 1500rpm for 2 minutes and discard wash buffer by inverting the Flow Cytometry tube as described above..

7. Permeabilize the cells by adding 100µl of saponin based wash buffer for 30 minutes R/T.

8. Wash with 3mls of saponin based wash buffer and pellet cells again.

9. Add **Click IT reaction cocktail** and add 500 µl per Flow Cytometry tube and incubate for 30 minutes R/T in the dark.

10. Wash once with PBS, pellet cells and add **DAPI solution** and incubate overnight at 4°C and analyse the following day for best results or leave at 4ºC for at least 2h for immediate FACS analysis.

CRITICAL STEP: We have tried different DNA dyes (PI, Hoechst33342, Click-iT EdU Cell Cycle 633-red, 7AAD, and in our hands the best cell cycle profiles in terms of lowest coefficients of variation for the G0/1 peak came up when using DAPI.

11. Assess a minimum of 10000 events at levels described in **Table 2.**

CRITICAL STEP: Check to ensure that you flow cytometry machine has PMT detectors that are Hamamatsu -15, which are very sensitive. If not higher powers of 100-200mW may be needed to detect DAPI.

Assessment of Apoptosis using DiLC by Flow Cytometry analysis.

We have assessed two methods for measuring apoptosis in pluripotent cells including DiLC and Annexin V. We found that DiLC gave the best results. Annexin V is not suitable for trypisination of pluripotent cells because it causes false positives **(see Figure 3 and Table 3).**

TIMING 2 hours.

12. The other sample of pluripotent cells split from the original is used to assess levels of apoptosis.

13. Use the MitoProbe DiLC Assay Kit for Flow Cytometry (M34151) from Invitrogen to measure mitochondrial membrane potential.

14. Tripsinize or scrape pluripotent cells from plate and pellet cells by centrifuge and place in pre-warmed (37°C) PBS.

CRITICAL STEP Maintain the cells at 37°C at all times in a water bath for stable membrane potential. Having access to a water bath in the flow cytometry machine room is advised.

15. Wash cells again in 1ml pre-warmed PBS in Flow Cytometry tubes and pellet.

16. For control tubes add 1uL of 50mM CCCP and incubate cells at 37°C for 5 minutes.

CRITICAL STEP: Including a CCCP (it is a metabolic inhibitor) control is essential to clearly define within the histogram analysis the cut-off between the apoptotic and alive populations in the first experiments and to determine that the apoptosis assay is working. Adding CCCP causes loss of mitochondrial membrane potential (MMP) and should cause a shift of cells out of the top left where alive cells can be found **(Figure 3).**

17. Add 5uL of 10µM DilC (can be added at same time with CCCP for controls) and incubate at 37°C, 5% CO_2 for 30 minutes).

18. Wash with 3 mls of pre-warmed PBS and pellet cells and discard wash by tipping once and drying edges (50uL of solution is left with this method).

19. Resuspend cells with 100uL of propidium iodide (PI) solution and incubate for 15 minutes at 37°C.

20. Proceed to analyser to assess percent of cells apoptotic/alive/dead (**see figure 3**).

21. Assess a minimum of 10,000 events.

CRITICAL STEP: samples must be analysed immediately to ensure the membrane is preserved. Heating the DAKO MoFlo flow cytometer tubing to 37°C is recommended. With the MoFlo, the sample port can be set at any temperature with a range 0ºC- 40º. Because the 37ºC is important in order to maintain the MMP, taking advantage of this feature in your flow cytometry machine will help maintain valid results.

Western Blot methodology

We include a list of antibodies that have been tried and tested for detecting cell cycle proteins and apoptosis proteins in pluripotent cells (**Table 4**). These selected antibodies, of some of the main cell cycle proteins, work with resolving SDS gels of 4-12% using between10-15 µg of total protein unless specified in **table 4.** If non resolving gels are used then use 8% gels for Rb, p107, cdc27 and MDM2, which are 80Kda or bigger proteins and 12% SDS gels for all others. See **figure 4** for an example of the expected results for pluripotent cells using some of these antibodies. Using 10 well gels, up to four lysates can be loaded twice on one gel, with protein molecular weight markers and four gels run at the same time (two gels per container). Each membrane can be blotted twice for two different antibodies from different species (i.e. first with mouse antibodies, and developed and then re-blotted with the rabbit primary antibodies and developed again) and a final time for alpha tubulin as a loading control (not listed). Therefore, up to 16 antibodies can be tested from the 4 gels using between 40 and 60 µg of total protein. If manipulating a cell cycle gene by gain of function (cDNA) or loss of function (shRNA), then protein lysates can be run alongside the ESC lane to determine the overall effect on core cell cycle protein expression levels.

DISCUSSION

Accurate cell cycle analysis has to be based on data from cells handled in a manner in which the least variation between experiments occurs. In our hands the reliability and validity of the described method for measurement of apoptosis and cell proliferation in the same sample is very good. In the past other methods have been developed to measure cell proliferation that provide an alternative approach **(see trouble shooting**

table 5). Specifically, the use of other DNA dyes may improve the method in different laboratories with different machines. Other DNA specific dye, such as propidium iodide (PI) can be added to the labelled cells for two-parameter analysis of EdU. We settled on DAPI (overnight at 4°C) giving the most reliable results. In our experience with EdU stainings for flow cytometry analysis, the CVs have remained low and reproducible with DAPI staining and not 7-AAD (a modification from the kit). To achieve this we recommend that factors such as cell culture conditions are maintained well, exposure time of substrate and concentration (as well as storage of substrate) is maintained well and that cell density is equal between experiments (**see figure 1**). Other methods for assessment of cell cycle have been published before. Krishan and Hamelik have modified the EdU procedure as an alternative method to the one we have described (20). In comparison to our method, the method involves a more laborious step of isolation of cell nuclei. Moreover, the requirements and complexicity of the method is more demanding. Therefore, to maintain simplicity and ease in use of the protocol with low CVs we prefer to use DAPI staining with EdU, and give the same results compared to using BRDU **(see Figure 2).**

We chose EdU click IT kit over standard BRDU staining for S phase analysis because it gave reliable results and was quicker to complete with the same results **(Figure 2).** It is important to note that the Click-it method breaks down GFP signal so we recommend to use an anti-GFP antibody to recognize GFP expression, since it uses copper sulfate and ascorbate to develop a signal. Other methods have suggested to fix the cells in dilute paraformaldehye which keeps the GFP intact prior to staining (21). We agree that fixing cells with dilute paraformaldehyde can preserve the GFP signal, however in our hands, using an anti-GFP AlexaFluor-488 antibody, a flurochrome that is not degraded during

the reaction cocktail step, helps to retrieve the GFP signal, a significant advantage with pluripotent cells that are so often hard to infect/transfect. Given that ESC are notoriously difficult for gain and loss of gene function studies, retrieving the GFP signal with an Alexaflour 488 GFP antibody, gives an advantage to attaining the best results form flow cytometry work.

Flow Cytometry machines available to researchers from lab to lab will vary and that different machines will require different power settings. The machine used in this protocol is a High Performance MoFlo Cell sorter. The MoFlo is equipped with 3 lasers, an Innova 90C UV laser from Coherent, a red diode 635nm and Lytcyt200s 488nm solid-state laser. The PMT detectors used are Hamamatsu -15; this is the most sensitive model and therefore low power levels at 30mW are used. If we work with 100-200mW of power the signal would be out of range. The best resolution of DNA signals may require more power using different machines; however, this would depend on DNA dye used. For example Hoechst dye exclusion assays to identify the side population in a bone marrow just require 20-30mW of UV power using a machine not equipped with a Hamamatsu-15 detector.

The faster cells proliferate when the cells are exposed to BrdU or EdU for a fixed amount of time means more cells labeled in late S, G_2 or M phases. The main data from EdU staining is S phase percentages but we thought to also highlight that the mean intensity of signal can also be used a secondary guide as well. When working with a fixed amount of time and EdU concentration as recommended in our protocol, the difference in the EdU Signal to Noise ratio (S/N) can be directly related with how fast they are growing. The more time exposure and the more concentration of EdU the

higher the S/N ratio and for this reason it is important to use pluripotent cells at around 50-60% confluency, the same concentration of EdU and also the same incubation time for all the treated samples. We recommend that 10uM EdU and 45 minutes to be used across the field for pluripotent cells. In that way coefficient of variation can be calculated intra-laboratory for many different pluripotent cell lines and we have found very little variation between experiments when this protocol is followed correctly.

CONCLUSIONS

At the end of the protocol a comprehensive analysis of the percent of cells in G_0/G_1 phase, S phase and G_2/M phase should reveal an expected percentages of cells in each phase as: 15%/65%/20% +/- 5%, respectively. Changes greater than 5% in the G_1 or G_2/M phases between samples of interest are considered significant and a change of 10% or more in the S Phase is considered significant. Further evidence of an effect on cell cycle can be done by performing a proliferation growth curve to show differences more clearly. In our experience, differences even less than 10% in S phase can be seen in proliferation curves maintained for over 2 to 3 weeks. Western Blot analysis should reveal a protein expression for the main cell cycle proteins as seen in **figure 4.** Apoptosis measurements by FACs should give a normal range of 70-75% of cells alive, 20% in transition and 5-10% apoptosis using DilC combined with PI methods. Overall, this protocol will give rise to a detailed analysis of the cell cycle and apoptosis status in human and mouse pluripotent cells, offering a standardized approach across the field. For more details of making lentivirus and infection of ESC, please see previous published work from our group (17-19).

COMPETING INTERESTS

The authors declare that they have no competing interests.

ACKNOWLEDGMENTS

The authors are indebted to Meritxell Carrió for expert assistance with cell culture techniques. Cristina Menchon is partly supported by a pre-doctoral grant from the Spanish Ministry (AP-2004-3523). This work was partially supported by grants from the Fondo de Investigaciones Sanitarias, Insituto Carlos III (P1071209), MICINN, Fundacion Cellex, CIBER, Sanofi-Aventis and the G. Harold and Leila Y. Mathers Charitable Foundation.

AUTHOR CONTRIBUTIONS

M.J.E. designed the overall protocol, wrote the manuscript after obtaining material from all authors. J.M.A.V. developed the flow cytometry protocol and performed low cytometry experiments. C.M. developed and tested the western blot methods. J.C.I.B. supervised the project.

All authors have read and approved the final manuscript.

REFERENCES.

1. Thomson JA, Itskovitz-Eldor J, Shapiro SS, Waknitz MA, Swiergiel JJ, Marshall VS, Jones JM: Embryonic stem cell lines derived from human blastocysts. *Science* 1998, 282:1145-1147.
2. Takahashi K, Yamanaka S: Induction of pluripotent stem cells from mouse embryonic and adult fibroblast cultures by defined factors. *Cell* 2006, 126:663-676.

3. Takahashi K, Tanabe K, Ohnuki M, Narita M, Ichisaka T, Tomoda K, Yamanaka S: Induction of pluripotent stem cells from adult human fibroblasts by defined factors. *Cell* 2007, 131:861-872.

4. Edel MJ, Menchon C, Menendez S, Consiglio A, Raya A, Izpisua Belmonte JC: Rem2 GTPase maintains survival of human embryonic stem cells as well as enhancing reprogramming by regulating p53 and cyclin D1. *Genes Dev* 2010, 24:561-573.

5. Zhao Y, Yin X, Qin H, Zhu F, Liu H, Yang W, Zhang Q, Xiang C, Hou P, Song Z, et al: Two supporting factors greatly improve the efficiency of human iPSC generation. *Cell Stem Cell* 2008, 3:475-479.

6. Li H, Collado M, Villasante A, Strati K, Ortega S, Canamero M, Blasco MA, Serrano M: The Ink4/Arf locus is a barrier for iPS cell reprogramming. *Nature* 2009, 460:1136-1139.

7. Kawamura T, Suzuki J, Wang YV, Menendez S, Morera LB, Raya A, Wahl GM, Belmonte JC: Linking the p53 tumour suppressor pathway to somatic cell reprogramming. *Nature* 2009, 460:1140-1144.

8. Hong H, Takahashi K, Ichisaka T, Aoi T, Kanagawa O, Nakagawa M, Okita K, Yamanaka S: Suppression of induced pluripotent stem cell generation by the p53-p21 pathway. *Nature* 2009, 460:1132-1135.

9. Marion RM, Strati K, Li H, Murga M, Blanco R, Ortega S, Fernandez-Capetillo O, Serrano M, Blasco MA: A p53-mediated DNA damage response limits reprogramming to ensure iPS cell genomic integrity. *Nature* 2009, 460:1149-1153.

10. Utikal J, Polo JM, Stadtfeld M, Maherali N, Kulalert W, Walsh RM, Khalil A, Rheinwald JG, Hochedlinger K: Immortalization eliminates a roadblock during cellular reprogramming into iPS cells. *Nature* 2009, 460:1145-1148.

11. Savatier P, Lapillonne H, Jirmanova L, Vitelli L, Samarut J: Analysis of the cell cycle in mouse embryonic stem cells. *Methods Mol Biol* 2002, 185:27-33.

12. Stead E, White J, Faast R, Conn S, Goldstone S, Rathjen J, Dhingra U, Rathjen P, Walker D, Dalton S: Pluripotent cell division cycles are driven by ectopic Cdk2, cyclin A/E and E2F activities. *Oncogene* 2002, 21:8320-8333.

13. White J, Dalton S: Cell cycle control of embryonic stem cells. *Stem Cell Rev* 2005, 1:131-138.

14. Becker KA, Ghule PN, Therrien JA, Lian JB, Stein JL, van Wijnen AJ, Stein GS: Self-renewal of human embryonic stem cells is supported by a shortened G1 cell cycle phase. *J Cell Physiol* 2006, 209:883-893.

15. Kalaszczynska I, Geng Y, Iino T, Mizuno S, Choi Y, Kondratiuk I, Silver DP, Wolgemuth DJ, Akashi K, Sicinski P: Cyclin A is redundant in fibroblasts but essential in hematopoietic and embryonic stem cells. *Cell* 2009, 138:352-365.

16. Faast R, White J, Cartwright P, Crocker L, Sarcevic B, Dalton S: Cdk6-cyclin D3 activity in murine ES cells is resistant to inhibition by p16(INK4a). *Oncogene* 2004, 23:491-502.

17. Tiscornia G, Singer O, Verma IM: Design and cloning of lentiviral vectors expressing small interfering RNAs. *Nat Protoc* 2006, 1:234-240.

18. Tiscornia G, Singer O, Verma IM: Production and purification of lentiviral vectors. *Nat Protoc* 2006, 1:241-245.

19. Raya A, Rodriguez-Piza I, Navarro S, Richaud-Patin Y, Guenechea G, Sanchez-Danes A, Consiglio A, Bueren J, Izpisua Belmonte JC: A protocol describing

the genetic correction of somatic human cells and subsequent generation of iPS cells. *Nat Protoc* 2010, 5:647-660.

20. Hamelik RM, Krishan A: Click-iT assay with improved DNA distribution histograms. *Cytometry A* 2009, 75:862-865.

21. Cappella P, Gasparri F, Pulici M, Moll J: Cell proliferation method: click chemistry based on BrdU coupling for multiplex antibody staining. *Curr Protoc Cytom* 2008, Chapter 7:Unit7 34.

FIGURE LEGENDS

Figure 1: Analysis of different DNA dyes in pluripotent cells.

Panel A: Comparison of FACs histograms of four different DNA dyes, staining of Jurkat cells, Human ESC and human IPS cells. We found that DAPI gave the best overall profile of the G1, S and G2/M phases of the cell cycle across different cell types described in the figure. **Panel B:** FACs histograms of DAPI staining of mouse ESC at day zero (undifferentiated pluripotent cells) and at different stages of differentiation using general differentiation cell culture conditions (Gelatin coated plates with 20% FCS in DMEM). Note the dramatic changes in the overall profile of the G1, S and G2/M phases of the cell cycle with differentiation.

Figure 2: Analysis of cell cycle.

Panel A: Photographs of hESC at different densities. The table below is an analysis of cell cycle profile using EdU for 30 minutes at 10uM. Note the differences in G1 and G2/M with different cell density. Using cells at 50-60% confluence is optimal. *Lower Panel:* Histogram of hESC treated with BRDU demonstrating a 50-60% of cells in S phase. **Panel B:** Flow cytometry histograms of cell cycle profile of hESC, human IPS

cells, mouse IPS cells and Jurkat cells treated with EdU and DAPI. *Note* the red box highlights the mean intensity of EdU signal that can also be used as an indicator of the proliferative state of the cells.

Figure 3: Analysis of Apoptosis using DiLC and PI.

Comparison of two different methods for measurement of apoptosis, DilC and Annexin V in human ESC (pluripotent cells) or Jurkat cells (Differentiated cells). Flow cytometry histogram of hESC assessed for apoptosis levels using DiLC, which measures the mitochondrial membrane potential. Note that the control ESC treated with CCCP (with DiLC at the same time) to show the shift in signal, demonstrating that the assay is working. Cyclosporin A was used in Annexin V assays to induce apoptosis (50uM for 20 hours).

Figure 4: Western blot analysis of cell cycle proteins.

Western blot of fourteen cell cycle antibodies described in table 4 using irradiated MEFs as a control and undifferentiated human ESC protein. Alpha-tubulin used as a loading control and Oct4 is used to determine pluripotent state. Note: a comprehensive analysis such as this one can be achieved in one week. sc: Santa Cruz; Cell Sign: Cell Signal antibodies.

Table 1: Modified working volumes for Click IT cocktail for EdU analysis of S phase.

Reaction components for Click IT cocktail	Number of reactions		
	2	**5**	**10**
10x Click-IT Reaction Buffer	87.5ul	219ul	438ul
CuSO4	20ul	50ul	100ul
Fluorescent dye	5ul	12.5ul	25ul
10x Reaction buffer additive	10ul	25ul	50ul
Water	877.5ul	2193.5ul	4387ul
TOTAL volume	1ml	2.5ml	5 ml

Table 2: MoFlo Instrument Settings the Flow Cytometry machine for detection of GFP, EdU and DAPI signals.

Laser	**Excitation wavelength & power**	**Band Pass Filters used for collection of emitted fluorescence (wavelength/power)**
Blue	488nm at 30mWatts	Green emission – 530/30 (from anti-GFP/Alexa Fluor 488)
Ultra violet	351nm at 20mWatts	Blue emission – 450/65 (from DAPI)
Red	633nm at 35mWatts	Red emission – 670/20 (from Alexa Fluor 647 azide linked to EdU)

Table 3: MoFlo Instrument Settings for detection of DilC and PI signal.

Laser	**Excitation wavelength & power**	**Band Pass Filters used for collection of emitted fluorescence (wavelength/power)**
Blue (PI)	488nm at 30mWatts	Orange emission – 580/30 (from PI) Red emission – 670/30 (from PI)
Red (DilC)	633nm at 35mWatts	Red emission – 670/20 (from DilC)

Table 4: Tested and working antibodies for analysis of cell cycle and apoptosis by western blot methodology. TIMING: 1 week.

Antibody name	Company and Cat #	Dilution and expected size (KDa).
P53	sc-126(DO-1) mouse	1:1000 5%milk/TBS. 53KDa
P19ARF	R562 Abcam Rabbit	1:1000 5%milk/TBS 25 Kda (30-50µg)
P16INK4a	M-156 (sc-Rabbit)	1:1000 5%milk/TBS 16 Kda
Rb	C15 (sc rabbit)	1:1000 5%milk/TBS 105 KDA
P107	C18 (sc Rabbit)	1:1000 5%milk/TBS. 107 KDa
Cyclin A	C19 (sc-rabbit)	1:1000 5%milk/TBS 54Kda
Cyclin A1	H-230 (sc rabbit)	1:1000 5%milk/TBS 54Kda
Cyclin A2	Epitomics E399 (rabbit)	1:500 5%milk/TBS 54Kda
Cyclin B1	Sc-245 (mouse)	1:1000 5%milk/TBS 60Kda
Cyclin D1	H-295 (sc rabbit)	1:1000 5%milk/TBS 34 KDa
Cyclin D2	M20 (sc rabbit)	1:1000 5%milk/TBS 34 KDa
Cyclin E	M20 (sc rabbit)	1:1000 5%milk/TBS 53 KDa
E2F1	Sc-251 (sc mouse)	1:1000 5%milk/TBS 55 KDa
P21CIP	F5 (sc mouse)	1:1000 5%milk/TBS 21KDa
P27KIP	(M-197) sc776 rabbit	1:1000 5%milk/TBS 27 KDa
CDK4	C22 (sc rabbit)	1:1000 5%milk/TBS 34 KDa
CDK2	H-298 (sc rabbit)	1:1000 5%milk/TBS 34 KDa
PCNA	PC-10 (sc. Mouse)	1:1000 5%milk/TBS 36 KDa
MDM2	Abcam 2A10 (mouse)	1:1000 5%milk/TBS 80 KDa(30-50µg)
Cleaved Casapse 3	Cell sign (rabbit) #9664	1:1000 5%milk/TBS 18 KDa
Cdc27	C4 (sc mouse)	1:1000 5%milk/TBS 102KDa

Table 5: Troubleshooting

Step	Problem	Possible reason and solution
	Low number of cells in S Phase	EdU substrate incubation too short or batch of substrate used too many times. Use fresh aliquoted EdU and incubate 15-30 minutes longer.
	No distinct G1/S/G2M phases	Cells not healthy or DAPI staining not working. Check that cells look healthy before starting experiment and leave DAPI staining overnight at 4°C (in the fridge). Also consider using a modified method using Hamelik and Krishan protocol by lysing cells (Hypotonic solution) for 1 minute followed by centrifugation and then using EdU reaction (Click iT)[20].
	DilC % apoptosis lower than expected or not working.	Check with CCCP control there is a shift in DilC positive cells to negative. Keep cells at 37°C at all times throughout the procedure and analyse immediately following PI staining.

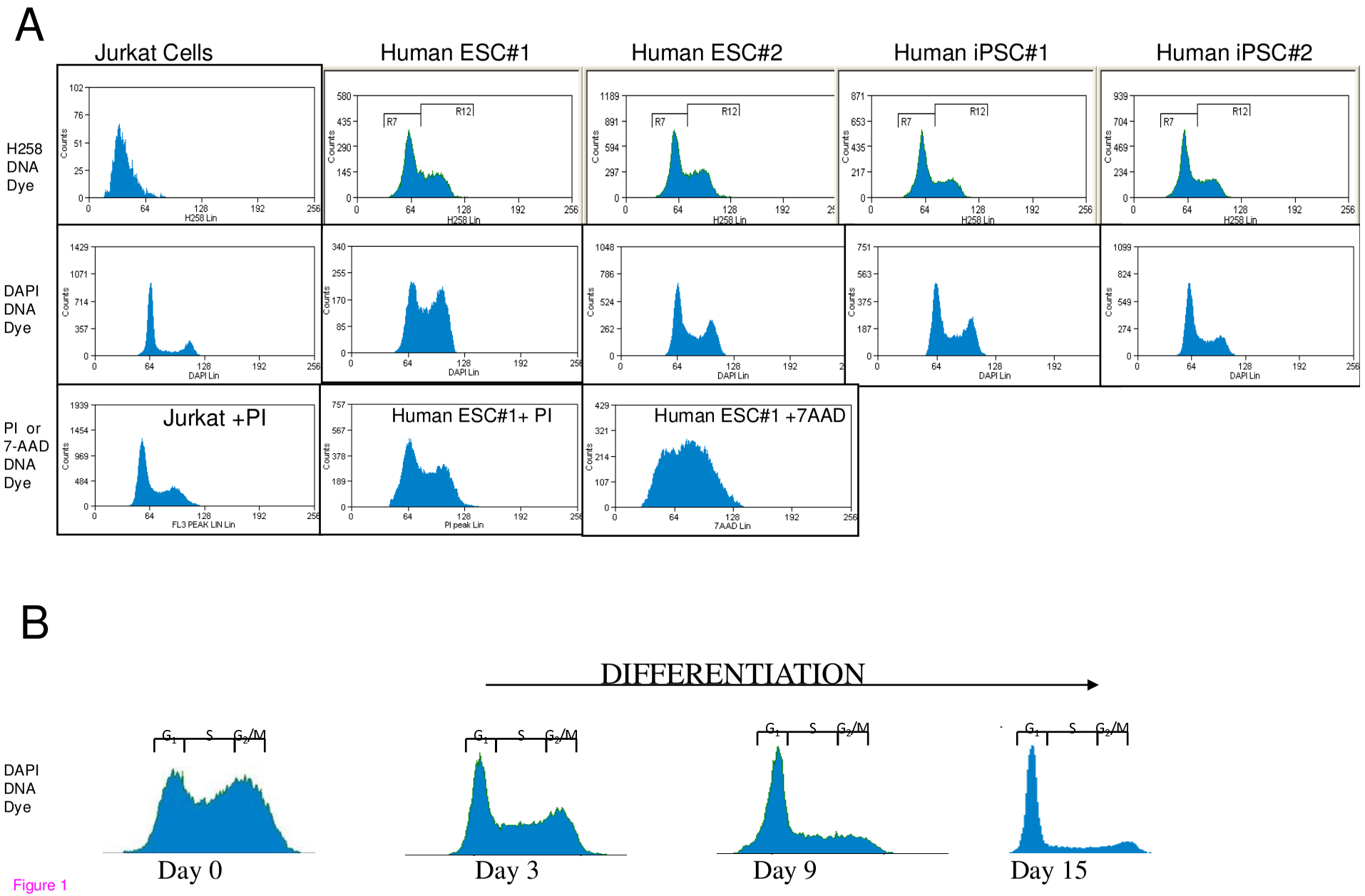
A
Jurkat Cells
Human ESC#1
Human ESC#2
Human iPSC#1
Human iPSC#2
H258 DNA Dye
DAPI DNA Dye
PI or 7-AAD DNA Dye
Jurkat +PI
Human ESC#1+ PI
Human ESC#1 +7AAD
R7
R12
Counts
H258 Lin
DAPI Lin
FL3 PEAK LIN Lin
PI peak Lin
7AAD Lin
B
DIFFERENTIATION
DAPI DNA Dye
G1 S G2/M
Day 0
Day 3
Day 9
Day 15

Figure 1

A

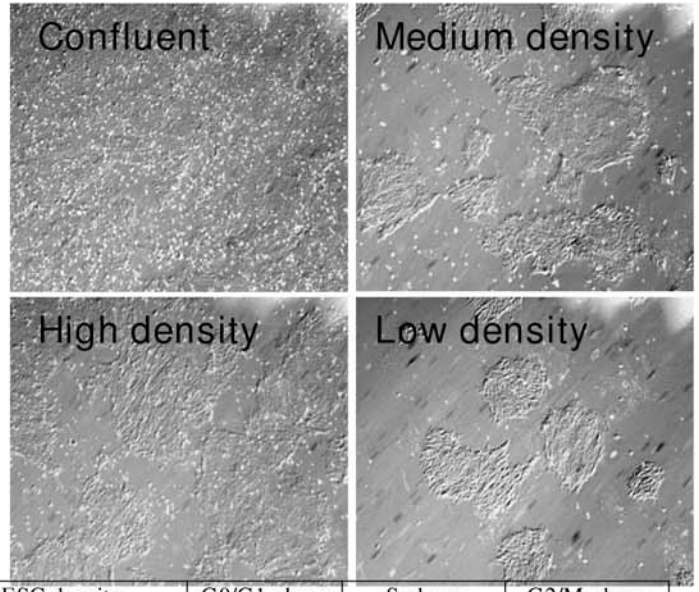

hESC density	G0/G1 phase	S phase	G2/M phase
Low (20%)	13%	54%	29%
Medium (50%)	16%	54%	22%
High (75%)	16%	53%	22%
Confluent (100%)	18%	53%	20%

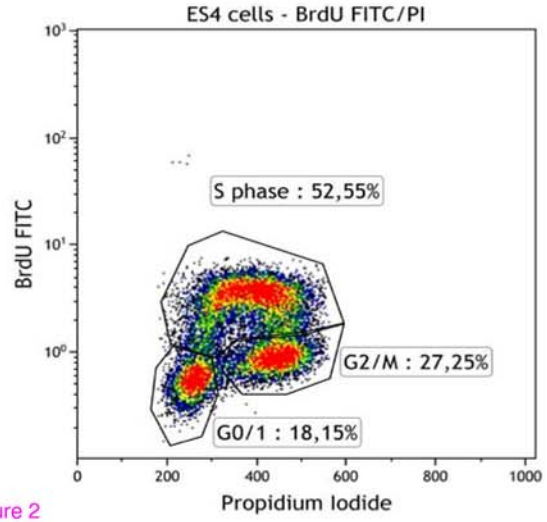

B

Mouse iPS cells (late passage)

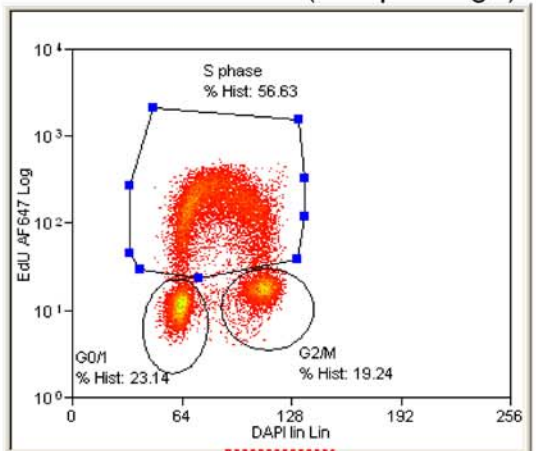

Region	% Hist	Mean	CV
Total	100.00	84.10, 98.50	24.08, 100.59
S phase	56.63	83.97, 163.33	20.24, 53.46
G0/1	23.14	62.94, 11.11	6.30, 29.07
G2/M	19.24	110.01, 16.91	5.70, 25.33

Human ESC

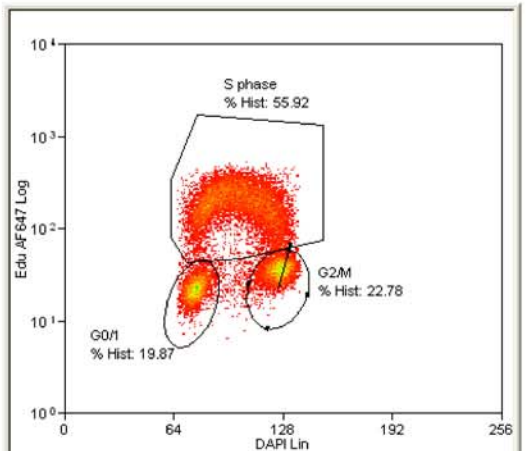

Region	% Hist	Mean	CV
Total	100.00	101.84, 119.31	20.00, 84.00
S phase	55.92	101.54, 190.41	16.53, 42.10
G0/1	19.87	76.72, 22.62	5.75, 26.75
G2/M	22.78	124.76, 34.88	4.63, 22.18

Human IPS cells (early passage)

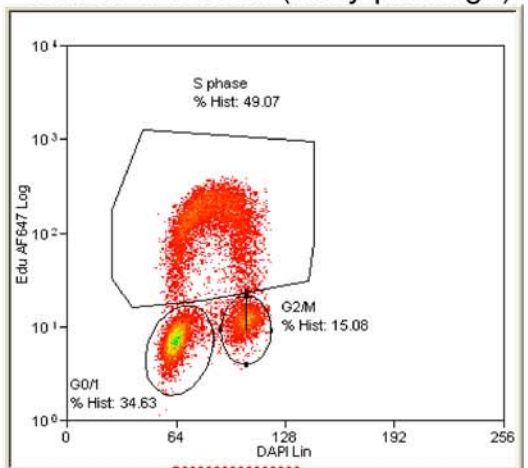

Region	% Hist	Mean	CV
Total	100.00	80.45, 74.98	21.81, 112.97
S phase	49.07	84.43, 143.67	17.40, 50.89
G0/1	34.63	64.14, 7.39	7.50, 30.63
G2/M	15.08	104.34, 11.60	5.02, 24.61

Jurkat cells

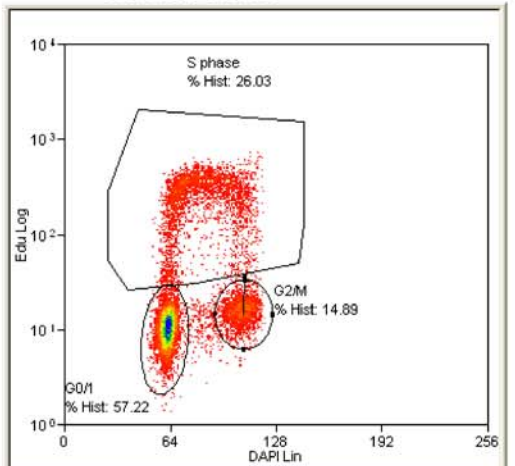

Region	% Hist	Mean	CV
Total	100.00	74.46, 75.93	24.95, 166.92
S phase	26.03	82.24, 258.48	20.18, 49.88
G0/1	57.22	62.12, 10.56	4.97, 36.64
G2/M	14.89	106.73, 15.98	5.63, 27.30

Figure 2

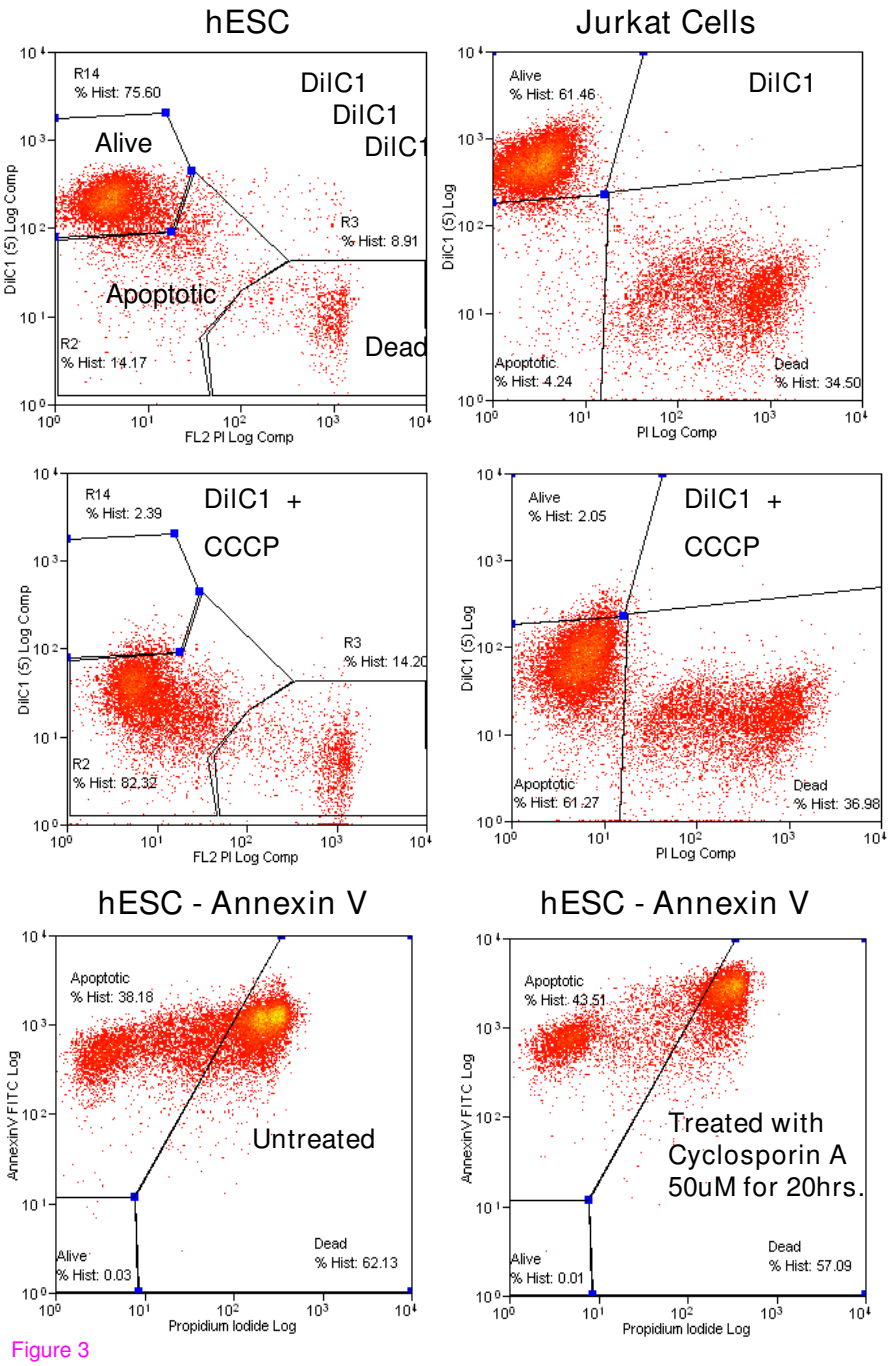
hESC
Jurkat Cells
R14
% Hist: 75.60
DilC1
DilC1
DilC1
Alive
R3
% Hist: 8.91
Apoptotic
Dead
R2
% Hist: 14.17
DilC1 (5) Log Comp
FL2 PI Log Comp
Alive
% Hist: 61.46
DilC1
Apoptotic
% Hist: 4.24
Dead
% Hist: 34.50
DilC1 (5) Log
PI Log Comp
R14
% Hist: 2.39
DilC1 +
CCCP
R3
% Hist: 14.20
R2
% Hist: 82.32
DilC1 (5) Log Comp
FL2 PI Log Comp
Alive
% Hist: 2.05
DilC1 +
CCCP
Apoptotic
% Hist: 61.27
Dead
% Hist: 36.98
DilC1 (5) Log
PI Log Comp
hESC - Annexin V
hESC - Annexin V
Apoptotic
% Hist: 38.18
Untreated
Alive
% Hist: 0.03
Dead
% Hist: 62.13
AnnexinV FITC Log
Propidium Iodide Log
Apoptotic
% Hist: 43.51
Treated with
Cyclosporin A
50uM for 20hrs.
Alive
% Hist: 0.01
Dead
% Hist: 57.09
AnnexinV FITC Log
Propidium Iodide Log

Figure 3

A

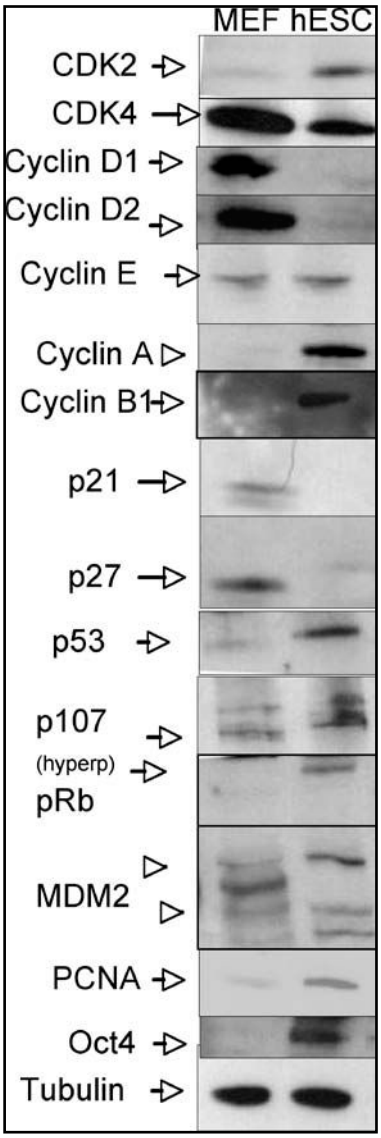
MEF hESC
CDK2
CDK4
Cyclin D1
Cyclin D2
Cyclin E
Cyclin A
Cyclin B1
p21
p27
p53
p107
(hyperp)
pRb
MDM2
PCNA
Oct4
Tubulin

Figure 4